MEASUREMENT OF TWO- AND THREE-PHASE RELATIVE PERMEABILITY

AND DISPERSION FOR MICELLAR FLUIDS IN

UNCONSOLIDATED SAND

APPROVED:

Gary A. Pope

Bruce A. Rouse

Robert S. Schechter

MEASUREMENT OF TWO- AND THREE-PHASE RELATIVE PERMEABILITY AND DISPERSION FOR MICELLAR FLUIDS IN UNCONSOLIDATED SAND

BY

DONALD JAMES MacALLISTER, B. S. CHEMISTRY

THESIS

Presented to the Faculty of the Graduate School of

The University of Texas at Austin

in Partial Fulfillment

of the Requirements

for the Degree of

MASTER OF SCIENCE IN PETROLEUM ENGINEERING

THE UNIVERSITY OF TEXAS AT AUSTIN

May, 1982

ACKNOWLEDGEMENT

I thank my supervising professor, Gary Pope, for his guidance and support. I am also grateful to Dr. R. S. Schechter and Dr. B. A. Rouse for serving on my graduate committee.

Appreciation is extended to my fellow graduate students and the many undergraduate laboratory technicians who helped me. I am grateful to Mike Breland, Mojdeh Delshad, Bruce Rouse, John Trowbridge, Lorie Werts, and Vito Zapata who are more friends than colleagues.

I am especially grateful to my beautiful wife Gayle for her understanding.

ABSTRACT

Experiments in sandpacks and Berea sandstone were performed to measure dispersion and steady-state relative permeabilities. Phase behavior, interfacial tension, and viscosity determinations were made using DS-10 and TRS 10-410 surfactants to formulate a suitable three-phase micellar mixture. Relative permeability measurements were made at steady-state on both high tension brine-oil pairs and a low tension three-phase brine-oil-surfactant-alcohol mixture followed by injection of radioactive and chemical tracer(s) to investigate dispersion. The classical solution to the convection-diffusion equation for single-phase flow is generalized to multiphase flow, allowing interpretation of the multiphase flow experiments. Dispersivity was a strong function of phase, phase saturation, porous medium, and interfacial tension. Dispersivity values varied over two orders of magnitude. Extremely early breakthrough of carbon-14 tracer in the high tension oil phases was an unexpected result. Tritium tracer breakthrough curves, however, were similar to 100% saturation breakthrough curves (except for a shift due to the oil saturation). Unlike the aqueous and oleic phases, the microemulsion phase dispersivity was not a function of saturation. Three-phase experiments indicated that the aqueous or oleic phase relative permeability is a function of its own saturation only. During three-phase flow, a change in wettability from the original water-wet state occurred.

TABLE OF CONTENTS

LIST OF TABLES

LIST OF FIGURES

INTRODUCTION

Among the approximations commonly made in constructing a chemical flood simulator are theoretical relative permeability curves of micellar fluid phases and negligible dispersion (or artificially-produced dispersion such as numerical dispersion). Errors in these approximations can lead to erroneous and misleading results, especially in compositional simulators[1] and when applying fractional flow theory.[2,3]

The objective of this study is to determine the relative permeability and dispersion in one-, two-, and three-phase flow for a three-phase micellar fluid composition. These data can then be incorporated into a chemical flood simulator so that more accurate predictions can be made.

To fulfill this objective, this investigation consists of five sections: the theoretical background of relative permeability and dispersion in porous media, a description of the physical properties of the fluid compositions under consideration, a description of the experimental apparatus and experimental procedures, a discussion of the experimental results, and a discussion of conclusions drawn from experimental evidence.

THEORETICAL BACKGROUND

The theoretical background of relative permeability and dispersion in porous media is an integral, although sparsely researched, aspect of chemical flooding. First, this chapter reviews relative premeability, its definition, the properties of high and low interfacial tension two-phase relative permeabilities, and the application of relative permeability to mobility design. Secondly, dispersion in porous media is discussed including its definition, single-phase dispersion, a theory for partitioning of tracers into multiple phases, two-phase dispersion, and, finally, three-phase dispersion.

Relative Permeability

Permeability is an average (macroscopic) property that measures the ability of a porous medium to transmit fluid. When two or more immiscible fluids are simultaneously flowing in a porous media, interference occurs which reduces the effective permeability of each fluid. This permeability reduction gives rise to the following relative permeability concept:

$$k_{r_j} = k_{e_j}/k \qquad 2.1$$

Due to fluid-fluid interference, relative permeability is a function of fluid saturation.[4-5] Figure 5.16

illustrates typical relative permeability curves. The relative permeability of the non-wetting phase at residual wetting phase saturation is always greater than the relative permeability of the wetting phase at residual non-wetting phase saturation.

The rapid decline of wetting phase relative permeability indicates that the larger pores are occupied first by the non-wetting phase.[4] As the non-wetting phase saturation increases, the average pore size saturated by the wetting phase decreases. As a result, the non-wetting phase occupies larger pores than the wetting phase. Oil/brine relative permeabilities, with high interfacial tension (IFT), exhibit a hysteresis effect for desaturation and resaturation processes.

Bardon and Longeron[6] studied a two-phase oil/vapor system and determined that oil/vapor relative permeabilities are independent of velocity. Two-phase oil/brine relative permeabilities are also independent of velocity except close to residual oil and residual brine saturations.[7,8] This exception is due to the dependence of residual oil and residual brine saturations on the capillary number, which is proportional to fluid velocity, and defined by the following ratio:

$$N_C = \frac{v\mu}{\sigma} \qquad 2.2$$

Interfacial tension-lowering additives have several effects on two-phase relative permeabilities:

Critical Interfacial Tension

Leverett[9] added amyl alcohol to a kerosene/7N sodium chloride solution to lower the IFT from 30 dynes/cm to 5 dynes/cm. This caused a small but significant increase in both oil and brine relative permeabilities in high permeability sandpacks. Amaefule and Handy[7] found a critical IFT occurs at 10^{-1} dyne/cm where an increase in relative permeability is apparent for several oil/brine/low concentration surfactant formulations in Berea sandstone. Bardon and Langeron[6] found a critical IFT of 0.04 dyne/cm is necessary to increase the relative permeabilities of a n-heptane/methane formulation at 71.1°C and 5,800 psig in Fountainebleau sandstone.

Klaus[10] found that aqueous phase relative permeability increased with decreasing IFT over the entire IFT range for soltrol 170/2.0 wt % calcium chloride brine/isopropyl alcohol two-phase compositions in Berea sandstone. Oleic phase relative permeability increased with decreasing IFT below 1.6 dynes/cm. Above 1.6 dynes/cm no change in oleic phase relative permeability occurred.

Residual Saturations

As noted earlier, residual oil and residual brine saturations decrease with increasing capillary number.

Since the capillary number is inversely proportional to IFT, residual oil and residual brine saturations should decrease with the addition of IFT-lowering additives. Several investigators[7,10-12] have confirmed this decrease.

Curvature

Relative permeability curvature decreases with decreasing IFT and tends to become a linear function of saturation as IFT approaches zero.[7,12,13] Batycky and McCaffery[14] observed this effect for n-decane/1.0 wt % NaCl brine/0.2 wt % TRS 10-80 two-phase compositions at 26.6°C in unconsolidated sand. Some curvature still exists at 0.02 dynes/cm indicating some interference between the fluids. Batycky and McCaffery postulate that only when residual oil and residual brine saturations are zero will wettability-determined preferential flow paths be eliminated and straight relative permeability curves occur. This postulation is confirmed for one case by Bardon and Longeron[6] who studied n-heptane/methane relative permeabilities. Relative permeability curves became straight lines at 10^{-3} dynes/cm where the residual oil and residual brine saturations were zero.

Hysteresis

At high IFT, relative permeability may be different for imbibition and drainage processes. This phenomenon is called hysteresis. Amaefule and Handy[7] found that hysteresis tends to diminish with decreasing IFT and is almost non-existent at ultra-low IFTs for several oil/brine/surfactant formulations in Berea sandstone. Batycky and McCaffery[14] observed the same effect for an n-decane/1.0 wt % NaCl brine/0.2 wt % TRS 10-80 two-phase fluid composition at 26.6°C in unconsolidated sand. Talash[13] reports similar results for two-phase crude oil/field brine compositions with four different low-concentration surfactants in Berea sandstone. Klaus,[10] on the other hand, found little or no change in relative permeability hysteresis with decreasing IFT for soltrol 170/2.0 wt % calcium chloride brine/isopropyl alcohol two-phase compositions in Berea sandstone. The absence of hysteresis may be due to an insufficiently decreased capillary number.

Wettability

The shape of relative permeability curves is dependent on the porous media wettability.[11,12,15,16] In addition, the nonwetting phase displacing the wetting phase leaves a lower residual saturation than the reverse.[11,12,16] Amaefule and Handy[7] determined that Berea sandstone surfaces were less water wet after flooding with sulfonate. This effect is evident in the relative permeability curves for fluids containing IFT-lowering additives for Berea sandstone,[10] polytetrafluoroethylene cores,[11] and unconsolidated sand.[14]

Mobility

Gogarty et al[17,18] investigated the effect of relative permeability in secondary and tertiary flooding. Gogarty utilized the mobility and total relative mobility concepts as a basis for field flood design. Mobility and total relative mobility are defined as follows:

$$M = \frac{k_e}{\mu} \qquad 2.3$$

$$M_{rT} = \sum_{j=1}^{3} \frac{k_{rj}}{\mu_j} \qquad 2.4$$

A minimum total relative mobility value is determined by plotting total relative mobility vs aqueous saturation (Figure 5.2). The minimum total relative mobility is used as a criterion for designing a fluid to efficiently displace an oil/brine bank. Chang et al[19] recently applied the minimum total relative mobility criterion in designing the mobility requirements of the El Dorado micellar-polymer demonstration project.

Dispersion in Porous Media

Consider a single fluid containing a non-adsorbing solute tracer and flowing through a porous medium. The tracer is identified by a physical property (radioactivity, color, etc.). As flow proceeds, the tracer spreads and forms an ever-widening transition zone of tracer concentration varying from injected concentration to zero. The transition zone extends beyond the region it is expected to occupy according to the average flow alone. When a small slug of fluid containing tracer is injected, a bell-shaped pulse forms. The height of the pulse decreases and its width increases as flow proceeds. This spreading of the tracer is termed dispersion.

Dispersion in Single-Phase Flow

This discussion considers only one-dimensional miscible dispersion of a liquid phase in porous media. For these assumptions, the material balance equation is:

$$\frac{\partial C_T}{\partial X} + \frac{q}{A\phi}\frac{\partial C_T}{\partial X} = \frac{\partial}{\partial X}\left(K_l \frac{\partial C_T}{\partial X}\right) \qquad 2.5$$

As outlined by Perkins and Johnston,[21] dispersion in porous media during laminar flow can be characterized by the dispersion tensor, $\underline{\underline{K}}$, as follows:

$$\underline{\underline{K}} = \begin{pmatrix} K_t & 0 & 0 \\ 0 & K_t & 0 \\ 0 & 0 & K_l \end{pmatrix} \qquad 2.6$$

(The axis is aligned with the flow.)

$$K_l = \frac{D_o}{F\phi} + \alpha_l\, v^{\beta} \tag{2.7a}$$

$$K_t = \frac{D_o}{F\phi} + \alpha_t\, v^{\beta} \tag{2.7b}$$

Several authors[20,22-25] have demonstrated that at frontal advance rates on the order of 0.5 to one foot per day the second term dominates for longitudinal dispersion. The magnitude of β varies between 1.0 and 1.4 with 1.2 considered a reasonable value for sandstone.[20,21,23,26]

For simplicity β is often assumed to be 1.0. This assumption, for the case where the second term of Equation 2.6 dominates, implies that longitudinal dispersion is proportional to velocity. This has been confirmed by several investigators.[24,26-28] At very low flow rates, dispersion is equal to the Fick's diffusion coefficient reduced by the factor $F\phi$. The factor $F\phi$ accounts for the tortuosity of the porous media.[25] In addition, longitudinal dispersivity is on the order of 30 times greater than transverse dispersivity.[21,25]

Normalize distance, time, and concentration as follows:

$$x_D = \frac{X}{L} \tag{2.8}$$

$$t_D = \frac{tq}{AL\phi} \tag{2.9}$$

$$C_D = \frac{C_T}{C_O} \tag{2.10}$$

The material balance equation now becomes:

$$\frac{\partial}{\partial t_D} C_D + \frac{\partial}{\partial X_D} C_D = \frac{K_1}{v_T L} \frac{\partial^2}{\partial X_D{}^2} C T \qquad 2.11$$

The well-known solution to Equation 3.7 for the following boundary conditions:

$$C_D = 0 \qquad X_D \rightarrow \pm \infty \qquad 2.12$$

is:

$$C_D = \frac{1}{2}\left[1 - \mathrm{erf}\left(\frac{X_D - t_D}{\sqrt{\frac{4K_1 t_D}{v_T L}}}\right)\right] \qquad 2.13$$

All of our measurements are performed on samples produced from the outflow end of the porous media ($X_D = 1$), therefore, Equation 3.9 is rewritten as:

$$C_D = \frac{1}{2}\left[1 - \mathrm{erf}\left(\frac{1}{\sqrt{\frac{4K_1}{v_T L}}} \cdot \frac{1 - t_D}{\sqrt{t_D}}\right)\right] \qquad 2.14$$

Brigham et al[20] outlined a method of calculating longitudinal dispersion from experimental data for single-phase miscibile displacement. Their analysis assumes longitudinal dispersion is governed by Equation 2.5. This equation is analogous to Fick's diffusion equation[21] with the dispersion coefficient substituted for the diffusion coefficient. Perkins and Johnston[21] further modified the approach and illustrate how longitudinal dispersion can be calculated by plotting normalized concentration against a function λ on probability paper. The function λ is defined as follows:

$$\lambda = \frac{t_D - 1}{\sqrt{t_D}} \qquad 2.15$$

This plot yields a straight line for fluids conforming to Equation 2.14. The longitudinal dispersion coefficient can then be calculated by graphically determining λ_{90} (λ at 90% of full strength effluent concentration) and λ_{10} from the best straight line through the data as follows (Figure 5.22):

$$K_l = v_T L \left(\frac{\lambda_{90} - \lambda_{10}}{3.625} \right)^2 \qquad 2.16$$

or

$$\alpha_l = L \left(\frac{\lambda_{90} - \lambda_{10}}{3.625} \right)^2 \quad (\beta = 1.0) \qquad 2.17$$

Note that at one pore volume ($t_D = 1$), $\lambda = 0$ and Equation 2.14 reduces to $C_D = 1/2$. Therefore, the 50% of full strength concentration will be produced at $t_D = 1$.

Tracer Partitioning

A tracer, when added to either the oleic or aqueous phase in a three-phase micellar fluid formulation, will partition into the microemulsion phase since all components of both oleic and aqueous phases are also in the microemulsion phase. As a result, tracer production data in which partitioning occurs must be corrected. This section develops a theory to account for two-phase partitioning of micellar fluids.

The flow of tracer through a porous medium is not pistonlike. The breakthrough time of tracer, t_D^{Bt}, will be defined as the time at which the tracer concentration reaches 50% of its injected value since this corresponds to the time at which a truly pistonlike concentration change would occur. Note this is true only for a symmetrically-produced concentration profile.[29] The breakthrough time for a nonpartitioning tracer in a phase whose velocity is defined as:

$$v_{Tj} = \frac{qf_j}{A\phi S_j} \tag{2.18}$$

is given by:

$$t^{Bt} = \frac{L}{v_{Tj}} \tag{2.19}$$

Normalizing using Equation 2.9 yields:

$$t_D^{Bt} = S_j/f_j \tag{2.20}$$

Note that phase saturation can be calculated from tracer data since both t_D^{Bt} and f_j are known.[30]

Neglecting dispersion, the material balance equation for a partitioning tracer at steady state is:

$$\phi A \frac{\partial}{\partial t}(S_1 C_{T_{11}} + S_2\, C_{T_{12}}) + q \frac{\partial}{\partial X}(f_1\, C_{T_{11}} + f_2\, C_{T_{12}}) = 0 \tag{2.21}$$

Define a tracer partition coefficient as follows (for tritium tracer):

$$K_{T1} = C_{T_{12}}/C_{T_{11}} \qquad 2.22$$

Assume K_{T1} is constant (this is true under some conditions e.g., radioactive tracers,[30] see Table 5.17). Equation 2.21 now becomes:

$$(S_1 + S_2 K_{T1}) \frac{\partial C_{T_{11}}}{\partial t} + \frac{q}{A\phi}(f_1 + f_2 K_{T1}) \frac{\partial C_{T_{11}}}{\partial X} = 0 \qquad 2.23$$

and

$$\left(\frac{\partial X}{\partial t}\right)_{C_{T_{11}}} = \frac{q}{A\phi}\left(\frac{f_1 + f_2 K_{T1}}{S_1 + S_2 K_{T1}}\right) \qquad 2.24$$

Employing Equations 2.9, 2.18, and 2.19, the breakthrough time is:

$$t_D^{Bt} = \frac{S_1 + S_2 K_{T1}}{f_1 + f_2 K_{T1}} \qquad 2.25$$

Analyses leading to equations similar to these have been performed by Pope[1] and Deans,[30] who appears to be the first to propose the use of tracers in relative permeability experiments. Since K_{T1}, f_1, and f_2 are measured, there is only one unknown in Equation 2.25 since $S_1 + S_2 = 1$. (This is not true when three phases are present, however.) When phase two is not flowing (at residual saturation S_{2r}), Equation 2.25 reduces to:

$$t_D^{Bt} = S_1 + S_{2r} K_{T1} \tag{2.26}$$

Dispersion in Two-Phase Flow

For two-phase flow with a partitioning tracer, the material balance for a tracer undergoing dispersion is: (Note that the theory is developed for aqueous phase ($j = 1$) and microemulsion phase ($j = 3$) with a partitioning tritium tracer ($i = 1$) but could be developed for any two phases with an appropriate partitioning tracer.)

$$\phi A \frac{\partial}{\partial t}(S_1 C_{T_{11}} + S_3 C_{T_{13}}) + q \frac{\partial}{\partial X}(f_1 C_{T_{11}} + f_3 C_{T_{13}}) =$$

$$A\phi \frac{\partial}{\partial X}\left(S_1 K_{11} \frac{\partial C_{T_{11}}}{\partial X} + S_3 K_{13} \frac{\partial C_{T_{13}}}{\partial X} \right) \tag{2.27}$$

For the same assumptions stated in the single-phase flow section and assuming steady state flow (saturations and fractional flows constant) the material balance equation is:

$$(S_1 + S_3 K_{T1}) \frac{\partial C_{T_{11}}}{\partial t} + \frac{q}{A\phi}(f_1 + f_3 K_{T1}) \frac{\partial C_{T_{11}}}{\partial X} =$$

$$(S_1 K_{11} + S_2 K_{13} K_{T1}) \frac{\partial^2 C_{T_{11}}}{\partial X^2} \tag{2.28}$$

Normalizing using Equations 2.9 and 2.10 and a new normalized time variable:

$$t_{Dt} = \frac{qtf_1}{AL\phi S_1} = \frac{t_D}{(S_1/f_1)} \qquad 2.29$$

yields:

$$\frac{\partial C_{D_{11}}}{\partial t_{Dt}} + \frac{\partial C_{D_{11}}}{\partial X_D} = \frac{\overline{K}_1}{v_T L} \frac{\partial^2 C_{D_1}}{\partial X_D^2} \qquad 2.30$$

$$v_T = \frac{q}{A\phi} \frac{f_1 + f_3 K_{T1}}{S_1 + S_3 K_{T1}} \qquad 2.31$$

$$\overline{K}_1 = \frac{S_1 K_{11} + S_3 K_{13} K_{T1}}{S_1 + S_3 K_{T1}} \qquad 2.32$$

$$\overline{\alpha}_1 = \frac{S_1 \alpha_{11} + S_3 \alpha_{13} K_{T1}}{S_1 + S_3 K_{T1}} \qquad 2.33$$

As before, at $X_D = 1$:

$$C_{D11} = 1/2 \left[1 - \text{erf}\left(\frac{1 - t_{Dt}}{\sqrt{\frac{4K_{11} S_1 t_{Dt}}{f_1 v_T L}}}\right)\right] \qquad 2.34$$

and

$$\overline{K}_1 = v_T L \left(\frac{\lambda_{1_{90}} - \lambda_{1_{10}}}{3.625}\right)^2 \qquad 2.35$$

$$\overline{\alpha}_1 = L \left(\frac{\lambda_{1_{90}} - \lambda_{1_{10}}}{3.625}\right)^2 \qquad 2.36$$

where

$$\lambda_1 = \frac{t_{Dt} - 1}{\sqrt{t_{Dt}}} \qquad 2.37$$

Equation 2.37 adjusts λ_1 so that t_{Dt}^{Bt} occurs at $\lambda_1 = 0$. Brigham[29] discusses why this is necessary.

Using different nomenclature, Stalkup[31] modified Equation 2.15 for miscible oleic phase displacements of several hydrocarbons (including propane) performed in the presence of 0.5 wt % $CaCl_2$ brine in Boise, Berea, and Torpedo sandstones, where t_D^{Bt} occurs at less than one pore volume ($t_D < 1$) as follows:

$$\lambda_f = \frac{\frac{V}{V_{Pf}} - 1}{\left(\frac{V}{V_{Pf}}\right)^{0.5}} \qquad 2.38$$

V = produced oleic phase volume = qtf_o

V_{Pf} = total mobile oleic phase volume = $AL\phi S_o$

or

$$\lambda_f = \frac{\frac{qtf_o}{AL\phi S_o} - 1}{\left(\frac{qtf_o}{AL\phi S_o}\right)^{0.5}} \qquad 2.38a$$

Applying Equations 2.9 and 2.29:

$$\lambda_f = \frac{t_{Dt} - 1}{\sqrt{t_{Dt}}} \qquad 2.39$$

Note that in light of Equation 2.39, Equation 2.38 is merely a special case of Equation 2.37 for oleic phase flowing at residual aqueous phase. Similarly Equation 2.37 reduces to Equation 2.15 for S = 1 and f = 1.

The measured dispersivity ($\overline{\alpha}_i$) is a weighted average of the actual phase dispersivities. (Note that for single-phase flow, Equation 2.33 reduces to $\overline{\alpha} = \alpha$.) Saturations are determined by Equation 2.25 and by material balance calculation and K_{Ti} is measured for static fluid samples. This leaves two unknowns in Equation 2.33 (α_{11} and α_{13}). Therefore, in order to determine the actual phase dispersivities where $K_{Ti} \neq 0$, two tracers are required. As illustrated in Figure 5.63, the data often deviate from an S-shaped convective configuration indicating a departure from Equation 2.5. This occurance has been observed by several investigators[21,24,29,32-34] with a variety of explantions. The phenomenon is more severe in the presence of another immiscible phase. It is also associated with early breakthrough of the nonwetting phase coupled with a long "tailing out" of nonwetting phase concentration. This has been attributed to a stagnant volume of nonwetting fluid trapped by wetting phase as discontinuous masses or in "dead end pores" and "dendritic structures." This stationary volume is gradually replaced by molecular diffusion. The tailing out is due to the slowness of the diffusion process relative to the convective process. The fact that the tailing out is less pronounced at a lower fluid velocity has lead some investigators[24,33] to conclude that a diffusion process is indeed responsible.

Coats and Smith[32] have constructed a three-parameter capacitance model that assumes a stagnant volume in communication with the mobile fraction by a first-order rate expression. Besides the longitudinal dispersion coefficient (K_l), additional parameters of flowing fluid fraction and mass transfer coefficient describe the displacement. For experimental data exhibiting early, asymmetrical production, the capacitance model better fits the data. Also, the capacitance model very nearly approximates those production curves matched closely by the convective model. The capacitance model separates the dispersion process from the capacitance effect. For this reason, the dispersion coefficient calculated by the capacitance model for early, asymmetrical production is smaller than that calculated by the convective model. Similar capacitance effects are discussed by Spence and Watkins[23] for limestone and Donaldson et al[35] for sandstone.

Thomas et al[34] found that dispersion in the wetting phase increases with decreasing wetting phase saturation in Boise sandstone at room temperature. Nonwetting phase dispersion was determined by a unique method. Boise sandstone was saturated at elevated temperature with hot liquid paraffin representing a wetting phase. Air was then injected to reduce the paraffin to a residual saturation. Different air pressures were applied to vary the residual paraffin saturation. After cooling to room temperature, the air was displaced with brine, which simulates a nonwetting phase. The resulting nonwetting phase dispersivities increased with decreasing nonwetting phase saturation.

Schuler[24] performed wetting phase miscible displacements in Berea sandstone at several wetting phase saturations. Longitudinal dispersion increased not only with velocity, but with decreasing wetting phase saturation as well. Raimondi et al[33] also observed an increase in non-wetting phase dispersion with decreasing nonwetting phase saturation for ethylbenzene displacing heptane and 8.0 wt % NaCl brine displacing 3.0 wt % brine at room temperature in Berea sandstone. A variance in the wetting phase dispersivity is apparent, but no coherent relationship with phase saturation exists. Stalkup[31] also reported increased dispersion in the nonwetting phase with decreasing non-wetting phase saturation for several hydrocarbons and 0.5 wt % $CaCl_2$ brine in several sandstones. Longitudinal dispersion coefficients divided by phase velocity and by the dispersion coefficient at 100% phase saturation are plotted vs phase saturation for the nonwetting phase in Figure 2.1 and for the wetting phase in Figure 2.2 for the variety of fluids and sandstones reported. Figure 2.1 gives a clear indication of the increased dispersion with decreasing nonwetting phase saturation. Figure 2.2 gives the same indication for the wetting phase from data reported by Schuler[24] and Thomas et al.[34] The data of Raimondi et al[33] show no correlation. No mention of dispersion in low tension systems was found in in the literature.

<u>Dispersion in Three-Phase Flow</u>

For the tracers used in this investigation, partitioning occurs only between excess brine and microemulsion and excess oil and microemulsion. Since none of the tracers partition to all three phases, the equations developed for two-phase flow apply. The only difference is that $S_1 + S_2 \neq 1$ and $f_1 + f_2 \neq 1$. There are three average dispersivity equations (Equation 2.33) for three phases and three unknowns (α_1, α_2, and α_3). Therefore, three tracers are required. In addition, at least two equations like Equation 2.25 are required to calculate saturation from tracer breakthrough data. Two tracers would appear to be sufficient for this purpose since the three saturations must add to unity and two t_D values can be measured, one for each tracer. This gives two equations and two unknowns (any two of the three saturations). However, unlike the two-phase cases, no independent tracer calculation is possible unless a third, non-partitioning tracer is used.

FIGURE 2.1
NORMALIZED DISPERSIVITY VS
NON-WETTING PHASE SATURATION
FOR PUBLISHED LITERATURE VALUES

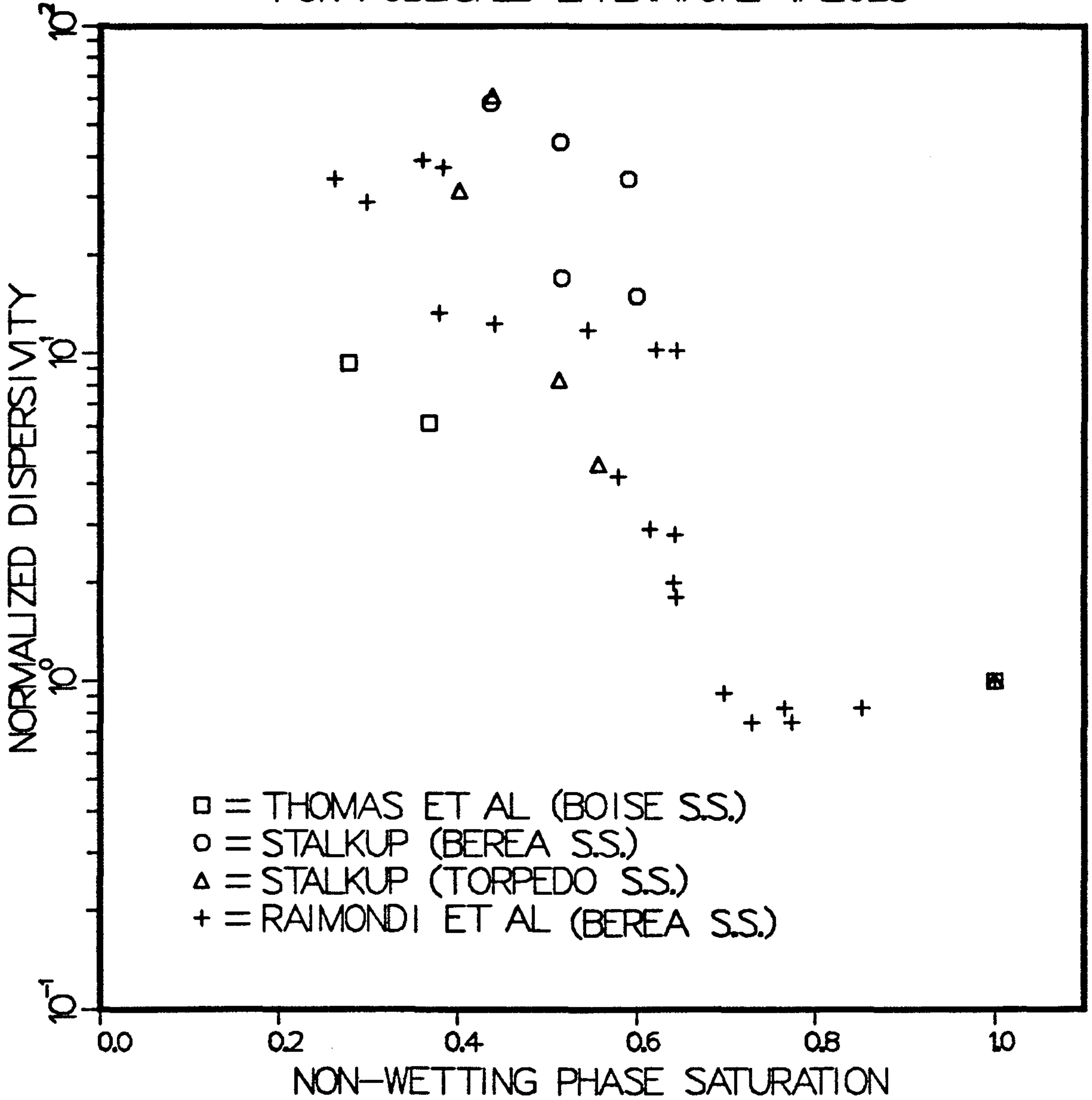

FIGURE 2.2
NORMALIZED DISPERSIVITY VS
WETTING PHASE SATURATION
FOR PUBLISHED LITERATURE VALUES

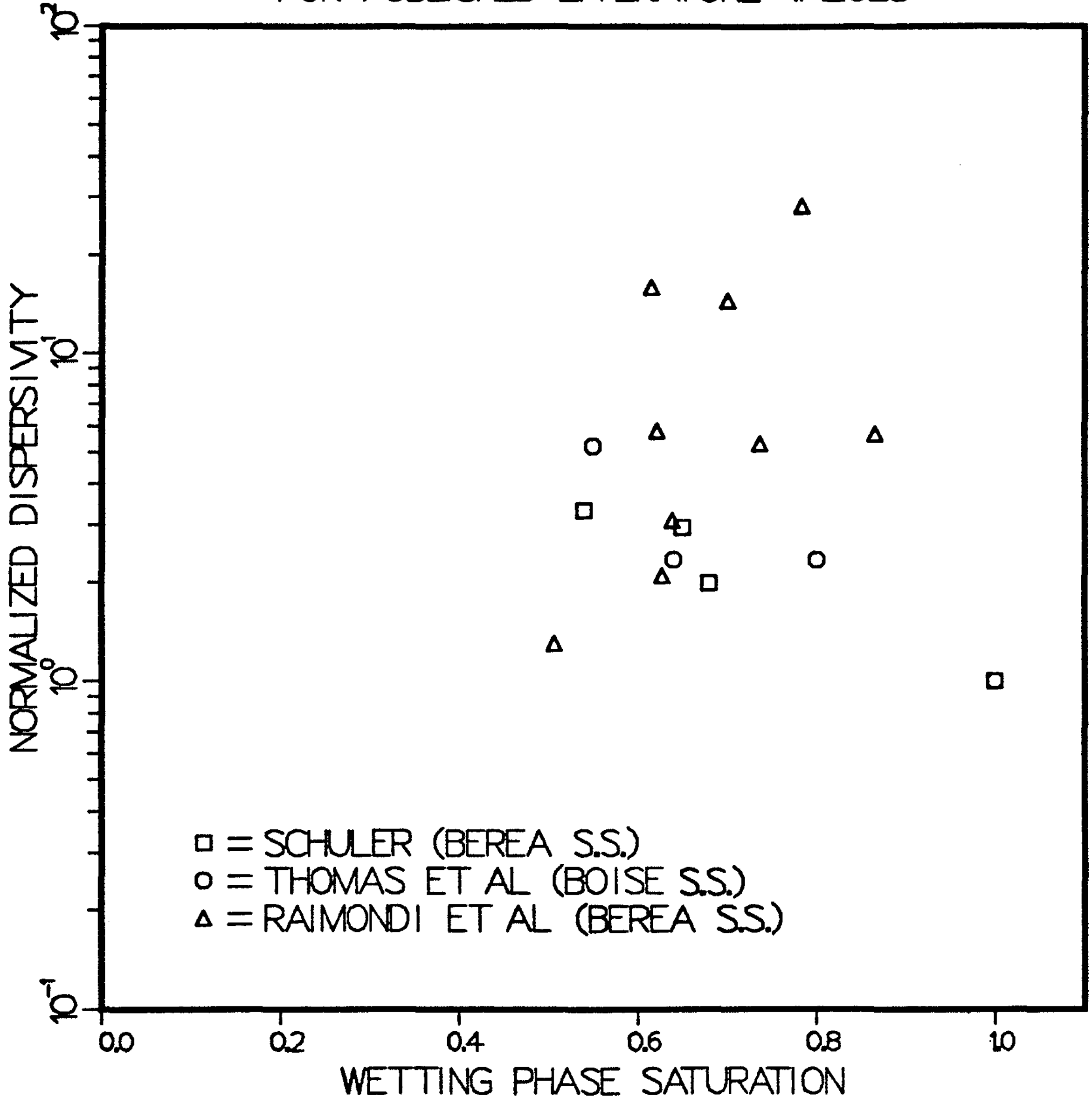

PHYSICAL SYSTEM

Phase behavior, interfacial tension (IFT), and viscosity are physical properties especially important in porous media flow experiments. In this chapter a brief introduction to phase behavior, IFT, and viscosity is presented followed by physical property data for Siponate DS-10 (sodium dodecyl benzene sulfonate) and Witco TRS 10-410 (a petroleum sulfonate).

As Figure 3.1 illustrates, three typical phase types are formed with changing salinity for surfactant/alcohol/oil/brine fluid compositions. At high surfactant concentration, all phase environments ideally are single phase. At lower surfactant concentration, three phase types exist. As indicated by the tie-lines in Figure 3-1, Type $II^{(+)}$ contains a two-phase region which is composed of an aqueous phase rich in amphiphilic species and containing some solubilized oil, and an oleic phase of almost pure oil. Type $II^{(-)}$ contains a two-phase region which is composed of an oleic phase rich in amphiphilic species and containing some solubilized brine, and an aqueous phase of almost pure brine. Type III contains the same two-phase regions, corresponding to Types $II^{(+)}$ and $II^{(-)}$ described above, and an additional three-phase region containing an oleic phase, an aqueous phase, and a middle (microemulsion) phase composed of the amphiphilic species and solubilized oil and brine. These trends have been discussed by many authors.[36-39,42-46]

Healy and Reed[38] demonstrated that the most efficient oil recovery occurs at or near the salinity where oleic/microemulsion phase IFT (γ_{mo}) and aqueous/microemulsion phase IFT (γ_{mw}) are equal and low. This salinity is, by one definition, the so-called optimal salinity for oil recovery. This salinity is close to the salinity at which the middle phase solubilizes equal volumes of oil and brine, which is another definition of optimal salinity.

Viscosity is important in calculating mobility, total relative mobility, and permeability. The first two are discussed in Chapter Two, Equations 2.3 and 2.4. Viscosity enters into the well-known Darcy equation[40] for calculating relative permeability as follows:

$$kk_{rj} = \frac{L\mu_j U_j}{\Delta\Phi_j} \qquad 3.1$$

Siponate DS-10, a highly purified sulfonate, was considered since its purity would facilitate analysis of effluent samples. Siponate DS-10 was investigated in combination with two alcohol co-surfactants, brine and iso-octane.

Unfortunately, DS-10 exhibited unacceptable phase behavior. Spontaneous precipitation was observed in some instances when samples equilibrated at elevated temperatures were opened at room conditions. This result was obtained by mixing various solutions containing sulfonate in screw-top vials and measuring their properties as outlined in the next chapter. The cause of the precipitation is unknown but may be related to thermodynamic instability at lower temperature and/or upon exposure to oxygen.

Siponate DS-10 samples containing s-pentanol and t-pentanol co-surfactants were equilibrated at 50°C. Both phase volume diagrams (Appendix 1) and pseudo-ternary diagrams (Appendix 2) were constructed.

The phase volume fractions for a 5.0 volume % DS-10, 5.0 volume % s-pentanol, 45.0 volume % iso-octane, 45.0 volume % NaCl brine composition are illustrated in Figure 3-2. One three-phase sample was observed at 3.0 wt % NaCl. Pseudo-ternary diagrams with iso-octane, 1:1 Siponate DS-10:s-pentanol, (by volume assuming 1.0 g/cm^3 sulfonate density), and brine pseudo-components are illustrated in Figures 3.3 to 3.6. The ternary diagram for 0.5 wt % NaCl (Figure 3.3) reflects suitable Type II$^{(-)}$ behavior. Problems occur with the 1.0 wt % NaCl compositions (Figure 3.4). Although Type III phase behavior is apparent, gels and precipitates developed as indicated. Type II$^{(+)}$ phase behavior is reflected in Figure 3.5 for 3.0 wt % NaCl and in Figure 3.6 for 6.0 wt % NaCl. Acceptable pseudo-ternary behavior is exhibited at 3.0 wt % NaCl but not at 6.0 wt % NaCl where departure from ideal pseudo-ternary behavior occurs on the brine/surfactant: alcohol axis. In this region, two-phase samples occur with s-pentanol apparently acting as an excess oleic phase.

In addition to the anomalous pseudo-ternary phase behavior encountered at 1.0 wt % NaCl and 6.0 wt % NaCl, difficulties occurred when viscosity measurements were attempted at room conditions. Many microemulsions became gel-like in the viscometer cup (marked "G") causing readings to go off scale. Soap-like bubbling also occurred, causing erratic and inconsistent viscometric measurements.

In light of these difficulties, samples were mixed using t-pentanol in place of s-pentanol. A phase volume fraction diagram appears in Figure 3.7. This diagram is more encouraging than Figure 3.2 because the middle phase microemulsion solubilizes greater volumes of oil and water. Unfortunately, problems develop with pseudo-ternary behavior. Figure 3.8 illustrates a pseudo-ternary phase diagram for 2.0 wt % NaCl. Precipitates or gels formed in the vials indicated.

At this point, investigation of Siponate DS-10 was suspended in favor of Witco TRS 10-410, a petroleum sulfonate investigated by Glinnsmann and Hedges[39,41] and many others.[28,42-46]

A fluid composition of 47.0 volume % of a 1.1 wt % NaCl brine, 1.5 volume % iso-butanol, 1.5 volume % of active TRS 10-410 sulfonate, and 50.0 volume % n-decane was determined to have acceptable physical properties. A volume fraction diagram appears in Figure 3.9. At 1.1 wt % NaCl almost equal volumes of oil and water are solubilized into the microemulsion phase. Figure 3.10 represents a Type III pseudo-ternary for 1.1 wt % NaCl brine. Interfacial tension as a function of salinity is plotted in Figure 3.11. At the optimal salinity of 1.1 wt % NaCl the IFT curves intersect at 10^{-3} dyne/cm. Viscosity data are illustrated in Figure 3.12. Viscosity is essentially constant at 1.1 wt % NaCl brine for shear rates greater than 1.0 sec^{-1}. Additional data at different salinities and with different oils, sacrifical agents, and alcohol co-surfactants are available.[28,41,47,48]

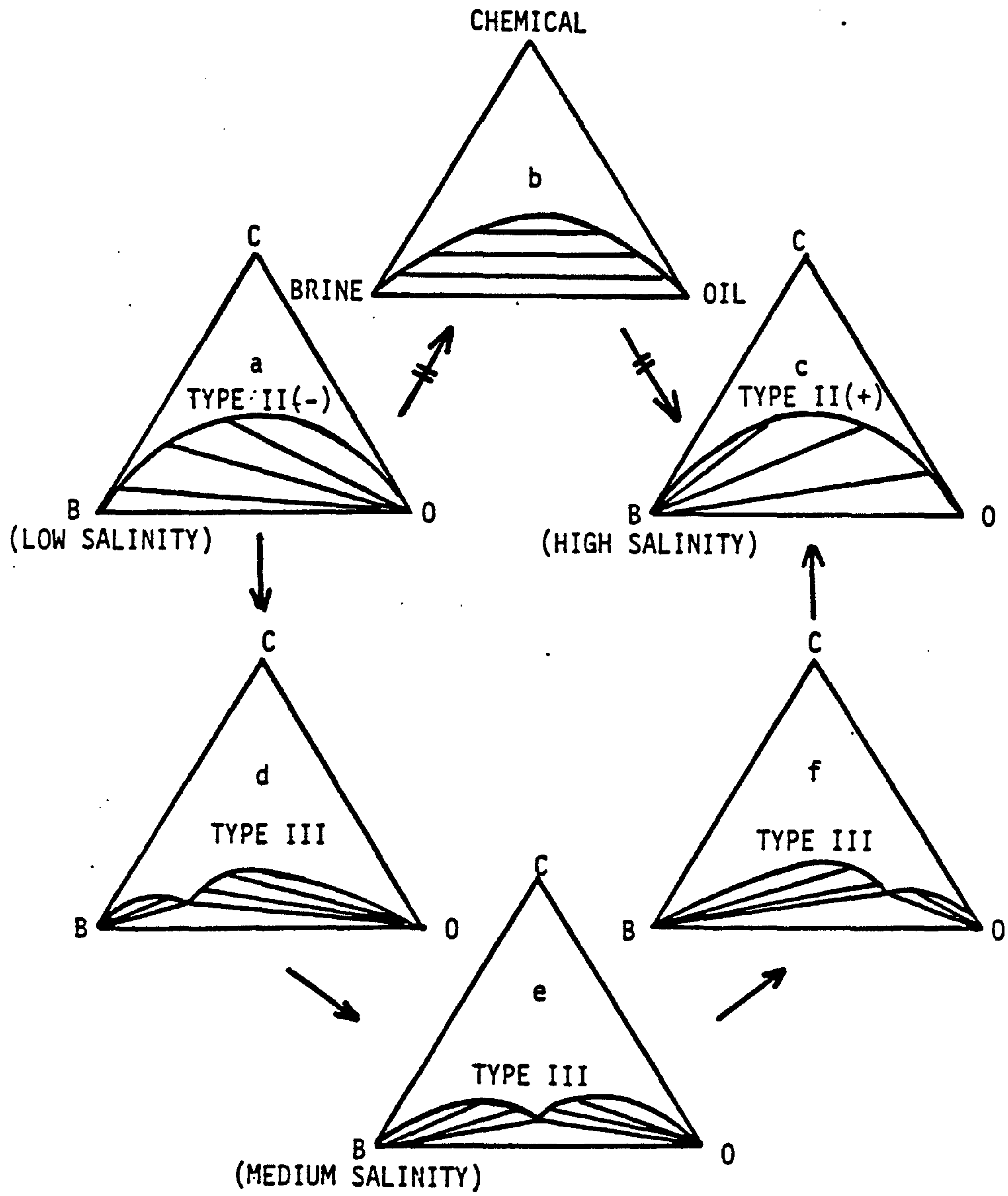

GENERALIZED PHASE DIAGRAMS ILLUSTRATING EFFECT OF CHANGING BRINE SALINITY

FIGURE 3.1

FIGURE 3.2

VOLUME FRACTION VS WEIGHT PERCENT
SODIUM CHLORIDE FOR DS-10
S-PENTANOL FORMULATION

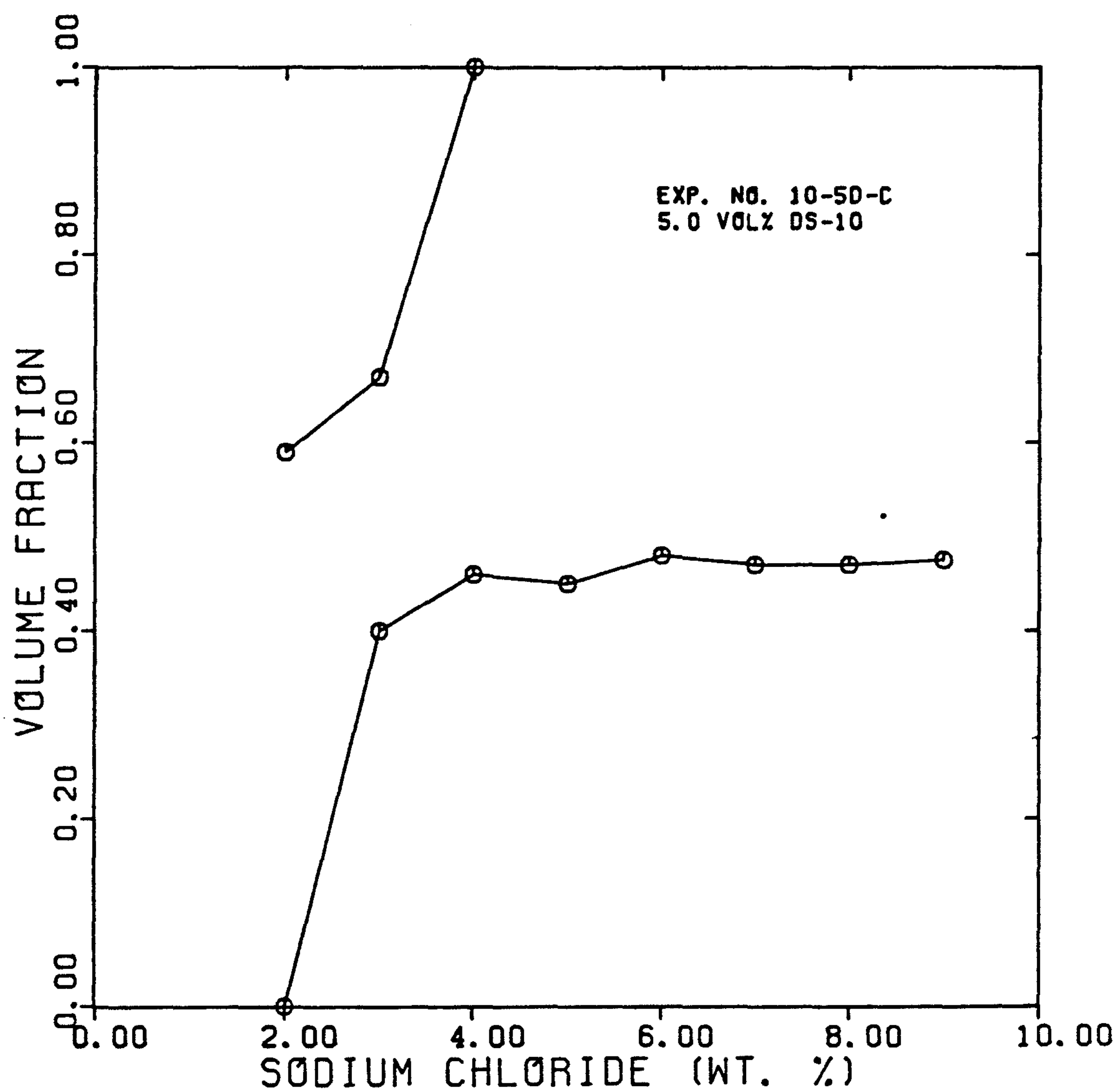

FIGURE 3.3 -- Pseudo-Ternary Behavior of 1:1 (by Volume) s-Pentanol: DS-10, 0.5 wt % NaCl Brine and iso-Octane

● 1Ø
⊙ 2Ø

Expt. No. 5-I-SP-T
5.0 vol % DS-10
5.0 vol % s-Pentanol
50°C

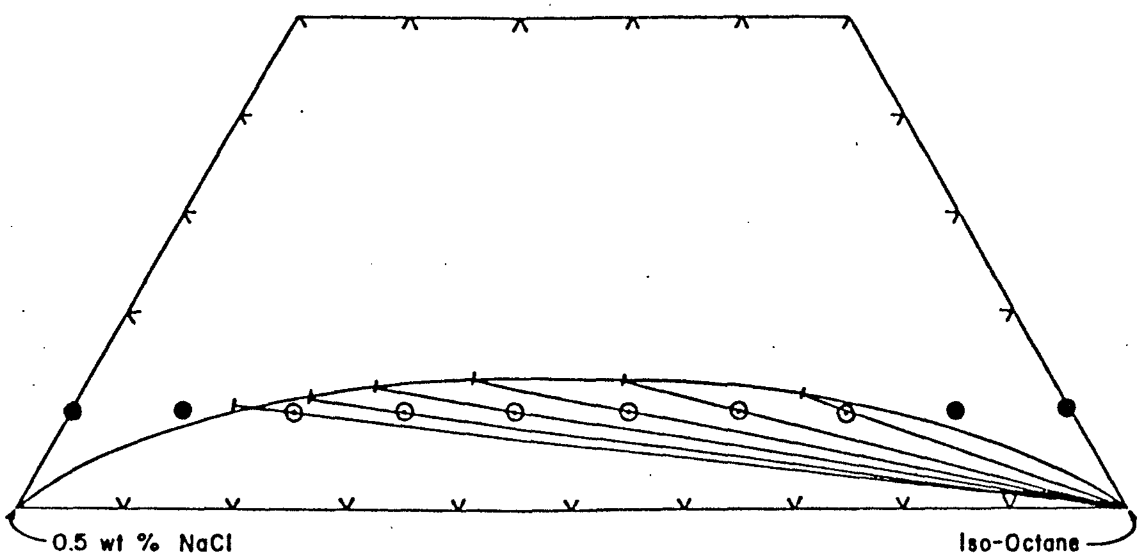

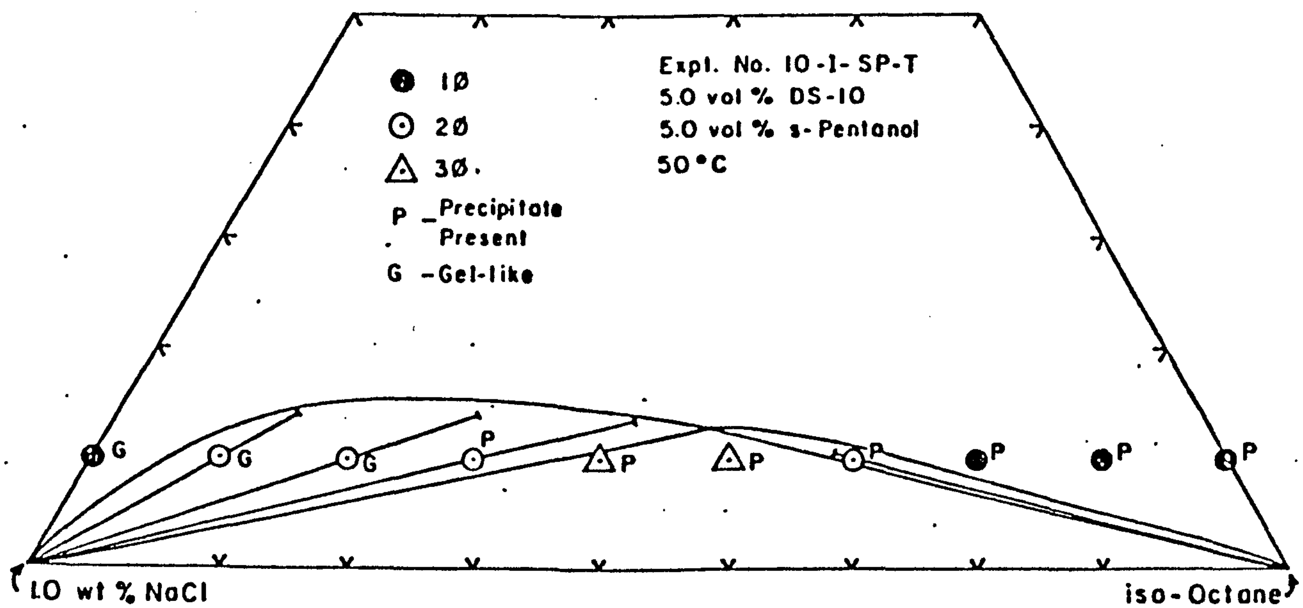

FIGURE 3.4 -- Pseudo-Ternary Behavior of 1:1 (by Volume) s-Pentanol: DS-10, 1.0 wt % NaCl Brine and iso-Octane

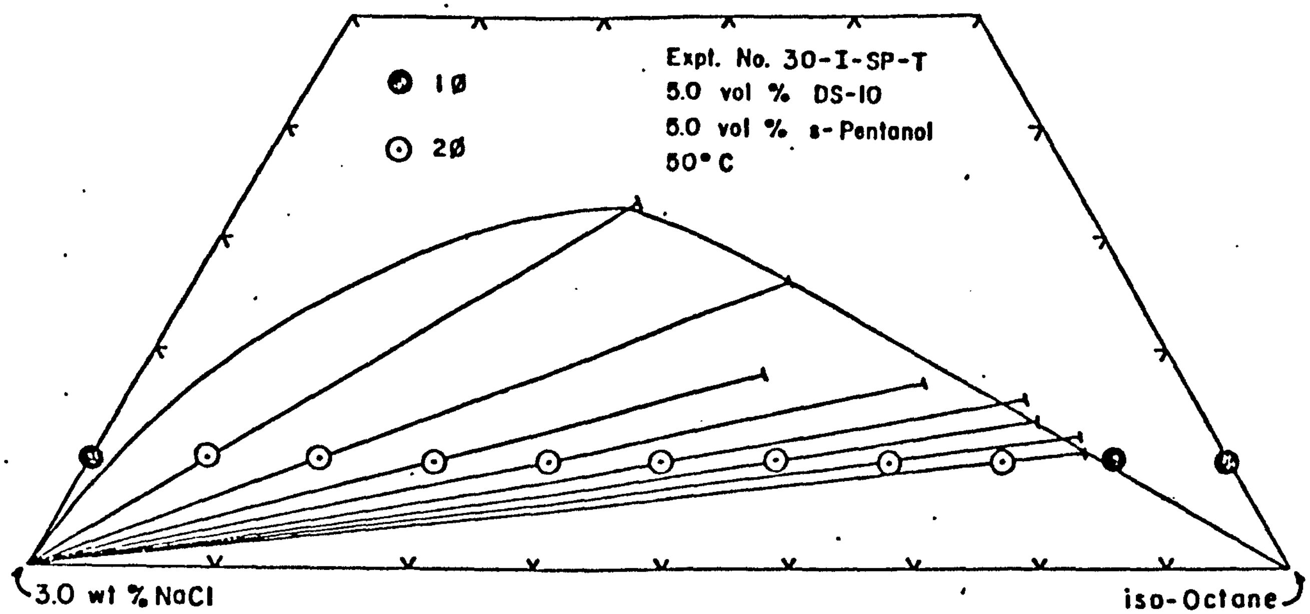

FIGURE 3.5 -- Pseudo-Ternary Behavior of 1:1 (by Volume) s-Pentanol: DS-10, 3.0 wt % NaCl Brine and iso-Octane

FIGURE 3.6 -- Pseudo-Ternary Behavior of 1:1 (by Volume) s-Pentanol:
DS-10, 6.0 wt % NaCl Brine and iso-Octane

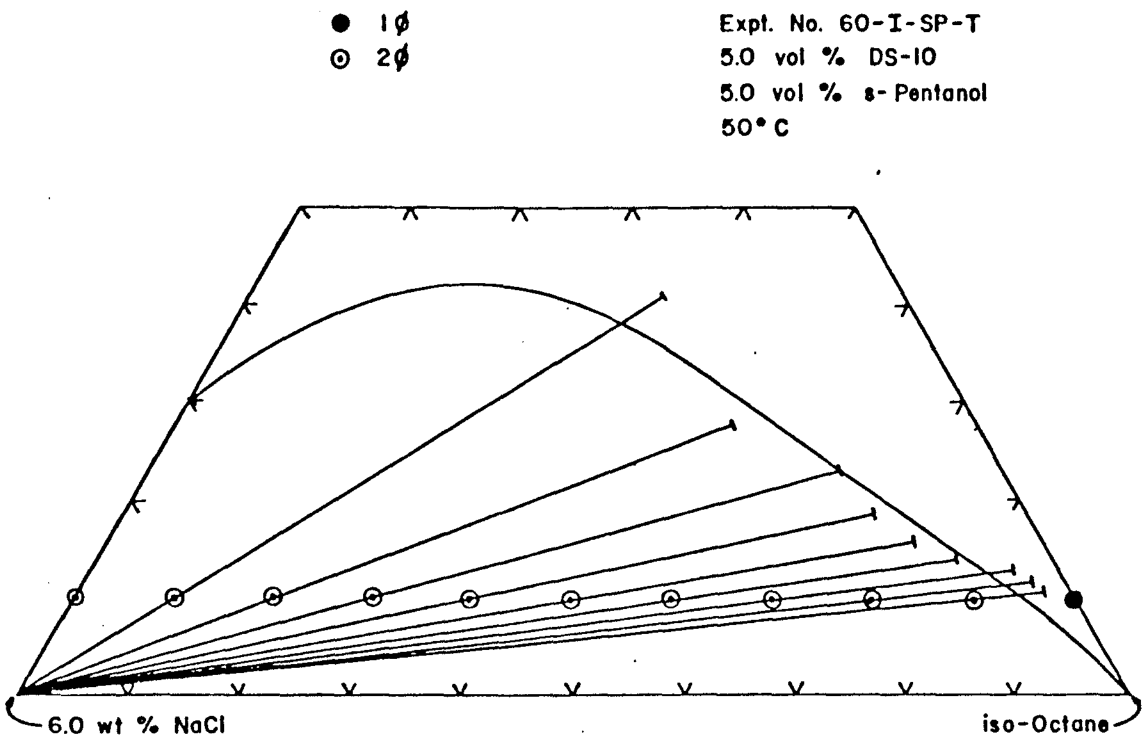

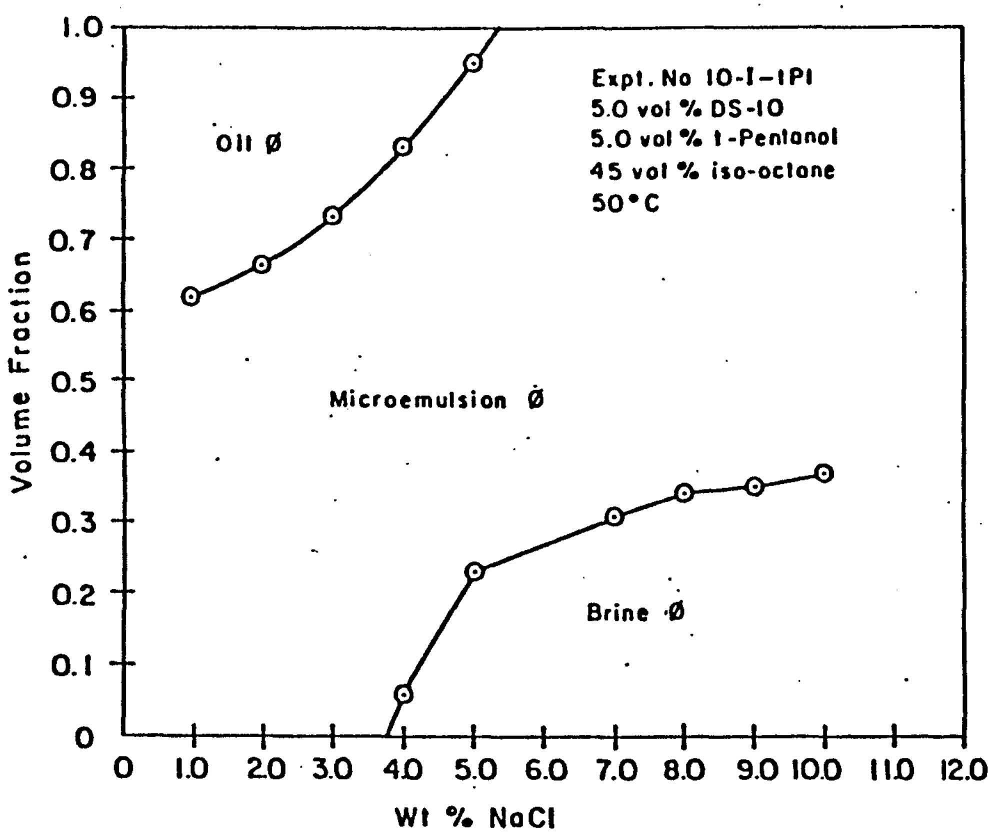

FIGURE 3.7 -- Volume Fraction vs Weight Percent Sodium Chloride for a DS-10, t-Pentanol Formulation

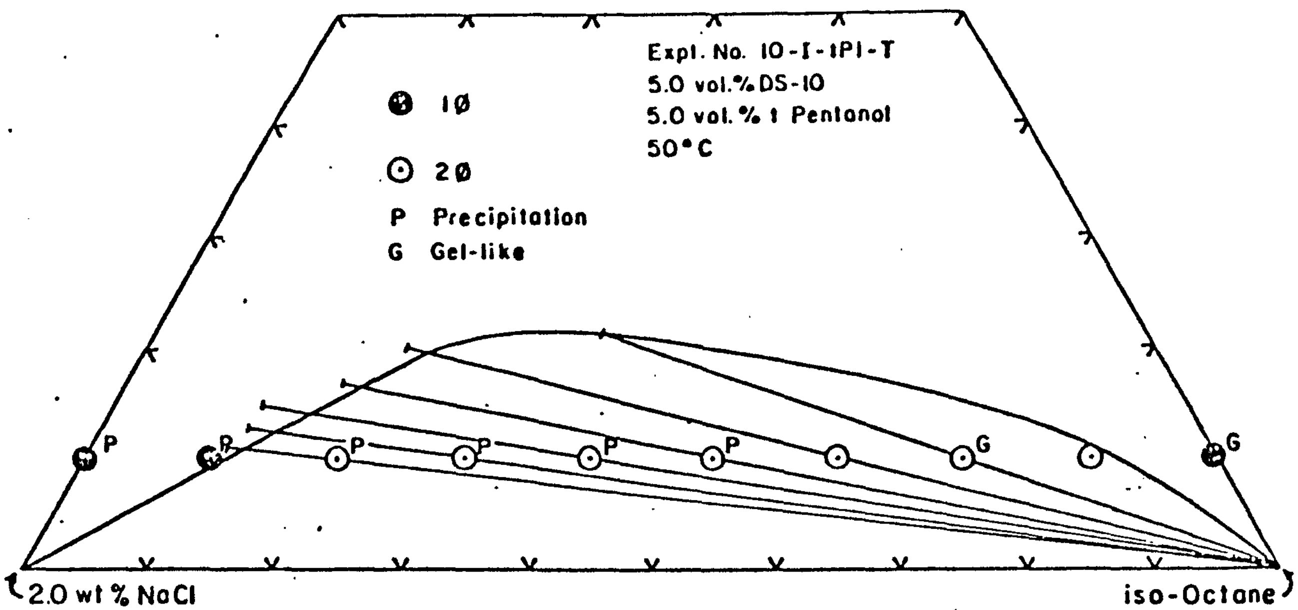

FIGURE 3.8 -- Pseudo-Ternary Behavior of 1:1 (by Volume) t-Pentanol: DS-10, 2.0 wt % NaCl Brine and iso-Octane

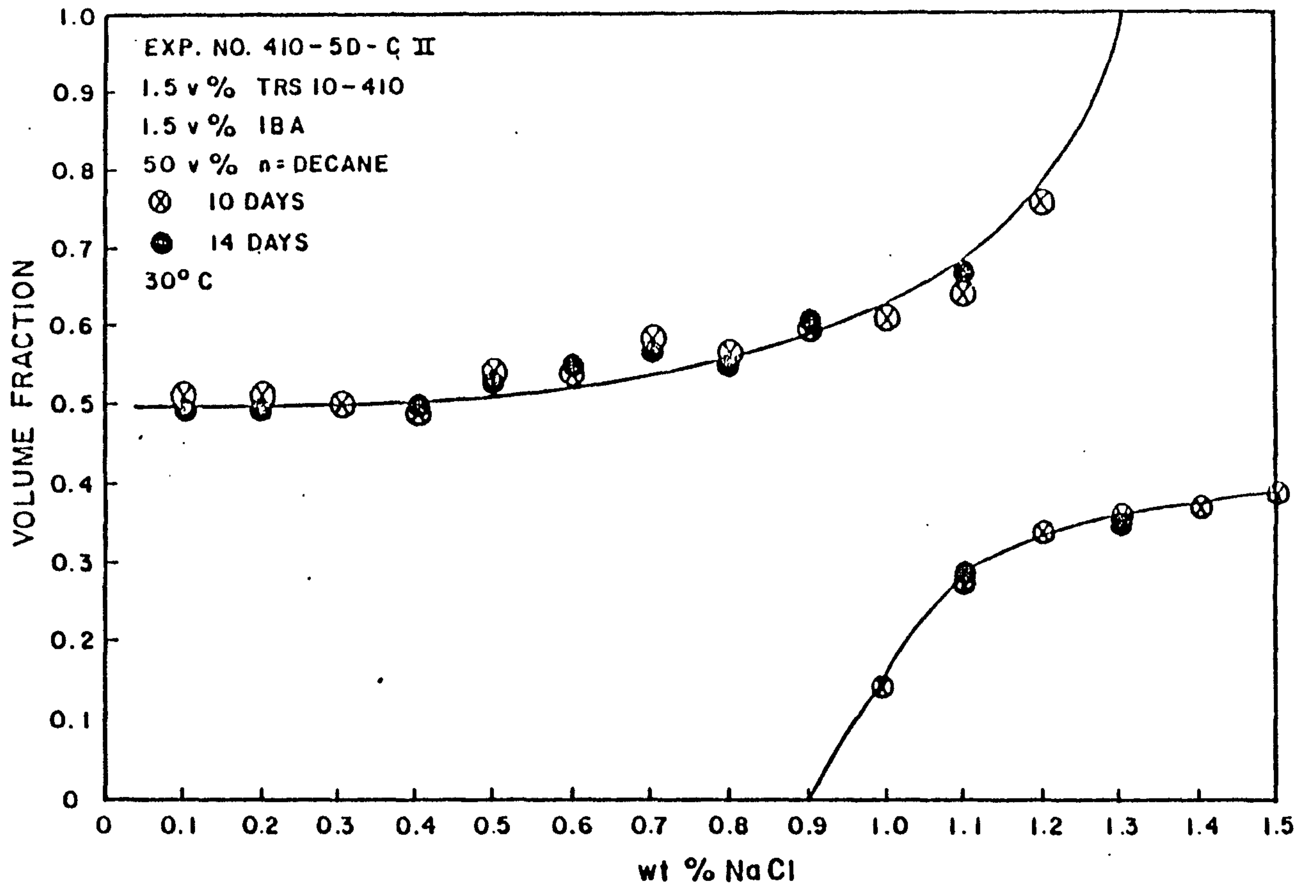

FIGURE 3.9 -- Volume Fraction vs Weight Percent Sodium Chloride for a TRS 10-410, i-Butanol Formulation

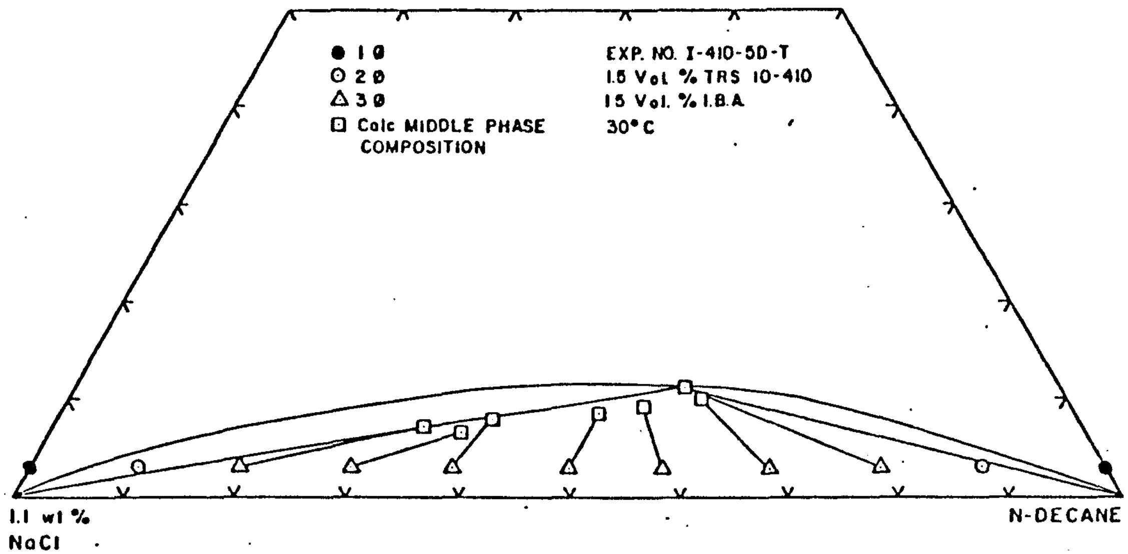

FIGURE 3.10 -- Pseudo-Ternary Behavior of 1:1 (By Volume) i-Butanol: TRS 10-410, 1.1 wt % Nacl Brine and n-Decane

FIGURE 3.11

Interfacial Tension vs Salinity for a

TRS 10-410, i-Butanol Formulation

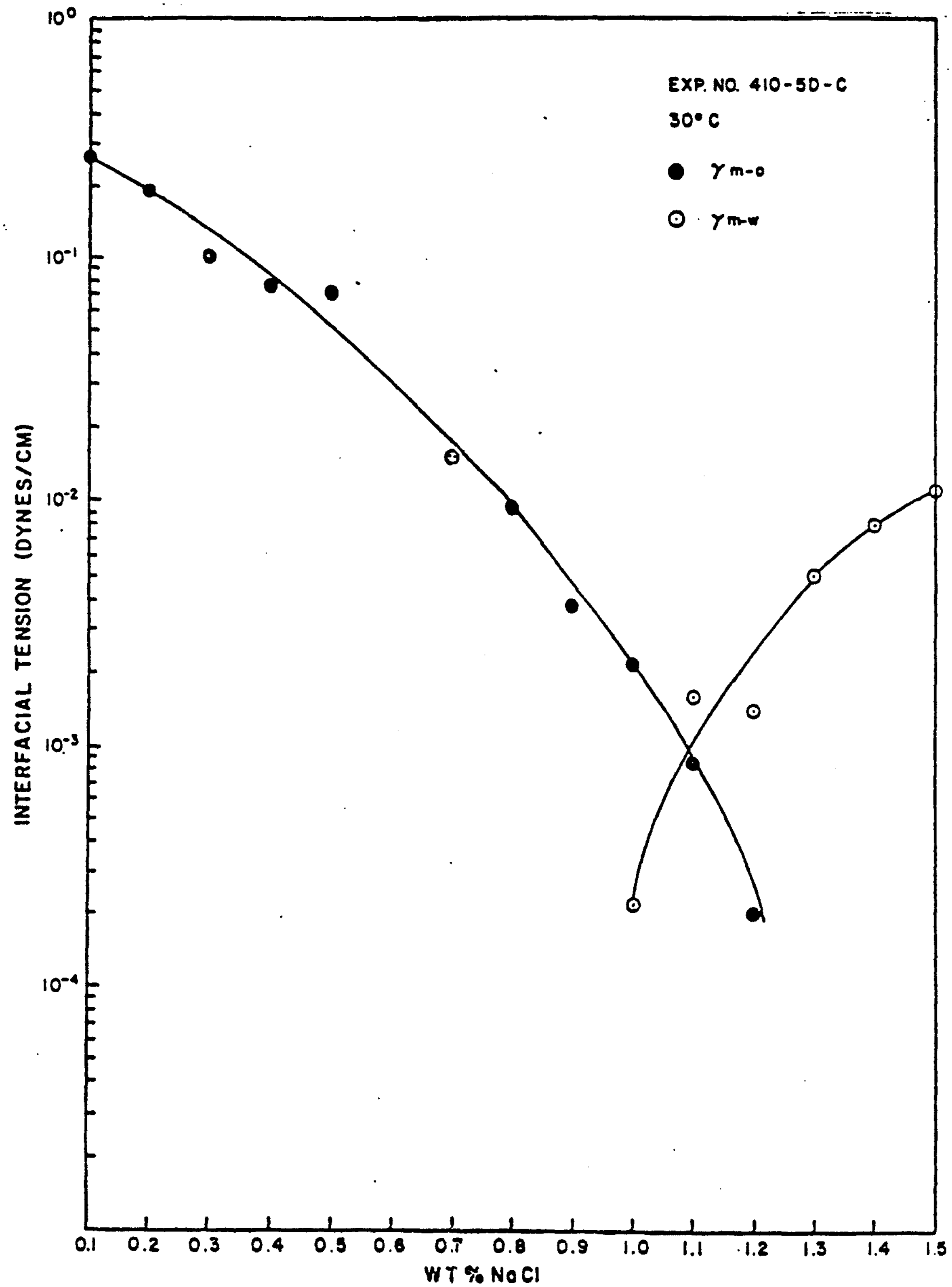

FIGURE 3.12

VISCOSITY VS SHEAR RATE OF TRS 10-410, IBA, N-DECANE, AND 1.1 WT% NACL BRINE IN THE MICROEMULSION PHASE

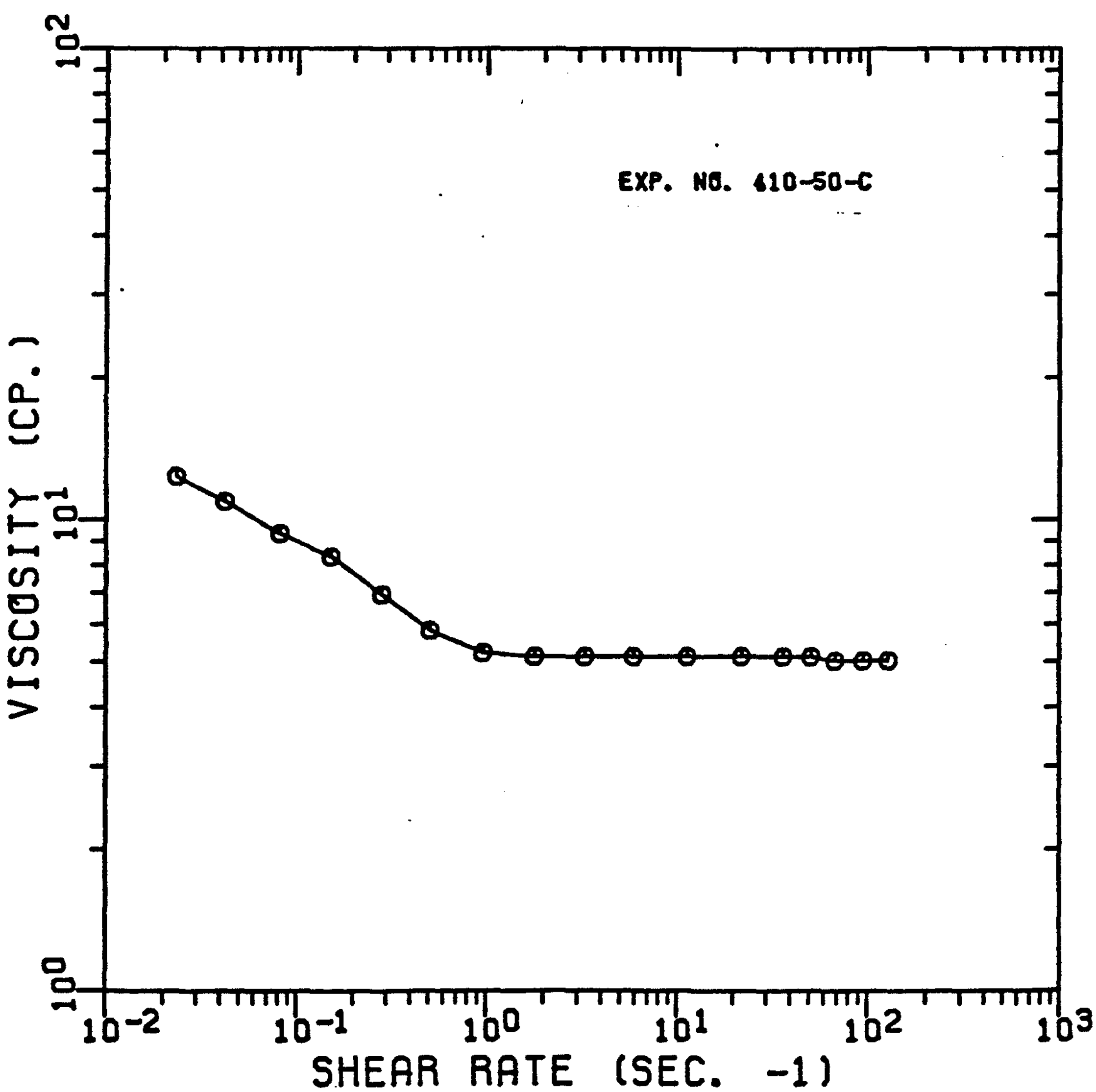

EQUIPMENT AND PROCEDURES

The major components of the flow apparatus as well as the analytical instruments used in characterizing the injected and produced fluids are briefly described. The experimental and analytical procedures employed are outlined next. Additional information for some of the equipment used is available.[28,47,48] Equipment manufacturers are listed in Table 4.1

A schematic diagram of the three-phase steady state flow apparatus appears in Figure 4.1. The major components are constant rate pumps, fluid reservoirs, porous medium, pressure detecting and recording equipment, sample collector, and temperature-controlled air bath.

Constant Rate Pump

Cheminert model CMP-2 metering pumps were employed in all flow experiments. The Cheminert pumps possess two rate selection potentiometers; one selects the maximum pump delivery rate (0.2, 0.4, 0.5, 1, and 2 ml/min), the second selects the fraction of the maximum flow rate. Although this fractional range is from .001 to 1.0, the practical rate selection limits are approximately 0.02 ml/min to 2.0 ml/min. Note that the pumps were not calibrated and flow rate was calculated from effluent production for each phase cut. The Cheminert pump has three independent pump chambers which are composed of a cylinder (Kel-F), piston (glass), and seal (Teflon). Two of the pistons are 180° out of phase to minimize pulsing. The third acts as a filling pump. Maximum output pressure is 500 psi. Due to swelling of Kel-F cylinders upon contact with some hydrocarbons only distilled water, brine, or equilibrated aqueous phases were pumped through the pistons. Piston cycles are coordinated with pneumatic valves which are switched from inlet to discharge. For this reason, a 60 psi compressed gas source is necessary for pump operation.

Fluid Reservoir

Glenco Chromatographic Series 3400 and 3500 glass columns were employed as fluid reservoirs. The column is 2.0 inches in diameter by 24.0 inches long with a volume of 1235.6 ml. The columns are constructed of borosilicate glass with polypropylene collars and end pieces. These reservoirs allow visualization of fluid levels and detection of air bubbles but are rated only to 80 psi. The Series 3500 end pieces are Teflon and are resistant to hydrocarbon swelling when in contact with the oleic and microemulsion phases. In addition, a vent plug in the end piece allows air to be easily removed from the column. Teflon pistons 2.0 inches thick by 1 15/16 inch diameter were cut in the University of Texas Petroleum Engineering Department. Two O-ring grooves are cut to fit two Parker 125 O-rings, providing a double seal and preventing torsion of the piston as it moves. The pistons are necessary to prevent contact of the pump drive fluid and the injected fluids.

Porous Media

Sandpacks and Berea sandstone were employed in this investigation. Berea sandstone (2.0 inches square) was cut to a 24.0 inch length. End pieces consisted of a 2.0 by 2.0 inch square of nylon screen (500 micron pore size) placed between the sandstone and a 2.0 by 2.0 inch square plexiglas end piece drilled and tapped in the center to accomodate a 1/8 inch NPT nylon Swagelok male connector. Connectors of the same size were used 6.0 inches from each end of the sandstone to serve as intermediate pressure taps. The taps and end pieces were held in place by three coats of epoxy (Appendix 3) which also served to seal the sandstone and confine injected fluids. Details of the epoxy procedure are contained in Appendix 3.

The sandpacks utilized in Experiments OWCL and OW were packed in Glenco Chromatographic glass columns (see Fluid Reservoir section). These columns are identical to the Series 3400 columns used as reservoirs except that the internal diameter is 1.0 inch. The packing procedure for sandpacks is outlined later in this chapter. The glass columns allow visualization of the fluids but are limited to 80 psi pressure and have no intermediate pressure taps.

Experiments OWZ, MO, MW, and PH3 were conducted in unconsolidated sand packed in a 2.0 inch internal diameter by 24.0 inch long stainless steel column. Details of the sand modification, cleaning and packing procedures appear later in this chapter. The column consists of 1/8 inch NPT male connectors, threaded endcaps, stainless steel mesh supports, 10 μm screens, O-rings, threaded steel column, and 1/8 inch tube fittings. Intermediate pressure ports are installed every 6.0 inches. End pieces are screwed on and form an O-ring seal. The column has been pressure tested successfully up to 1,000 psi.

Pressure Detecting and Recording Equipment

Diaphragm-type pressure tranducers were employed for all pressure measurements. Diaphragm-type transducers consist of rigid, fixed supports holding a magnetically permeable metal plate which deforms under a pressure differential. The magnetic inductance changes as the gap between support and deformable plate changes. The inductance is converted by an AC bridge to a voltage proportional to the applied pressure differential. Validyne model DP15 transducers were used with 80, 50, 10, 5, and 1 pounds per square inch maximum pressure differential transducer plates. A model MC 1-10 module case holding up to ten Validyne CD-19 demodulators was used. Each demodulator has a six position gain switch and a gain potentiometer. The voltage position gain switch and a gain potentiometer. The voltage is converted to a DC signal which is recorded by a Texas Instruments multipoint self-balancing recorder. The recorder is capable of recording on twelve separate channels. The pressure measuring apparatus is calibrated as follows:

1. Apply pressure equal to full scale (measured by a known, accurate source, such as a mecury manometer).
2. Adjust gain on the demodulator to register full scale on the recorder.
3. Release pressure and adjust zero settings.
4. Repeat Steps 2 and 3 until no adjustment is necessary.
5. Check at least three intermediate pressures to check linearity of pressure response.

Fraction Collector

Incremental volumes collected for an adjustable time interval were obtained with an Isco model 328 fraction collector. Time intervals from 0.1 to 99.9 minutes in increments of 0.1 min (6 sec) are available. Graduated test tubes of 15 ml or 10 ml volume in 0.1 ml increments were utilized.

Temperature-Controlled Air Bath

Flow experiments conducted at 30°C were performed in a fiberglass hood. The hood is 72.0 inches long by 60.0 inches high by 36.0 inches deep outside dimensions, and consists of 0.5 inch urethane sandwiched between two 1/8-inch thick fiberglass sheets. Access to the inside is gained through a vertically sliding glass door 60.0 inches long and 30.0 inches high. The hood is heated by two heaters controlled by an Athena model 74-6 proportional band temperature controller (0 to 300°F) and a continuously running blower for each heater. Temperature is monitored by a mercury thermometer.

Several components and properties of both injected and produced fluids were analyzed including water, isobutanol, decane, and nonane concentration (gas chromatography); calcium ion concentration (atomic absorption); radioactivity (scintillation counter); viscosity (viscometer); and IFT (spinning drop interfacial tensiometer). A brief description of each of these instruments follows.

Gas Chromatography

A Tracor Model 560 gas chromatograph with a Model 770 auto sampler was employed to analyze water, isobutanol, nonane, and decane. Samples are vaporized and passed through a thermal conductivity detector for water analysis followed by flame ionization. The flame ionization detector detects nonane, decane, and isobutanol. Table 4.2 lists operating conditions for the 36.0 inch by 1/8 inch column packed with 80/100 Porapak Q. Standard samples are prepared and analyzed for each component each time the chromatograph is used. The standard samples allow standard curves to be constructed and quantitative interpretation to be performed.

Atomic Absorption

A Perkin-Elmer model 360 spectrophotometer with a calcium, magnesium, aluminum lamp is used to detect calcium ion concentration utilizing a standard addition technique. Two 1.5 ml aliquots of brine phase are taken. One is diluted to 25.0 ml with distilled water and the second has calcium ion added and is diluted to give 2 ppm added calcium ion. Calcium concentration in both samples is read and the concentration in the original 1.5 ml aliquot calculated.

Scintillation Counter

Radioactivity was determined for carbon-14 labelled decane (^{14}C) and tritium (T_2O) tracers employed in this investigation using a Packard model 3400 liquid scintillation counter. Scintillation samples were prepared for counting by adding 0.25 ml of the appropriate liquid phase (aqueous, microemulsion, or oleic) to 10.0 ml of scintillation cocktail

(Universal® J. T. Baker Chemical Company) and cooling for two hours prior to counting. Samples are counted at least twice for two minutes with an external standard. Previously constructed quench curves using an external standard ratio method for ^{14}C and T_2O efficiency are incorporated into a computer program which is employed to separate ^{14}C and T_2O counts and to convert raw counts into disintegrations per minute. This separation is necessary since the micro-emulsion phase often contains both tracers.

The same procedure was utilized for both tritium (T_2O) and carbon-14 (^{14}C) tracer radioactivity determinations. The concentration of ^{14}C labelled n-decane was 20 μCi/ml and was diluted with n-decane to about 1,100 cpm/ml (0.2 ml concentrated ^{14}C to one liter of n-decane). The concentration of T_2O was 250 μCi/ml and was diluted with 1.1 wt % NaCl brine to about 16,000 cpm/ml (0.15 ml concentrated T_2O to one liter of brine). Nonane tracer was added in the amount of 1.0 volume % to n-decane. Whenever radioactive tracer was used vinyl gloves were worn and other safety precautions observed.

1. Measure 10.0 ml of liquid scintillation cocktail (Baker Universal® LSC) into 20 ml polyethylene vials.
2. Pipette 0.25 ml of appropriate phase into vial and securely tighten lid to avoid evaporation or spillage of radioactive material.

3. Cool samples to 5°C for two hours prior to counting to minimize chemoluminescent effects.
4. Load in scintillation counter and measure radioactivity.

Viscometer

Fluid viscosity was measured with a Contraves low shear model LS 30 viscometer. The LS 30 operates on a couette principle which analyzes stresses between two concentric cylinders. The instrument has five range settings and 30 fixed angular velocities for a shear rate range of 0.0174 to 128.5 sec^{-1} (for the available cup and bob). By multiplying shear rate by the appropriate calibration factor supplied by the manufacturer, viscosity is determined. Temperature control is maintained by a circulating water bath and monitored with a mercury thermometer placed in the viscometer cup. The operating procedure used follows:

1. Circulate water until the desired temperature is attained.
2. Place 1.0 ml of sample into the cup and insert the bob being careful to avoid air bubbles.
3. Adjust zero without rotation of the cup.
4. Take a reading at every other speed setting until reading is greater than 150.
5. Change to next higher range and repeat Step 4.

6. After all rotational speeds have been read, convert readings to viscosity with the appropriate calibration factors.

Spinning Drop Interfacial Tensiometer

Interfacial tension was measured by the method of Cayias.[49] In this technique, a small drop of the less dense liquid is placed in a bulk volume of the denser liquid in a tube. The tube is sealed and rotated along its longitudunal axis. Centrifugal force causes the drop to move to the center and elongate along the axis of rotation. For a drop whose length is greater than four times its diameter, a limiting condition is achieved and IFT is proportional to the density difference times the drop diameter squared divided by the rotational velocity to the third power. Density measurements are made with a Mettler/Paar model DMA 46 densitometer. The interfacial tensiometers were constructed by the University of Texas Department of Chemistry. Samples are spun for a minimum of eight hours or until equilibrium is achieved.

Procedures are outlined for the preparation of fluids and porous media and the experimental sequences. Preparation of samples for delineating the physical system, cleaning procedure for clay-free sand, sand packing, preparation of injection fluids, preparation of scintillation samples, determination of porous media basic properties, as well as the experimental procedures, are described.

Samples used in determining physical properties were prepared from 30.0 volume % surfactant: 30.0 volume % alcohol, and 3.695 wt % NaCl in water stock solutions. Stock solutions were prepared as follows:

1. Heat surfactant in original container in a 50°C water bath for one and a half hours.
2. Manually stir sulfonate to ensure homogeneity. (Note Steps 1 and 2 are skipped for DS-10 since it is already homogeneous.)
3. Weigh 300 ml of active* sulfonate and 300 ml of co-surfactant based on density into a 1,500 ml Erlinmeyer flask.
4. Add distilled water to make 1,000 ml of solution.
5. Mix 15 hours by magnetic stirrer in the stoppered flask.
6. Weigh 36.95 g anhydrous NaCl into a 1,500 ml Erlinmeyer flask.
7. Add 963.05 g of distilled water to the flask.
8. Mix with a magnetic stirrer for one hour.

Physical property samples were mixed by the following procedure:

*Active refers to the amount of material that is actually sulfonate exclusive of water, unreacted oil, etc.

1. Pipette appropriate amount of 30.0 volume % surfactant (30.0 volume % co-surfactant stock) into 30 ml screwtop vials.
2. Pipette appropriate volume of distilled water.
3. Pipette appropriate volume of 3.695 wt % brine stock.
4. Pipette appropriate volume of oil and screw lid on tightly to prevent evaporation. (Note Steps 1 through 4 are performed in order since this sequence results in the fastest equilibration times.)
5. Invert vial three times to ensure mixing and place in 30°C air bath.

To remove any effect from clay, the unconsolidated sand used in Experiments OWZ, MO, MW, and PH3 was cleaned as described below:

1. Immerse sand completely in concentrated (as is) hydrochloric acid and agitate to ensure all sand surfaces are contacted.
2. Allow sand to settle for two hours.
3. Decant acid and wash repeatedly with distilled water (with agitation) until pH 7.0 is achieved. (At least ten washes are usually required.)
4. Sonify sand for two hours in distilled water.
5. Dry sand in 110°C air bath for 48 hours.

A discussion of which sands were used and why appears in the next chapter. An outline of sandpacking technique follows. The sand was packed by allowing it to fall through a series of four (for Experiments OWCL and OW) or seven (for Experiments OWZ, MO, MW, and PH3) 850 µm screens. Sand is contained in a separatory funnel reservoir and allowed to trickle out at a slow rate. The screens are held in a tube the same diameter as the column and are attached directly to one end. An FMC heavy duty vibrator is also attached to the assembly to assure an even pack. The flow of sand must be continuous during the entire packing procedure to ensure a homogeneous pack.

1. Sift sand through 150 mesh (100 micron) screen to break up any consolidation.
2. Weigh dry sand.
3. Assemble packing apparatus and use plumb-bob to make the column vertical.
4. Allow sand to fall at a slow rate with vibration.
5. Refill sand reservoir as needed to maintain continuous sand flow.
6. Stop sand flow and vibration when sand level is past the end of the column.
7. Remove screens and level sand at the end of the column with a straightedge.
8. Glue a 10 µm screen on the end of the column with silicon cement and allow to dry for 24 hours.

9. Carefully brush away all sand from threads and O-ring groove. (Stray sand grains can cause leakage.)
10. Weigh unused sand for calculation of pore volume (described later in this chapter).
11. Screw end piece with O-ring on hand tight.

Preparation of injection fluids consisted of mixing and filtering the phases of interest. Procedures for both are described. Fluids used in Experiments OWCL, OW, OWZ, and BAOW consisted of n-decane or iso-octane oil phase and various sodium chloride brines. Brine solutions were mixed on a weight percentage of salt in distilled water basis as described in the section on physical system sample preparation and will not be further discussed. Oils were used as is. Components used in mixing the three-phase micellar formulations were prefiltered. The filtering procedure follows:

1. 300 ml of fluid is loaded in a Fann model 12 BL filter container with a 0.45 micron filter (Millipore type HA).
2. The containter is placed in the accompanying filter press at 40 psi.
3. Effluent is collected in a 500 ml Erlenmeyer flask.

Micellar fluids used in flow experiments were mixed from stock solutions as follows:

1. Heat TRS 10-410 surfactant in original container in 50°C water bath for 1.5 hours.
2. Manually stir surfactant to ensure homogeneity.
3. Weigh 1,935.5 g TRS 10-410, 969.6 g IBA, and 864.5 g of distilled water into a four-liter flask (Stock I).
4. Cover and stir with magnetic stirrer for 24 hours.
5. Weigh 147.46 g of anhydrous NaCl and 3,852.54 g distilled water into a second four-liter flask (Stock II).
6. Cover and stir with magnetic stirrer for two hours.
7. Dilute 800 g of Stock I with 5,000 g distilled water in an eight-liter flask to facilitate filtering (Stock ID).
8. Filter Stock ID, Stock II, and 6,000.0 g n-decane as outlined above.
9. Combine 5,437.5 g of Stock ID, 2,100.0 g of Stock II, and 5,475.0 g of n-decane to make 15 liters total in a five-gallon glass jar.
10. Cap and invert jar four times to mix components.
11. Replace cap with stopper containing two glass tubes.
12. Evacuate, invert, and place jar in 30°C air bath.
13. Allow to equilibrate for at least seven days.
14. Release vacuum, separate phases by gravity drainage and store in one-liter containers at 30°C.

The porous media is characterized by determining the porosity, permeability, and homogeneity. A procedure is outlined for this characterization.

1. Close the valve at one end of the column and cap all pressure ports.
2. Connect the other end to a vacuum pump for 30 minutes. Stop vacuum pump and monitor vacuum gauge for evidence of leakage. If no leakage is evident, restart vacuum pump.
3. Fill a Burette with the degassed saturation brine and take an initial volume reading.
4. Open closed end of column to Burette and close off vacuum.
5. Allow fluid to enter column until the level in the Burette stops changing.
6. Take final Burette reading and subtract from initial reading to obtain saturated pore volume. (This value can be compared to the bulk pore volume calculated from the weight of packed sand--Apendix 4.)
7. Calculate bulk volume (cross-sectional area times length) and determine porosity (pore volume divided by bulk volume).
8. Attach pressure monitoring equipment and brine pump and flood with brine until a steady-state pressure drop is obtained.

9. Calculate single-phase brine permeability from Darcy's law based on intermediate and total pressure taps to determine if end effects are present.
10. Flow tritium-labelled brine under steady-state conditions through the medium. Collect and analyze effluent samples.
11. Calculate saturated pore volume (Equation 2.20) as a third check of pore volume. (Note: a smooth S-shaped effluent tracer concentration curve is a good indication of homogeneity.)

An experimental procedure is outlined for dispersion and relative permeability experiments. In practice these two experiments were performed simultaneously so one outline is presented in the order that each step was carried out.

1. Pump brine phase at a constant rate through the brine saturated medium until a constant pressure drop is obtained.
2. Drain outlet line and flush inlet lines with tritiated brine.
3. Inject 1.5 pore volume of tritiated brine at the same constant rate used in Step 1 and collect effluent in graduated test tubes in a fraction collector.

4. Calculate permeability from Darcy's law using equilibrium pressure drop, average tube volume and time setting of fraction collector.
5. Drain outlet line and flush inlet line with oil phase.
6. Drive oil phase through the porous medium at 15 psid/foot while collecting all effluent (for material balance) until no more brine is produced.
7. Pump oil phase at the same constant rate as Step 1 until a constant pressure drop is obtained.
8. Drain outlet line and flush inlet lines with labelled oil phase.
9. Pump 1.5 pore volumes of labelled oil phase at the constant rate used in Step 1 and collect effluent in graduated test tubes in a fraction collector.
10. Calculate effective permeability from equilibrium pressure drop, average tube volume and time setting of fraction collector.
11. Drain outlet line and flush input lines with two or three fluid phases at the desired fractional flow.
12. Pump phases at the same total constant flow rate until a constant pressure drop is achieved and all tagged components have been displaced (check effluent radioactivity). In addition, collect all effluent for material balance until output fractional flows equal input fractional flows.

13. Drain outlet line and flush input lines with tagged phases at the same fractional flows.
14. Pump tagged phases at the previously used rate until 0.75 to 1.0 pore volume more than t_D^{Bt} of fluid (based on material balance saturations and Equation 2.20) is flushed through the porous medium. Collect effluent in graduated test tubes in a fraction collector.
15. Calculate the effective permeability of each phase from equilibrium pressure drop, average phase volumes and time setting of fraction collector.
16. Change to the next phase cuts and repeat Steps 11 through 15.
17. Analyze selected test tube samples for phase volumes, tracer concentration, IFT, calcium ion concentration, and component concentrations.

TABLE 4.1

EQUIPMENT LIST AND TYPE

EQUIPMENT	MODEL	MANUFACTURER
Zenith Pump	QM/BPB	The Zenith Corporation 432 Cherry Street West Newton, MA 02165
Ruska Pump	1446 WI	Ruska Instrument Corp. P. O. Box 36010 Houston, TX 77036
Cheminert Pump	CMP-3	Laboratory Data Control P. O. Box 10235 Interstate Industrial Park Riverea Beach, FL 33404
Pressure Transducer	DP15	Validyne Engineering Corp. 19414 Londelius Street Northridge, CA 91324
Demodulator	CD-19	Validyne Engineering Corp. 19414 Londelius Street Northridge, CA 91324
Sample Collector	Isco Model 328	Instrumentation Specialities Company P. O. Box 5347 Lincoln, NE 68505
Solution Reservoir (packed column)	Glenco 3400, 3500	Glenco Scientific Inc. 2802 White Oak Drive Houston, TX 77007
Pressure Recorder	FMWSE6C	Texas Instruments Inc. Recorder Department 12203 Southwest Freeway Stafford, TX 77477
Air Bath		Contemporary Products, Inc. P. O. Box 6249 2204 East 6th Street Austin, TX 78762
Temperature Controller	Athena 74-6	Athena Controls Inc. W. Conshohocken, PA 19476

TABLE 4.1 continued

EQUIPMENT LIST AND TYPE

EQUIPMENT	MODEL	MANUFACTURER
Scintillation Counter	Packard 3400	Packard Instrument Company 2200 West Arrenville Road Downers Grove, IL 60515
Gas Chromatograph	Tracor Model 560	Tracor, Inc. 6500 Tracor Lane Austin, TX 78721

TABLE 4.2

OPERATING CONDITIONS EMPLOYED

FOR GAS CHROMATOGRAPHIC ANALYSIS

Carrier Gas Flow (Helium)	30 cc/min
Thermal Conductivity Reference Flow (Helium)	30 cc/min
Flame Ionization Detector Gas Flow (Hydrogen)	30 cc/min
Flame Ionization Support Gas Flow (Compressed Air)	470 cc/min
Injection Port Temperature	250°C
Thermal Conductivity Detector Temperature	250°C
Flame Ionization Detector Temperature	250°C
Initial Oven Temperature	110°C
Final Oven Temperature	225°C
Program Temperature Change Rate	20°C/min
Initial Hold	5 min
Final Hold	20 min
F.I.D. Electrometer	
Input Range	X 1000
Output Attenuator	16
Output Connection	10 mv Full Scale
Recorder Attenuator	1 mv/volt
T. C. Detector	
Sensitivity	low
Filament Current	110 mA
Output Attenuation	8

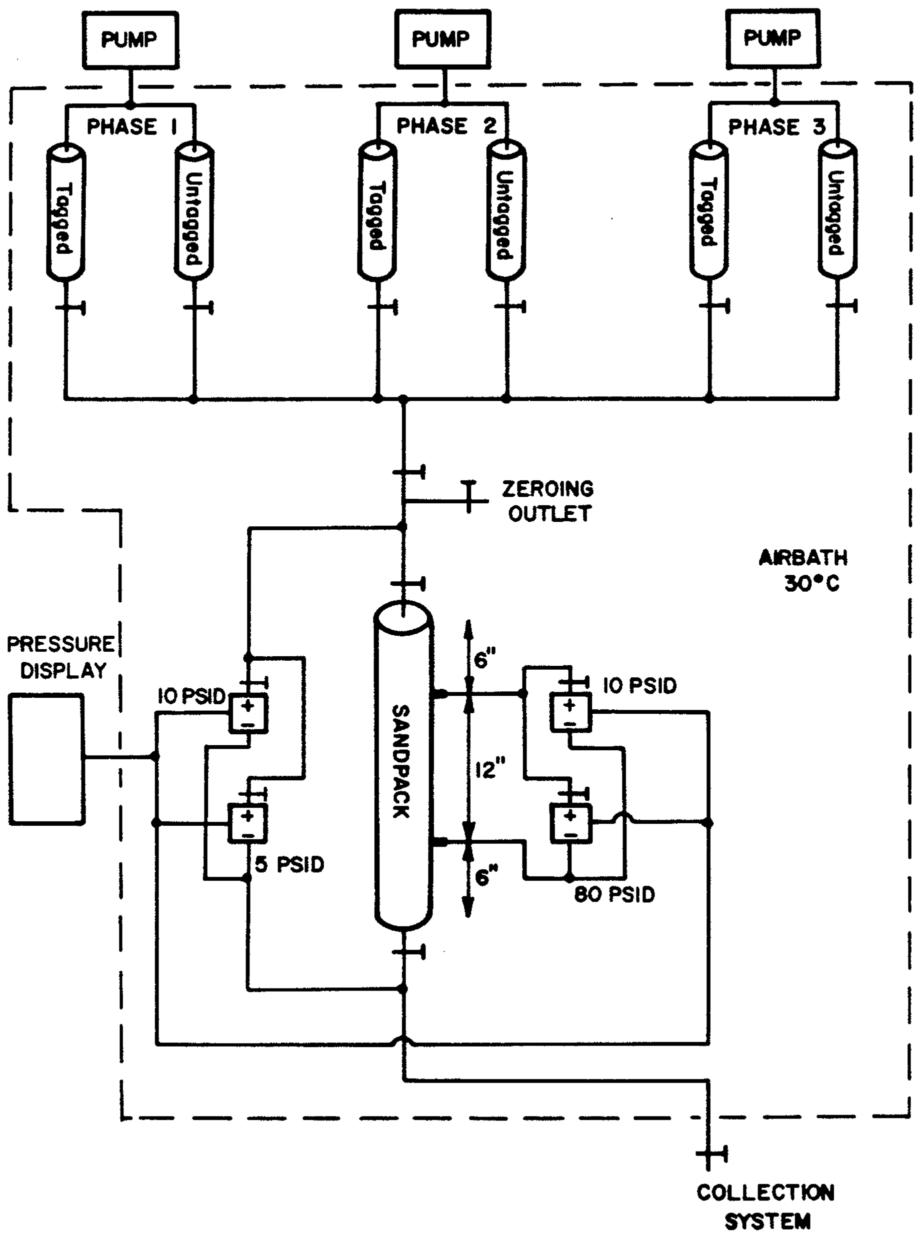

SCHEMATIC OF EXPERIMENTAL SETUP

FIGURE 4.1

EXPERIMENTAL RESULTS

The results of the seven flow experiments conducted are discussed in this chapter (Table 5.1). They consist of: 1) brine/iso-octane drainage in a high permeability sandpack with chloride ion tracer (Experiment OWCL), 2) 1.0 wt % NaCl brine/iso-octane drainage in a high permeability sandpack with tritium tracer (Experiment OW), 3) 1.1 wt % NaCl brine/n-decane imbibition in Berea sandstone with tritium and carbon-14 tracers (Experiment BAOW), 4) 1.1 wt % NaCl brine/n-decane imbibition in a low permeability sandpack with tritium, carbon-14 and n-nonane tracers (Experiment OWZ), 5) microemulsion phase/oleic phase imbibition in a low permeability sandpack with tritium and carbon-14 tracers (Experiment MO), 6) aqueous phase/microemulsion phase drainage in a low permeability sandpack with tritium and carbon-14 tracers (Experiment MW), and 7) aqueous phase/microemulsion phase/oleic phase three-phase flow in a low permeability sandpack with tritium, carbon-14, and n-nonane tracers (Experiment PH3).

Experiment OWCL

Experiment OWCL was conducted at a nominal rate of 3.5 cc/min at 27°C using a glass column packed with Oklahoma No. 1, a course silica sand (Table 5.2). The pack was initially saturated with 1.0 wt % NaCl brine and displaced with 3.0 wt % NaCl brine. Chloride ion concentration was monitored with a chloride ion specific ion electrode.

Due to calibration problems, only the 100% brine saturation was monitored with the electrode. The remainder of the flow experiment was conducted using 1.0 wt % NaCl brine and iso-octane. Fluid and sandpack data are detailed in Table 5.3. The experimental results are summarized in Tables 5.4 and 5.5 and Figures 5.1 to 5.5.

Figure 5.1 reflects typical waterwet drainage relative permeability curves. The residual brine saturation is 0.149 and relative permeability to iso-octane at residual brine is 0.377. The total relative mobility curve (Figure 5.2) is also typical of a high tension, waterwet sandpack. The minimum is 0.408 cp^{-1} at 0.490 brine saturation. The experimental fractional flow diagram (Figure 5.3) is typical for high IFT fluids. The S-shaped breakthrough curve for 100% brine saturated sandpack (Figure 5.4) indicates a homogeneous pack was achieved and the breakthrough time implies that the pore volume is very close to 50.4 cc (Equation 2.9). This close agreement with the pore volume by saturation and by weight (Table 5.3) is another indication of a well-packed sandpack. The single-phase brine dispersivity is 0.250 cm (Figure 5.5).

Experiment OW

Experiment OW was conducted as a nominal rate of 2.0 cc/min at 27°C using a glass column packed with silica sand (Tables 5.2 and 5.6). The pack was initially saturated with 1.0 wt % NaCl brine. Dispersion in the aqueous phase was determined using a tritium tracer in 1.0 wt % NaCl brine for three of the six brine/iso-octane cuts (OW_1, OW_2, and OW_4). Fluid and sandpack data are given in Table 5.6. The experimental results appear in Tables 5.7 and 5.8 and Figures 5.6 to 5.15.

As expected, Figure 5.6 reflects typical waterwet drainage relative permeability curves. The residual brine saturation is 0.117 and relative permeability to iso-octane at residual brine is 0.204. The total relative mobility curve (Figure 5.7) is also typical of a high tension, waterwet sandpack. The minimum is 0.181 cp^{-1} at 0.308 brine saturation. The experimental fractional flow curve (Figure 5.8) is typical of high IFT fluids. The S-shaped breakthrough curve for 100% brine saturated sandpack (Figure 5.9) indicates a homogeneous pack was achieved and the breakthrough time implies that the pore volume is very close to 113.0 cc (Equation 2.9). The close agreement with the pore volume by saturation and by weight (Table 5.6) is another indication of a well-packed sandpack. The single-phase brine phase dispersivity is 0.342 cm (Figure 5.10). The breakthrough curve for cut OW_2 appears in Figure 5.11.

There is considerable scatter in the initial points but the S-shaped portion is reasonable. Figure 5.13 for cut OW_4 is similar. The brine saturations calculated from the breakthrough times are slightly different than saturations calculated by material balance (Table 5.7) with OW_2 being 0.071 pore volume less and OW_4 being 0.076 pore volume greater than the corresponding material balance calculations. Due to this discrepancy, all subsequent dispersions were conducted from low to high concentration. Dispersivities are 0.965 cm and 1.387 cm for OW_2 and OW_4 respectively (Figures 5.12 and 5.14 and Table 5.8). Brine phase dispersivity as a function of brine phase saturation is illustrated in Figure 5.15. Brine phase dispersivity increases as brine phase saturation decreases.

Experiment BAOW

Experiment BAOW was conducted at 2.0 cc/min nominal flow rate at 30°C using Berea sandstone (Table 5.9). The core was initially saturated with 1.1 wt % NaCl brine. Dispersion in the aqueous phase was determined using a tritium tracer in 1.1 wt % NaCl brine. Dispersion in the oleic phase was determined using carbon-14 labelled n-decane in untagged n-decane. Fluid and core data are contained in Table 5.9. The experimental results appear in Tables 5.10 and 5.11 and Figures 5.16 to 5.40.

Figure 5.16 reflects typical waterwet imbibition relative permeability curves with the high residual saturations characteristic of Berea sandstone. Figure 5.17 illustrates the same curves along with a set from another Berea experiment conducted by Deshad[29] using the same fluids, but in a horizontal configuration. The curves are very close except for the location of the endpoints. Total relative mobility data is illustrated in Figure 5.18. The minimum total relative mobility is 0.0498 cp^{-1} (at residual oil saturation, $S_{ro} = 0.367$). A fractional flow diagram (Figure 5.19) for both cores shows excellent correlation and also illustrates the rapid increase in brine saturation with brine phase fractional flow increasing up to 0.1. Brine phase fractional flow greater than 0.1 causes relatively small further increases in brine saturation.

Figure 5.20 demonstrates the calcium ion leaching that occurred. Initial effluent volumes contained up to 50.1 ppm calcium ion which quickly dropped to about 12.0 ppm $\pm$ 2.0 ppm where it remained. Figures 5.21 to 5.38 contain the dispersion plots for the six different cuts used.

The narrow S-shaped curve for 100% brine saturation (Figure 5.21) indicates that the core contains no significant systematic heterogeneities and the breakthrough time implies a pore volume that is very close to 304.8 cc. The close agreement with the saturation pore volume (Table 5.9) is another indication of homogeneity. The single-phase dispersivity is 0.128 cm (Figure 5.22). The aqueous phase dispersion curves are S-shaped and brine phase saturations calculated from frontal breakthrough (Equation 2.20) are 90% to 97% of the material balance brine phase saturations (Table 5.11). However, the n-decane dispersion curves demonstrate a skewed "capacitance"-type profile (Chapter 2). The n-decane dispersion curve at residual brine (Figure 5.23) has a breakthrough time that yields a saturation that is 97% of material balance saturation. However, oil phase breakthrough times where two phases are flowing yield oil phase saturations much less than material balance saturations. Brine and oil phase dispersivities as a function of brine phase saturation are illustrated in Figure 5.39. For both phases, dispersivity increases as phase saturation decreases. Dispersivities for the Berea core Delshad used are included in Figure 5.40. Although less pronounced than in Figure 5.39, the brine phase dispersivity increases as brine phase saturation decreases. Delshad did not use an oil tracer in this particular experiment, so no comparison of oil dispersion can be made.

Experiment OWZ

Experiment OWZ was conducted at 2.0 cc/min nominal flow rate at 30°C using a specially prepared sandpack (Appendix 5 and Table 5.2) in a 2.0 inch diameter steel column. The sandpack was initially saturated with 1.1 wt % NaCl brine.

Dispersion was determined using tritium in the brine phase and carbon-14 labelled n-decane and n-nonane in the n-decane phase. Fluid and sandpack data are contained in Table 5.12. The experimental results appear in Tables 5.13 and 5.14 and Figures 5.41 to 5.76.

Imbibition relative permeability curves for n-decane and brine appear in Figure 5.41. Saturation from tritium breakthrough in the brine phase agrees closely with material balance saturations. Oil saturations by isotope breakthrough, however, are skewed to the right perhaps due to stagnant fluid saturations (Chapter 2). Total relative mobility data is illustrated in Figure 5.42. The minimum is $0.106 cp^{-1}$ and is skewed to the right occurring at residual oil saturation (S_{or} = 0.134). The fractional flow diagram (Figure 5.43) is typical of low permeability waterwet unconsolidated sand. The change in shape of total relative mobility and fractional flow curves for the low permeability sandpack compared to a high permeability pack (Figures 5.7 and 5.8) is due to a change in the pore distribution with a much more restrictive flow environment (especially with multiple saturations present) occurring in the low permeability pack.

Table 5.15 contains calcium leaching data from the sandpack for Experiment OWZ. Although some calcium ion is picked up in initial samples it quickly falls to an undetectable concentration (< 5 ppm) and appears to be no problem. The clay removal prior to packing removes most of the calcium ion source (Appendix 5). Figures 5.44 to 5.48 contain sandpack property determination data and Figures 5.49 to 5.74 contain dispersion data.

The narrow S-shaped curve for 100% brine saturation (Figure 5.44) indicates that the pack contains no significant heterogeneities and the breakthrough time implies that the pore volume is very close to 472.5 cc (Equation 2.9). The close agreement with the saturation pore volume (Table 5.12) is another indication of homogeneity. The single-phase dispersivity is 0.274 cm (Figure 5.45). The next cut consisted of 100% n-decane and resulted in the dispersion curve labelled Tracer A in Figure 5.46. Although early breakthrough and non-ideal S-shape curves were later observed for the oleic phase dispersions in Berea sandstone, the unusual shape of Tracer A was at this time not understood, so the possibility that it was due to heterogeneity of the sandpack was investigated. The sandpack was flooded to residual oil and the resulting dispersion curve (Figure 5.47) is smooth and S-shaped indicating a good pack. The pack was flooded back to residual water with n-decane and a second dispersion (Tracer B) was conducted (Figure 5.46). A third dispersion curve (Tracer C) was determined, this time utilizing a n-nonane tracer. All three curves are essentially identical. At this point the sandpack was cleaned of oil and brine by flushing the pack with four pore volumes of ethylbenzene followed by four pore volumes of methanol and finally ten pore volumes of 1.1 wt % NaCl brine. This was done to determine if heterogeneity had developed since the initial 100% brine dispersion was determined. The second 100% brine dispersion (OW1Z) appears in Figure 5.49. The curve is smooth and S-shaped indicating a good homogeneous pack. At this juncture, the core was judged to contain no heterogeneity and the unusual appearance of Figure 5.46 was thought to be due to some other mechanism. Note that relative permeability, fractional flow, and mobility data were determined after the cleaning discussed above. A final dispersion curve for oil at residual water appears in Figure 5.51. This curve is similar to those in Figure 5.46 (any differences are probably due to a change in wettability during the cleaning process). The aqueous phase dispersion curves are smooth and S-shaped and brine phase saturations calculated from frontal breakthrough (Equation 2.20) are 0.9 (OW4Z) to 1.3 times the material balance saturations (Table 5.14). The oil phase dispersions, like the high tension Berea results (BAOW), exhibit very early breakthrough and skewed, "capacitance"-type curves. Brine and oil phase dispersivities as a function of brine phase saturation are illustrated in Figure 5.75. Unlike the other experimental results in this investigation, there is little correlation between phase dispersivity and phase saturation. Oil phase dispersivity is two orders of magnitude greater than for the brine phase.

Experiment MO

Experiment MO was conducted in the same sandpack utilized in Experiment OWZ (Appendix 5). The investigation was carried out at 2.0 cc/min nominal flow rate at 30°C using pre-equilibrated oleic and microemulsion phases from a three-phase system. A complete recovery of all oil and brine phases was accomplished by flooding with the microemulsion phase and the flooding series began, therefore, at 100% microemulsion saturation. Carbon-14 labelled n-decane was used as a tracer for the oil phase and tritium for the microemulsion phase. Note that the carbon-14 tracer partitions into the microemulsion phase (see Chapter 2). Fluid and sandpack data are contained in Table 5.16. The partition coefficient determination is given in Table 5.17. The experimental results appear in Tables 5.18 to 5.20 and Figures 5.76 to 5.103.

Relative permeability curves appear in Figure 5.76. Note that although the curves span the entire saturation range, they are not straight lines. In addition, the oil relative permeability curve is more concave than the microemulsion curve. There is a fairly good agreement between the saturation by material balance calculation and the saturation by tritium breakthrough. Also, the 100% oil permeability and 100% microemulsion permeability were both 0.154 Darcy which is lower than the 100% brine permeability (0.467 Darcy). The 100% oleic phase saturation permeability from Experiment MO and 100% microemulsion phase saturation permeabilities from Experiments MO and MW (Tables 5.18 and 5.21) are all very close to 0.154 Darcy. This fact, along with the observation of rust in initial effluent samples after the porous medium was shut in, leads to suspicion of permeability reduction from the original 100% brine permeability (0.467 Darcy). As a result all effective permeabilities are normalized by 100% microemulsion permeability in Experiments MO, MW, and PH3 to obtain relative permeability. Figure 5.77 compares the relative permeability curves with the high tension experiment (OWZ) relative permeability curves. Microemulsion relative permeability is higher than brine phase relative permeability. Oleic phase relative permeability, on the other hand, is approximately equal to n-decane relative permeability. The range of saturation increases to encompass the entire range. Total relative mobility data is illustrated in Figure 5.78. The minimum is 0.213 cp^{-1} and occurs at 0.831 microemulsion saturation. A fractional flow diagram appears in Figure 5.79 and is linear from approximately 0.30 to 1.0 microemulsion saturation. Figure 5.80 illustrates the widening of the saturation range for micellar fluids compared to high IFT fluids. Table 5.20 contains calcium leaching data. As for Experiment OWZ, calcium leaching is not significant. Dispersion data for Experiment MO appears in Figures 5.81 to 5.102.

The narrow S-shaped curve for 100% microemulsion saturation (Figure 5.81) indicates once again that the sandpack was homogeneous. The single-phase dispersivity is 0.274 cm (Figure 5.82). The microemulsion dispersion curves are smooth and S-shaped. Microemulsion phase saturations calculated from frontal breakthrough (Equation 2.20) are 1.1 to 1.3 times the material balance saturations (Table 5.19). The oil phase dispersions, unlike high tension oil phases, do not exhibit early breakthrough times and are more S-shaped. The 100% oleic phase dispersion (Figure 5.101) again reflects a homogeneous pack. The single-phase oleic dispersivity is 0.21 cm (Figure 5.102). Oleic phase dispersivity based on Equation 2.33 and measured from apparent carbon-14 dispersivity ($\bar{\alpha}$) in both phases yields essentially the same result. The equations for cut MO4 appear below:

$$2.09 = \frac{0.577\ \alpha_{22} + (0.443)\ \alpha_{23}\ (0.486)}{0.577 + (0.443)(0.486)} \tag{5.1}$$

$$1.98 = \frac{0.577\ \alpha_{22} + (0.443)\ \alpha_{23}\ (0.486)}{0.577 + (0.443)(0.486)} \tag{5.2}$$

$$0.229 = \frac{0.443\ \alpha_{13} + (0.557)\ \alpha_{12}\ (0)}{0.443 + (0.557)(0)} \tag{5.3}$$

Equations 5.1 and 5.2 yield the same result. Since there are three unknown quantities (α_{22}, α_{23}, α_{13}) and three equations, the system is determinate. Since two equations are the same, this implies that two unknowns are also the same. Oleic phase dispersivity and microemulsion phase dispersivity are not equal. Therefore microemulsion phase dispersivity measured by tritium (α_{13}) is equal to microemulsion phase dispersivity measured by carbon-14 (α_{23}).

Oleic phase saturations calculated by Equation 2.25 are negative. A negative value has no physical meaning so the theory apparently does not apply in this case. Oleic phase saturations based on a non-partitioning tracer (Equation 2.20), however, are in close agreement for both microemulsion and oleic phases (Table 5.19).

Microemulsion and oleic phase dispersivities as a function of microemulsion phase saturation are illustrated in Figure 5.103. As before, oleic phase dispersion increases as oleic phase saturation decreases. Microemulsion phase dispersivity, on the other hand, remains approximately constant with changing microemulsion phase saturation.

A comparison of high and low IFT dispersivities appears in Figure 5.104. Microemulsion and brine dispersivities are approximately equal. Oleic phase dispersivity is about equal to microemulsion dispersivity at 100% oleic phase saturation and increases, approaching the n-decane dispersivity values, as the oleic phase saturation decreases.

Table 5.16 contains data on injected phase compositions. Figures 5.105 and 5.106 illustrate the composition (by gas chromatography) of effluent phases for steady-state dispersion determinations. Figure 5.107 contains interfacial tension data for these same cuts. It appears that steady-state was achieved for this experiment.

Experiment MW

Experiment MW was also carried out in the same sandpack (Appendix 5). The investigation was conducted at a nominal flow rate of 2.0 cc/min at 30°C using pre-equilibrated brine and microemulsion phases from the same three-phase system as before. The fluids were injected in the direction of decreasing brine cuts. Carbon-14 labelled n-decane was utilized as a tracer for the microemulsion phase and tritium for the aqueous phase. Note that the tritium tracer partitions into the microemulsion phase (see Chapter 2) while the carbon-14 tracer is non-partitioning. Fluid and sandpack data are contained in Table 5.16. Partition coefficient determination data are given in Table 5.17.

Relative permeability curves appear in Figure 5.108. The curves indicate a residual microemulsion saturation of 0.113. The 100% microemulsion permeability is 0.154 Darcy, which is lower than the 100% brine permeability (see Experiment MO). Material balance saturations and saturation by carbon-14 breakthrough are very close. Figure 5.109

compares high IFT relative permeabilities with those obtained in this experiment. Aqueous phase relative permeability is higher and covers a larger saturation range. The micro-emulsion phase, although it covers a larger saturation range, is very close to n-decane relative permeability. Total relative mobility data is illustrated in Figure 5.110. The minimum is 0.213 cp^{-1} at 0.137 aqueous phase saturation. A fractional flow diagram appears in Figure 5.111. The shape of the curve has a convex character. High IFT brine-phase fractional flow is compared to low tension aqueous-phase fractional flow in Figure 5.112. The widening of saturation range and change in shape is apparent. Table 5.20 contains calcium leaching data. As before, calcium leaching is not significant. Dispersion data for Experiment MW appears in Figures 5.113 to 5.134.

The microemulsion dispersion curves are smooth and S-shaped. Microemulsion phase saturations calculated from frontal breakthrough times (Equation 2.20) are 1.02 to 1.2 times the saturations calculated by material balance (Table 5.22). The aqueous phase dispersion curves are more irregularly shaped than the microemulsion phase curves. As in Experiment MO, aqueous phase saturations calculated by Equation 2.25 are negative values. The theory apparently does not apply in this case. Saturations based on a non-partitioning tracer yield fairly good approximations of material balance saturations being 1.1 to 1.4 times greater than saturations calculated from material balance (Table 5.22). Aqueous phase dispersivities calculated from the partitioning tritium tracer are in close agreement for both microemulsion and aqueous phases. Microemulsion and aqueous phase dispersivities as a function of aqueous phase saturation are illustrated in Figure 5.135. Aqueous phase dispersivity increases as aqueous phase saturation decreases. Microemulsion phase dispersivity remains essentially unchanged with decreasing saturation. A comparison of high and low IFT dispersivities appears in Figure 5.136. As before, microemulsion and brine dispersivities are approximately equal. As aqueous phase saturation decreases, the magnitude of aqueous phase dispersivity increases to the same magnitude as n-decane dispersivity. Table 5.16 contains data on injected phase compositions. Figures 5.137 and 5.138 illustrate the composition (by gas chromatography) of effluent phases for steady-state dispersion determinations. Figure 5.139 contains IFT data for these same cuts. It appears that steady-state was achieved for this experiment.

Experiment PH3

Experiment PH3 utilized the same specially prepared sandpack (Appendix 5). The investigation was conducted at 2.0 cc/min nominal flow rate at 30°C using pre-equilibrated aqueous, microemulsion, and oleic phases from a three-phase system. The experimental flooding sequence proceeds from predominantly oleic phase saturation to predominantly aqueous phase saturation with approximately constant microemulsion saturation. This was done to resemble the imbibition phenomenon. Carbon-14 labelled n-decane in microemulsion phase, n-nonane in oleic phase, and tritium in aqueous phase were the tracers utilized. Note that tritium partitions between microemulsions and aqueous phases while n-nonane and carbon-14 labelled n-decane partition between microemulsion and oleic phases (see Chapter 2). Fluid and sandpack data are contained in Table 5.16. Partition coefficient data is contained in Table 5.17.

The saturation history of PH3 appears in Figure 5.140. There are three two-phase endpoints and three three-phase points.

Relative permeability of phase j as a function of phase j saturation for oleic, microemulsion, and aqueous phases appears in Figure 5.141. As expected, the microemulsion phase relative permeabilities are essentially unchanged since the microemulsion cut was kept constant during the experiment. Aqueous and oleic phase relative permeabilities, on the other hand, appear to be approximately equal and dependent on their individual saturations. Oleic and aqueous phase saturations are about the same as in the two-phase experiments (Figures 5.76 and 5.108). Total relative mobility as a function of aqueous phase saturation is illustrated in Figure 5.142. The minimum is 0.149 cp^{-1}

at 0.324 aqueous, 0.515 microemulsion, and 0.161 oleic phase saturations. Fraction flow of phase j as a function of phase j saturation appears in Figure 5.143. Aqueous and oleic phase fractional flows are approximately equal. Additional data at different microemulsion cuts will be necessary before its behavior can be characterized. Calcium leaching was insignificant (Table 5.20). Dispersion data appears in Figures 5.144 to 5.177.

Single aqueous phase dispersion at residual microemulsion (Figure 5.144) is smooth and S-shaped. Oleic phase dispersion at residual aqueous phase saturation (Figure 5.146) is also smooth and S-shaped and demonstrates that n-nonane works well as a non-partitioning tracer. The dispersion curves for three-phase flow with partitioning tracers are all S-shaped. Tracers that partition into the microemulsion phase (n-nonane and tritium) tend to demonstrate more scatter in the microemulsion phase. N-nonane in microemulsion was not measured due to insufficient phase volumes and carbon-14 dispersion in cut PH35 in the oleic phase was not measured due to loss of samples. Finally, aqueous phase at residual microemulsion (Figure 5.176) is very close to the initial saturation (Figure 5.144). Saturations calculated from frontal breakthrough times (Equation 2.20) are very close to material balance saturations for cuts PH31, PH32, PH33, and PH36. Aqueous phase saturations are moderately larger in PH34 and substantially larger in PH35. The reverse is true of microemulsion saturation at these two cuts. Oleic saturations are within 20 percent of material balance saturations in PH34 and PH35 (Table 5.24). Saturations calculated by Equation 2.25 are negative. As before, the theory apparently does not apply in this case. Dispersivity of tracer i as a function of phase j saturation is illustrated in Figures 5.178 and 5.179. Ideally, three tracers are needed to calculate three dispersivities. Using Equation 2.33 to calculate dispersivity results in negative values. The n-nonane tracer gave inconsistent average dispersivities and apparently is not suitable where partitioning occurs. Since microemulsion dispersivity is approximately 0.2 cm in Experiments MO and MW, it will be assumed to be this value in this experiment as well. Oleic and aqueous phase dispersivities are calculated from Equation 2.33 using this microemulsion phase dispersivity. It would appear that phase dispersivity increases as phase saturation decreases for the oleic and aqueous phases. It is also apparent that inconsistent results occur for the n-nonane tracer. Table 5.23 contains data on injected phase compositions. Figures 5.180 to 5.182 illustrate the composition (by gas chromatography) of effluent phases for steady state dispersion determinations. Figures 5.183 and 5.184 contain IFT data for these same cuts. It appears that steady state was achieved for this experiment.

General Comments

If a material balance is performed on those high IFT oleic phase cases in BAOW and OWZ where early oleic phase tracer breakthrough occurred, it would appear that more tracer is produced than injected. This anomaly can be explained if the plateau tracer concentration is lower than injected concentration. This situation is confirmed in Table 5.26 which contains data on those cuts where these two concentrations were measured. Brine phase plateau concentrations are close to injected, but oleic phase concentrations are significantly lower. This suggests that some of the oleic phase (presumed non-wetting) is being bypassed during the flooding.

A comparison of residual phase saturations as a function of capillary number (defined two different ways) appears in Figures 5.185 and 5.186. At the high capillary numbers attained in this investigation, all residual saturations are zero except for residual microemulsion saturation to brine which is, however, much lower than residual microemulsion saturation to brine in Berea.[28] This would imply that microemulsion is the wetting phase.

TABLE 5.1

Flow Experiments

EXPERI-MENT	TYPE	PHASES	TRACERS	POROUS MEDIUM
OWCL	Drainage	1.0 wt % NaCl brine iso-Octane	Chloride ---	HPS
OW	Drainage	1.0 wt % NaCl brine iso-Octane	Tritium ---	HPS
BAOW	Imbibition	1.1 wt % NaCl brine n-decane	Tritium Carbon-14	Berea
OWZ	Imbibition	1.1 wt % NaCl brine n-decane	Tritium Carbon-14 n-Nonane	LPS
MO	Imbibition	Microemulsion Oleic	Tritium Carbon-14	LPS
MW	Drainage	Aqueous Microemulsion	Tritium Carbon-14	LPS
PH3	"Imbibition"	Aqueous Microemulsion Oleic	Tritium Carbon-14 n-Nonane	LPS

HPS = High Permeability Sandpack
LPS = Low Permeability Sanpack
Berea = Berea Sandstone

TABLE 5.2

Sand Mesh Sizes

SCREEN MESH	GRAIN SIZE MICRON	PERCENT STOPPED BY SCREENS OKLAHOMA NO. 1	OTTAWA F140	FISHER SILICA FLOUR 140
50	300	0.4	2.3	---
100	150	45.4	19.3	---
140	106	44.2	49.5	0.5
170	90	7.2	13.8	0.7
200	75	---	---	1.2
230	63	2.2	8.3	0.8
270	53	0.7	5.0	8.5
325	45	0.2	1.8	3.2
thru 325	<45	---	---	85.0

40-50 Mesh Seasand; 425-300 micron

TABLE 5.3

Sandpack and Fluid Data for Iso-Octane/Brine Imbibition

(Experiment OWCL)

Sand (Table 5.2)	- Oklahoma No. 1
Weight of sand	- 300.54 g
Column length	- 11.50 in (29.21 cm)
Cross-sectional area	- 0.785 in^2 (5.07 cm^2)
Bulk volume	- 148.0 cc
Pore volume (grain density)	- 47.7 cc
Pore volume (saturation volume)	- 50.4 cc
Porosity (saturation volume)	- 0.341
100% brine permeability	- 5.17 Darcies
100% brine dispersivity	- 0.250 cm
Temperature	- 27°C
Measured viscosity:	
of 3.0 wt % NaCl brine	- 0.95 cp
of 1.0 wt % NaCl brine	- 0.92 cp
of iso-Octane	- 0.54 cp

TABLE 5.4

Material Balance for Iso-Octane/Brine Imbibition

(Experiment OWCL)

CUT	BRINE FRACTIONAL FLOW, f_w	OIL FRACTIONAL FLOW, f_o	BRINE VOLUME IN PACK (cc)	BRINE SATURATION S_w	OIL VOLUME IN PACK (cc)	OIL SATURATION S_o	PRODUCED BRINE VOLUME (cc)	PRODUCED OIL VOLUME (cc)	TOTAL PRODUCED VOLUME (cc)
OWCL1	1.0	0.0	50.4	1.0	0.0	0.0	43.95	0.0	43.95
OWCL2	0.758	0.242	30.2	0.599	20.2	0.401	127.35	14.00	141.35
OWCL3	0.476	0.524	24.7	0.490	25.7	0.510	37.75	30.05	67.80
OWCL4	0.246	0.754	19.5	0.387	30.9	0.613	24.20	52.95	77.15
OWCL5	0.0	1.0	7.5	0.149	42.9	0.851	12.03	154.92	166.95

TABLE 5.5

Experimental Results for Iso-Octane/Brine Imbibition (Experiment OWCL)

CUT	FRACTIONAL FLOW BRINE f_w	FRACTIONAL FLOW OIL f_o	SATURATION BY MATERIAL BALANCE BRINE S_w	SATURATION BY MATERIAL BALANCE OIL S_o	BRINE SATURATION BY TRACER BREAKTHROUGH S_w	TOTAL FLOW RATE q(cc/min)	POTENTIAL DIFFERENCE $\Delta\Phi$ (psi)	RELATIVE PERMEABILITY BRINE k_{rw}	RELATIVE PERMEABILITY OIL k_{ro}
OWCL1	1.0	0.0	1.0	0.0	1.002	3.52	0.86	1.0	0.0
OWCL2	0.758	0.242	0.599	0.401	---	3.50	1.98	0.329	0.064
OWCL3	0.476	0.524	0.490	0.510	---	3.34	2.00	0.193	0.130
OWCL4	0.246	0.754	0.387	0.613	---	3.54	1.95	0.110	0.201
OWCL5	0.0	1.0	0.149	0.851	---	3.52	1.38	0.0	0.377

CUT	TOTAL RELATIVE MOBILITY M_T (cp^{-1})	CHLORIDE DISPERSIVITY IN THE BRINE PHASE α_{11} (cm)
OWCL1	1.087	0.250
OWCL2	0.476	---
OWCL3	0.451	---
OWCL4	0.492	---
OWCL5	0.698	---

100% Brine Permeability = 0.467 Darcy

TABLE 5.6

Sandpack and Fluid Data for Iso-Octane/Brine Imbibition

(Experiment OW)

Sand (Table 5.2)	- Oklahoma No. 1 (100-170 mesh)
Weight of sand	- 297.15 g
Column length	- 23.75 in (60.33 cm)
Cross-sectional area	- 0.795 in^2 (5.06 cm^2)
Bulk volume	- 305.5 cc
Pore volume (grain density)	- 112.9 cc
Pore volume (saturation volume)	- 113.0 cc
Porosity (saturation volume)	- 0.370
100% brine permeability	- 10.4 Darcies
100% brine dispersivity	- 0.342 cm
Temperature	- 27°C
Measured viscosity:	
of 1.0 wt % NaCl brine	- 0.92 cp
of Iso-octane	- 0.54 cp

TABLE 5.7

Material Balance for Iso-Octane/Brine Imbibition

(Experiment OW)

CUT	BRINE FRACTIONAL FLOW, f_w	OIL FRACTIONAL FLOW, f_o	BRINE VOLUME IN PACK (cc)	BRINE SATURATION S_w	OIL VOLUME IN PACK (cc)	OIL SATURATION S_o	PRODUCED BRINE VOLUME (cc)	PRODUCED OIL VOLUME (cc)	TOTAL PRODUCED VOLUME (cc)
OW1	1.0	0.0	113.0	1.0	0.0	0.0	170.8	0.0	170.8
OW2	0.837	0.134	76.5	0.677	36.5	0.323	403.75	20.30	424.05
OW3	0.730	0.270	68.0	0.602	45.0	0.398	164.45	49.20	213.65
OW4	0.497	0.508	54.8	0.485	58.2	0.515	139.60	117.40	257.00
OW5	0.246	0.754	34.8	0.308	78.2	0.692	74.50	146.85	221.35
OW6	0.0	1.0	13.2	0.117	99.8	0.883	21.6	214.55	236.15

TABLE 5.8

Experimental Results for Iso-Octane/Brine Imbibition (Experiment OW)

CUT	FRACTIONAL FLOW BRINE f_w	FRACTIONAL FLOW OIL f_o	SATURATION BY MATERIAL BALANCE BRINE S_w	SATURATION BY MATERIAL BALANCE OIL S_o	BRINE SATURATION BY TRACER BREAKTHROUGH S_w	TOTAL FLOW RATE q(cc/min)	POTENTIAL DIFFERENCE $\Delta\Phi$ (psi)	RELATIVE PERMEABILITY BRINE k_{rw}	RELATIVE PERMEABILITY OIL k_{ro}
OW1	1.0	0.0	1.0	0.0	1.010	1.96	0.52	1.0	0.0
OW2	0.837	0.134	0.677	0.323	0.605	1.96	2.45	0.179	0.0162
OW3	0.730	0.27	0.602	0.398	---	1.98	2.53	0.147	0.0320
OW4	0.497	0.508	0.485	0.515	0.523	1.97	2.61	0.0957	0.0580
OW5	0.246	0.754	0.308	0.692	---	1.97	3.05	0.0410	0.0737
OW6	0.0	1.0	0.117	0.883	---	2.00	1.48	0.0	0.204

CUT	TOTAL RELATIVE MOBILITY M_T (cp^{-1})	TRITIUM DISPERSIVITY IN BRINE PHASE α_{11} (cm)
OW1	1.087	0.342
OW2	0.225	0.965
OW3	0.219	---
OW4	0.211	1.387
OW5	0.181	---
OW6	0.378	---

100% Brine Permeability = 0.467 Darcy x 10.4 Darcy

TABLE 5.9

Core and Fluid Data for n-Decane/Brine Imbibition

(Experiment BAOW)

Porous medium	- Berea
Rock length	- 24.00 in (60.96 cm)
Cross-sectional area	- 4.00 in^2 (25.81 cm^2)
Bulk volume	- 1573.2 cc
Pore volume (fluid saturation)	- 304.8 cc
Porosity	- 0.194
100% brine permeability	- 0.193 Darcy
100% brine dispersivity	- 0.269 cm
Temperature	- 30°C
Measured viscosity:	
of 1.1 wt % NaCl brine	- 0.903 cp
of n-decane	- 0.863 cp

TABLE 5.10

Material Balance for n-Decane/Brine Imbibition

(Experiment BAOW)

CUT	BRINE FRACTIONAL FLOW, f_w	OIL FRACTIONAL FLOW, f_o	BRINE VOLUME IN PACK (cc)	BRINE SATURATION S_w	OIL VOLUME IN PACK (cc)	OIL SATURATION S_o	PRODUCED BRINE VOLUME (cc)	PRODUCED OIL VOLUME (cc)	TOTAL PRODUCED VOLUME (cc)
BAOW1	1.0	0.0	304.8	1.0	0.0	0.0	618.3	0.0	618.3
BAOW2	0.0	1.0	138.1	0.453	166.7	.547	166.7	775.3	942.0
BAOW3	0.0855	0.9145	174.0	0.571	130.8	.429	30.3	743.7	774.0
BAOW4	0.1895	0.8105	179.2	0.588	125.6	.412	48.7	235.6	284.3
BAOW7	0.484	0.516	184.4	0.605	120.4	.395	103.2	120.8	224.0
BAOW8	1.0	0.0	192.9	0.633	111.9	.367	1279.1	8.5	1287.6

TABLE 5.11

Experimental Results for n-Decane/Brine Imbibition (Experiment BAOW)

CUT	FRACTIONAL FLOW BRINE f_w	FRACTIONAL FLOW OIL f_o	SATURATION BY MATERIAL BALANCE BRINE S_w	SATURATION BY MATERIAL BALANCE OIL S_o	SATURATION BY TRACER BREAKTHROUGH BRINE S_w	SATURATION BY TRACER BREAKTHROUGH OIL S_o	TOTAL FLOW RATE q(cc/min)	POTENTIAL DIFFERENCE $\Delta\Phi$ (psi)	RELATIVE PERMEABILITY BRINE k_{rw}	RELATIVE PERMEABILITY OIL k_{ro}
BAOW1	1.0	0.0	1.0	0.0	1.007	---	1.91	5.17	1.0	0.0
BAOW2	0.0	1.0	0.453	0.547	---	0.533	1.85	6.33	0.0	0.756
BAOW3	0.0855	0.9145	0.571	0.429	0.534	0.325	0.982	8.30	0.0274	0.290
BAOW4	0.1895	0.8105	0.588	0.412	0.529	0.219	0.486	6.80	0.0367	0.144
BAOW7	0.484	0.516	0.605	0.395	0.577	0.108	0.670	19.8	0.0443	0.0445
BAOW8	1.0	0.0	0.633	0.367	0.617	---	0.541	20.9	0.0701	0.0

CUT	TOTAL RELATIVE MOBILITY M_T (cp^{-1})	DISPERSIVITY IN THE BRINE PHASE TRITIUM α_{11} (cm)	DISPERSIVITY IN THE BRINE PHASE CARBON-14 α_{22} (cm)
BAOW1	1.107	0.269	---
BAOW2	0.876	---	0.548
BAOW3	0.366	1.46	2.81
BAOW4	0.208	0.632	3.63
BAOW7	0.101	0.660	4.67
BAOW8	0.0776	0.498	---

100% Brine Permeability = 0.193 Darcy

TABLE 5.12

Sandpack and Fluid Data for n-Decane/Brine Imbibition

(Experiment OWZ)

Porous medium	- Ottawa sand (Appendix 5)
Length	- 60.96 cm
Cross-sectional area	- 20.27 cm^2
Bulk volume	- 1235.6 cc
Pore volume	- 472.5 cc
Porosity	- 0.382
100% brine permeability	- 0.467 Darcy
100% brine dispersivity	- 0.274 cm
Temperature	- 30°C
Measured viscosity:	
of 1.1 wt % NaCl brine	- 0.903 cp
of n-decane	- 0.863 cp

TABLE 5.13

Material Balance for n-Decane/Brine Imbibition

(Experiment OWZ)

CUT	BRINE FRACTIONAL FLOW, f_w	OIL FRACTIONAL FLOW, f_o	BRINE VOLUME IN PACK (cc)	BRINE SATURATION S_w	OIL VOLUME IN PACK (cc)	OIL SATURATION S_o	PRODUCED BRINE VOLUME (cc)	PRODUCED OIL VOLUME (cc)	TOTAL PRODUCED VOLUME (cc)
OW1Z	1.0	0.0	472.5	1.0	0.0	0.0	673.2	0.0	673.2
OW2Z	0.0	1.0	175.8	0.372	296.7	0.628	296.7	715.3	1012.0
OW3Z	0.108	0.892	212.6	0.450	259.9	0.550	150.2	1581.1	1731.3
OW4Z	0.198	0.802	257.5	0.545	215.0	0.455	247.7	1230.2	1477.9
OW5Z	0.300	0.700	308.1	0.652	164.4	0.348	452.4	1224.3	1676.7
OW6Z	0.512	0.488	357.2	0.756	115.3	0.244	190.1	277.1	467.2
OW7Z	0.761	0.239	403.5	0.854	69.0	0.146	601.6	249.8	851.4
OW8Z	1.0	0.0	409.2	0.889	63.3	0.134	298.3	5.7	304.0

TABLE 5.14

Experimental Results for n-Decane/Brine Imbibition (Experiment OWZ)

	FRACTIONAL FLOW		SATURATION BY MATERIAL BALANCE		SATURATION BY TRACER BREAKTHROUGH		TOTAL	POTENTIAL	RELATIVE PERMEABILITY	
	BRINE	OIL	BRINE	OIL	BRINE	OIL	FLOW RATE	DIFFERENCE	BRINE	OIL
CUT	f_w	f_o	S_w	S_o	S_w	S_o	q(cc/min)	$\Delta\Phi$ (psi)	k_{rw}	k_{ro}
OW1Z	1.0	0.0	1.0	0.0	0.997	---	1.83	2.61	1.0	0.0
OW2Z	0.0	1.0	0.372	0.628	---	0.488	1.91	7.26	0.0	0.358
OW3Z	0.108	0.892	0.450	0.550	0.585	0.229	1.98	9.43	0.0323	0.266
OW4Z	0.198	0.802	0.545	0.455	0.514	0.073	1.97	11.5	0.0485	0.190
OW5Z	0.300	0.700	0.652	0.348	0.786	0.083	1.94	14.4	0.0574	0.129
OW6Z	0.512	0.488	0.756	0.244	0.834	0.027	1.70	17.4	0.0713	0.0653
OW7Z	0.761	0.239	0.854	0.146	0.908	0.018	1.74	20.4	0.0925	0.0279
OW8Z	1.0	0.0	0.866	0.134	0.889	---	1.92	28.7	0.0953	0.0

	TOTAL RELATIVE MOBILITY	DISPERSIVITY IN THE BRINE PHASE	
		TRITIUM	CARBON-14
CUT	M_T (cp^{-1})	α_{11} (cm)	α_{22} (cm)
OW1Z	1.107	0.063	---
OW2Z	0.415	---	11.5
OW3Z	0.344	0.085	18.5
OW4Z	0.274	0.131	34.4
OW5Z	0.213	0.287	24.4
OW6Z	0.155	0.197	13.7
OW7Z	0.135	0.172	9.35
OW8Z	0.106	0.252	---

100% Brine Permeability = 0.467 Darcy

TABLE 5.15

Calcium Ion Concentration in Sandpack

Steady State Effluent

(Experiment OWZ)

CUT	PORE VOLUMES	CALCIUM ION CONCENTRATION (ppm)
OW1Z	0.024	66.1
	0.678	20.3
	1.404	<5.0
	1.825	<5.0
OW2Z	0.051	<5.0
	1.731	<5.0
OW3Z	0.062	7.1
	2.136	<5.0
OW4Z	0.018	<5.0
	1.763	<5.0
OW5Z	0.026	<5.0
	2.014	<5.0
OW6Z	0.041	6.3
	1.231	<5.0
OW7Z	0.053	<5.0
	1.468	<5.0
OW8Z	0.021	<5.0
	1.231	<5.0

TABLE 5.16

Sandpack and Fluid Data for Two Micellar Phase Flow Experiments (Experiments MO and MW)

Porous media	- Ottawa sand (Appendix 5)
Length	- 60.96 cm
Cross-sectional area	- 20.27 cm^2
Bulk volume	- 1235.6 cc
Pore volume	- 472.5 cc
Porosity	- 0.382
100% brine permeability	- 0.467 Darcy
100% brine dispersivity	- 0.274 cm
Temperature	- 30°C
Measured viscosity:	
Oleic phase	- 0.87 cp
Microemulsion phase	- 4.37 cp
Aqueous phase	- 0.93 cp

Injection Phase Composition by Gas Chromatography

PHASE	N-DECANE (vol %)	WATER (vol %)	ISOBUTANOL (vol %)	*TRS 10-410 (vol %)
Oleic	99.2	0.0	0.0	0.8
Microemulsion	39.1	47.0	4.1	9.8
Aqueous	0.0	97.6	3.1	0.0

*TRS 10-410 by material balance

TABLE 5.17

Partition Coefficient Determinations

for Two Micellar Phase Flow Experiments

(Experiments MO and MW)

EXPERIMENT	TRACER	OLEIC OR AQUEOUS PHASE (dpm)	MICROEMULSION PHASE (dpm)	K_T
*Standard	Carbon-14	3451	1688	0.489
MO2	Carbon-14	2394	1263	0.528
MO3	Carbon-14	2564	1418	0.553
MO4	Carbon-14	2381	1158	0.486
*Standard	Tritium	5835	2362	0.405
MW2	Tritium	6268	2965	0.473
MW3	Tritium	8081	2319	0.287
MW4	Tritium	6395	2666	0.417

*Standard = standard samples mixed independently from experimenal fluids

TABLE 5.18

Material Balance for Oleic/Microemulsion Phase Imbibition

(Experiment MO)

	FRACTIONAL FLOW		VOLUME IN PACK		SATURATION		PRODUCED VOLUME		TOTAL
CUT	MICRO-EMULSION F_{me}	OIL f_o	MICRO-EMULSION (cc)	OIL (cc)	MICRO-EMULSION S_{me}	OIL S_o	MICRO-EMULSION (cc)	OIL (cc)	PRODUCED VOLUME (cc)
MO1	1.0	0.0	472.5	0.0	1.0	0.0	708.8	0.0	708.8
MO2	0.772	0.228	392.6	79.9	0.831	0.169	584.4	69.1	653.5
MO3	0.516	0.484	307.1	165.4	0.650	0.350	468.4	273.6	742.0
MO4	0.258	0.742	209.3	263.2	0.443	0.557	306.9	503.4	810.3
MO5	0.0	1.0	1.9	470.6	0.004	0.996	207.4	967.2	1174.6

TABLE 5.19

Experimental Results for Oleic/Microemulsion Phase Imbibition (Experiment MO)

CUT	FRACTIONAL FLOW MICRO-EMULSION f_{me}	FRACTIONAL FLOW OIL f_o	SATURATION BY MATERIAL BALANCE MICRO-EMULSION S_{me}	SATURATION BY MATERIAL BALANCE OIL S_o	MICROEMULSION SATURATION BY TRITIUM BREAK-THROUGH IN MICRO-EMULSION, S_{me}	OIL SATURATION BY TRITIUM BREAKTHROUGH IN MICROEMULSION, S_o	OIL SATURATION BY CARBON-14 BREAKTHROUGH IN OIL, S_o
MO1	1.0	0.0	1.0	0.0	1.023	---	---
MO2	0.772	0.228	0.831	0.169	0.918	0.159	0.161
MO3	0.516	0.484	0.650	0.350	0.772	0.347	0.317
MO4	0.258	0.742	0.443	0.557	0.567	0.578	0.606
MO5	0.0	1.0	0.004	0.996	---	1.003	---

CUT	TOTAL FLOW RATE q(cc/min)	POTENTIAL DIFFERENCE $\Delta\Phi$(psi)	RELATIVE PERMEABILITY MICROEMULSION k_{rme}	RELATIVE PERMEABILITY OIL k_{ro}	TOTAL RELATIVE MOBILITY M_T (cp^{-1})	TRITIUM DISPERSIVITY IN MICRO-EMULSION PHASE α_{13} (cm)	CARBON-14 DISPERSIVITY MICRO-EMULSION PHASE α_{23} (cm)	CARBON-14 DISPERSIVITY OIL PHASE α_{22} (cm)
MO1	1.94	54.6	1.007	0.0	0.230	0.274	---	---
MO2	2.00	60.5	0.723	0.0431	0.213	0.182	8.76	6.89
MO3	2.01	55.0	0.534	0.0998	0.237	0.176	4.28	3.73
MO4	2.10	41.1	0.374	0.217	0.335	0.229	2.81	2.65
MO5	1.93	10.6	0.0	1.031	1.185	---	---	0.205

100% Microemulsion Permeability = 0.154 Darcy

TABLE 5.20

Calcium Ion Concentration in

Microemulsion Steady-State Effluent

(Experiments MO, MW, PH3)

CUT	PORE VOLUMES	CALCIUM ION CONCENTRATION (ppm)
MO1	0.048	8.3
	1.050	<5.0
MO2	0.055	9.1
	1.441	<5.0
MO3	0.040	7.2
	1.701	<5.0
MO4	0.061	<5.0
	1.689	<5.0
MW1	0.054	6.1
	1.177	<5.0
MW2	0.056	7.2
	1.250	<5.0
MW3	0.060	<5.0
	1.783	<5.0
MW4	0.059	<5.0
	2.168	<5.0
PH33	0.057	6.1
	1.752	<5.0
PH34	0.068	<5.0
	1.366	<5.0
PH35	0.058	<5.0
	1.968	<5.0

TABLE 5.21

Material Balance for Microemulsion/Aqueous Phase Drainage

(Experiment MW)

CUT	FRACTIONAL FLOW BRINE f_w	FRACTIONAL FLOW MICRO-EMULSION f_{me}	VOLUME IN PACK BRINE (cc)	VOLUME IN PACK MICRO-EMULSION (cc)	SATURATION BRINE S_w	SATURATION MICRO-EMULSION S_{me}	PRODUCED VOLUME BRINE (cc)	PRODUCED VOLUME MICRO-EMULSION (cc)	TOTAL PRODUCED VOLUME (cc)
MW1	0.0	1.0	0.0	472.5	0.0	1.0	0.0	684.2	684.2
MW2	0.230	0.770	64.7	407.8	0.137	0.863	134.6	731.9	866.5
MW3	0.511	0.489	142.2	330.3	0.301	0.699	359.9	496.1	856.0
MW4	0.764	0.236	254.7	217.8	0.539	0.461	622.4	339.5	961.9
MW5	1.0	0.0	419.1	53.4	0.887	0.113	1006.5	164.4	1170.9

TABLE 5.22

Experimental Results for Microemulsion/Aqueous Phase Drainage (Experiment MW)

	FRACTIONAL FLOW		SATURATION BY MATERIAL BALANCE		BRINE SATURATION BY TRITIUM BREAKTHROUGH		MICROEMULSION SATURATION BY CARBON-14 BREAKTHROUGH IN MICROEMULSION, S_{me}	TOTAL FLOW RATE q(cc/min)
CUT	BRINE f_w	MICRO-EMULSION f_{me}	BRINE S_w	MICRO-EMULSION S_{me}	BRINE S_w	MICRO-EMULSION S_w		
MW1	0	1.0	0	1.0	---	---	1.020	1.94
MW2	0.230	0.770	0.137	0.863	0.193	0.186	0.943	1.95
MW3	0.511	0.489	0.301	0.699	0.371	0.377	0.759	2.02
MW4	0.764	0.236	0.539	0.461	0.570	0.595	0.564	2.16
MW5	1.0	0.0	0.887	0.113	0.884	---	---	2.03

CUT	POTENTIAL DIFFERENCE $\Delta\Phi$ (psi)	RELATIVE PERMEABILITY BRINE k_{rw}	RELATIVE PERMEABILITY MICROEMULSION k_{rme}	TOTAL RELATIVE MOBILITY M_T (cp^{-1})	TRITIUM DISPERSIVITY BRINE PHASE α_{11} (cm)	TRITIUM DISPERSIVITY MICROEMULSION PHASE α_{13} (cm)	CARBON-14 DISPERSIVITY IN THE MICROEMULSION PHASE α_{23} (cm)
MW1	38.9	0.0	1.001	0.229	---	---	0.211
MW2	36.2	0.0552	0.670	0.213	27.2	18.6	0.276
MW3	44.2	0.104	0.470	0.219	5.34	3.42	0.143
MW4	37.7	0.195	0.283	0.274	0.617	1.25	0.203
MW5	20.3	0.446	0.0	0.480	0.289	---	---

100% Microemulsion Permeability = 0.154 Darcy

TABLE 5.23

Fluid Data for Three Micellar Phase Flow Experiments

Temperature	- 30°C
Measured viscosity:	
Oleic phase	- 0.86 cp
Microemulsion phase	- 4.34 cp
Aqueous phase	- 0.92 cp

Injection Phase Composition by Gas Chromatography

PHASE	N-DECANE (vol %)	WATER (vol %)	ISOBUTANOL (vol %)	*TRS 10-410 (vol %)
Oleic	98.9	0.0	0.0	1.1
Microemulsion	43.9	44.9	3.6	7.6
Aqueous	0.0	95.1	2.5	2.4

*TRS 10-410 by material balance

TABLE 5.24

Material Balance for Three-Phase Flow

(Experiment PH3)

CUT	FRACTIONAL FLOW BRINE f_w	FRACTIONAL FLOW MICRO-EMULSION f_{me}	FRACTIONAL FLOW OIL f_o	VOLUME IN PACK BRINE (cc)	VOLUME IN PACK MICRO-EMULSION (cc)	VOLUME IN PACK OIL (cc)	SATURATION BRINE S_w	SATURATION MICRO-EMULSION S_{me}	SATURATION OIL S_o
PH31	1.0	0.0	0.0	414.4	58.1	0.0	0.877	0.123	0.0
PH32	0.0	0.0	1.0	95.4	0.0	377.1	0.202	0.0	0.798
PH33	0.196	0.212	0.592	109.2	189.8	173.5	0.231	0.402	0.367
PH34	0.392	0.230	0.378	133.9	215.4	123.2	0.283	0.456	0.261
PH35	0.587	0.233	0.180	153.1	243.2	76.2	0.324	0.515	0.161
PH36	1.0	0.0	0.0	371.2	101.3	0.0	0.786	0.214	0.0

CUT	PRODUCED VOLUME BRINE (cc)	PRODUCED VOLUME MICRO-EMULSION (cc)	PRODUCED VOLUME OIL (cc)	TOTAL PRODUCED VOLUME (cc)
PH31	573.2	0.0	0.0	573.2
PH32	319.0	58.2	660.3	1037.4
PH33	278.6	126.5	1086.7	1491.8
PH34	369.2	205.5	430.1	1004.8
PH35	610.8	222.3	240.2	1073.2
PH36	1451.3	141.9	76.7	1669.4

TABLE 5.25

Experimental Results for Three-Phase Flow

(Experiment PH3)

CUT	FRACTIONAL FLOW: BRINE f_w	FRACTIONAL FLOW: MICRO-EMULSION f_{me}	FRACTIONAL FLOW: OIL f_o	SATURATION BY MATERIAL BALANCE: BRINE (cc)	SATURATION BY MATERIAL BALANCE: MICRO-EMULSION (cc)	SATURATION BY MATERIAL BALANCE: OIL (cc)	BRINE SATURATION BY TRITIUM BREAKTHROUGH: BRINE S_w	BRINE SATURATION BY TRITIUM BREAKTHROUGH: MICRO-EMULSION S_w	MICROEMULSION SATURATION BY CARBON-14 BREAK-THROUGH IN MICRO-EMULSION, S_{me}
PH31	1.0	0.0	0.0	0.877	0.123	0.0	0.852	---	---
PH32	0.0	0.0	1.0	0.202	0.0	0.798	---	---	---
PH33	0.196	0.212	0.592	0.231	0.402	0.367	0.232	0.189	0.421
PH34	0.392	0.230	0.378	0.283	0.456	0.261	0.344	0.361	0.368
PH35	0.587	0.233	0.180	0.324	0.515	0.161	0.722	0.644	0.330
PH36	1.0	0.0	0.0	0.786	0.214	0.0	0.779	---	---

CUT	OIL SATURATION BY CARBON-14 BREAKTHROUGH IN OIL, S_o	TOTAL FLOW RATE q(cc/min)	POTENTIAL DIFFERENCE $\Delta\Phi$ (psi)	RELATIVE PERMEABILITY: BRINE k_{rw}	RELATIVE PERMEABILITY: MICRO-EMULSION k_{rmw}	RELATIVE PERMEABILITY: OIL k_{ro}	TOTAL RELATIVE MOBILITY M_T (cp^{-1})
PH31	---	1.94	8.4	0.596	0.0	---	0.366
PH32	0.810	1.96	14.0	0.0	---	0.336	0.221
PH33	0.334	1.99	15.3	0.0655	0.374	0.198	0.219
PH34	0.202	1.99	19.7	0.102	0.269	0.0955	0.161
PH35	0.197	1.96	20.5	0.144	0.267	0.0390	0.149
PH36	---	1.91	9.6	0.513	0.0	---	0.315

100% Microemulsion Permeability = 0.267 Darcy

TABLE 5.25 continued

Experimental Results for Three-Phase Flow

(Experiment PH3)

CUT	TRITIUM DISPERSIVITY BRINE PHASE α_{11} (cm)	TRITIUM DISPERSIVITY MICRO-EMULSION PHASE α_{13} (cm)	ASSUMED CARBON-14 DISPERSIVITY IN THE MICROEMULSION PHASE α_{23} (cm)	DISPERSIVITY IN THE OIL PHASE CARBON-14 α_{22} (cm)	DISPERSIVITY IN THE OIL PHASE N-NONANE $\alpha_{2'2}$ (cm)
PH31	0.194	---	---	---	---
PH32	---	---	---	0.505	---
PH33	1.97	2.02	0.2	0.984	2.40
PH34	1.62	1.69	0.2	1.30	5.23
PH35	0.441	0.447	0.2	1.45	0.573
PH36	0.223	---	---	---	---

TABLE 5.26

Injected and Plateau Tracer Concentrations

CUT	TRACER	INJECTED CONCENTRATION (dpm)	PLATEAU CONCENTRATION (dpm)	PERCENT OF INJECTED
BAOW1	TRITIUM	3734	3517	94
BAOW3AQ	TRITIUM	9935	9632	97
BAOW3OL	CARBON-14	2052	1787	87
BAOW4AQ	TRITIUM	7686	7560	98
BAOW4OL	CARBON-14	2015	1881	93
BAOW7AQ	TRITIUM	9237	8802	95
BAOW7OL	CARBON-14	2062	1690	82
BAOW8	TRITIUM	3734	3791	102
OW1Z	TRITIUM	19127	19060	100
OW2Z	CARBON-14	2330	2143	92
OW4AQ	TRITIUM	17371	17179	99
OW4ZOL	CARBON-14	2527	2227	88
OW5ZOL	CARBON-14	2654	2288	86
OW6ZOL	CARBON-14	1645	1572	96
OW7ZOL	CARBON-14	1457	1329	91
OW8Z	TRITIUM	8631	8497	98

FIGURE 5.1

RELATIVE PERMEABILITY OF ISO-OCTANE
AND BRINE IN UNCONSOLIDATED SAND
(EXPERIMENT OWCL)

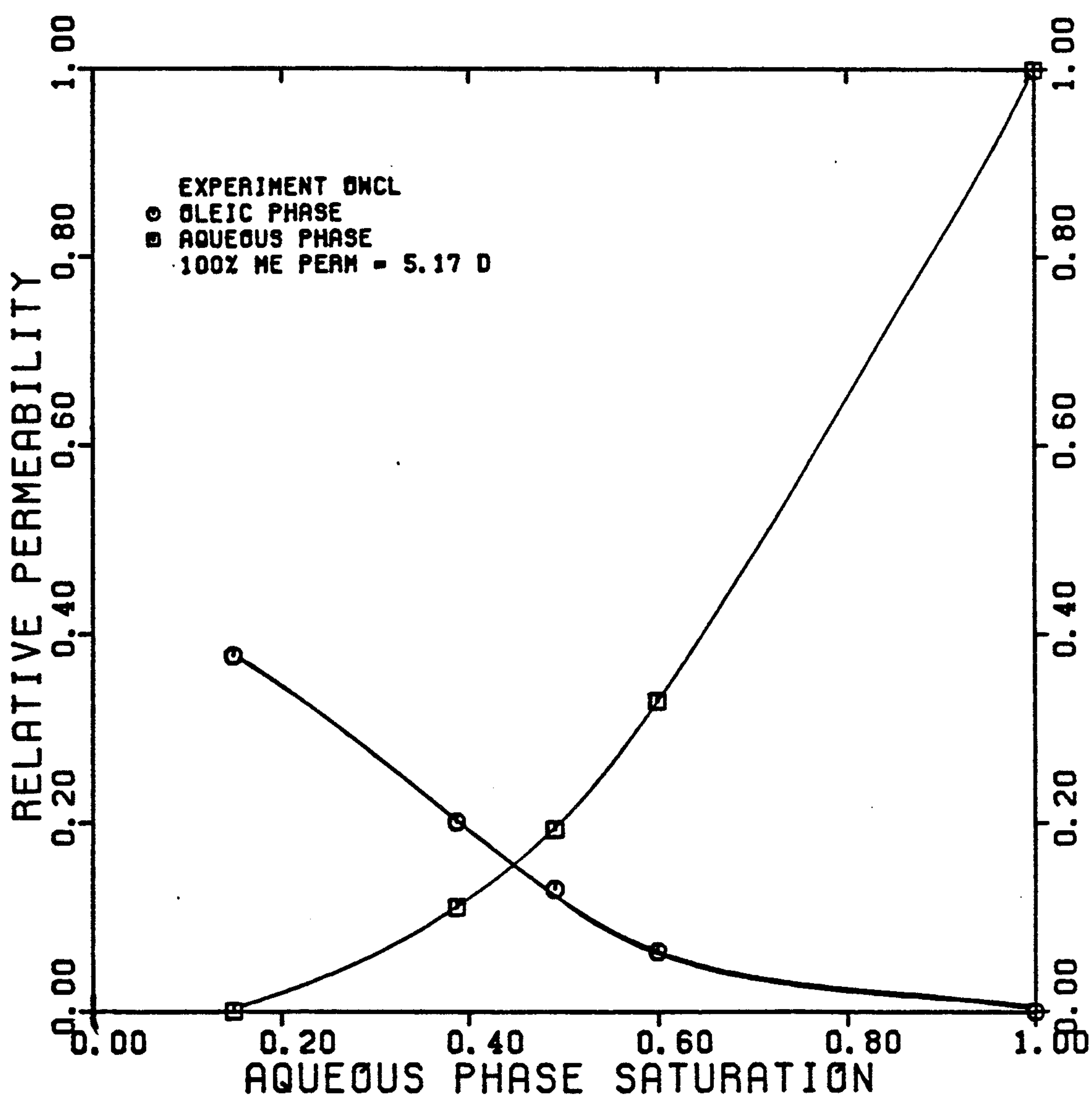

FIGURE 5.2

TOTAL RELATIVE MOBILITY OF BRINE AND
ISO-OCTANE IN UNCONSOLIDATED SAND
(EXPERIMENT OWCL)

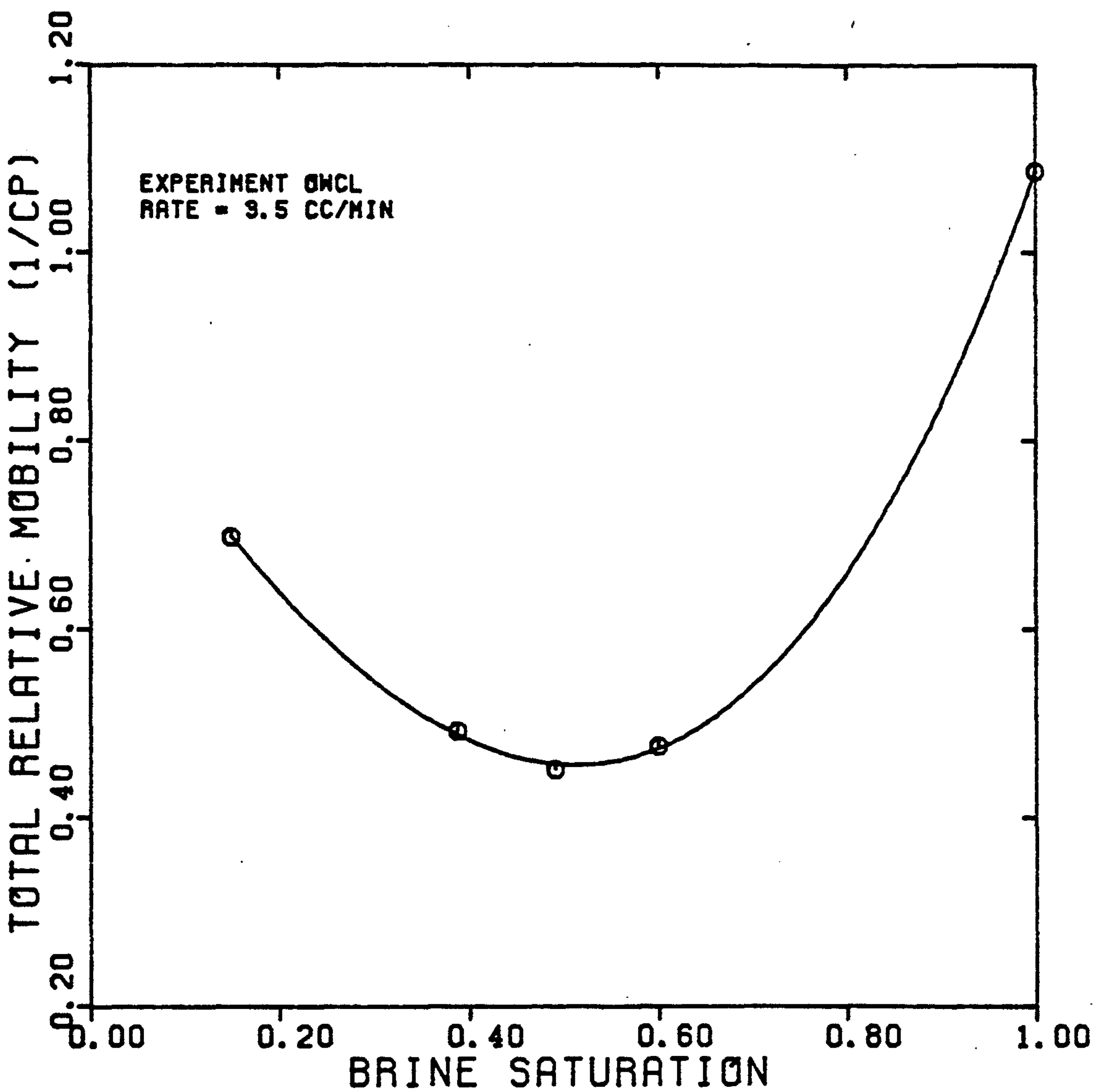

FIGURE 5.3

FRACTIONAL FLOW FOR THE AQUEOUS PHASE IN UNCONSOLIDATED SAND (EXPERIMENT OWCL)

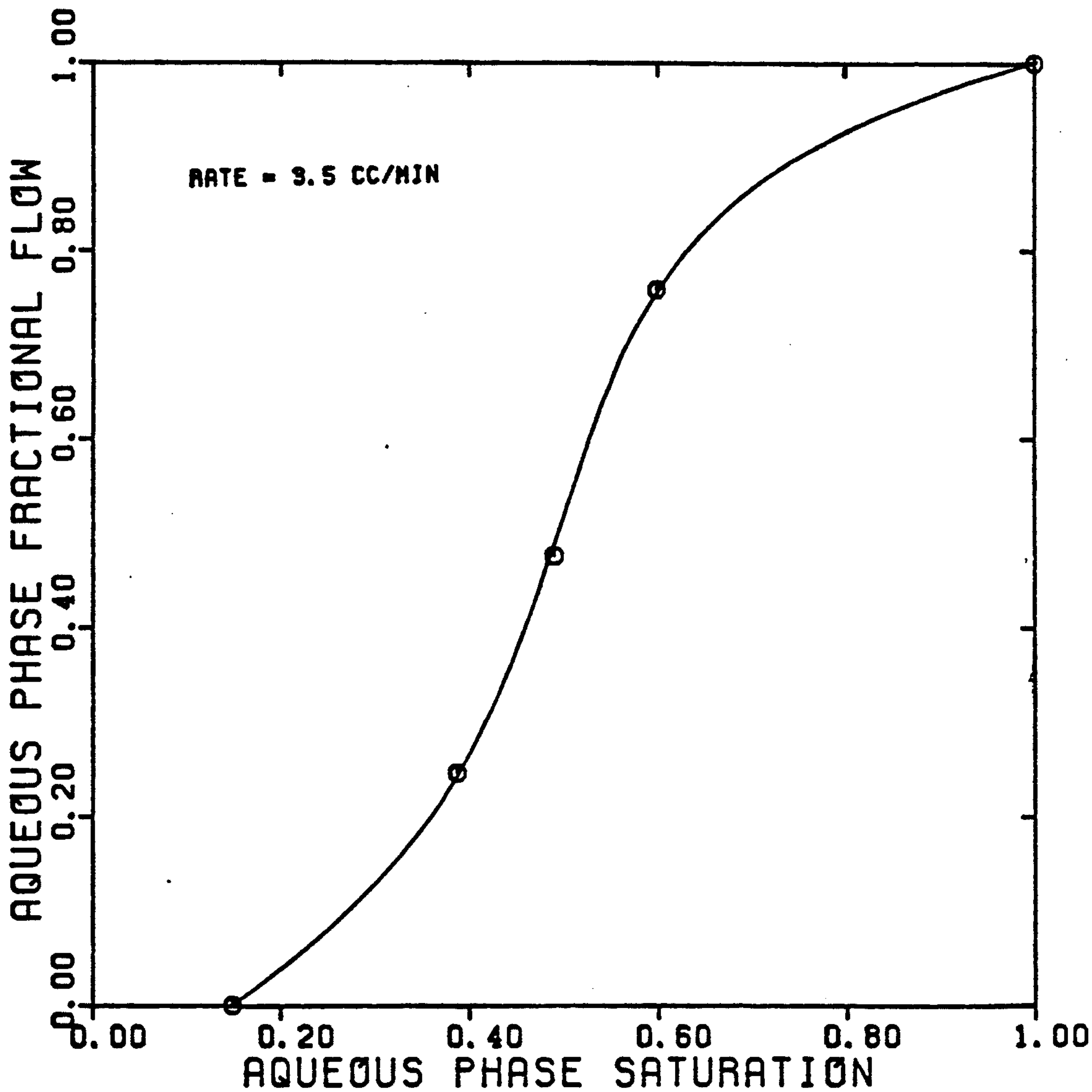

FIGURE 5.4

SANDPACK BREAKTHROUGH CURVE FOR CHLORIDE ION TRACER IN THE AQUEOUS PHASE (EXPERIMENT OWCL1)

$S_w = 1.0 \quad f_w = 1.0$

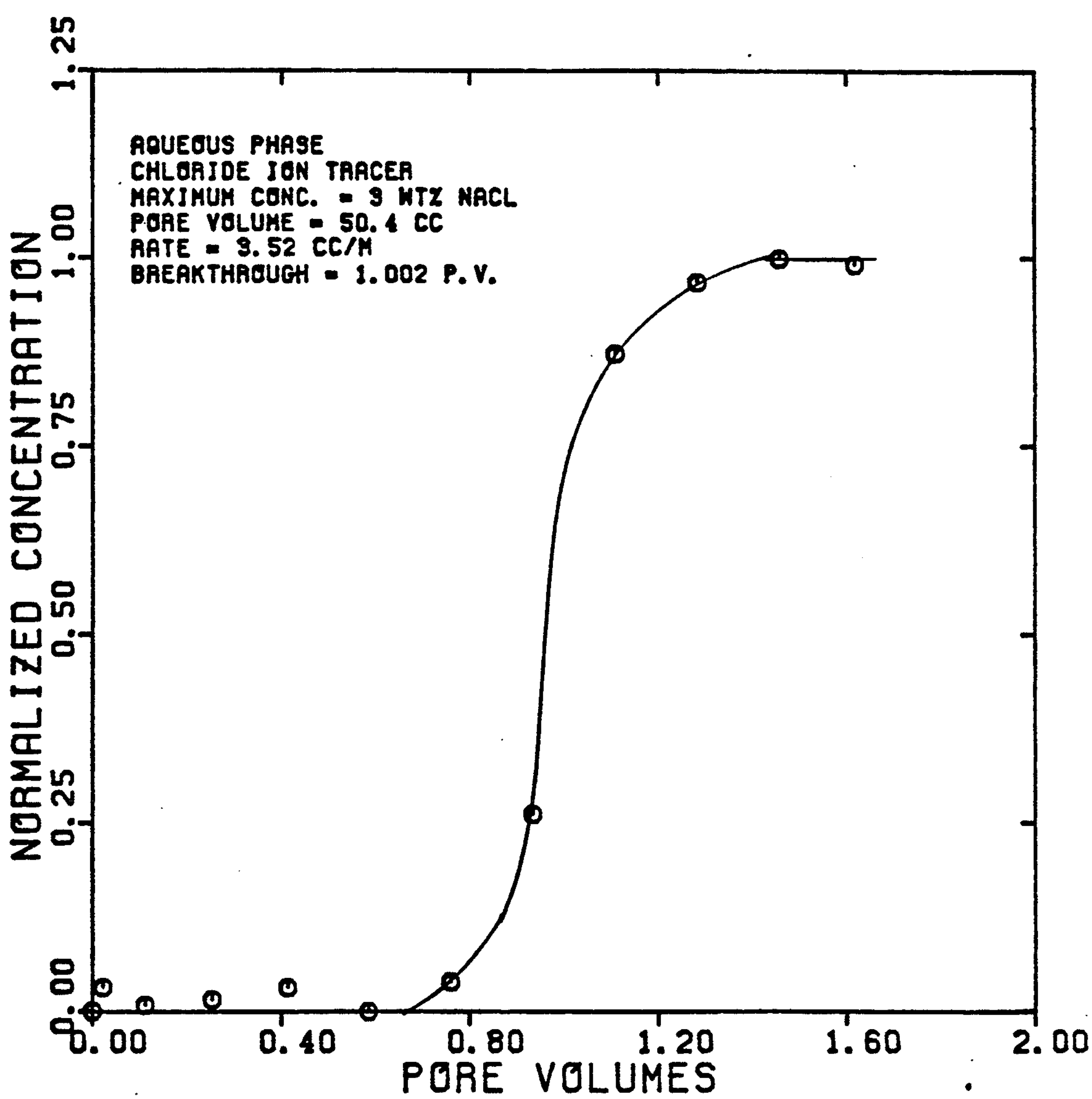

FIGURE 5.5

DISPERSIVITY OF CHLORIDE ION
TRACER IN THE AQUEOUS PHASE
(EXPERIMENT OWCL1)

$S_w = 1.0 \quad f_w = 1.0$

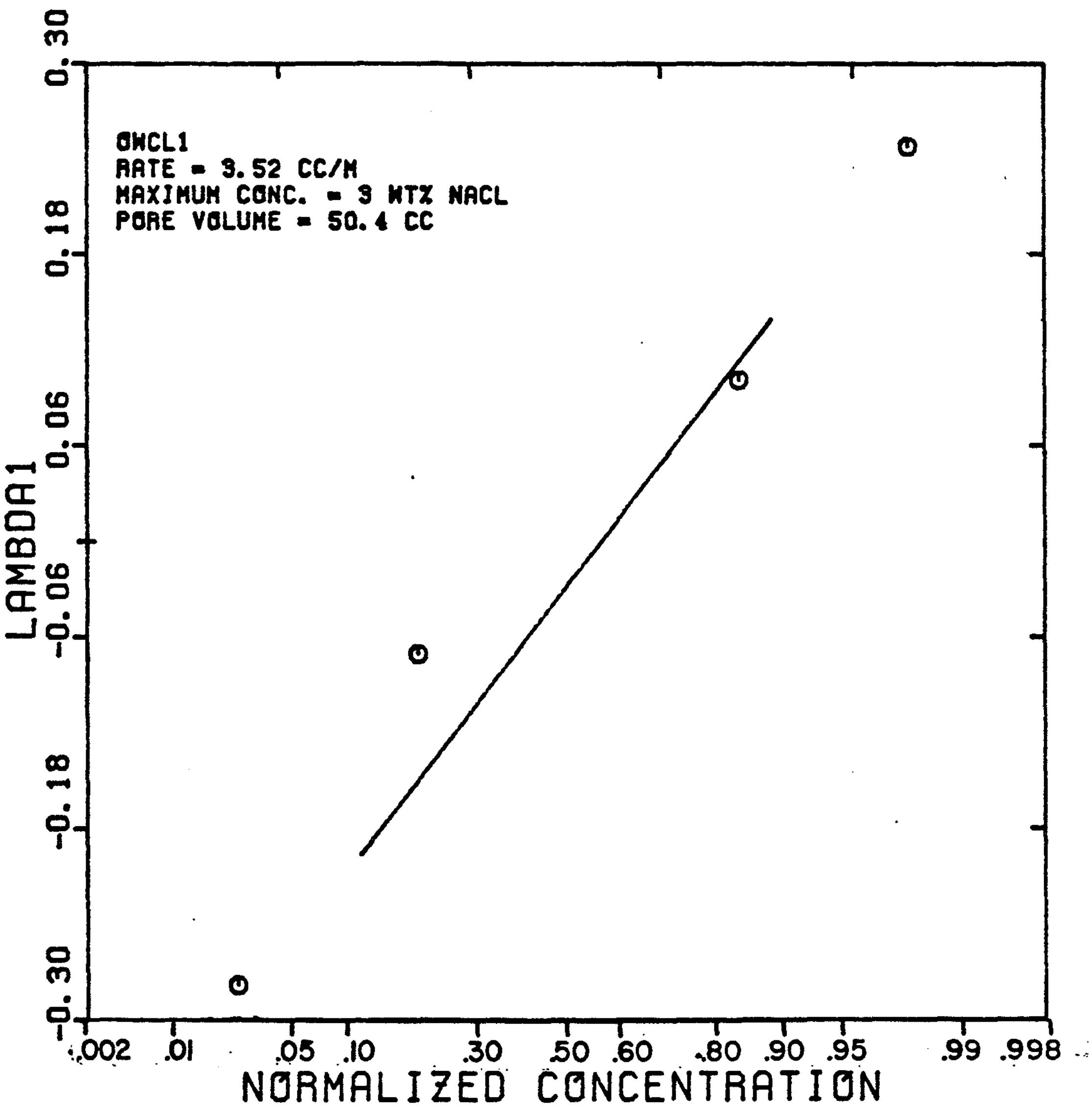

FIGURE 5.6

RELATIVE PERMEABILITY OF ISO-OCTANE
AND BRINE IN UNCONSOLIDATED SAND
(EXPERIMENT OW)

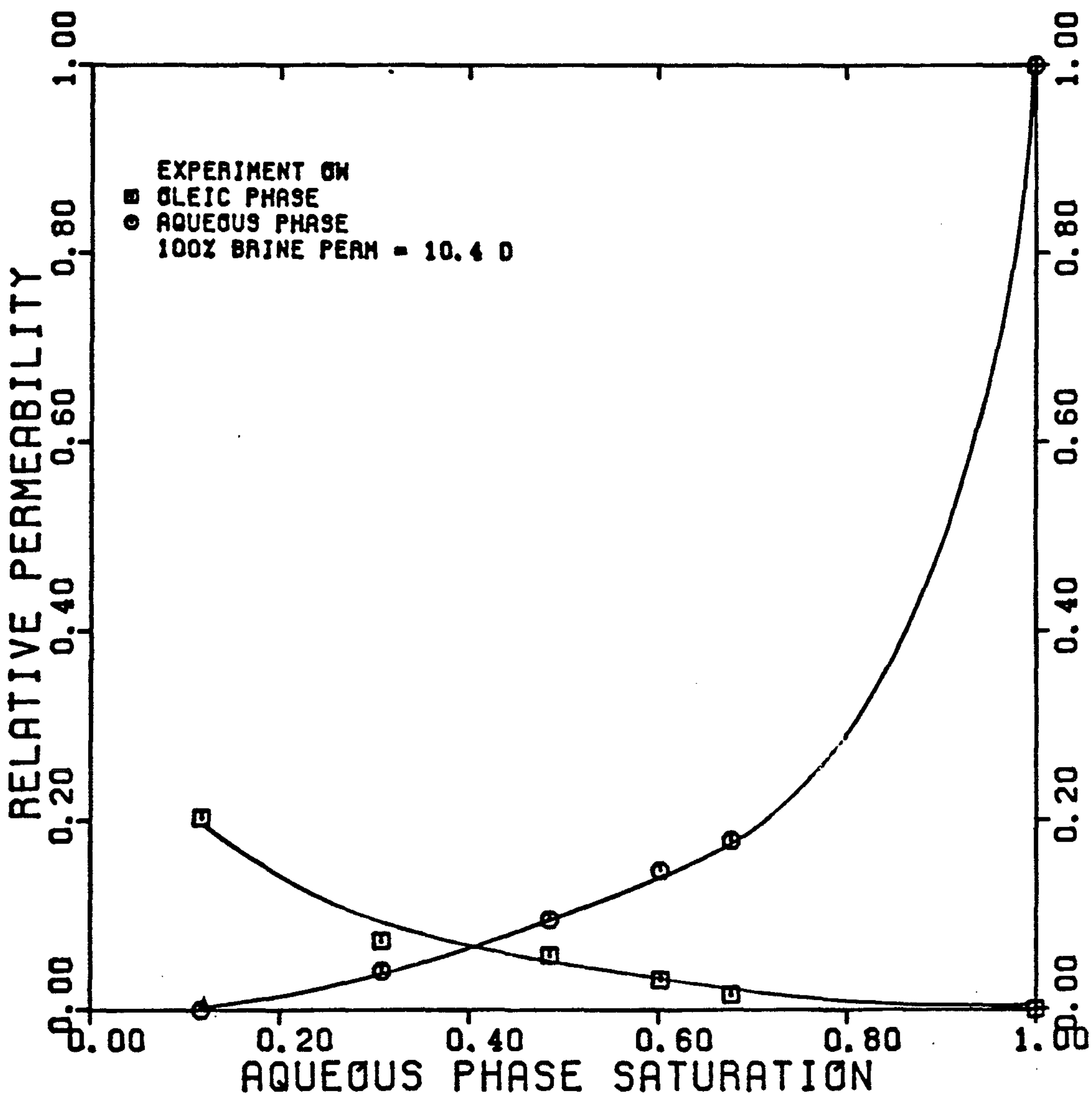

FIGURE 5.7

TOTAL RELATIVE MOBILITY OF BRINE AND
ISO-OCTANE IN UNCONSOLIDATED SAND
(EXPERIMENT OW)

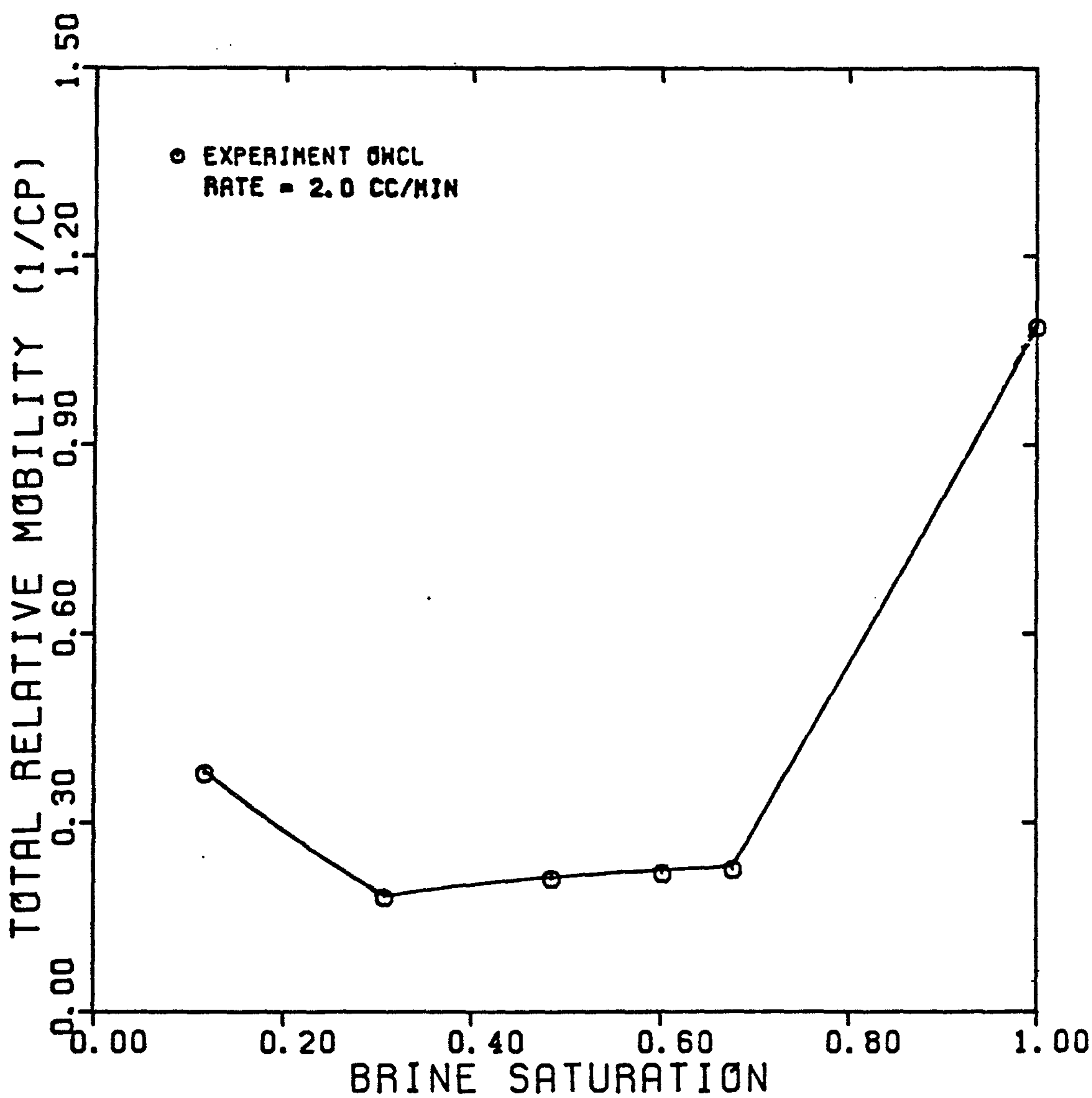

FIGURE 5.8

FRACTIONAL FLOW FOR THE AQUEOUS PHASE IN UNCONSOLIDATED SAND (EXPERIMENT OW)

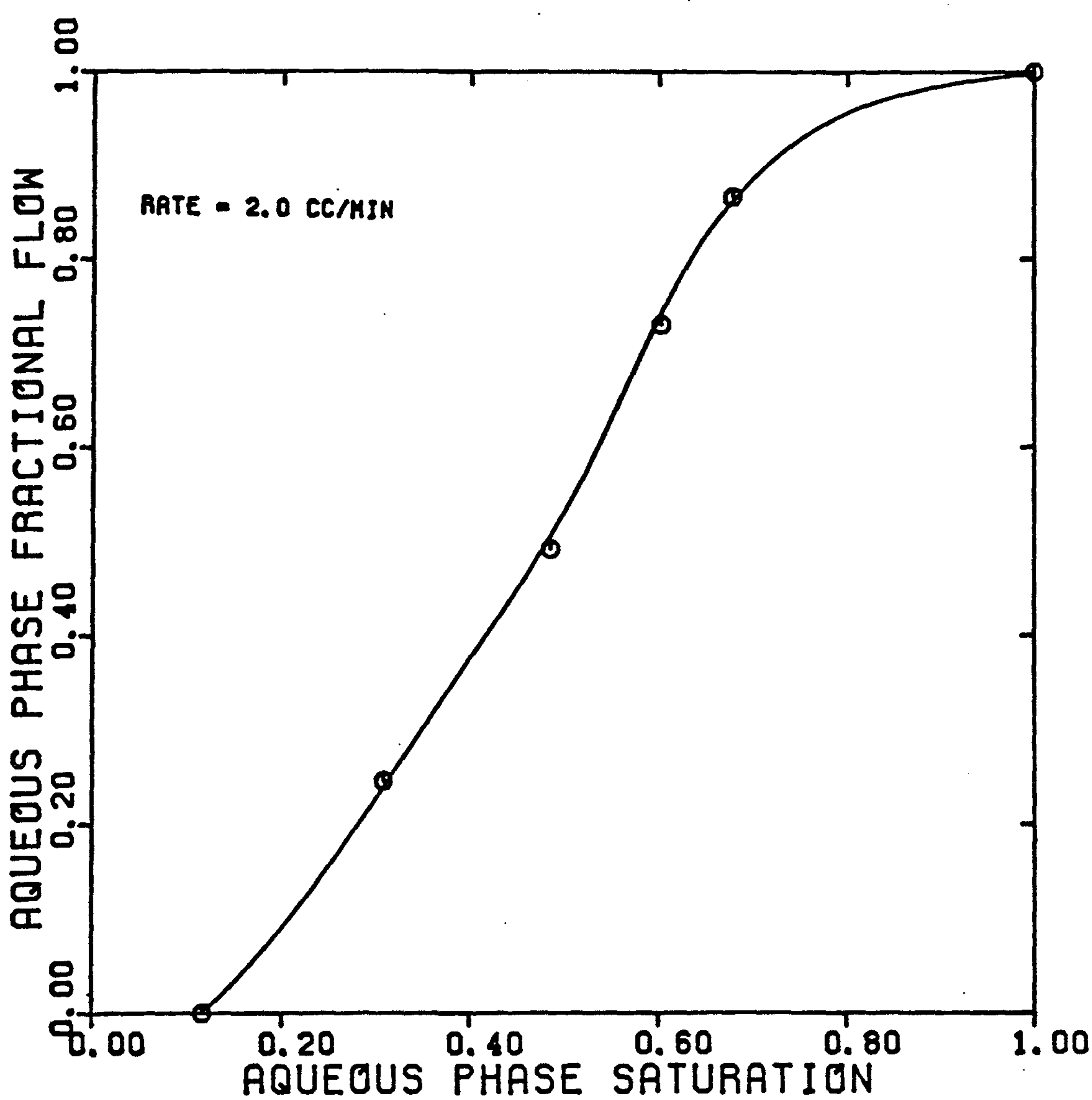

FIGURE 5.9

SANDPACK BREAKTHROUGH CURVE FOR TRITIUM
TRACER IN THE AQUEOUS PHASE
(EXPERIMENT OW1)

$S_w = 1.0 \quad f_w = 1.0$

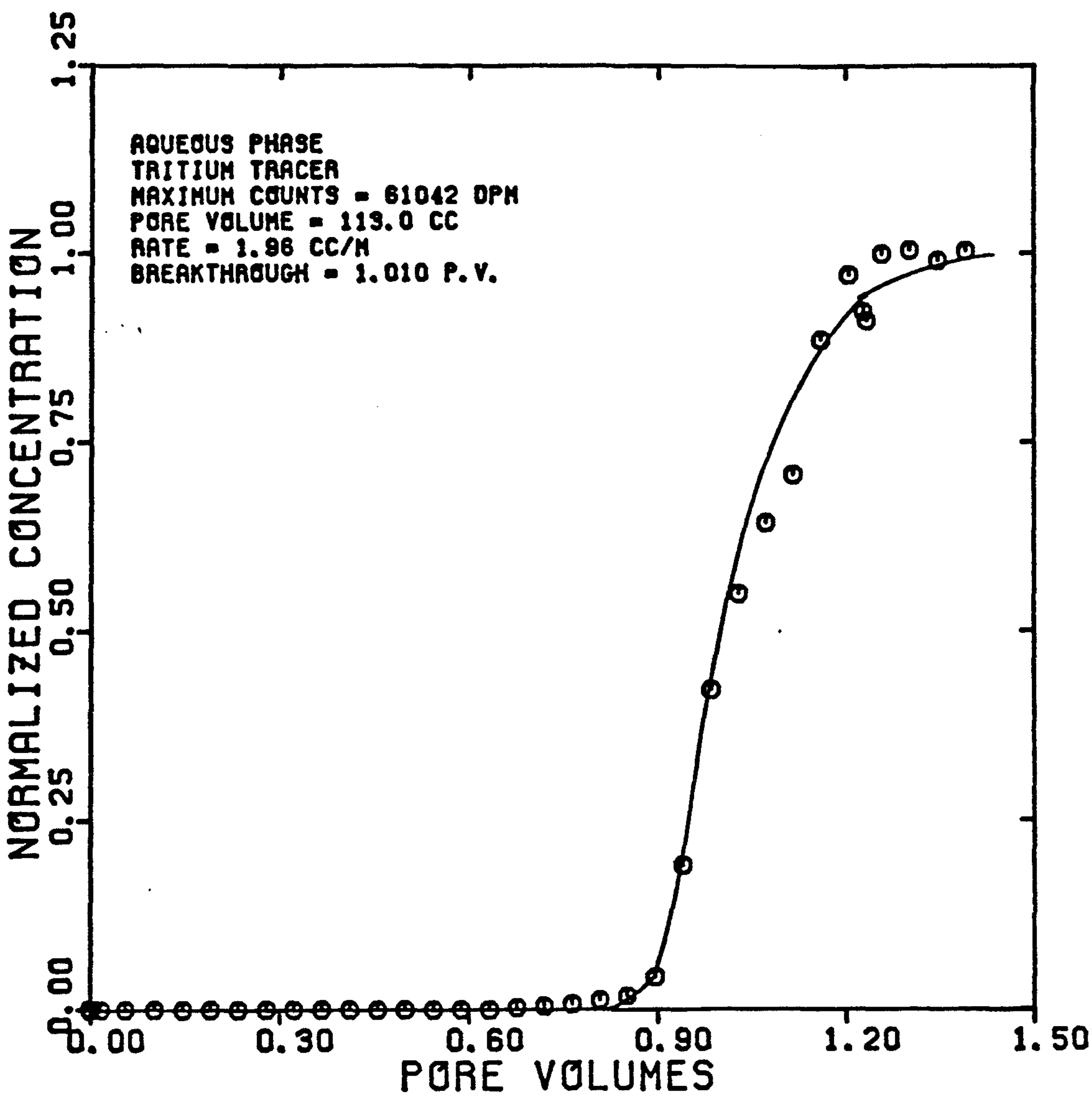

FIGURE 5.10

DISPERSIVITY OF TRITIUM
TRACER IN THE AQUEOUS PHASE
(EXPERIMENT OW1)

$S_w = 1.0 \quad f_w = 1.0$

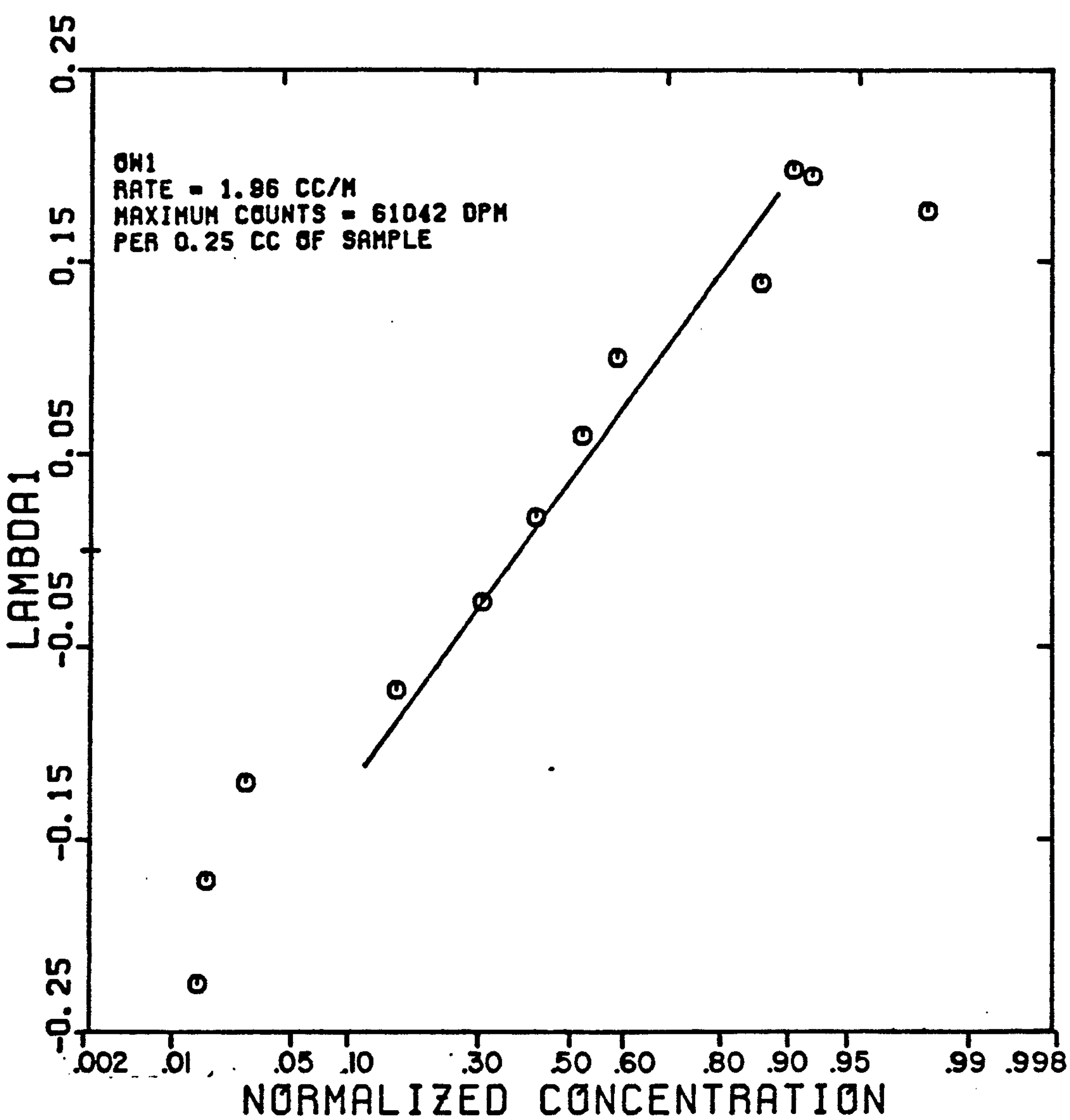

FIGURE 5.11

SANDPACK BREAKTHROUGH CURVE FOR TRITIUM TRACER IN THE AQUEOUS PHASE (EXPERIMENT OW2)

$S_w = 0.677 \quad f_w = 0.837$

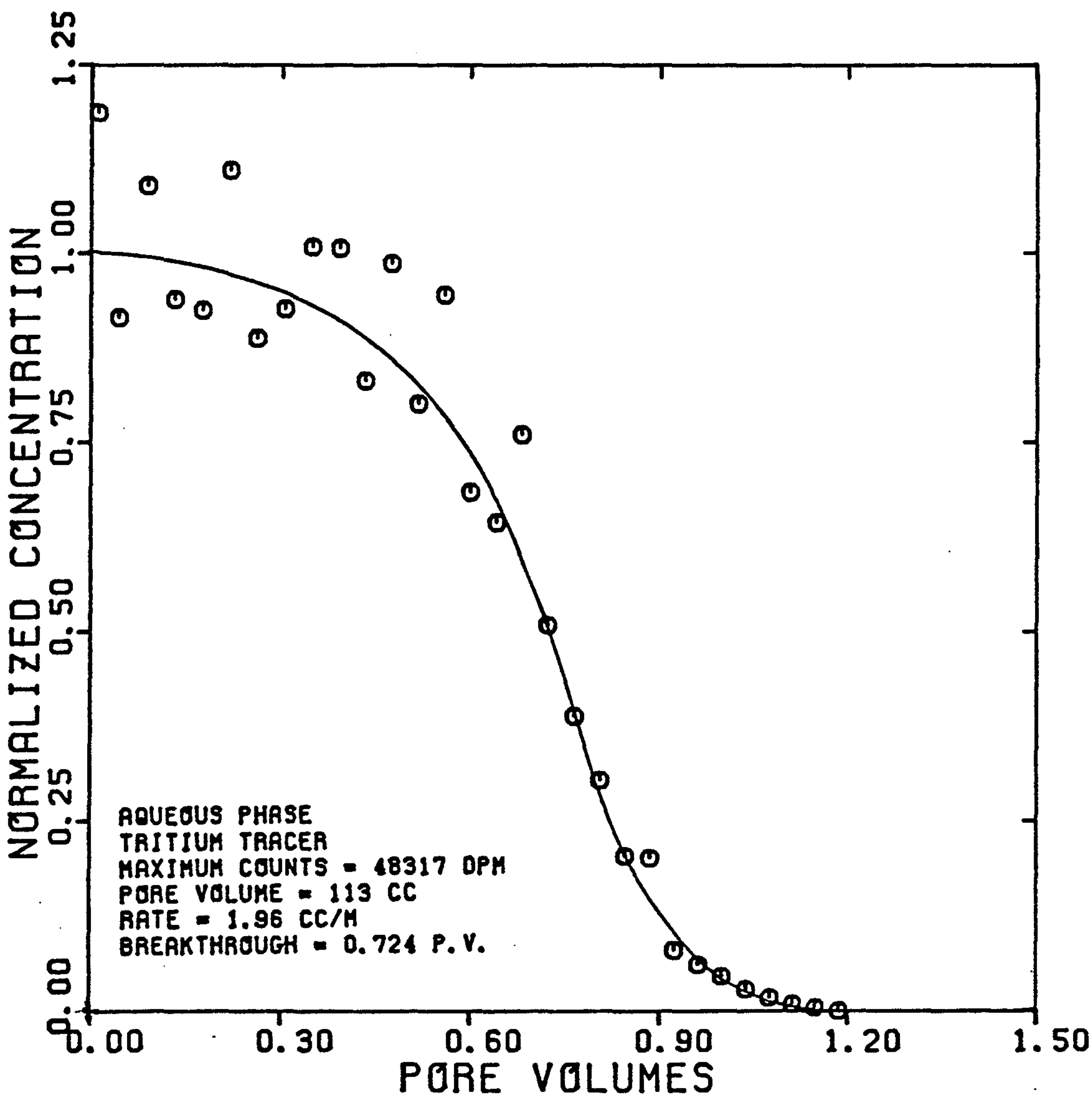

FIGURE 5.12

DISPERSIVITY OF TRITIUM
TRACER IN THE AQUEOUS PHASE
(EXPERIMENT OW2)

$S_w = 0.677 \quad f_w = 0.837$

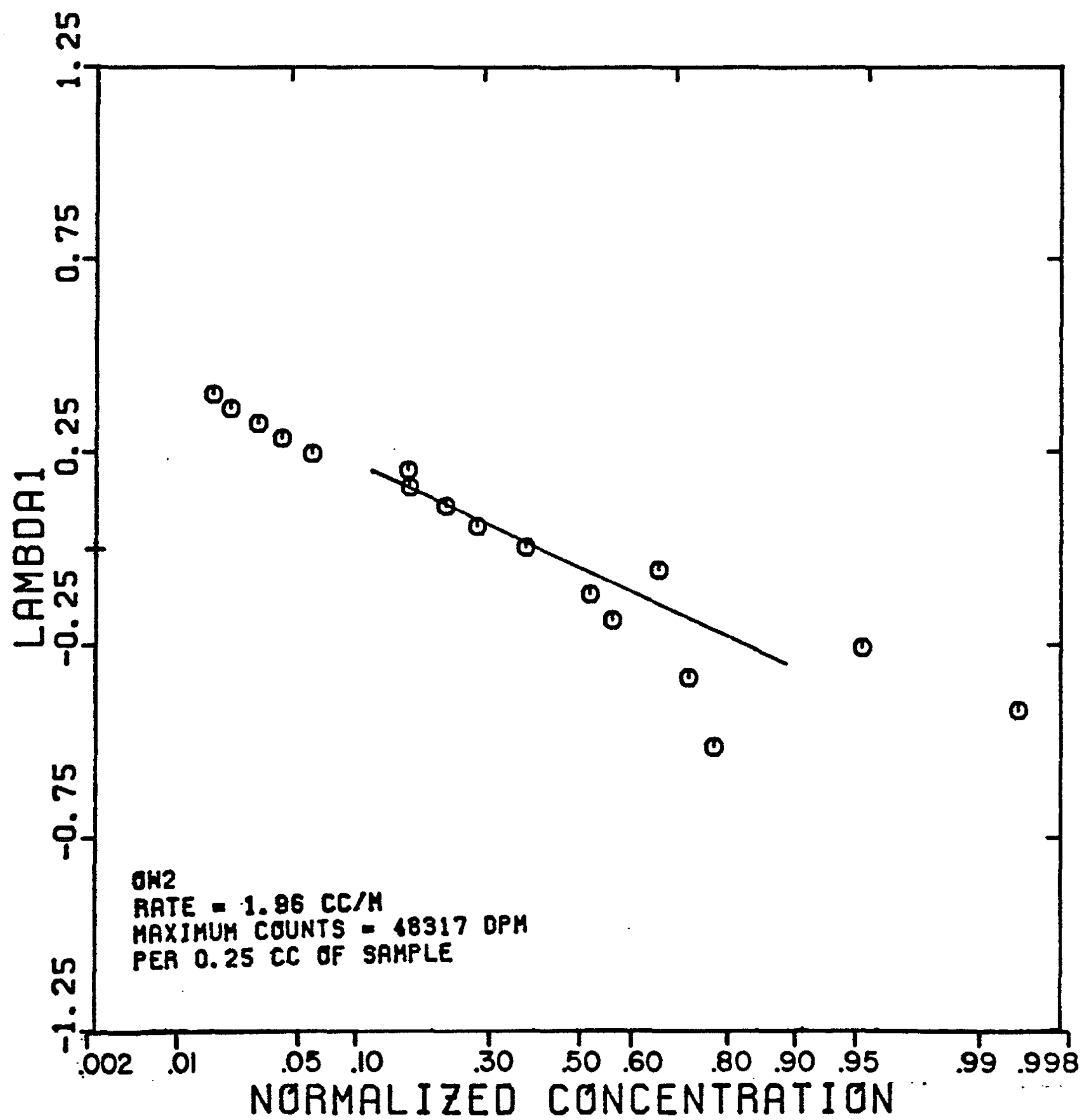

FIGURE 5.13
SANDPACK BREAKTHROUGH CURVE FOR TRITIUM
TRACER IN THE AQUEOUS PHASE
(EXPERIMENT OW4)

$S_w = 0.485 \quad f_w = 0.497$

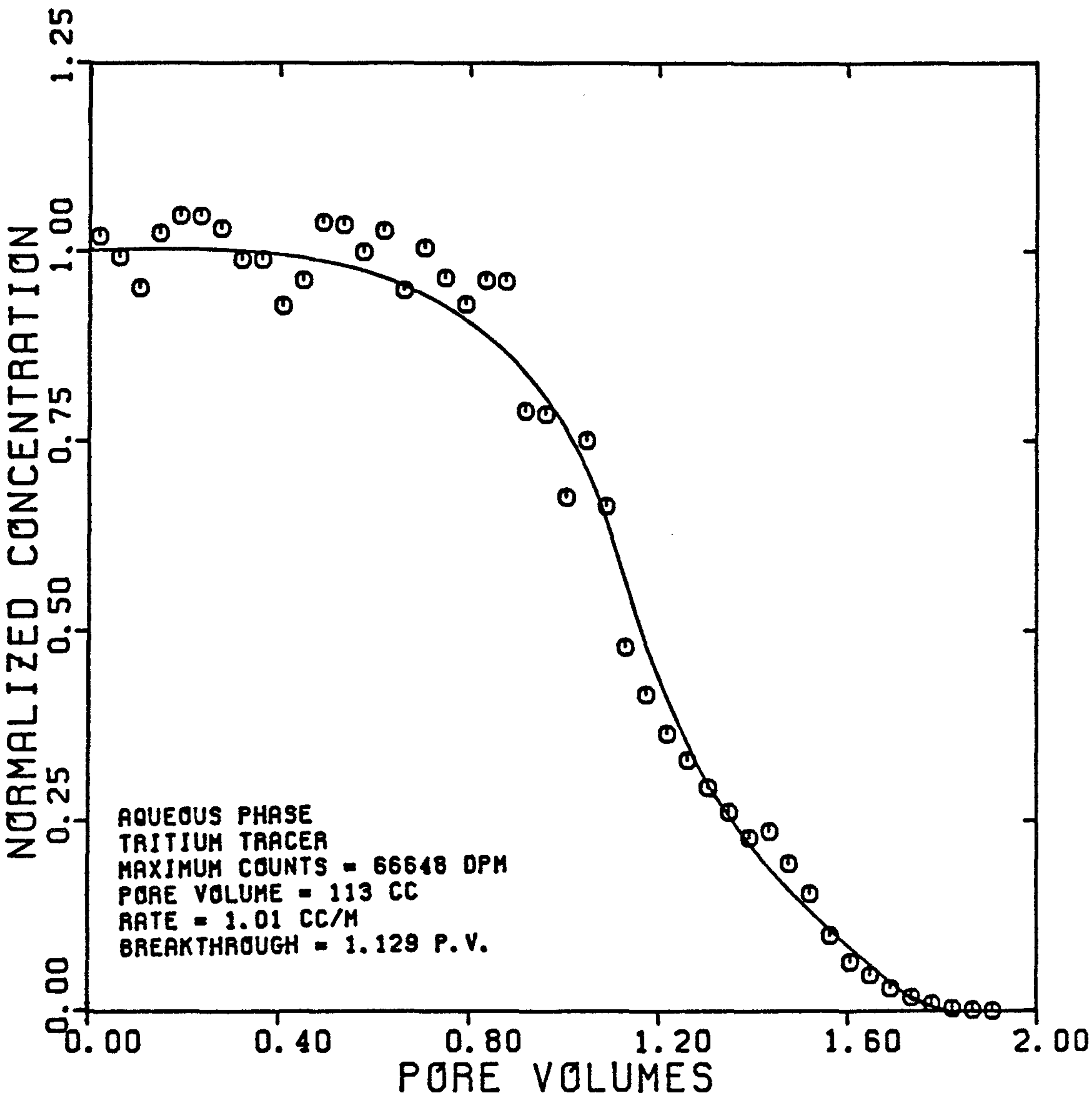

FIGURE 5.14

DISPERSIVITY OF TRITIUM
TRACER IN THE AQUEOUS PHASE
(EXPERIMENT OW4)

$S_w = 0.485 \quad f_w = 0.497$

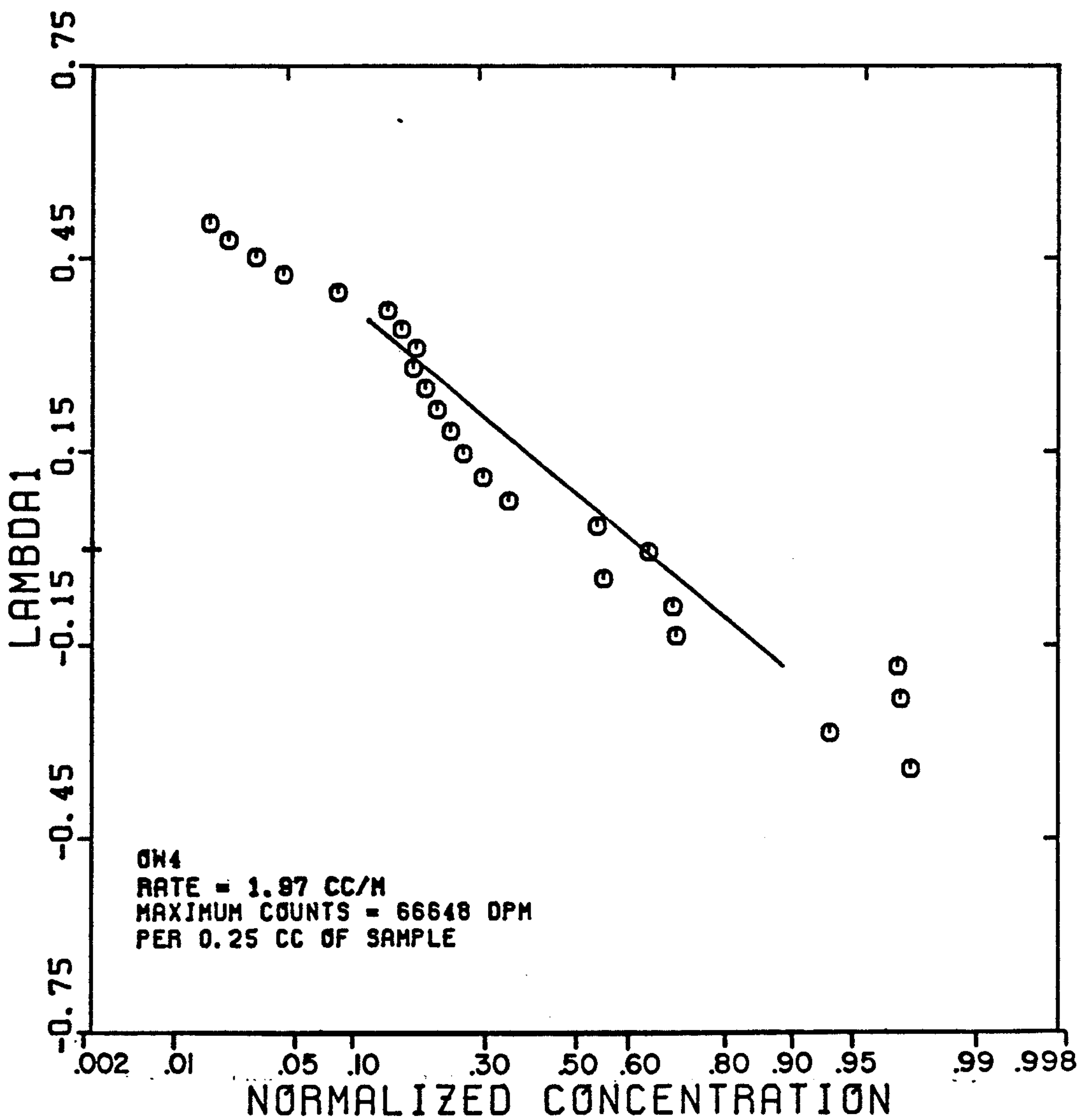

FIGURE 5.15

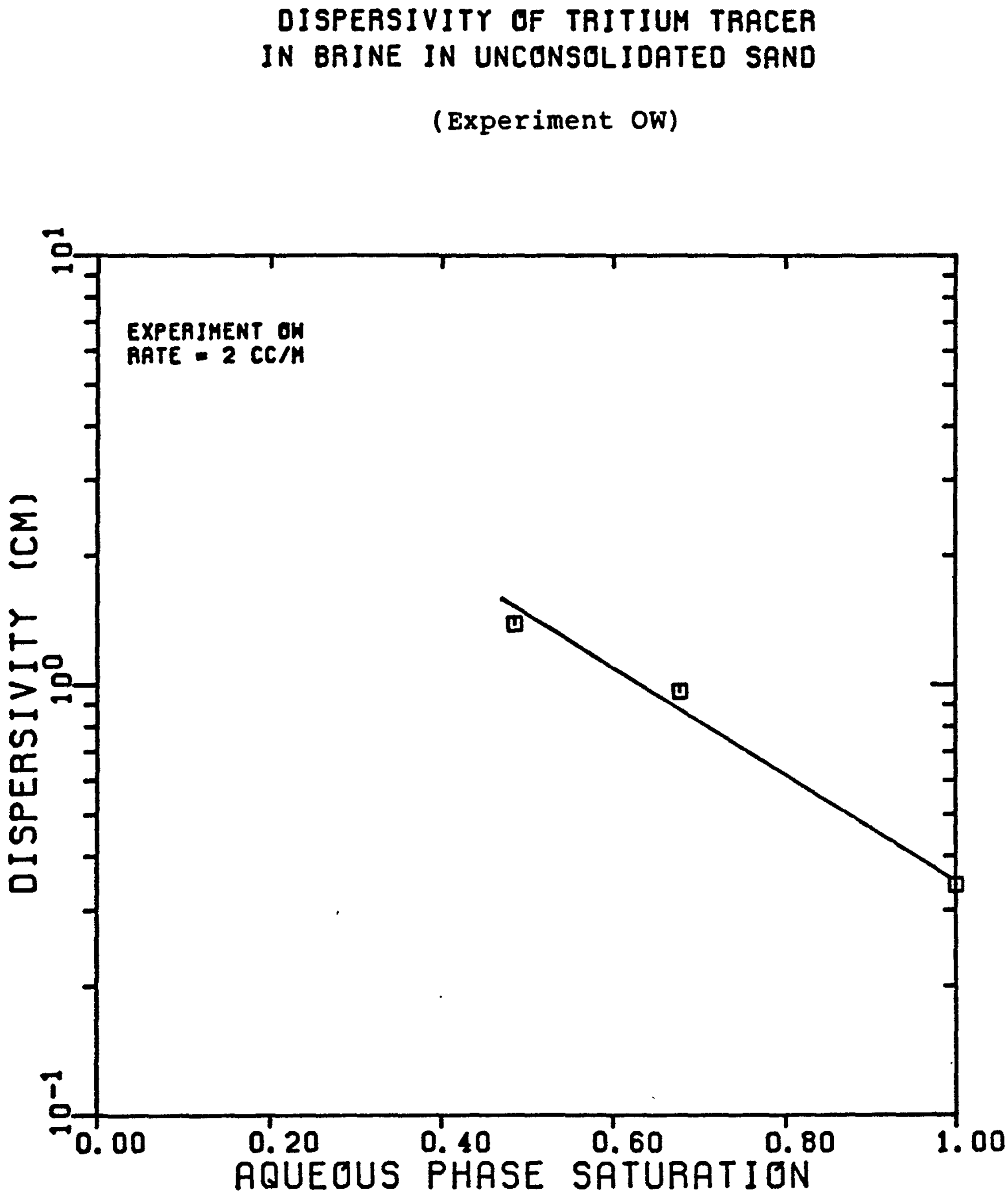

(Experiment OW)

FIGURE 5.16

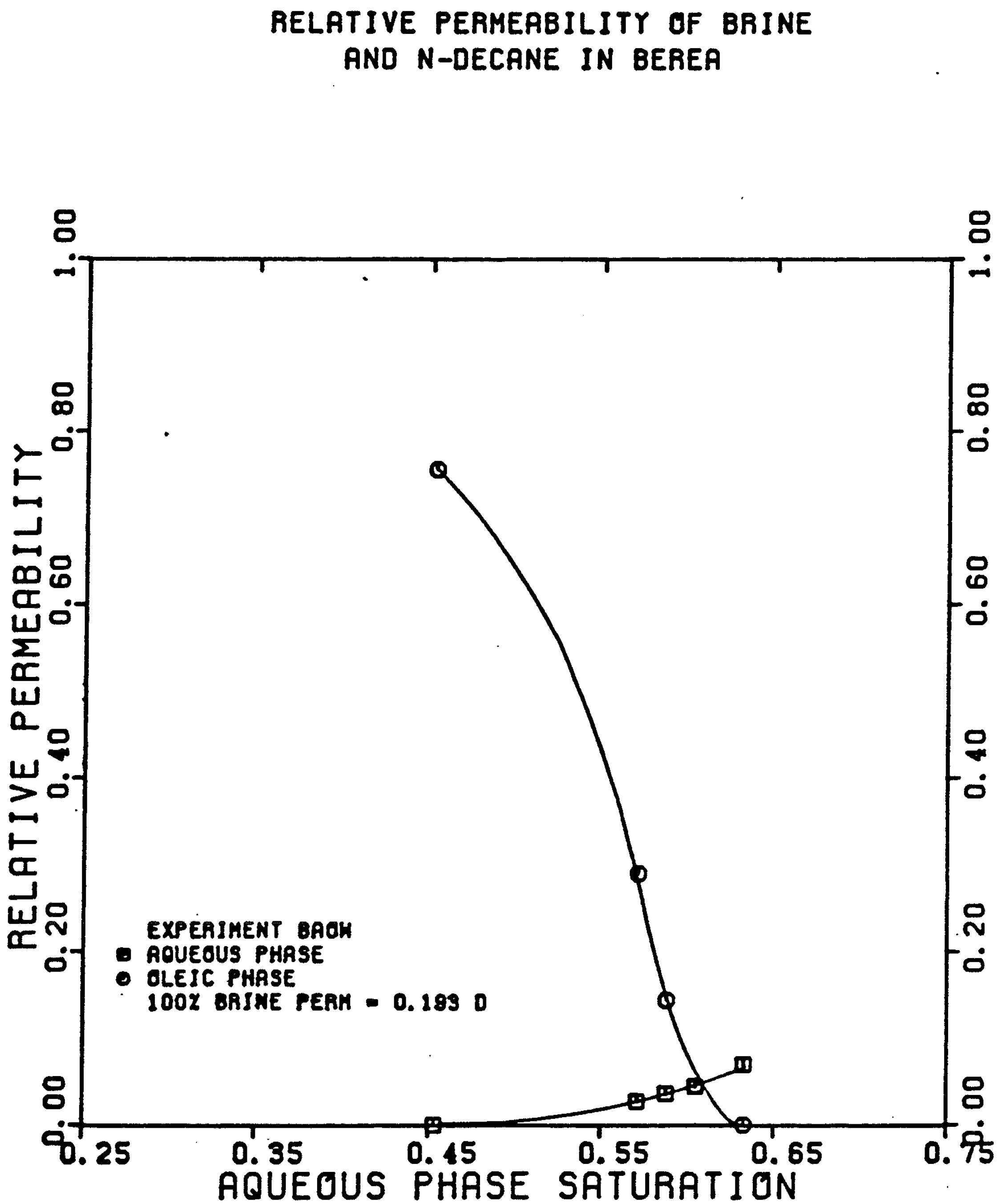
RELATIVE PERMEABILITY OF BRINE
AND N-DECANE IN BEREA
RELATIVE PERMEABILITY
AQUEOUS PHASE SATURATION
EXPERIMENT BAOW
AQUEOUS PHASE
OLEIC PHASE
100% BRINE PERM = 0.193 D
0.00
0.20
0.40
0.60
0.80
1.00
0.25
0.35
0.45
0.55
0.65
0.75

FIGURE 5.17

RELATIVE PERMEABILITY OF BRINE
AND N-DECANE IN BEREA
(EXPERIMENTS BAOW AND I-B/D)

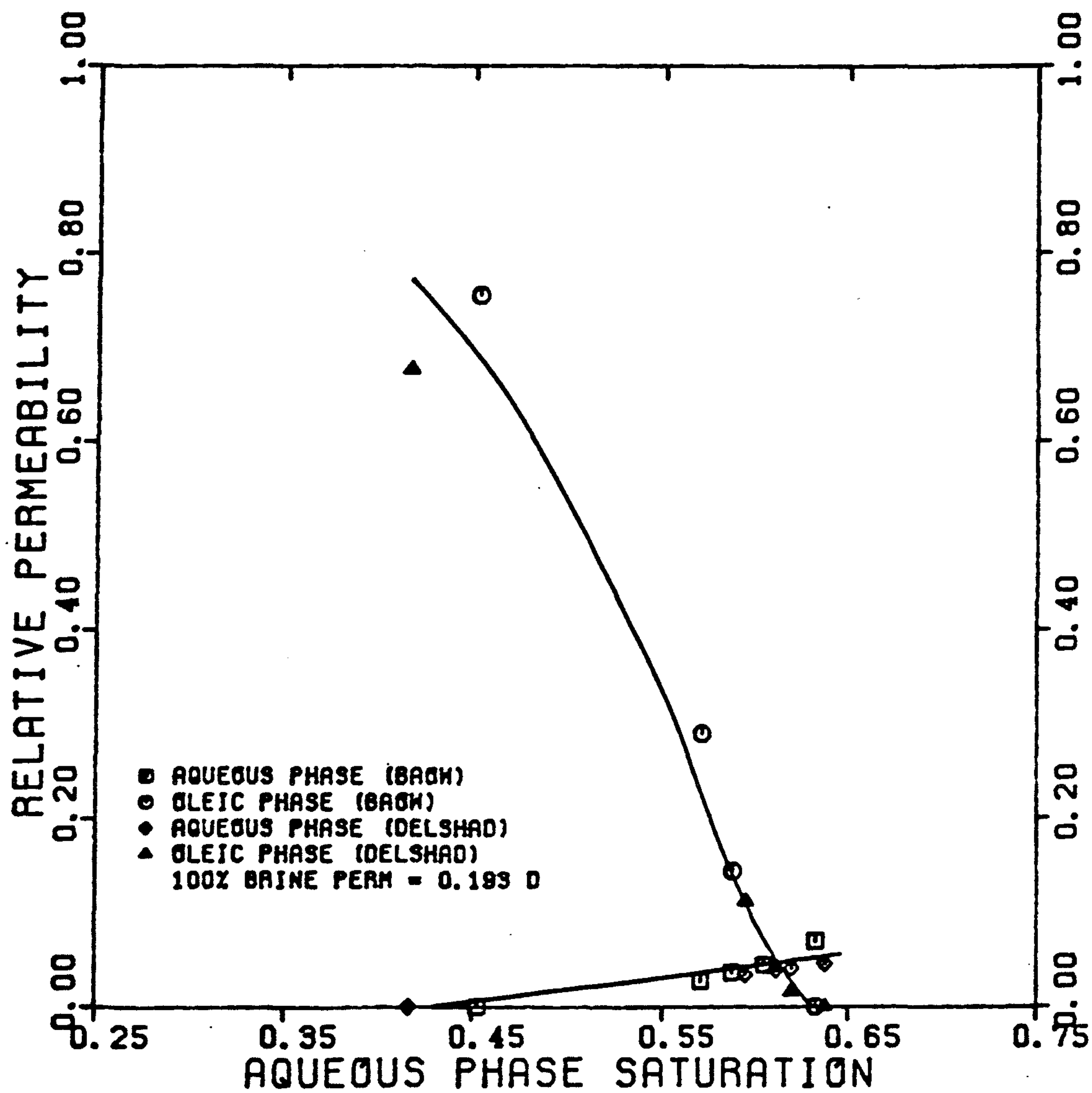

FIGURE 5.18

TOTAL RELATIVE MOBILITY OF BRINE AND
N-DECANE IN BEREA SANDSTONE
(EXPERIMENT BAOW)

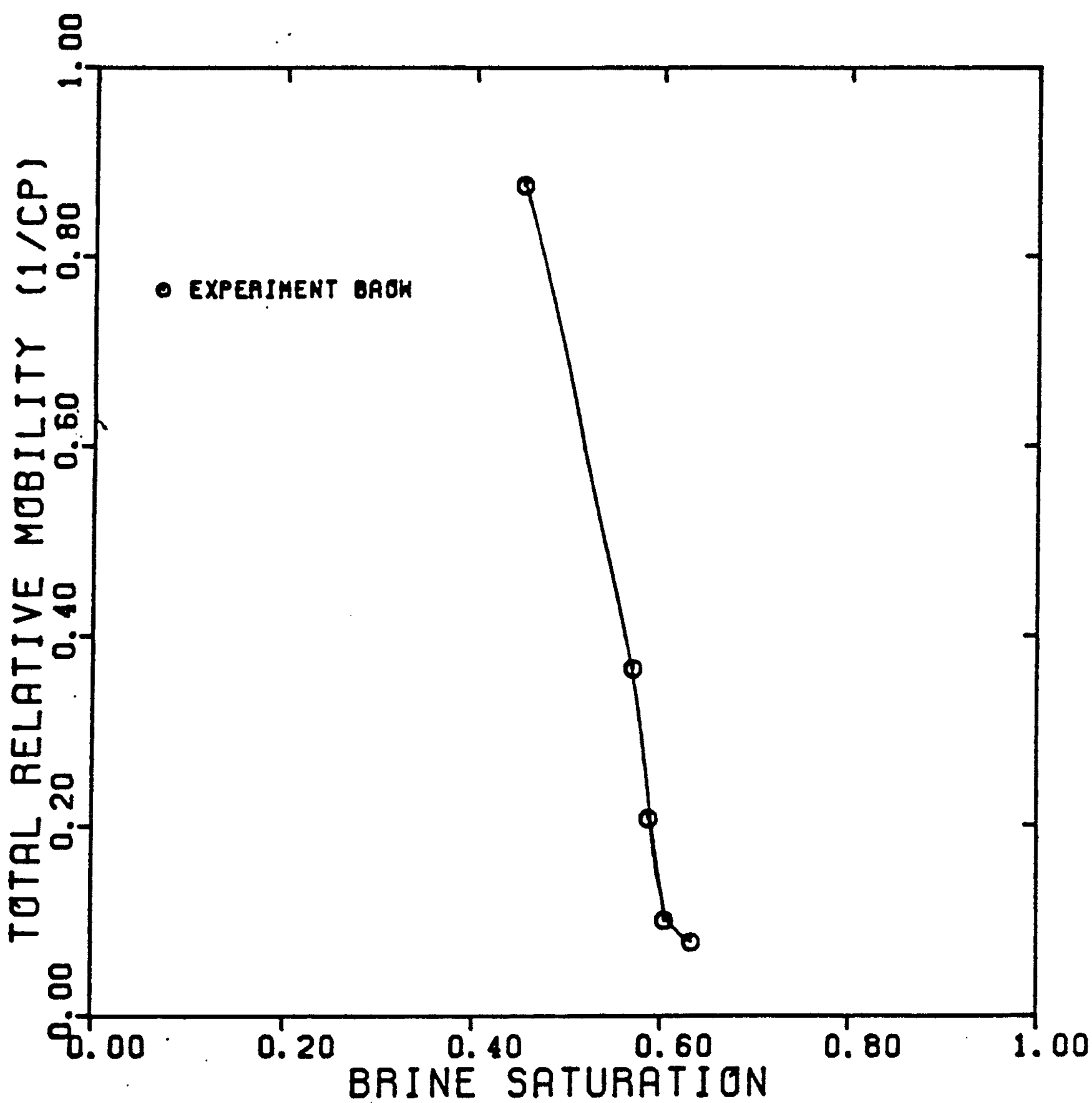

FIGURE 5.19

FRACTIONAL FLOW FOR N-DECANE
AND BRINE IN BEREA SANDSTONE

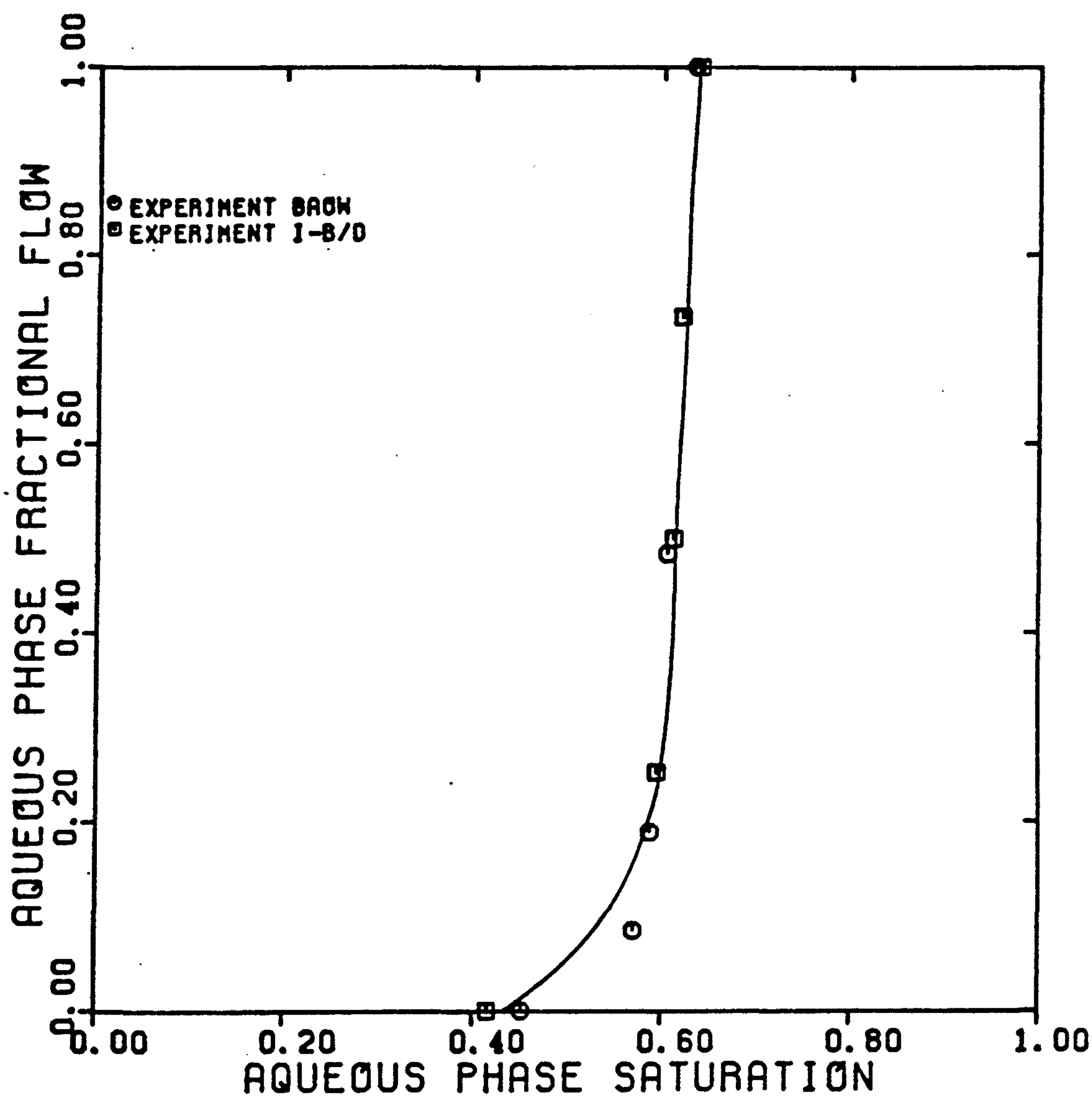

FIGURE 5.20

CALCIUM ION CONCENTRATION
IN STEADY-STATE BRINE
EFFLUENT

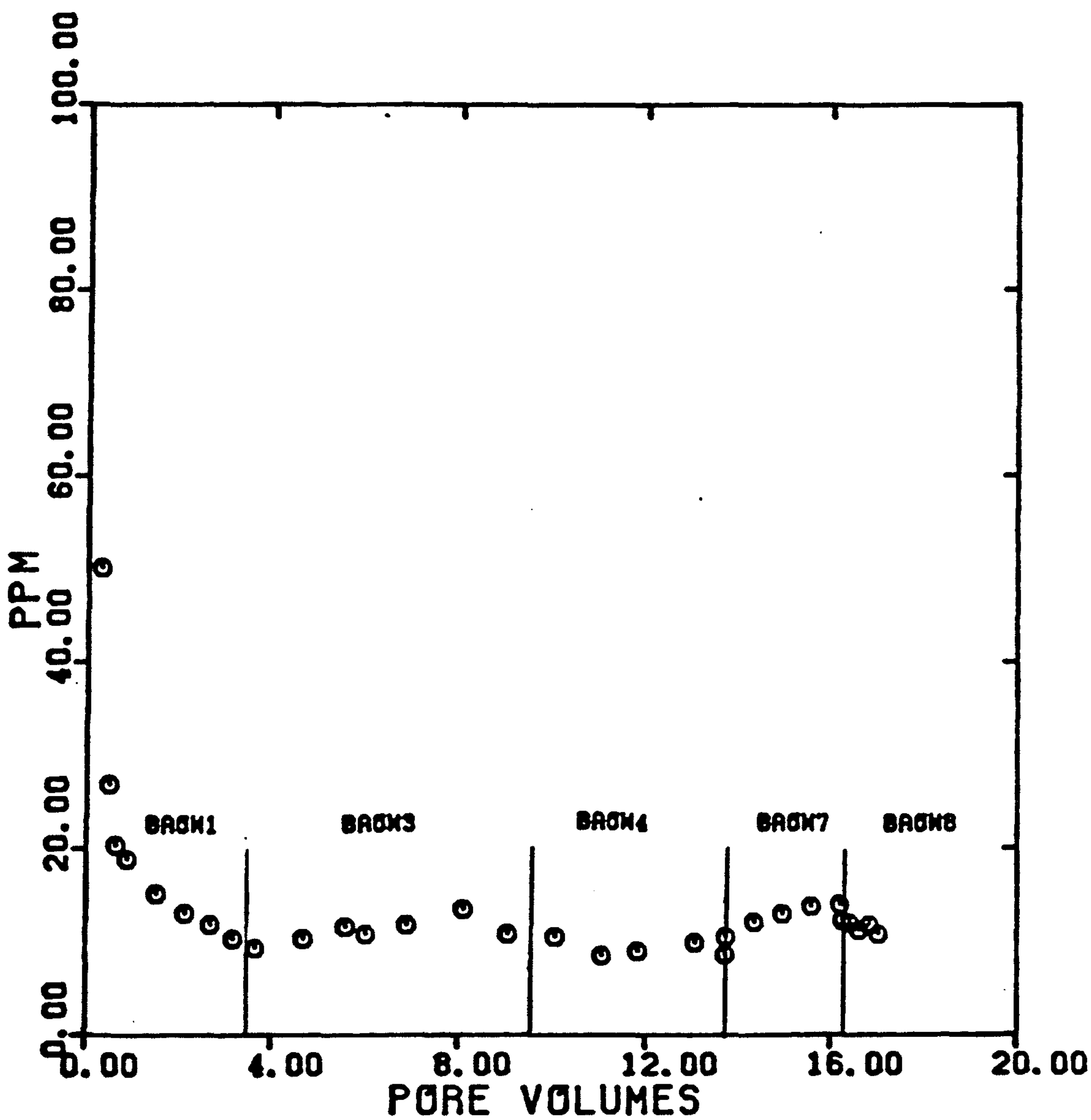

FIGURE 5.21

BEREA BREAKTHROUGH CURVE FOR TRITIUM TRACER IN THE AQUEOUS PHASE (EXPERIMENT BAOW1)

$S_w = 1.0 \quad f_w = 1.0$

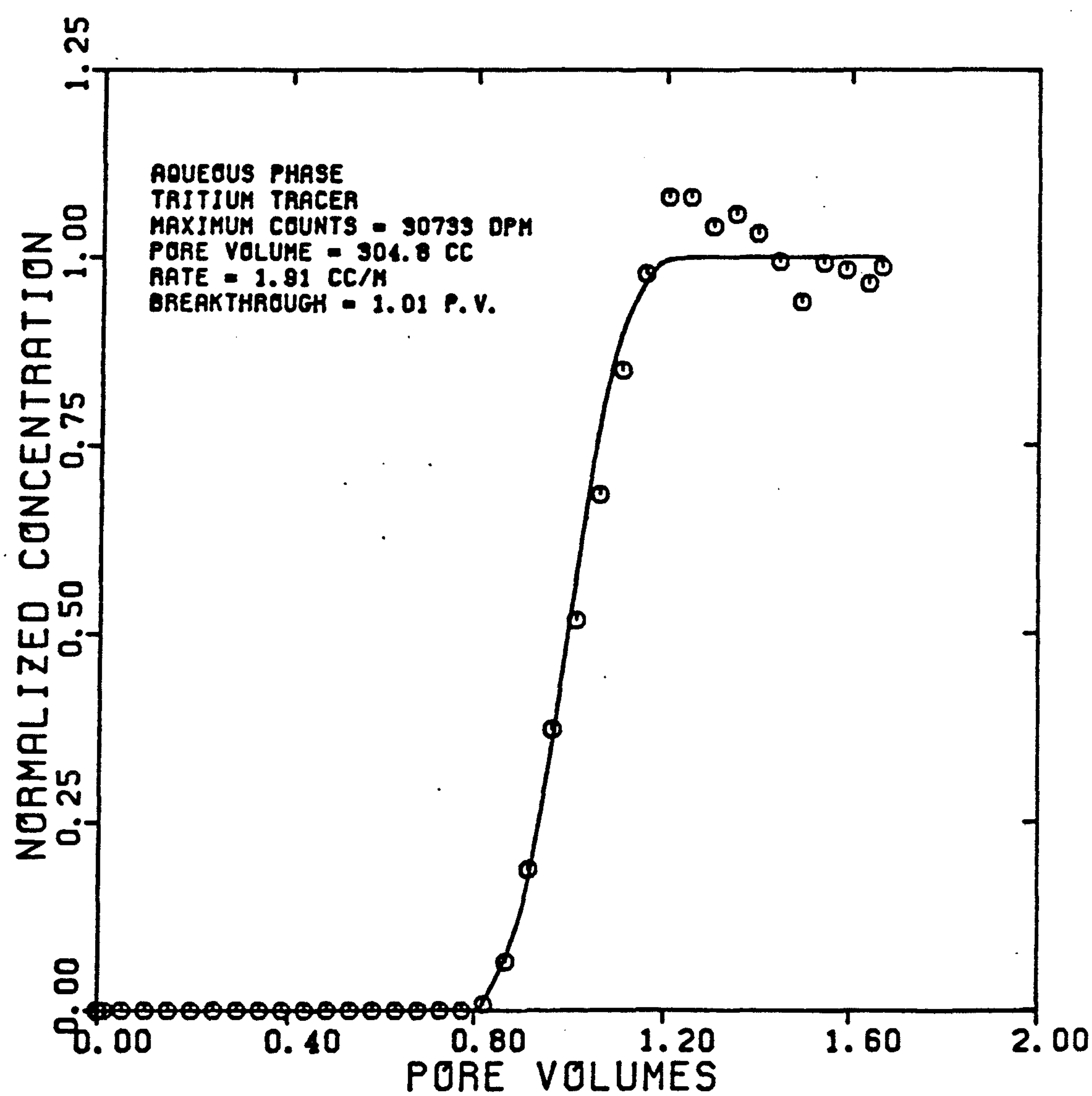

FIGURE 5.22

DISPERSIVITY OF TRITIUM
TRACER IN THE AQUEOUS PHASE
(EXPERIMENT BAOW1)

$S_w = 1.0 \quad f_w = 1.0$

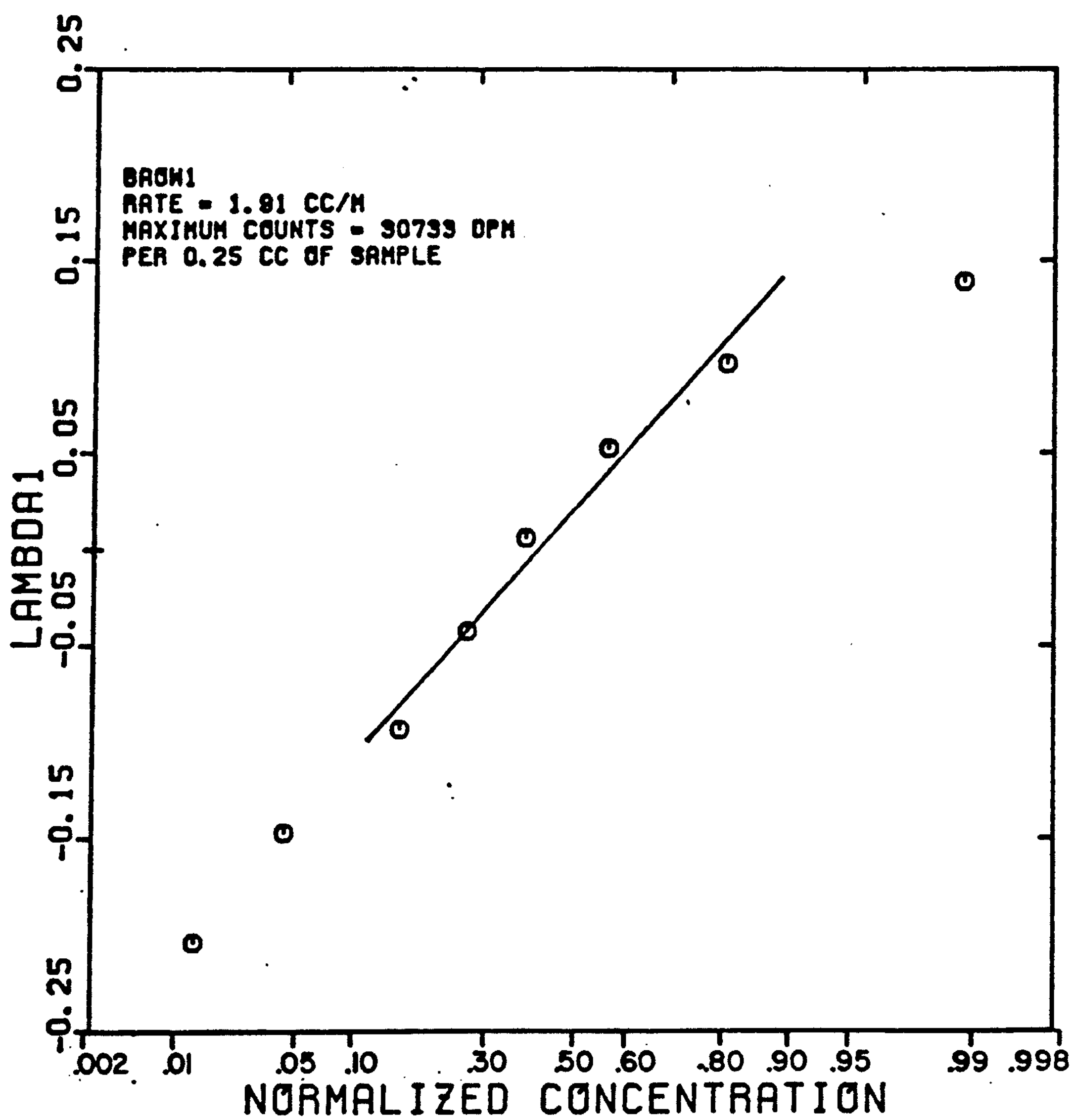

FIGURE 5.23

BEREA BREAKTHROUGH CURVE FOR N-NONANE
TRACER IN THE OLEIC PHASE
(EXPERIMENT BAOW2)

$S_o = 0.547 \quad f_o = 1.0$

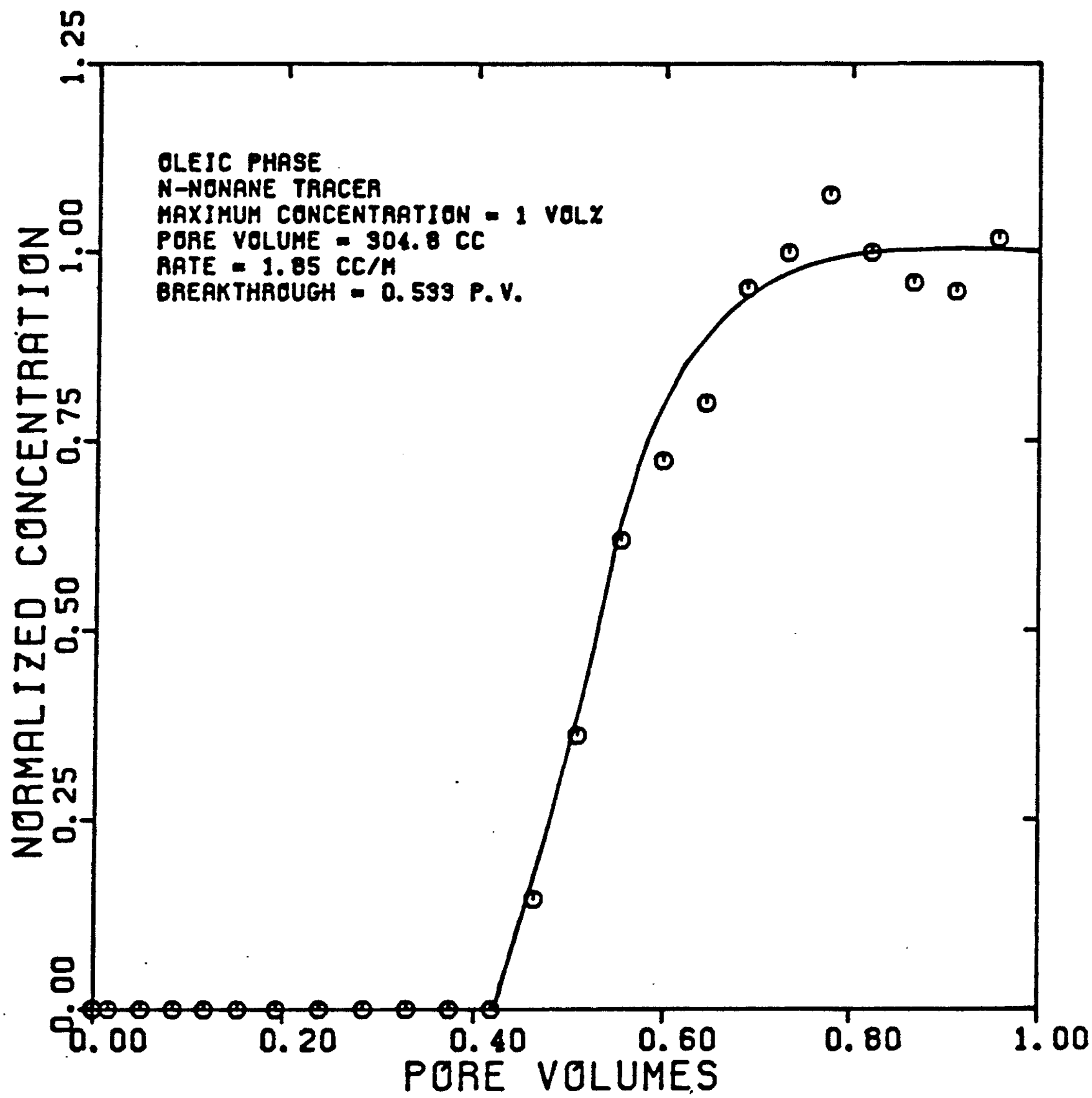

FIGURE 5.24

DISPERSIVITY OF N-NONANE
TRACER IN THE OLEIC PHASE
(EXPERIMENT BAOW2)

$S_o = 0.547 \quad f_o = 1.0$

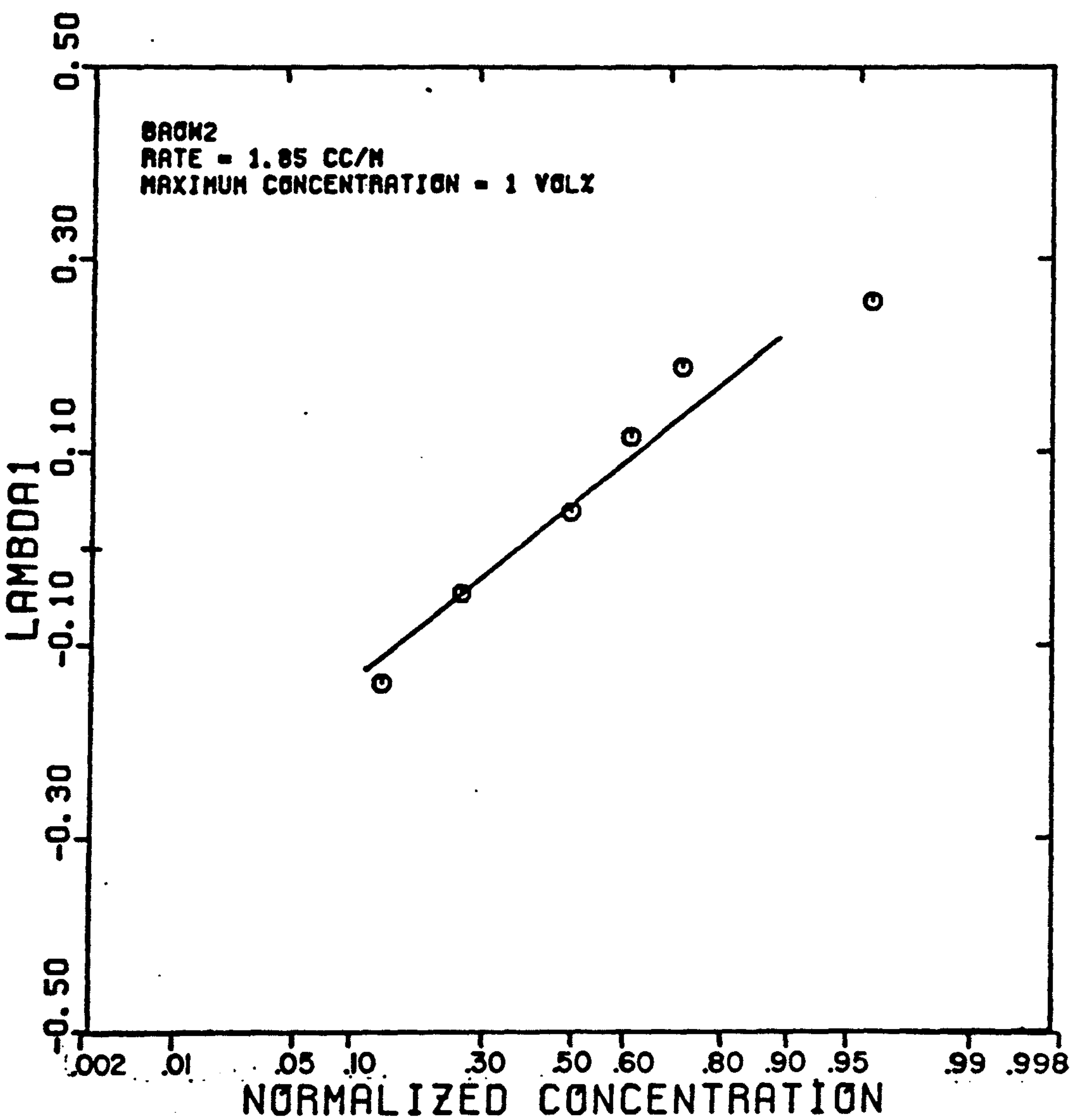

FIGURE 5.25

BEREA BREAKTHROUGH CURVE FOR TRITIUM
TRACER IN THE AQUEOUS PHASE
(EXPERIMENT BAOW3AQ)

$S_w = 0.571 \quad f_w = 0.0855$

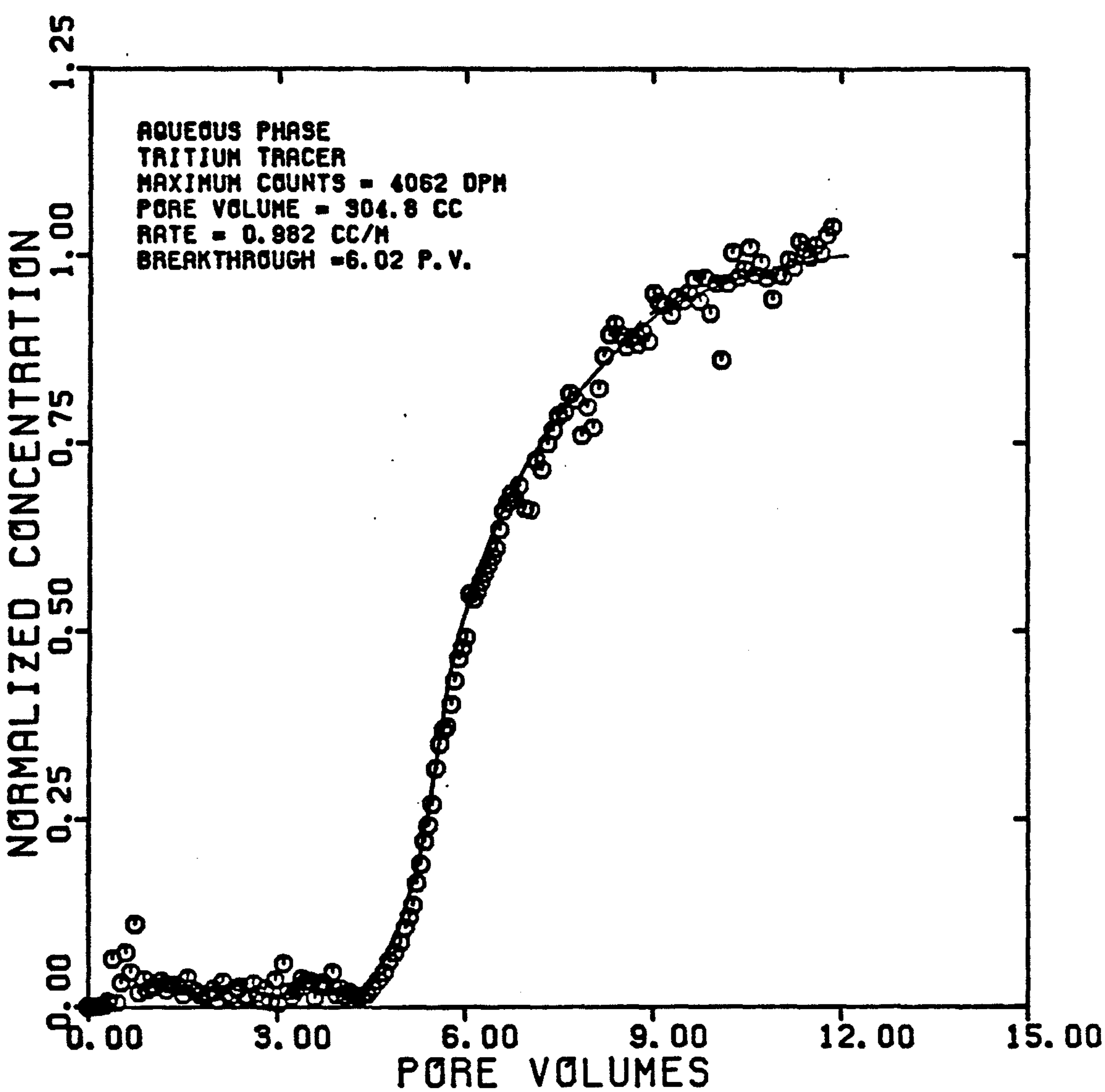

FIGURE 5.26

DISPERSIVITY OF TRITIUM TRACER IN THE AQUEOUS PHASE (EXPERIMENT BAOW3AQ)

$S_w = 0.571 \quad f_w = 0.0855$

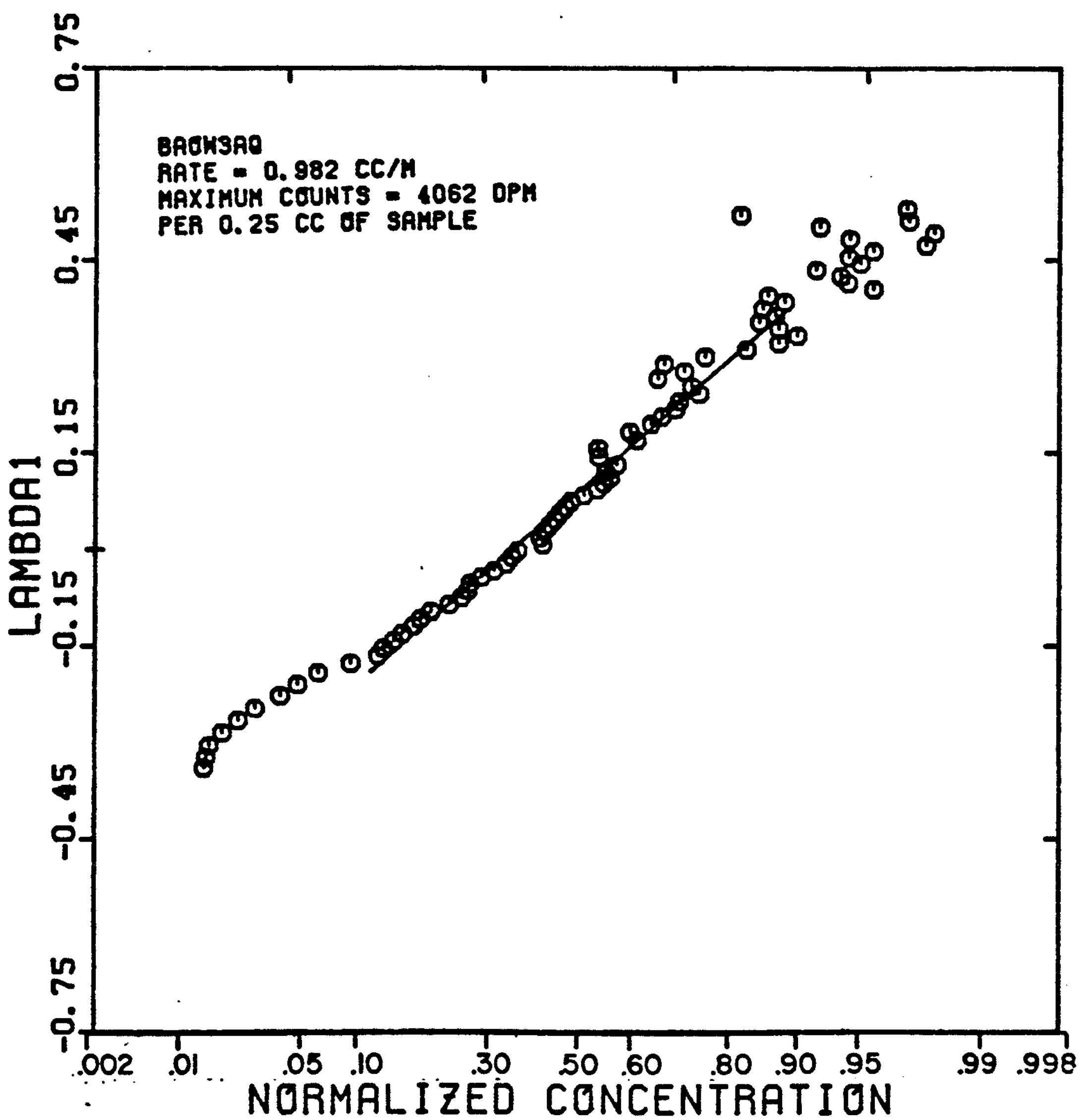

FIGURE 5.27

BEREA BREAKTHROUGH CURVE FOR CARBON 14
TRACER IN THE OLEIC PHASE
(EXPERIMENT BAOW3OL)

$S_o = 0.429 \quad f_o = 0.9145$

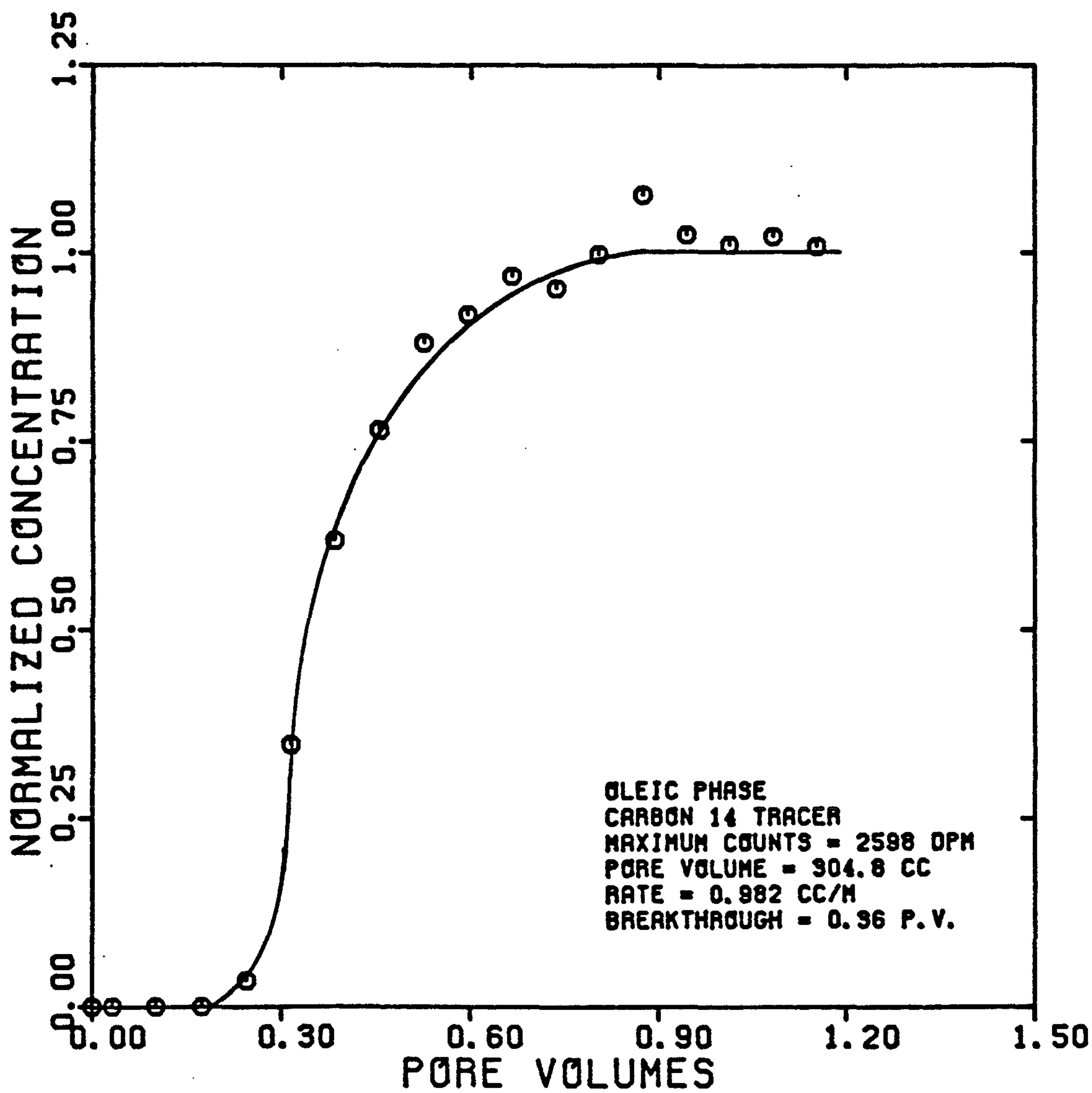

FIGURE 5.28

DISPERSIVITY OF CARBON 14
TRACER IN THE OLEIC PHASE
(EXPERIMENT BAOW30L)

$S_o = 0.429 \quad f_o = 0.9145$

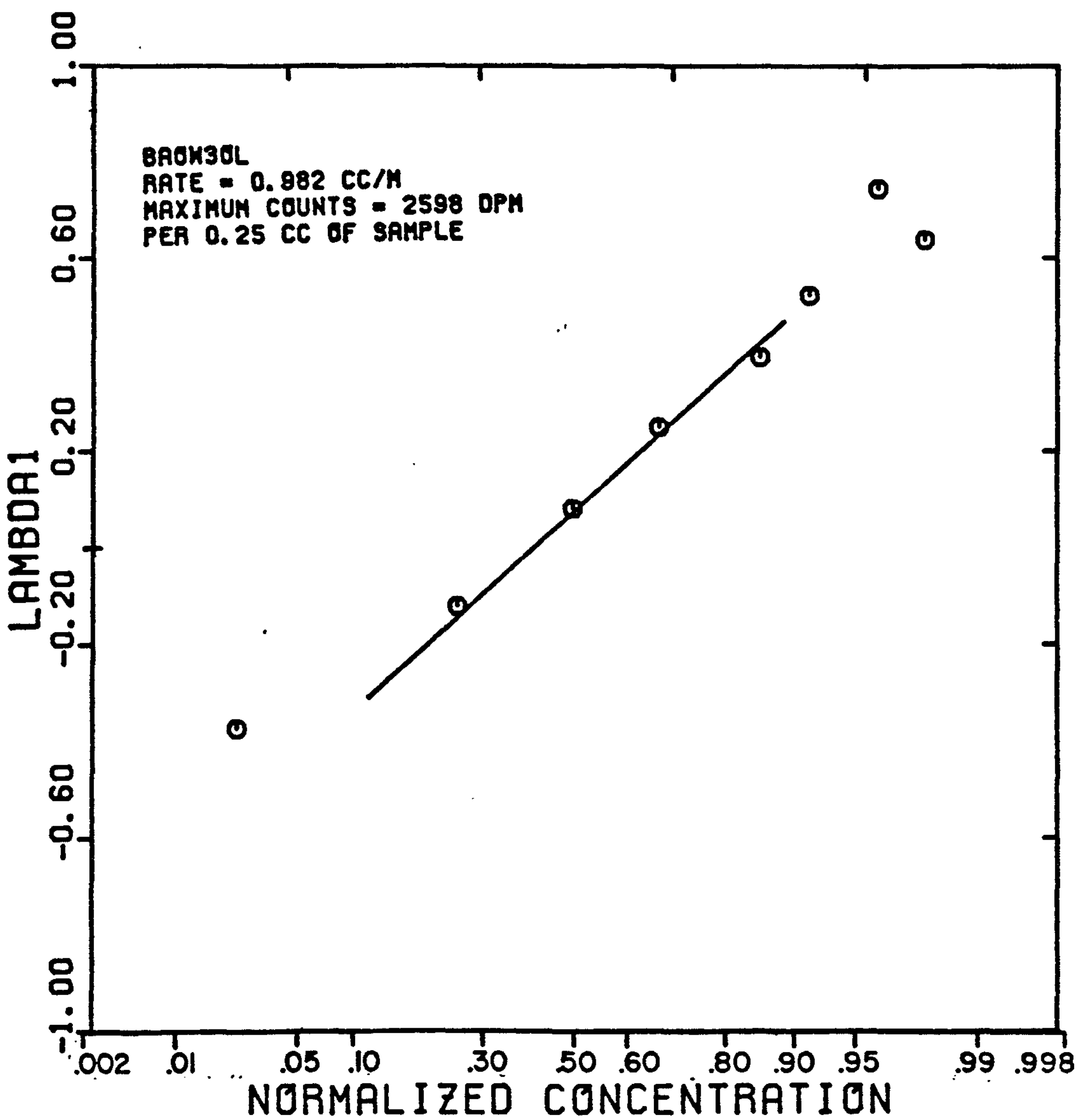

FIGURE 5.29

BEREA BREAKTHROUGH CURVE FOR TRITIUM TRACER IN THE AQUEOUS PHASE (EXPERIMENT BAOW4AQ)

$S_w = 0.588$ $f_w = 0.1895$

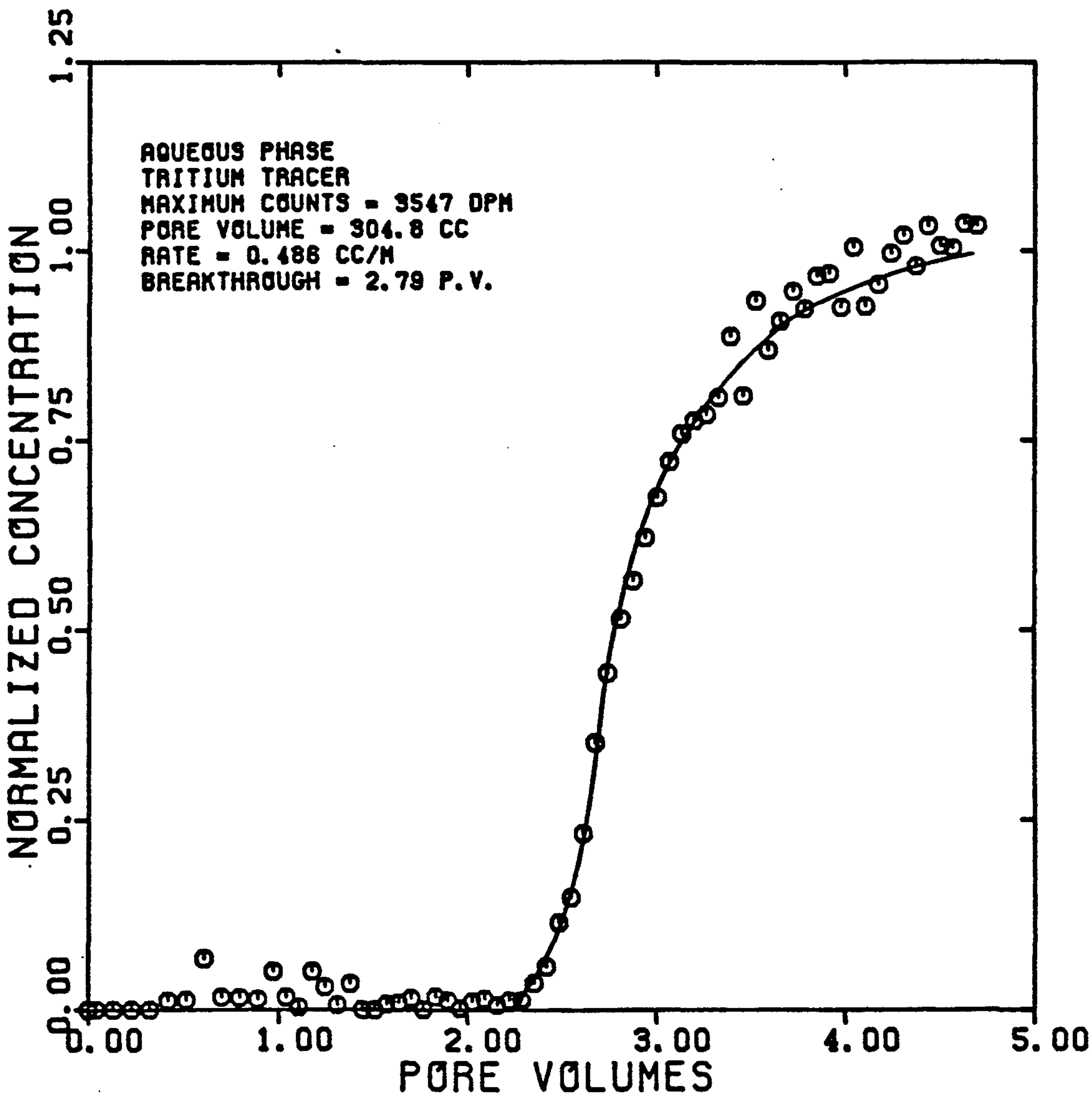

FIGURE 5.30

DISPERSIVITY OF TRITIUM
TRACER IN THE AQUEOUS PHASE
(EXPERIMENT BAOW4AQ)

$S_w = 0.588 \quad f_w = 0.1895$

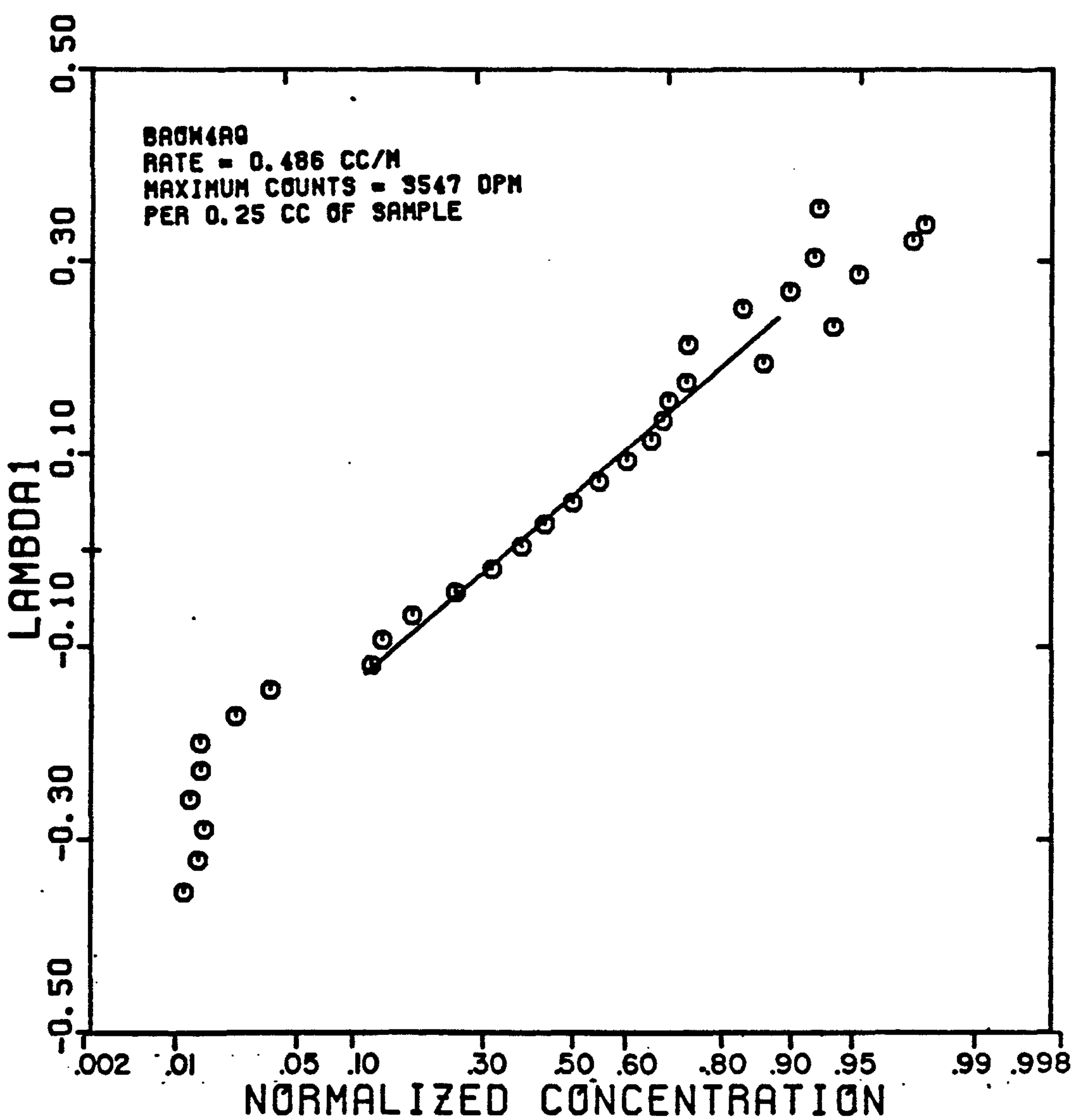

FIGURE 5.31

BEREA BREAKTHROUGH CURVE FOR CARBON 14
TRACER IN THE OLEIC PHASE
(EXPERIMENT BAOW4OL)

S_o = 0.412 f_o = 0.8105

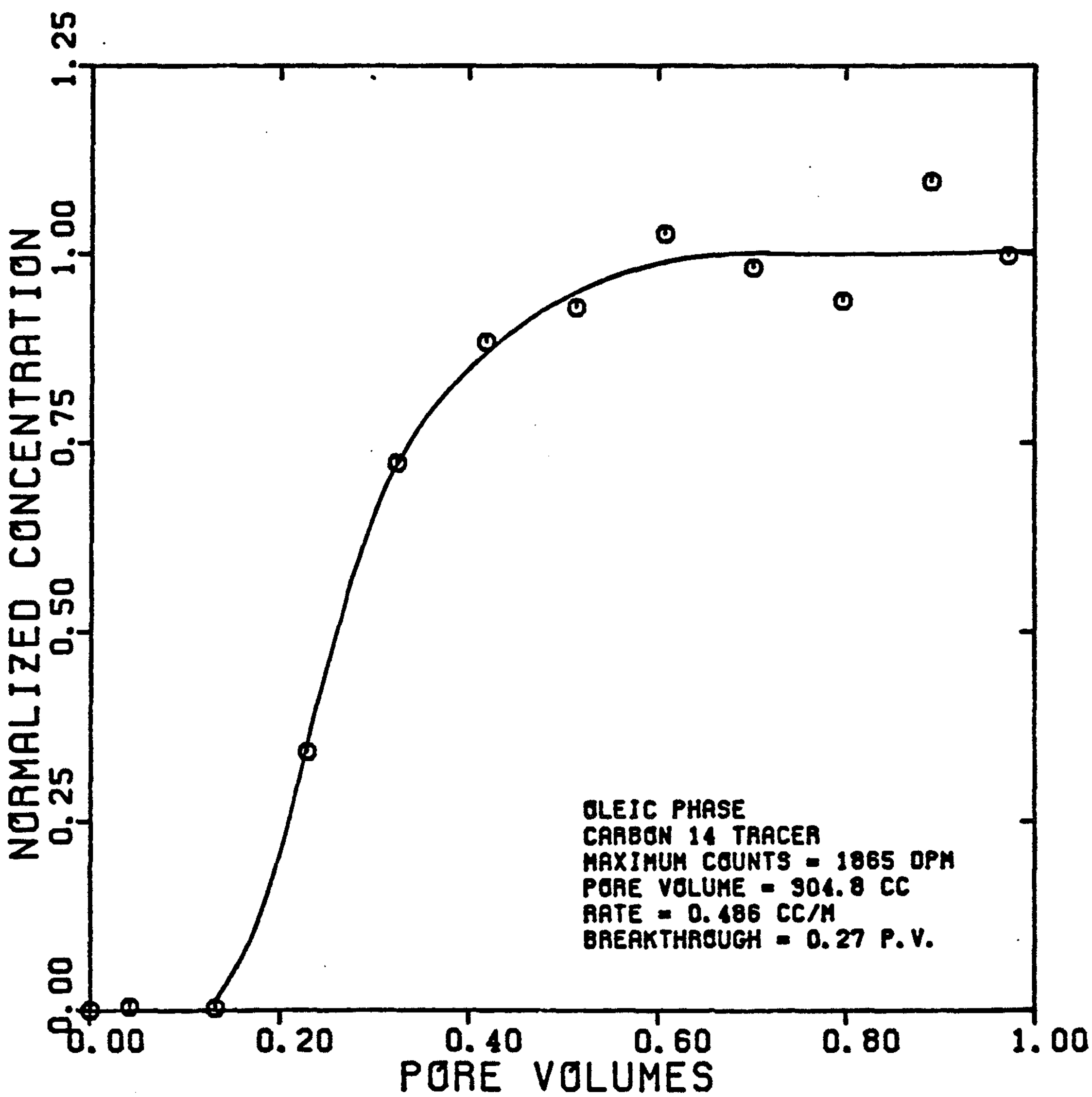

FIGURE 5.32

DISPERSIVITY OF CARBON 14
TRACER IN THE OLEIC PHASE
(EXPERIMENT BAOW4OL)

$S_o = 0.412 \quad f_o = 0.8105$

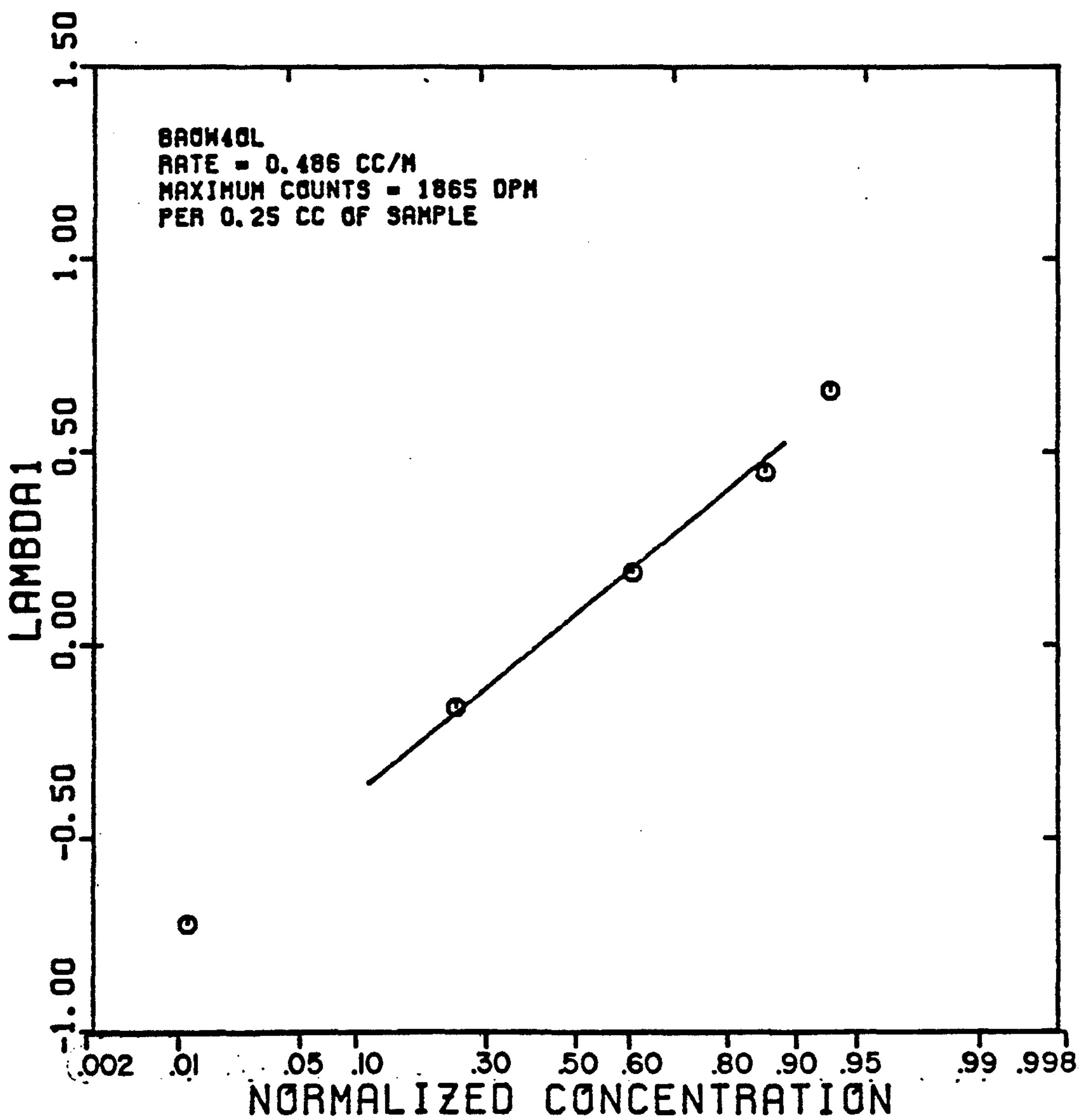

FIGURE 5.33

BEREA BREAKTHROUGH CURVE FOR TRITIUM TRACER IN THE AQUEOUS PHASE (EXPERIMENT BAOW7AQ)

$S_w = 0.605 \quad f_w = 0.484$

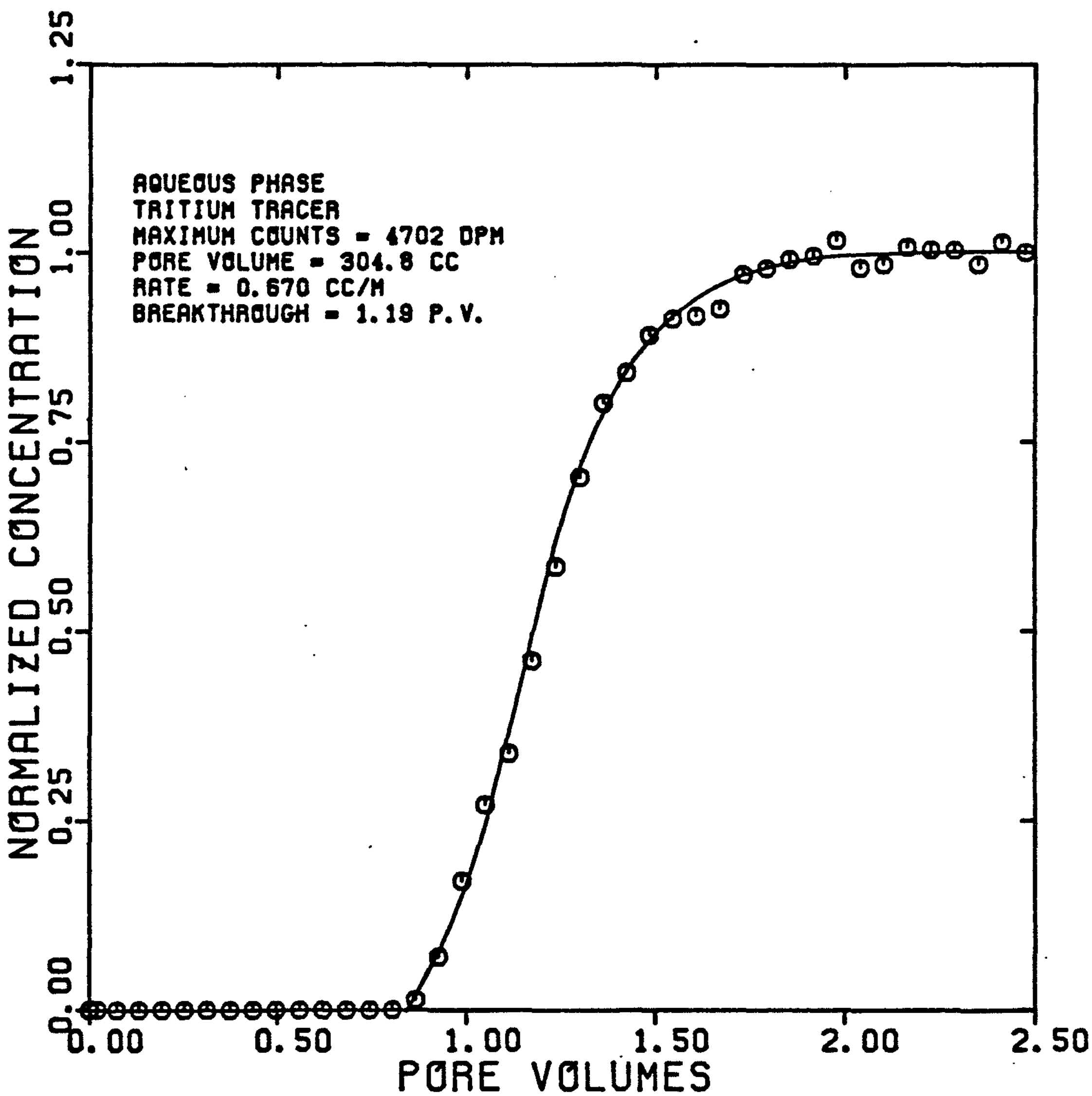

FIGURE 5.34

DISPERSIVITY OF TRITIUM
TRACER IN THE AQUEOUS PHASE
(EXPERIMENT BAOW7AQ)

$S_w = 0.605 \quad f_w = 0.484$

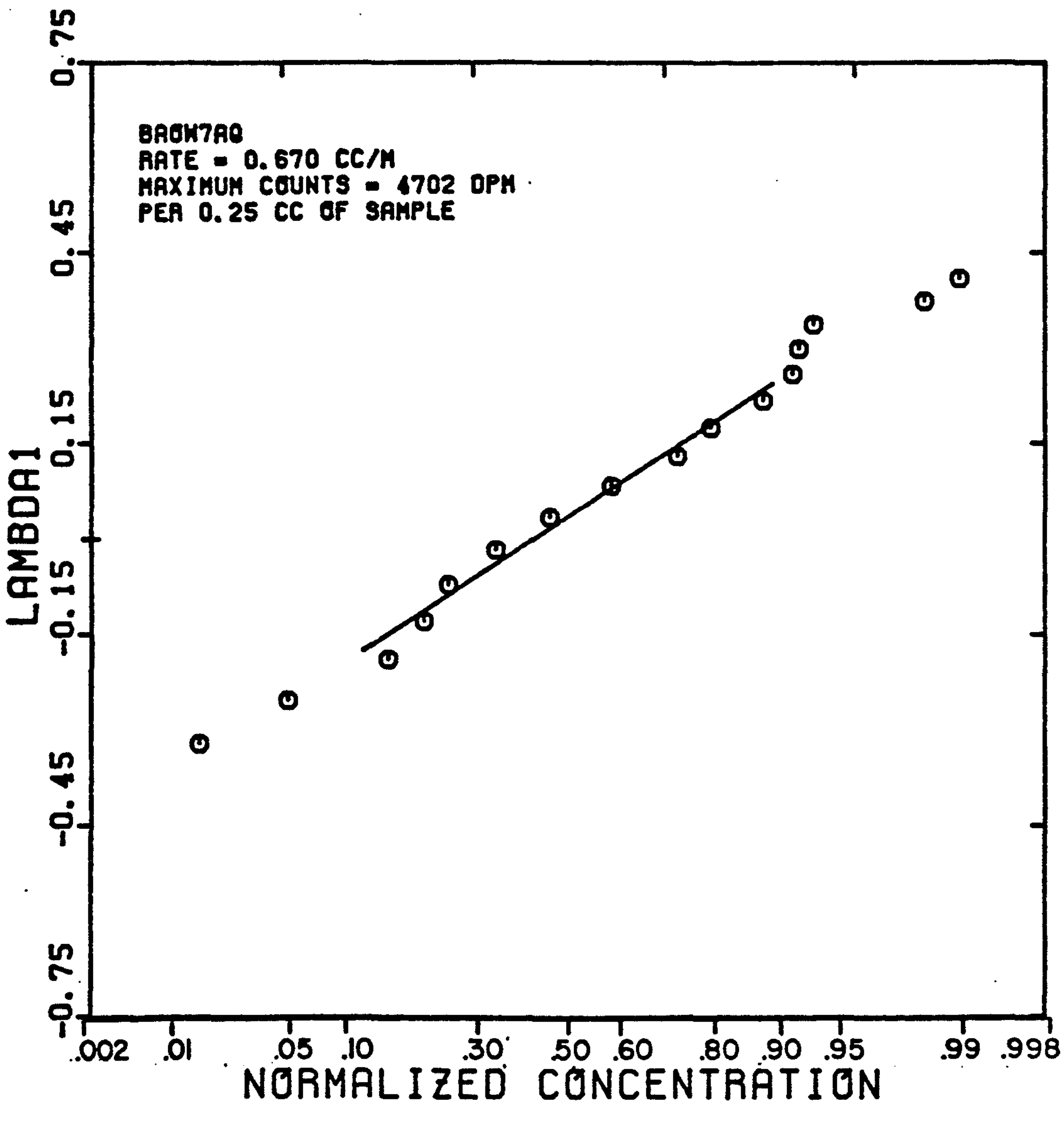

FIGURE 5.35

BEREA BREAKTHROUGH CURVE FOR CARBON 14
TRACER IN THE OLEIC PHASE
(EXPERIMENT BAOW7OL)

S_o = 0.395 f_o = 0.516

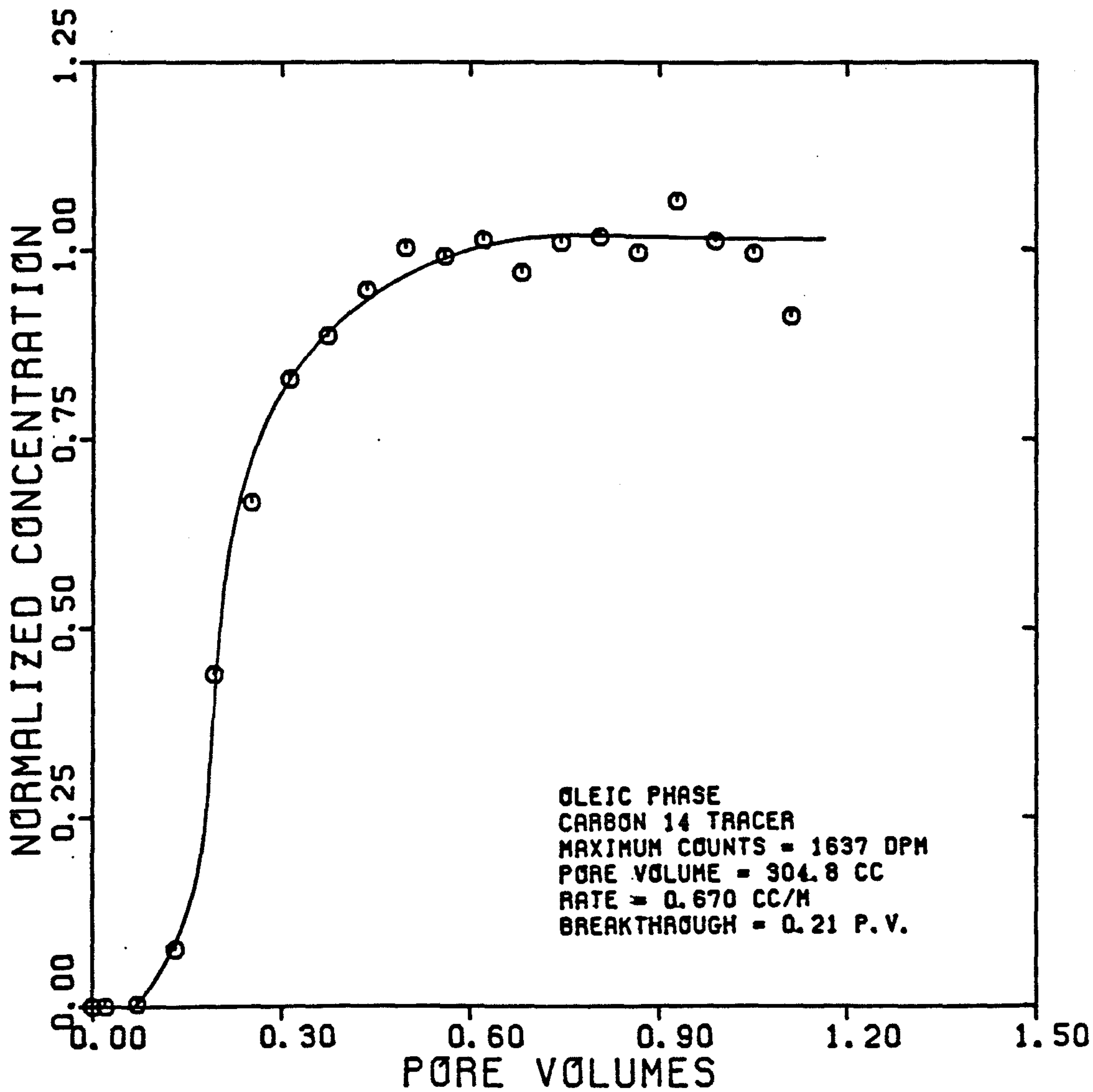

FIGURE 5.36

DISPERSIVITY OF CARBON 14
TRACER IN THE OLEIC PHASE
(EXPERIMENT BAOW70L)

$S_o = 0.395 \quad f_o = 0.516$

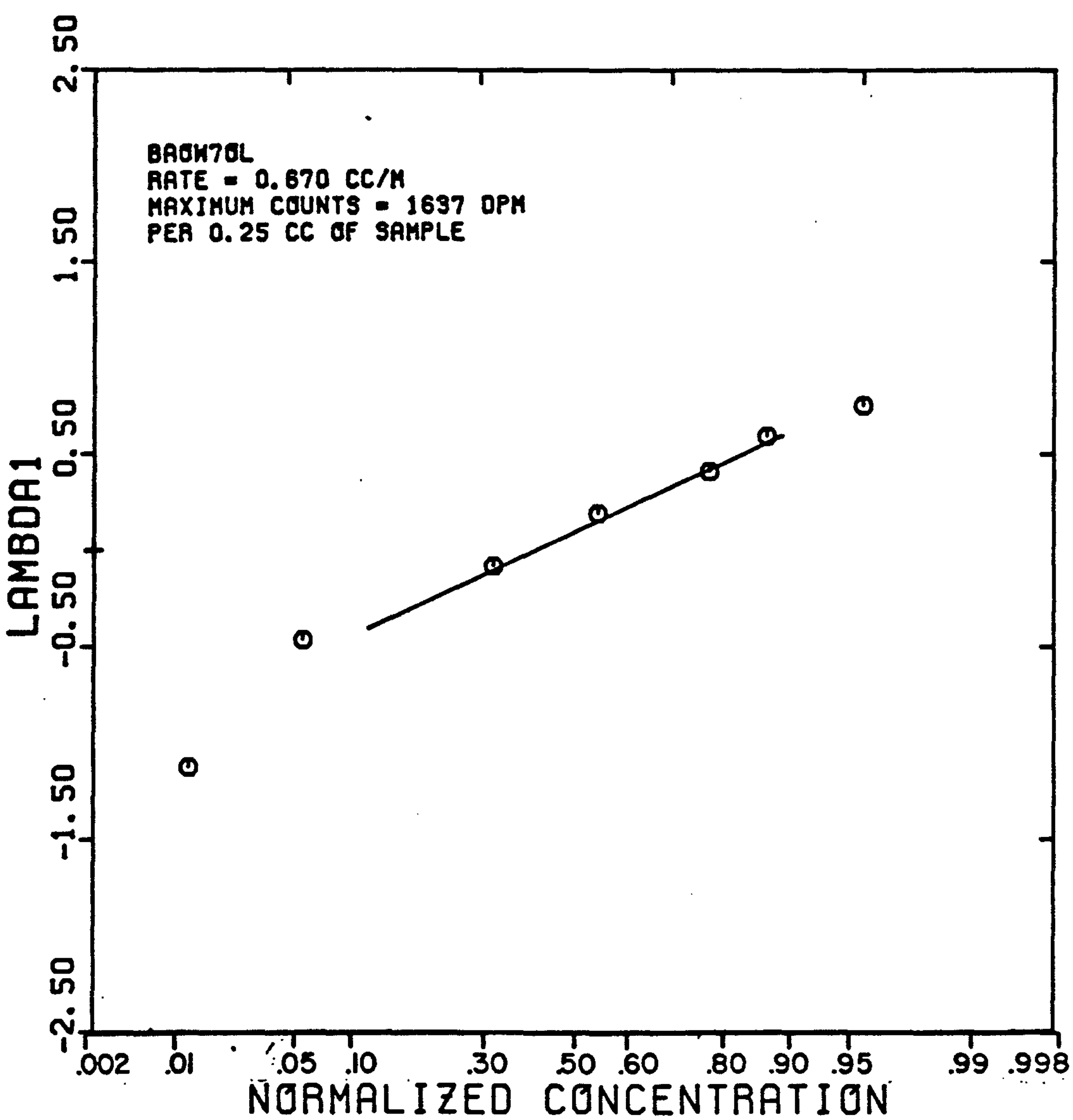

FIGURE 5.37

BEREA BREAKTHROUGH CURVE FOR TRITIUM
TRACER IN THE AQUEOUS PHASE
(EXPERIMENT BAOW8)

$S_w = 0.633 \quad f_w = 1.0$

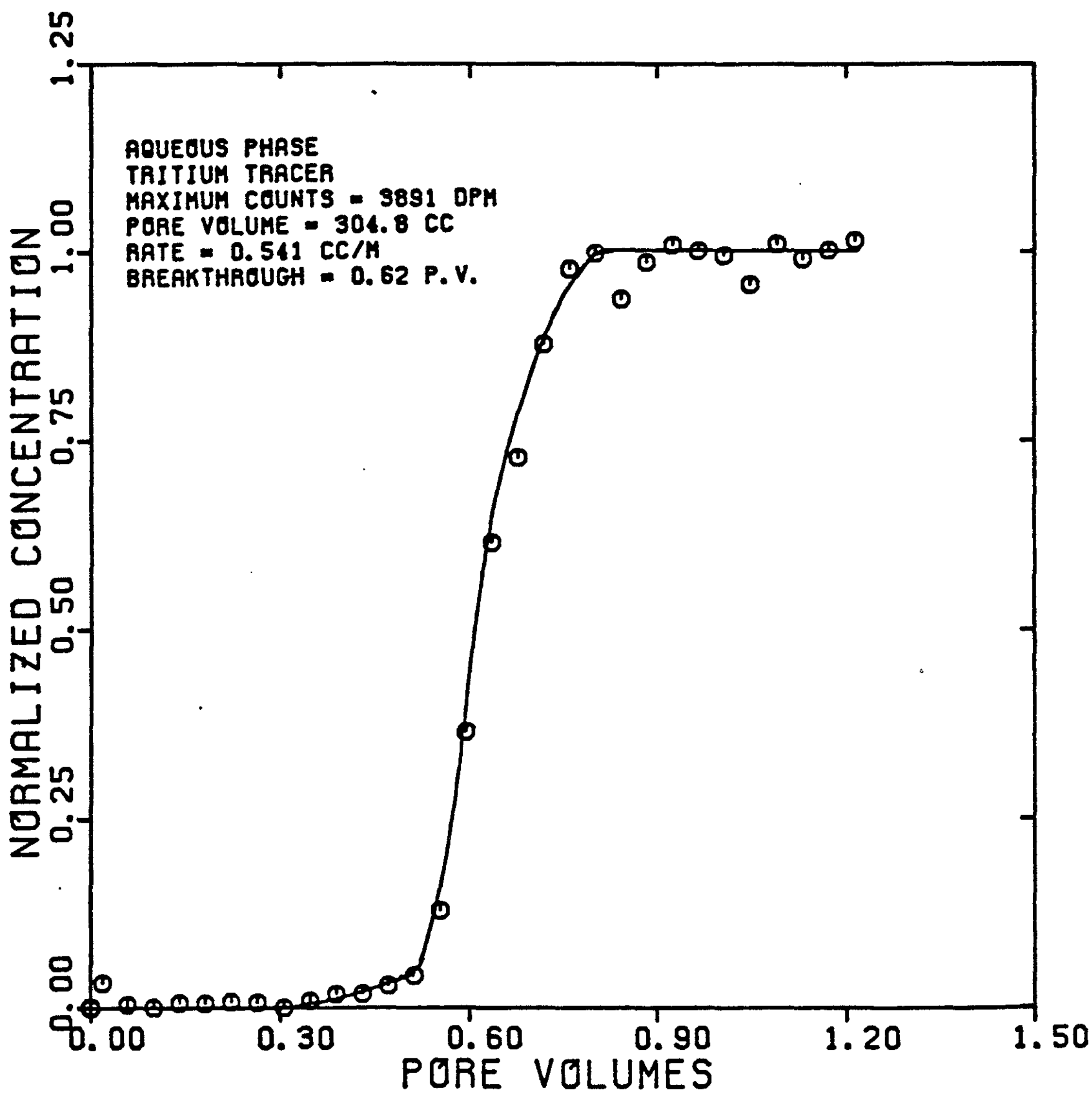

FIGURE 5.38

DISPERSIVITY OF TRITIUM
TRACER IN THE AQUEOUS PHASE
(EXPERIMENT BAOW8)

$S_w = 0.633 \quad f_w = 1.0$

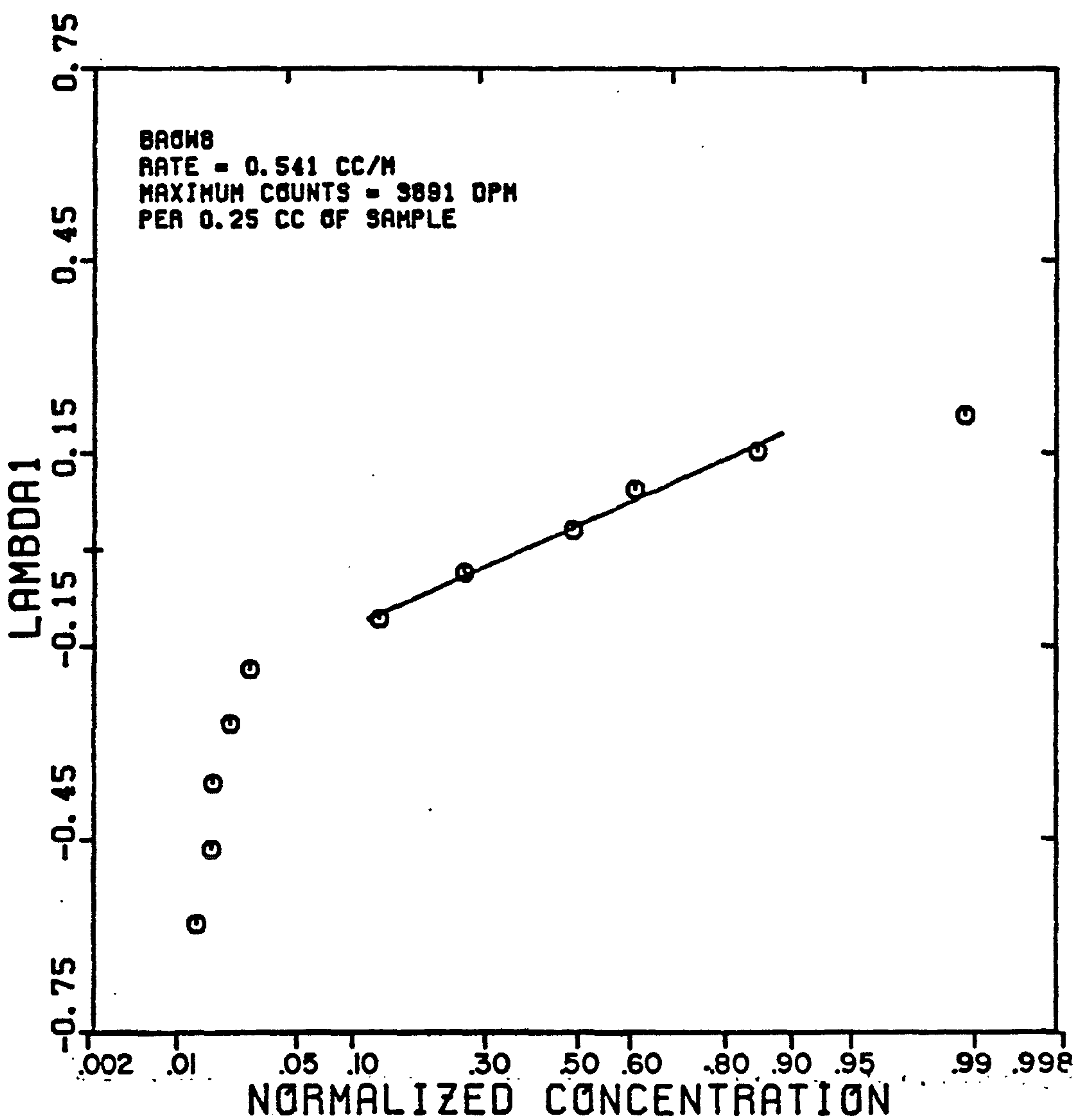

FIGURE 5.39

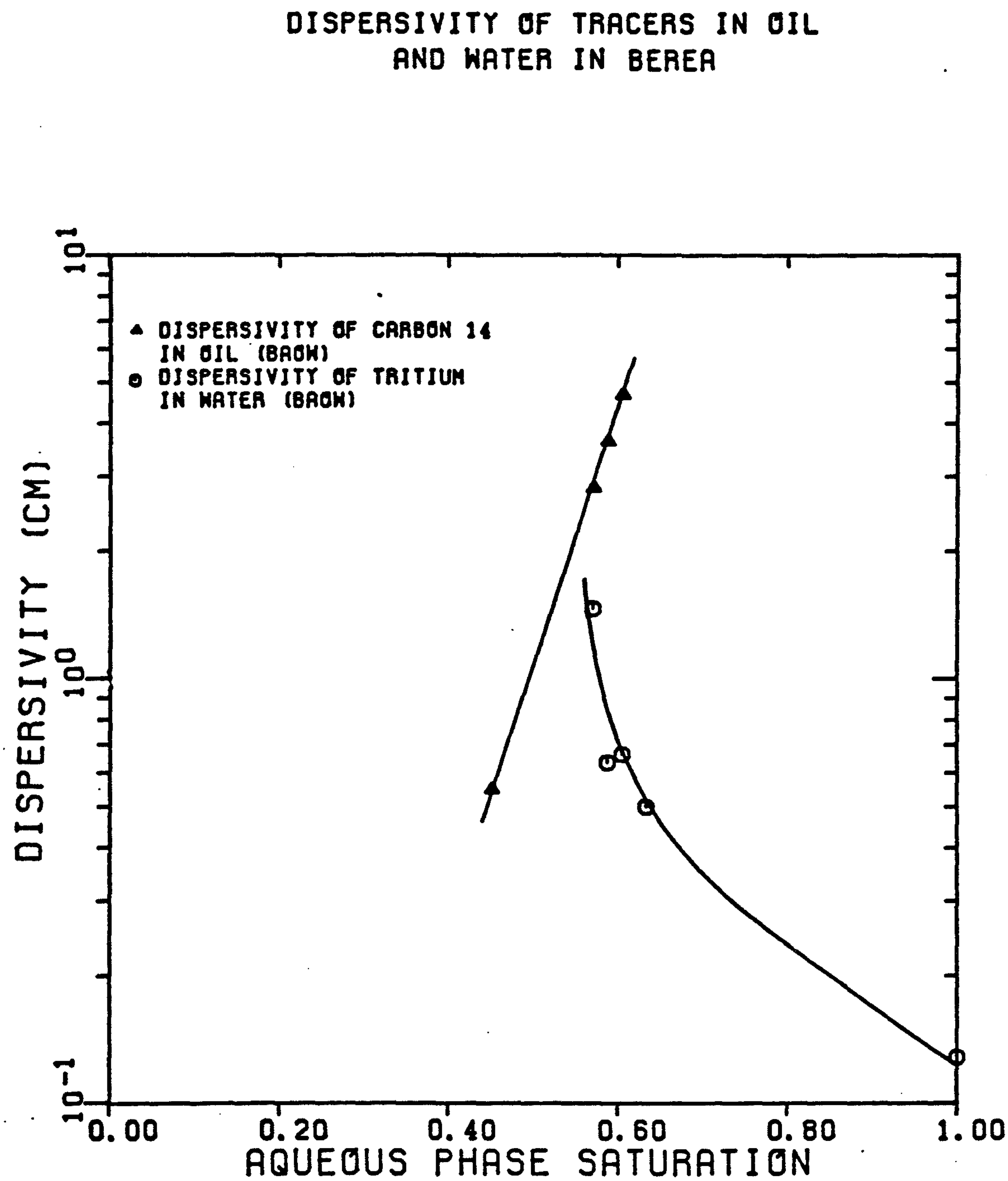
DISPERSIVITY OF TRACERS IN OIL
AND WATER IN BEREA
DISPERSIVITY OF CARBON 14
IN OIL (BAOW)
DISPERSIVITY OF TRITIUM
IN WATER (BAOW)
DISPERSIVITY (CM)
10^1
10^0
10^-1
0.00
0.20
0.40
0.60
0.80
1.00
AQUEOUS PHASE SATURATION

FIGURE 5.40

DISPERSIVITY OF N-DECANE AND BRINE
IN BEREA SANDSTONE
(EXPERIMENTS BAOW AND I-B/D)

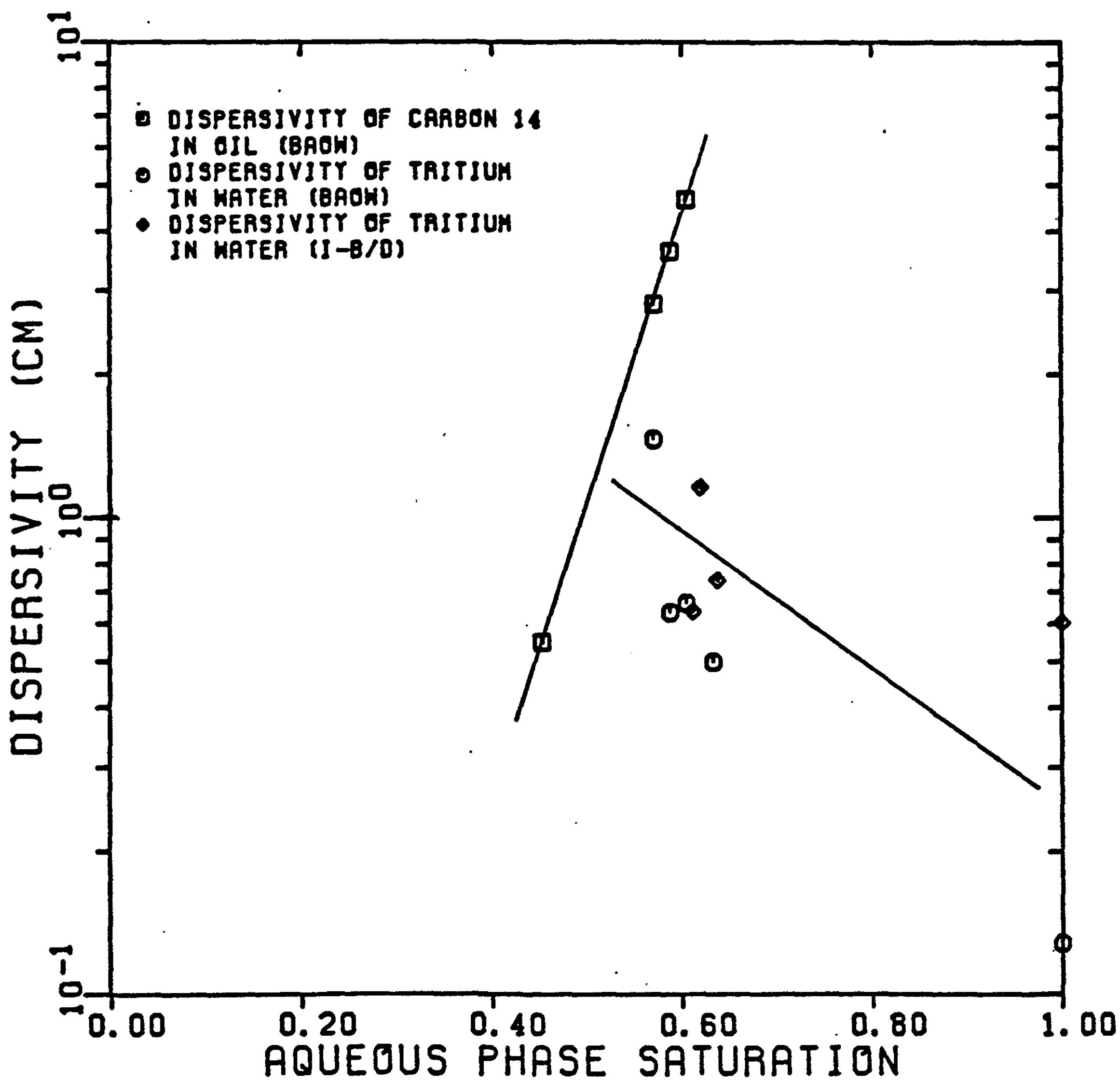

FIGURE 5.41

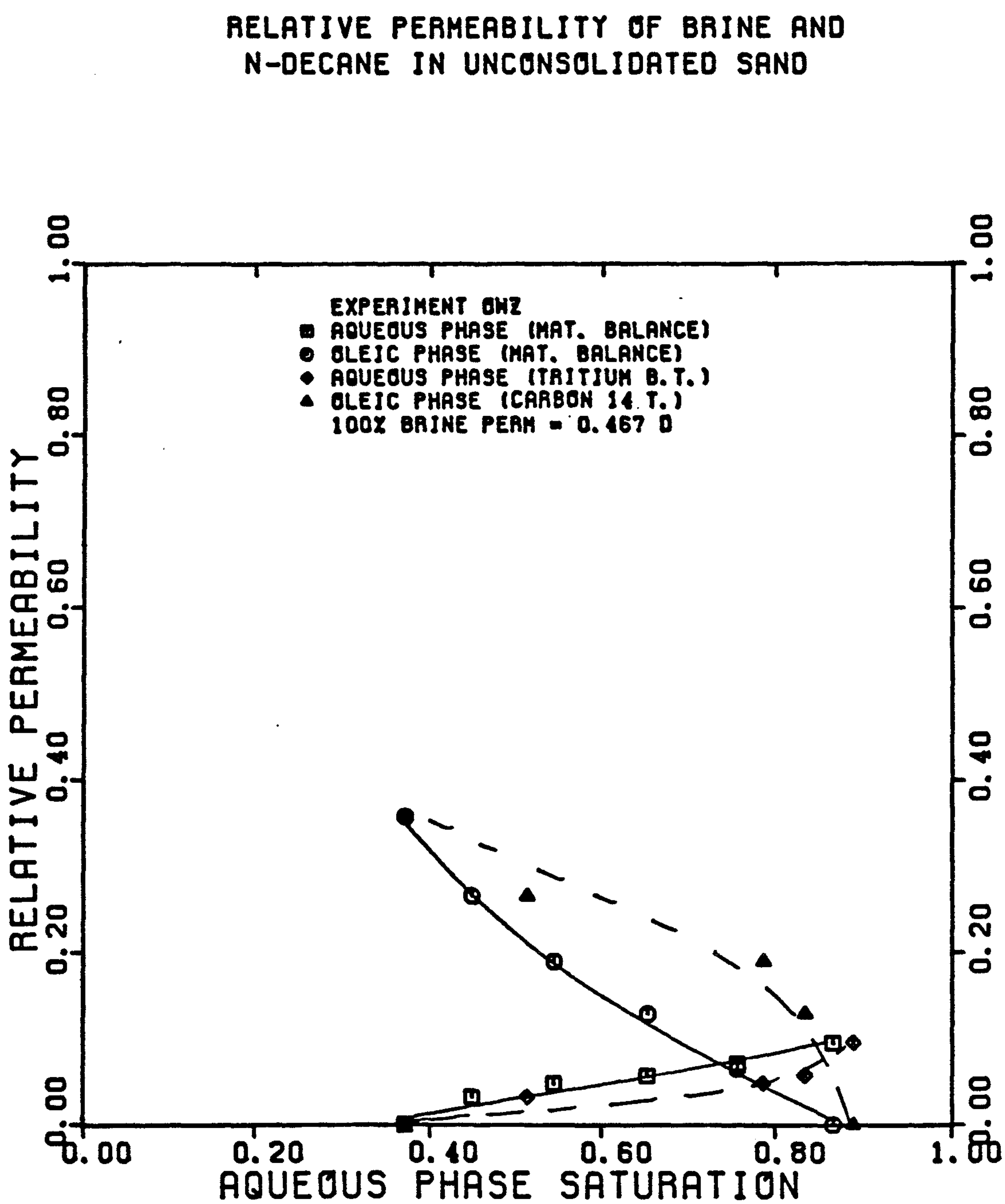
RELATIVE PERMEABILITY OF BRINE AND
N-DECANE IN UNCONSOLIDATED SAND
EXPERIMENT OWZ
AQUEOUS PHASE (MAT. BALANCE)
OLEIC PHASE (MAT. BALANCE)
AQUEOUS PHASE (TRITIUM B.T.)
OLEIC PHASE (CARBON 14 T.)
100% BRINE PERM = 0.467 D
RELATIVE PERMEABILITY
0.00
0.20
0.40
0.60
0.80
1.00
AQUEOUS PHASE SATURATION

FIGURE 5.42

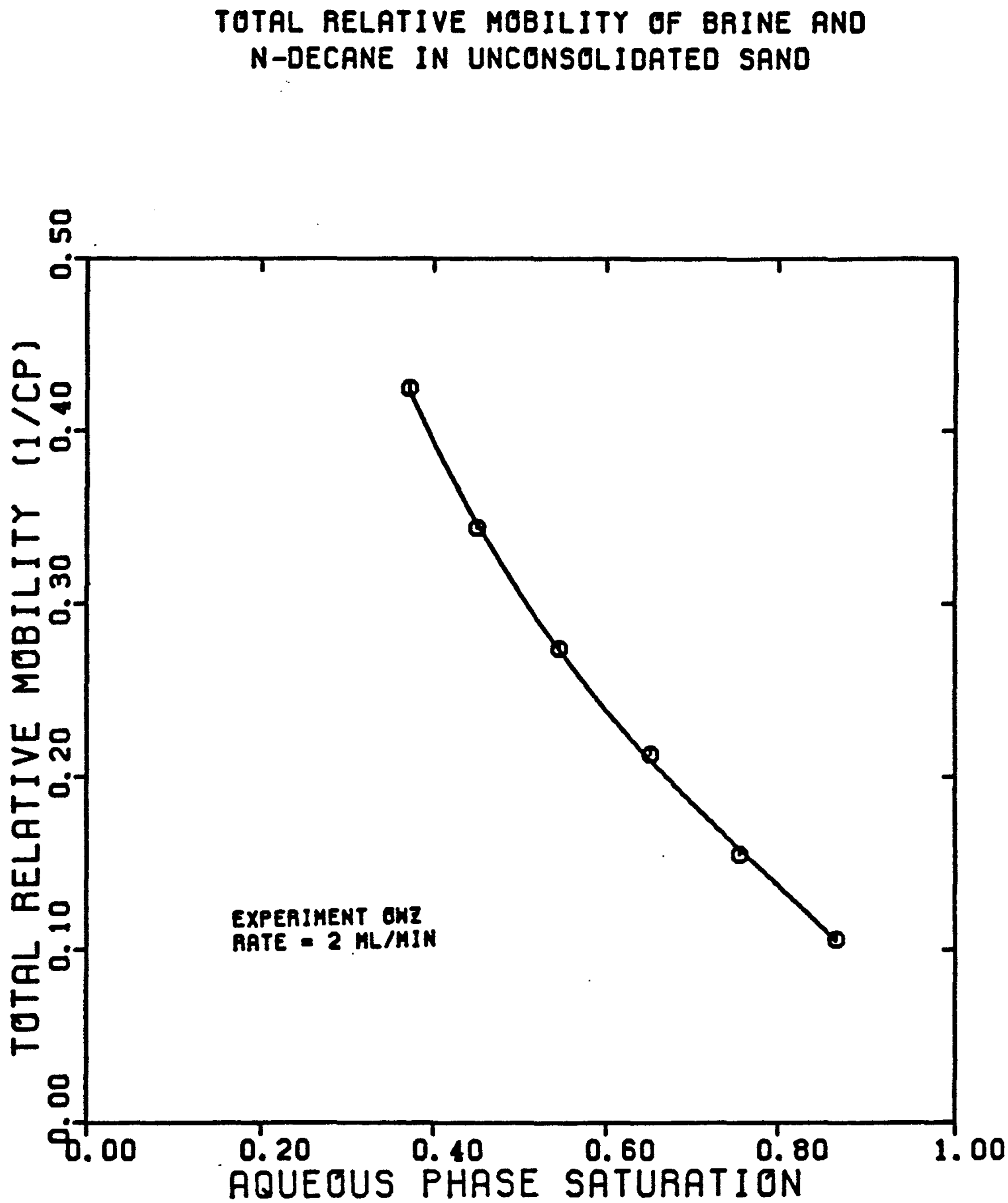
TOTAL RELATIVE MOBILITY OF BRINE AND
N-DECANE IN UNCONSOLIDATED SAND
TOTAL RELATIVE MOBILITY (1/CP)
0.00
0.10
0.20
0.30
0.40
0.50
0.00
0.20
0.40
0.60
0.80
1.00
AQUEOUS PHASE SATURATION
EXPERIMENT 6WZ
RATE = 2 ML/MIN

FIGURE 5.43

FRACTIONAL FLOW FOR THE AQUEOUS PHASE IN UNCONSOLIDATED SAND (EXPERIMENT OWZ)

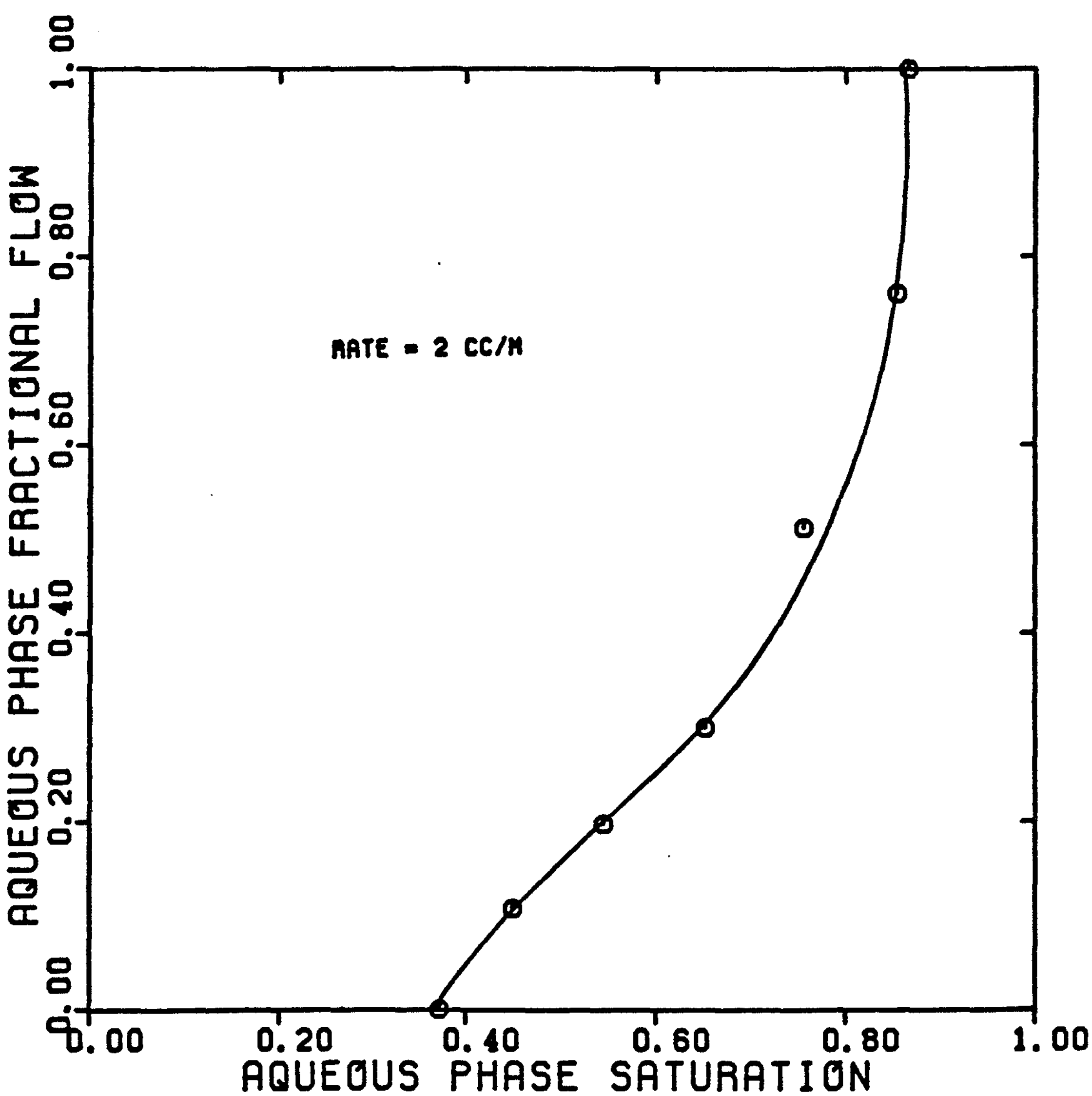

FIGURE 5.44

SANDPACK BREAKTHROUGH CURVE FOR TRITIUM TRACER IN THE AQUEOUS PHASE (EXPERIMENT OW1ZA)

$S_w = 1.0 \quad f_w = 1.0$

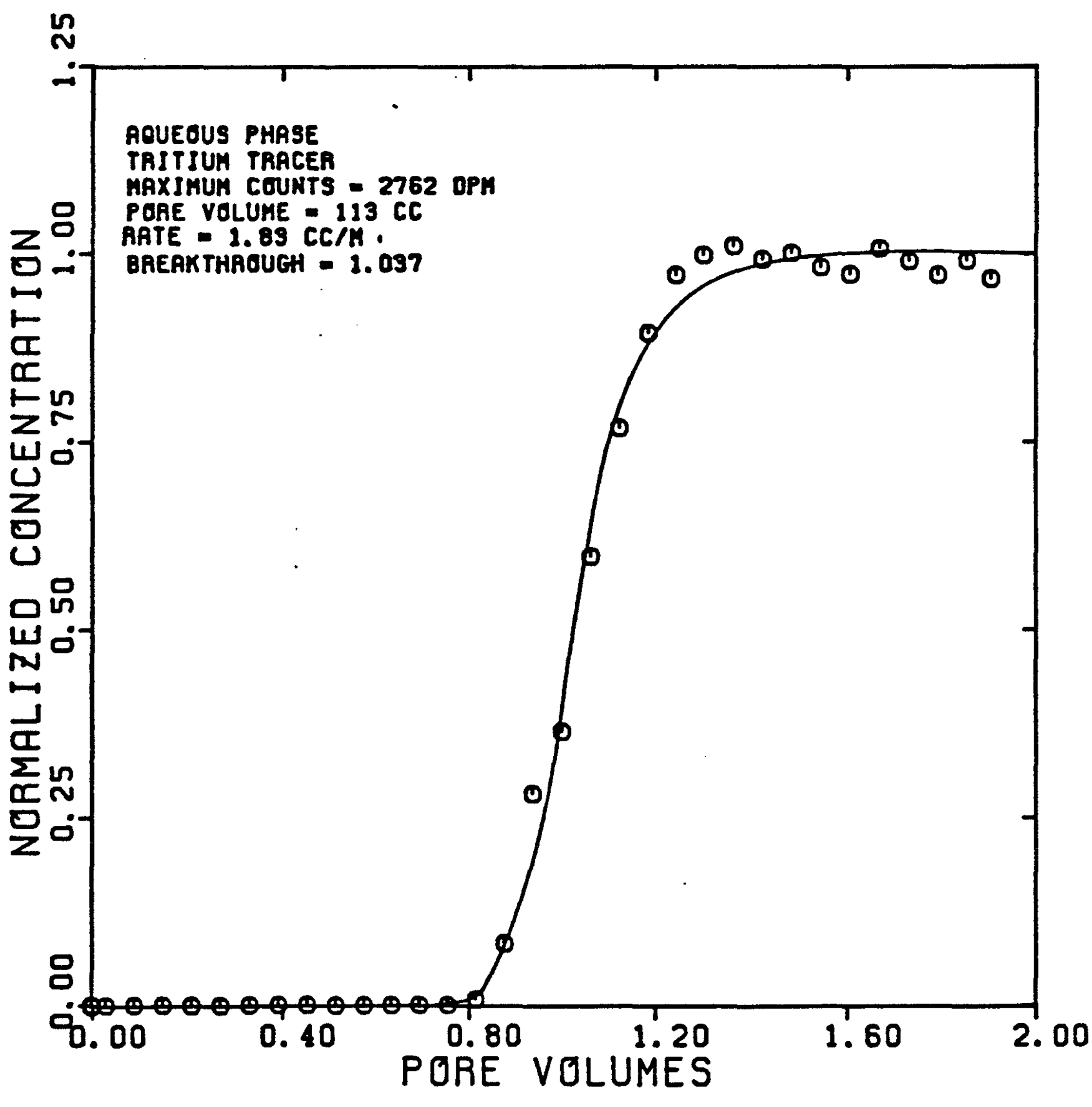

FIGURE 5.45

DISPERSIVITY OF TRITIUM TRACER IN THE AQUEOUS PHASE (EXPERIMENT OW1ZA)

$S_w = 1.0 \quad f_w = 1.0$

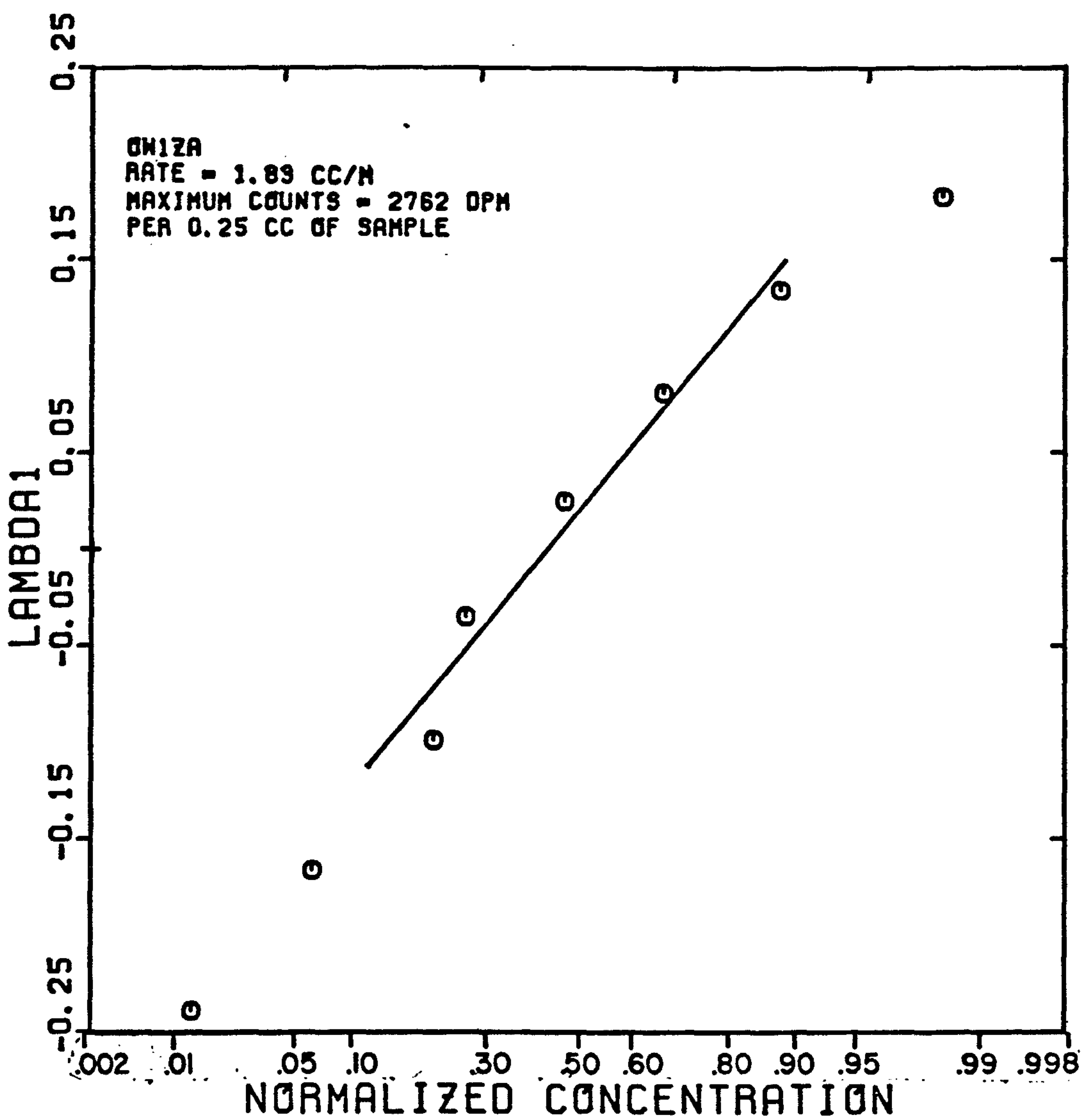

FIGURE 5.46

SANDPACK BREAKTHROUGH CURVE FOR CARBON 14 AND N-NONANE TRACERS IN THE OLEIC PHASE (EXPERIMENT OWZ2A)

$S_o = 0.628 \quad f_o = 1.0$

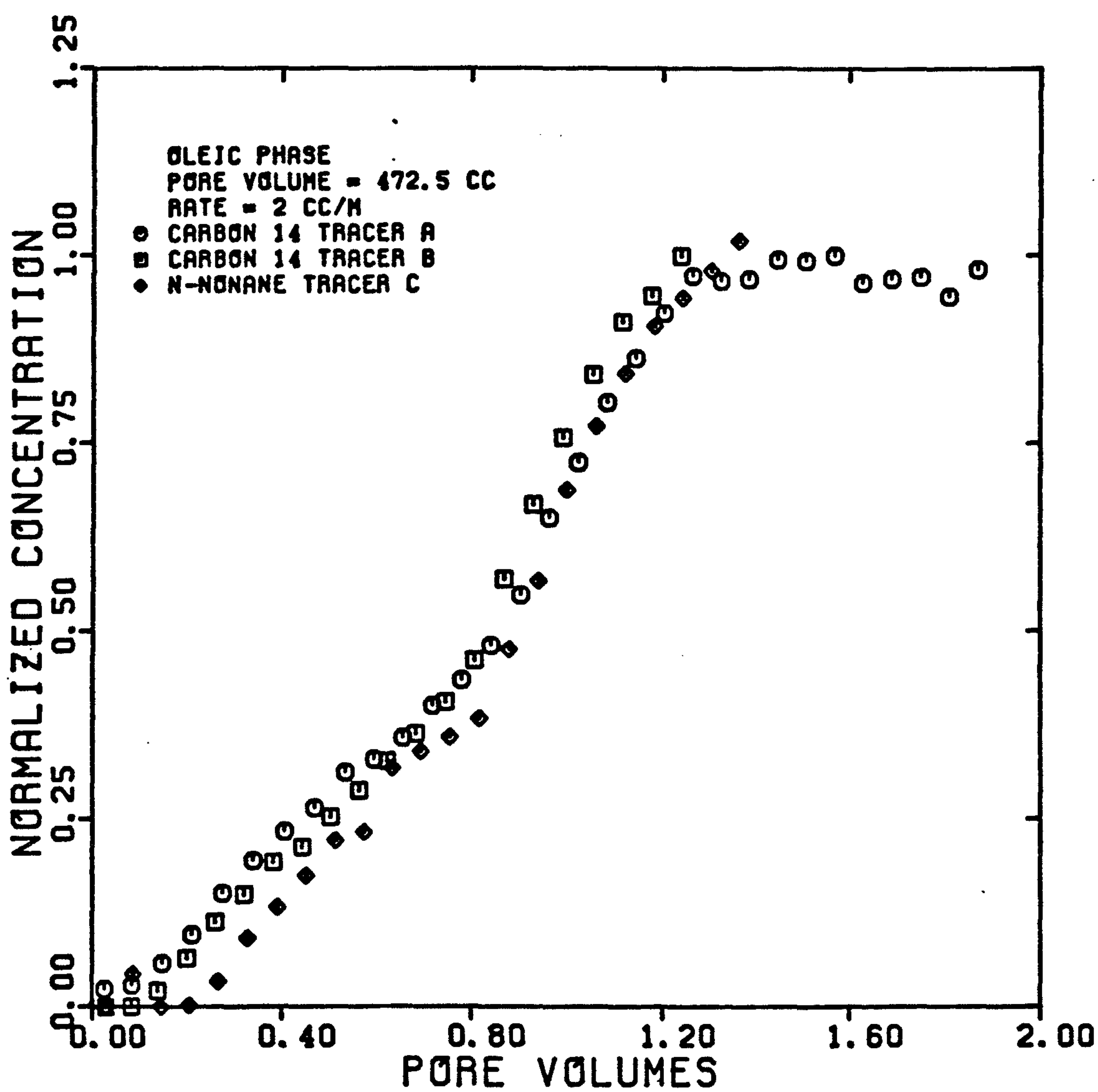

FIGURE 5.47

SANDPACK BREAKTHROUGH CURVE FOR TRITIUM TRACER IN THE AQUEOUS PHASE (EXPERIMENT OW8ZA)

$S_w = 0.871 \quad f_w = 1.0$

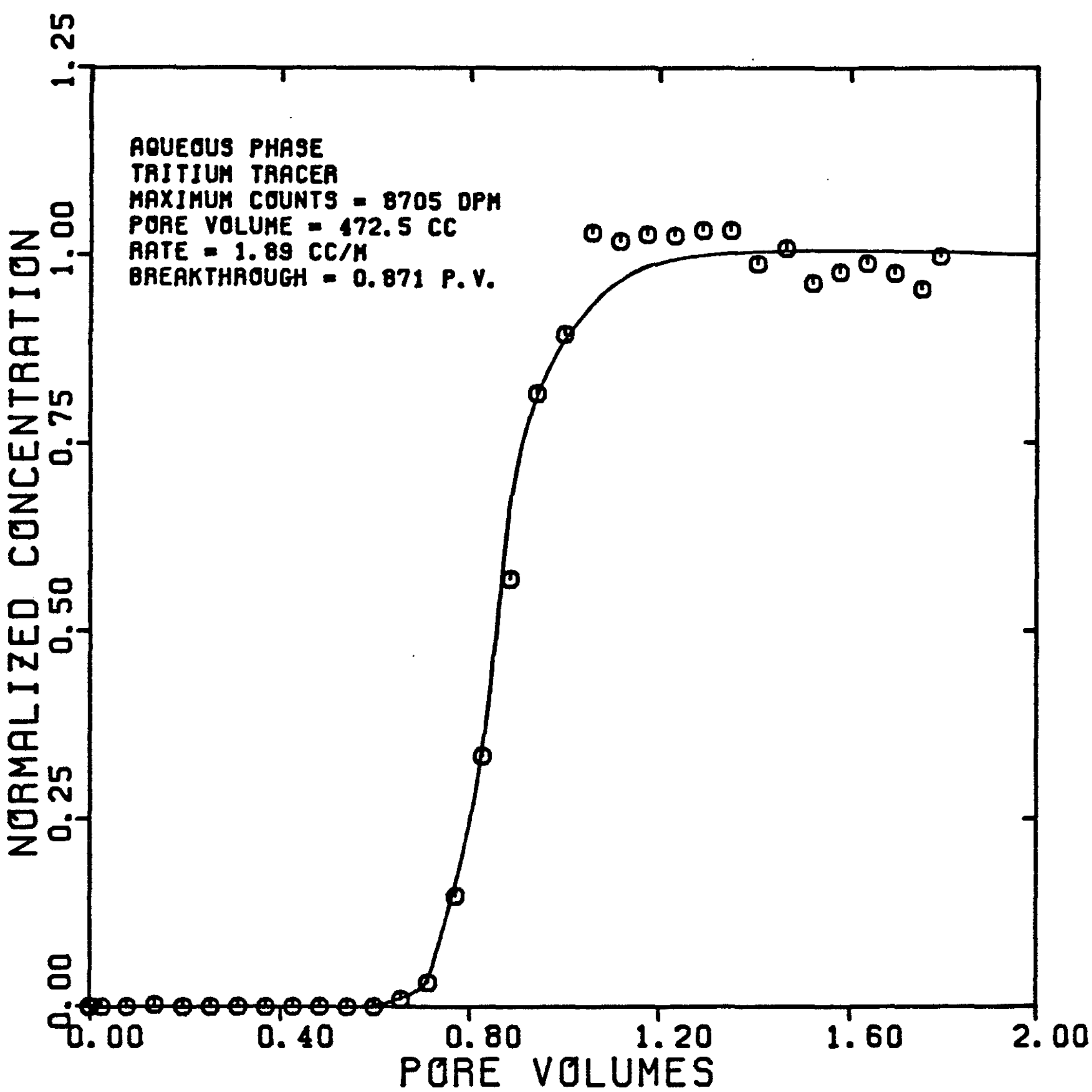

FIGURE 5.48

DISPERSIVITY OF TRITIUM
TRACER IN THE AQUEOUS PHASE
(EXPERIMENT OW8ZA)

$S_w = 0.871 \quad f_w = 1.0$

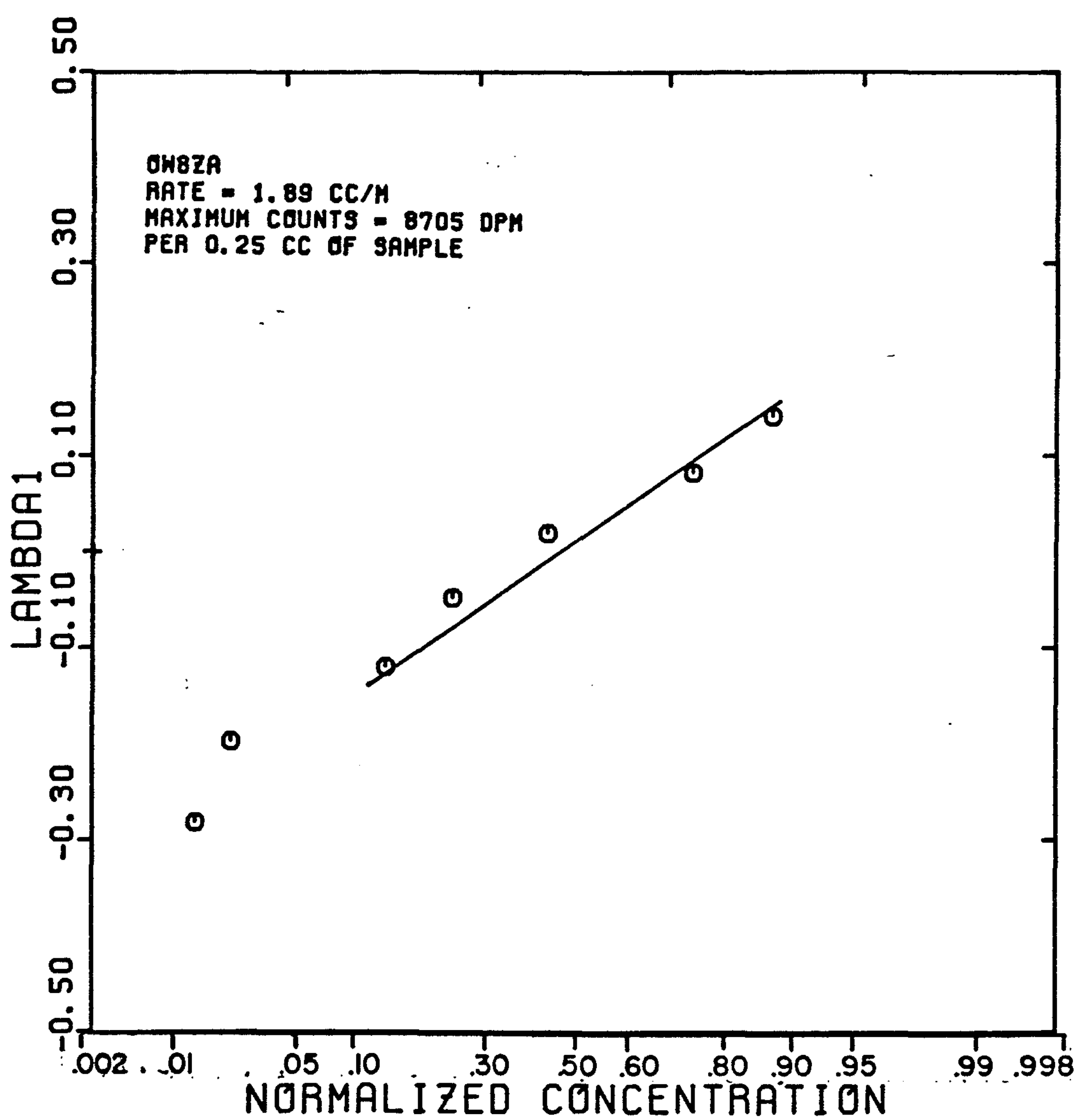

FIGURE 5.49

SANDPACK BREAKTHROUGH CURVE FOR TRITIUM TRACER IN THE AQUEOUS PHASE (EXPERIMENT OW1Z)

$S_w = 1.0 \quad f_w = 1.0$

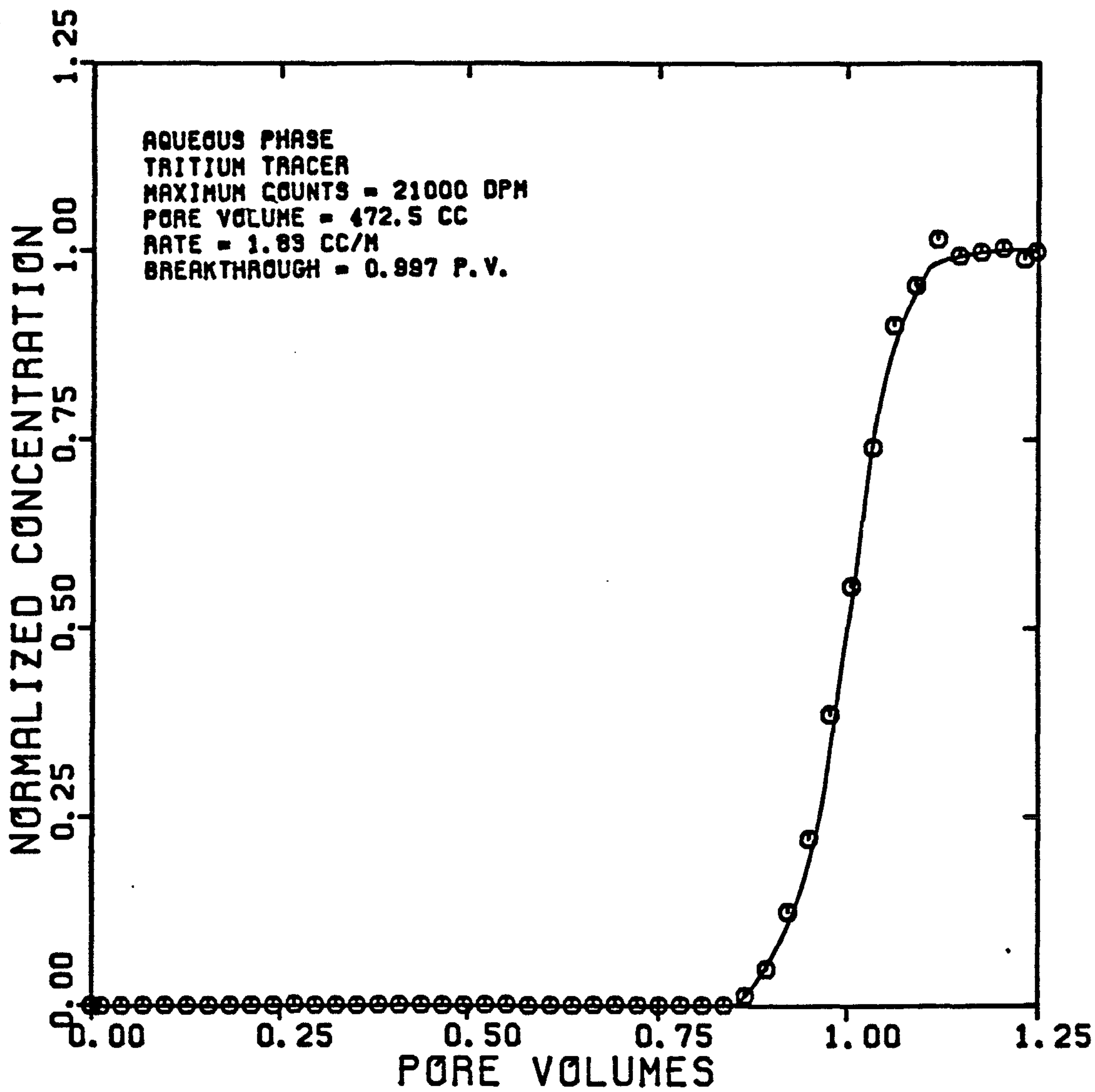

FIGURE 5.50

DISPERSIVITY OF TRITIUM
TRACER IN THE AQUEOUS PHASE
(EXPERIMENT OW1Z)

$S_w = 1.0 \quad f_w = 1.0$

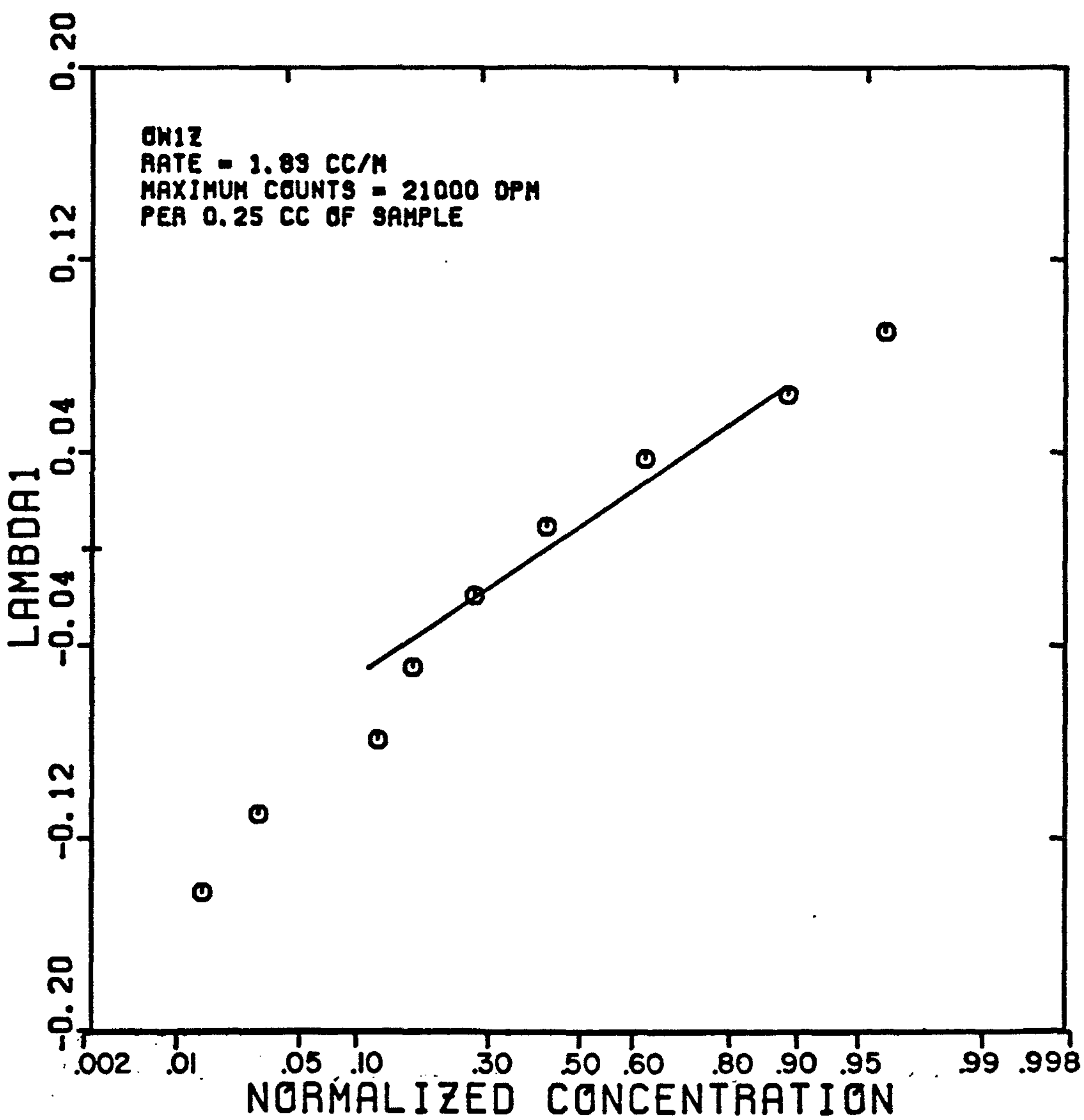

FIGURE 5.51

SANDPACK BREAKTHROUGH CURVE FOR CARBON 14 TRACER IN THE OLEIC PHASE (EXPERIMENT OW2Z)

$S_o = 0.628 \quad f_o = 1.0$

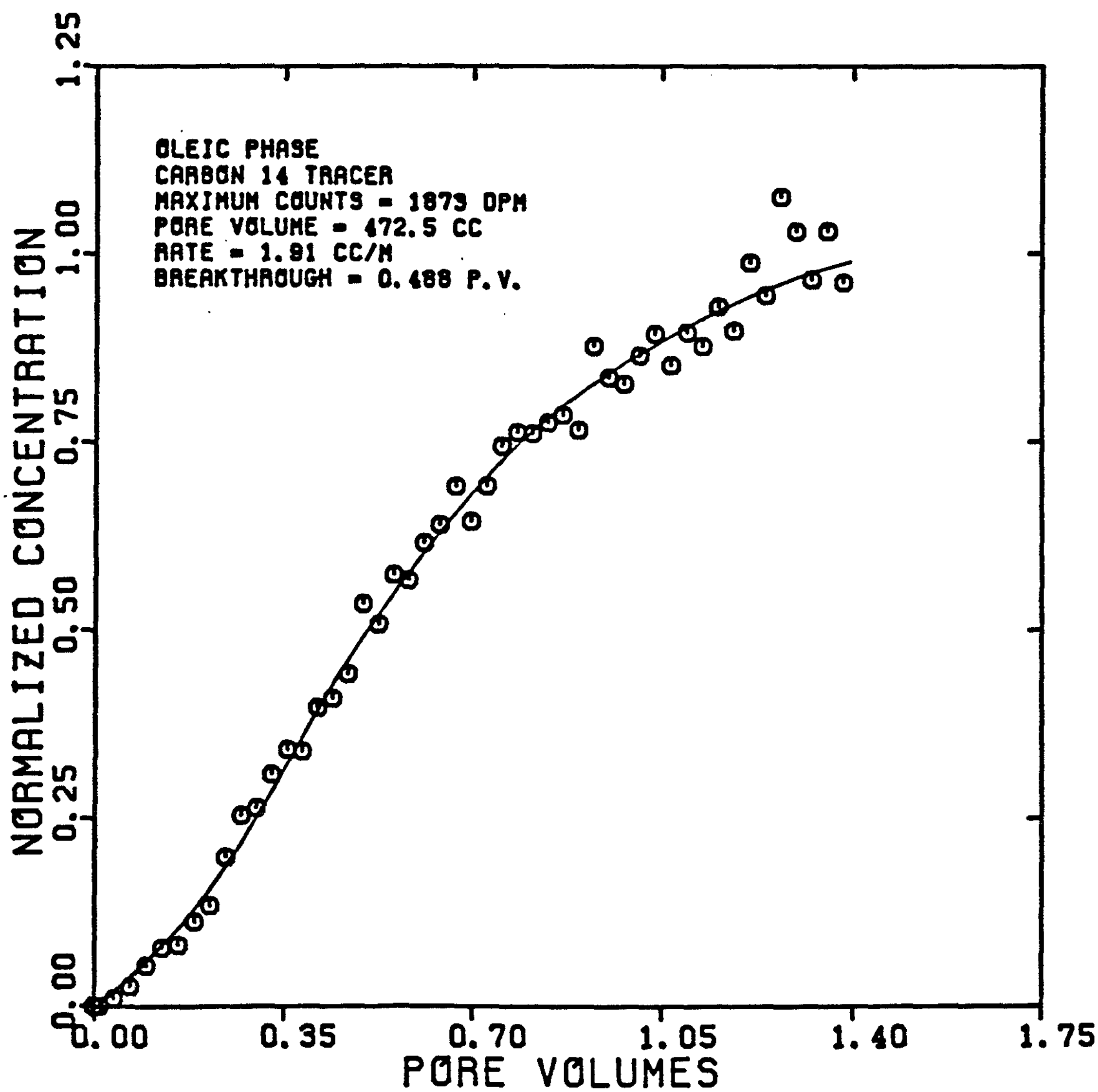

FIGURE 5.52

DISPERSIVITY OF CARBON 14
TRACER IN THE OLEIC PHASE
(EXPERIMENT OW2Z)

S_o = 0.628 f_o = 1.0

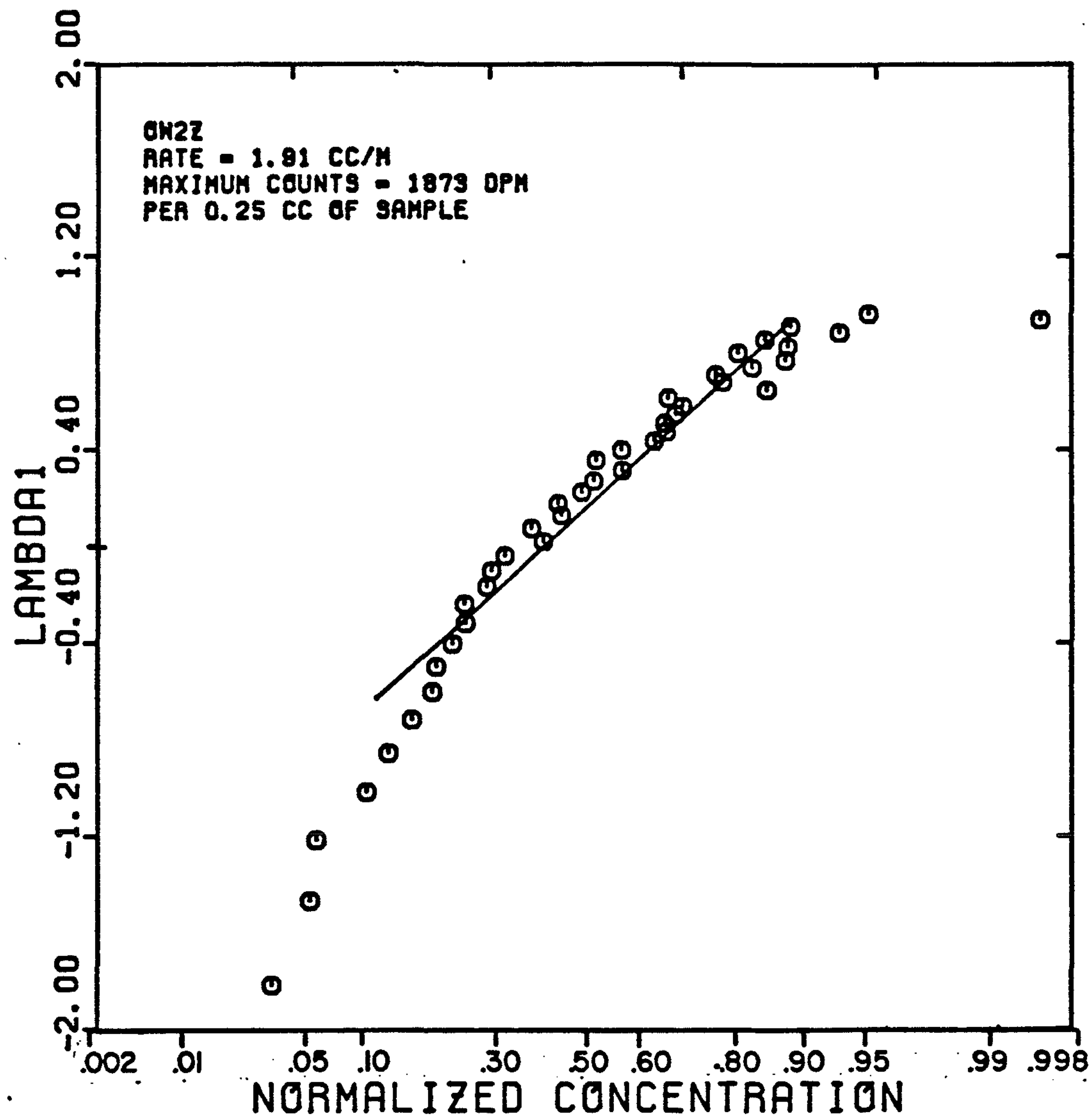

FIGURE 5.53

SANDPACK BREAKTHROUGH CURVE FOR TRITIUM
TRACER IN THE AQUEOUS PHASE
(EXPERIMENT OW3ZAQ)

$S_w = 0.450 \quad f_w = 0.108$

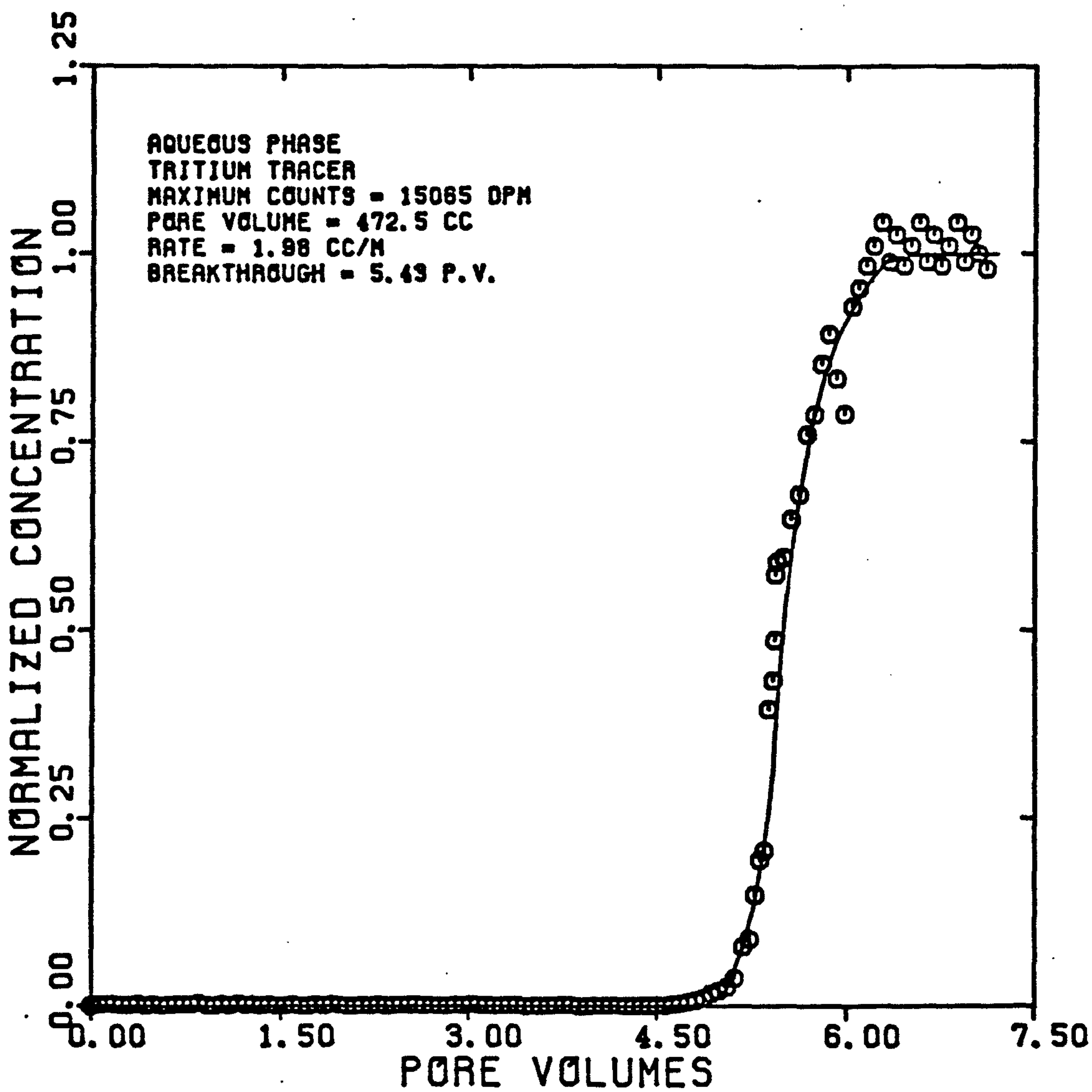

FIGURE 5.54

DISPERSIVITY OF TRITIUM
TRACER IN THE AQUEOUS PHASE
(EXPERIMENT OW3ZAQ)

$S_w = 0.450$ $f_w = 0.108$

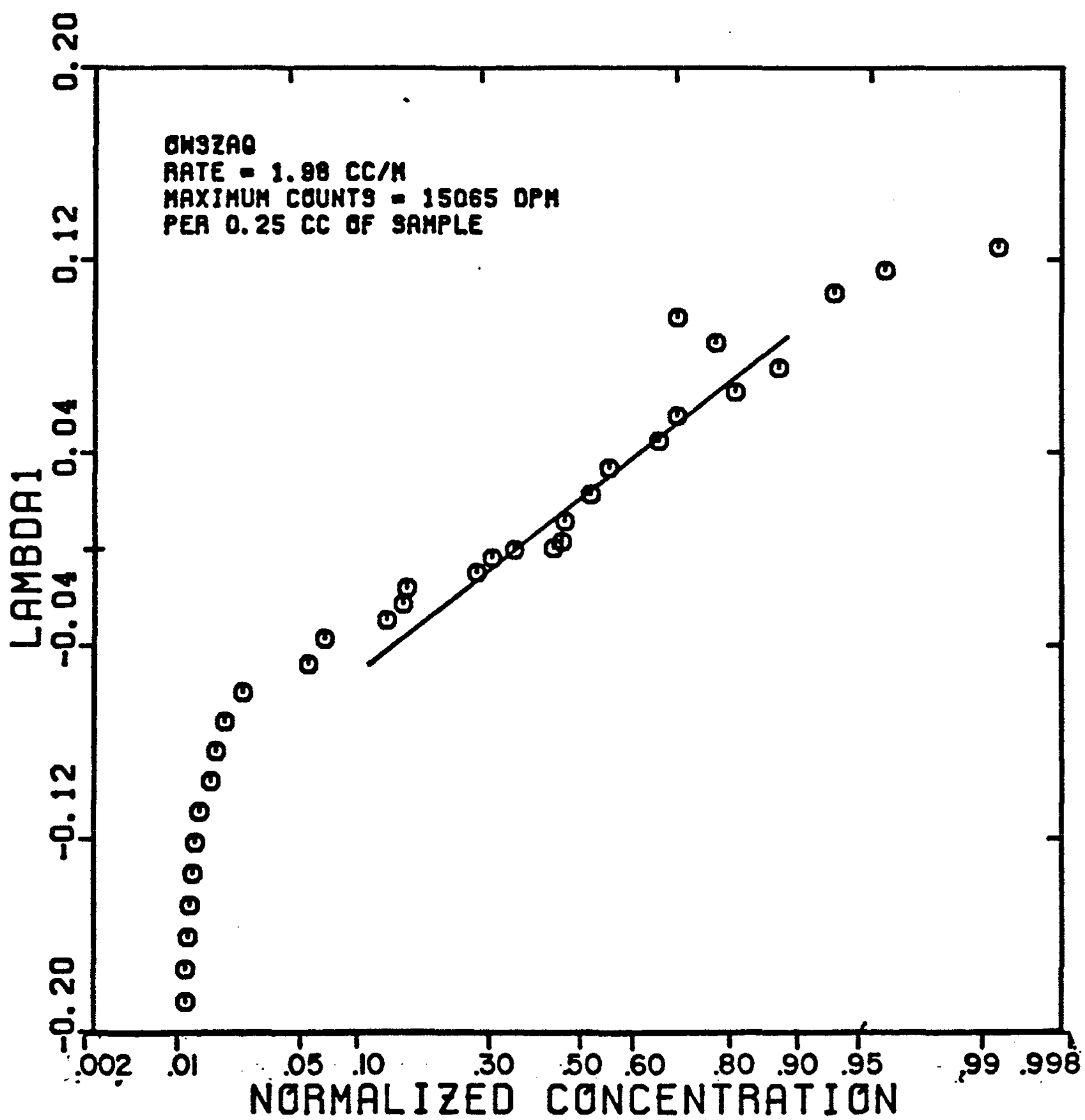

FIGURE 5.55

SANDPACK BREAKTHROUGH CURVE FOR CARBON 14
TRACER IN THE OLEIC PHASE
(EXPERIMENT OW3ZOL)

$S_o = 0.550 \quad f_o = 0.892$

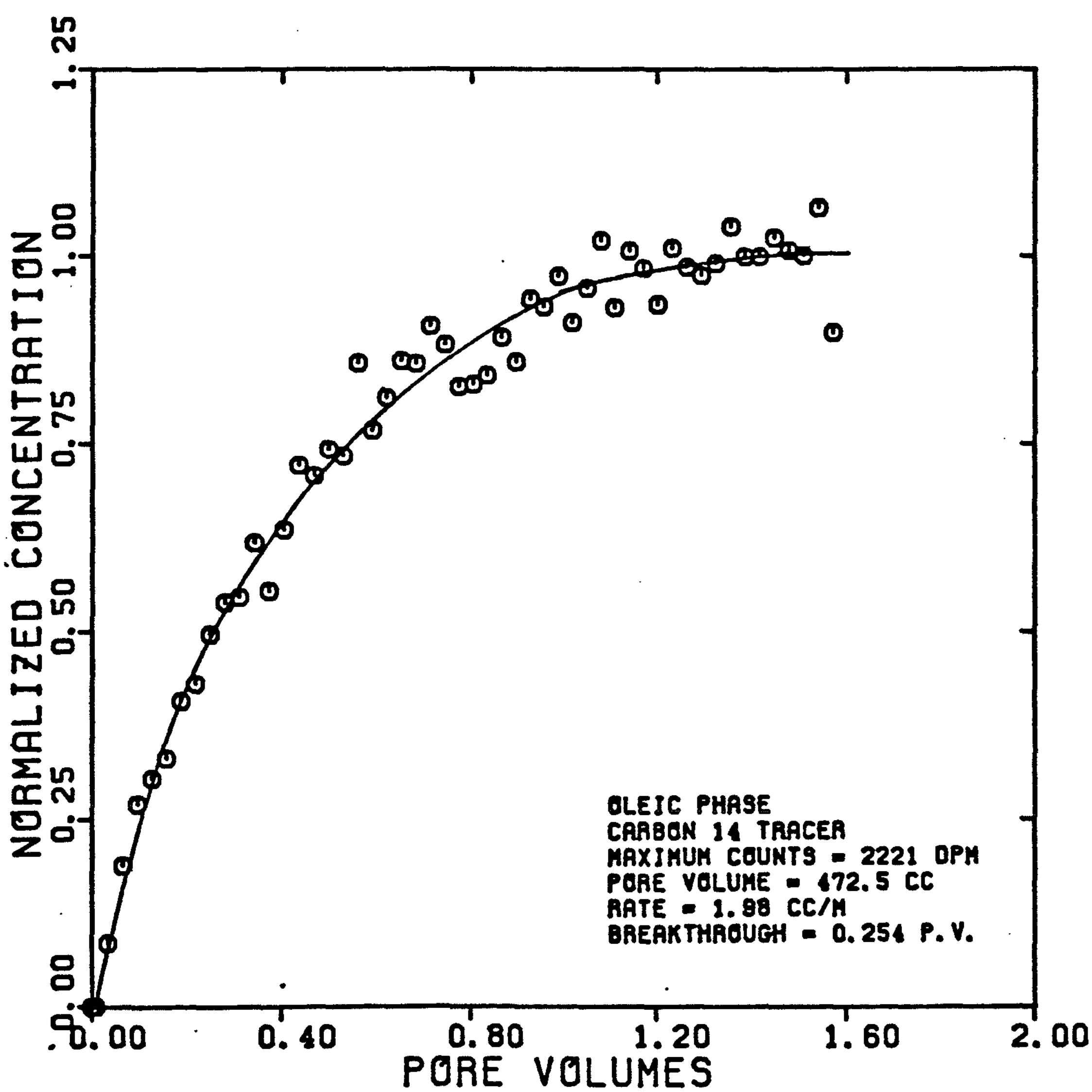

FIGURE 5.56

DISPERSIVITY OF CARBON 14
TRACER IN THE OLEIC PHASE
(EXPERIMENT OW3ZOL)

$S_o = 0.550 \quad f_o = 0.892$

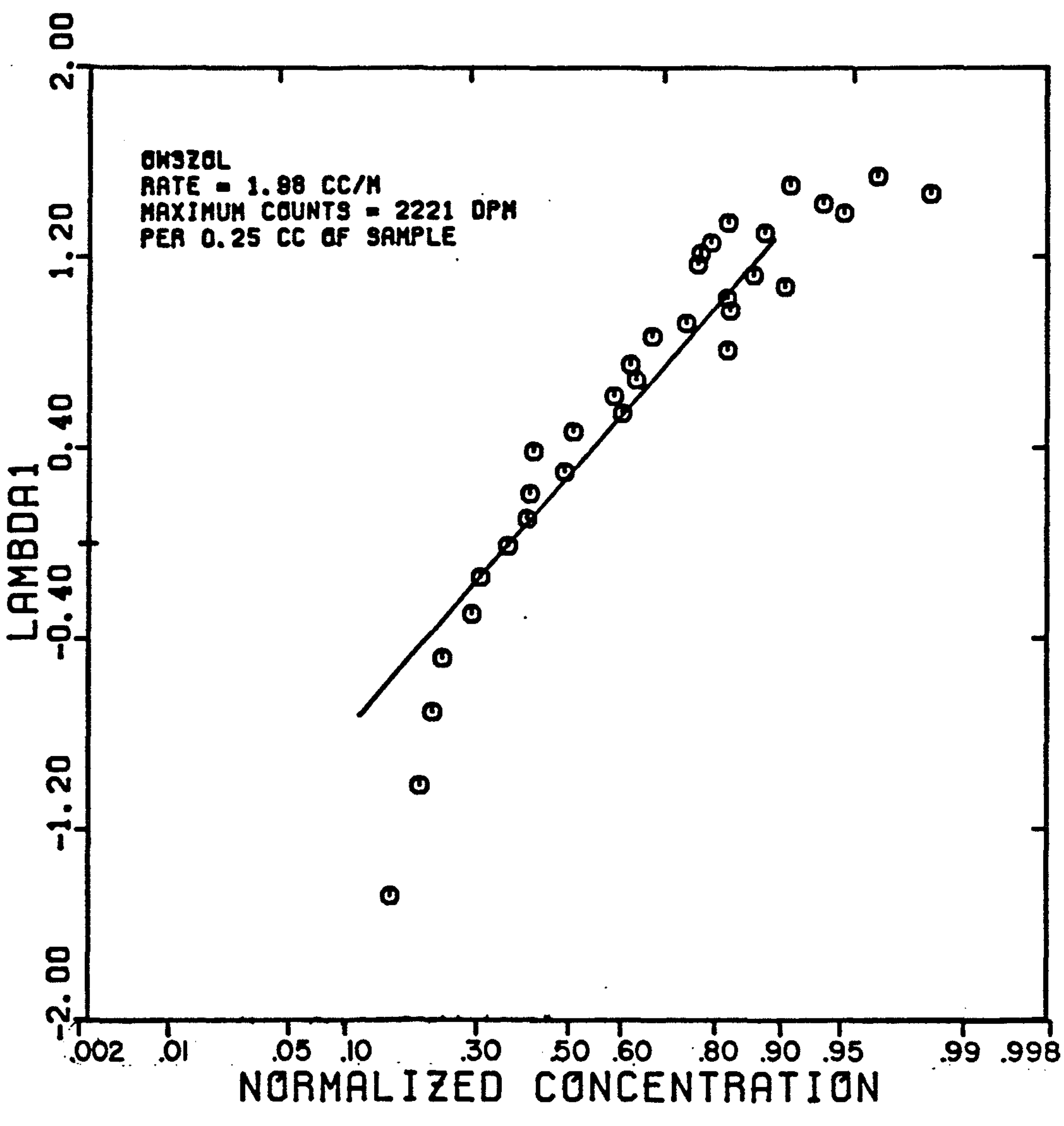

FIGURE 5.57

SANDPACK BREAKTHROUGH CURVE FOR TRITIUM
TRACER IN THE AQUEOUS PHASE
(EXPERIMENT OW4ZAQ)

$S_w = 0.545 \quad f_w = 0.198$

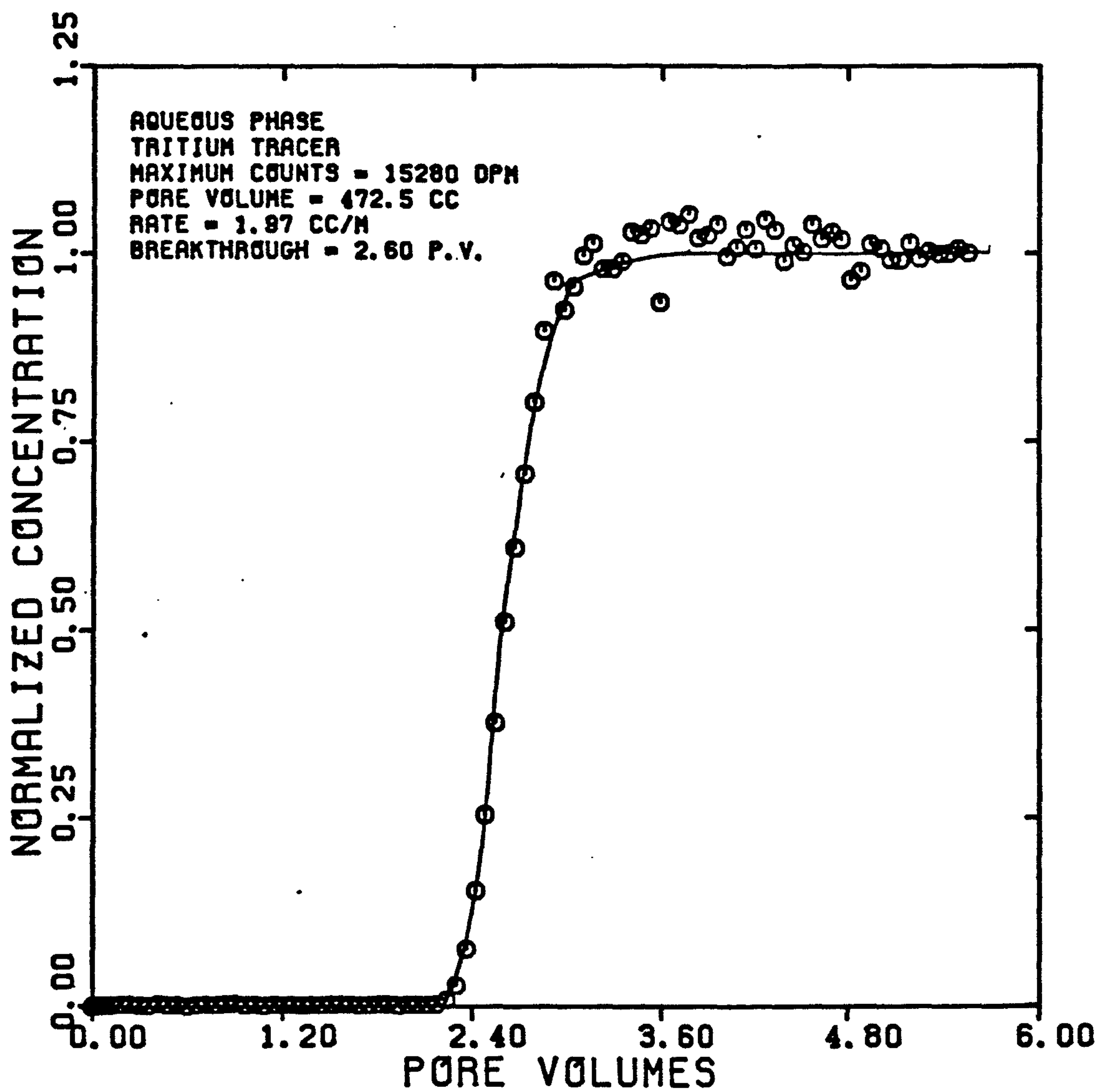

FIGURE 5.58

DISPERSIVITY OF TRITIUM TRACER IN THE AQUEOUS PHASE (EXPERIMENT OW4ZAQ)

$S_w = 0.545 \quad f_w = 0.198$

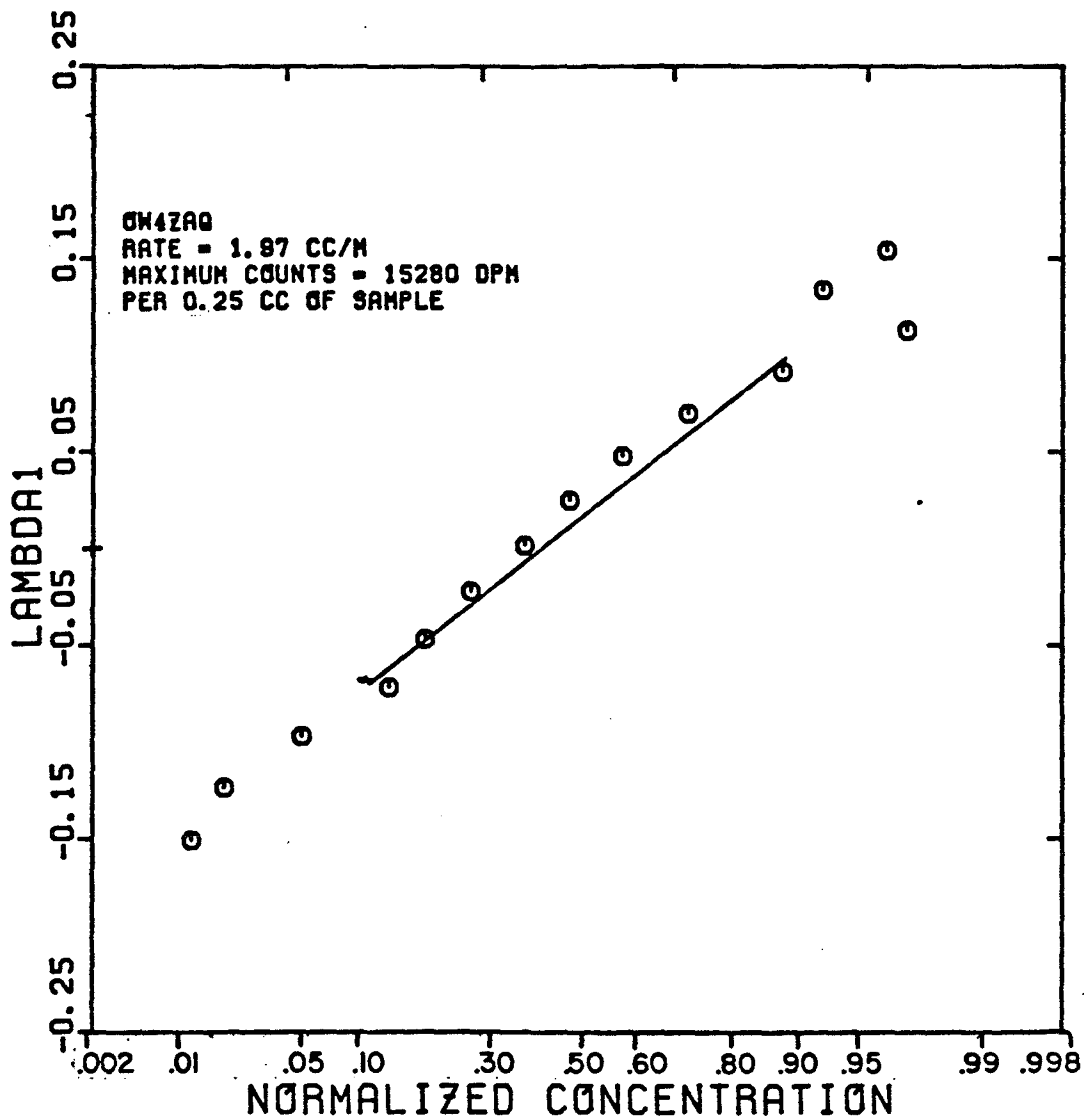

FIGURE 5.59

SANDPACK BREAKTHROUGH CURVE FOR CARBON 14
TRACER IN THE OLEIC PHASE
(EXPERIMENT OW4ZOL)

$S_o = 0.455 \quad f_o = 0.802$

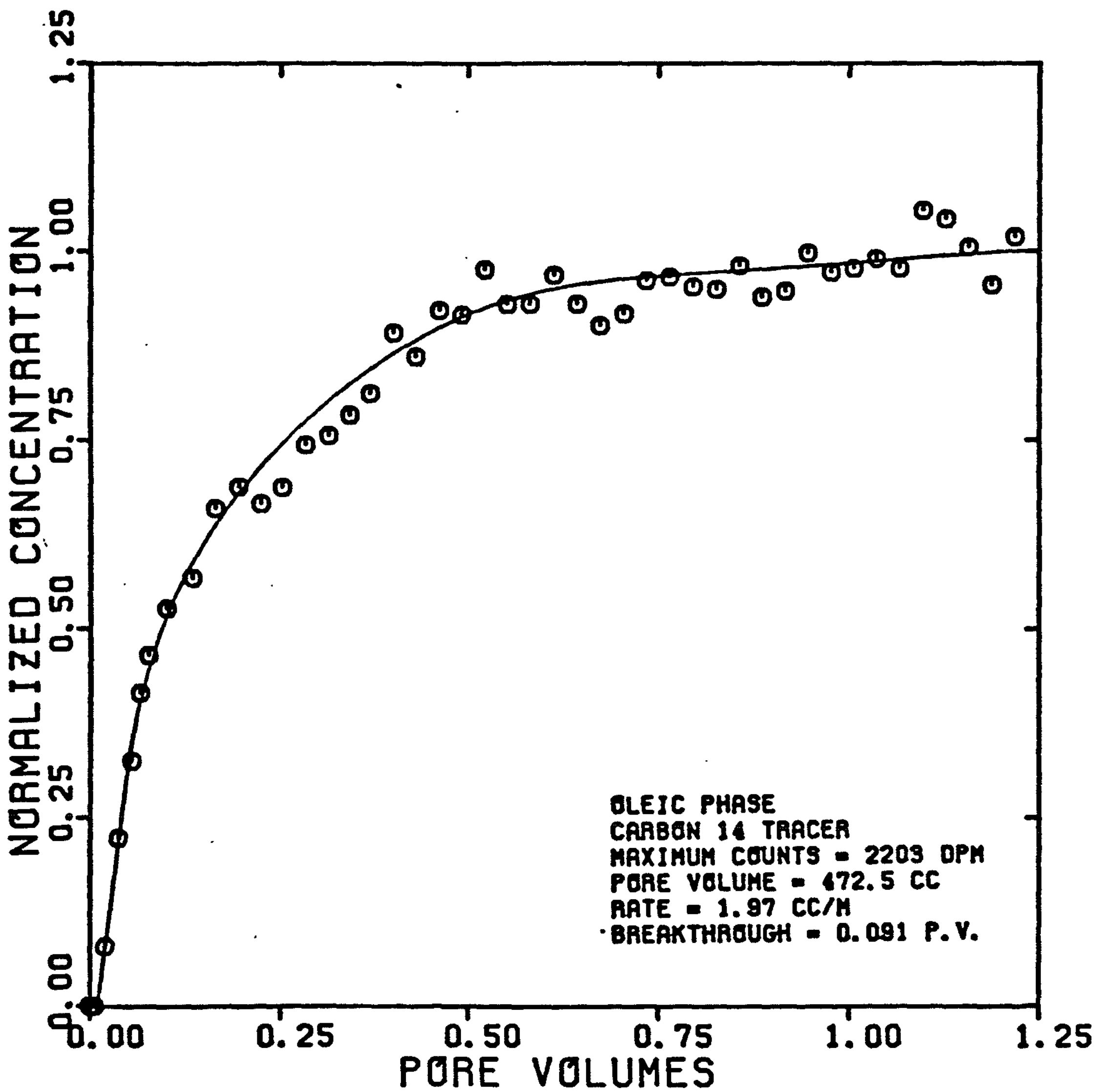

FIGURE 5.60

DISPERSIVITY OF CARBON 14
TRACER IN THE OLEIC PHASE
(EXPERIMENT OW4ZOL)

$S_o = 0.455 \quad f_o = 0.802$

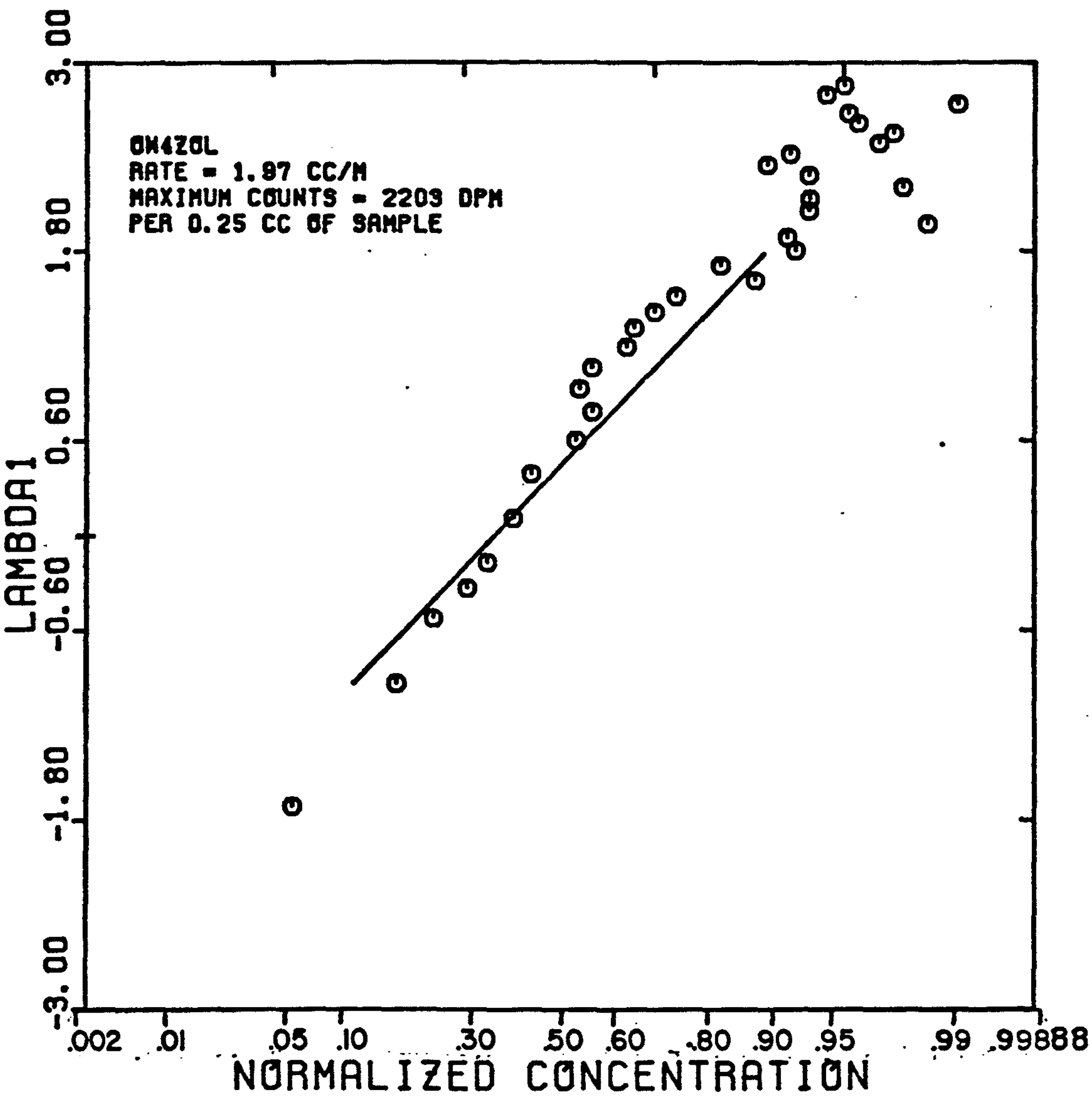

FIGURE 5.61

SANDPACK BREAKTHROUGH CURVE FOR TRITIUM
TRACER IN THE AQUEOUS PHASE
(EXPERIMENT OW5ZAQ)

$S_w = 0.652 \quad f_w = 0.300$

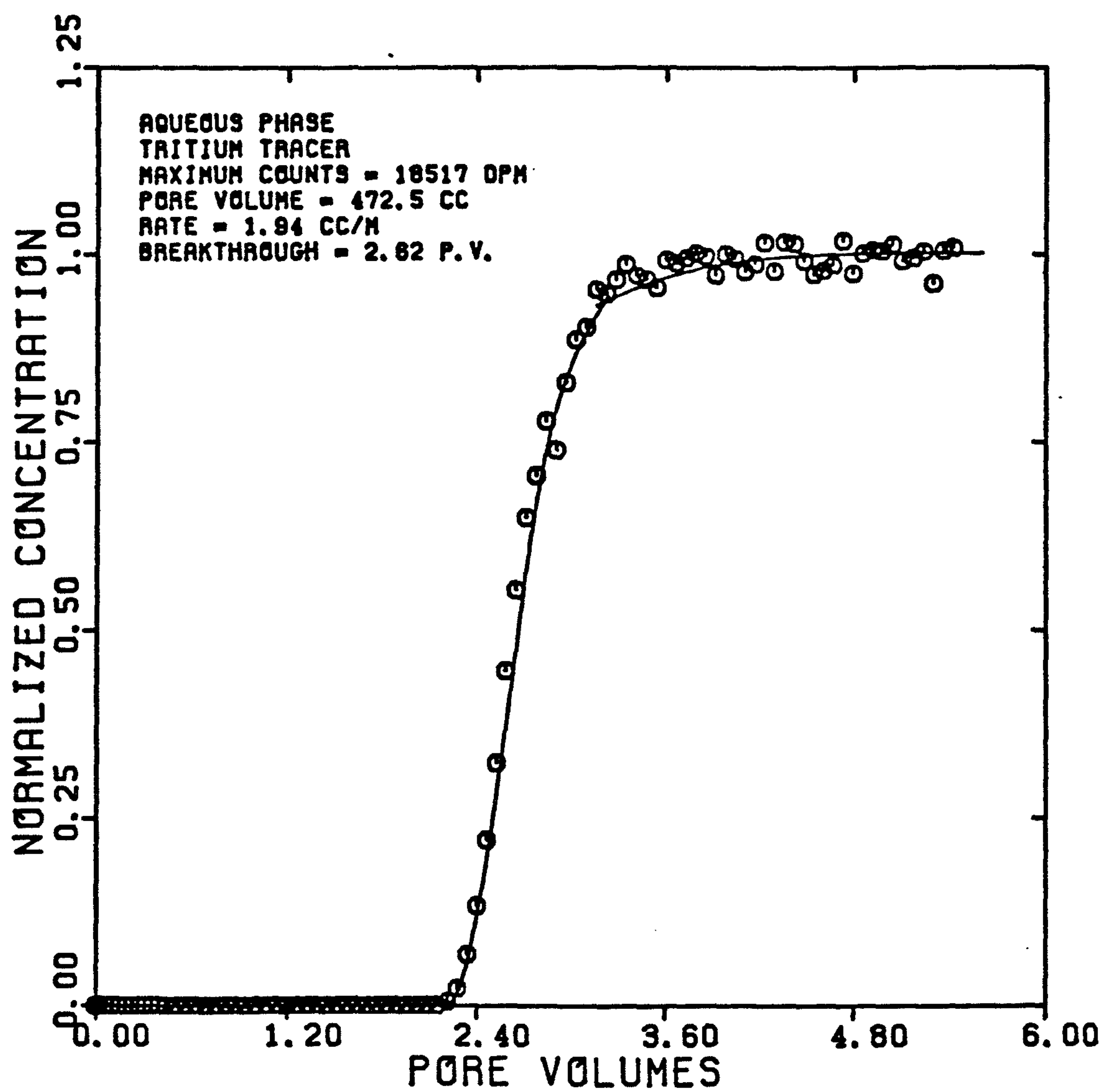

FIGURE 5.62

DISPERSIVITY OF TRITIUM
TRACER IN THE AQUEOUS PHASE
(EXPERIMENT OW5ZAQ)

$S_w = 0.652 \quad f_w = 0.300$

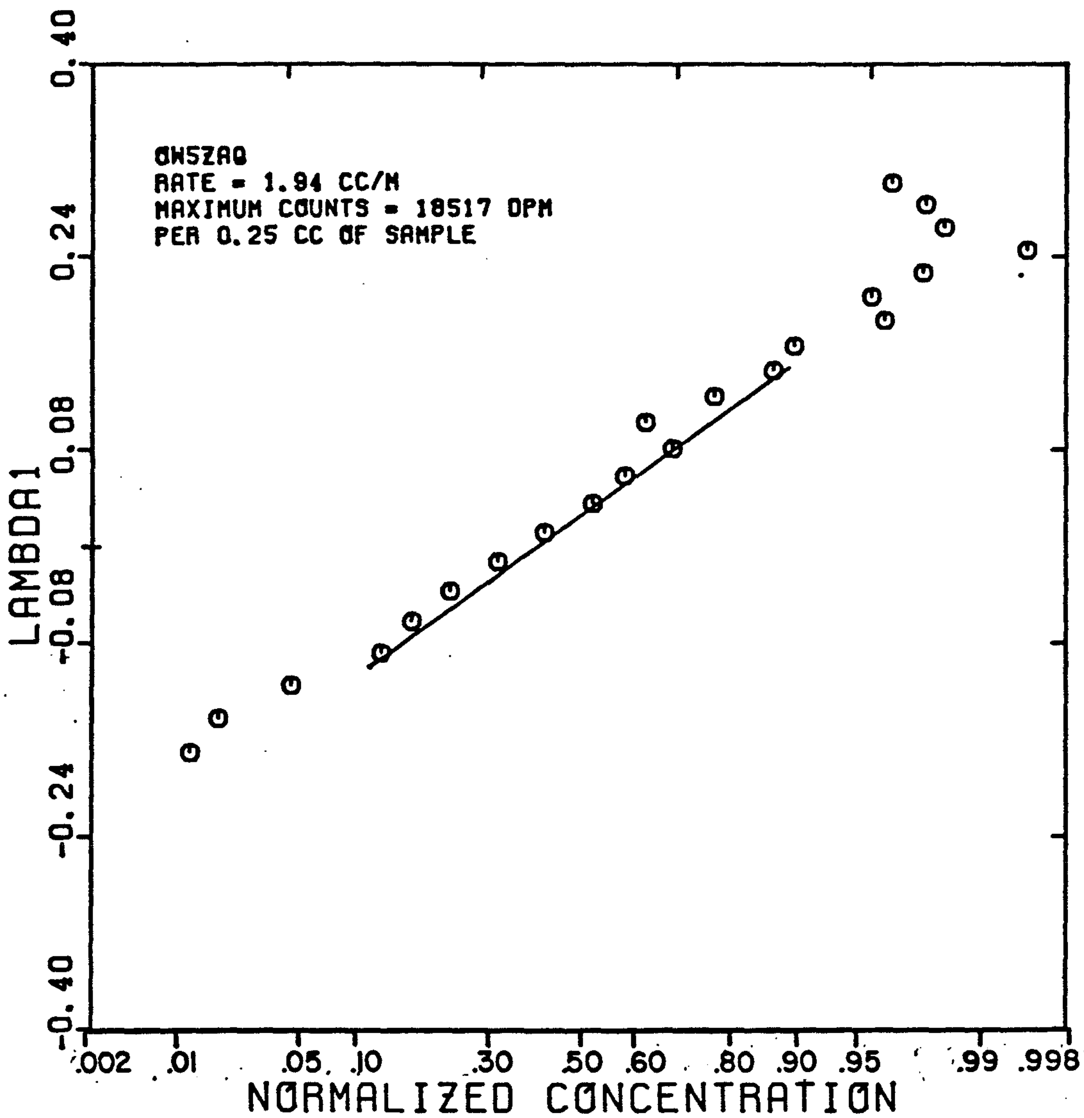

FIGURE 5.63

SANDPACK BREAKTHROUGH CURVE FOR CARBON 14
TRACER IN THE OLEIC PHASE
(EXPERIMENT OW5ZOL)

$S_o = 0.348 \quad f_o = 0.700$

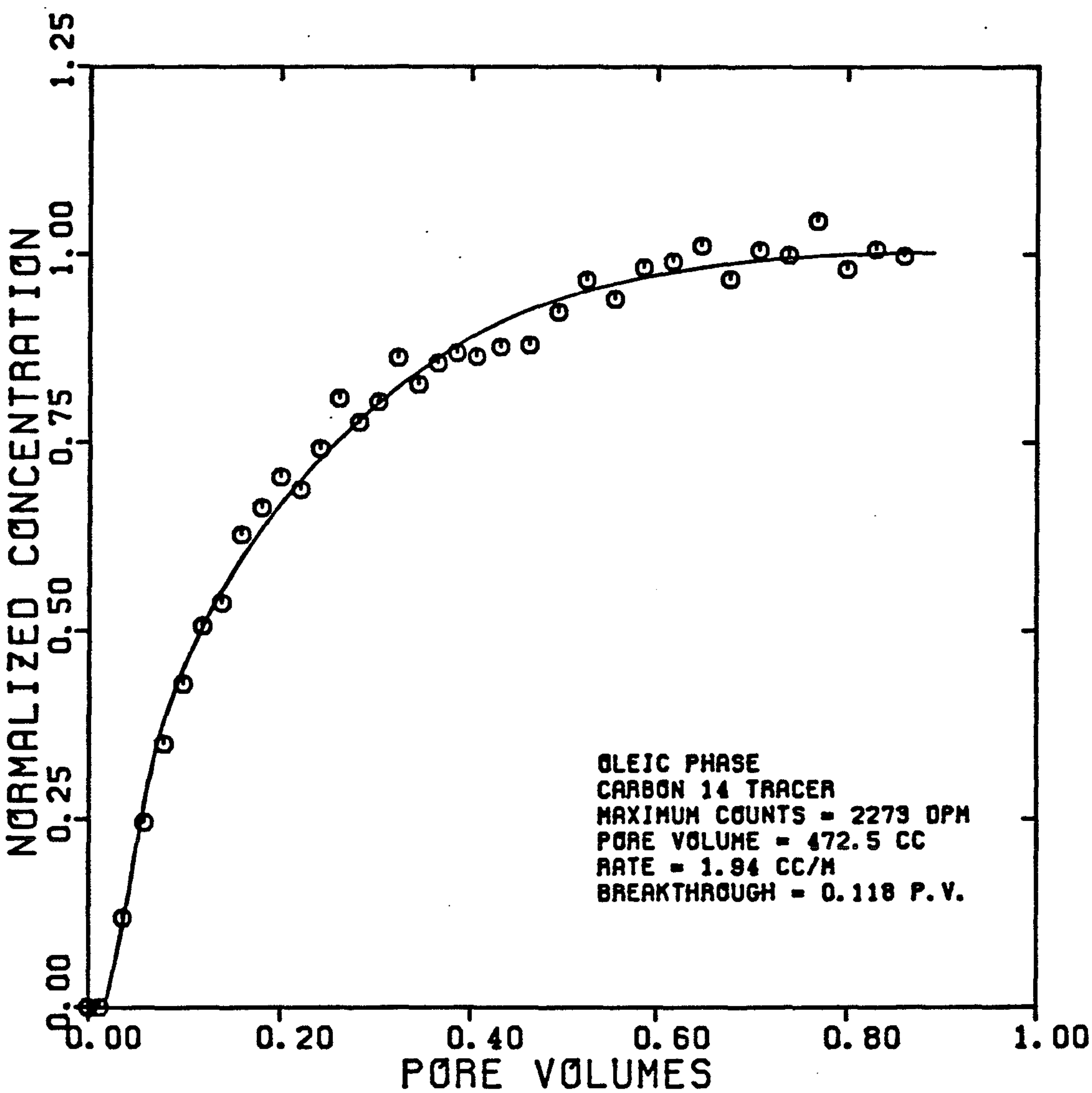

FIGURE 5.64

DISPERSIVITY OF CARBON 14
TRACER IN THE OLEIC PHASE
(EXPERIMENT OW5ZOL)

$S_o = 0.348 \quad f_o = 0.700$

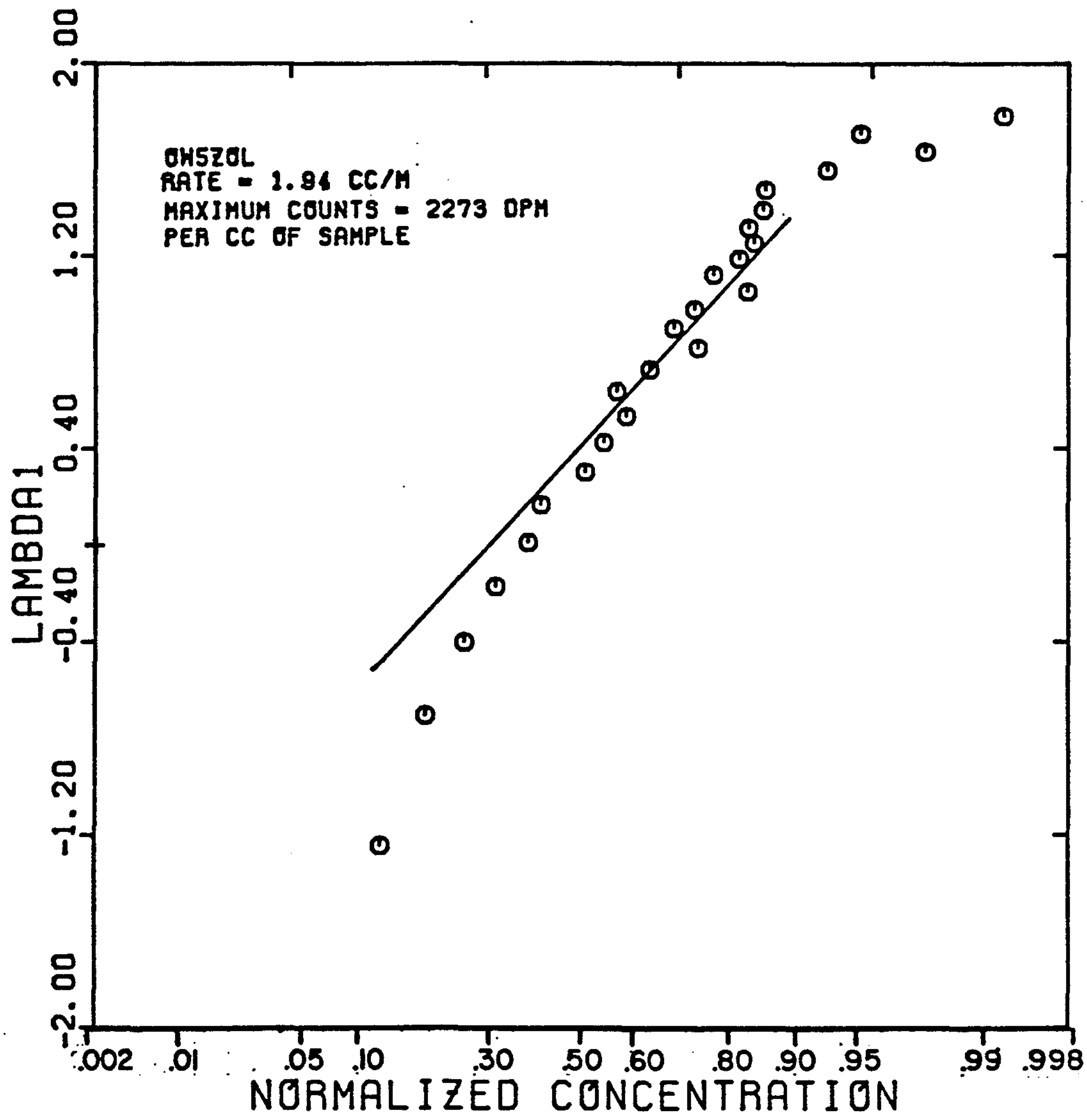

FIGURE 5.65

SANDPACK BREAKTHROUGH CURVE FOR TRITIUM
TRACER IN THE AQUEOUS PHASE
(EXPERIMENT OW6ZAQ)

$S_w = 0.756 \quad f_w = 0.512$

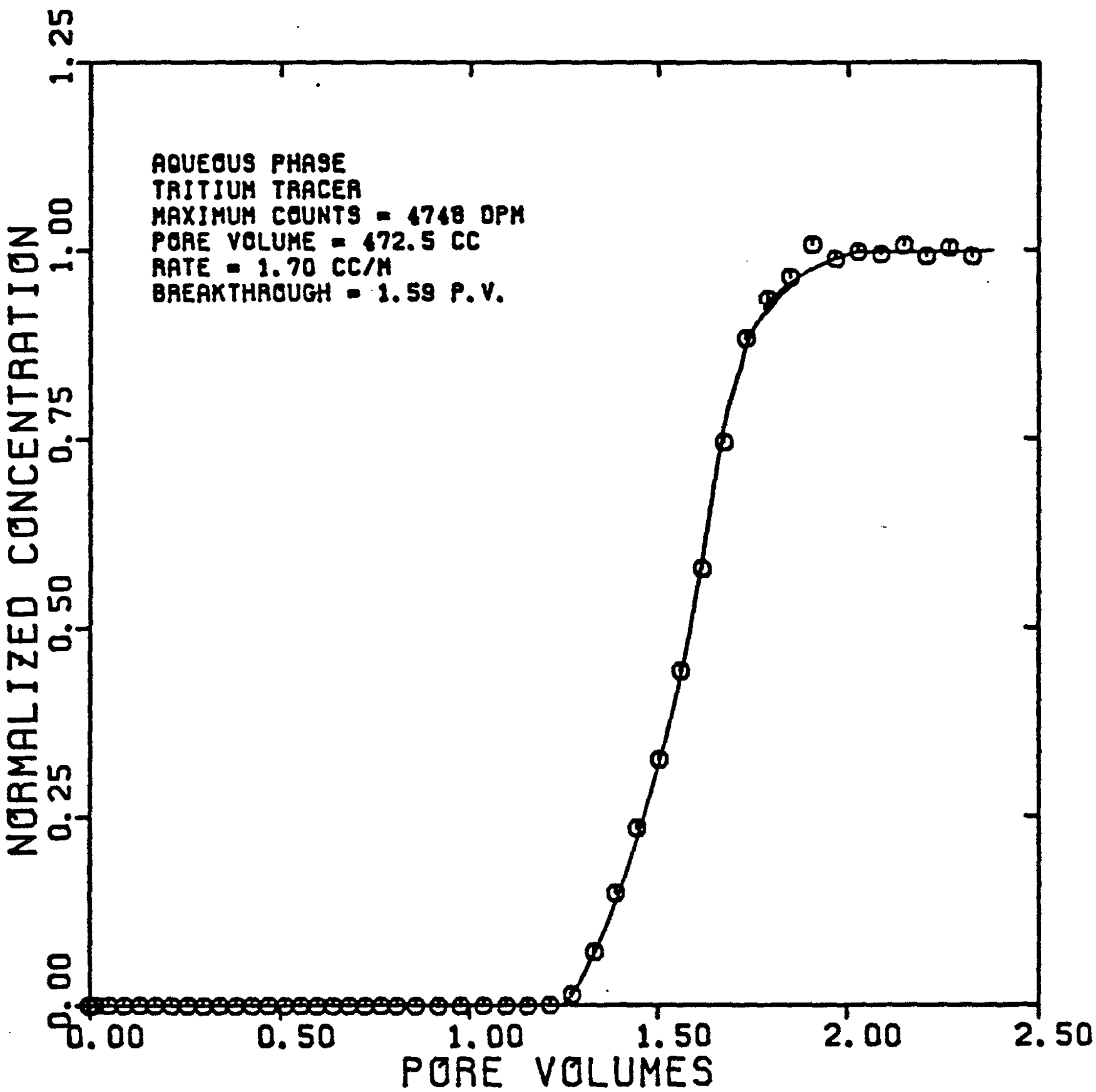

FIGURE 5.66

DISPERSIVITY OF TRITIUM
TRACER IN THE AQUEOUS PHASE
(EXPERIMENT OW6ZAQ)

$S_w = 0.756 \quad f_w = 0.512$

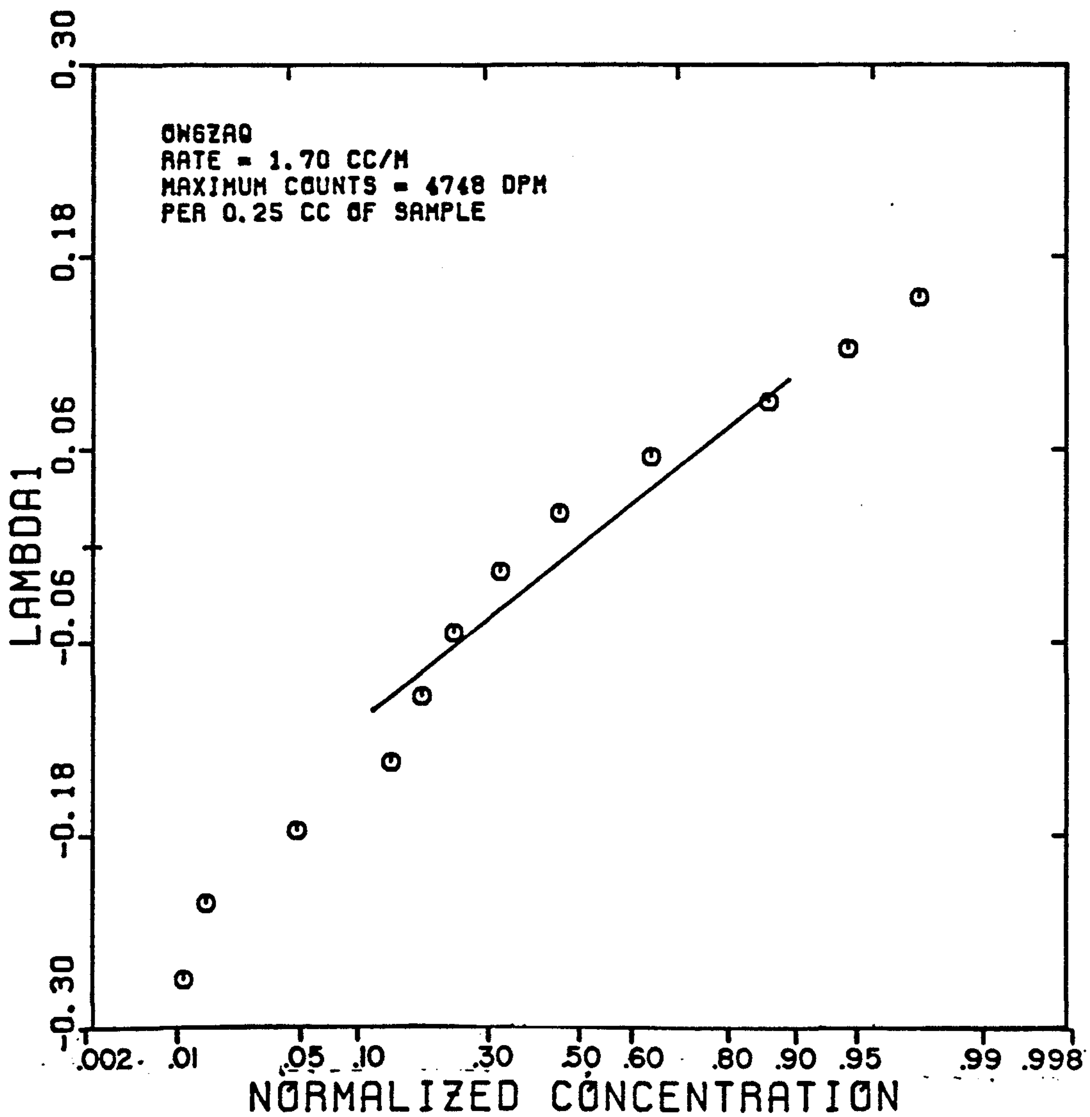

FIGURE 5.67

SANDPACK BREAKTHROUGH CURVE FOR CARBON 14
TRACER IN THE OLEIC PHASE
(EXPERIMENT OW6ZOL)

S_o = 0.244 f_o = 0.488

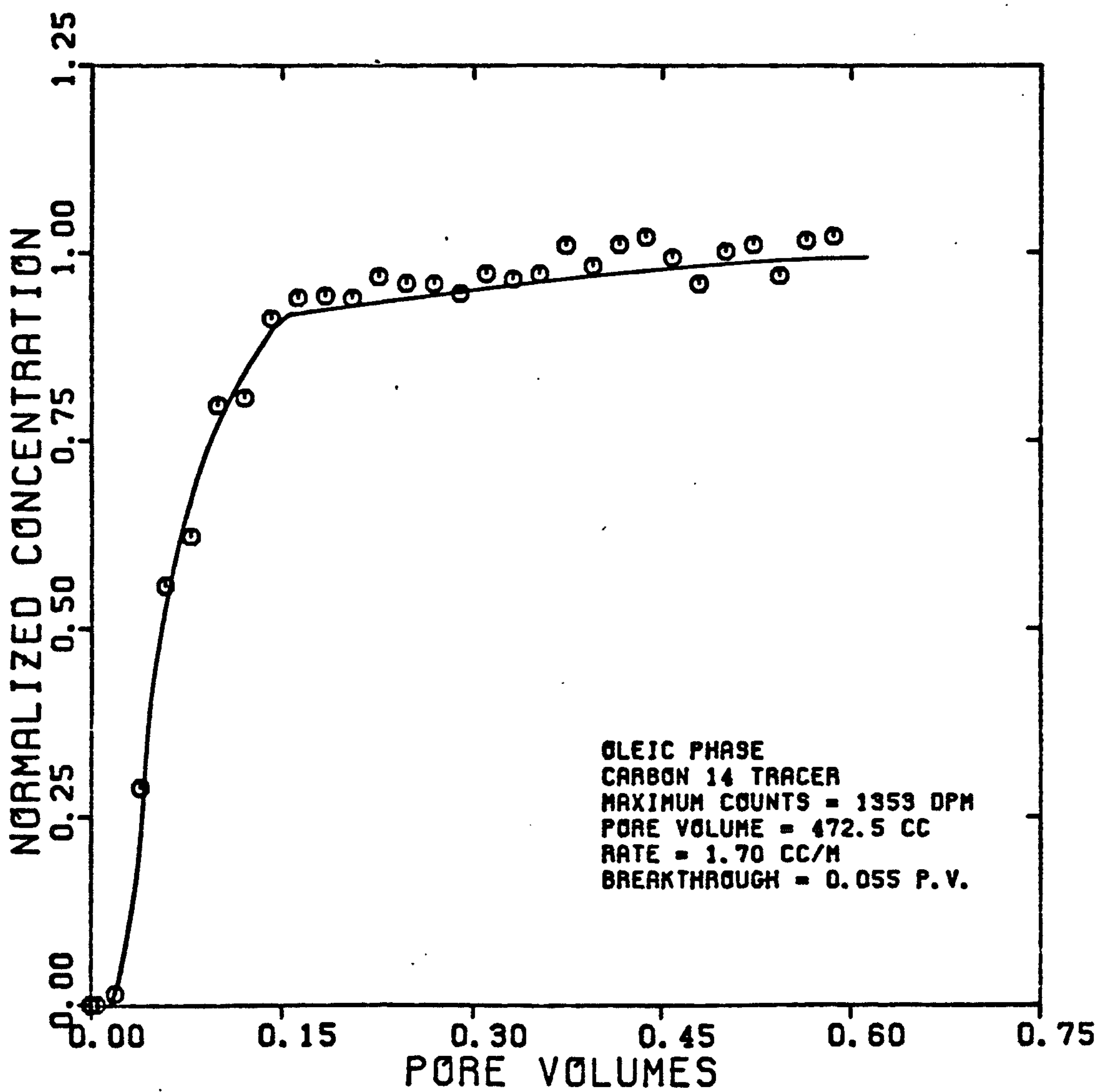

FIGURE 5.68

DISPERSIVITY OF CARBON 14
TRACER IN THE OLEIC PHASE
(EXPERIMENT OW6ZOL)

$S_o = 0.244 \quad f_o = 0.488$

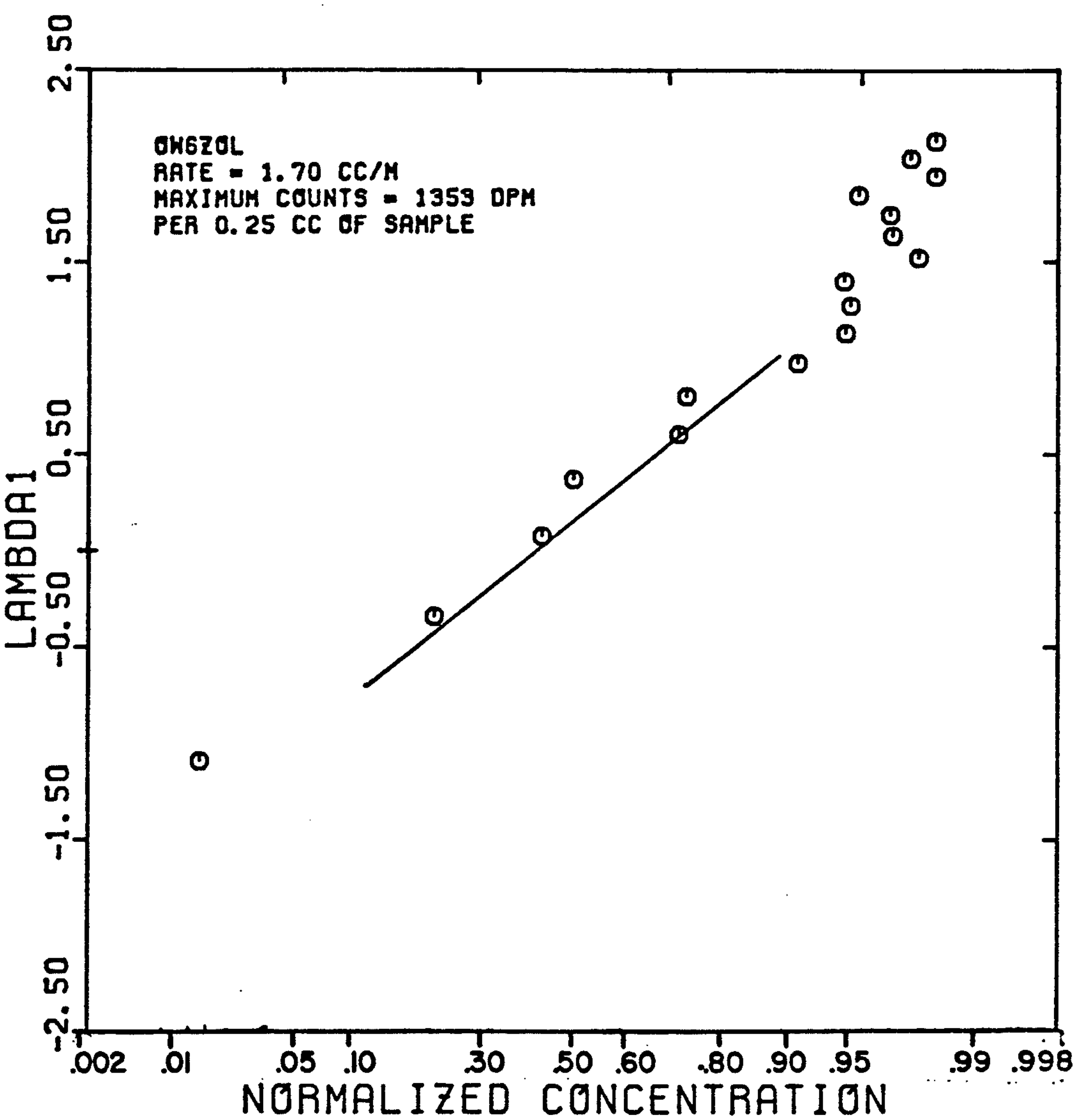

FIGURE 5.69

SANDPACK BREAKTHROUGH CURVE FOR TRITIUM
TRACER IN THE AQUEOUS PHASE
(EXPERIMENT OW7ZAQ)

$S_w = 0.854 \quad f_w = 0.761$

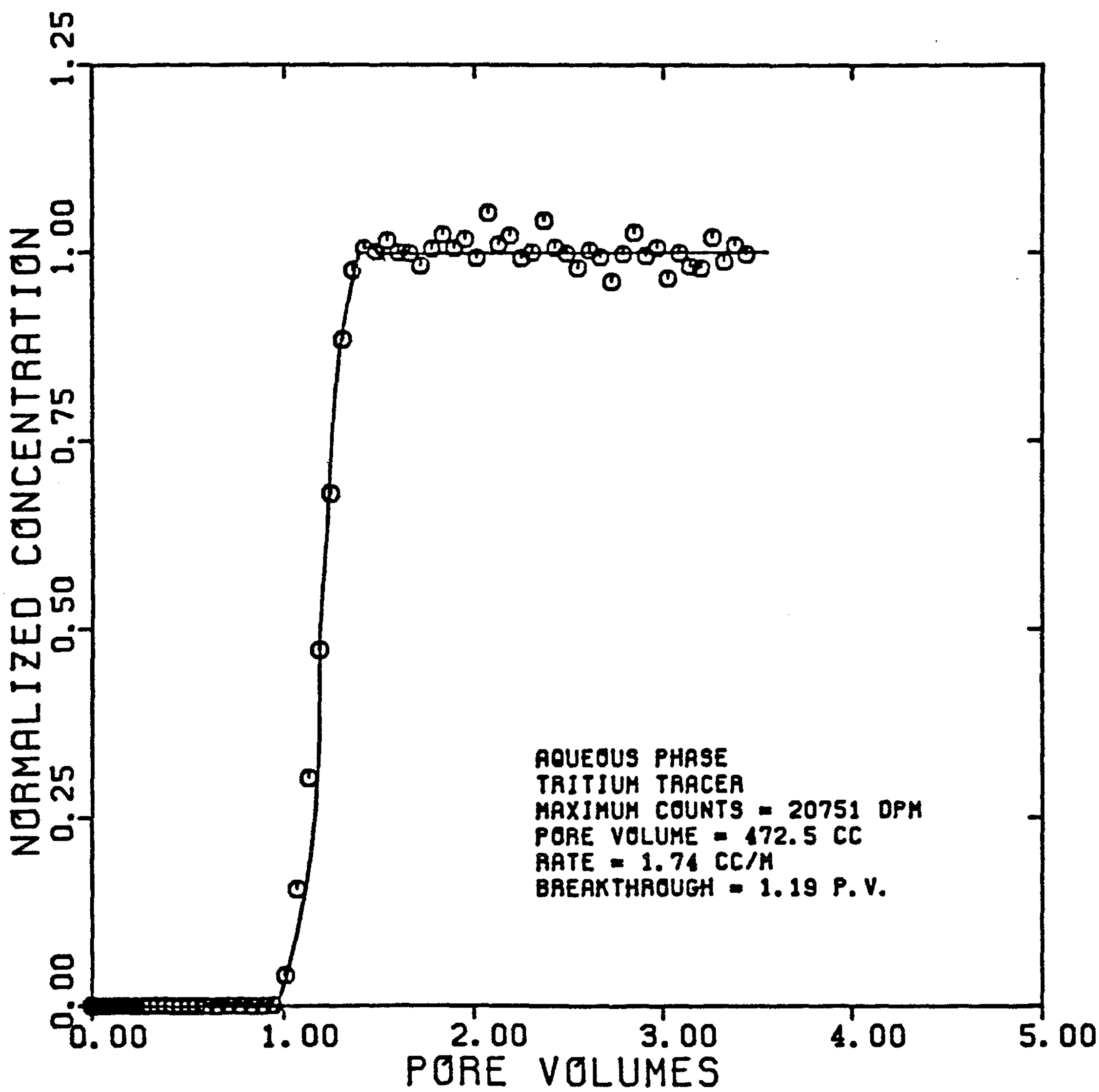

FIGURE 5.70

DISPERSIVITY OF TRITIUM
TRACER IN THE AQUEOUS PHASE
(EXPERIMENT OW7ZAQ)

$S_w = 0.854 \quad f_w = 0.761$

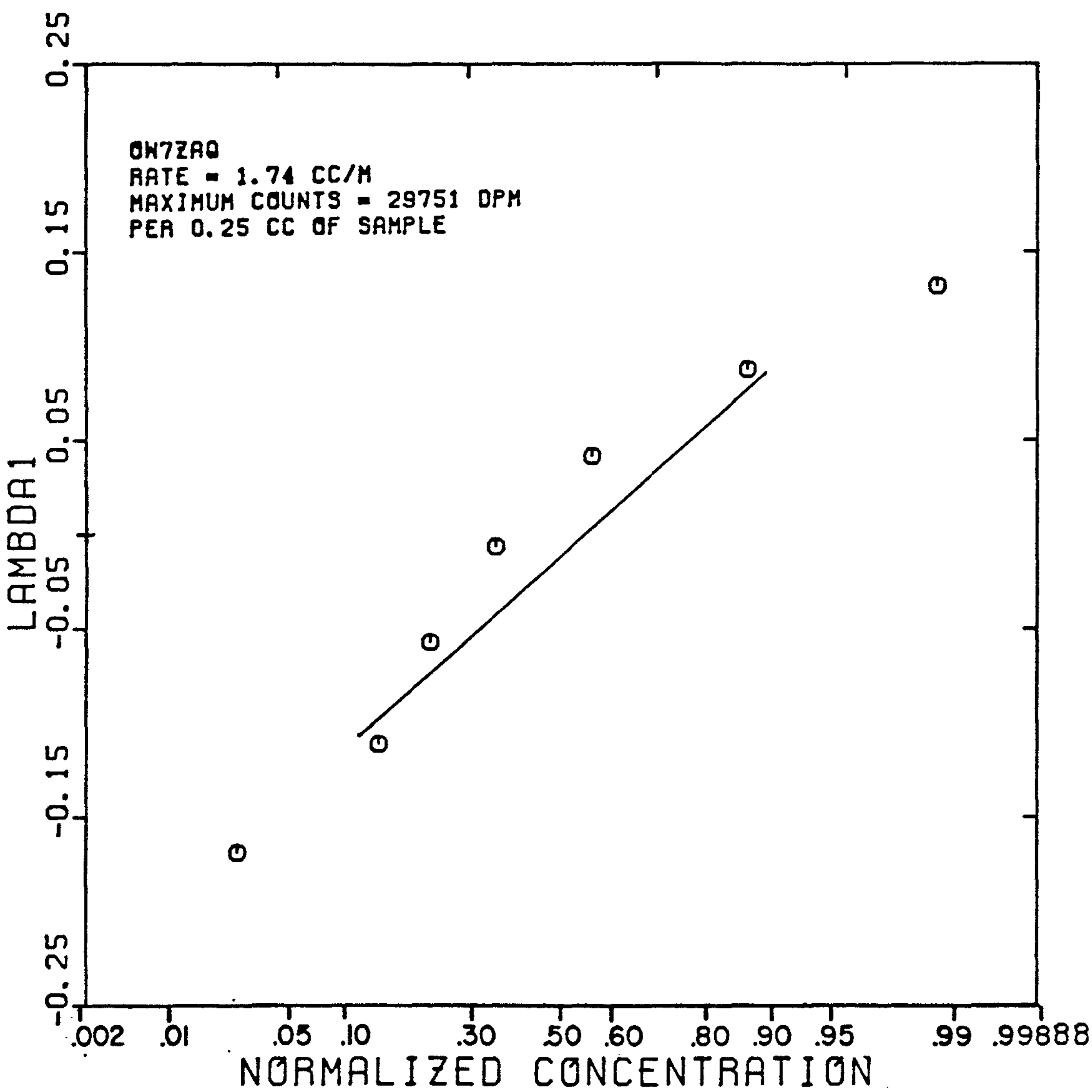

FIGURE 5.71

SANDPACK BREAKTHROUGH CURVE FOR CARBON 14
TRACER IN THE OLEIC PHASE
(EXPERIMENT OW7ZOL)

$S_o = 0.146 \quad f_o = 0.239$

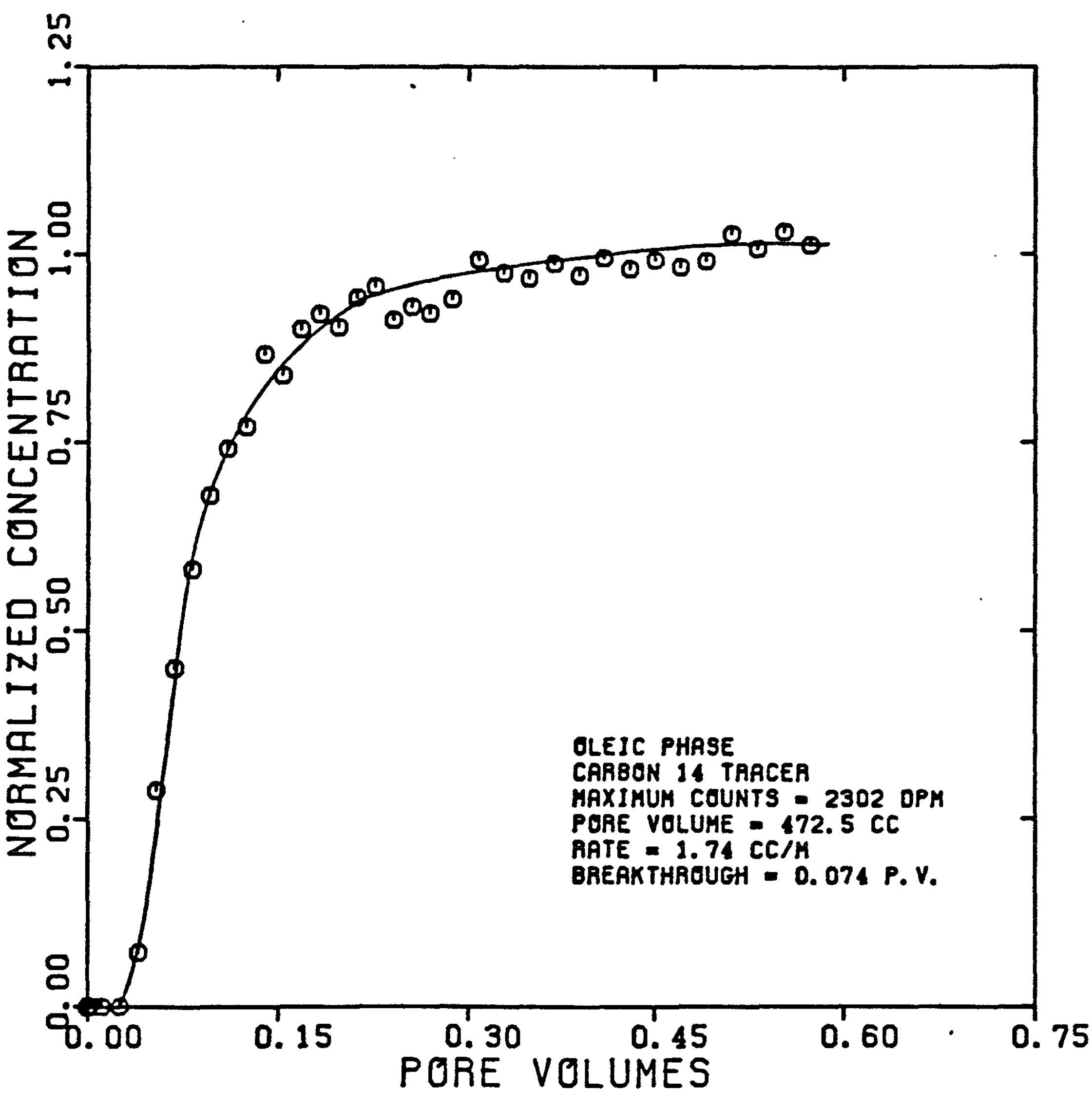

FIGURE 5.72

DISPERSIVITY OF CARBON 14
TRACER IN THE OLEIC PHASE
(EXPERIMENT OW7ZOL)

$S_o = 0.146 \quad f_o = 0.239$

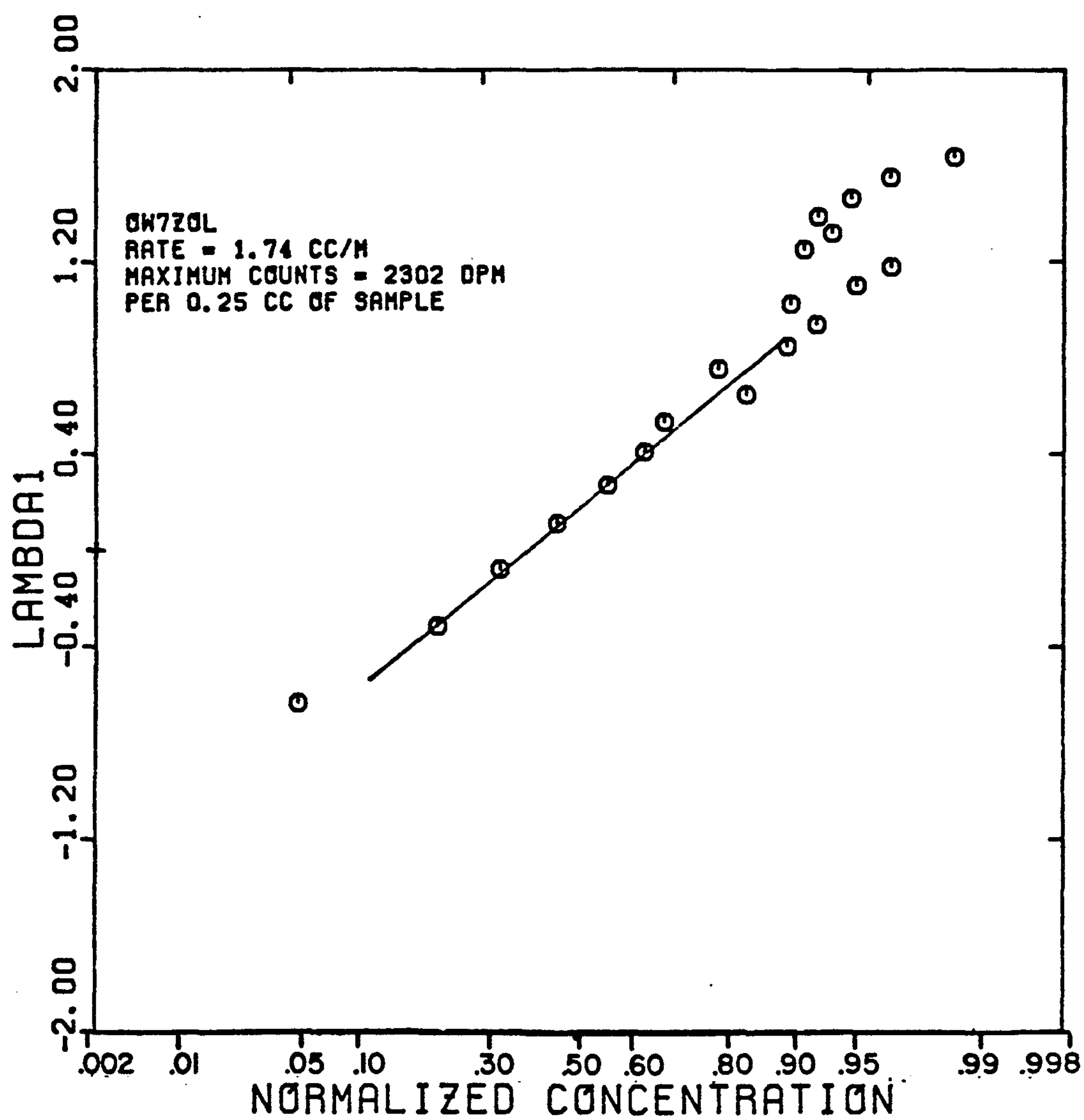

FIGURE 5.73

SANDPACK BREAKTHROUGH CURVE FOR TRITIUM TRACER IN THE AQUEOUS PHASE (EXPERIMENT OW8Z)

$S_w = 0.889 \quad f_w = 1.0$

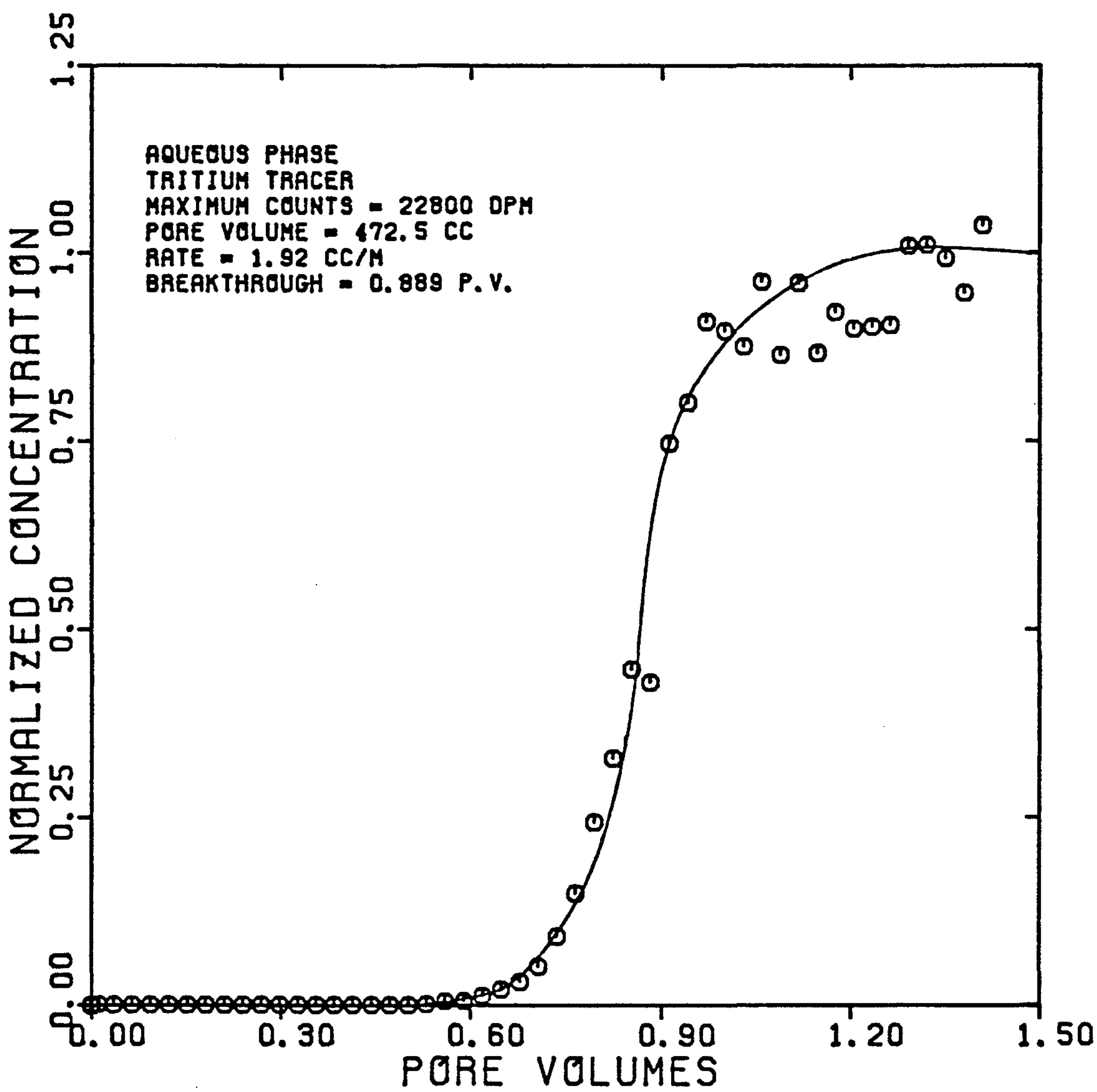

FIGURE 5.74

DISPERSIVITY OF TRITIUM
TRACER IN THE AQUEOUS PHASE
(EXPERIMENT OW8Z)

$S_w = 0.889 \quad f_w = 1.0$

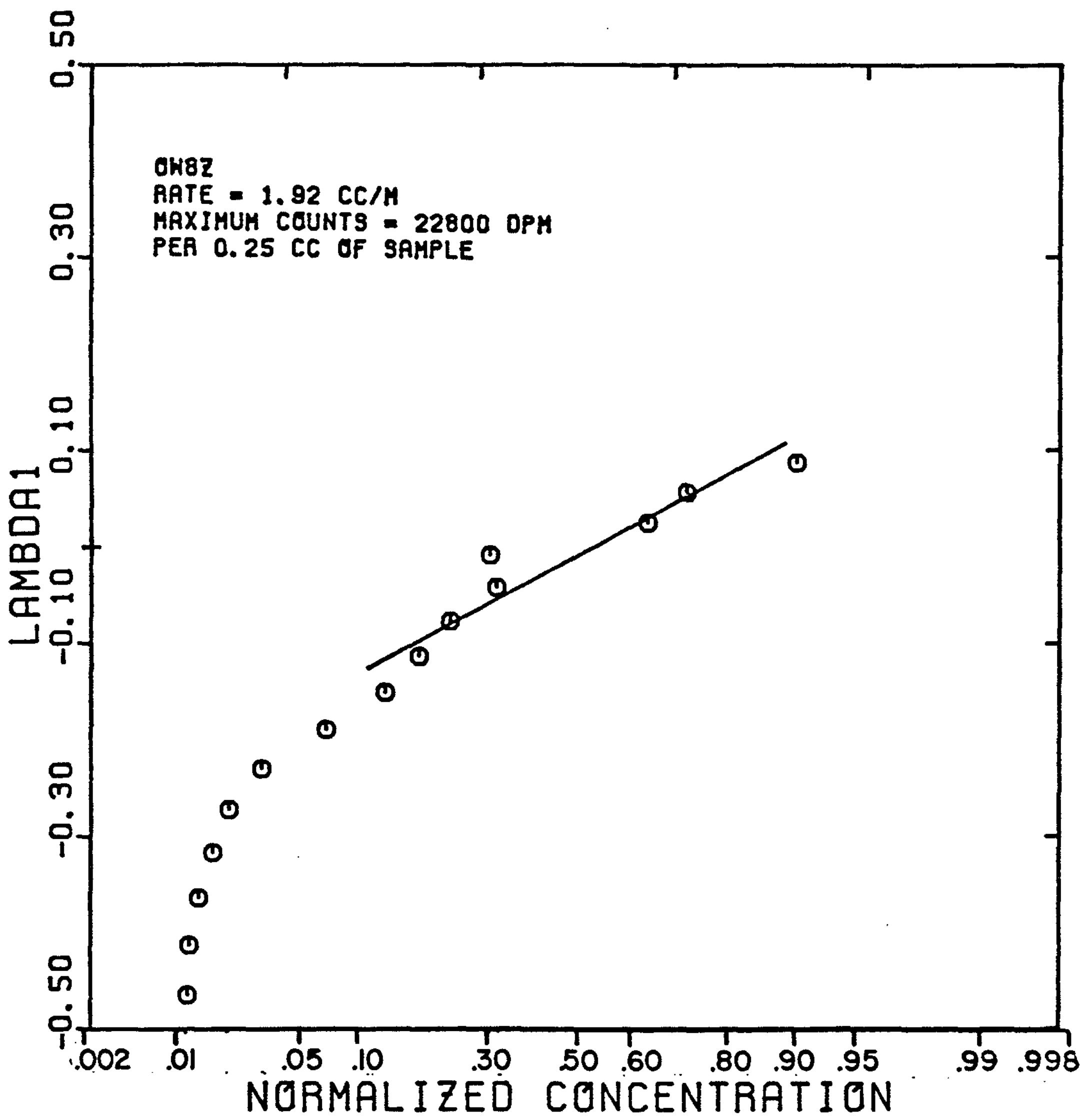

FIGURE 5.75

DISPERSIVITY OF BRINE AND N-DECANE
IN UNCONSOLIDATED SAND

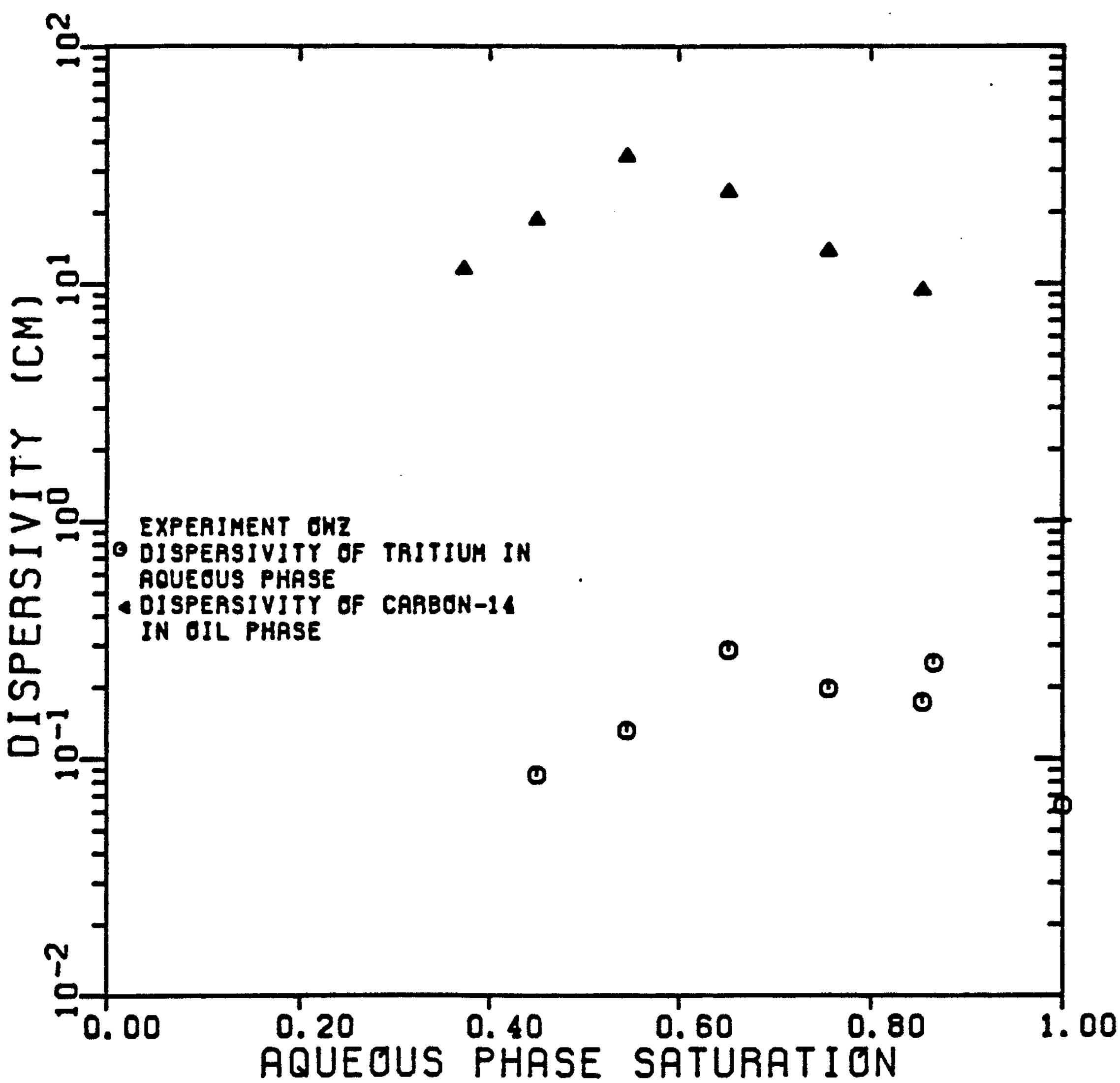

FIGURE 5.76

RELATIVE PERMEABILITY OF MICROEMULSION
AND OIL IN UNCONSOLIDATED SAND

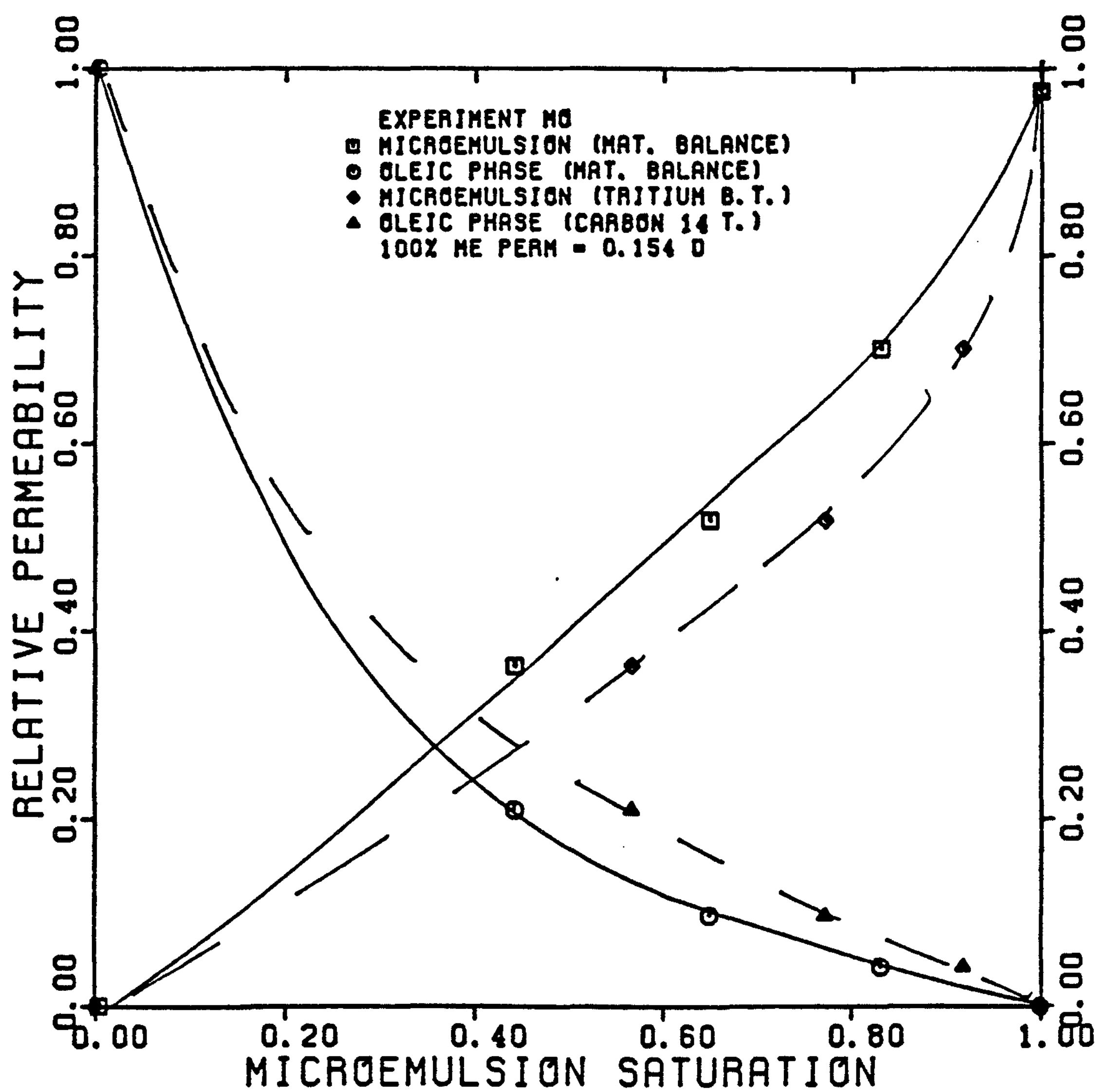

FIGURE 5.77

RELATIVE PERMEABILITY FOR HIGH AND LOW IFT SYSTEMS IN UNCONSOLIDATED SAND (EXPERIMENTS OWZ AND MO)

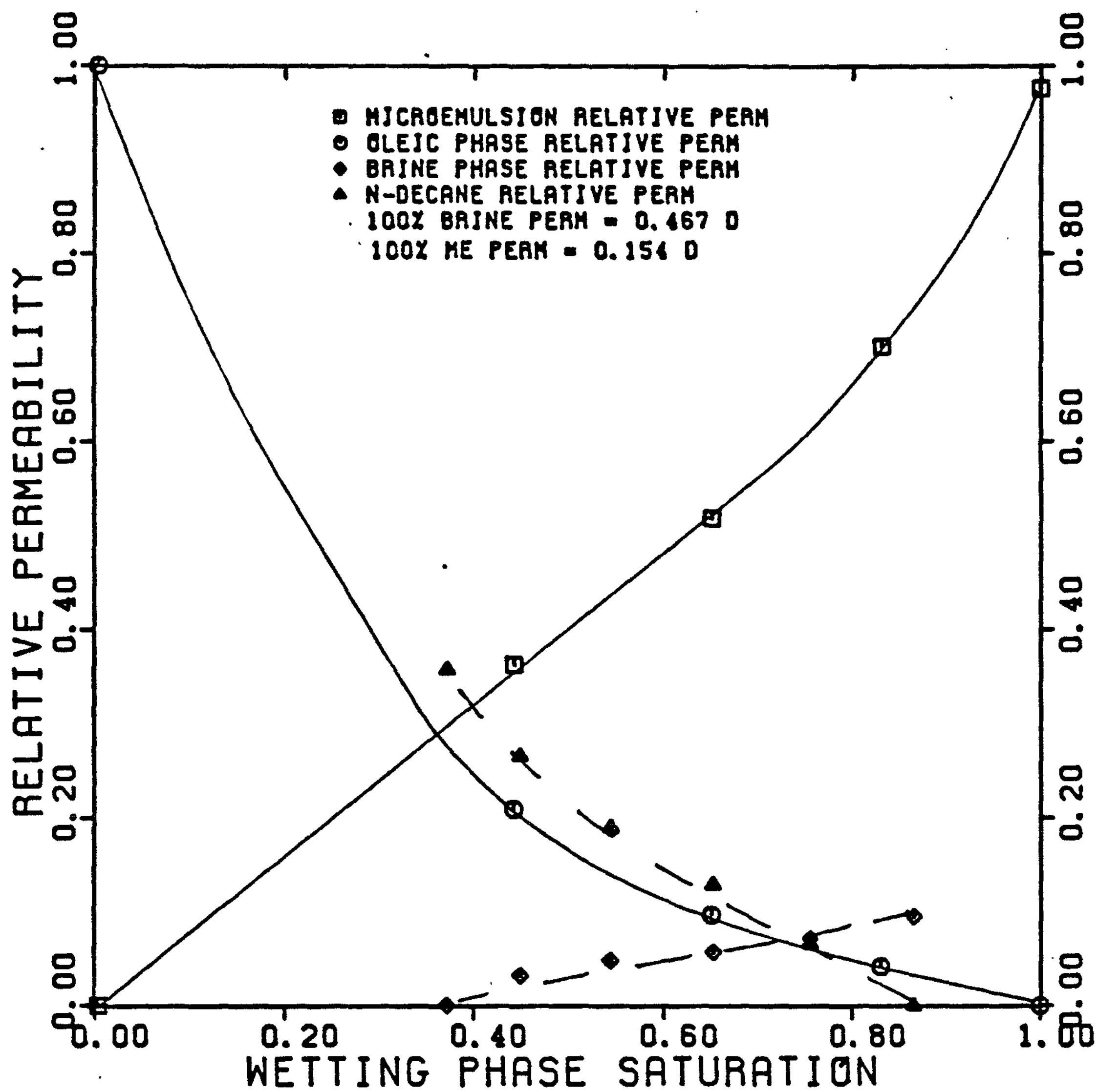

FIGURE 5.78

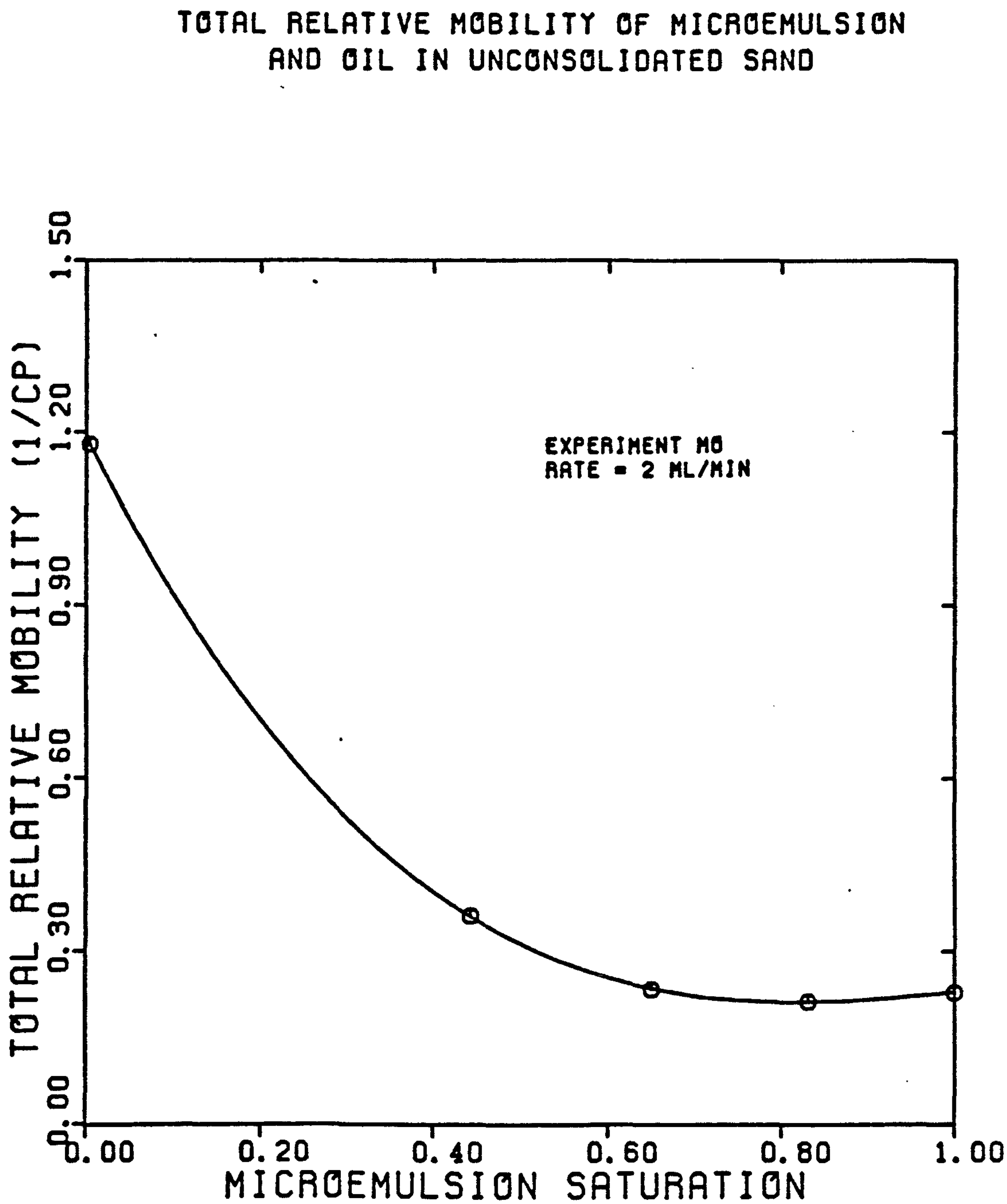
TOTAL RELATIVE MOBILITY OF MICROEMULSION
AND OIL IN UNCONSOLIDATED SAND
EXPERIMENT M8
RATE = 2 ML/MIN
TOTAL RELATIVE MOBILITY (1/CP)
0.00
0.30
0.60
0.90
1.20
1.50
0.00
0.20
0.40
0.60
0.80
1.00
MICROEMULSION SATURATION

FIGURE 5.79

FRACTIONAL FLOW FOR THE MICROEMULSION
PHASE IN UNCONSOLIDATED SAND
(EXPERIMENT MO)

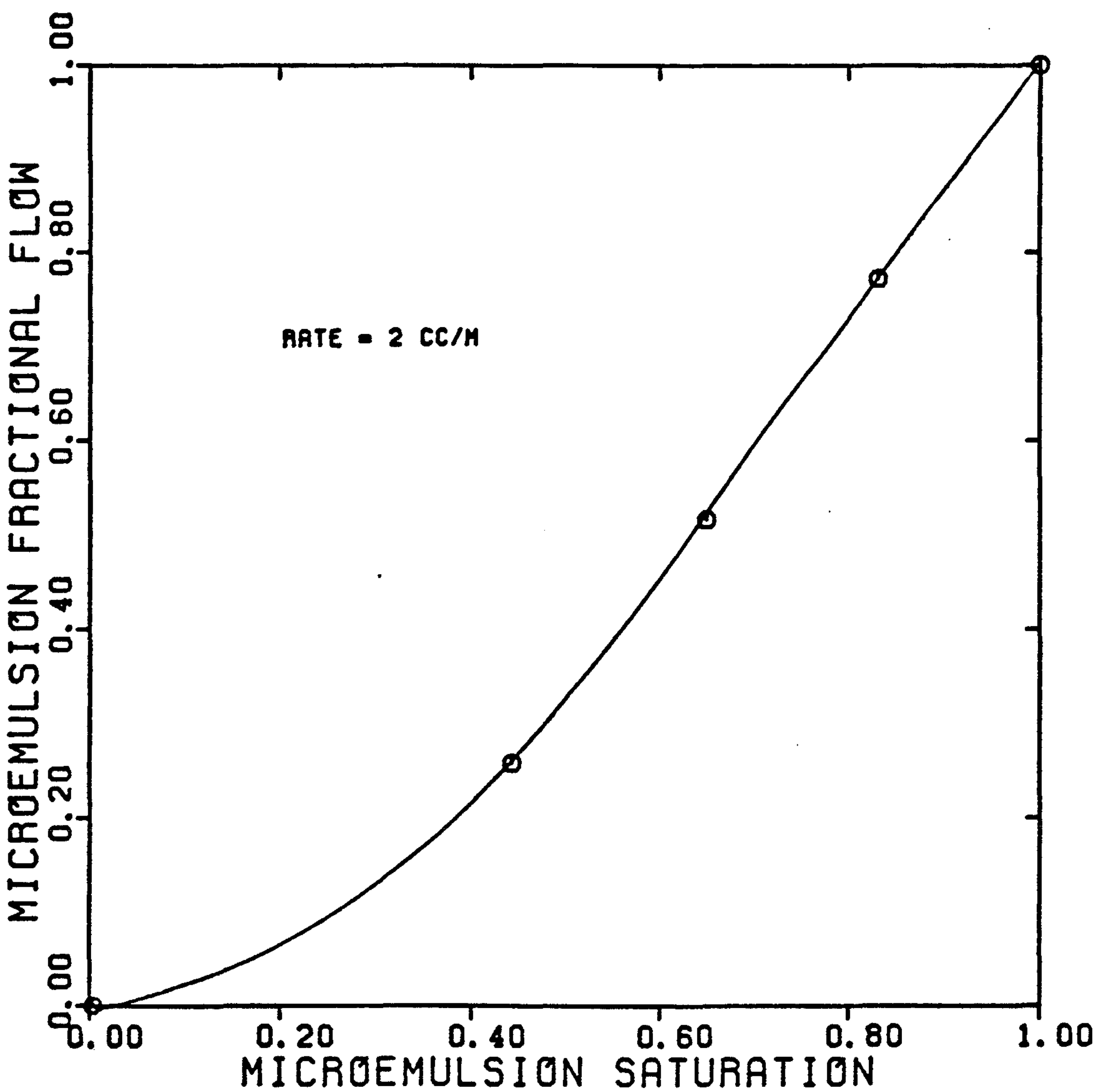

FIGURE 5.80

FRACTIONAL FLOW OF HIGH AND LOW IFT
SYSTEMS IN UNCONSOLIDATED SAND
(EXPERIMENTS OWZ AND MO)

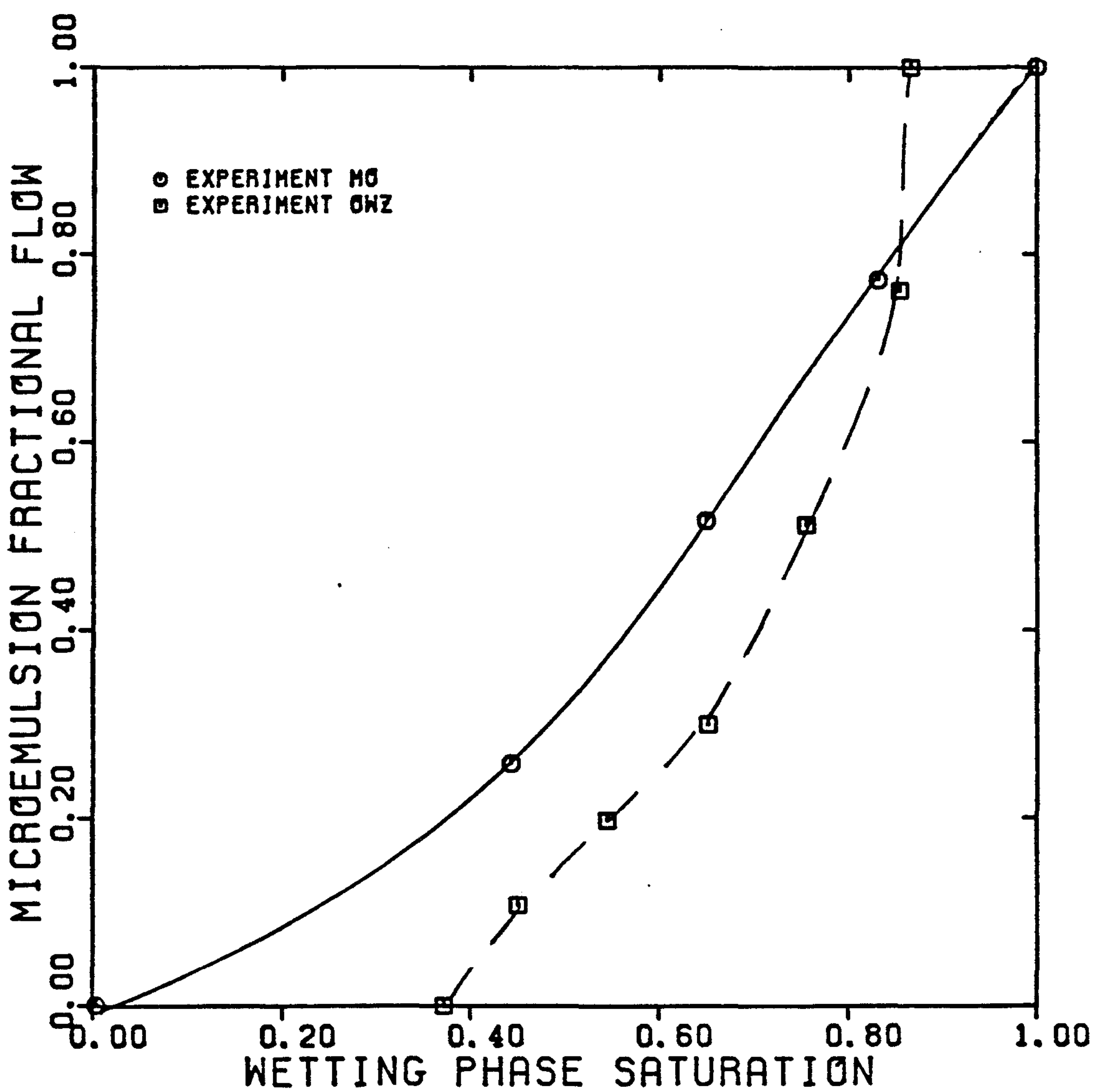

FIGURE 5.81

SANDPACK BREAKTHROUGH CURVE FOR TRITIUM TRACER IN THE MICROEMULSION PHASE (EXPERIMENT M01)

$S_{me} = 1.0 \quad f_{me} = 1.0$

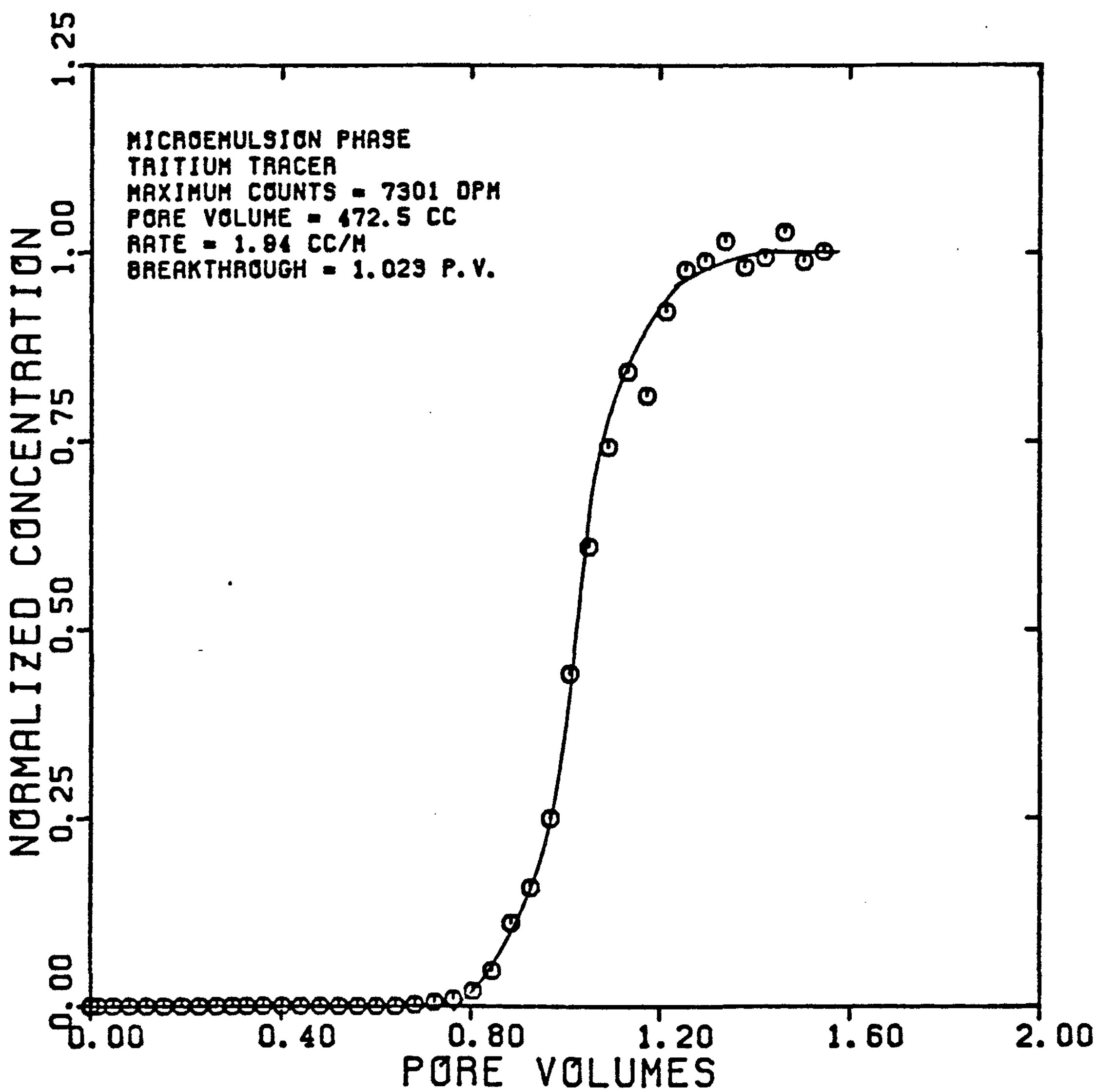

FIGURE 5.82

DISPERSIVITY OF TRITIUM
TRACER IN THE MICROEMULSION PHASE
(EXPERIMENT MO1)

$S_{me} = 1.0 \quad f_{me} = 1.0$

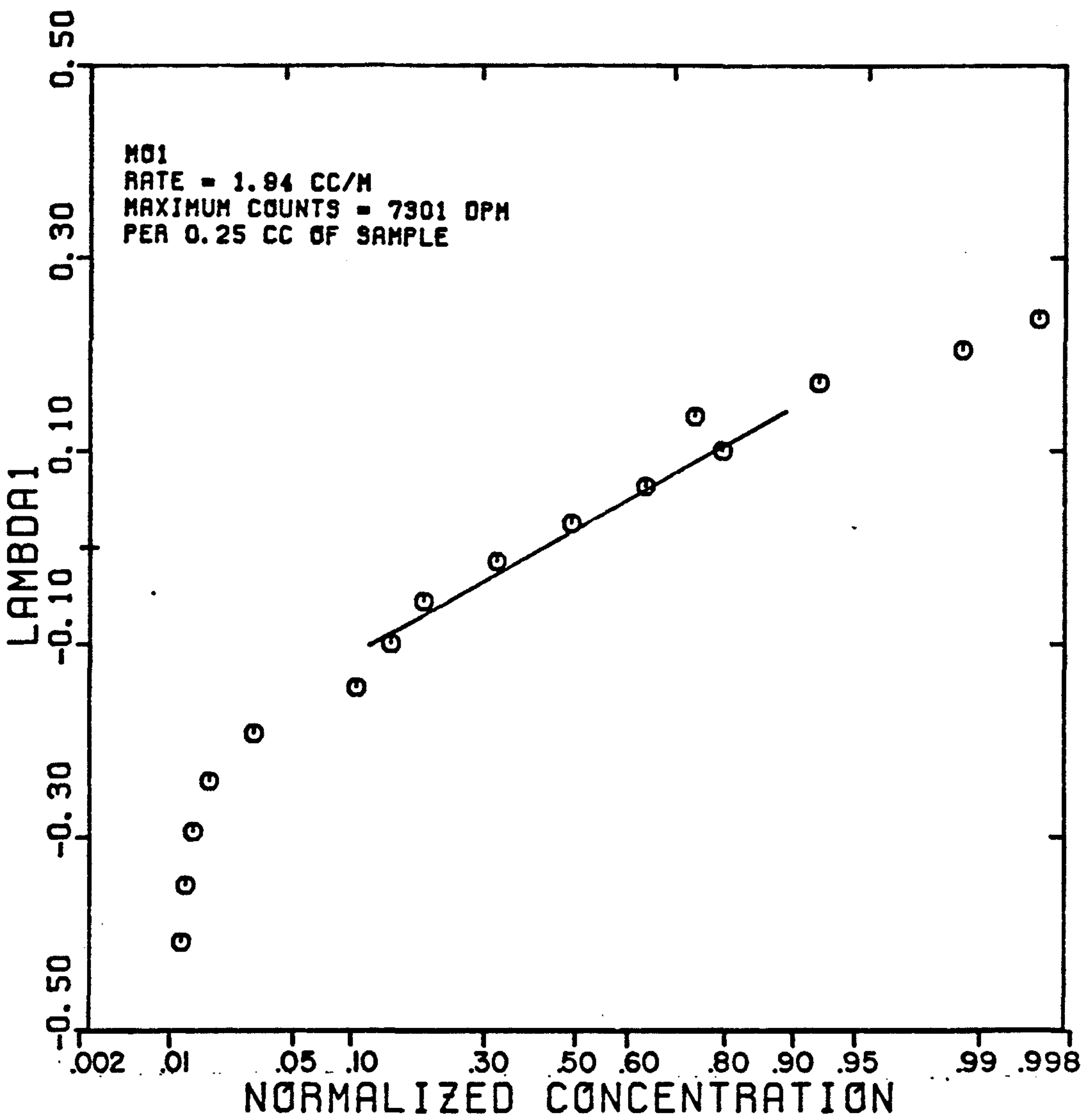

FIGURE 5.83

SANDPACK BREAKTHROUGH CURVE FOR TRITIUM TRACER IN THE MICROEMULSION PHASE (EXPERIMENT M02L0)

S_{me} = 0.831 f_{me} = 0.772

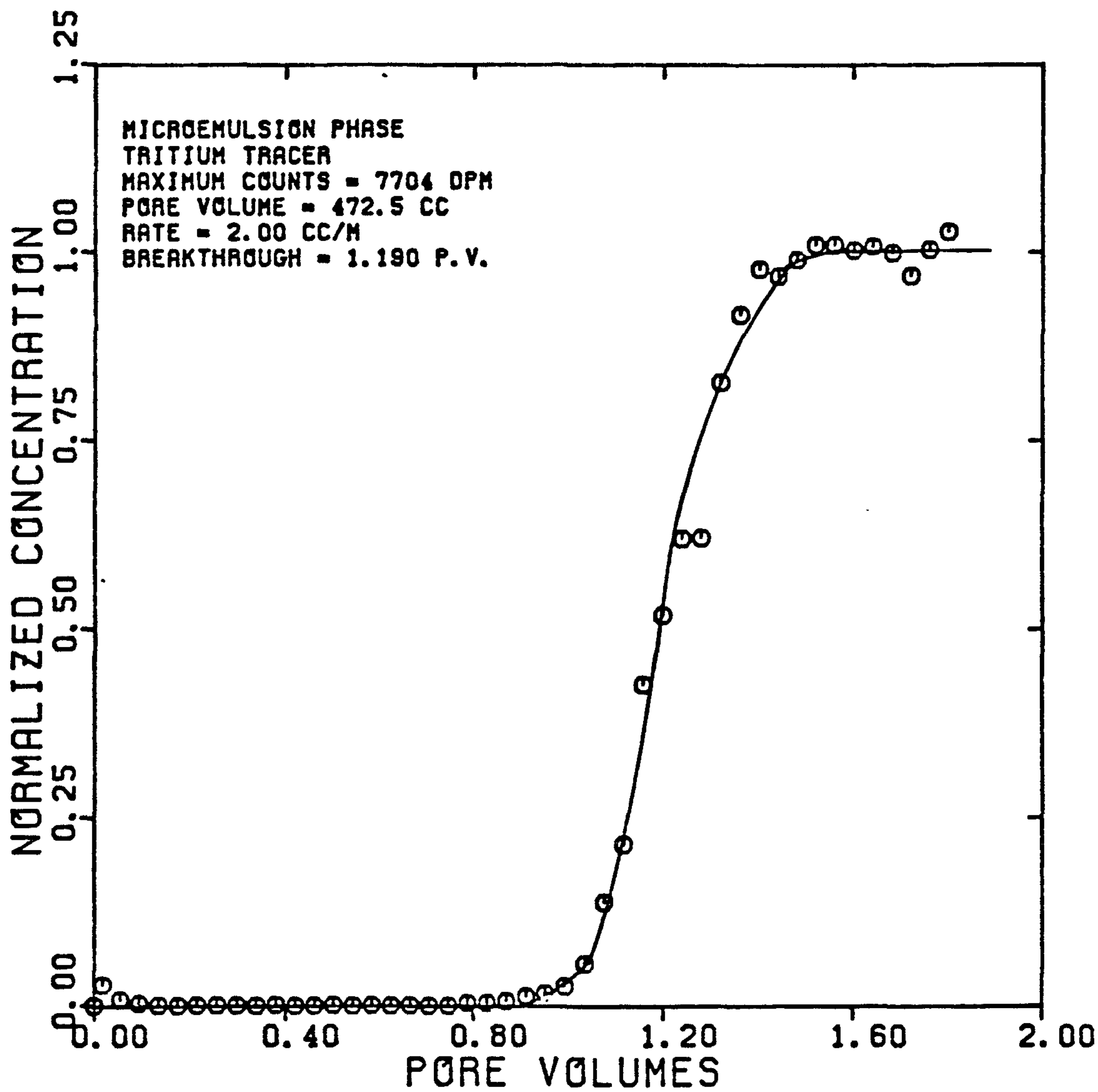

FIGURE 5.84

DISPERSIVITY OF TRITIUM
TRACER IN THE MICROEMULSION PHASE
(EXPERIMENT M02L0)

$S_{me} = 0.831 \quad f_{me} = 0.772$

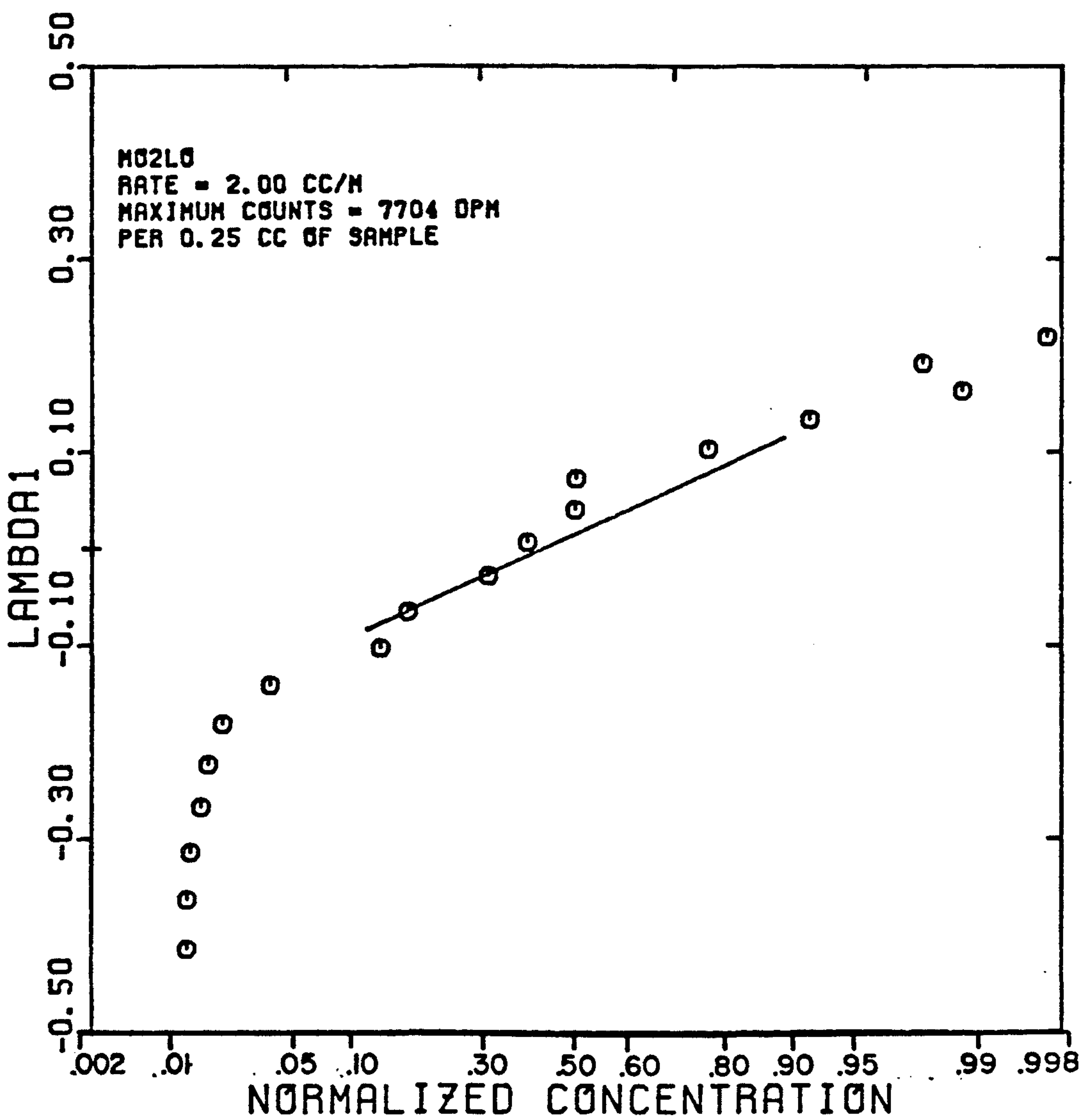

FIGURE 5.85

SANDPACK BREAKTHROUGH CURVE FOR CARBON 14
TRACER IN THE MICROEMULSION PHASE
(EXPERIMENT M02PART)

S_{me} = 0.831 f_{me} = 0.772

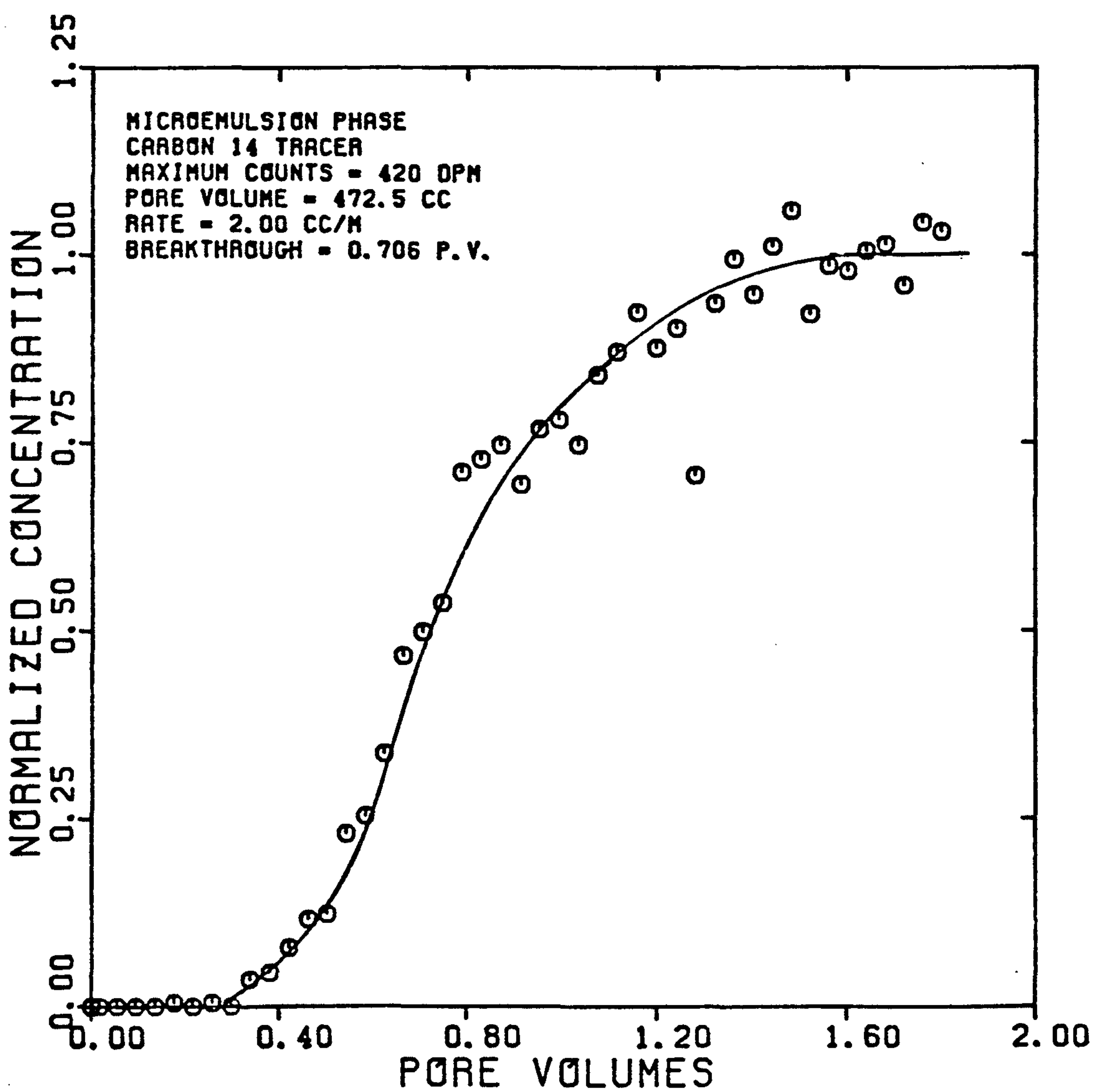

FIGURE 5.86

DISPERSIVITY OF CARBON 14
TRACER IN THE MICROEMULSION PHASE
(EXPERIMENT MO2PART)

S_{me} = 0.831 f_{me} = 0.772

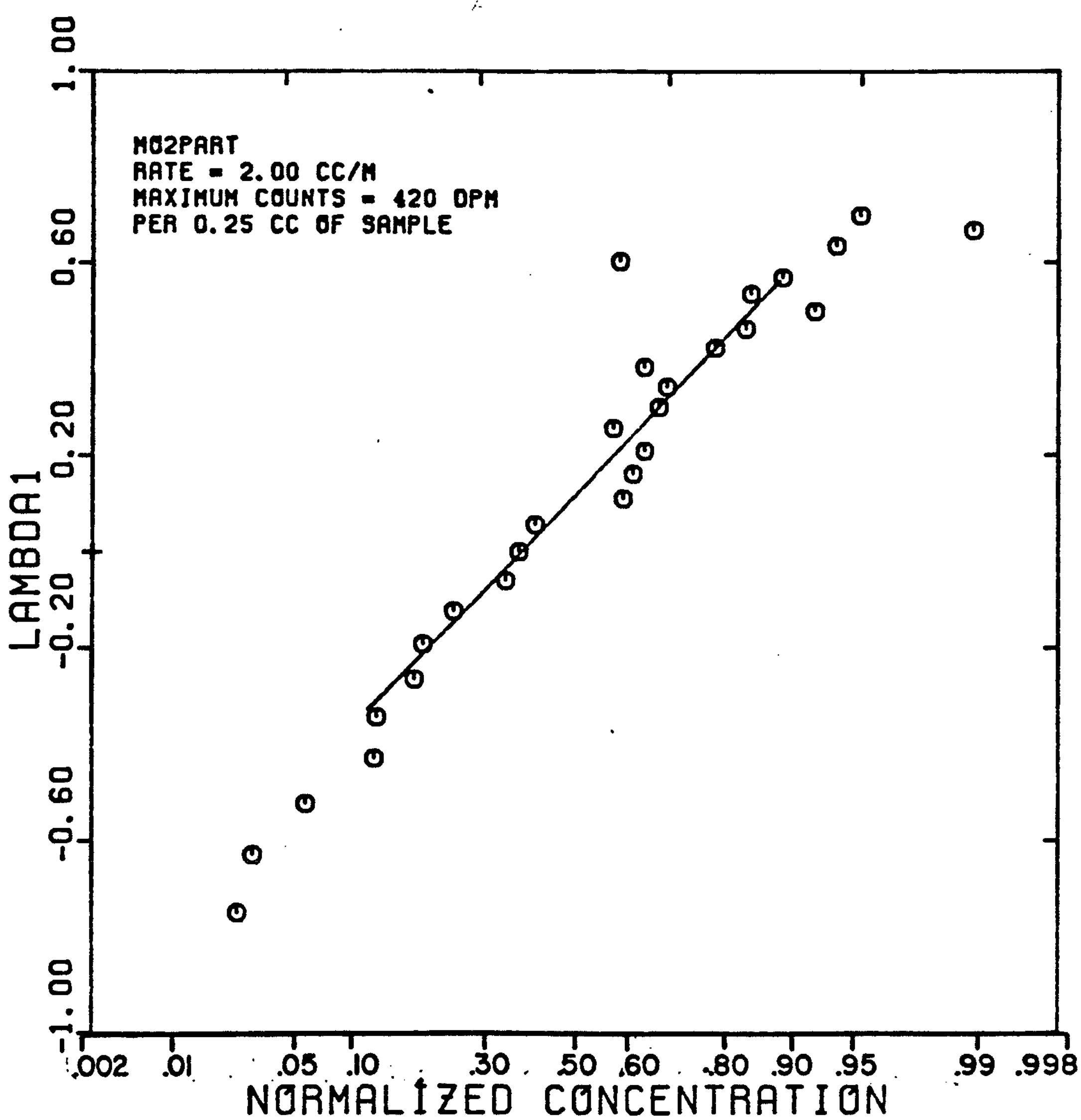

FIGURE 5.87

SANDPACK BREAKTHROUGH CURVE FOR CARBON 14
TRACER IN THE OLEIC PHASE
(EXPERIMENT M02UP)

$S_o = 0.169 \quad f_o = 0.228$

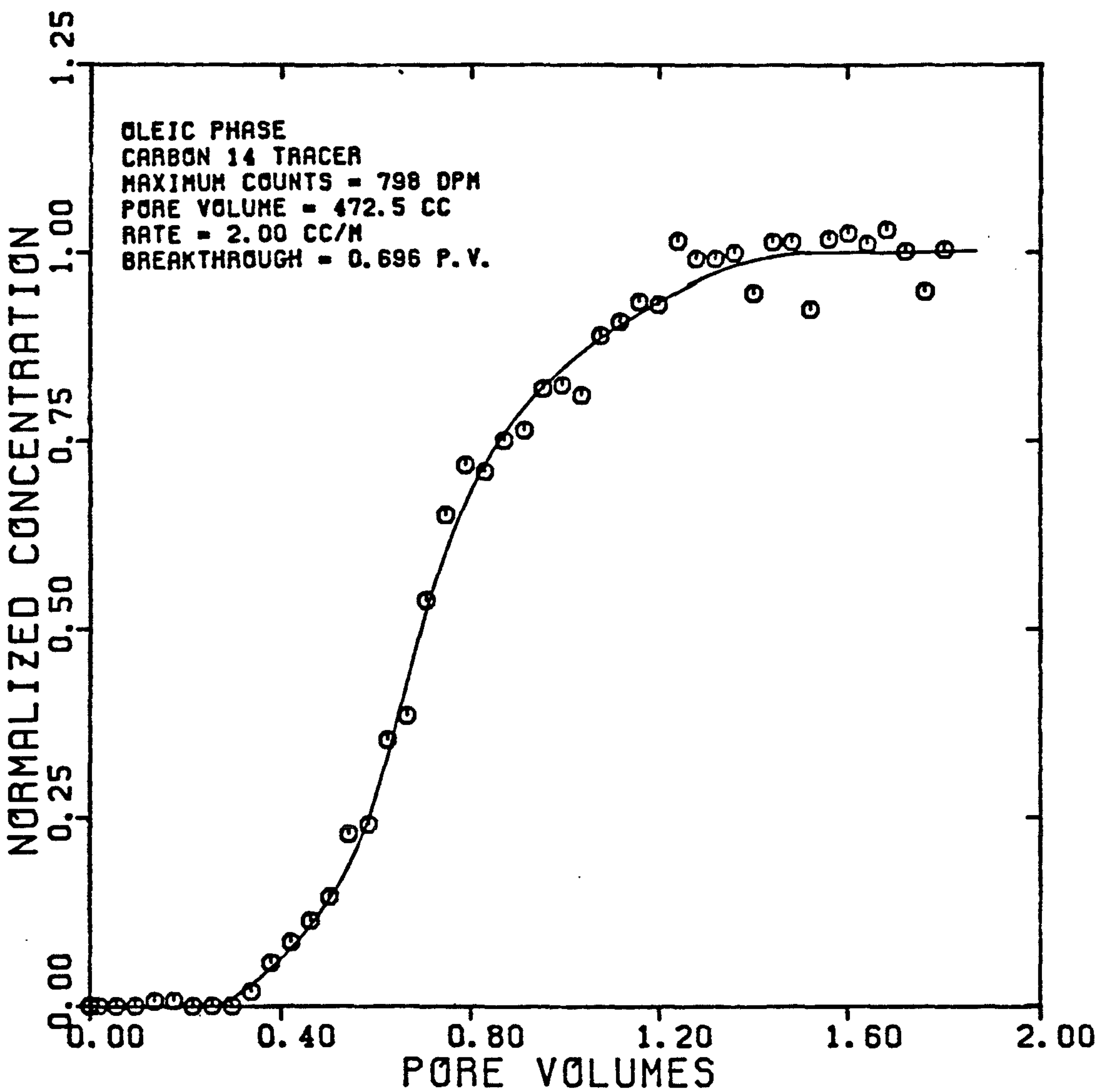

FIGURE 5.88

DISPERSIVITY OF CARBON 14
TRACER IN THE OLEIC PHASE
(EXPERIMENT MO2UP)

$S_o = 0.169 \quad f_o = 0.228$

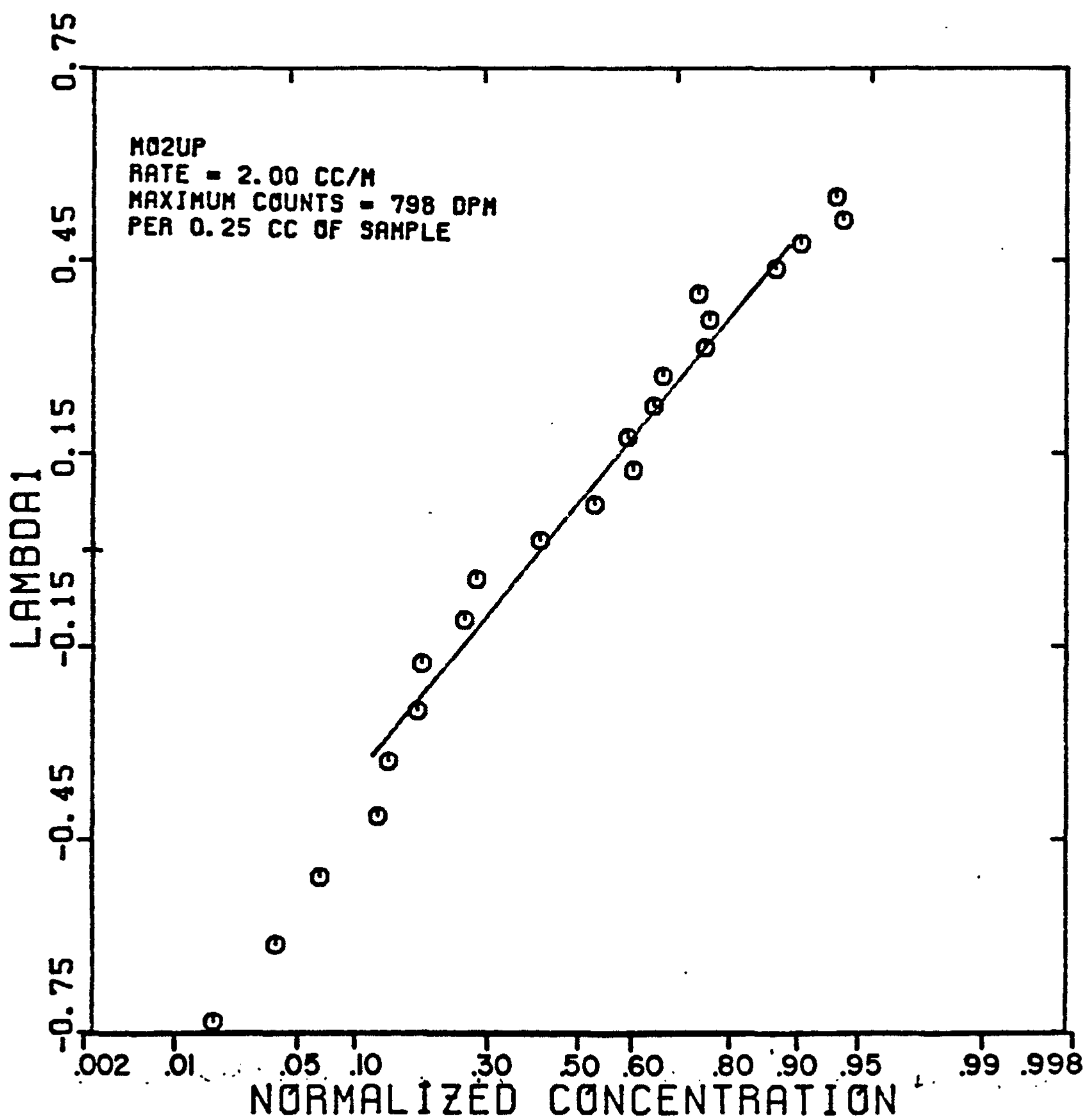

FIGURE 5.89

SANDPACK BREAKTHROUGH CURVE FOR TRITIUM TRACER IN THE MICROEMULSION PHASE (EXPERIMENT M03L0)

$S_{me} = 0.650 \quad f_{me} = 0.516$

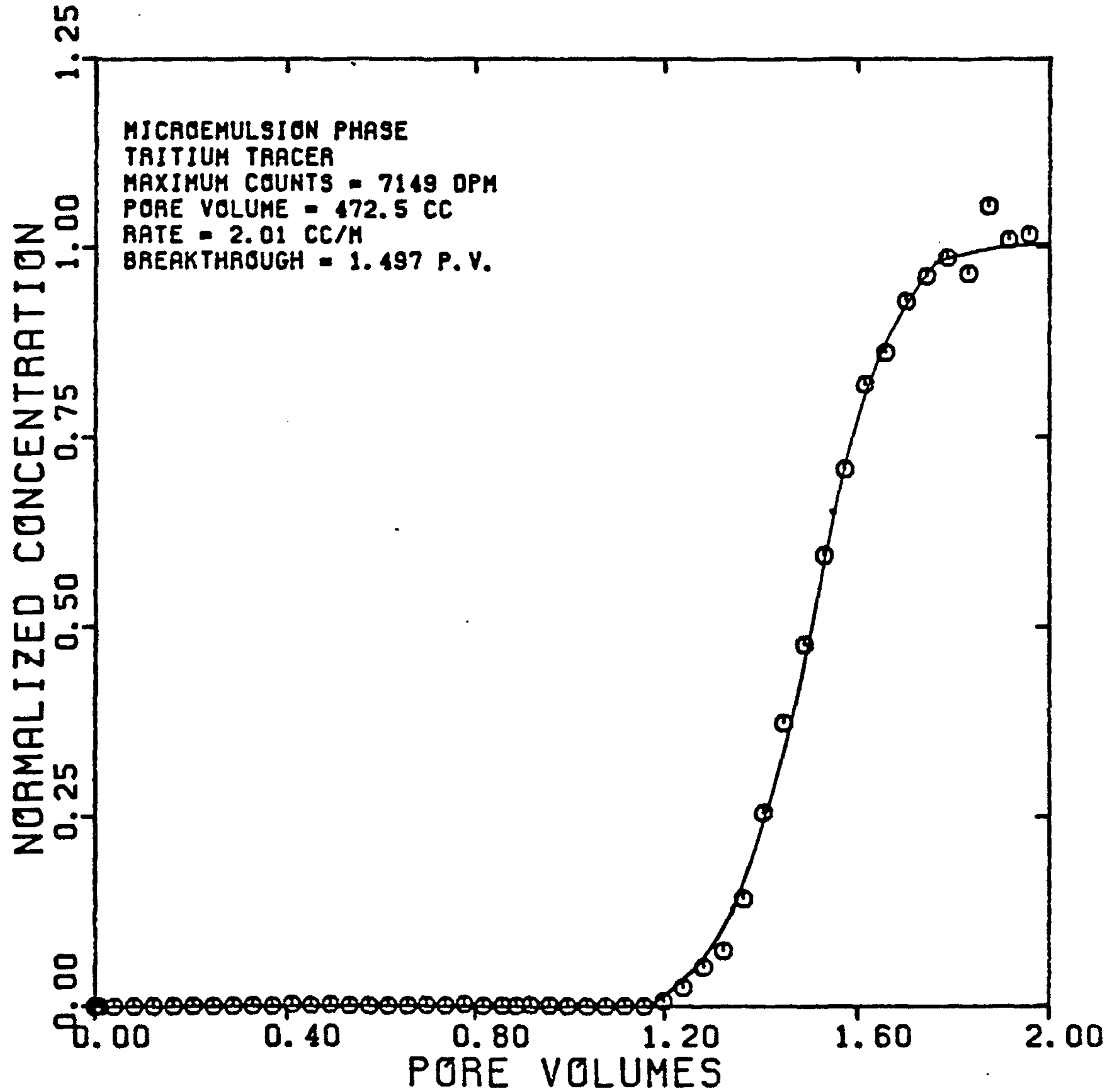

FIGURE 5.90

DISPERSIVITY OF TRITIUM
TRACER IN THE MICROEMULSION PHASE
(EXPERIMENT M03L0)

S_{me} = 0.650 f_{me} = 0.516

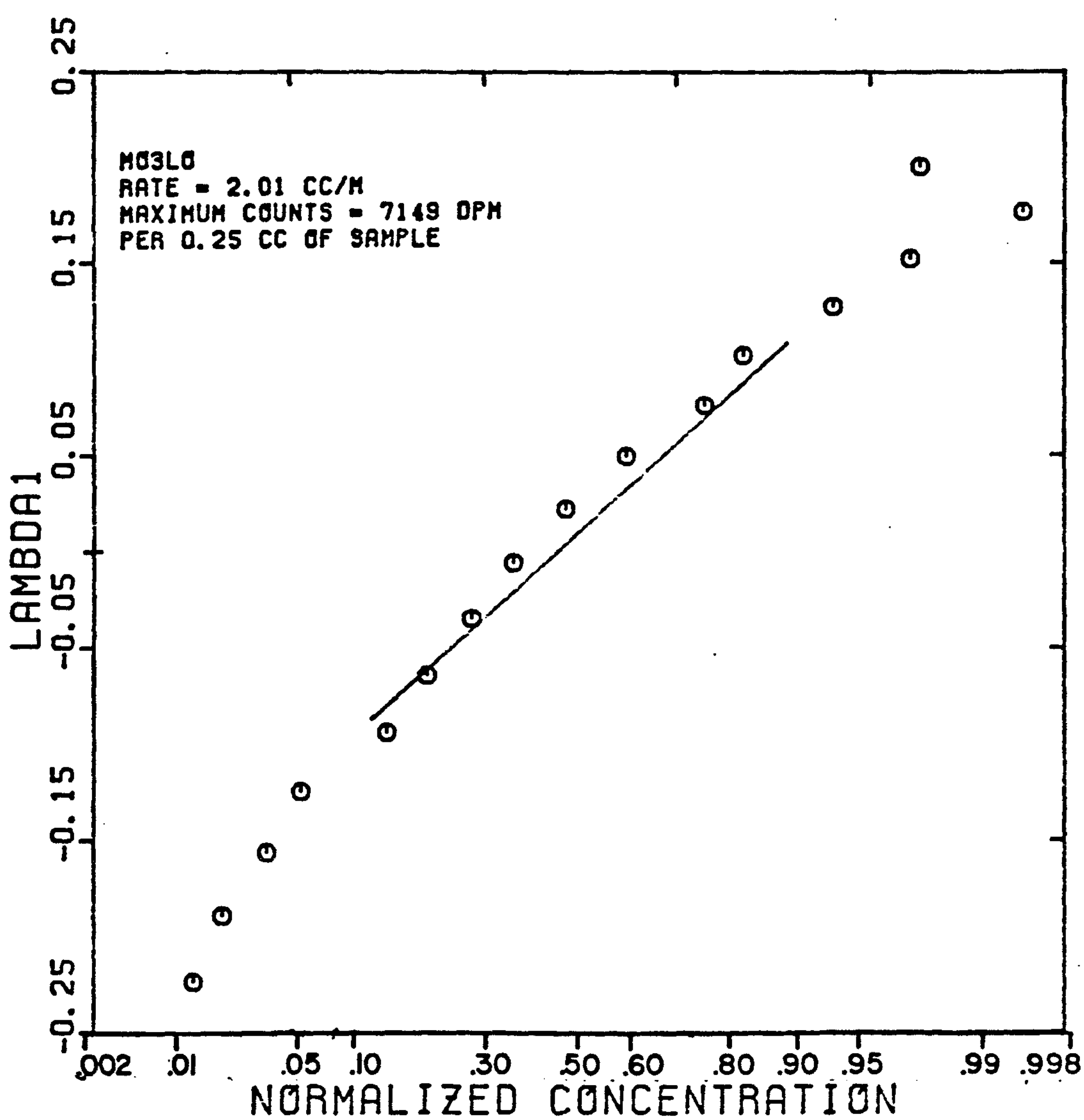

FIGURE 5.91

SANDPACK BREAKTHROUGH CURVE FOR CARBON 14
TRACER IN THE MICROEMULSION PHASE
(EXPERIMENT M03PART)

S_{me} = 0.650 f_{me} = 0.516

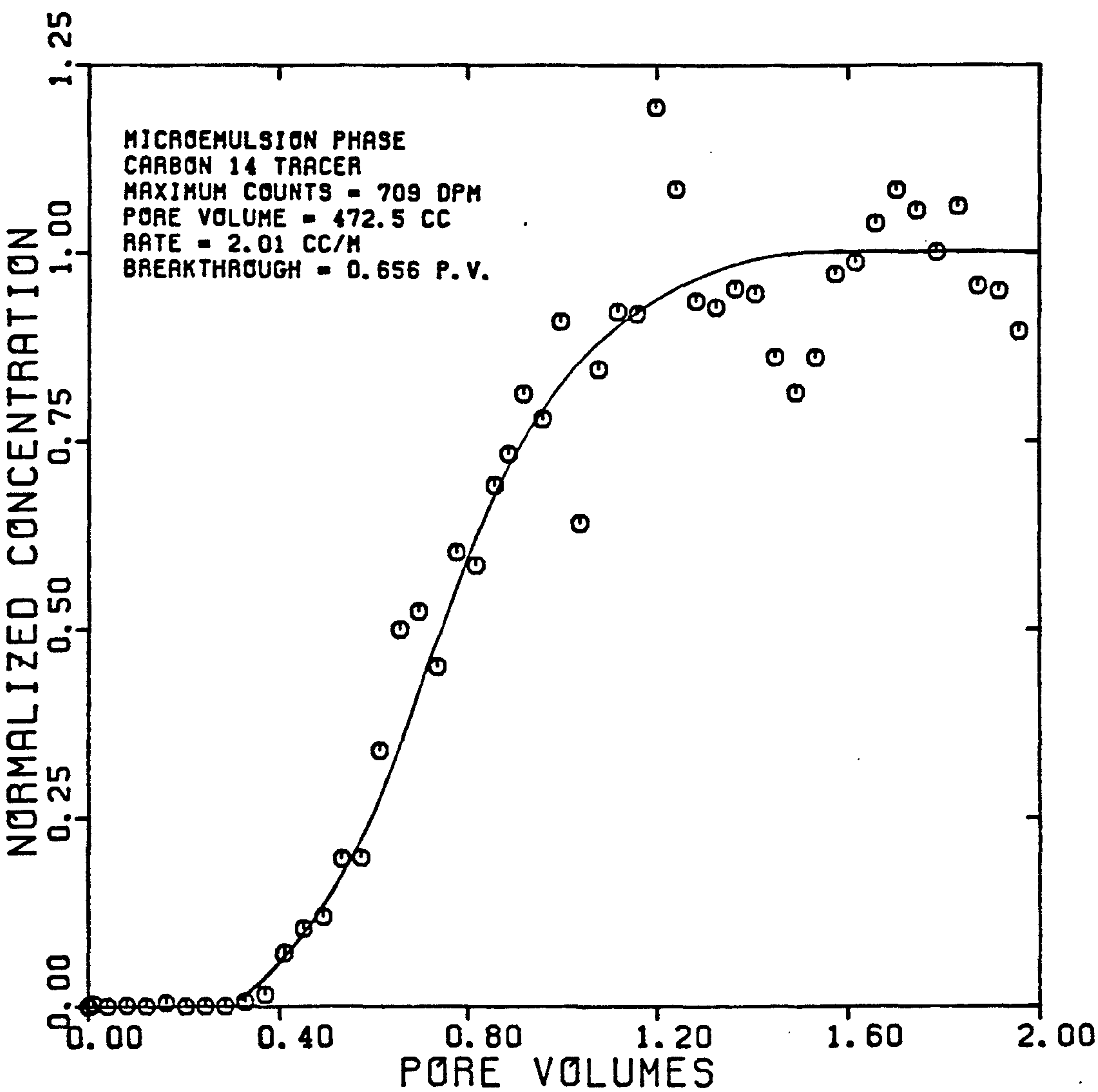

FIGURE 5.92

DISPERSIVITY OF CARBON 14
TRACER IN THE MICROEMULSION PHASE
(EXPERIMENT MO3PART)

S_{me} = 0.650 f_{me} = 0.516

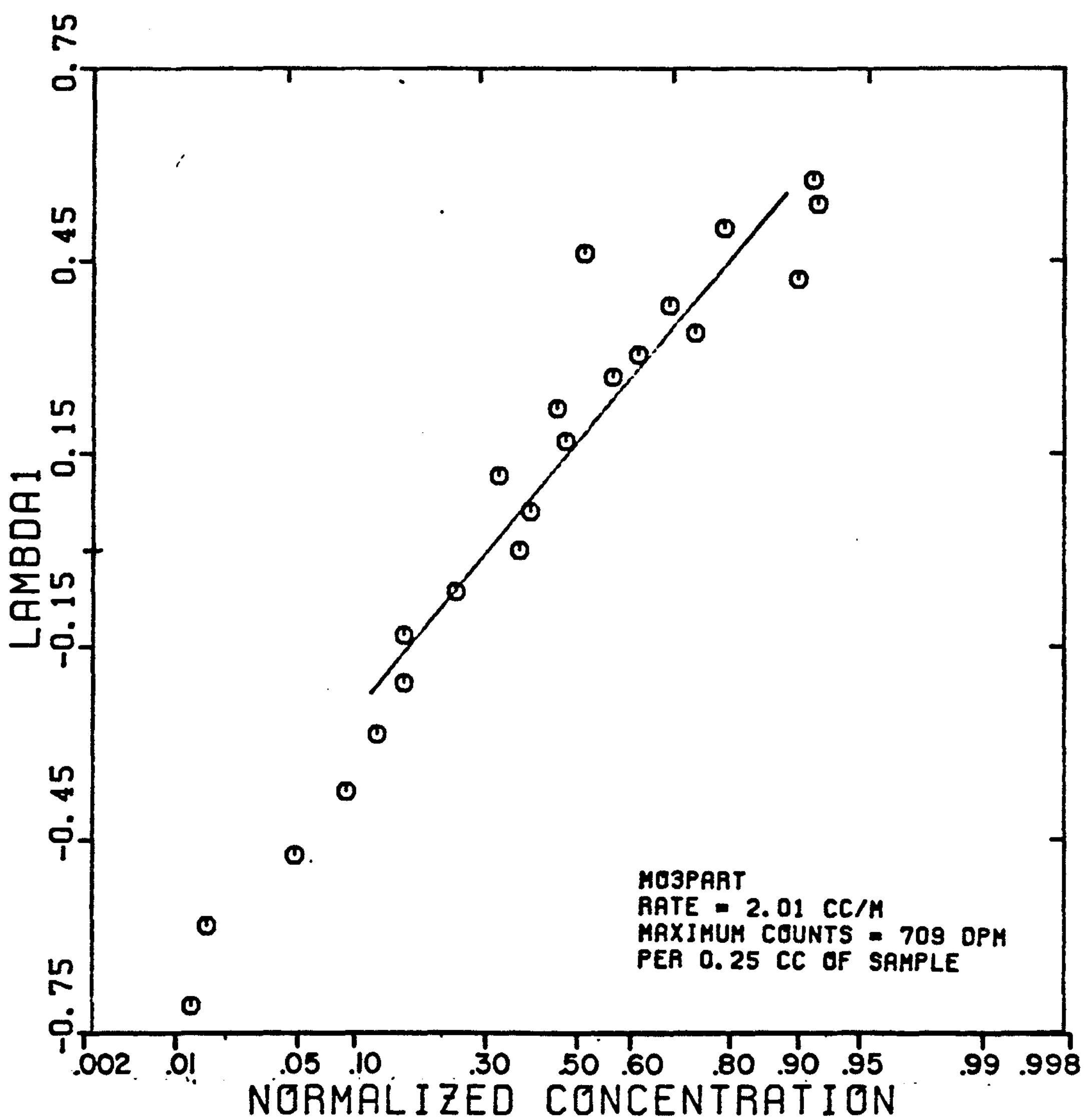

FIGURE 5.93

SANDPACK BREAKTHROUGH CURVE FOR CARBON 14
TRACER IN THE OLEIC PHASE
(EXPERIMENT MO3UP)

S_o = 0.350 f_o = 0.484

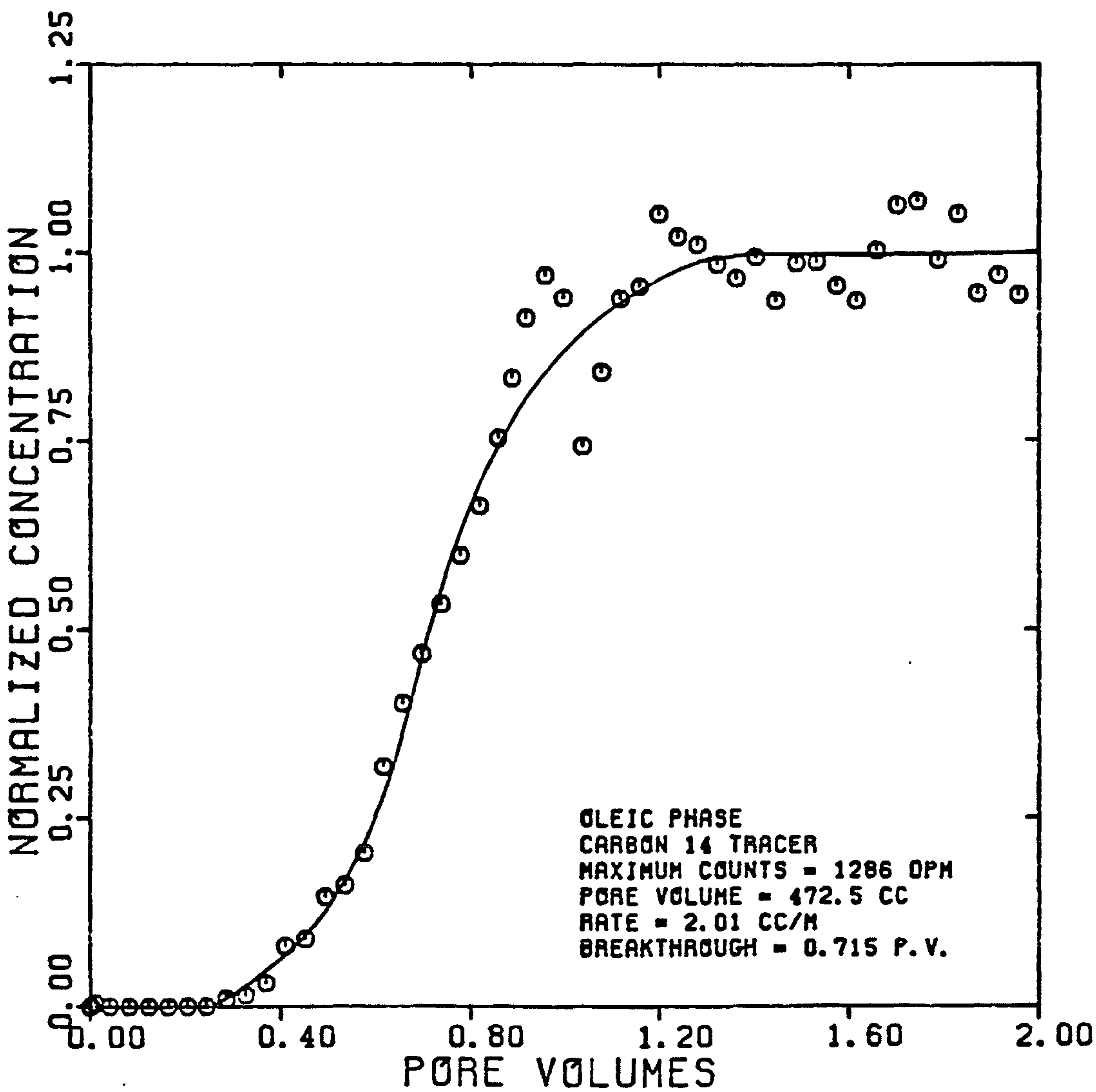

FIGURE 5.94

DISPERSIVITY OF CARBON 14
TRACER IN THE OLEIC PHASE
(EXPERIMENT MO3UP)

$S_o = 0.350 \quad f_o = 0.484$

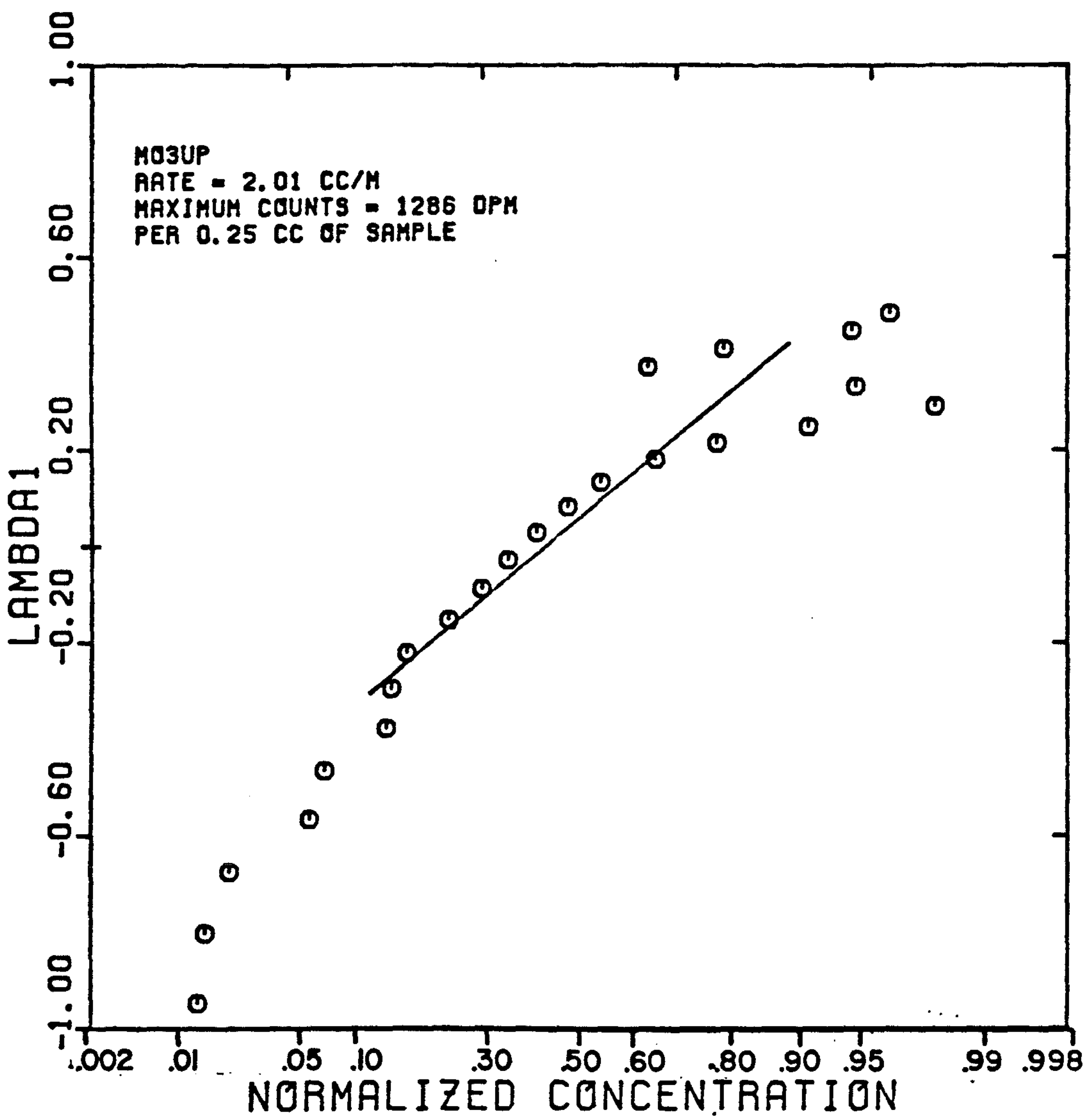

FIGURE 5.95

SANDPACK BREAKTHROUGH CURVE FOR TRITIUM
TRACER IN THE MICROEMULSION PHASE
(EXPERIMENT M04L0)

$S_{me} = 0.443 \quad f_{me} = 0.258$

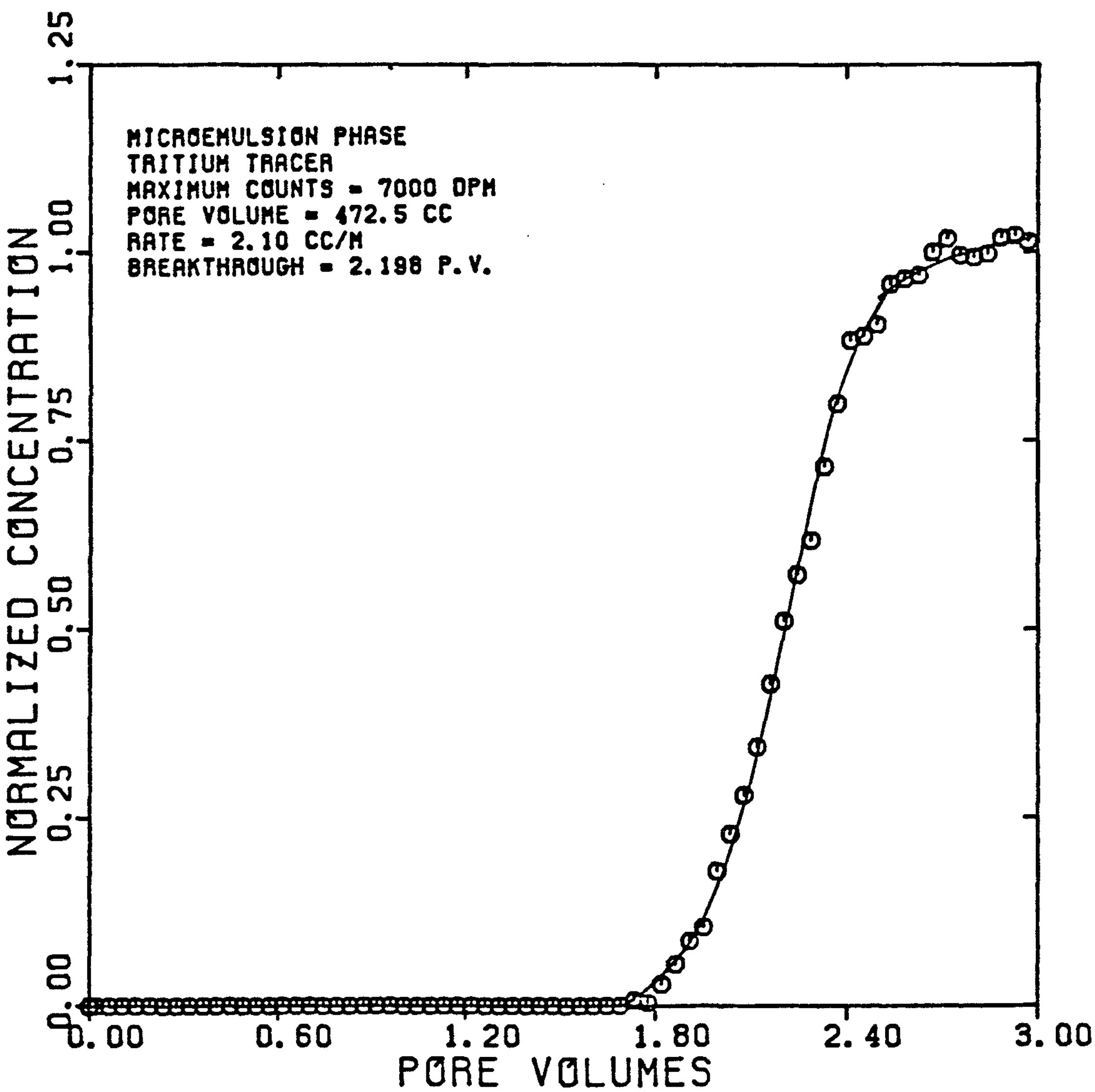

FIGURE 5.96

DISPERSIVITY OF TRITIUM
TRACER IN THE MICROEMULSION PHASE
(EXPERIMENT M04L0)

S_{me} = 0.443 f_{me} = 0.258

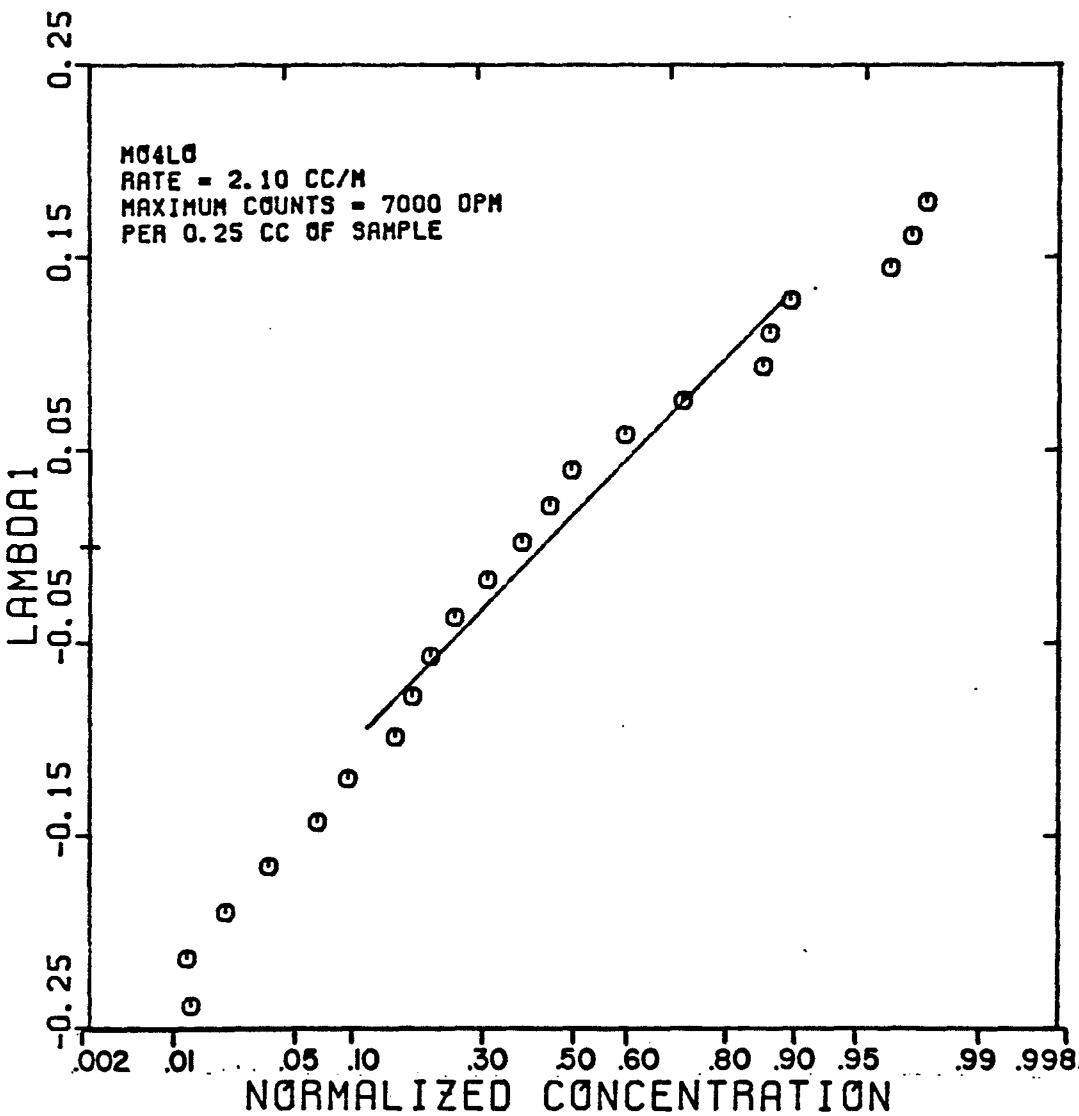

FIGURE 5.97

SANDPACK BREAKTHROUGH CURVE FOR CARBON 14
TRACER IN THE MICROEMULSION PHASE
(EXPERIMENT M04PART)

S_{me} = 0.443 f_{me} = 0.258

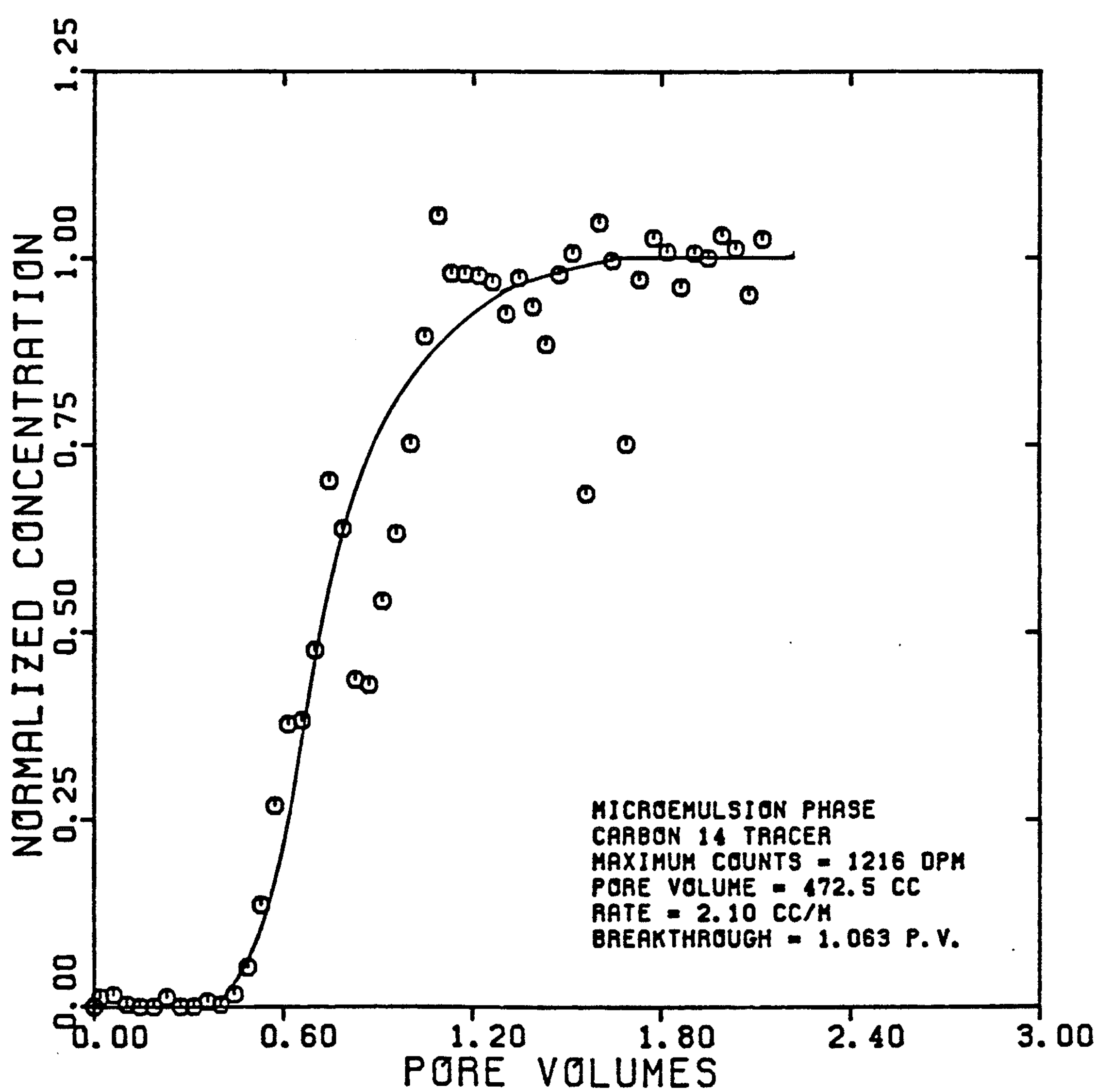

FIGURE 5.98

DISPERSIVITY OF CARBON 14
TRACER IN THE MICROEMULSION PHASE
(EXPERIMENT MO4PART)

$S_{me} = 0.443 \quad f_{me} = 0.258$

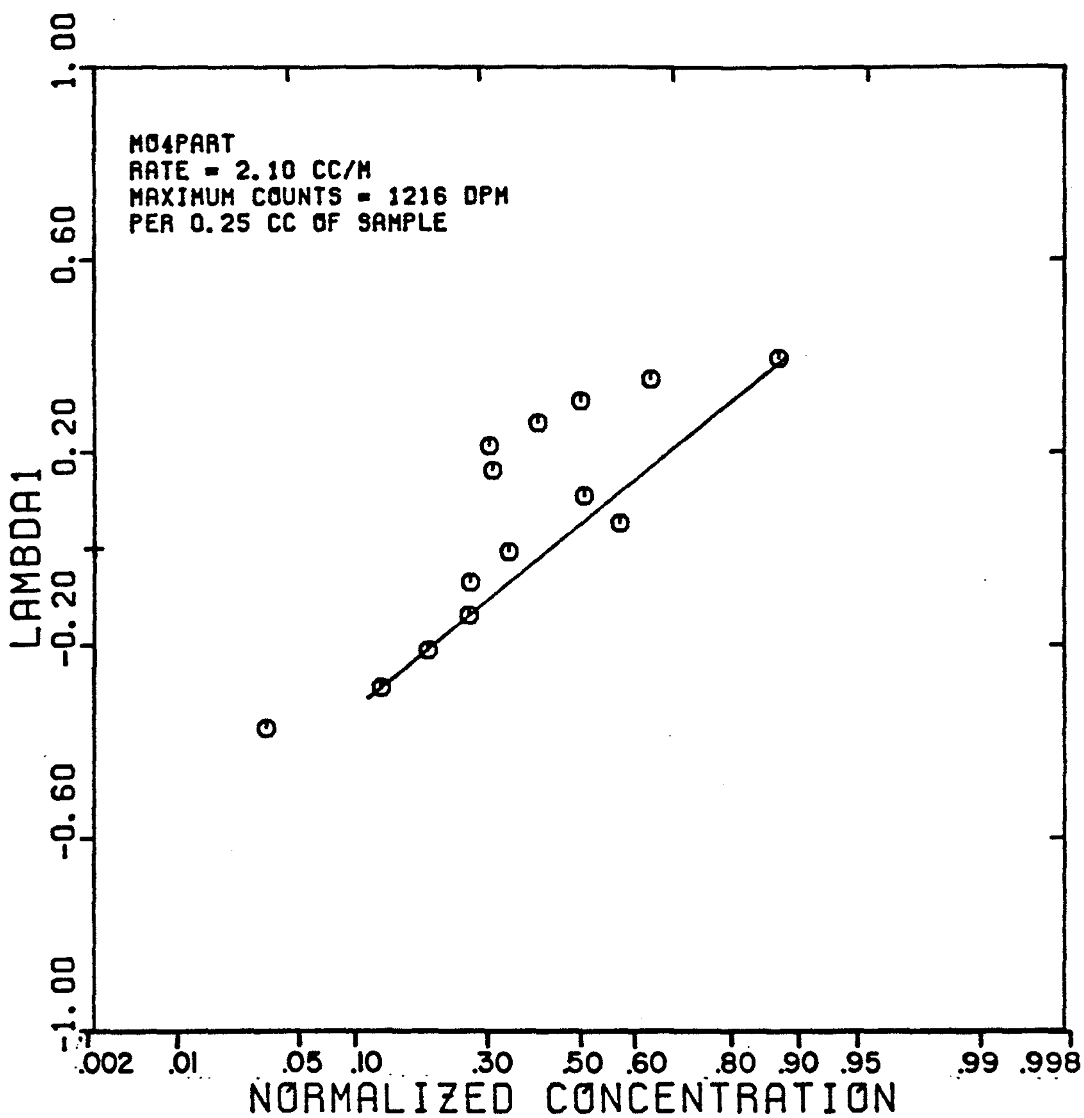

FIGURE 5.99

SANDPACK BREAKTHROUGH CURVE FOR CARBON 14
TRACER IN THE OLEIC PHASE
(EXPERIMENT MO4UP)

S_o = 0.557 f_o = 0.742

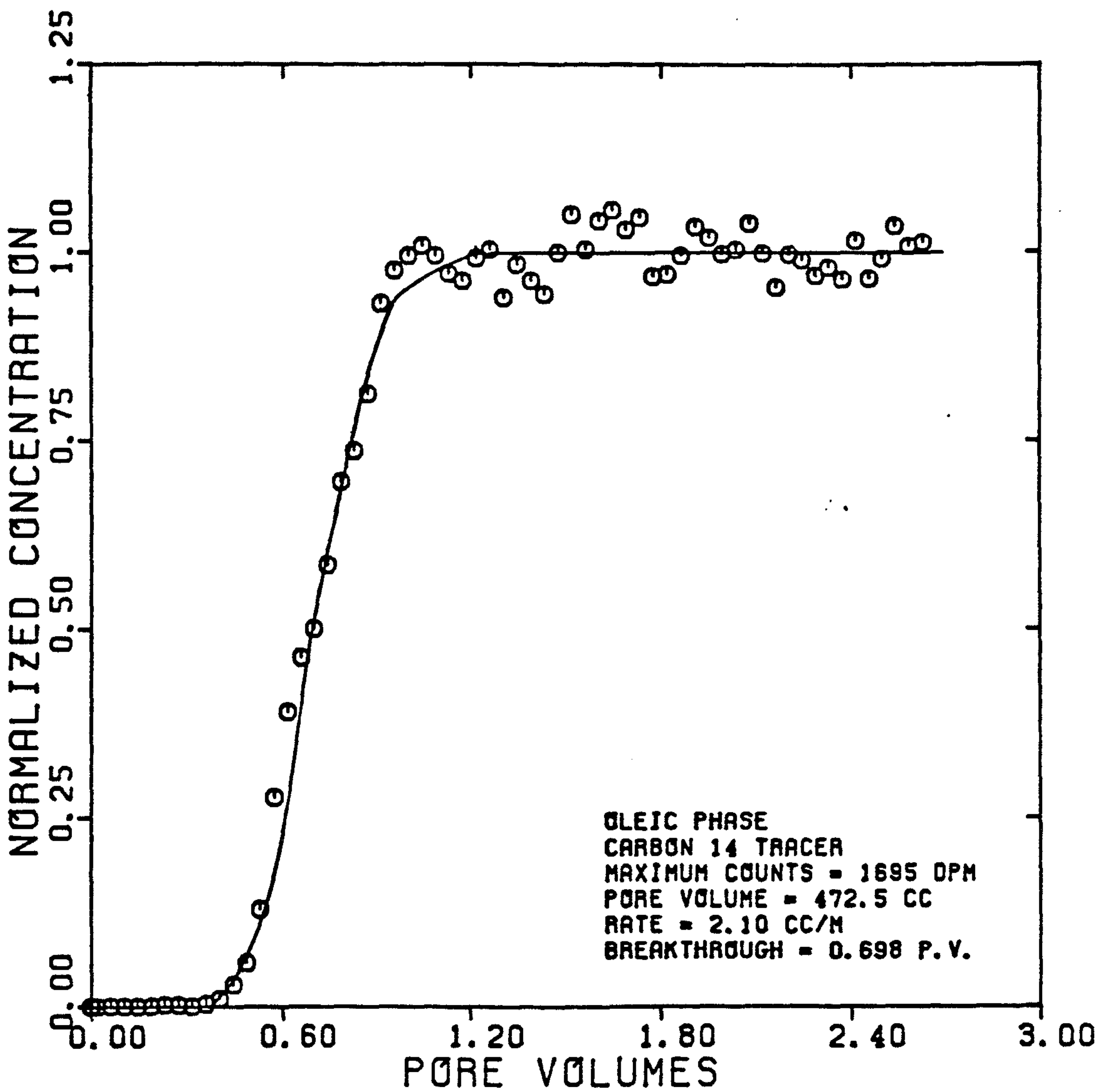

FIGURE 5.100

DISPERSIVITY OF CARBON 14
TRACER IN THE OLEIC PHASE
(EXPERIMENT M04UP)

$S_o = 0.557 \quad f_o = 0.742$

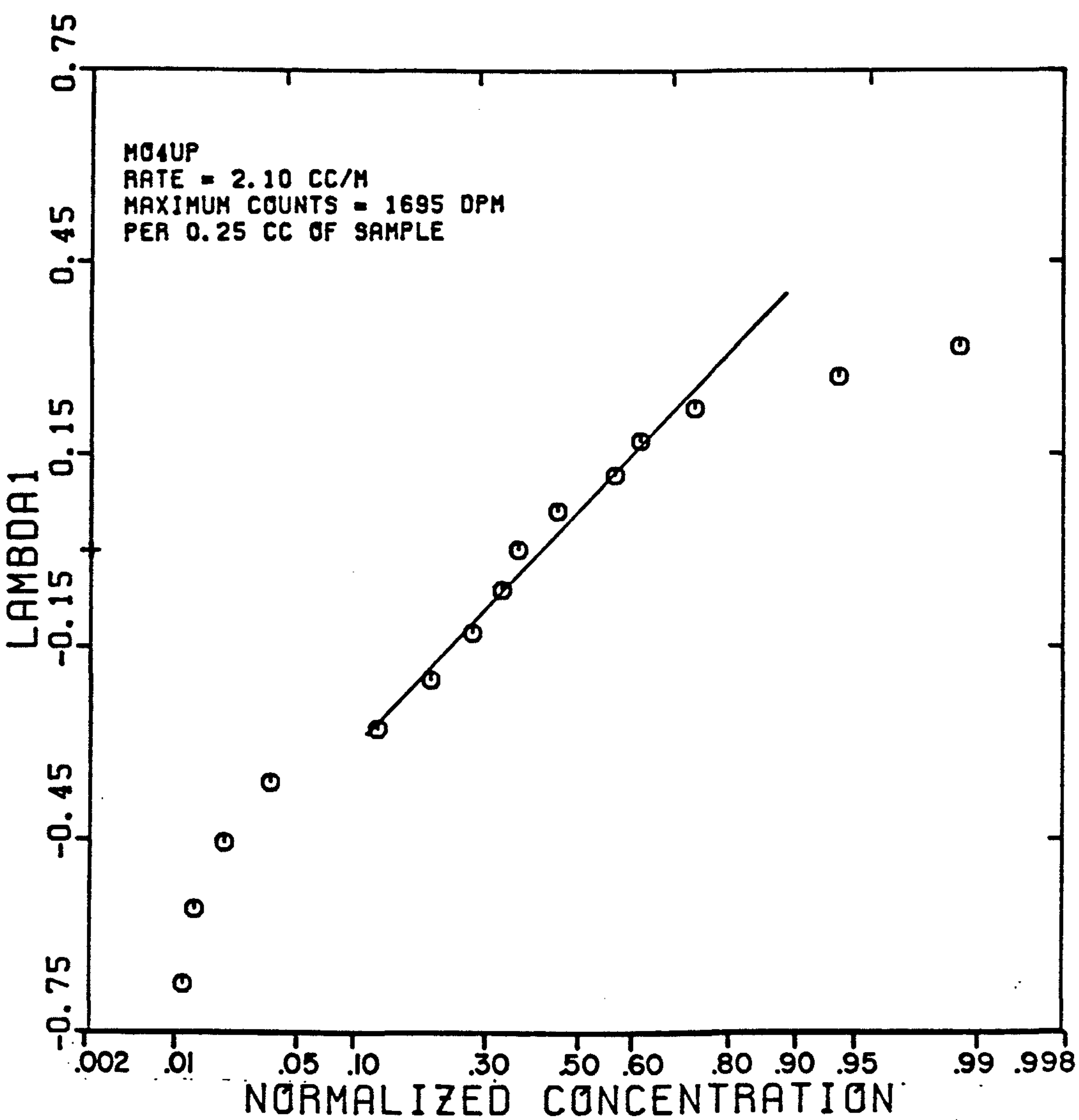

FIGURE 5.101

SANDPACK BREAKTHROUGH CURVE FOR CARBON 14
TRACER IN THE OLEIC PHASE
(EXPERIMENT M05)

$S_o = 0.996 \quad f_o = 1.0$

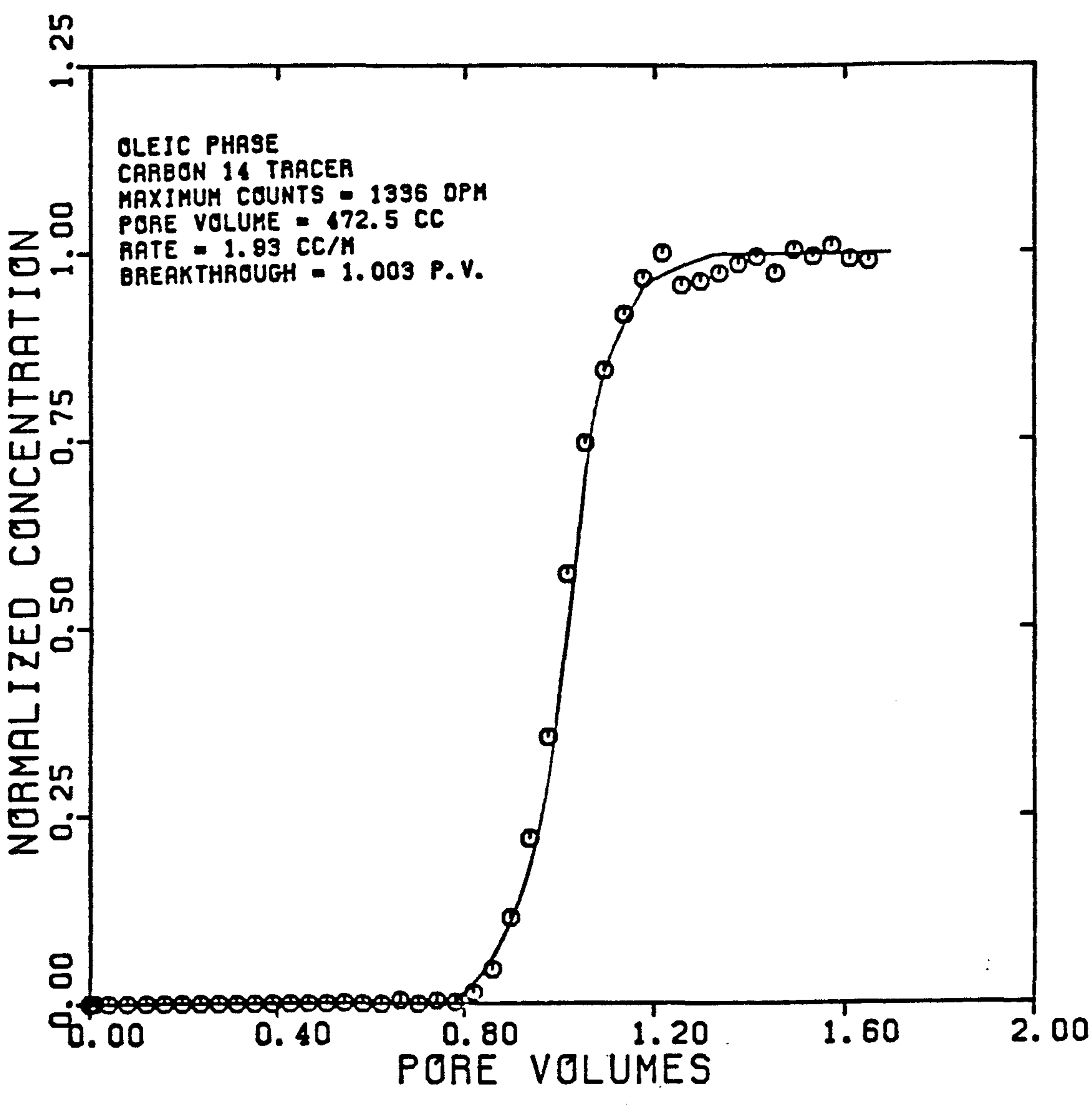

FIGURE 5.102

DISPERSIVITY OF CARBON 14
TRACER IN THE OLEIC PHASE
(EXPERIMENT M05)

$S_o = 0.996 \quad f_o = 1.0$

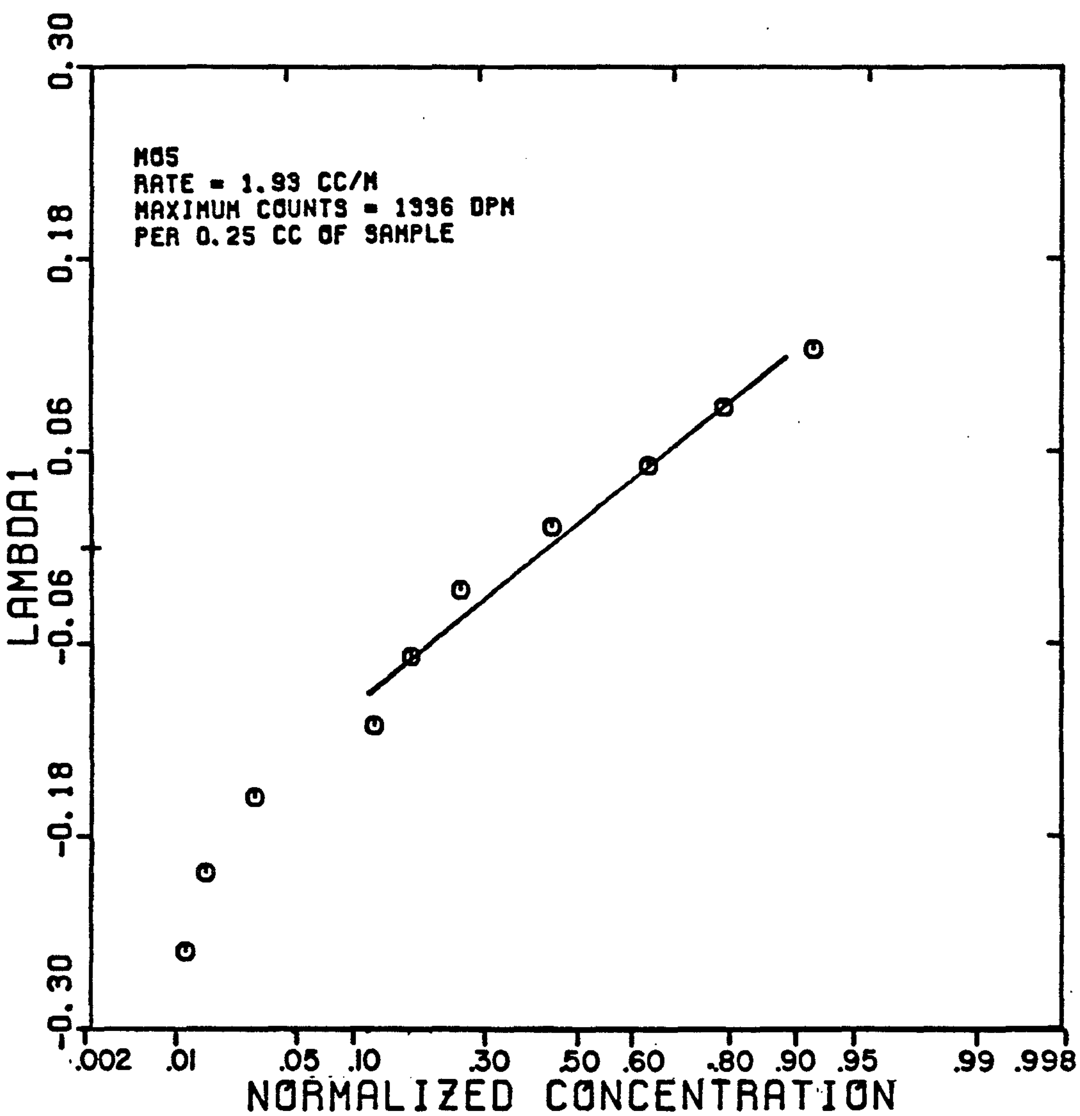

FIGURE 5.103

DISPERSIVITY OF MICROEMULSION AND
OIL IN UNCONSOLIDATED SAND
(EXPERIMENT MO)

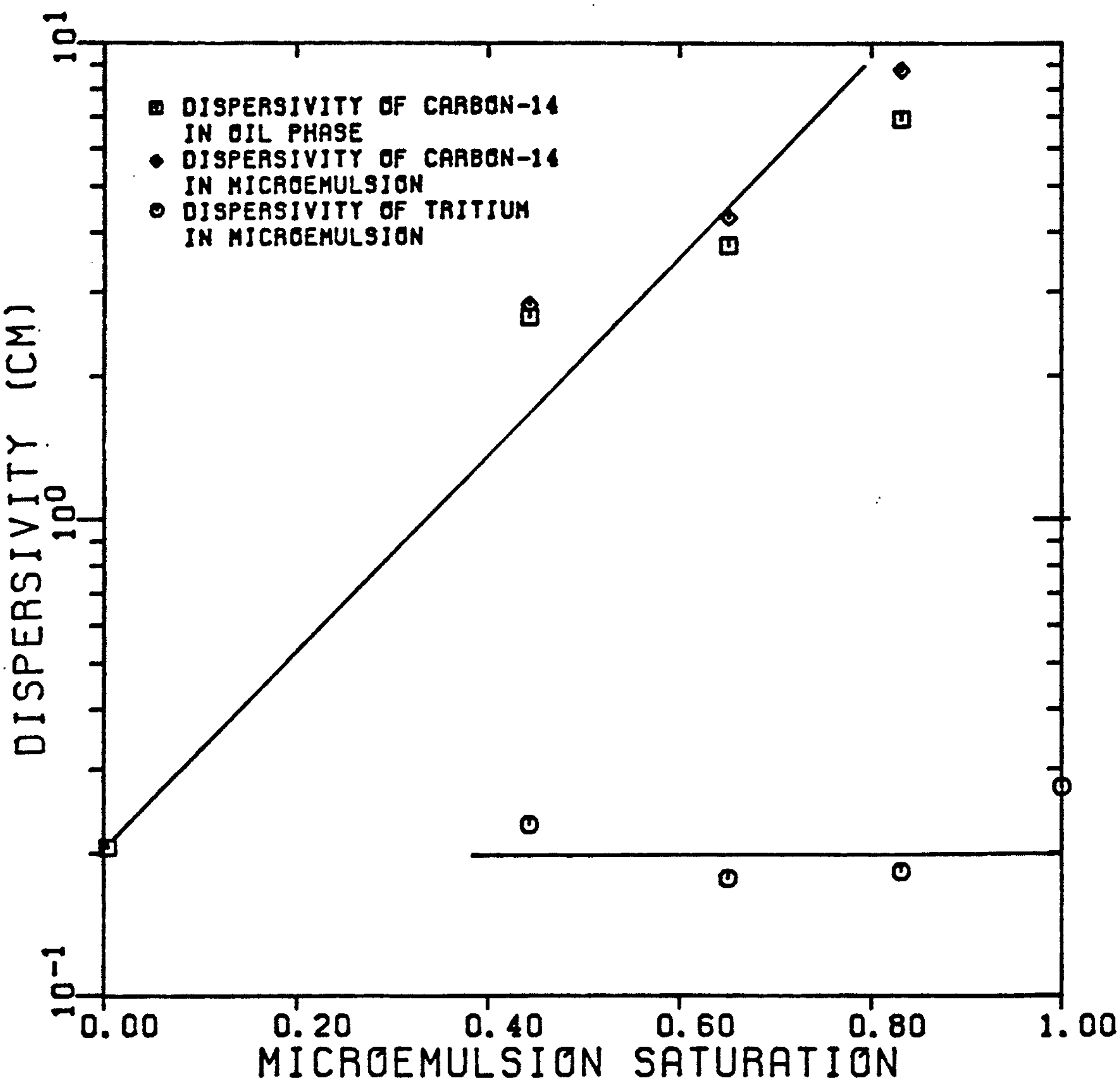

FIGURE 5.104
DISPERSIVITY OF HIGH AND LOW IFT
SYSTEMS IN UNCONSOLIDATED SAND
(EXPERIMENTS OWZ AND MO)

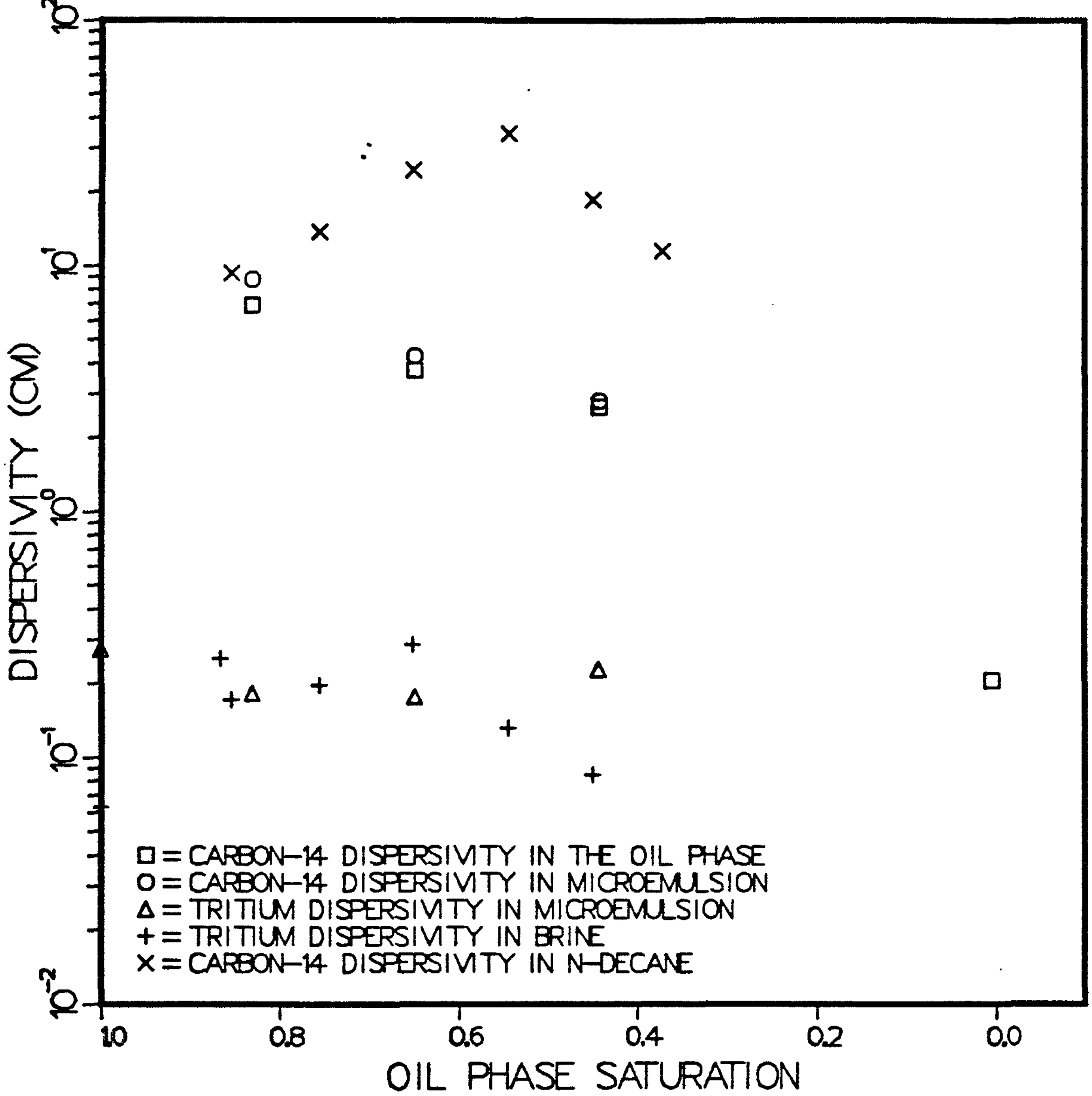

FIGURE 5.105

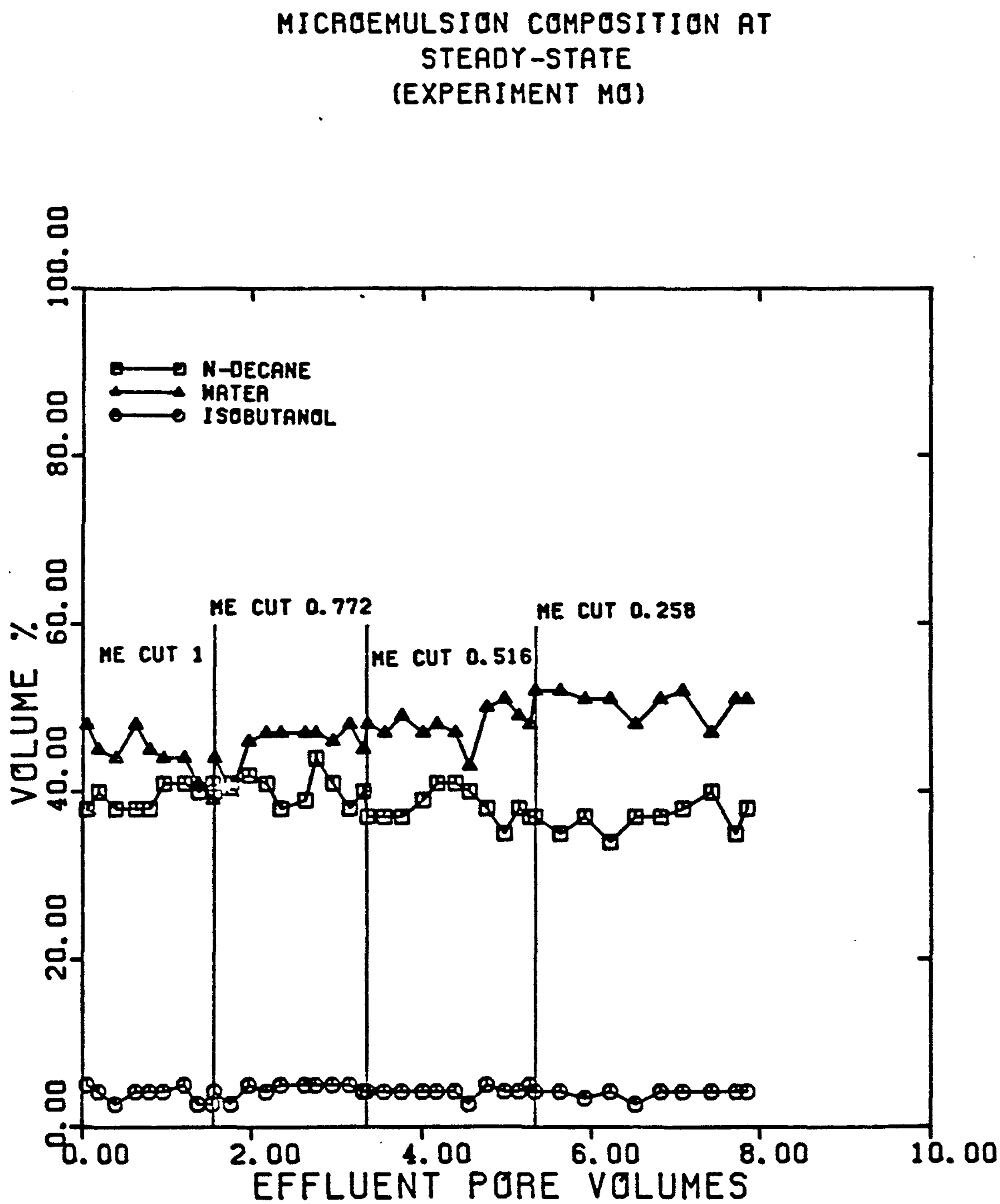
MICROEMULSION COMPOSITION AT
STEADY-STATE
(EXPERIMENT M0)
N-DECANE
WATER
ISOBUTANOL
ME CUT 1
ME CUT 0.772
ME CUT 0.516
ME CUT 0.258
VOLUME %
0.00
20.00
40.00
60.00
80.00
100.00
0.00
2.00
4.00
6.00
8.00
10.00
EFFLUENT PORE VOLUMES

FIGURE 5.106

OLEIC PHASE COMPOSITION AT
STEADY-STATE
(EXPERIMENT MO)

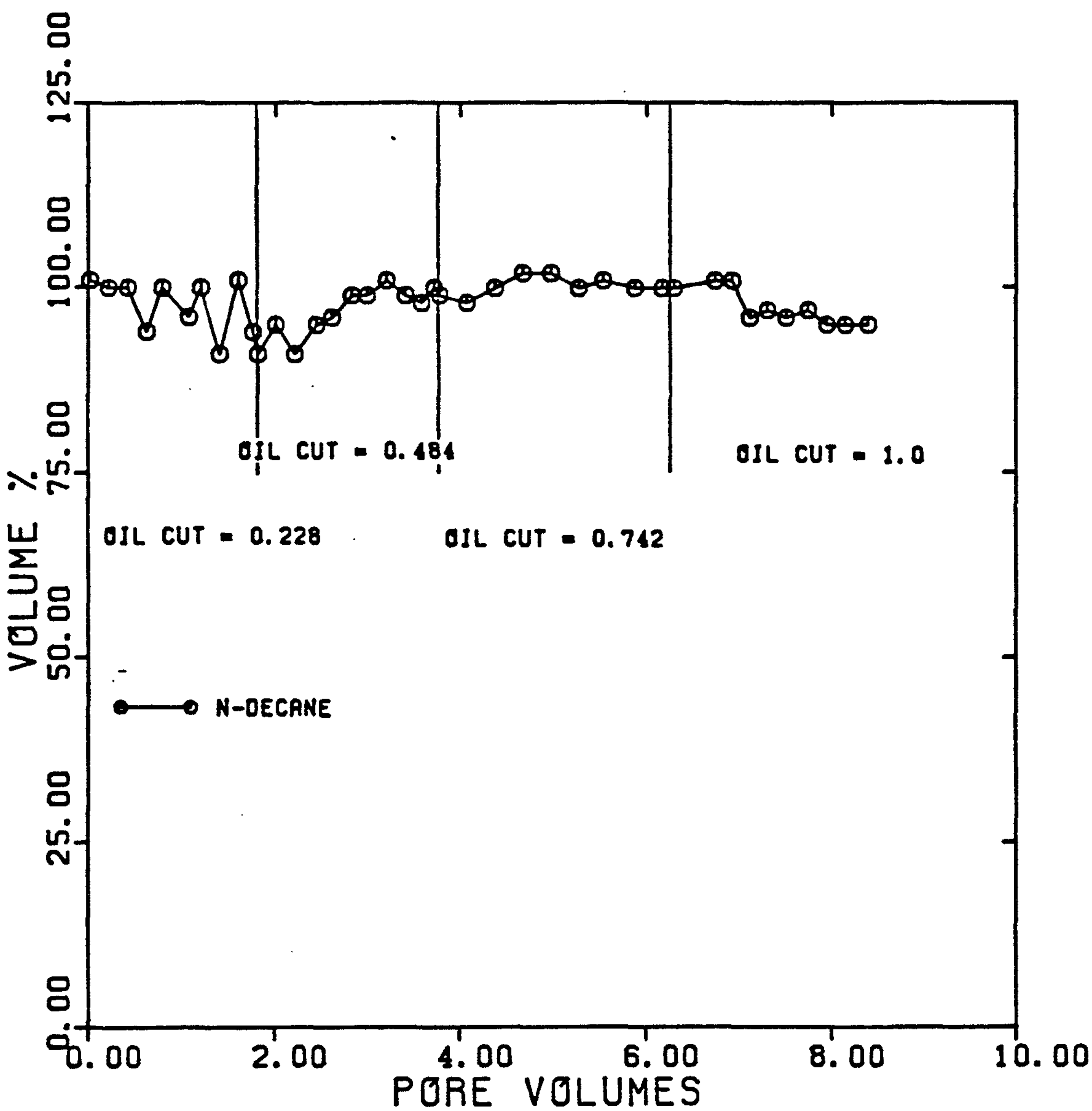

FIGURE 5.107

INTERFACIAL TENSION BETWEEN PRODUCED MICROEMULSION AND OIL AT STEADY-STATE (EXPERIMENT MO)

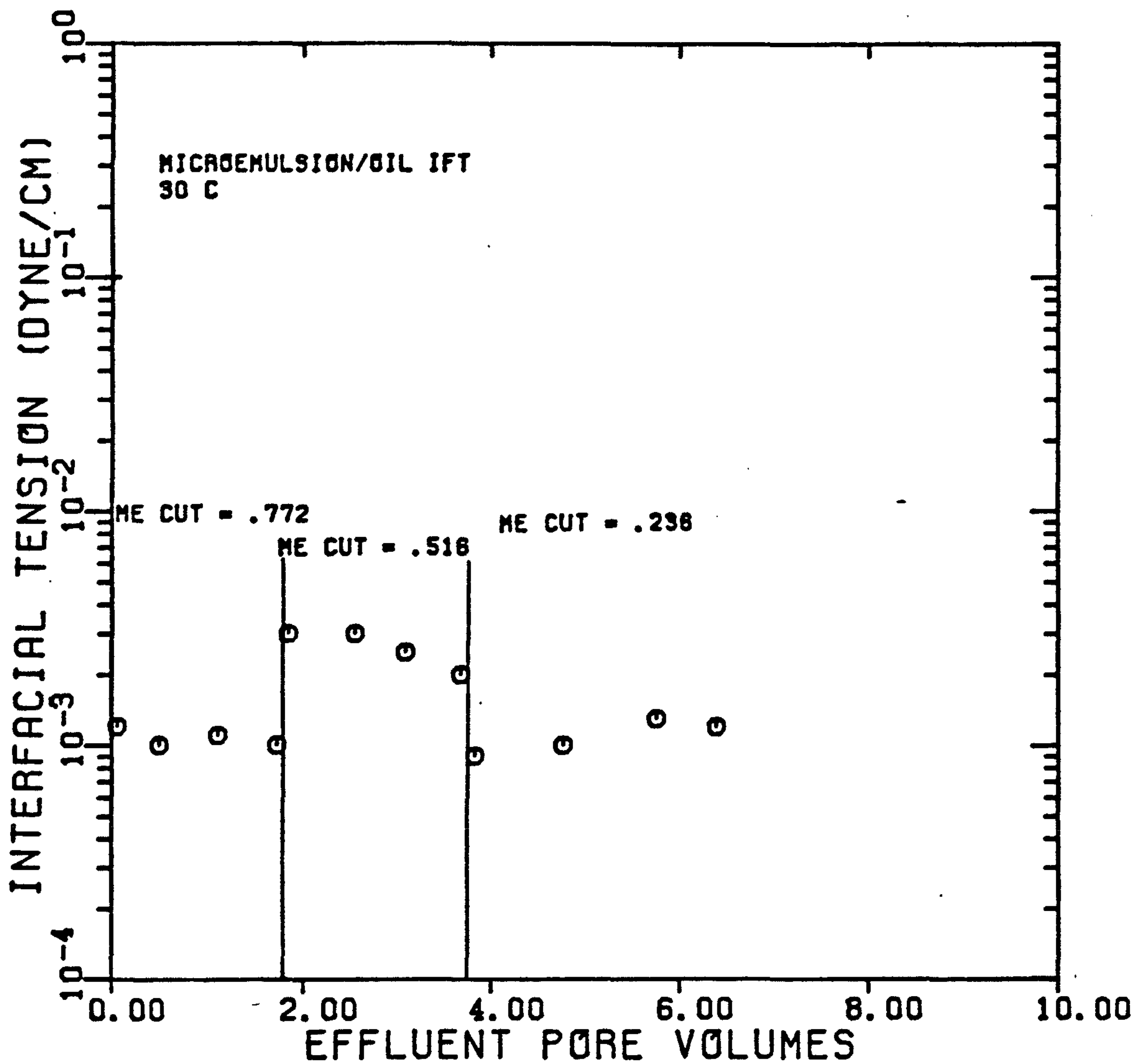

FIGURE 5.108

RELATIVE PERMEABILITY OF MICROEMULSION
AND BRINE IN UNCONSOLIDATED SAND

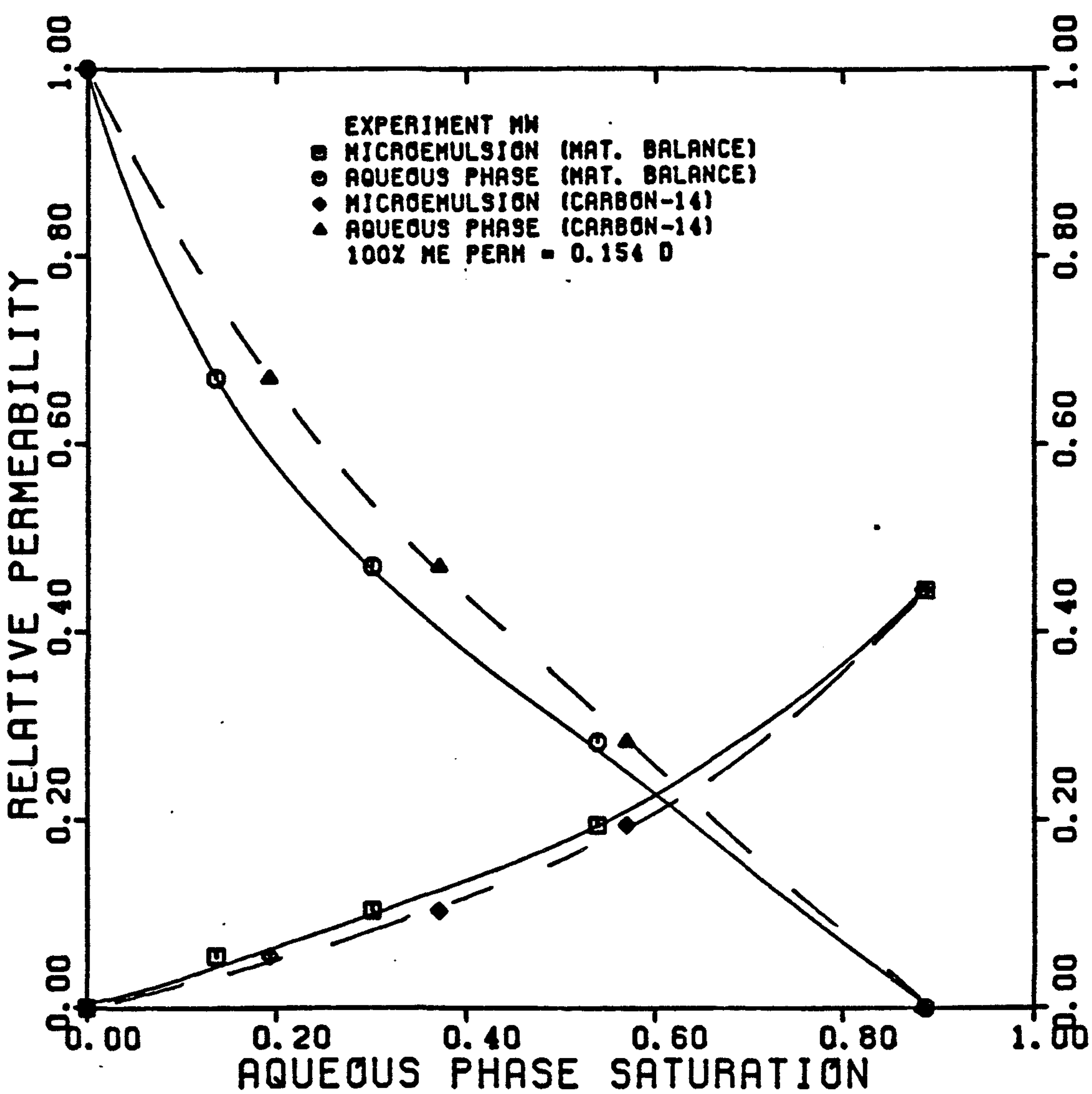

FIGURE 5.109

RELATIVE PERMEABILITY FOR HIGH AND LOW IFT SYSTEMS IN UNCONSOLIDATED SAND (EXPERIMENTS OWZ AND MW)

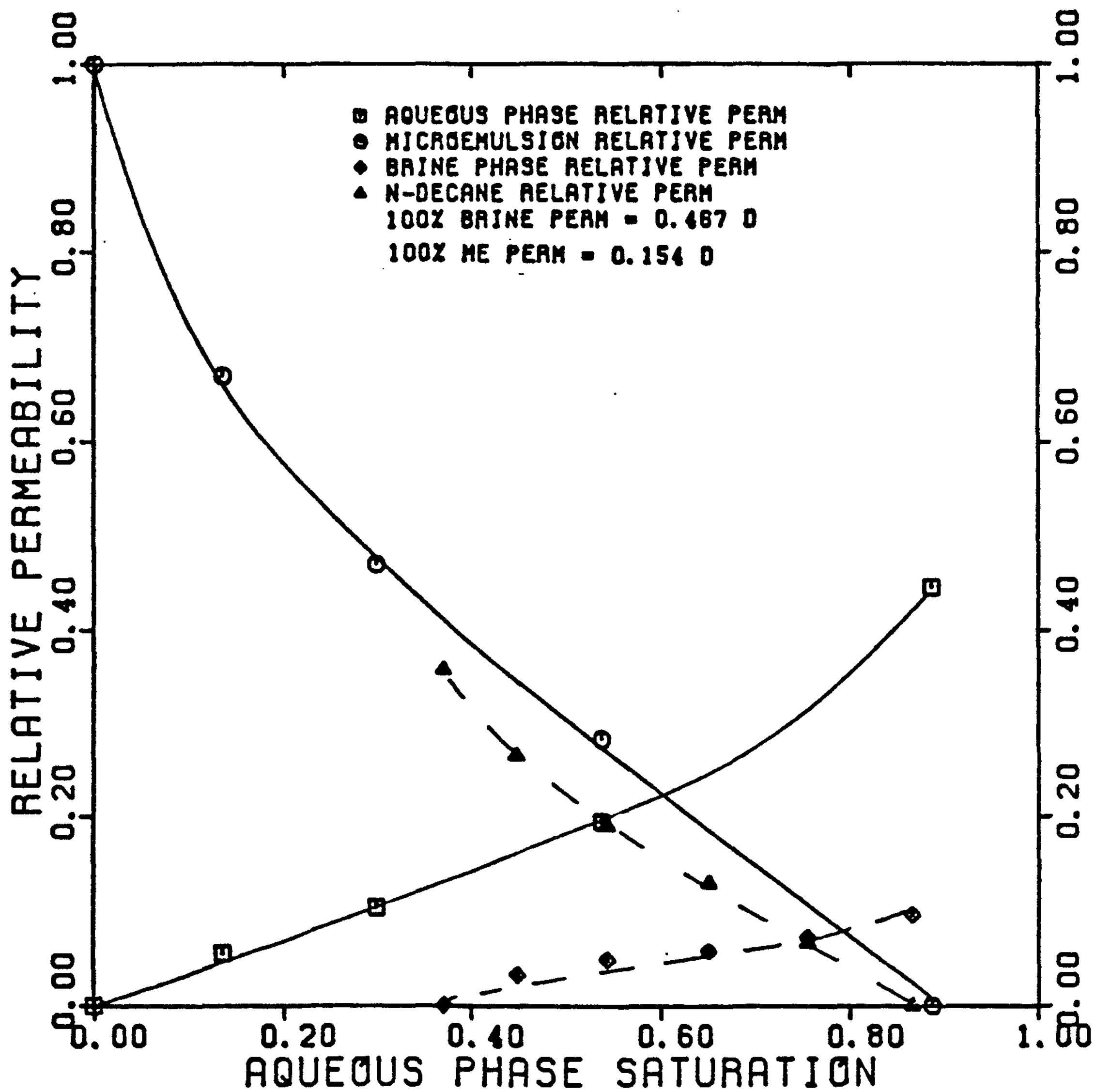

FIGURE 5.110

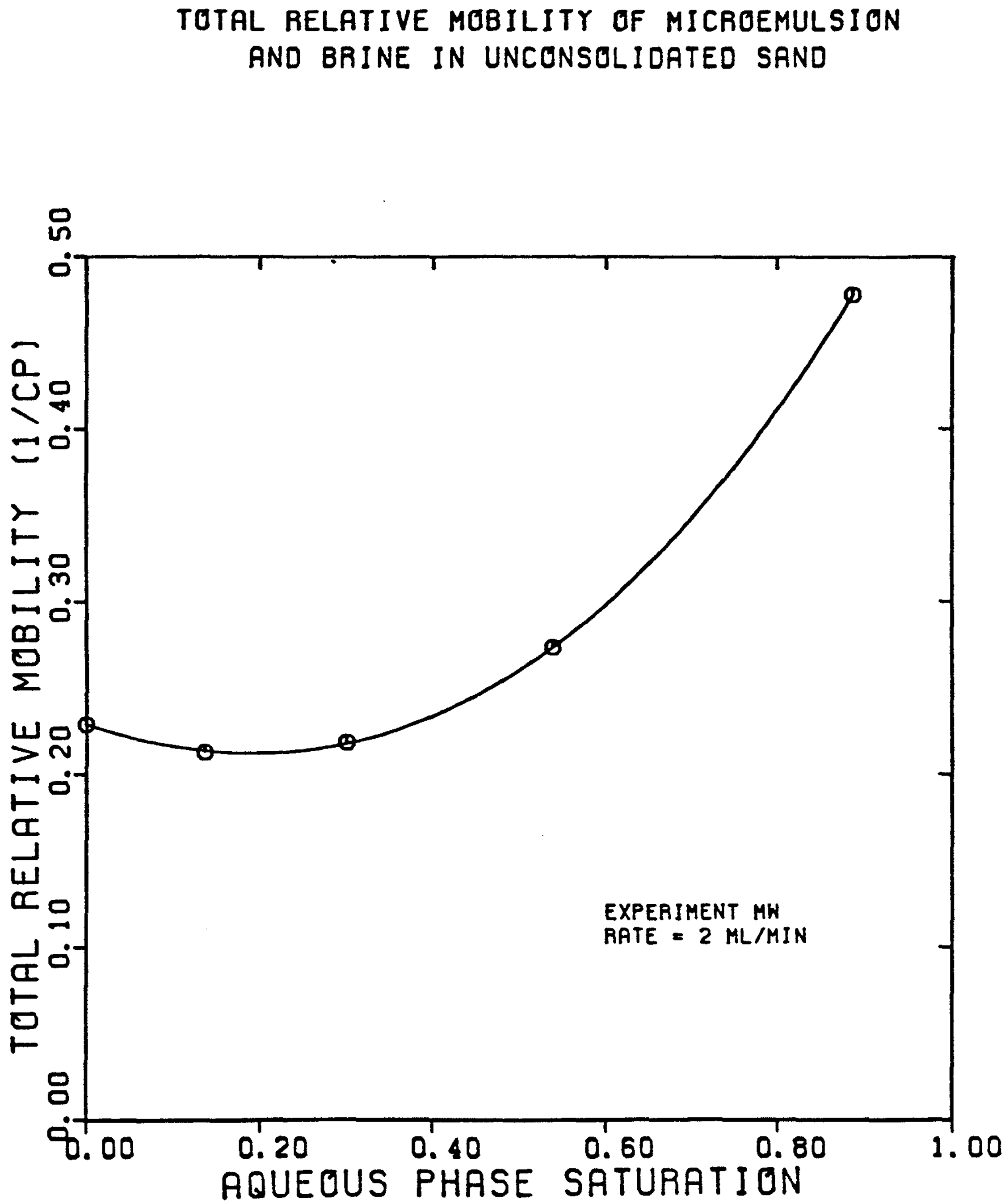
TOTAL RELATIVE MOBILITY OF MICROEMULSION
AND BRINE IN UNCONSOLIDATED SAND
TOTAL RELATIVE MOBILITY (1/CP)
0.00
0.10
0.20
0.30
0.40
0.50
0.00
0.20
0.40
0.60
0.80
1.00
AQUEOUS PHASE SATURATION
EXPERIMENT MW
RATE = 2 ML/MIN

FIGURE 5.111

FRACTIONAL FLOW FOR THE AQUEOUS PHASE IN UNCONSOLIDATED SAND (EXPERIMENT MW)

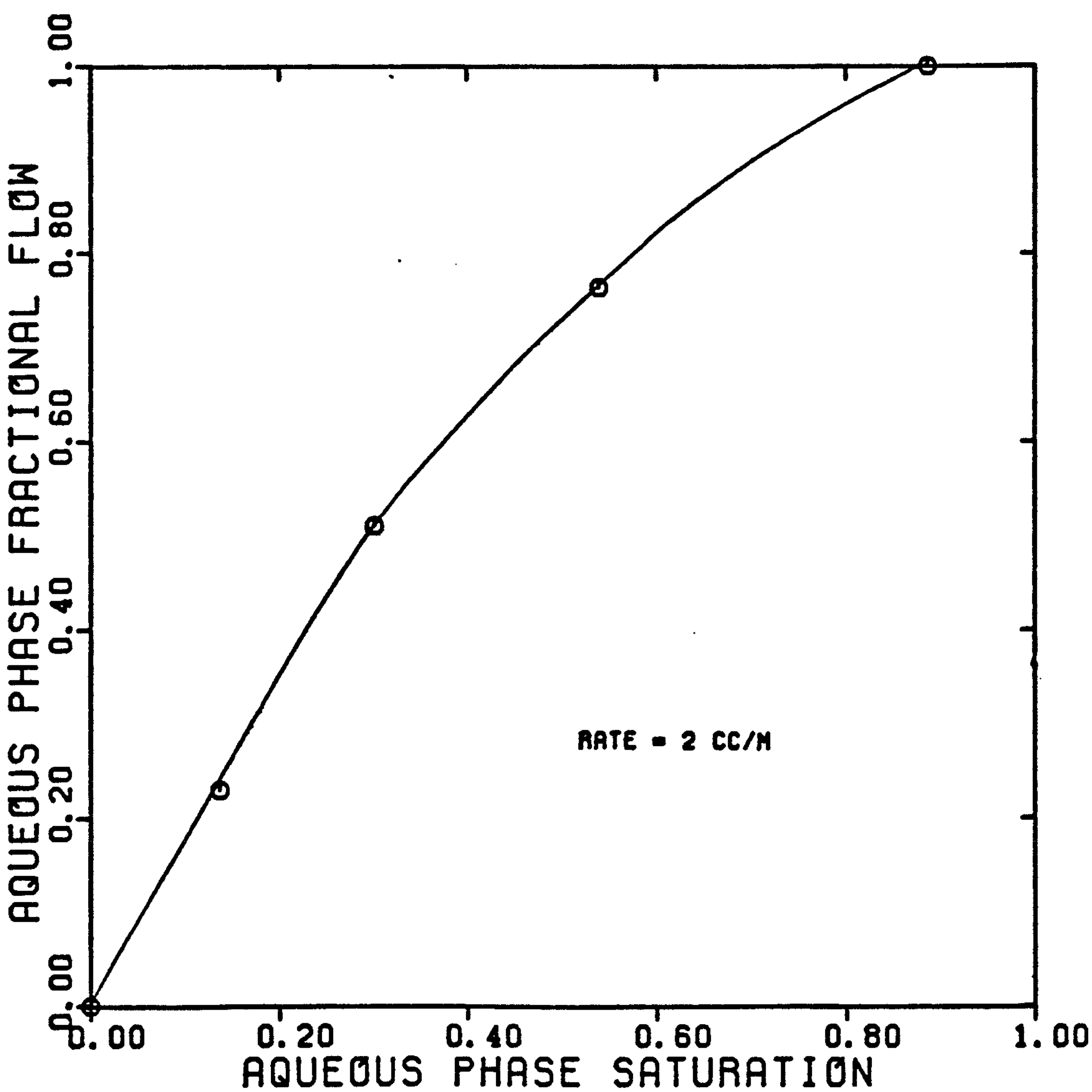

FIGURE 5.112

FRACTIONAL FLOW OF HIGH AND LOW IFT
SYSTEMS IN UNCONSOLIDATED SAND
(EXPERIMENTS OWZ AND MW)

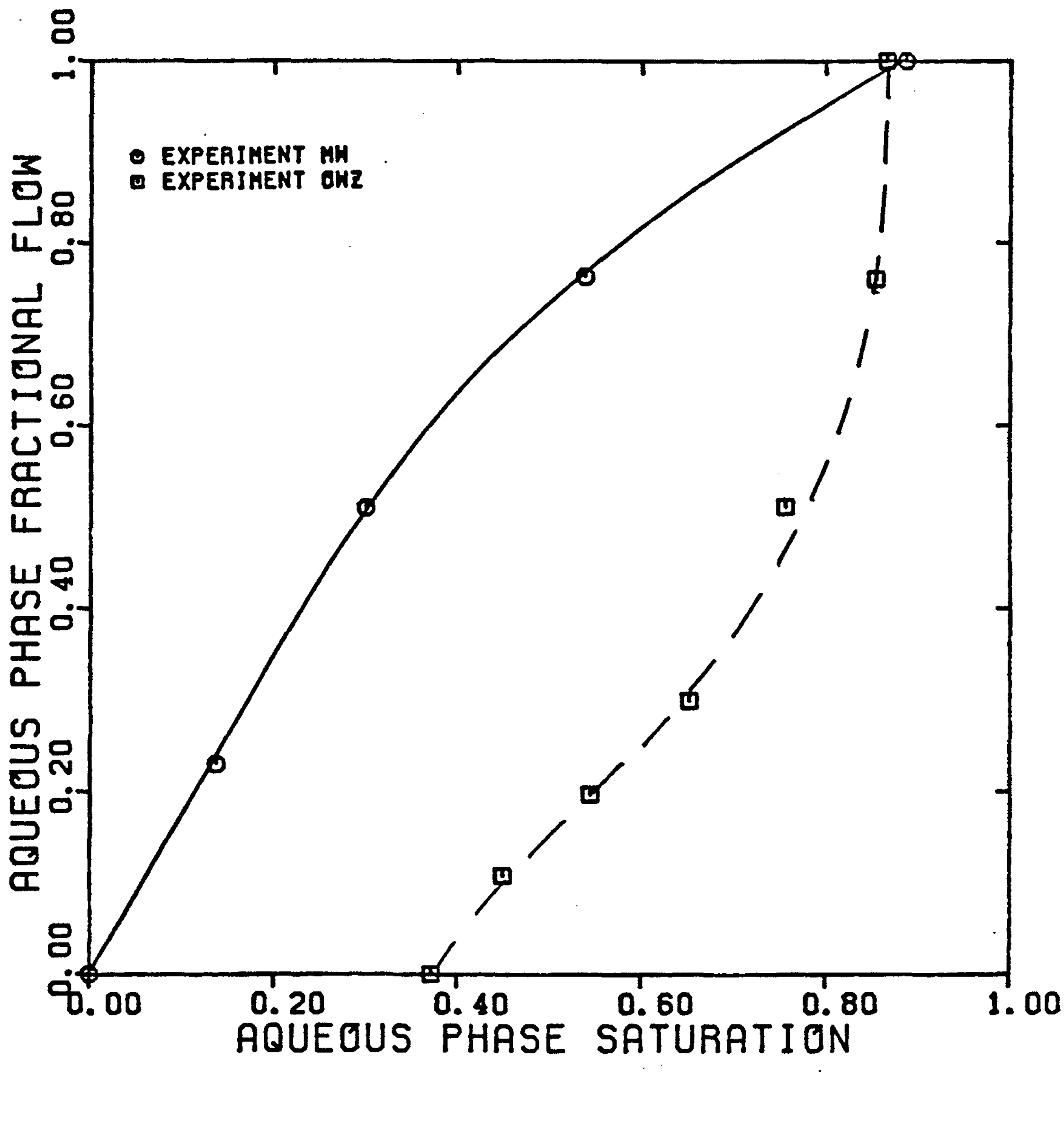

FIGURE 5.113

SANDPACK BREAKTHROUGH CURVE FOR CARBON 14
TRACER IN THE MICROEMULSION PHASE
(EXPERIMENT MW1)

$S_{me} = 1.0 \quad f_{me} = 1.0$

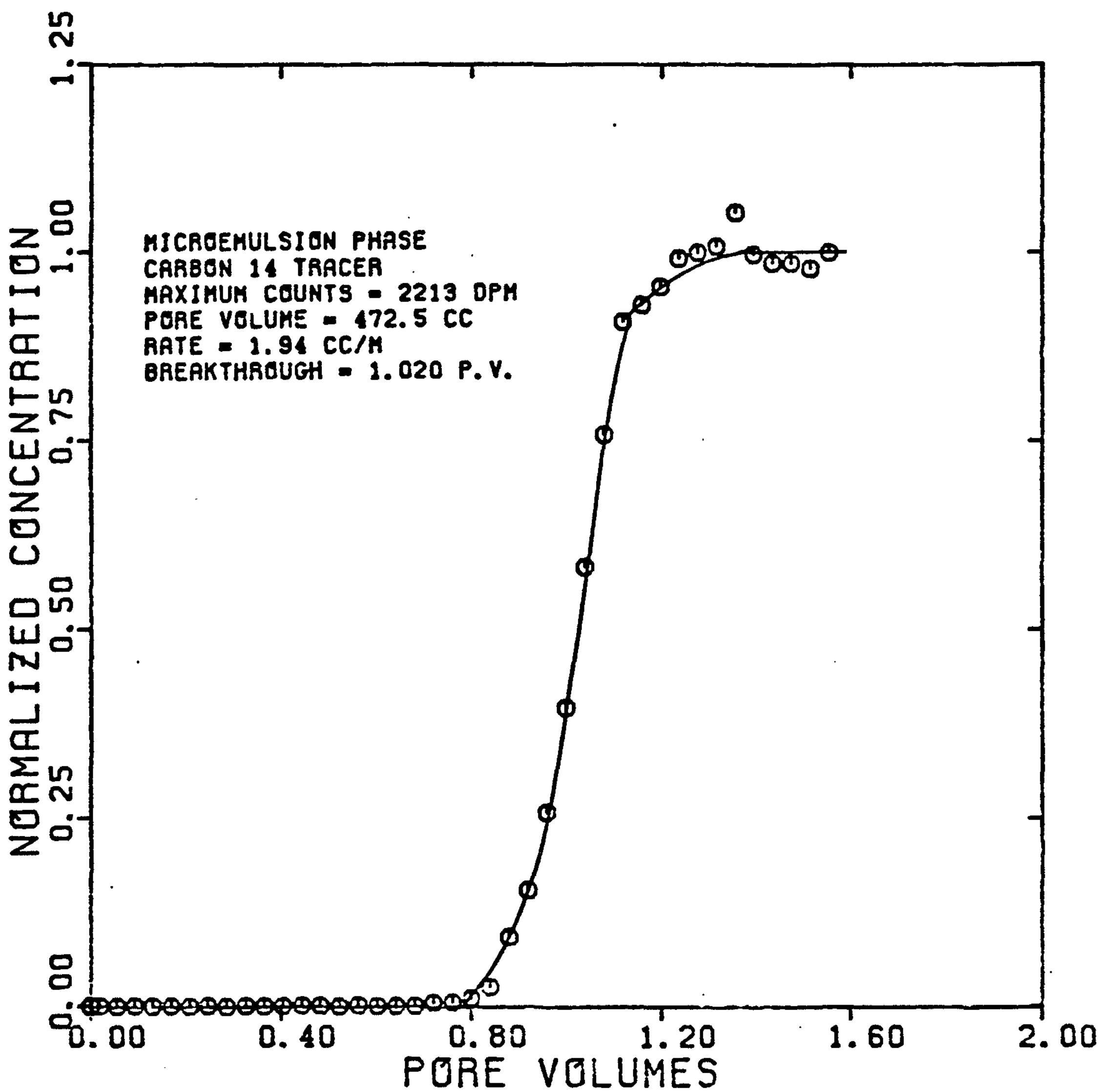

FIGURE 5.114

DISPERSIVITY OF CARBON 14
TRACER IN THE MICROEMULSION PHASE
(EXPERIMENT MW1)

$S_{me} = 1.0 \quad f_{me} = 1.0$

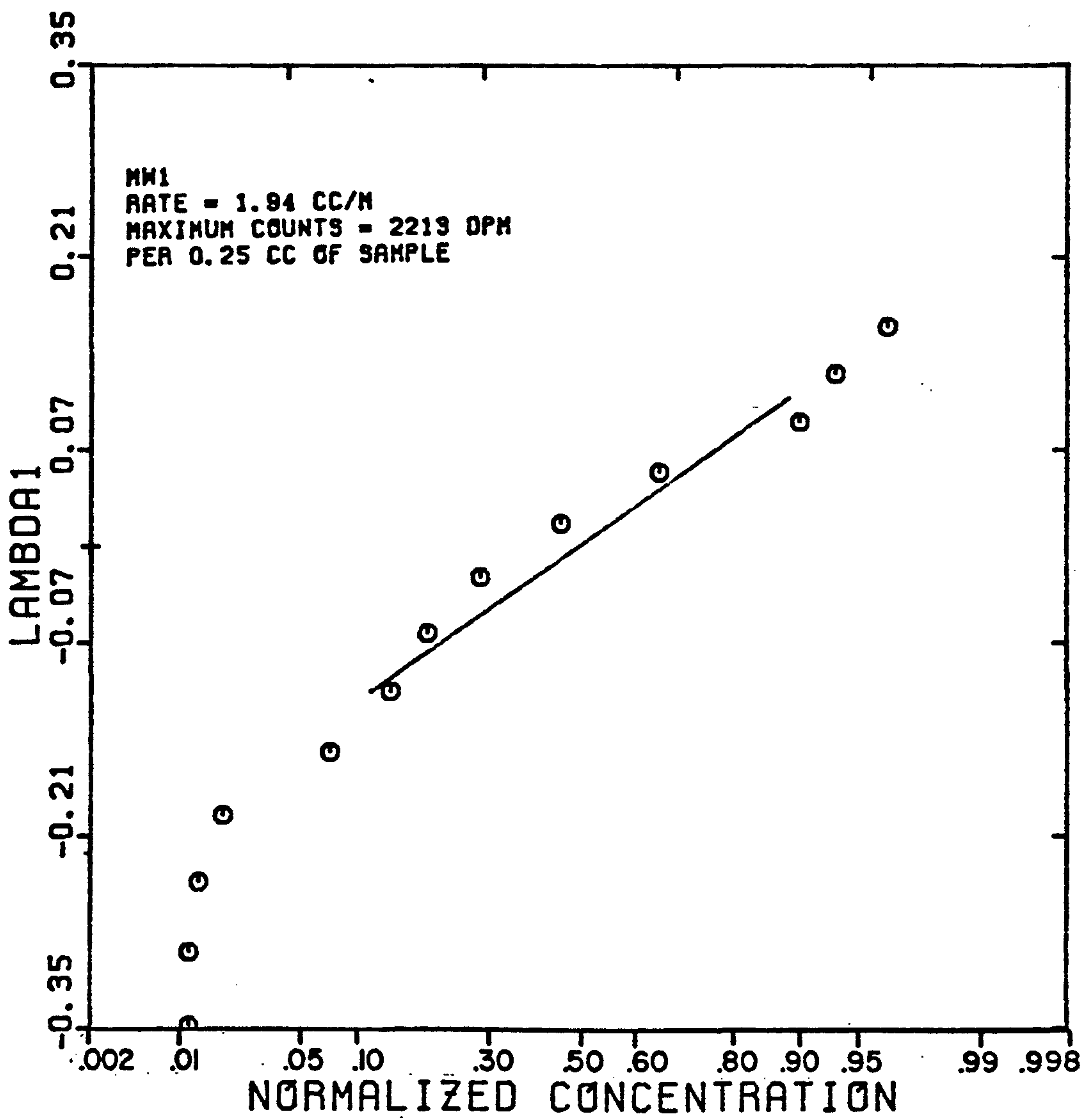

FIGURE 5.115

SANDPACK BREAKTHROUGH CURVE FOR TRITIUM
TRACER IN THE AQUEOUS PHASE
(EXPERIMENT MW2LO)

S_w = 0.137 f_w = 0.230

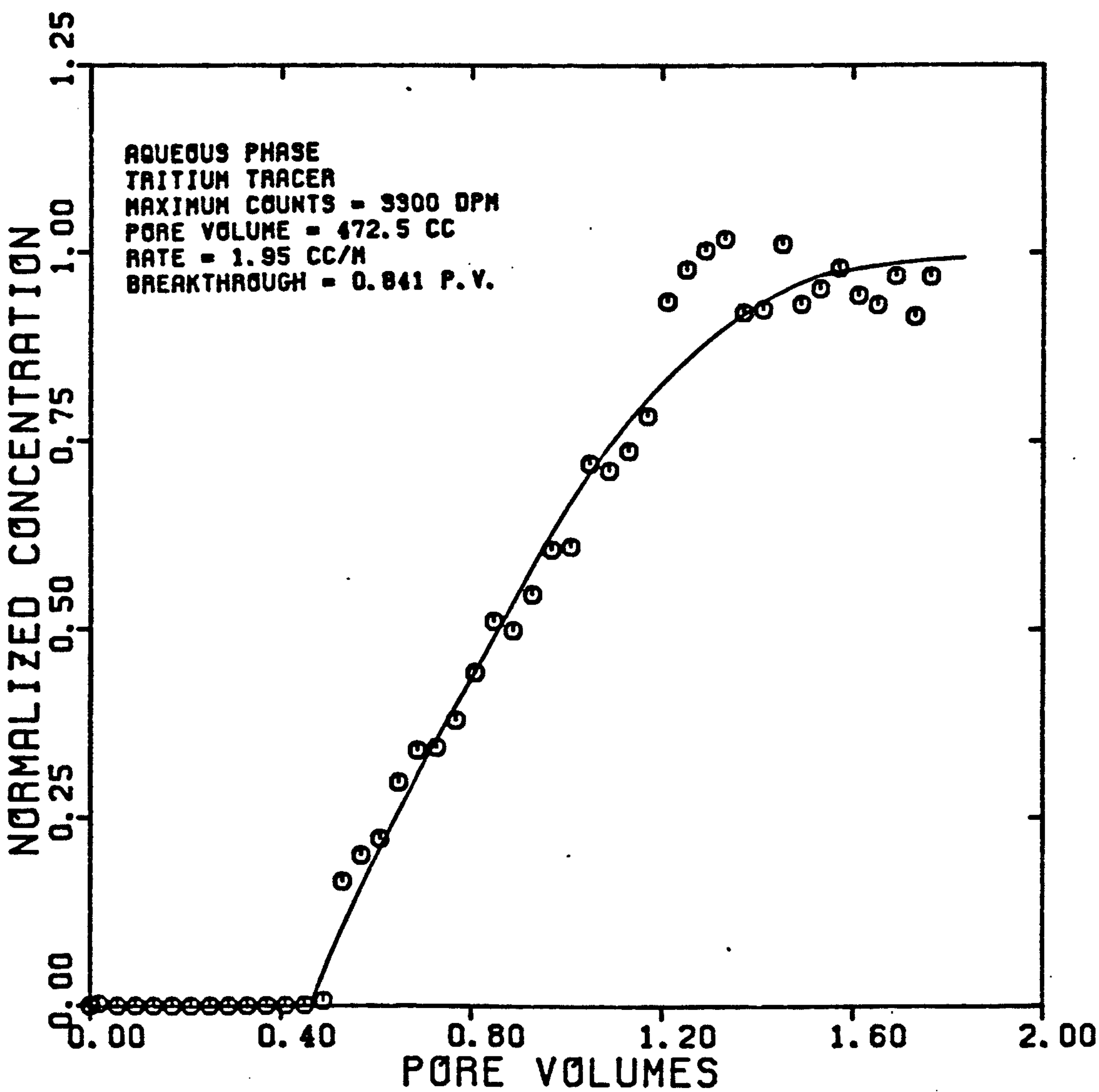

FIGURE 5.116

DISPERSIVITY OF TRITIUM
TRACER IN THE AQUEOUS PHASE
(EXPERIMENT MW2L0)

$S_w = 0.137 \quad f_w = 0.230$

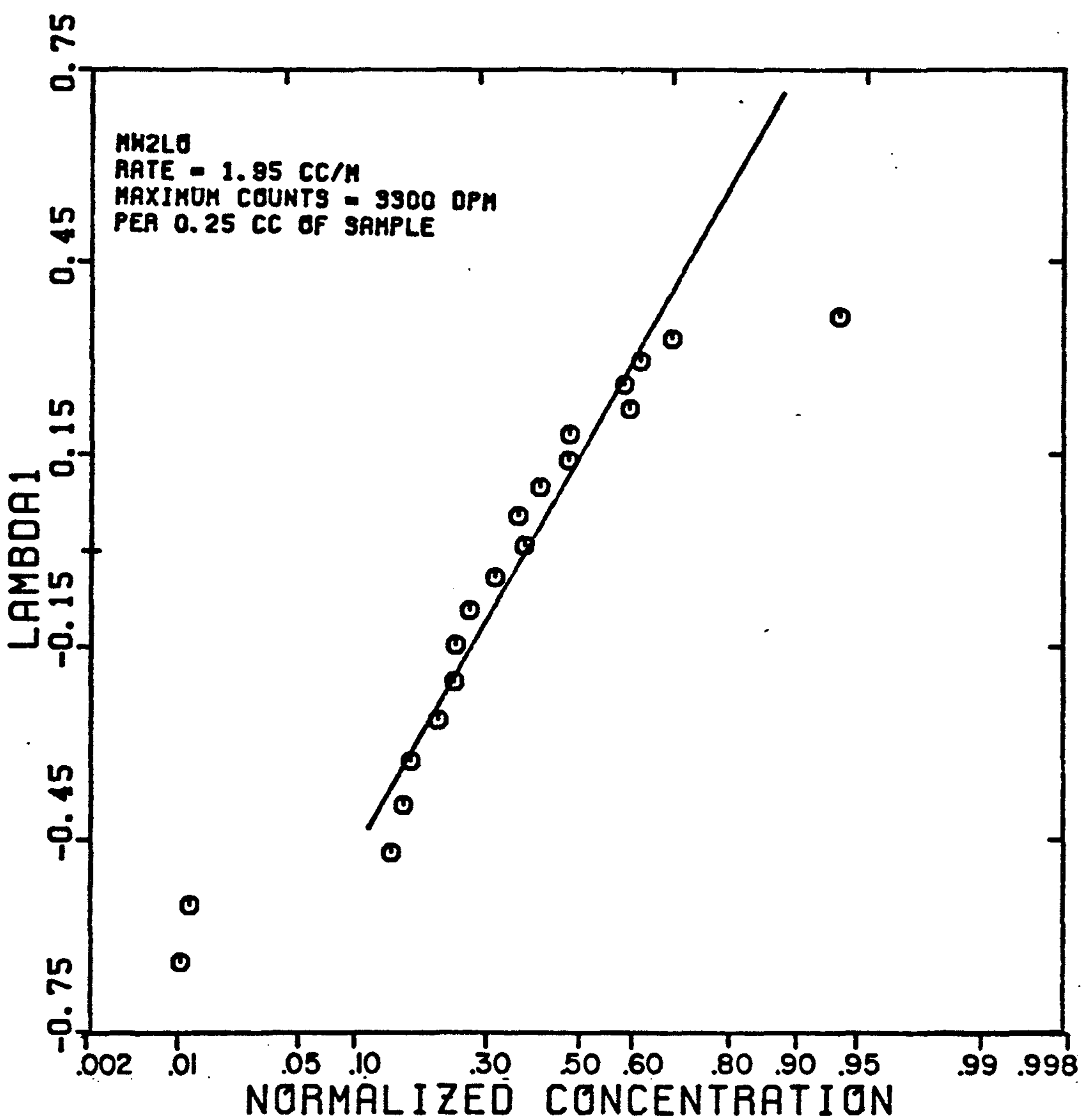

FIGURE 5.117

SANDPACK BREAKTHROUGH CURVE FOR TRITIUM
TRACER IN THE MICROEMULSION PHASE
(EXPERIMENT MW2PART)

$S_{me} = 0.863 \quad f_{me} = 0.770$

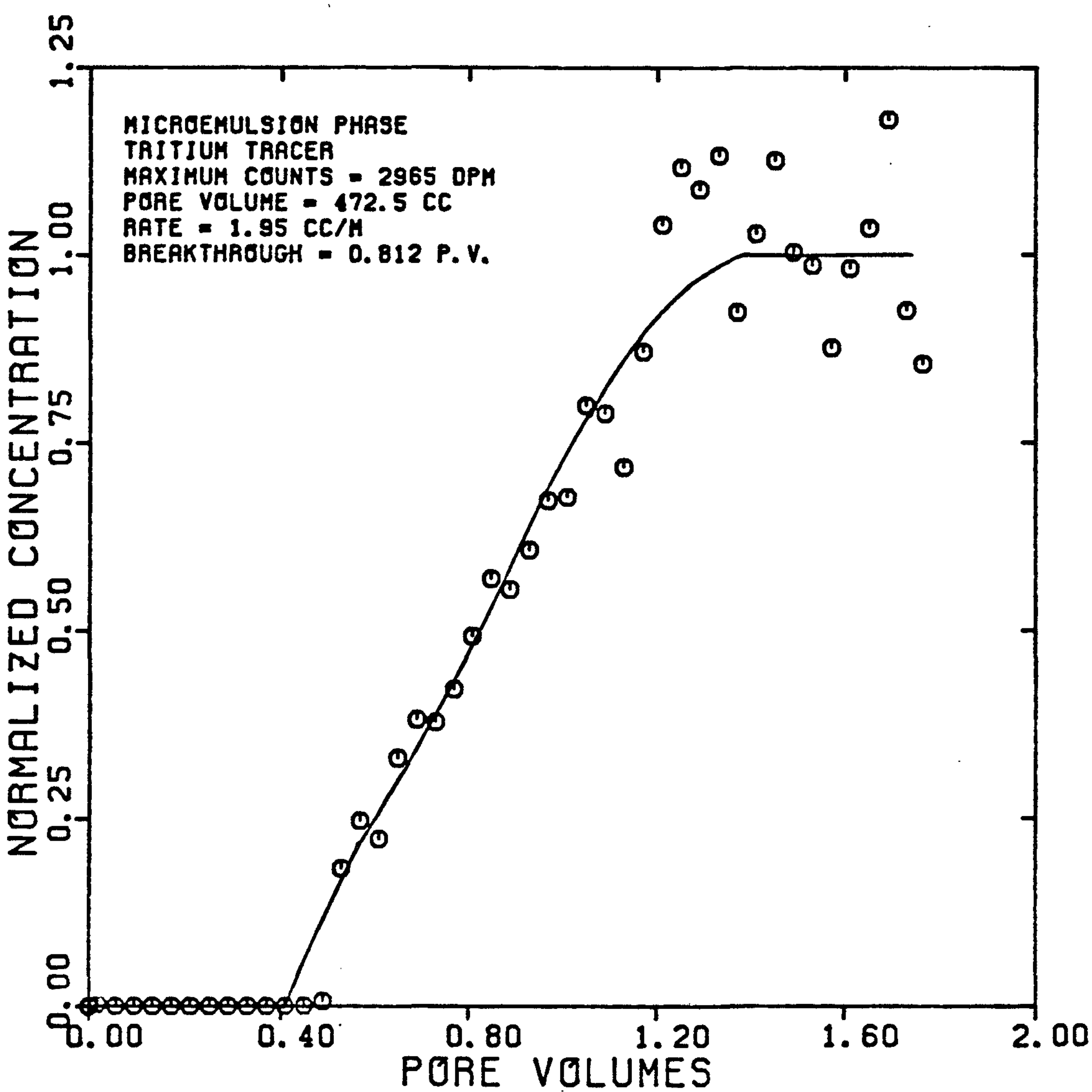

FIGURE 5.118

DISPERSIVITY OF TRITIUM
TRACER IN THE MICROEMULSION PHASE
(EXPERIMENT MW2PART)

$S_{me} = 0.863 \quad f_{me} = 0.770$

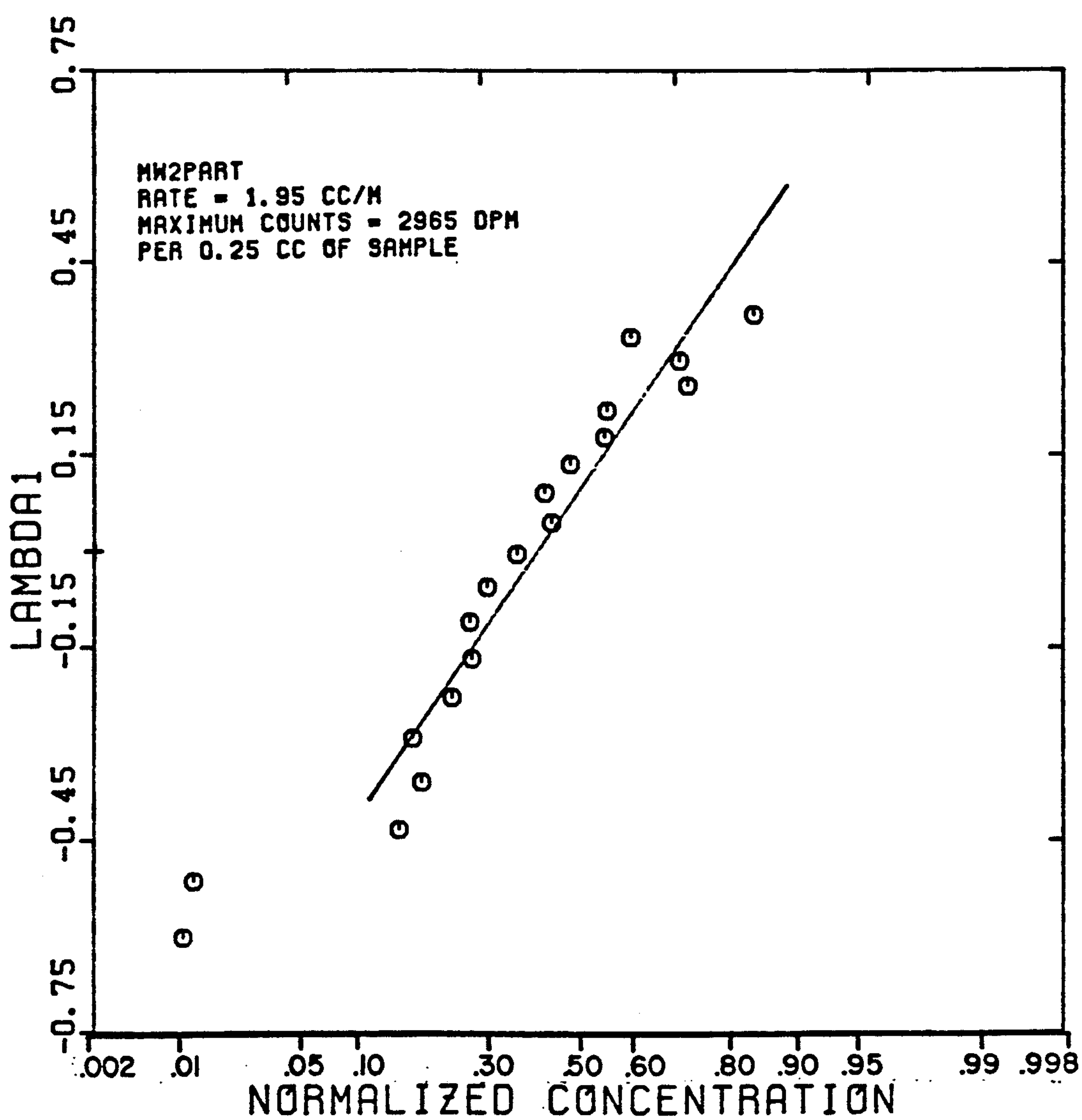

FIGURE 5.119

SANDPACK BREAKTHROUGH CURVE FOR CARBON 14
TRACER IN THE MICROEMULSION PHASE
(EXPERIMENT MW2UP)

$S_{me} = 0.863 \quad f_{me} = 0.770$

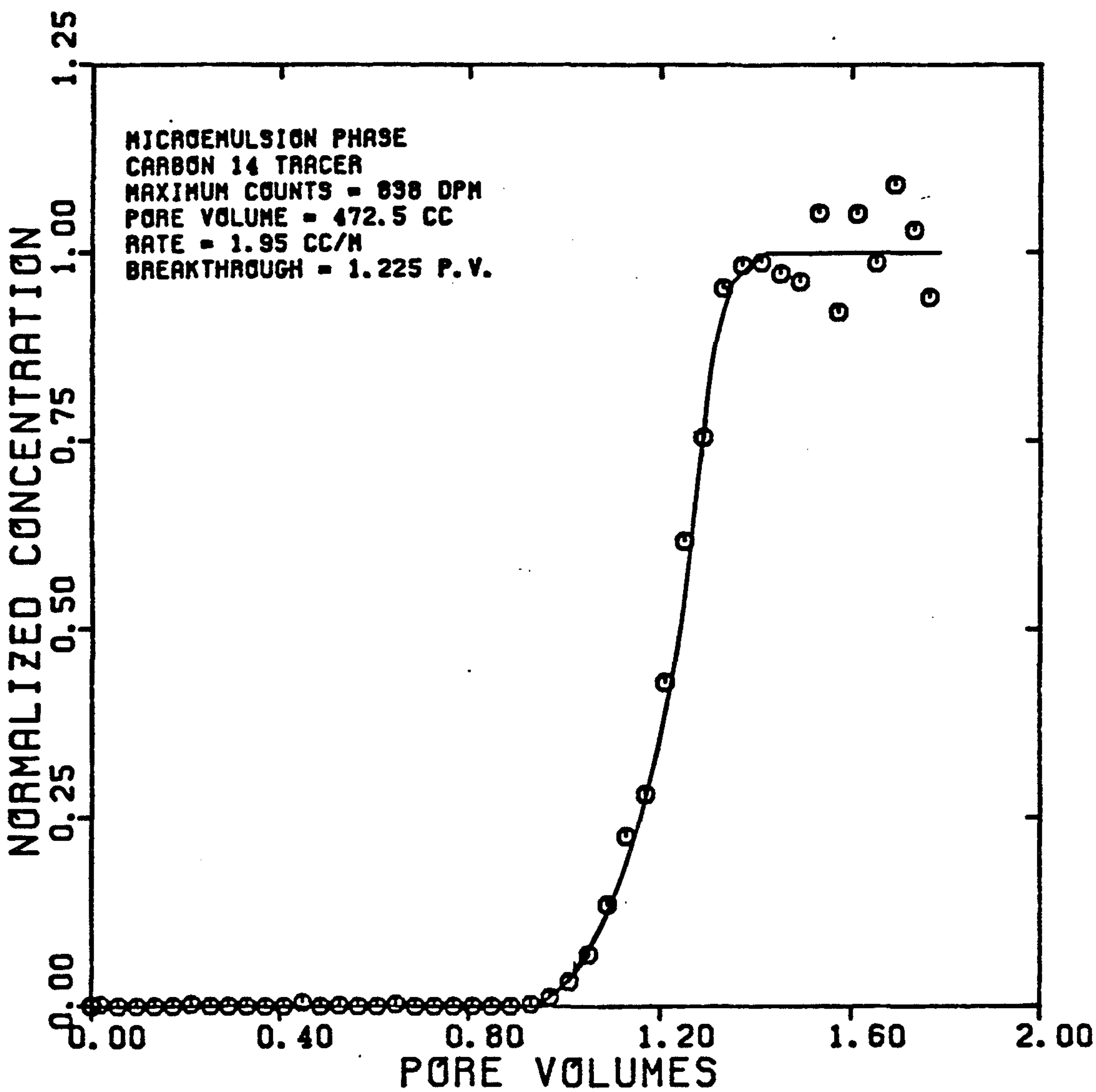

FIGURE 5.120

DISPERSIVITY OF CARBON 14
TRACER IN THE MICROEMULSION PHASE
(EXPERIMENT MW2UP)

S_{me} = 0.863 f_{me} = 0.770

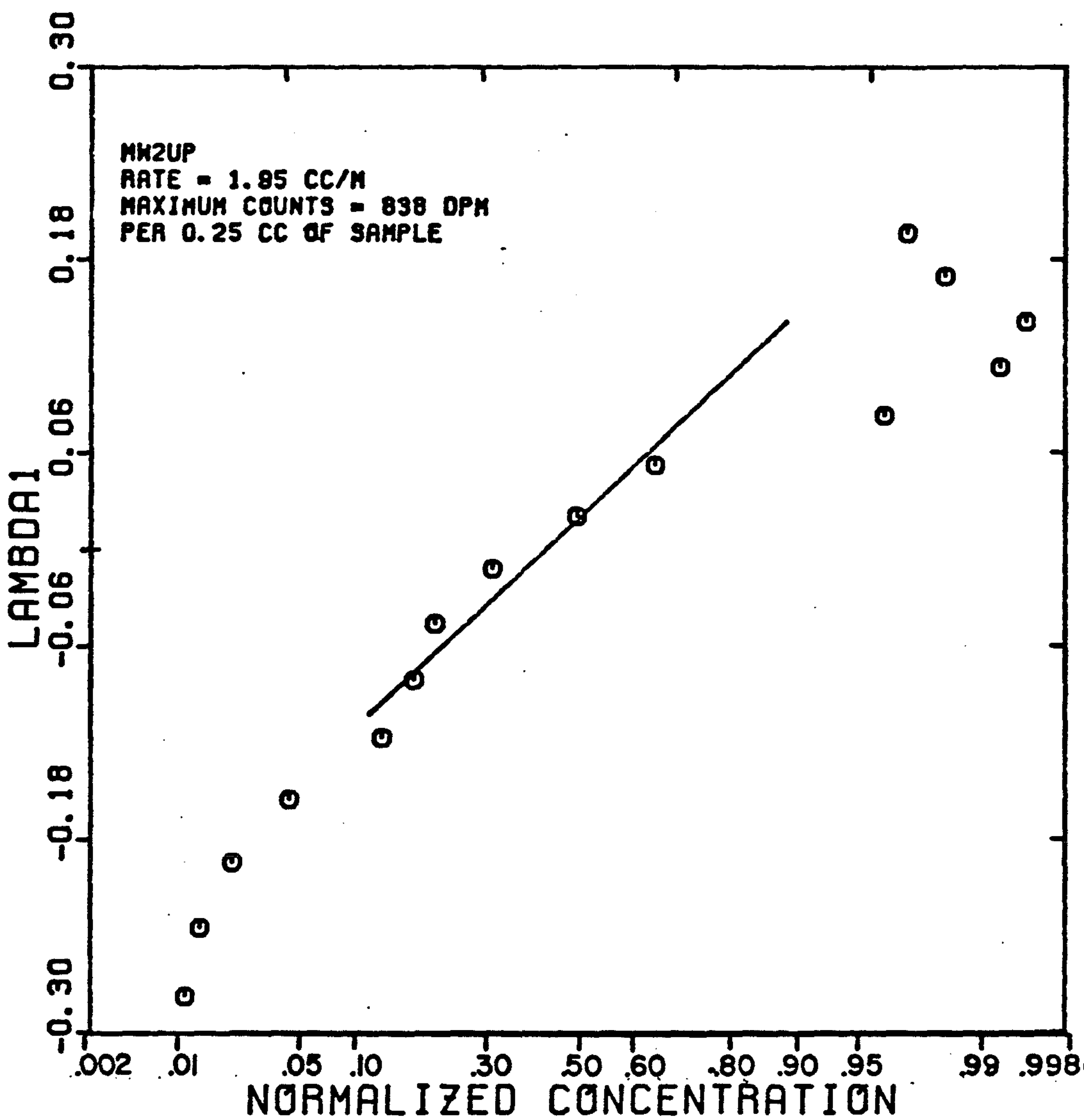

FIGURE 5.121

SANDPACK BREAKTHROUGH CURVE FOR TRITIUM
TRACER IN THE AQUEOUS PHASE
(EXPERIMENT MW3L0)

$S_w = 0.301 \quad f_w = 0.511$

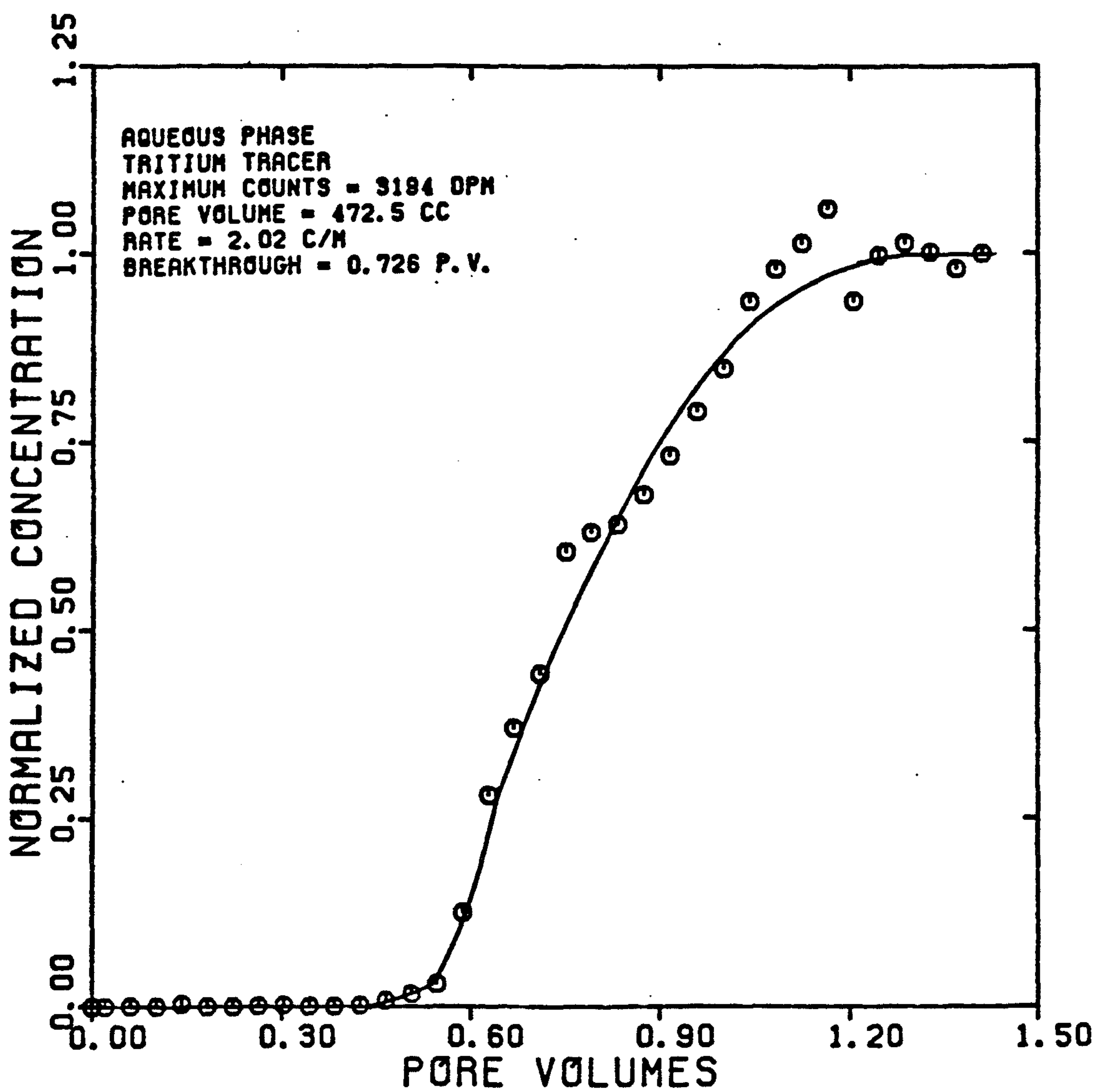

FIGURE 5.122

DISPERSIVITY OF TRITIUM
TRACER IN THE AQUEOUS PHASE
(EXPERIMENT MW3L0)

S_w = 0.301 f_w = 0.511

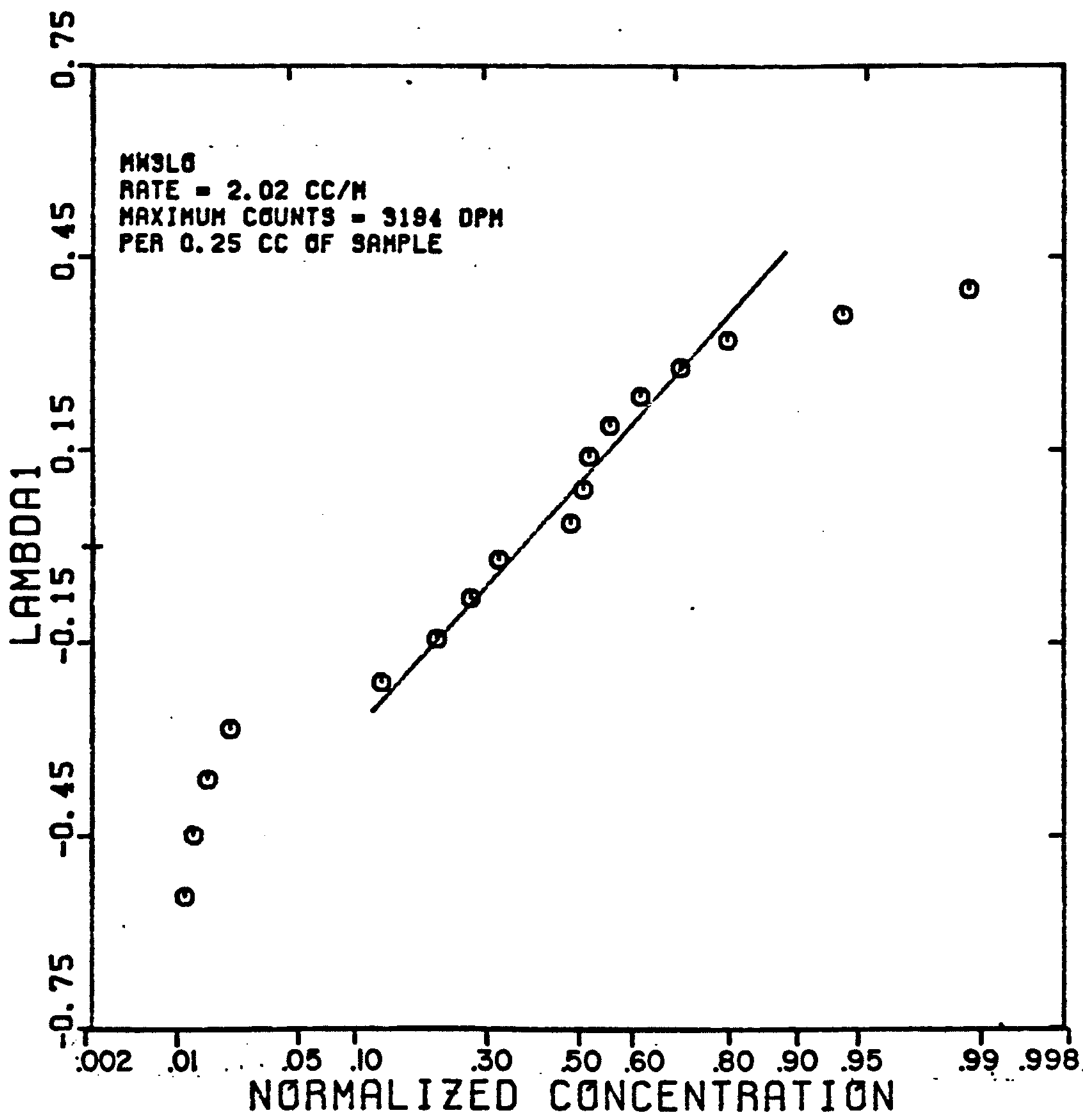

FIGURE 5.123

SANDPACK BREAKTHROUGH CURVE FOR TRITIUM
TRACER IN THE MICROEMULSION PHASE
(EXPERIMENT MW3PART)

S_{me} = 0.699 f_{me} = 0.489

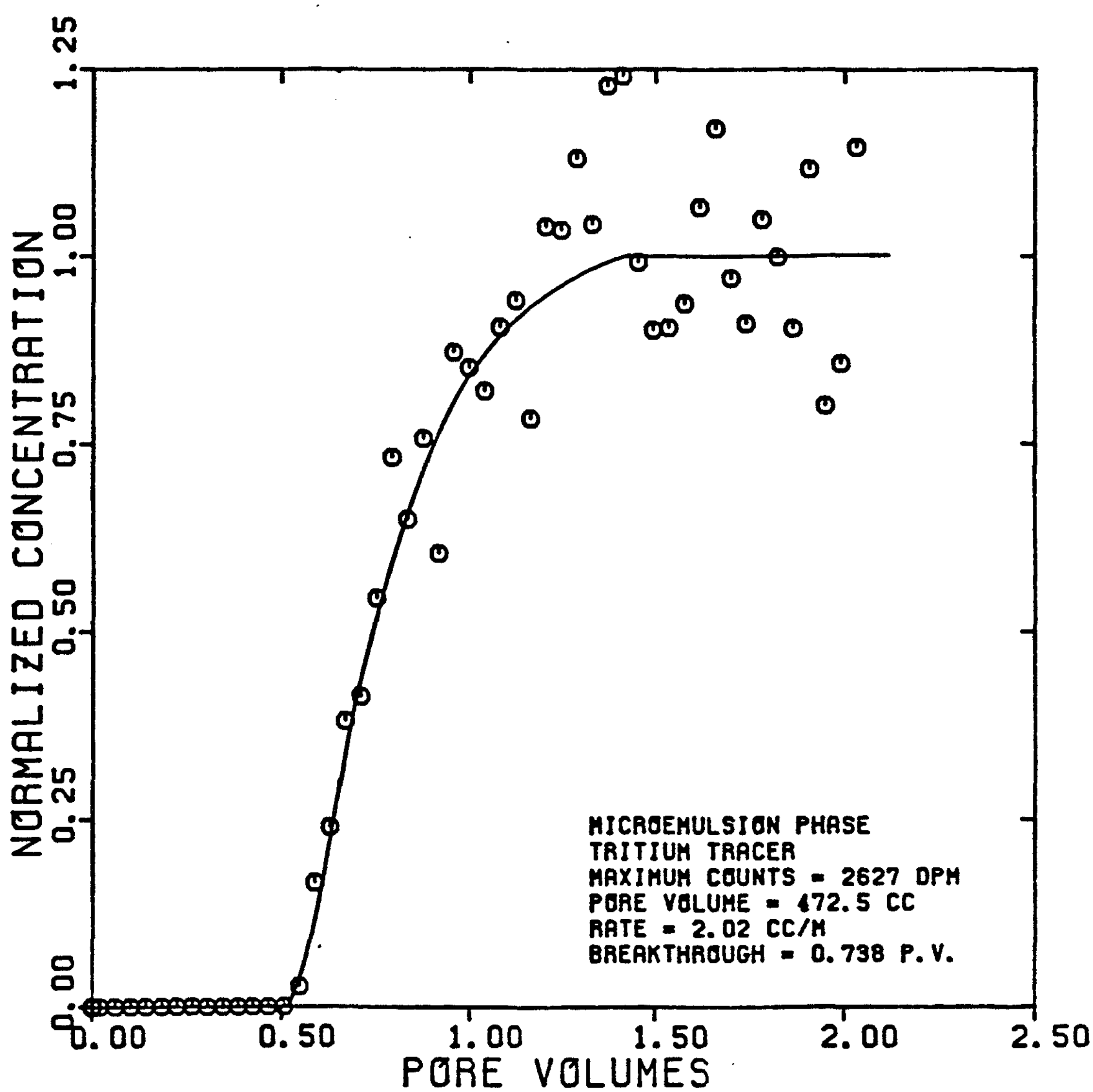

FIGURE 5.124

DISPERSIVITY OF TRITIUM
TRACER IN THE MICROEMULSION PHASE
(EXPERIMENT MW3PART)

$S_{me} = 0.699 \quad f_{me} = 0.489$

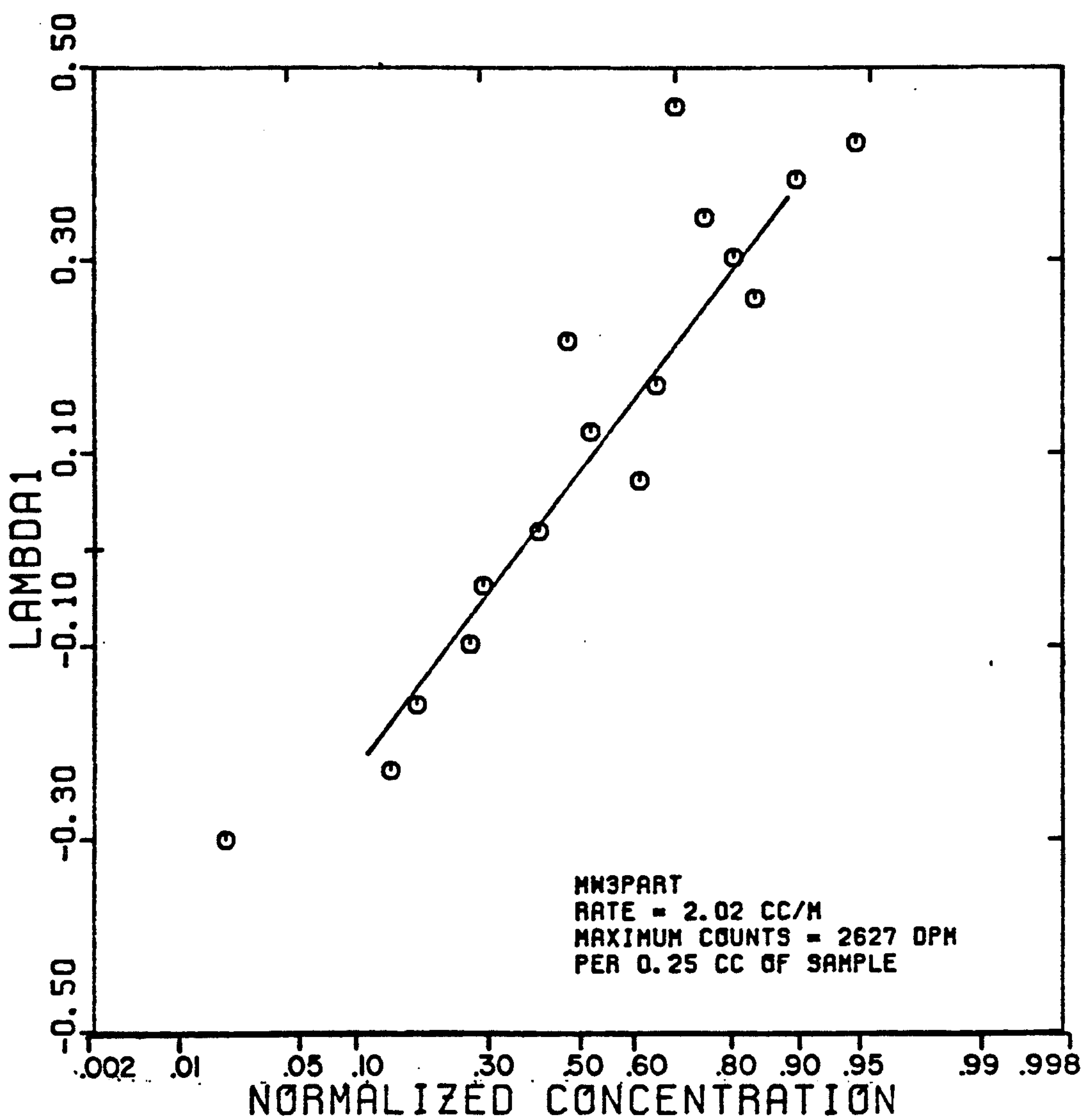

FIGURE 5.125

SANDPACK BREAKTHROUGH CURVE FOR CARBON 14
TRACER IN THE MICROEMULSION PHASE
(EXPERIMENT MW3UP)

$S_{me} = 0.699 \quad f_{me} = 0.489$

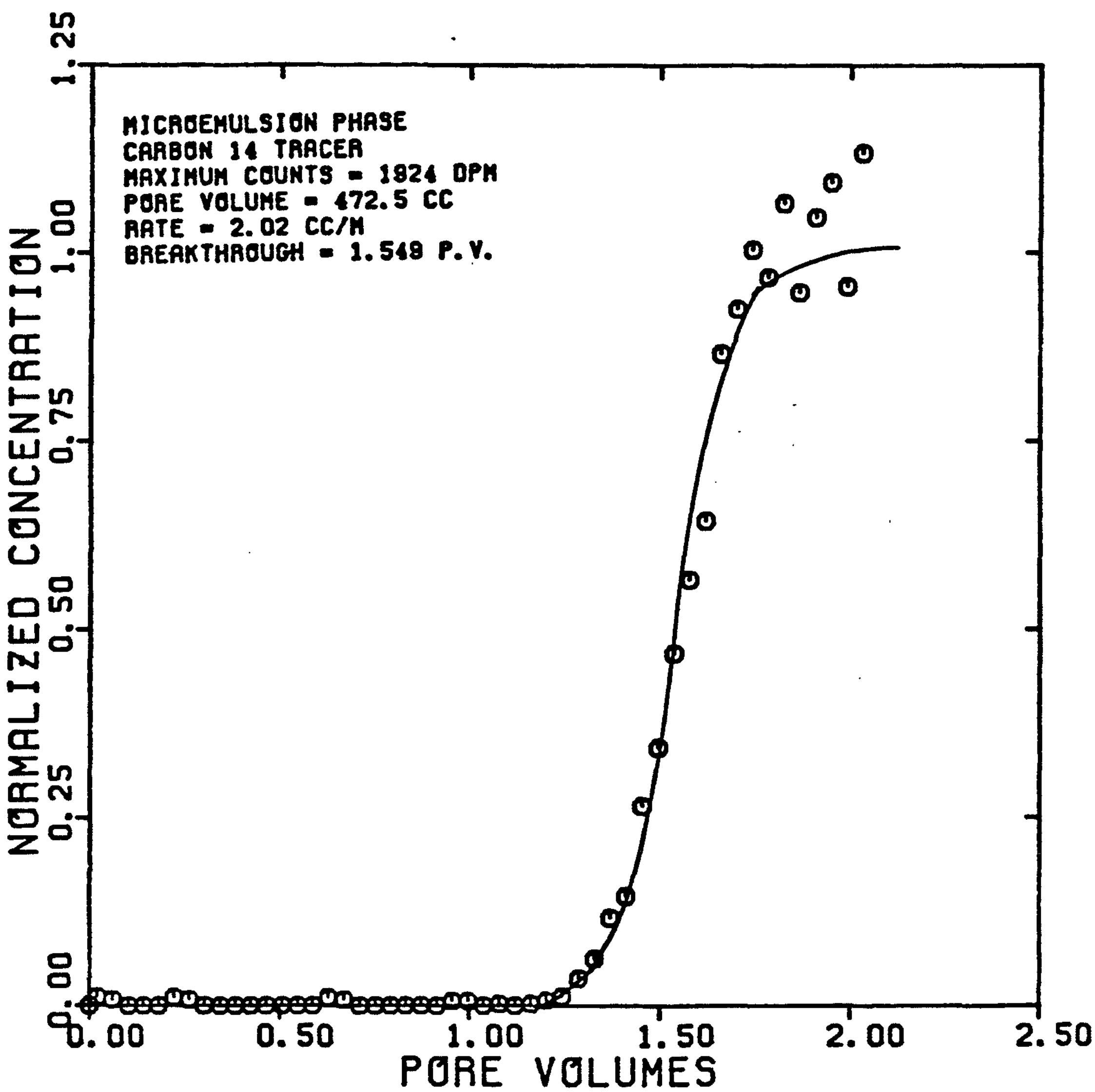

FIGURE 5.126

DISPERSIVITY OF CARBON 14
TRACER IN THE MICROEMULSION PHASE
(EXPERIMENT MW3UP)

S_{me} = 0.699 f_{me} = 0.489

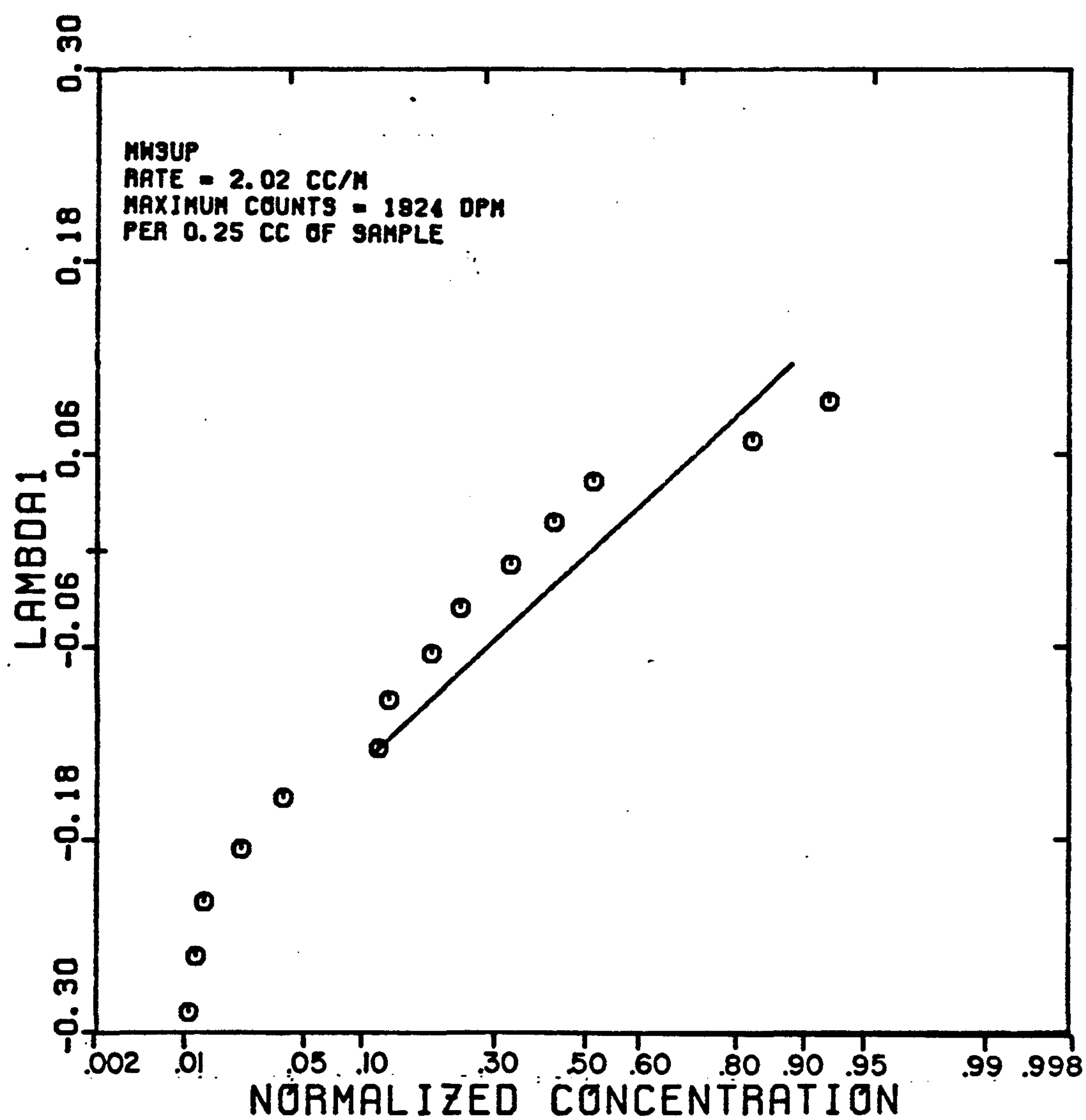

FIGURE 5.127

SANDPACK BREAKTHROUGH CURVE FOR TRITIUM
TRACER IN THE AQUEOUS PHASE
(EXPERIMENT MW4L0)

$S_w = 0.539 \quad f_w = 0.764$

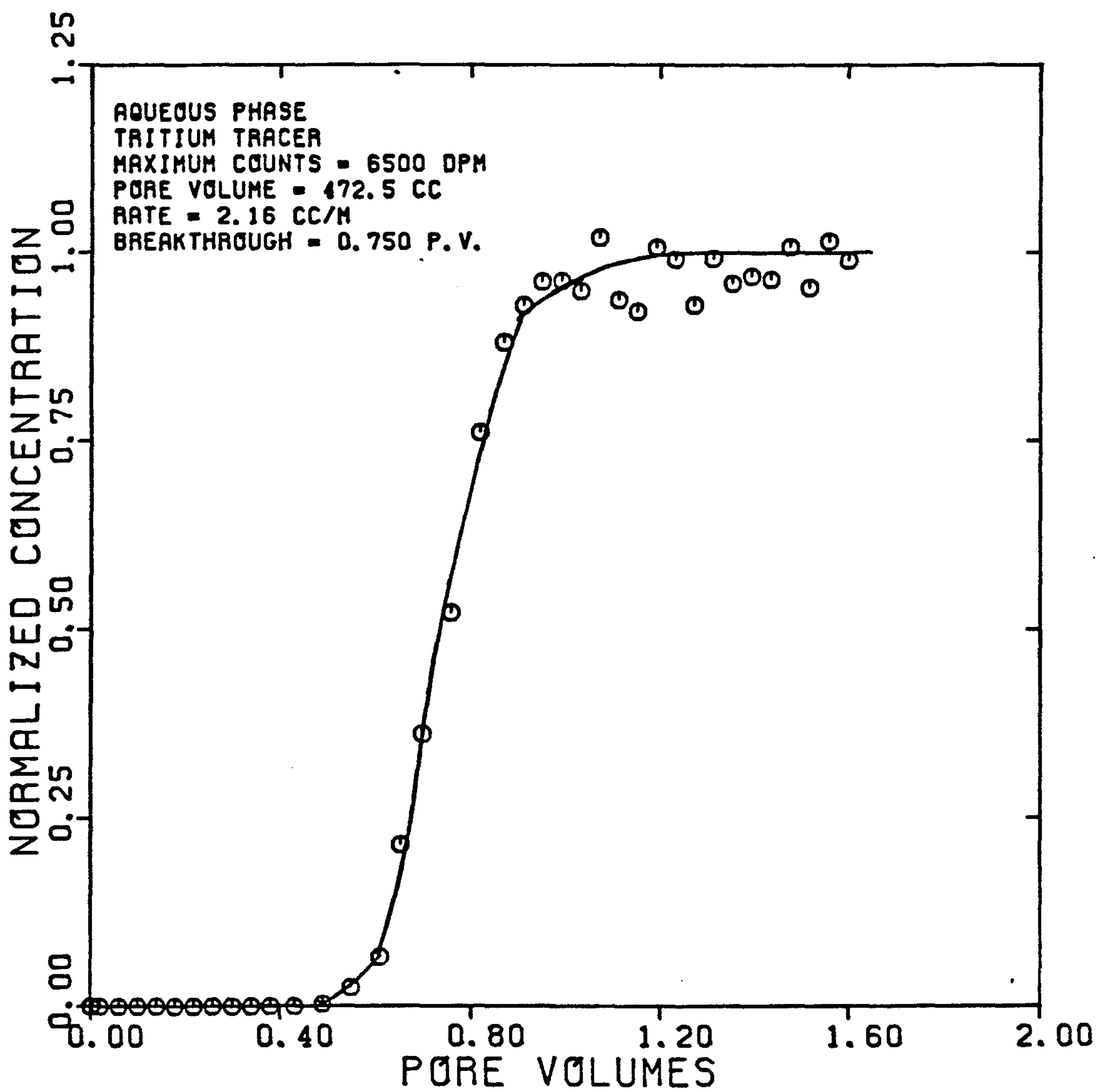

FIGURE 5.128

DISPERSIVITY OF TRITIUM
TRACER IN THE AQUEOUS PHASE
(EXPERIMENT MW4L0)

$S_w = 0.539 \quad f_w = 0.764$

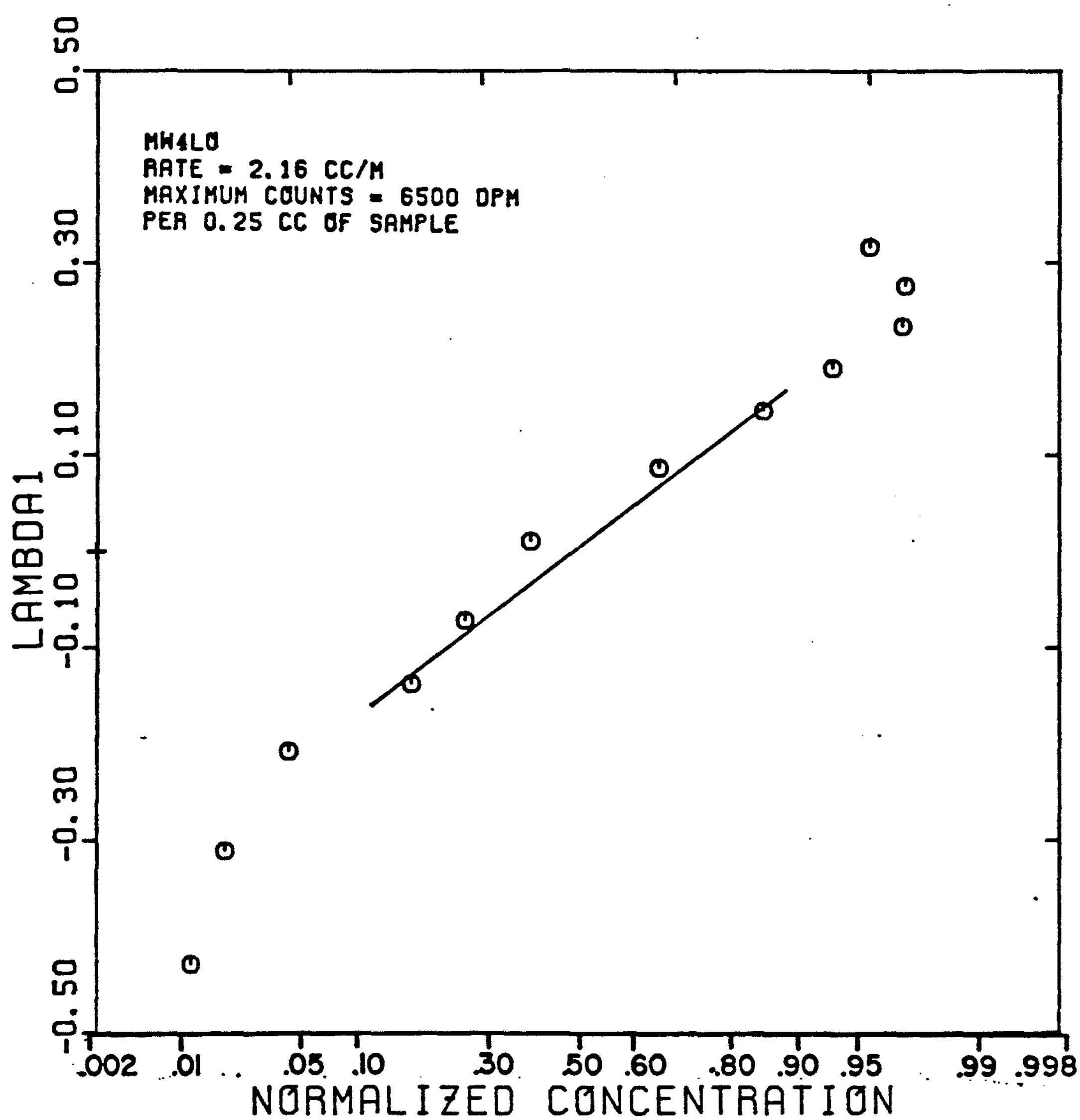

FIGURE 5.129

SANDPACK BREAKTHROUGH CURVE FOR TRITIUM TRACER IN THE MICROEMULSION PHASE (EXPERIMENT MW4PART)

$S_{me} = 0.461 \quad f_{me} = 0.236$

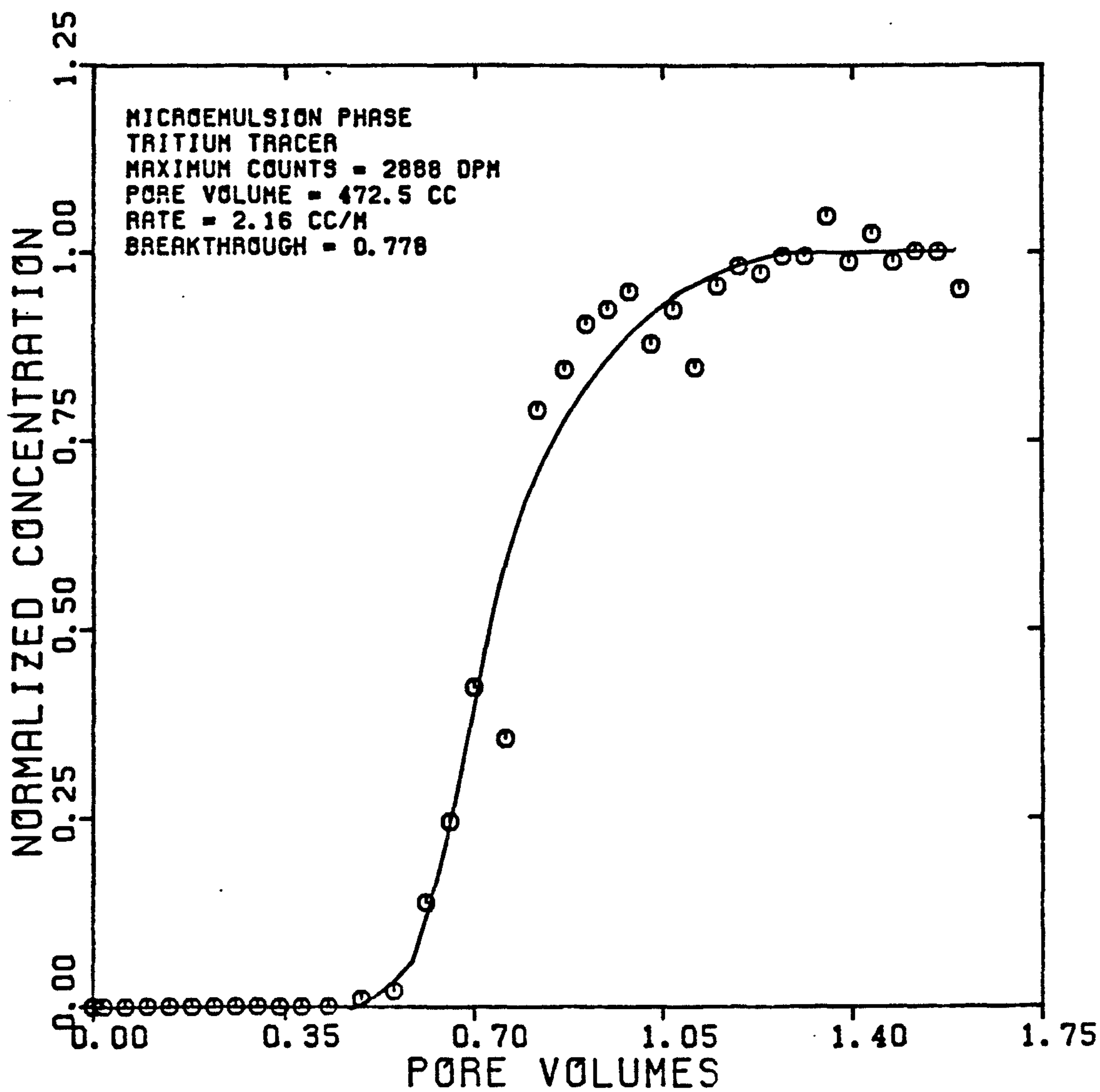

FIGURE 5.130

DISPERSIVITY OF TRITIUM
TRACER IN THE MICROEMULSION PHASE
(EXPERIMENT MW4PART)

$S_{me} = 0.461 \quad f_{me} = 0.236$

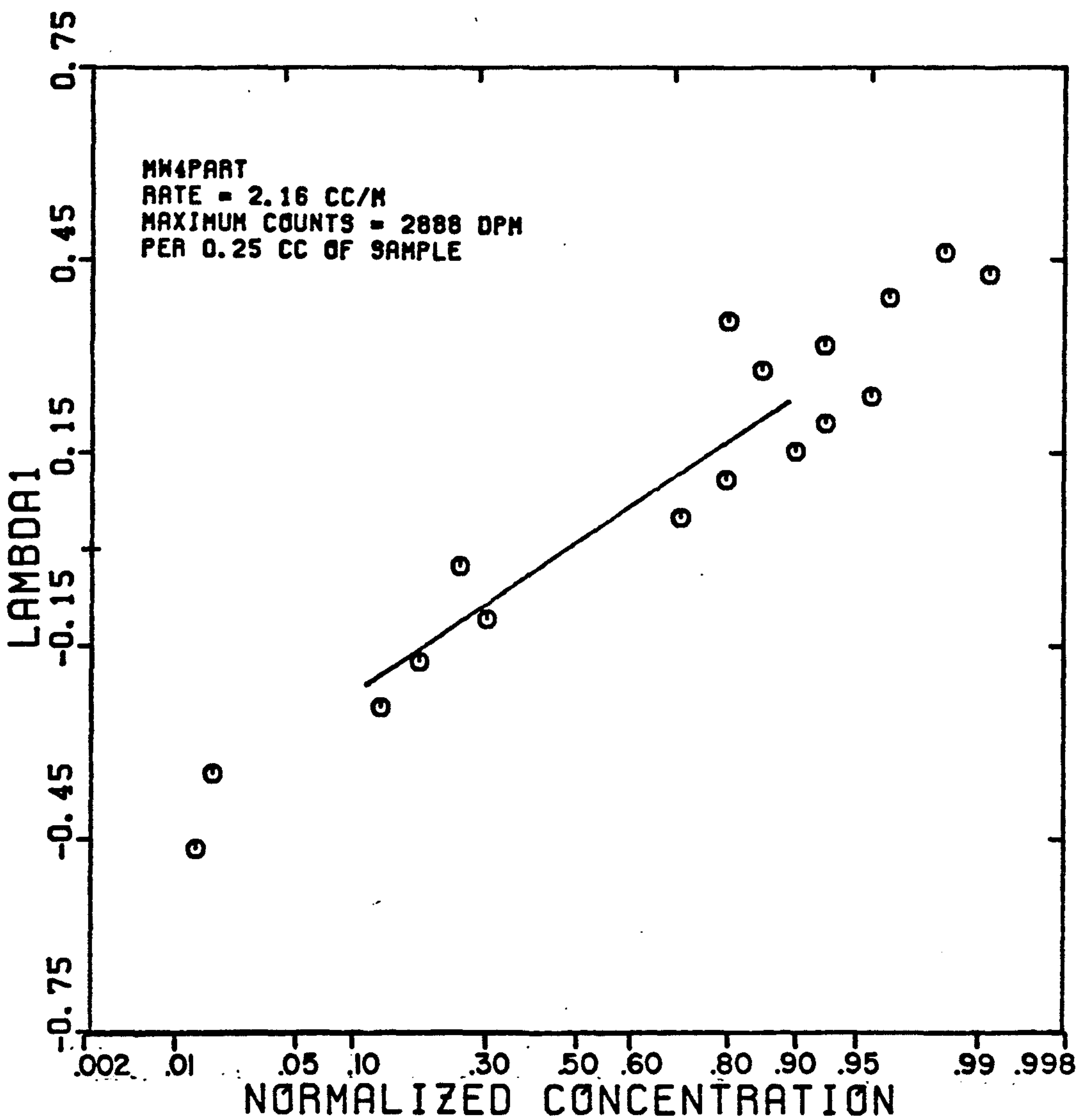

FIGURE 5.131

SANDPACK BREAKTHROUGH CURVE FOR CARBON 14
TRACER IN THE MICROEMULSION PHASE
(EXPERIMENT MW4UP)

$S_{me} = 0.461 \quad f_{me} = 0.236$

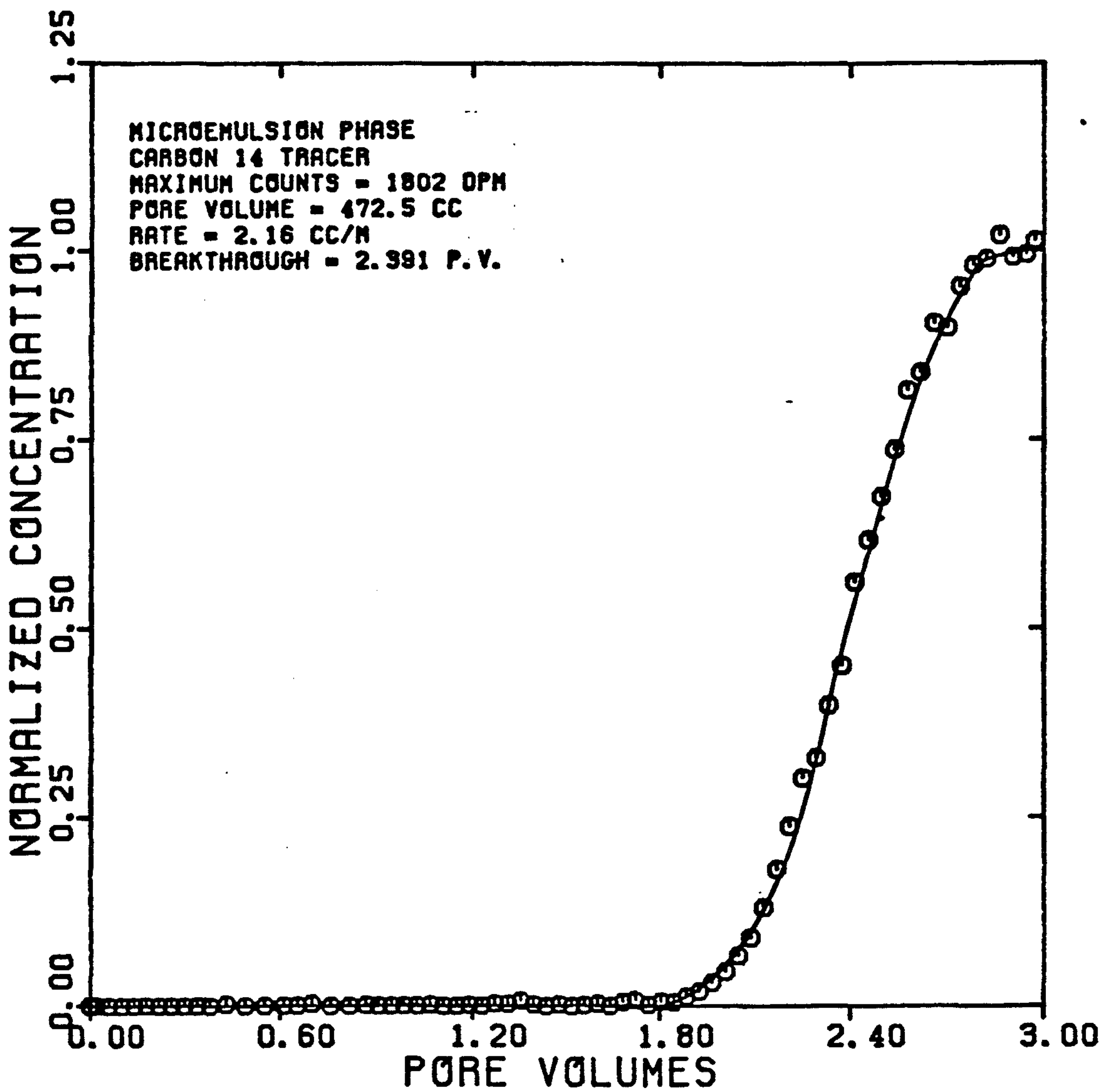

FIGURE 5.132

DISPERSIVITY OF CARBON 14
TRACER IN THE MICROEMULSION PHASE
(EXPERIMENT MW4UP)

$S_{me} = 0.461 \quad f_{me} = 0.236$

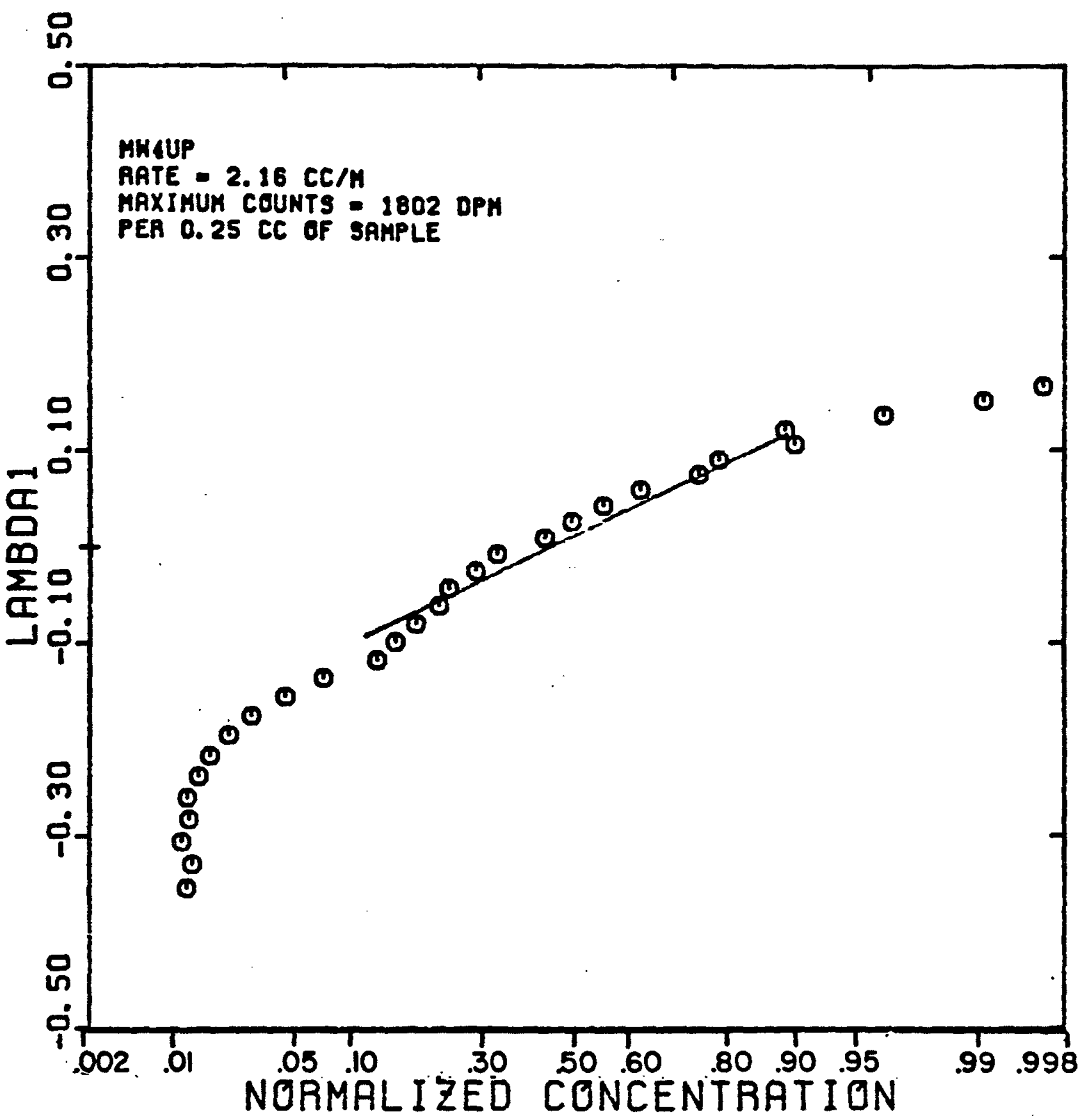

FIGURE 5.133

SANDPACK BREAKTHROUGH CURVE FOR TRITIUM
TRACER IN THE AQUEOUS PHASE
(EXPERIMENT MW5)

$S_w = 0.887 \quad f_w = 1.0$

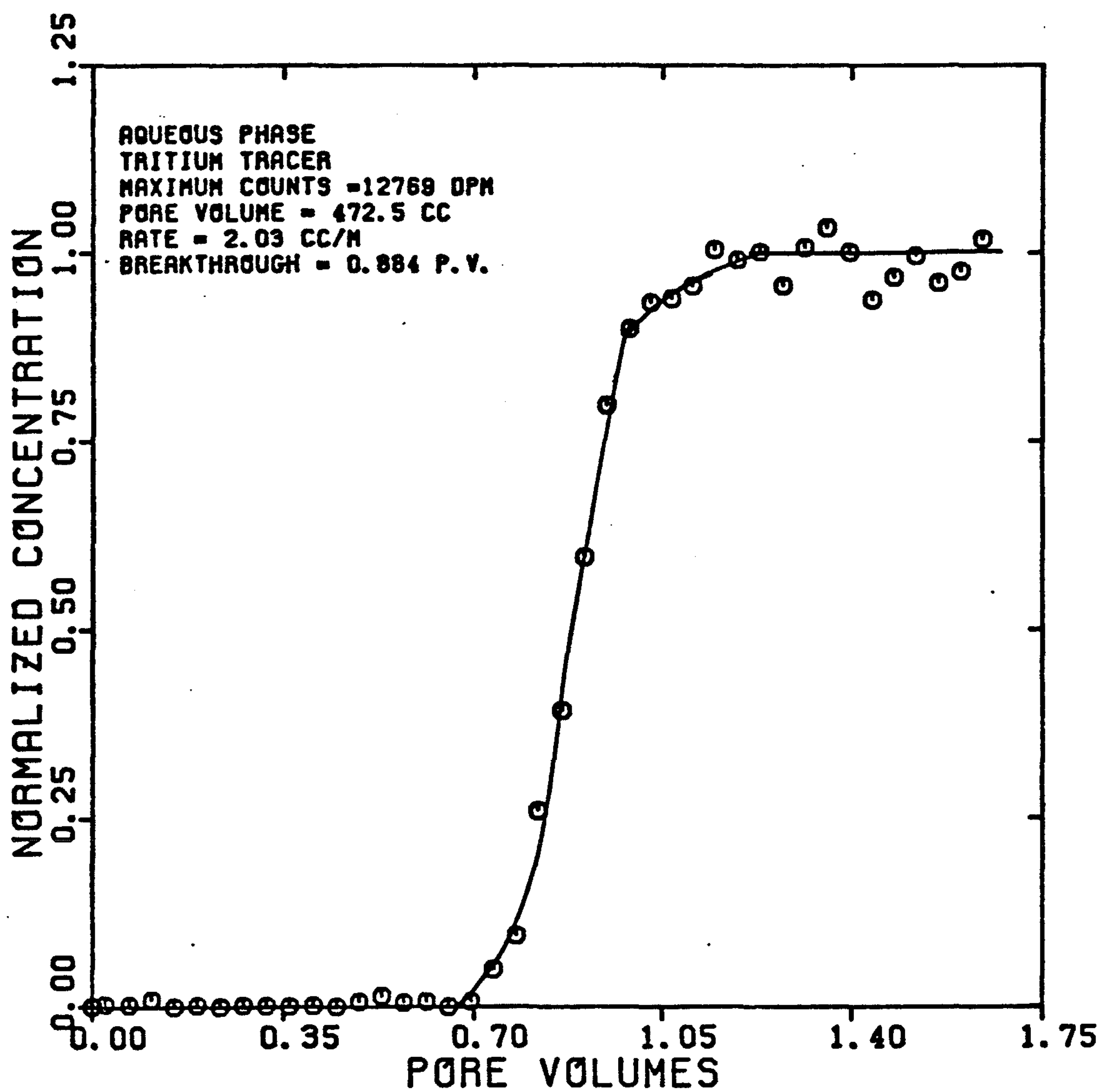

FIGURE 5.134

DISPERSIVITY OF TRITIUM
TRACER IN THE AQUEOUS PHASE
(EXPERIMENT MW5)

$S_w = 0.887 \quad f_w = 1.0$

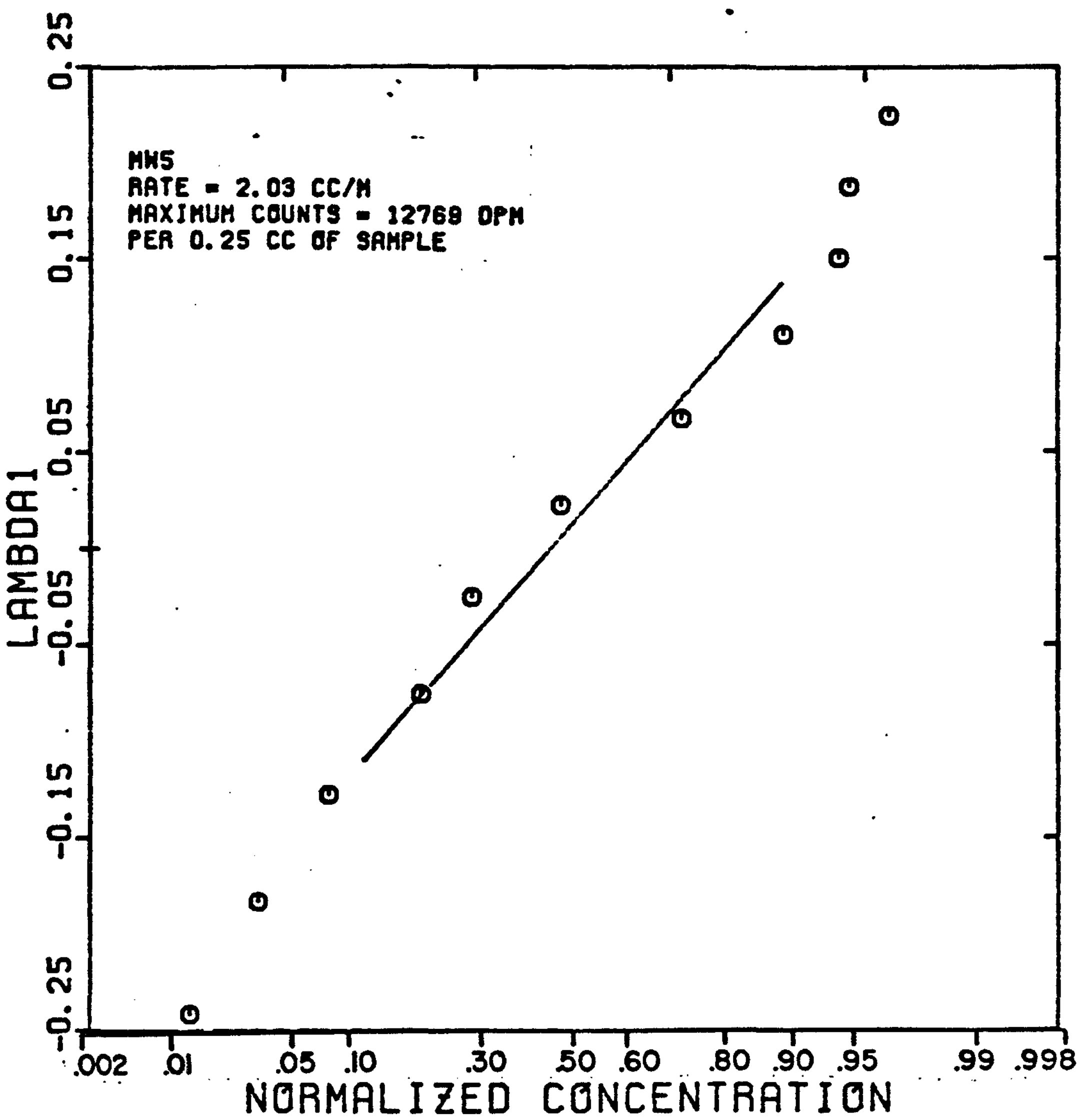

FIGURE 5.135

DISPERSIVITY OF MICROEMULSION AND
BRINE IN UNCONSOLIDATED SAND
(EXPERIMENT MW)

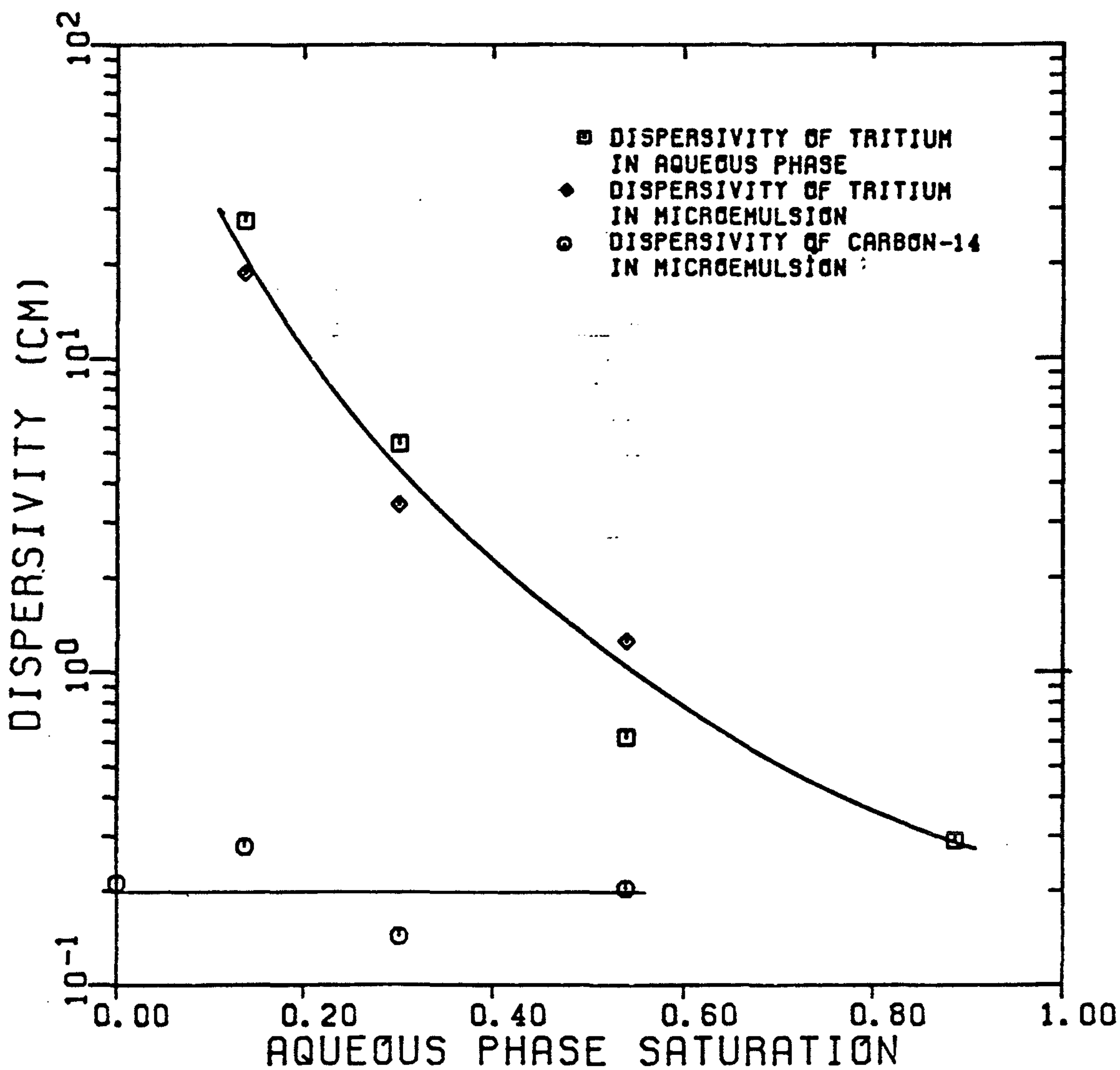

FIGURE 5.136
DISPERSIVITY OF HIGH AND LOW IFT SYSTEMS IN UNCONSOLIDATED SAND (EXPERIMENTS OWZ AND MW)

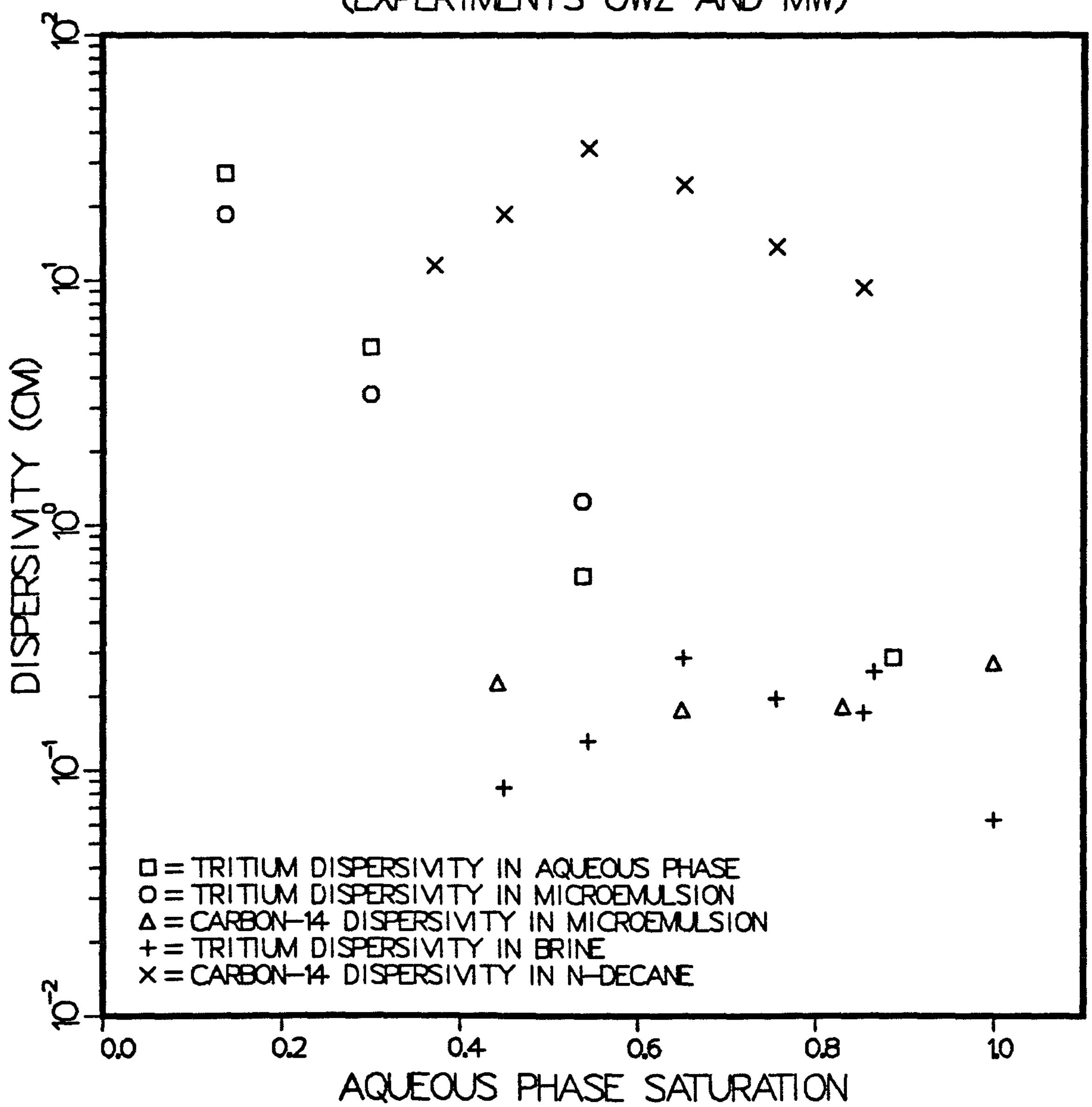

FIGURE 5.137

MICROEMULSION COMPOSITION AT
STEADY-STATE
(EXPERIMENT MW)

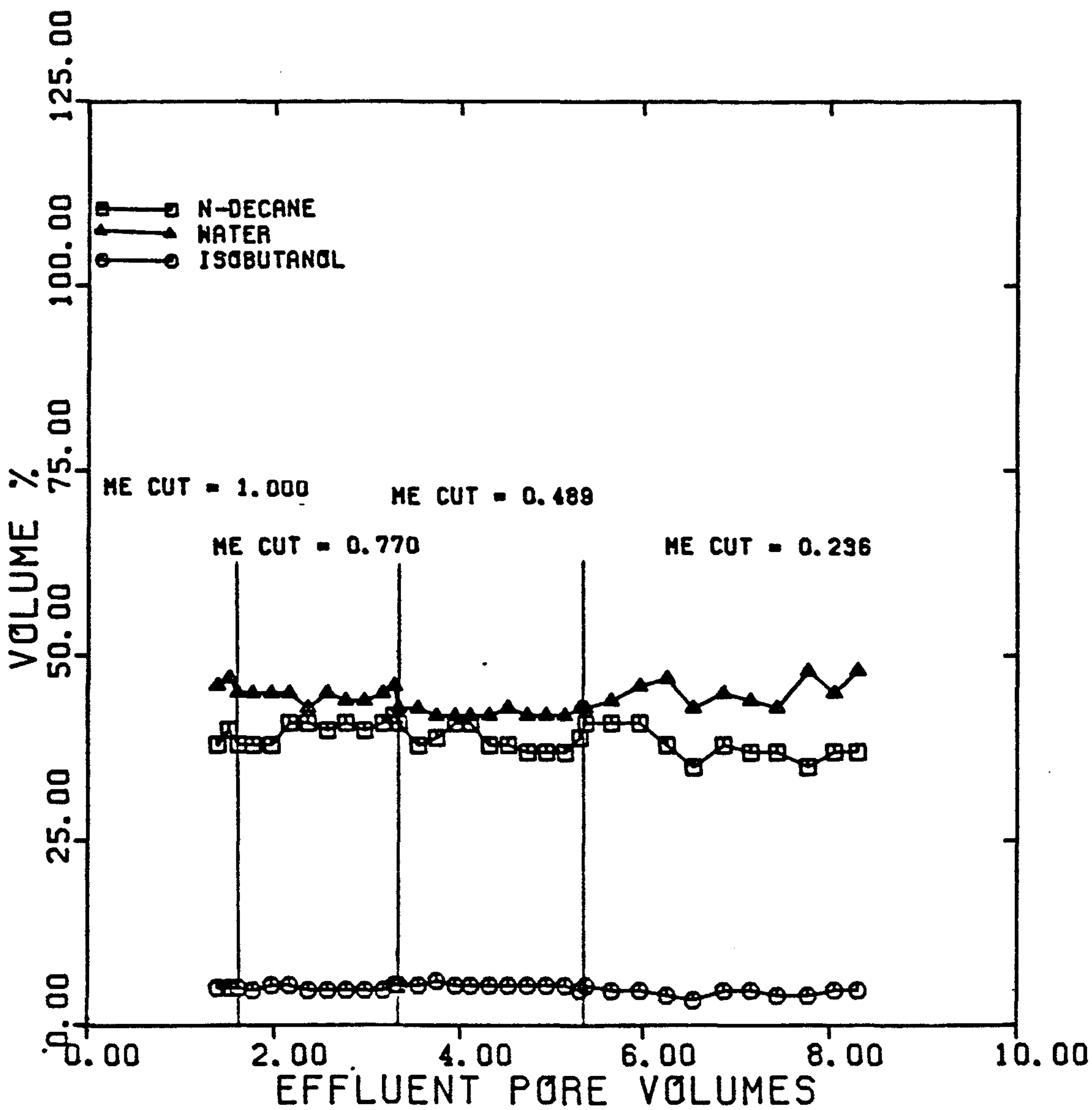

FIGURE 5.138

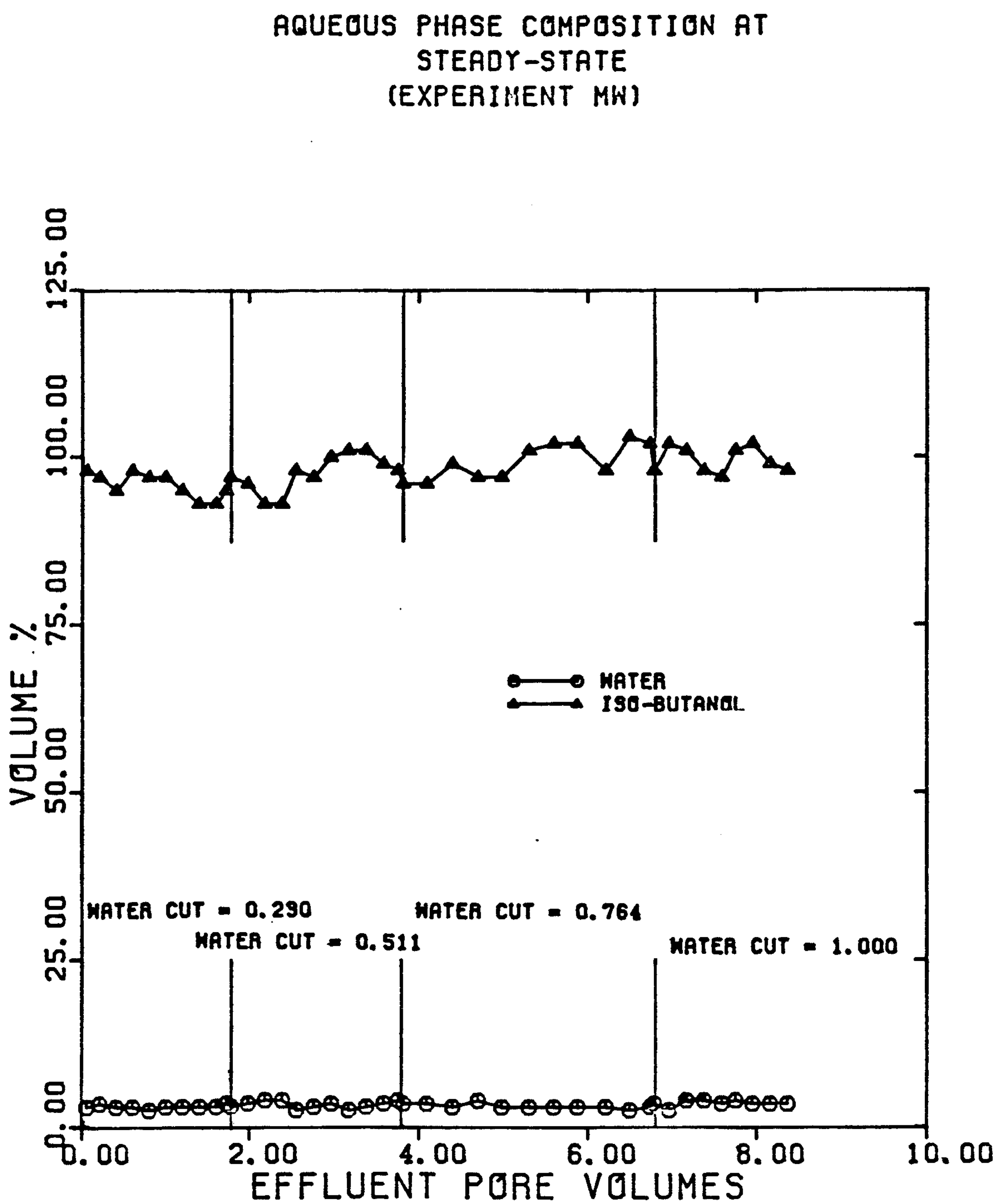
AQUEOUS PHASE COMPOSITION AT
STEADY-STATE
(EXPERIMENT MW)
VOLUME %
0.00
25.00
50.00
75.00
100.00
125.00
WATER
ISO-BUTANOL
WATER CUT = 0.290
WATER CUT = 0.511
WATER CUT = 0.764
WATER CUT = 1.000
0.00
2.00
4.00
6.00
8.00
10.00
EFFLUENT PORE VOLUMES

FIGURE 5.139

INTERFACIAL TENSION BETWEEN PRODUCED MICROEMULSION AND BRINE AT STEADY-STATE (EXPERIMENT MW)

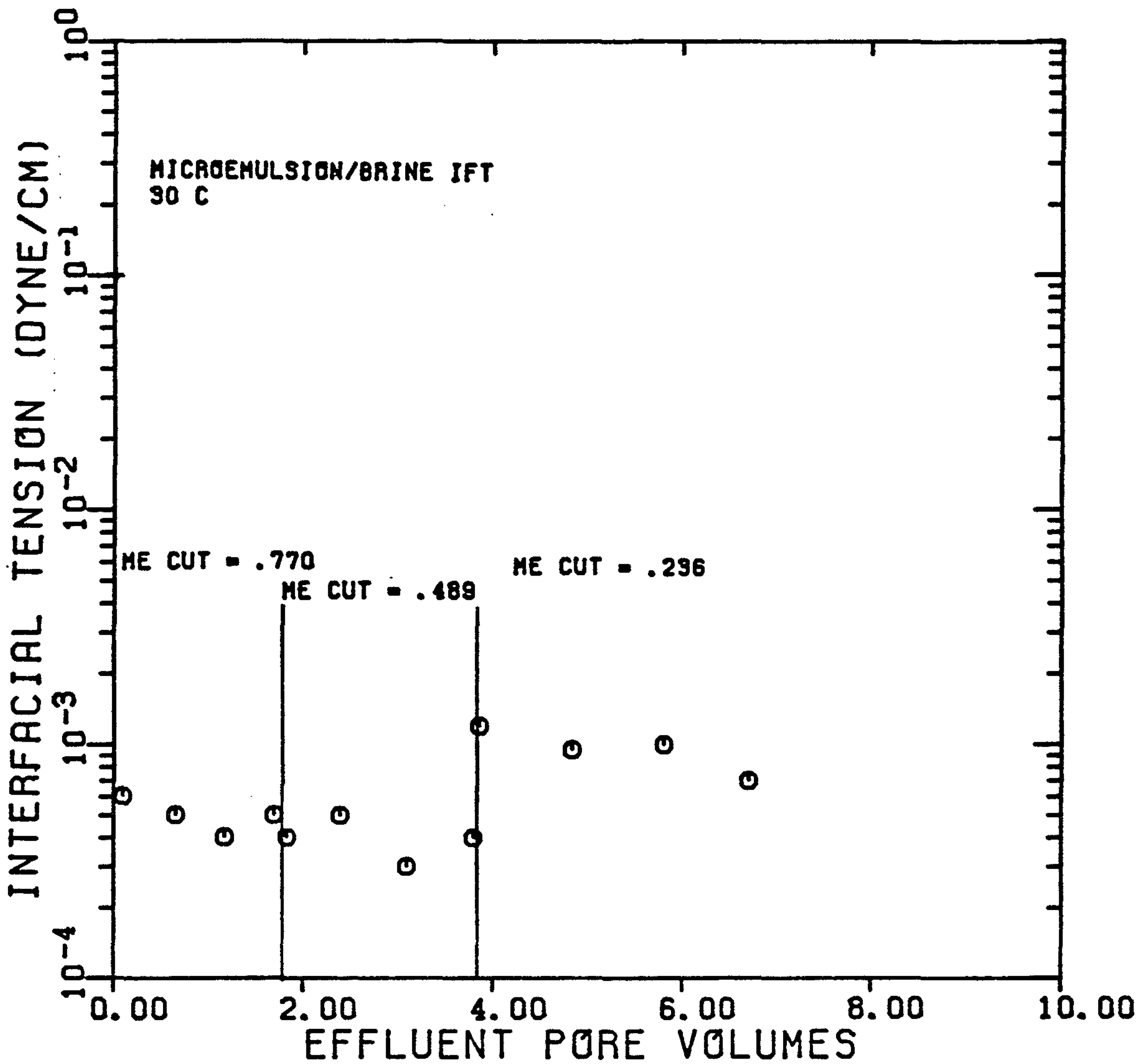

FIGURE 5.140

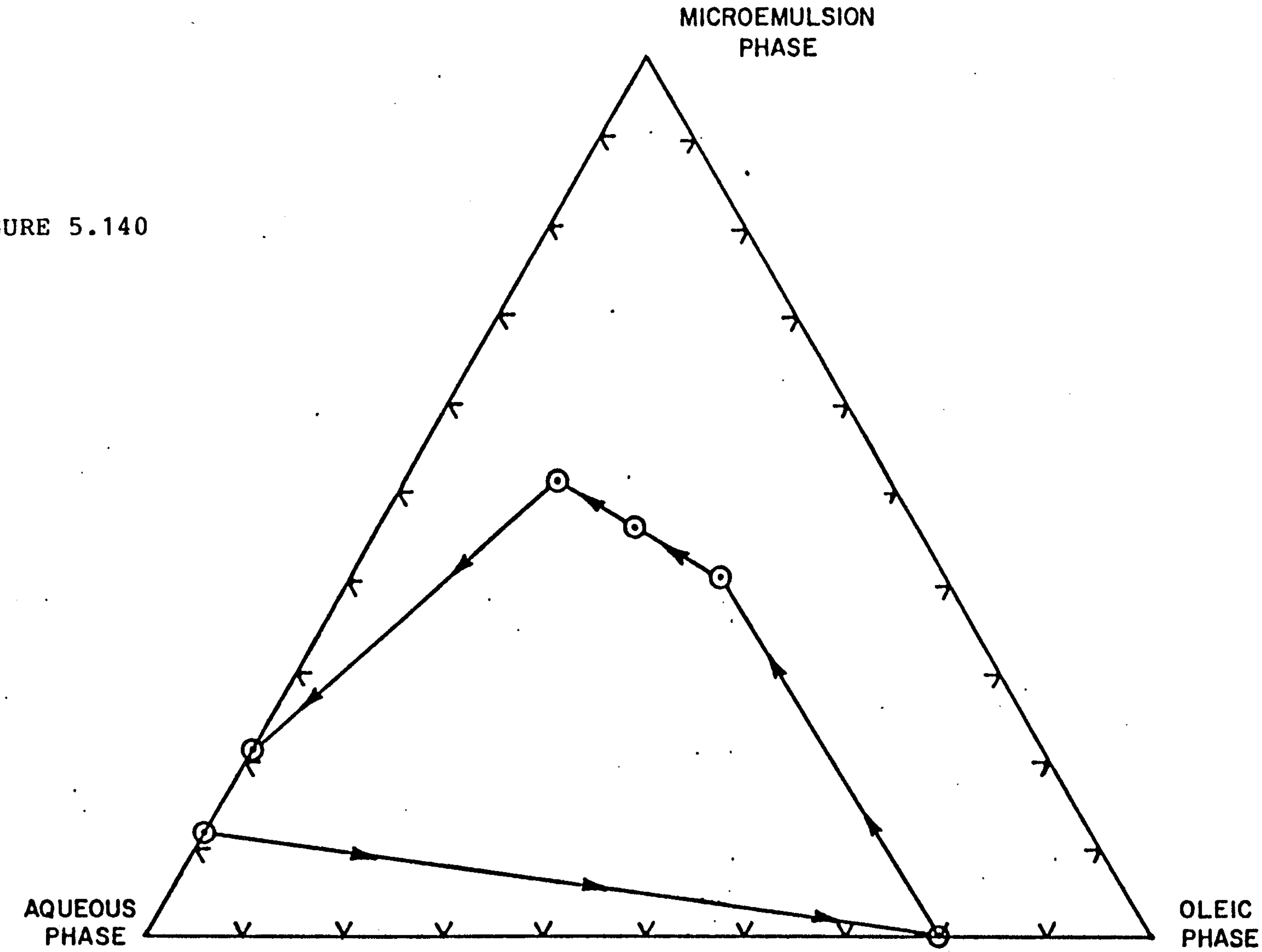

SATURATION DIAGRAM FOR THREE-PHASE FLOW

FIGURE 5.141

RELATIVE PERMEABILITY OF MICELLAR PHASES IN UNCONSOLIDATED SAND

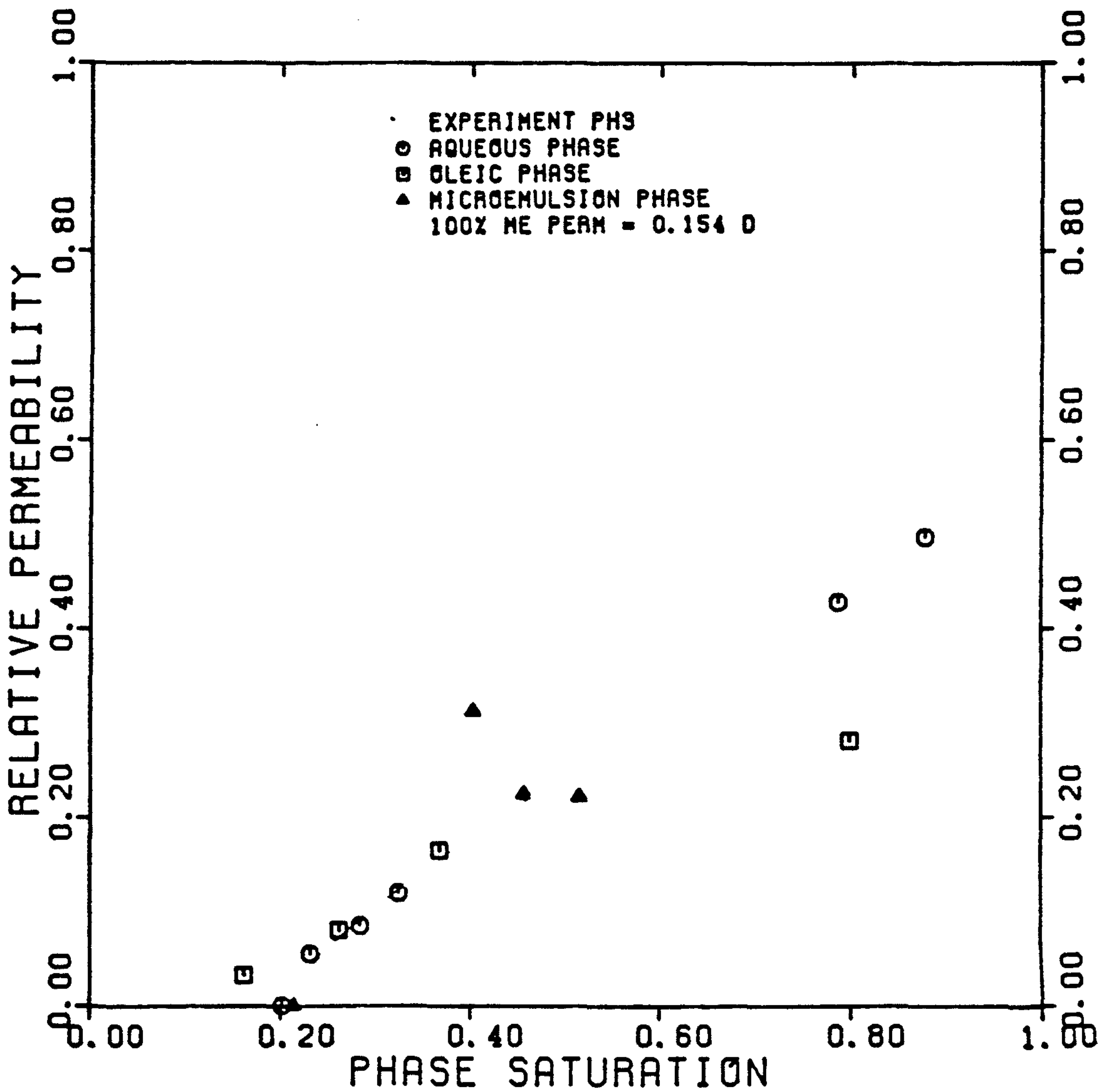

FIGURE 5.142

TOTAL RELATIVE MOBILITY OF MICELLAR PHASES IN UNCONSOLIDATED SAND

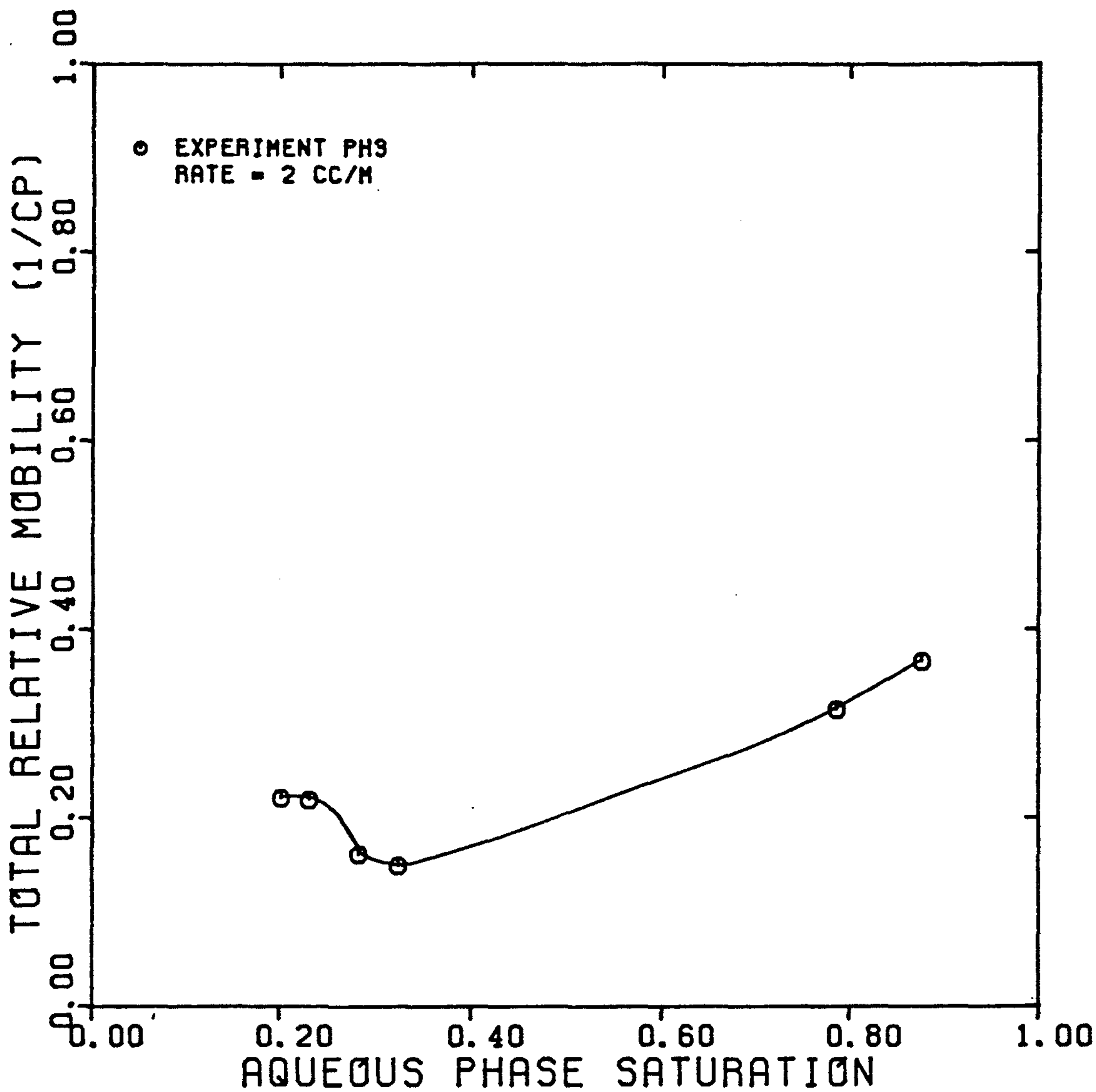

FIGURE 5.143

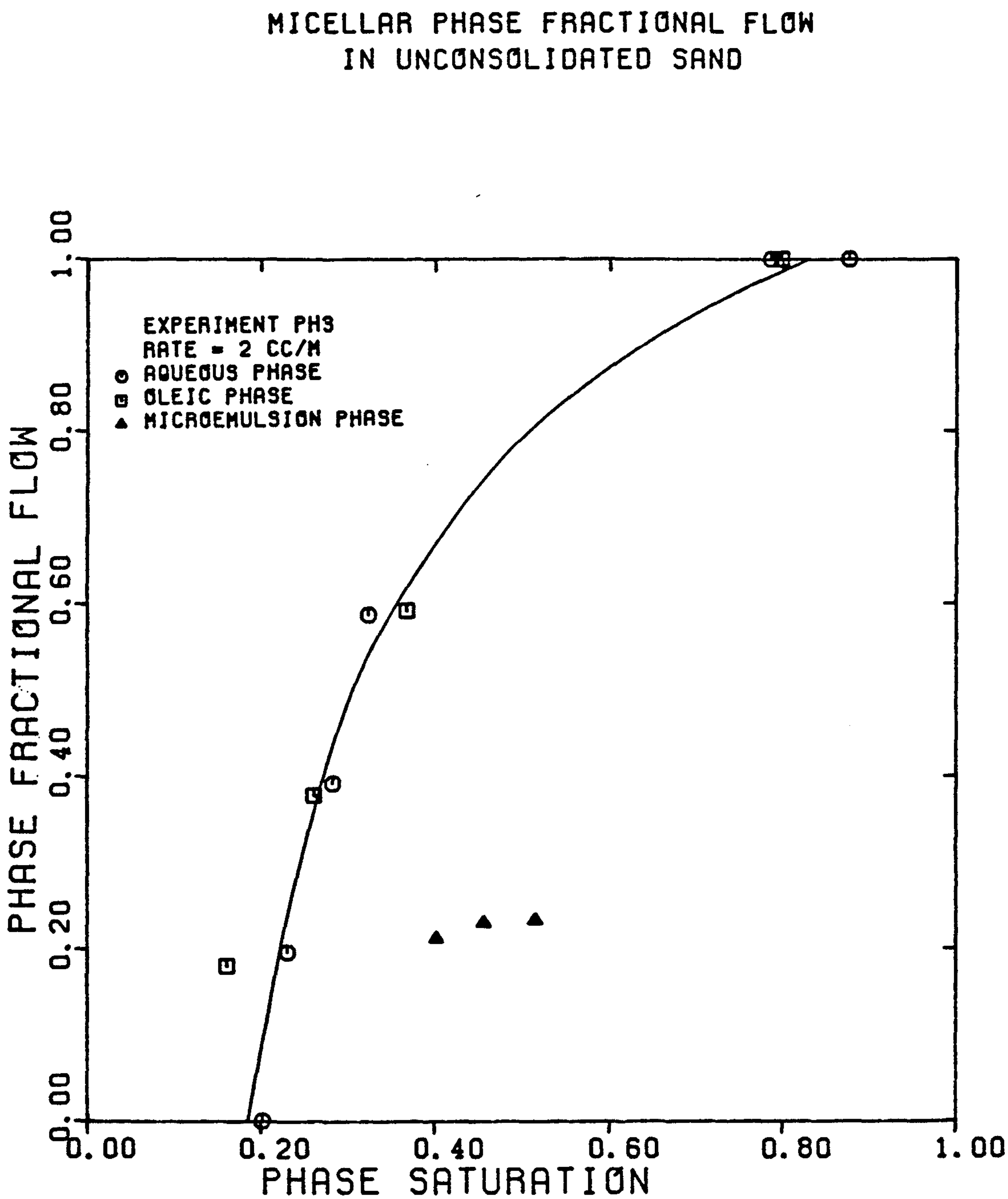
MICELLAR PHASE FRACTIONAL FLOW
IN UNCONSOLIDATED SAND
EXPERIMENT PH3
RATE = 2 CC/M
AQUEOUS PHASE
OLEIC PHASE
MICROEMULSION PHASE
PHASE FRACTIONAL FLOW
0.00
0.20
0.40
0.60
0.80
1.00
PHASE SATURATION
0.00
0.20
0.40
0.60
0.80
1.00

FIGURE 5.144

SANDPACK BREAKTHROUGH CURVE FOR TRITIUM
TRACER IN THE AQUEOUS PHASE
(EXPERIMENT PH31)

$S_w = 0.877 \quad f_w = 1.0$

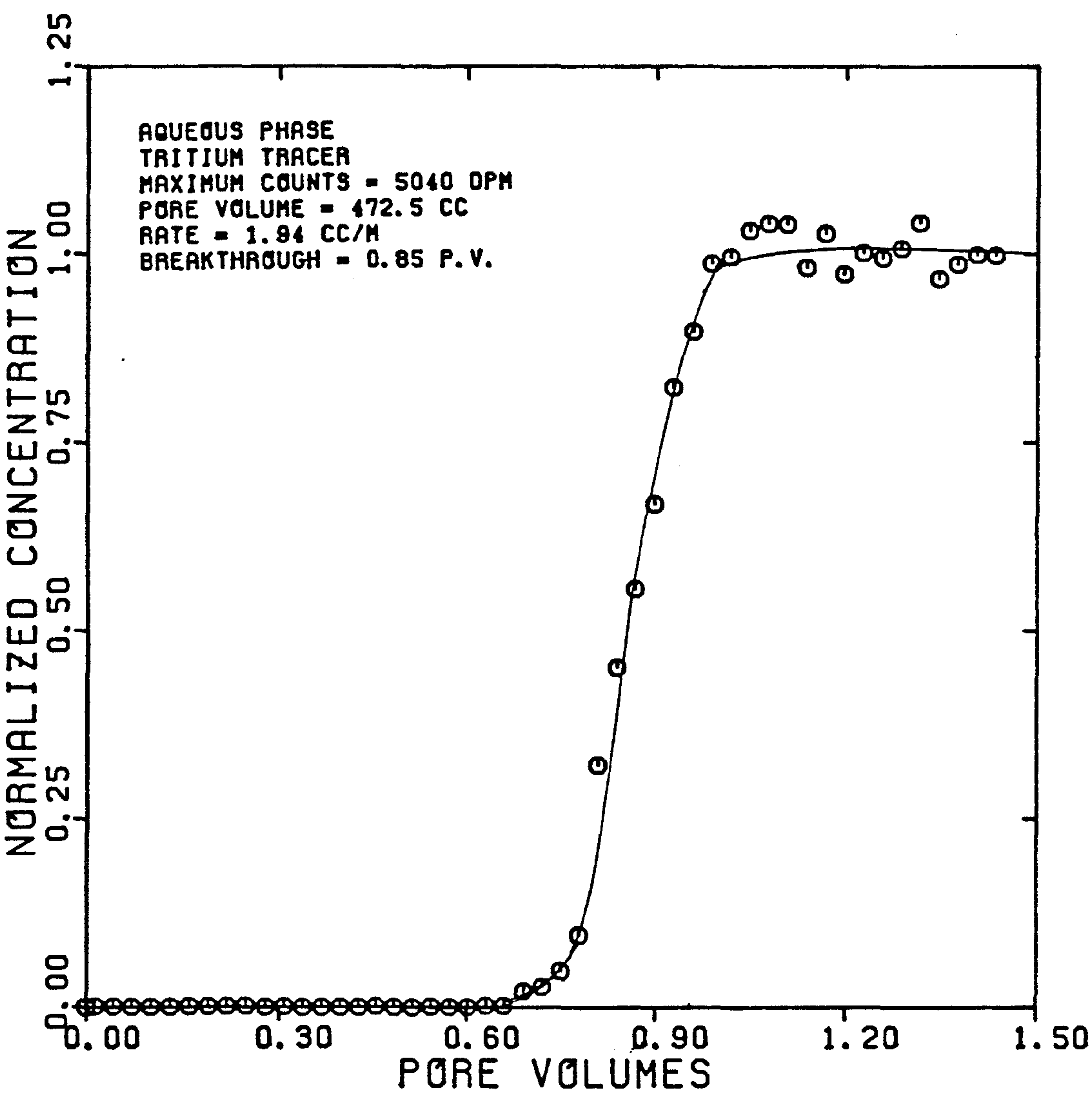

FIGURE 5.145

DISPERSIVITY OF TRITIUM
TRACER IN THE AQUEOUS PHASE
(EXPERIMENT PH31)

$S_w = 0.877 \quad f_w = 1.0$

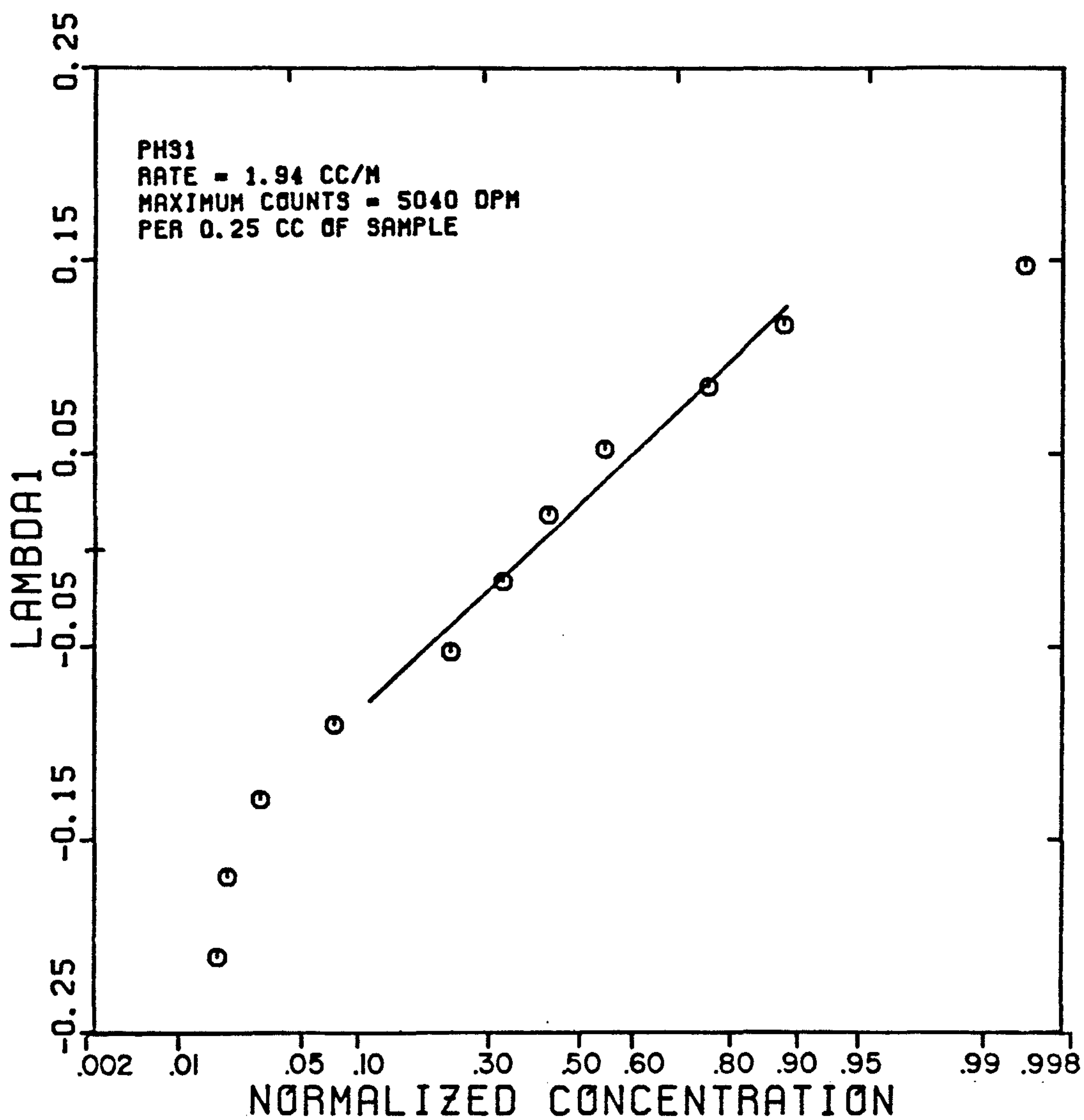

FIGURE 5.146

SANDPACK BREAKTHROUGH CURVE FOR N-NONANE TRACER IN THE OLEIC PHASE (EXPERIMENT PH32)

$S_o = 0.798 \quad f_o = 1.0$

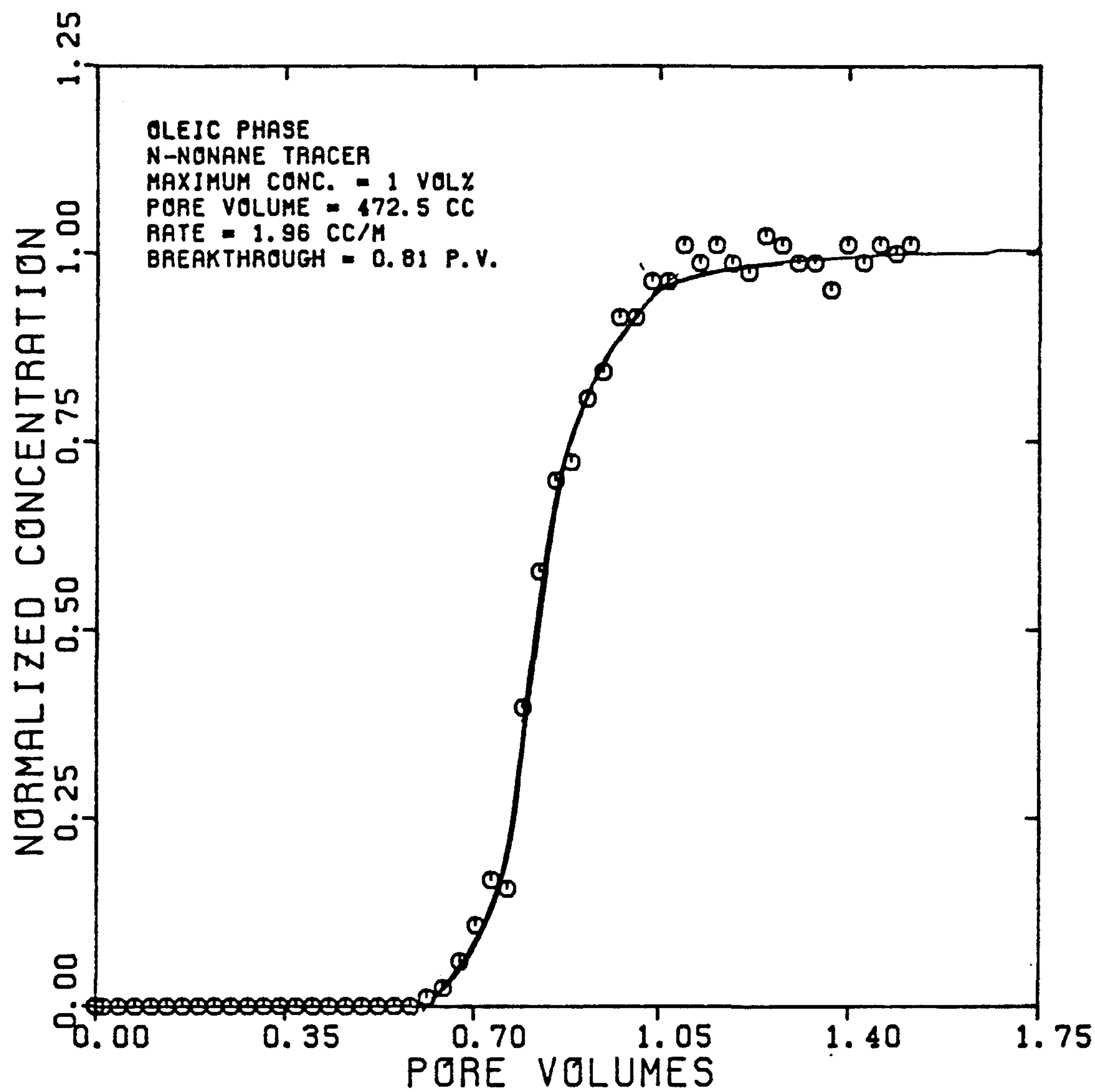

FIGURE 5.147

DISPERSIVITY OF N-NONANE
TRACER IN THE OLEIC PHASE
(EXPERIMENT PH32)

$S_o = 0.798 \quad f_o = 1.0$

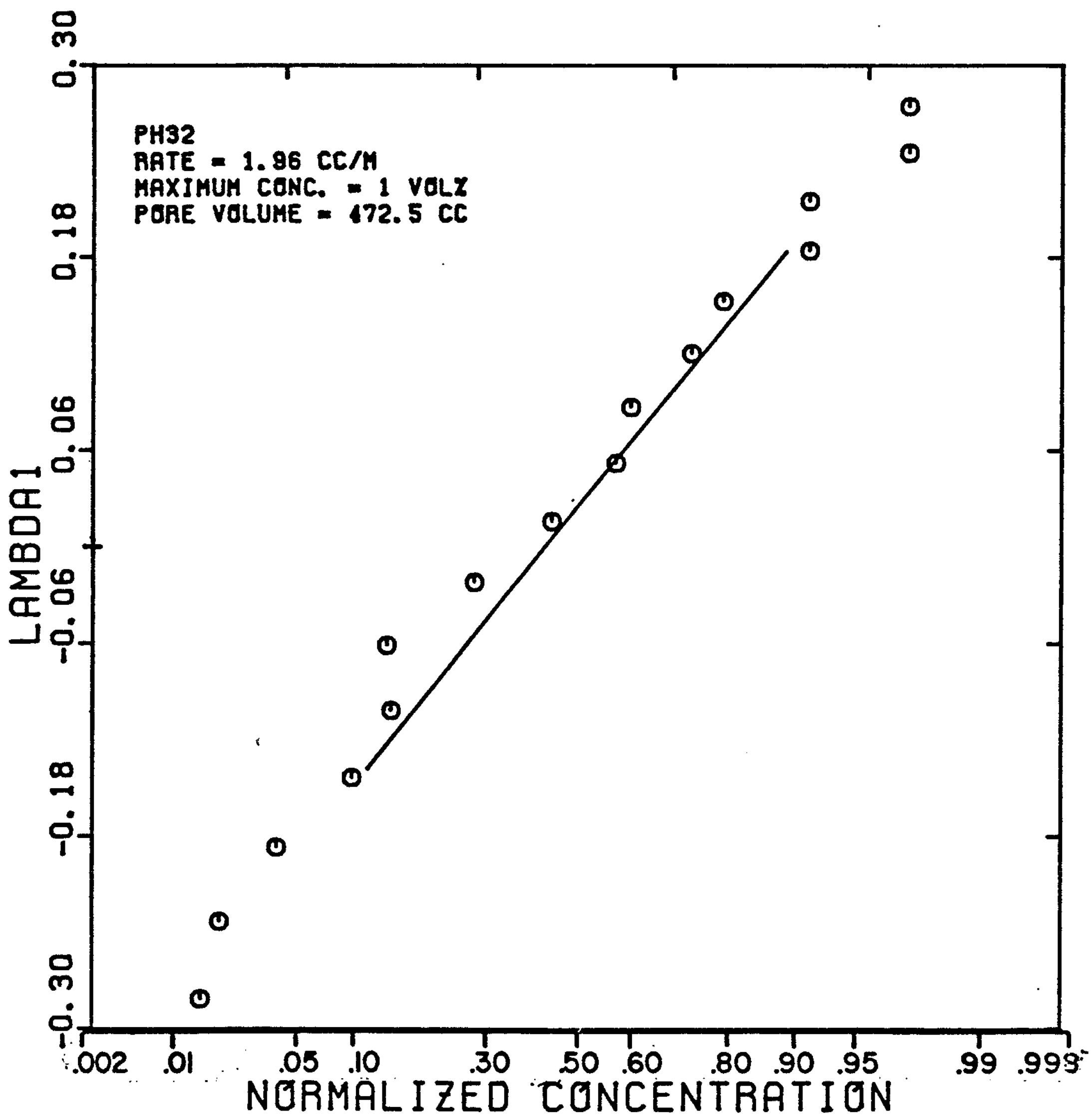

FIGURE 5.148

SANDPACK BREAKTHROUGH CURVE FOR TRITIUM
TRACER IN THE AQUEOUS PHASE
(EXPERIMENT PH33AQ)

$S_w = 0.231 \quad f_w = 0.196$

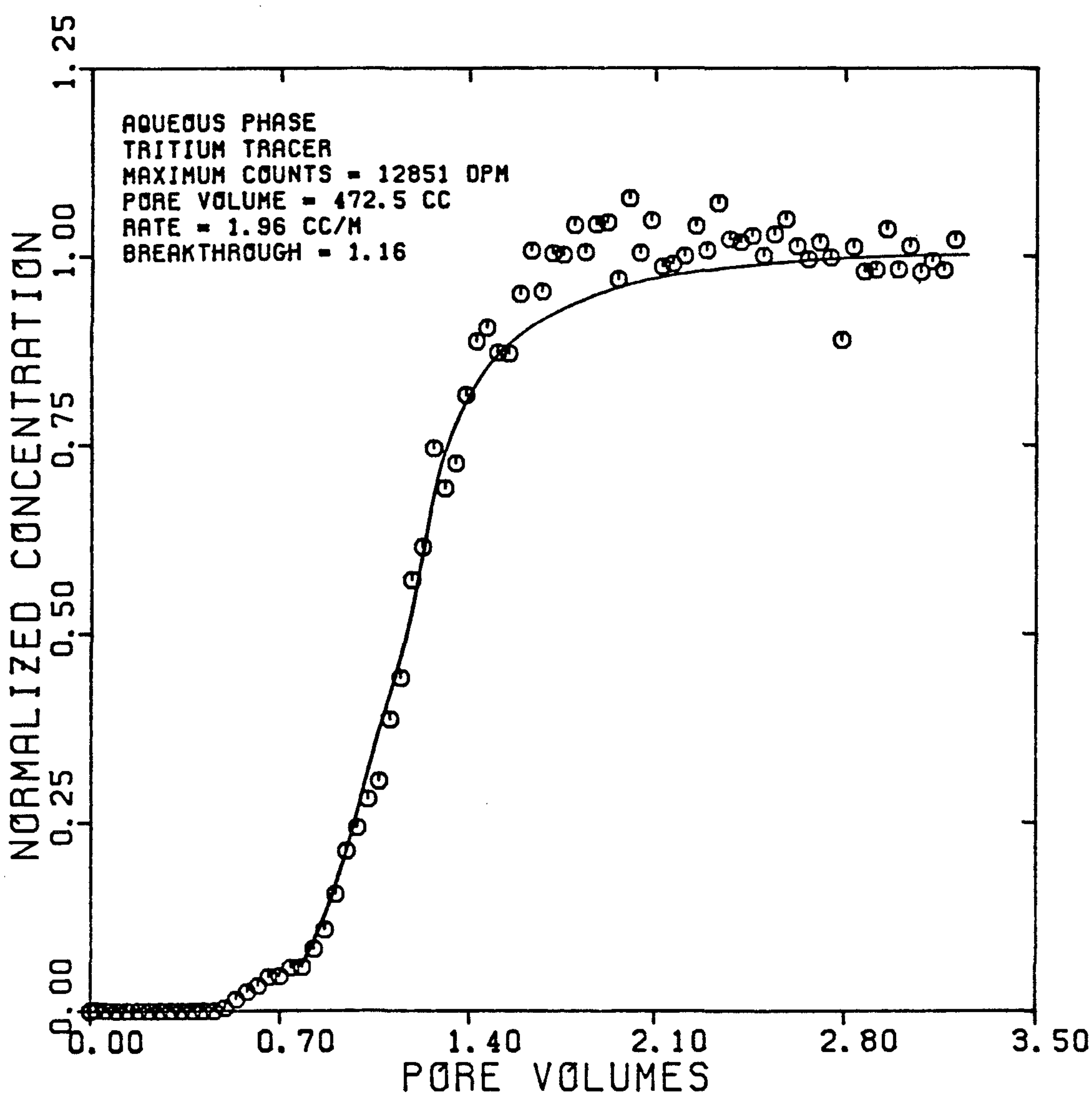

FIGURE 5.149

DISPERSIVITY OF TRITIUM
TRACER IN THE AQUEOUS PHASE
(EXPERIMENT PH33AQ)

S_w = 0.231 f_w = 0.196

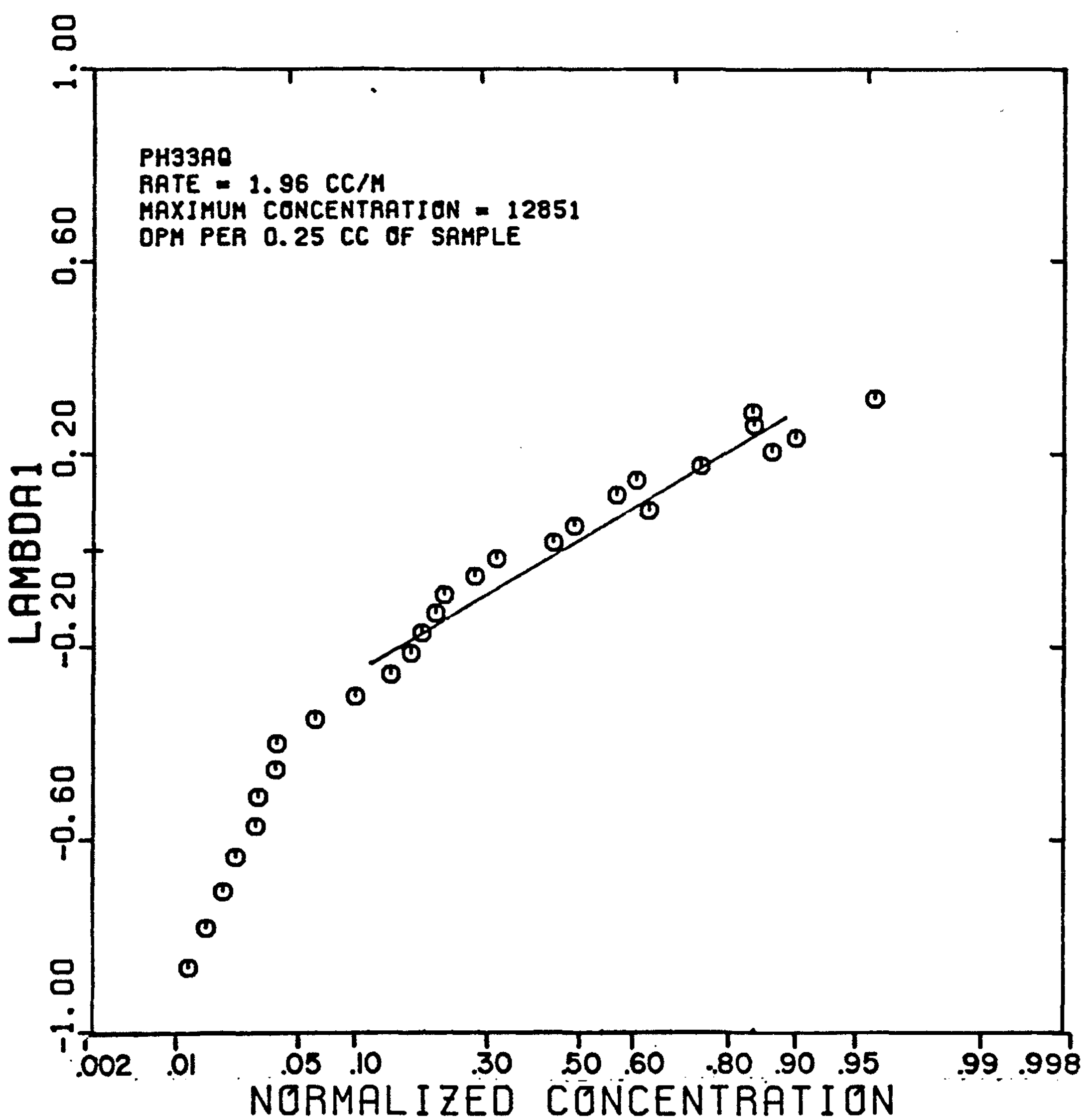

FIGURE 5.150

SANDPACK BREAKTHROUGH CURVE FOR TRITIUM TRACER IN THE MICROEMULSION PHASE (EXPERIMENT PH33MET)

S_{me} = 0.402 f_{me} = 0.212

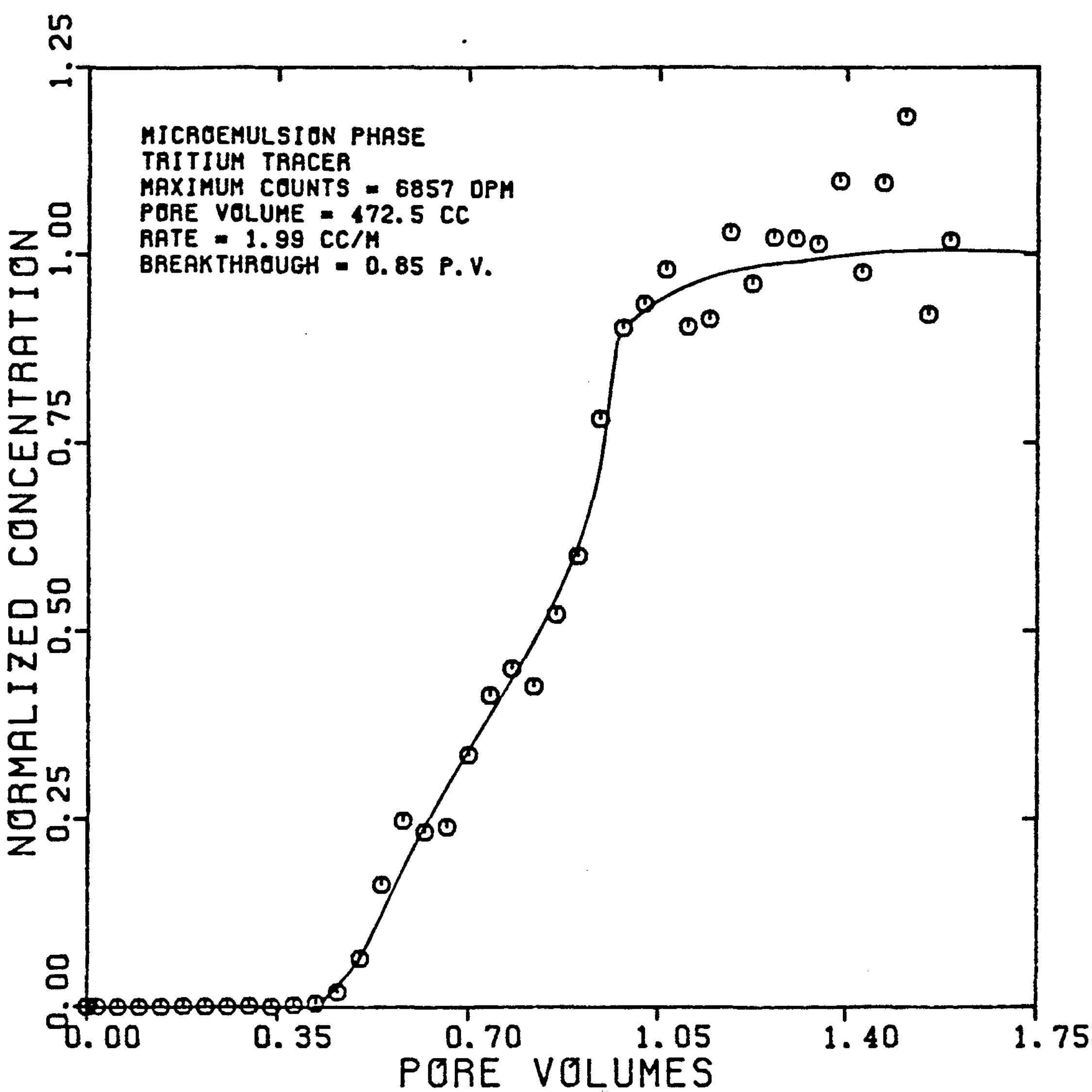

FIGURE 5.151

DISPERSIVITY OF TRITIUM
TRACER IN THE MICROEMULSION PHASE
(EXPERIMENT PH33MET)

$S_{me} = 0.402 \quad f_{me} = 0.212$

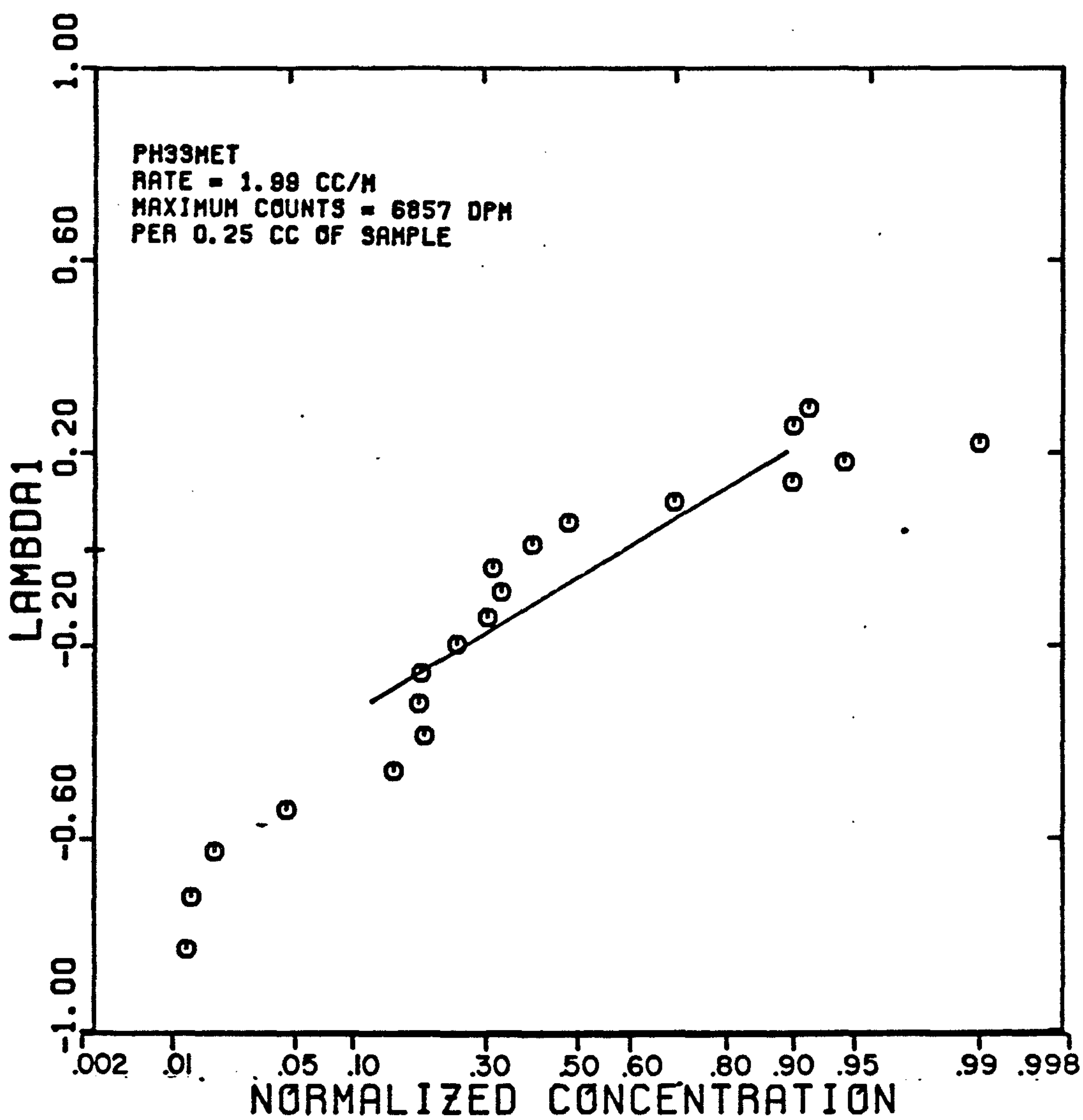

FIGURE 5.152

SANDPACK BREAKTHROUGH CURVE FOR CARBON 14
TRACER IN THE MICROEMULSION PHASE
(EXPERIMENT PH33MEC)

$S_{me} = 0.402 \quad f_{me} = 0.212$

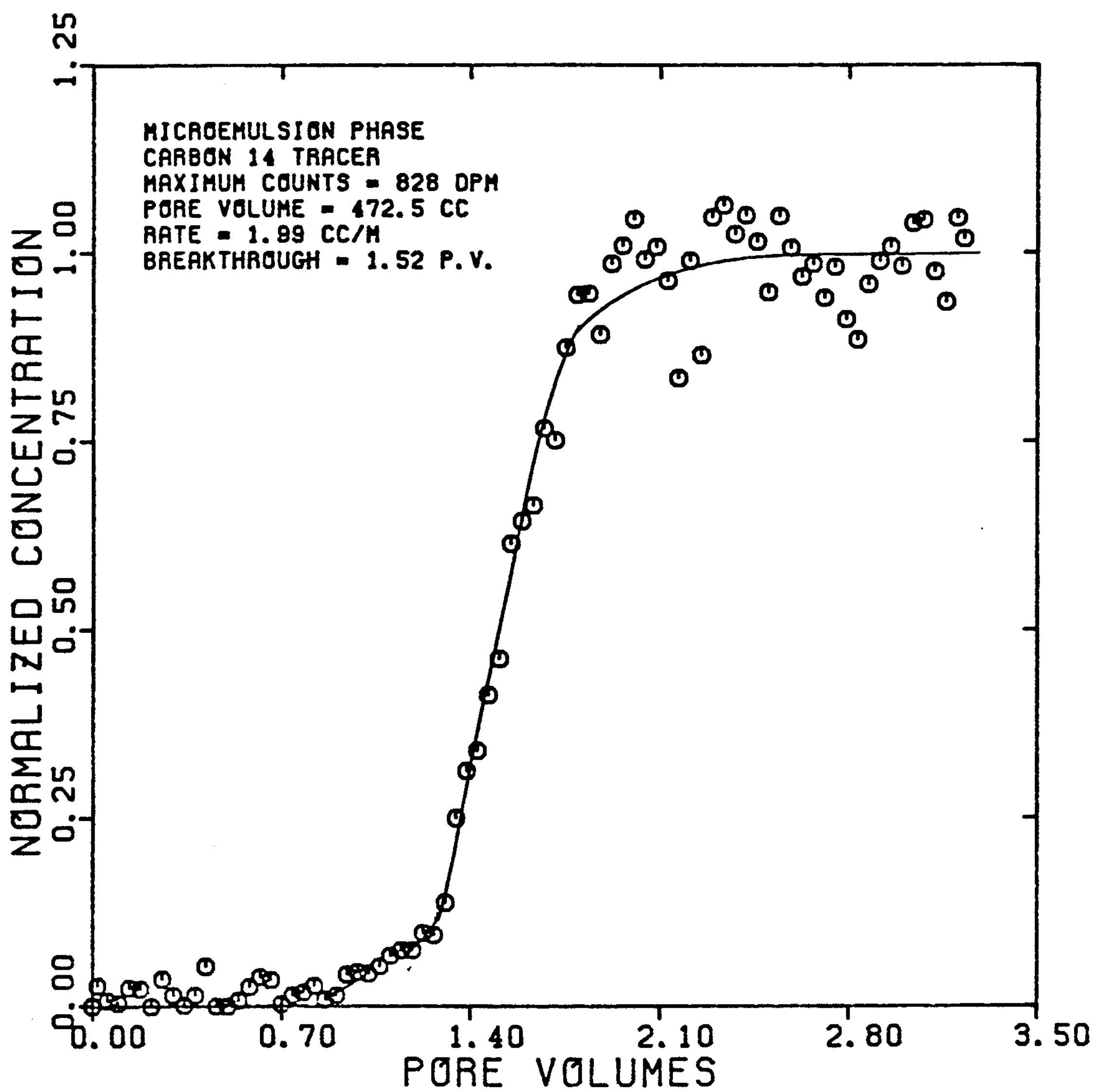

FIGURE 5.153

DISPERSIVITY OF CARBON 14
TRACER IN THE MICROEMULSION PHASE
(EXPERIMENT PH33MEC)

$S_{me} = 0.402 \quad f_{me} = 0.212$

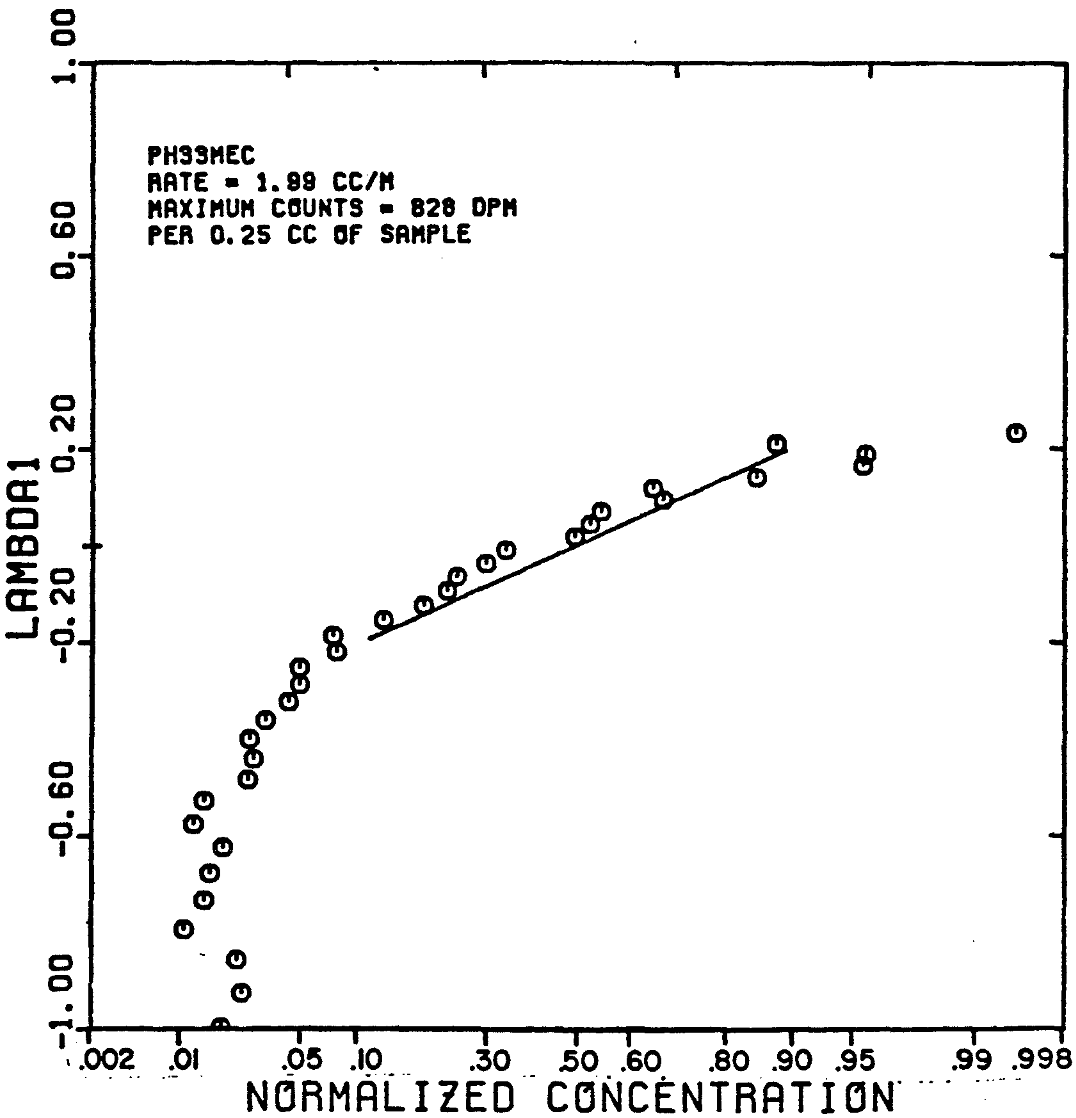

FIGURE 5.154

SANDPACK BREAKTHROUGH CURVE FOR N-NONANE TRACER IN THE OLEIC PHASE (EXPERIMENT PH33OL)

$S_o = 0.367 \quad f_o = 0.592$

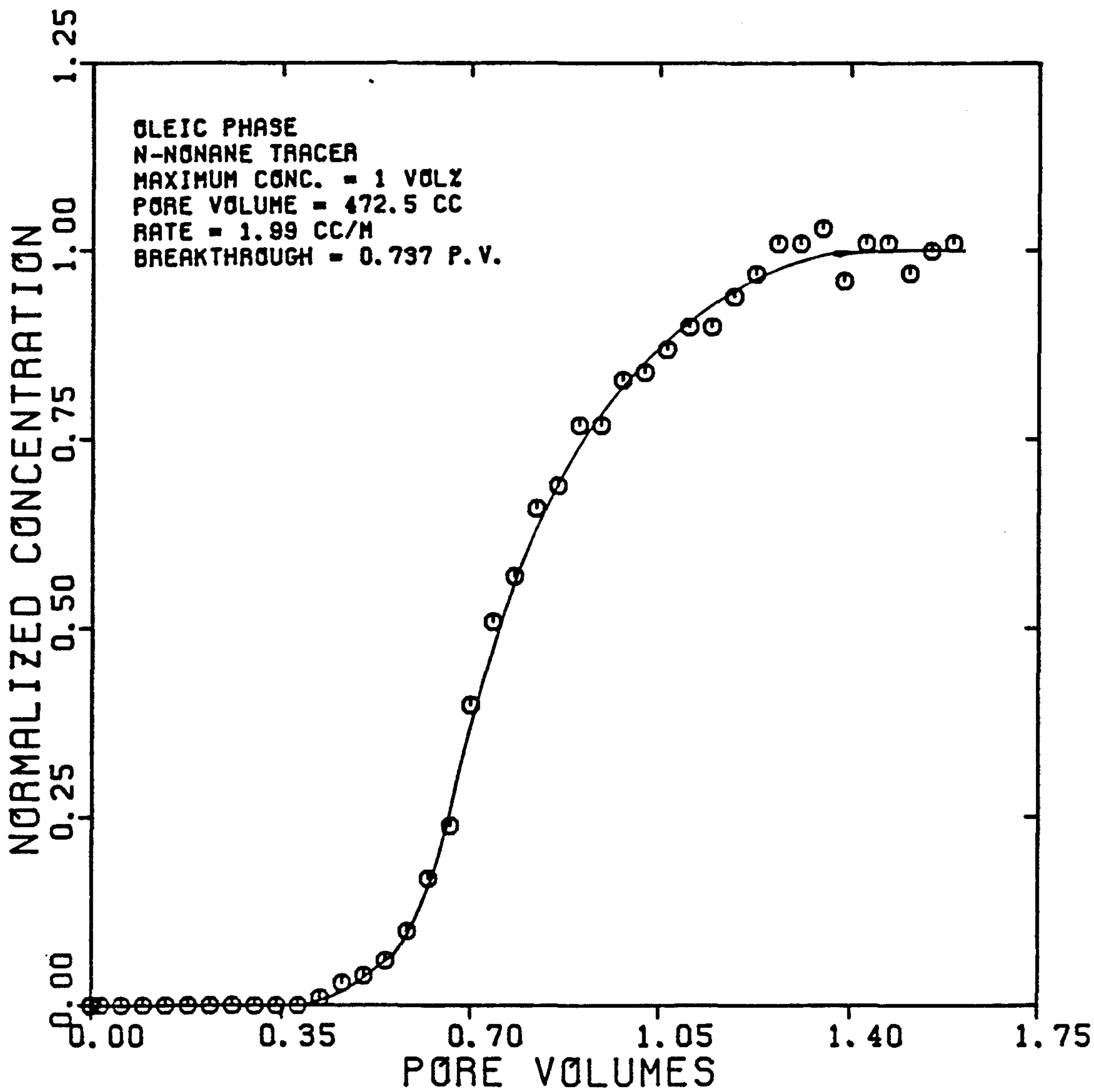

FIGURE 5.155

DISPERSIVITY OF N-NONANE
TRACER IN THE OLEIC PHASE
(EXPERIMENT PH33OL)

$S_o = 0.367 \quad f_o = 0.592$

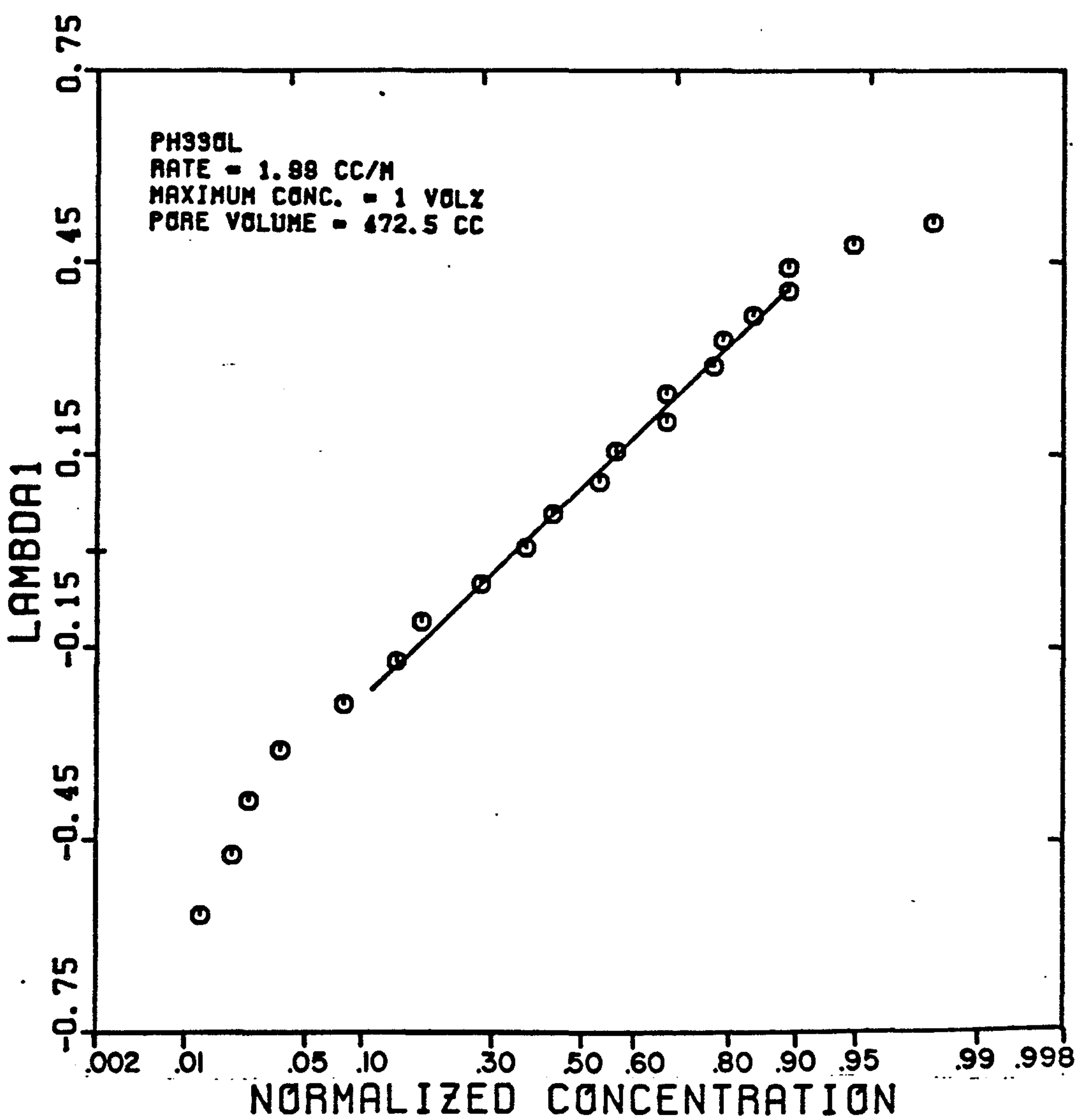

FIGURE 5.156

SANDPACK BREAKTHROUGH CURVE FOR CARBON 14
TRACER IN THE OLEIC PHASE
(EXPERIMENT PH330LC)

$S_o = 0.367 \quad f_o = 0.592$

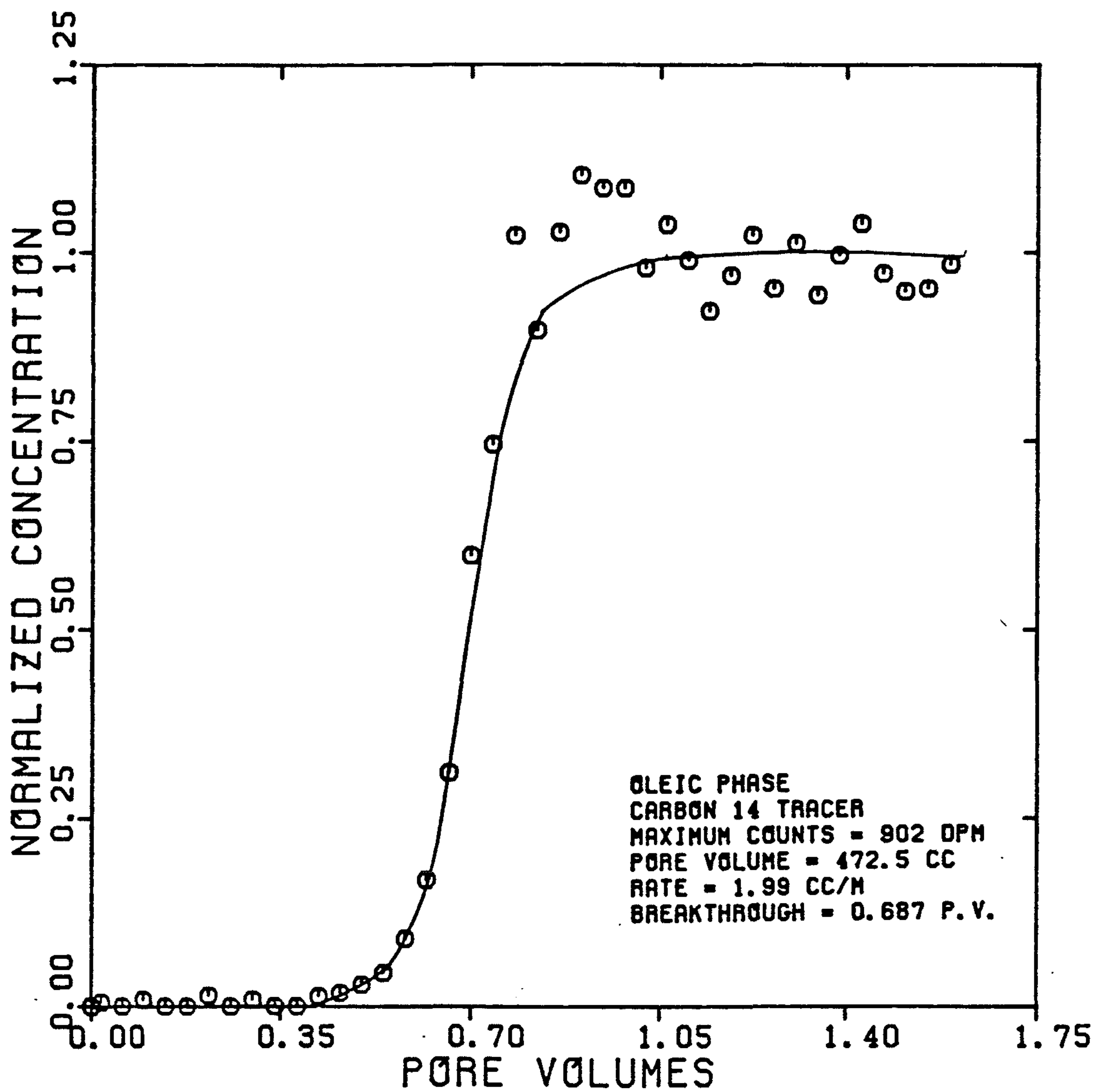

FIGURE 5.157

DISPERSIVITY OF CARBON 14
TRACER IN THE OLEIC PHASE
(EXPERIMENT PH330LC)

$S_o = 0.367 \quad f_o = 0.592$

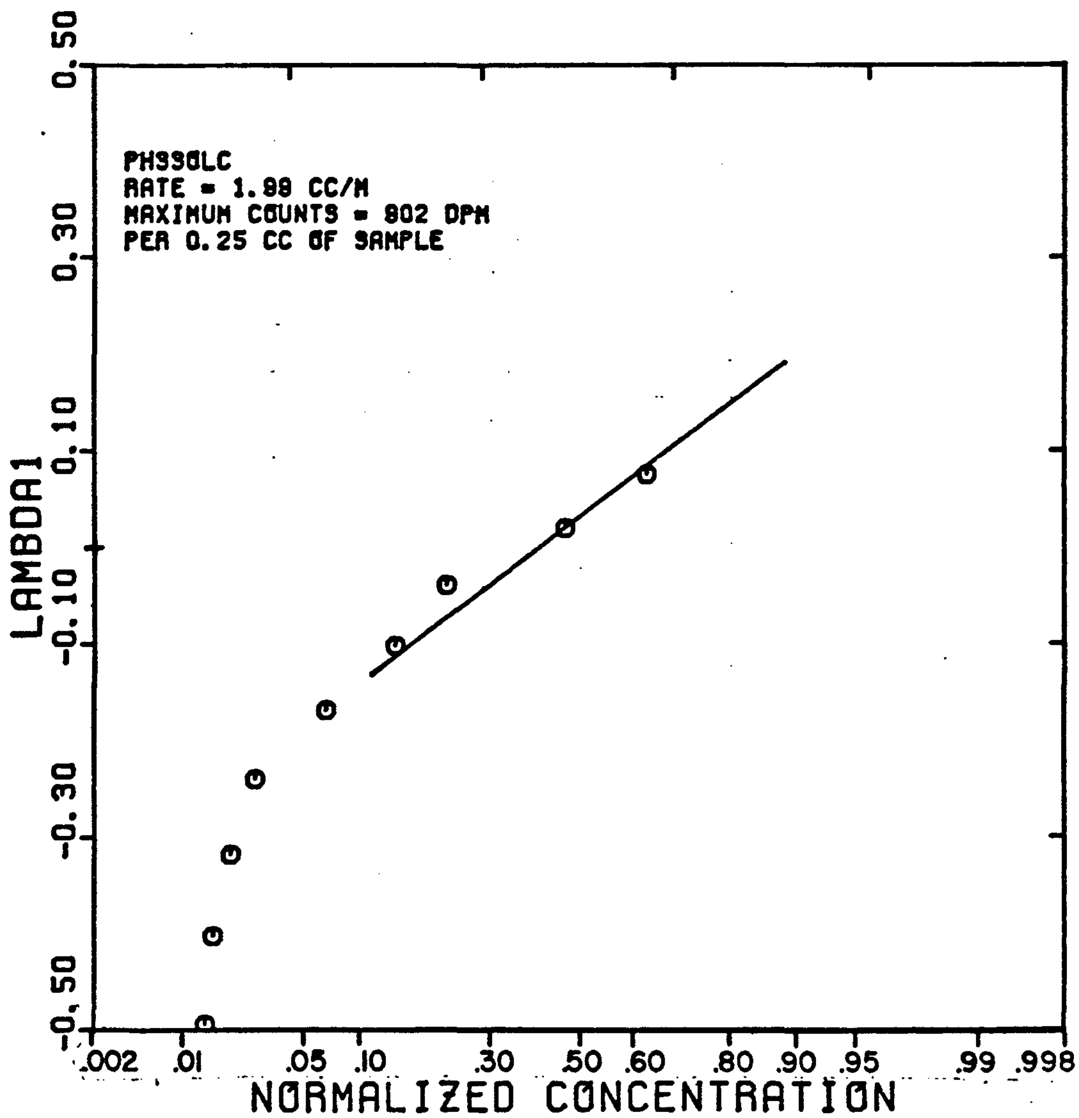

FIGURE 5.158

SANDPACK BREAKTHROUGH CURVE FOR TRITIUM
TRACER IN THE AQUEOUS PHASE
(EXPERIMENT PH34AQ)

$S_w = 0.238 \quad f_w = 0.392$

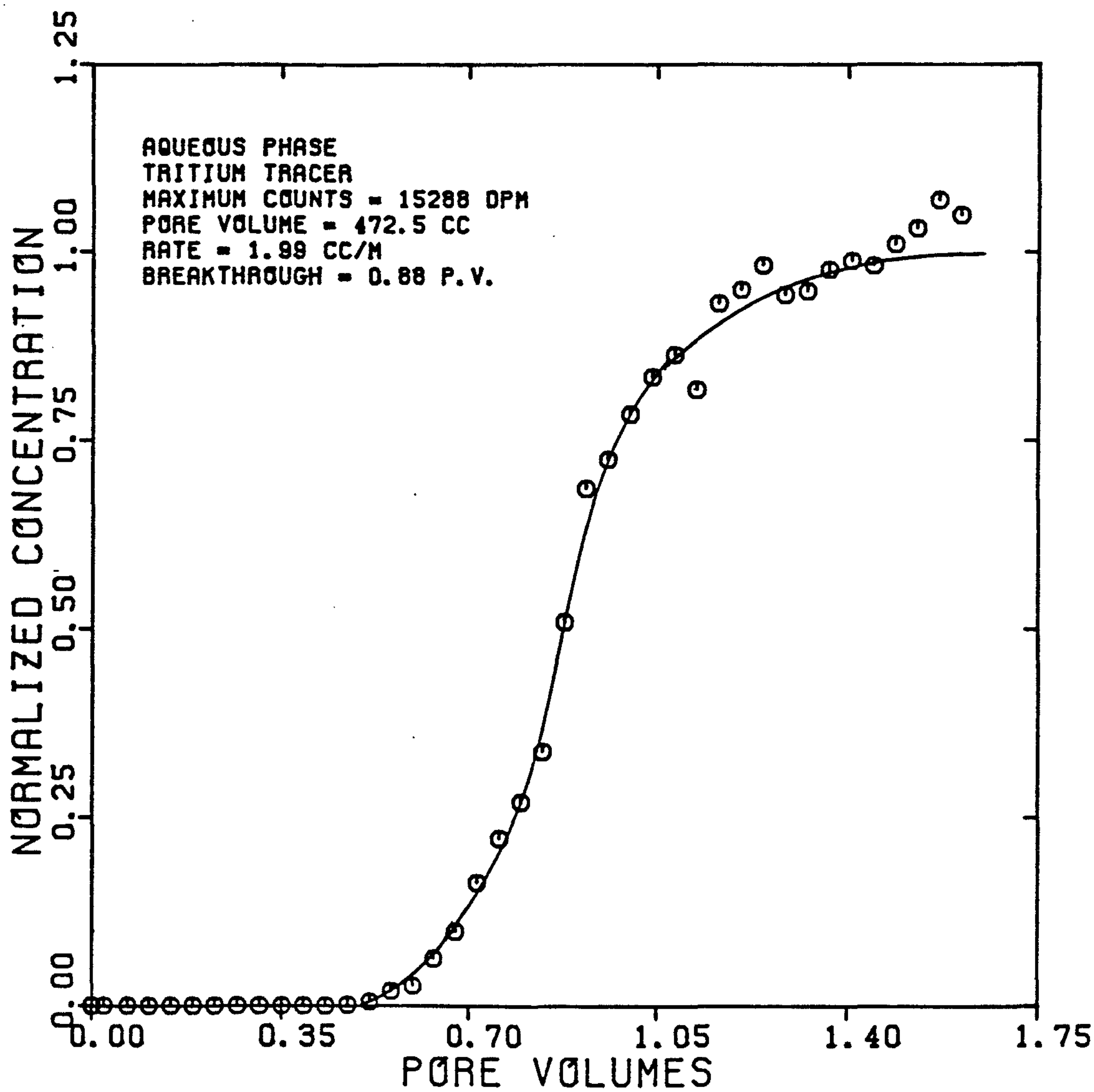

FIGURE 5.159

DISPERSIVITY OF TRITIUM
TRACER IN THE AQUEOUS PHASE
(EXPERIMENT PH34AQ)

$S_w = 0.238 \quad f_w = 0.392$

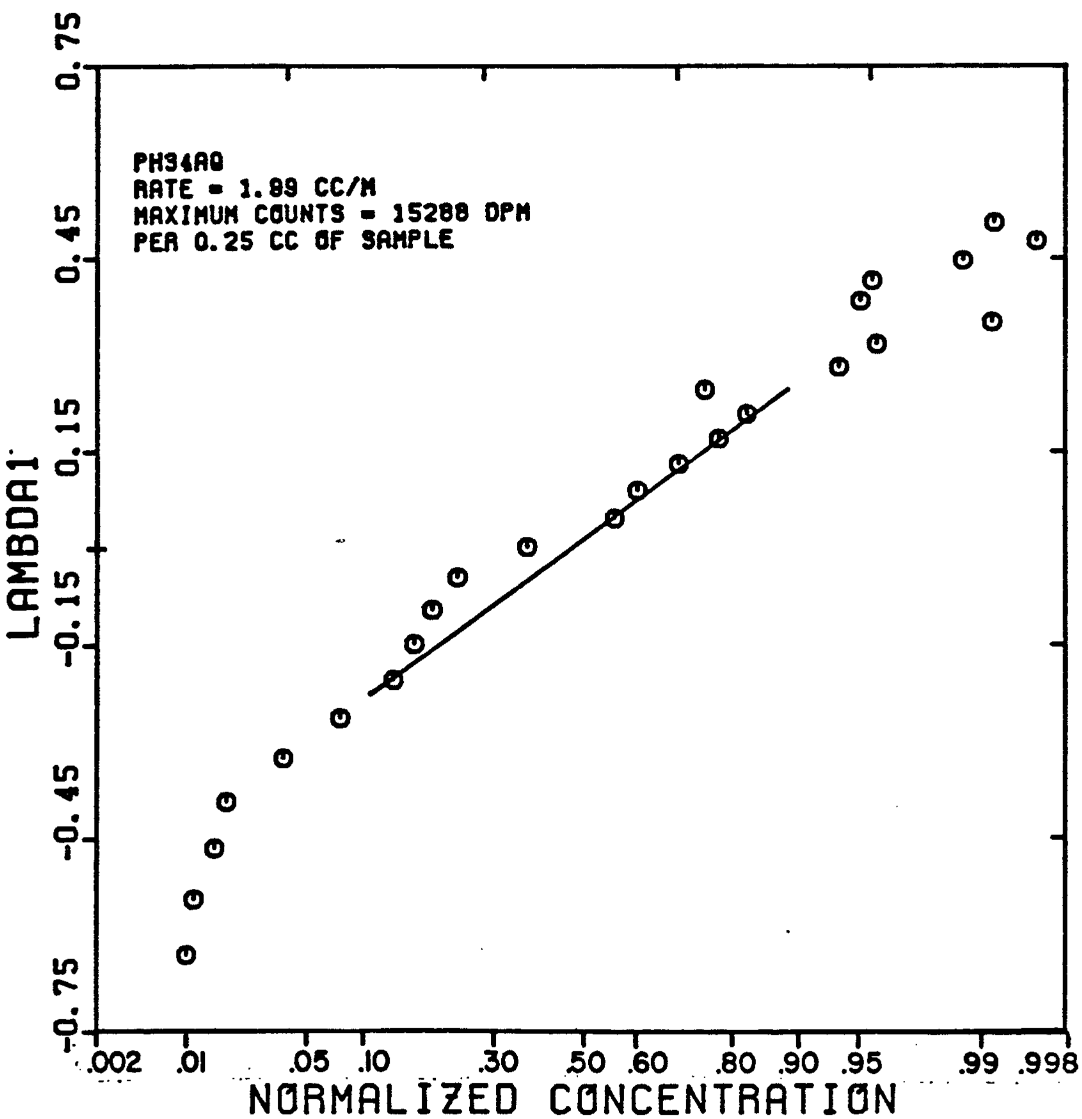

FIGURE 5.160

SANDPACK BREAKTHROUGH CURVE FOR TRITIUM TRACER IN THE MICROEMULSION PHASE (EXPERIMENT PH34MET)

S_{me} = 0.456 f_{me} = 0.230

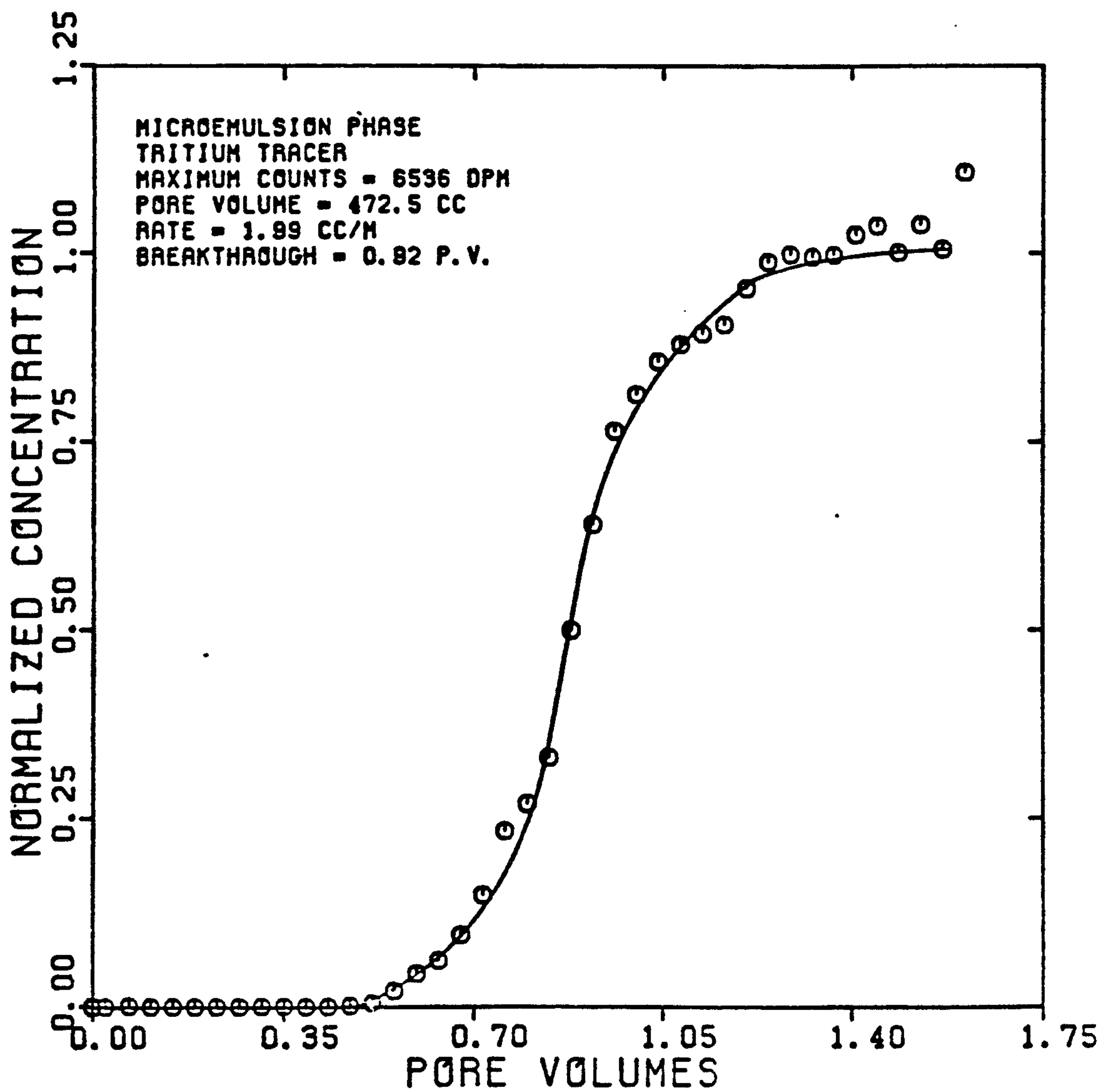

FIGURE 5.161

DISPERSIVITY OF TRITIUM
TRACER IN THE MICROEMULSION PHASE
(EXPERIMENT PH34MET)

S_{me} = 0.456 f_{me} = 0.230

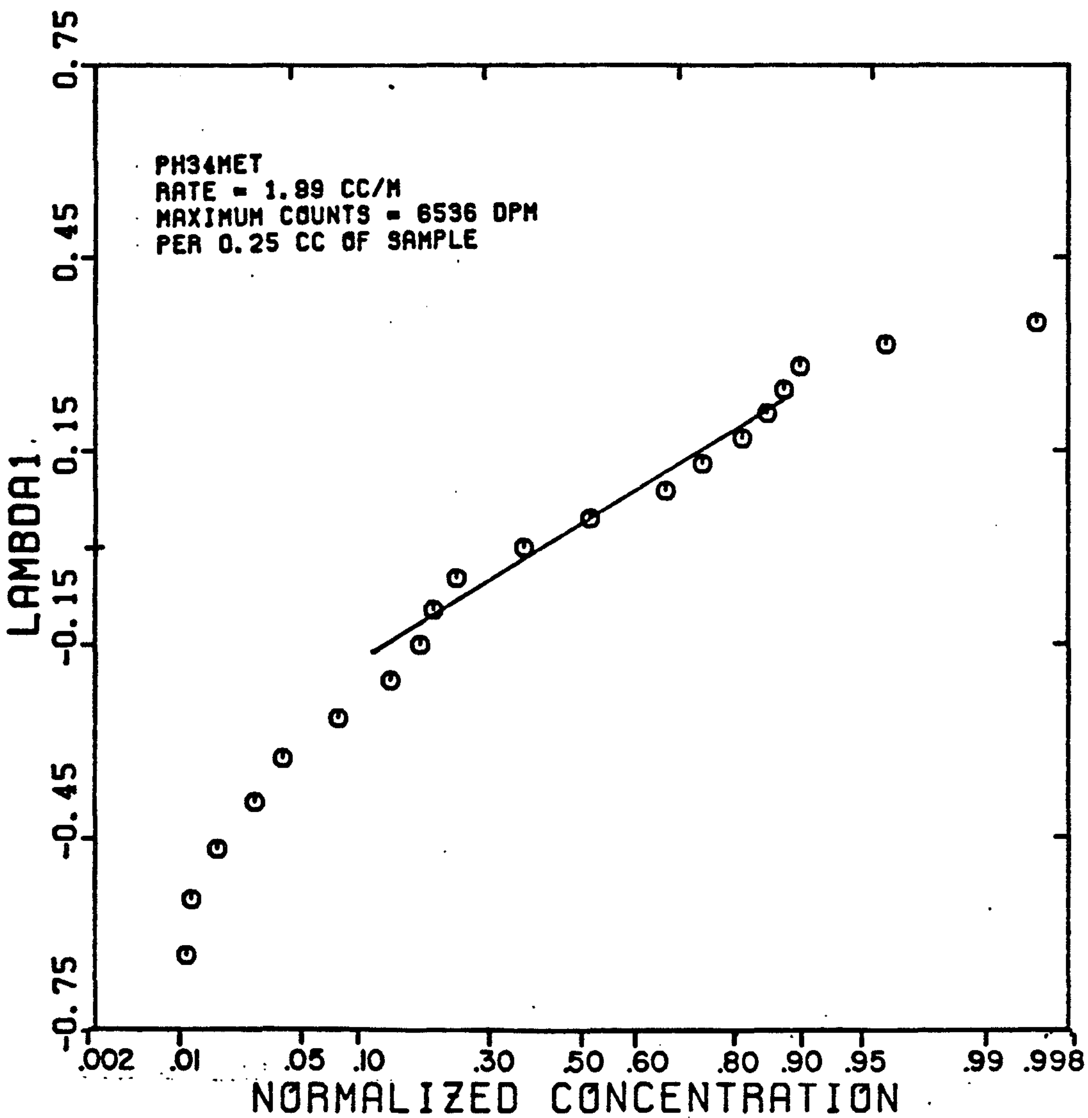

FIGURE 5.162

SANDPACK BREAKTHROUGH CURVE FOR CARBON 14
TRACER IN THE MICROEMULSION PHASE
(EXPERIMENT PH34MEC)

S_{me} = 0.456 f_{me} = 0.230

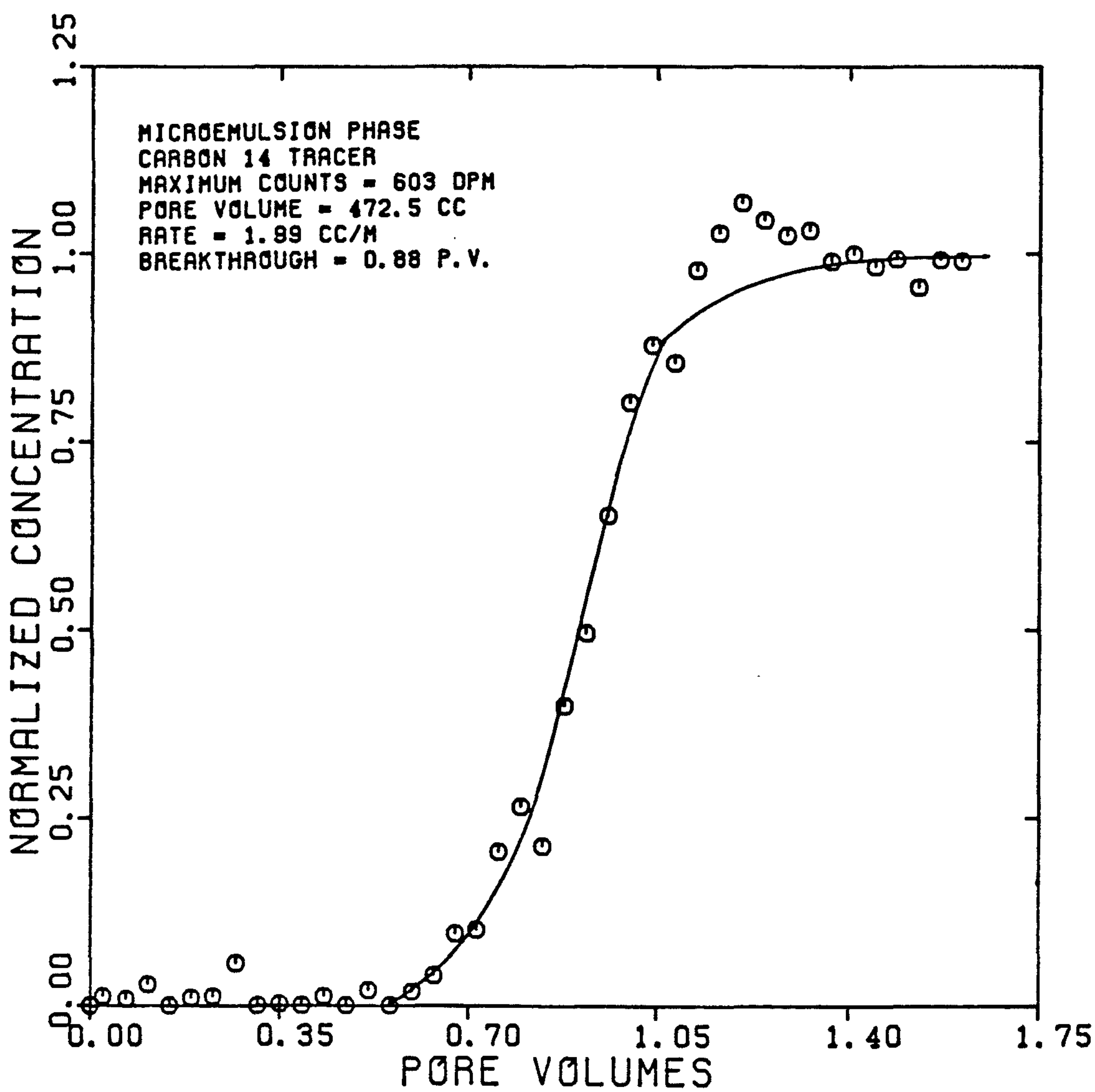

FIGURE 5.163

DISPERSIVITY OF CARBON 14
TRACER IN THE MICROEMULSION PHASE
(EXPERIMENT PH34MEC)

$S_{me} = 0.456 \quad f_{me} = 0.230$

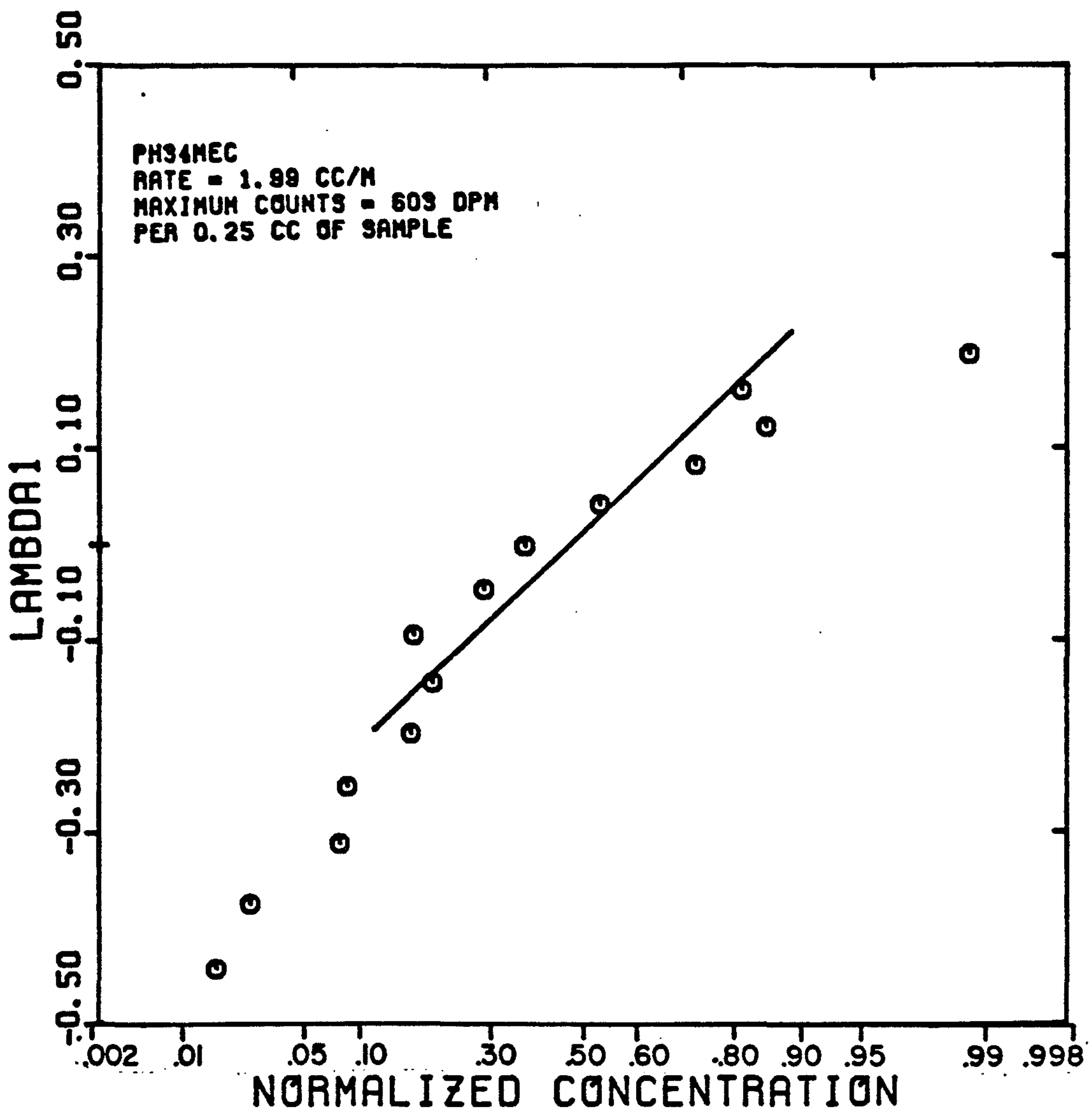

FIGURE 5.164

SANDPACK BREAKTHROUGH CURVE FOR N-NONANE
TRACER IN THE OLEIC PHASE
(EXPERIMENT PH340L)

$S_o = 0.261 \quad f_o = 0.378$

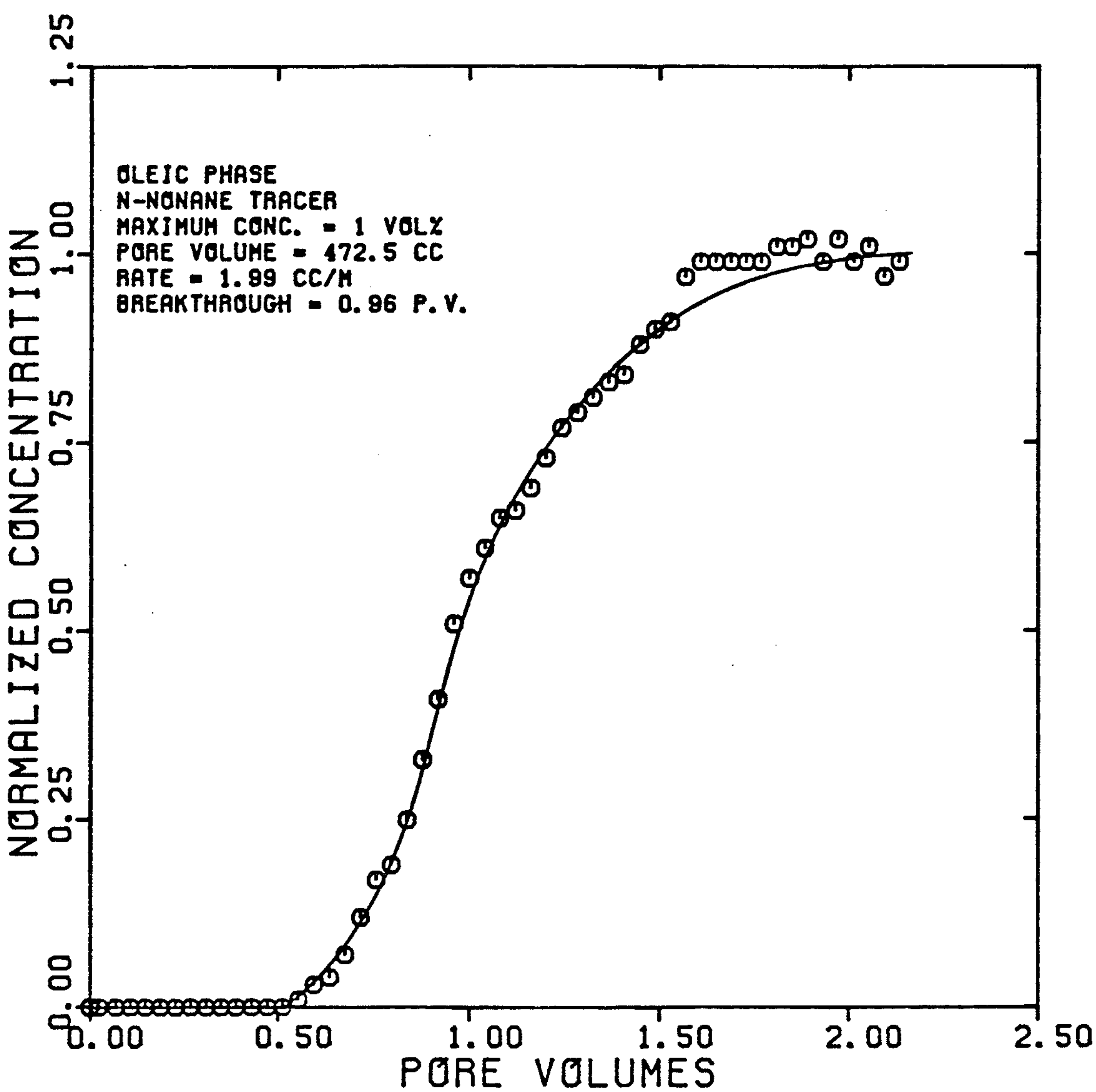

FIGURE 5.165

DISPERSIVITY OF N-NONANE
TRACER IN THE OLEIC PHASE
(EXPERIMENT PH340L)

$S_o = 0.261 \quad f_o = 0.378$

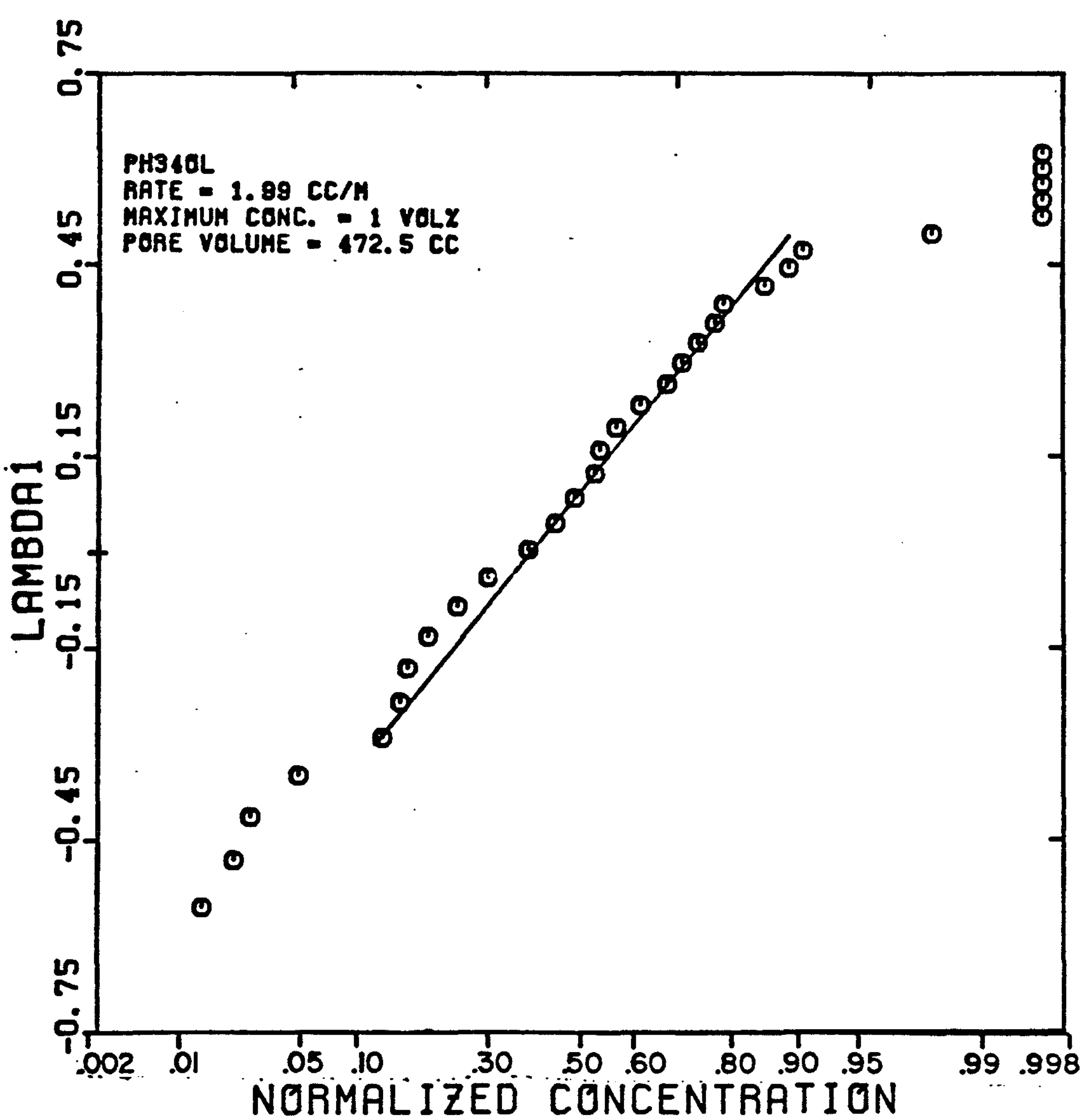

FIGURE 5.166

SANDPACK BREAKTHROUGH CURVE FOR CARBON 14
TRACER IN THE OLEIC PHASE
(EXPERIMENT PH340LC)

S_o = 0.261 f_o = 0.378

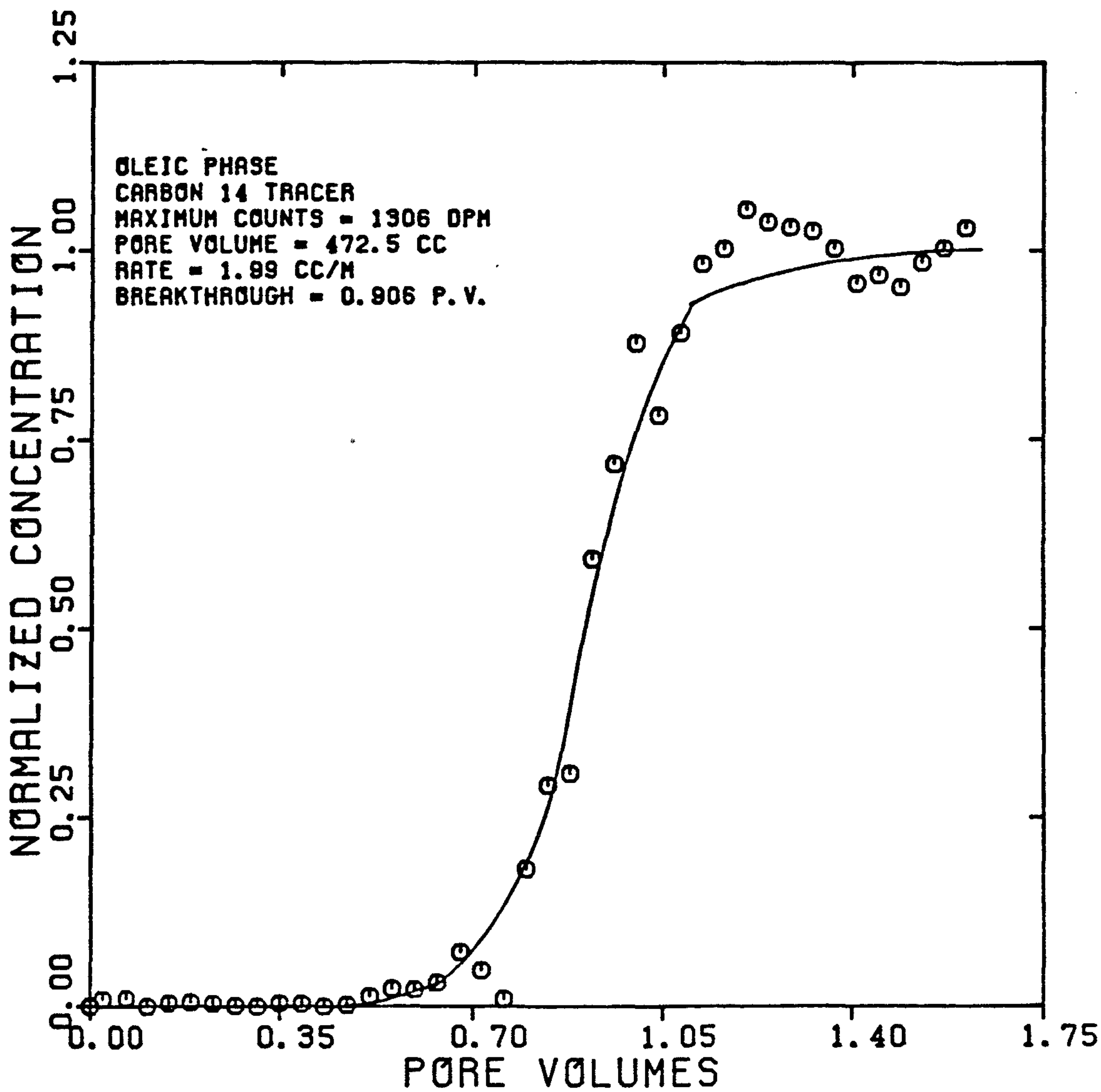

FIGURE 5.167

DISPERSIVITY OF CARBON 14
TRACER IN THE OLEIC PHASE
(EXPERIMENT PH34OLC)

$S_o = 0.261 \quad f_o = 0.378$

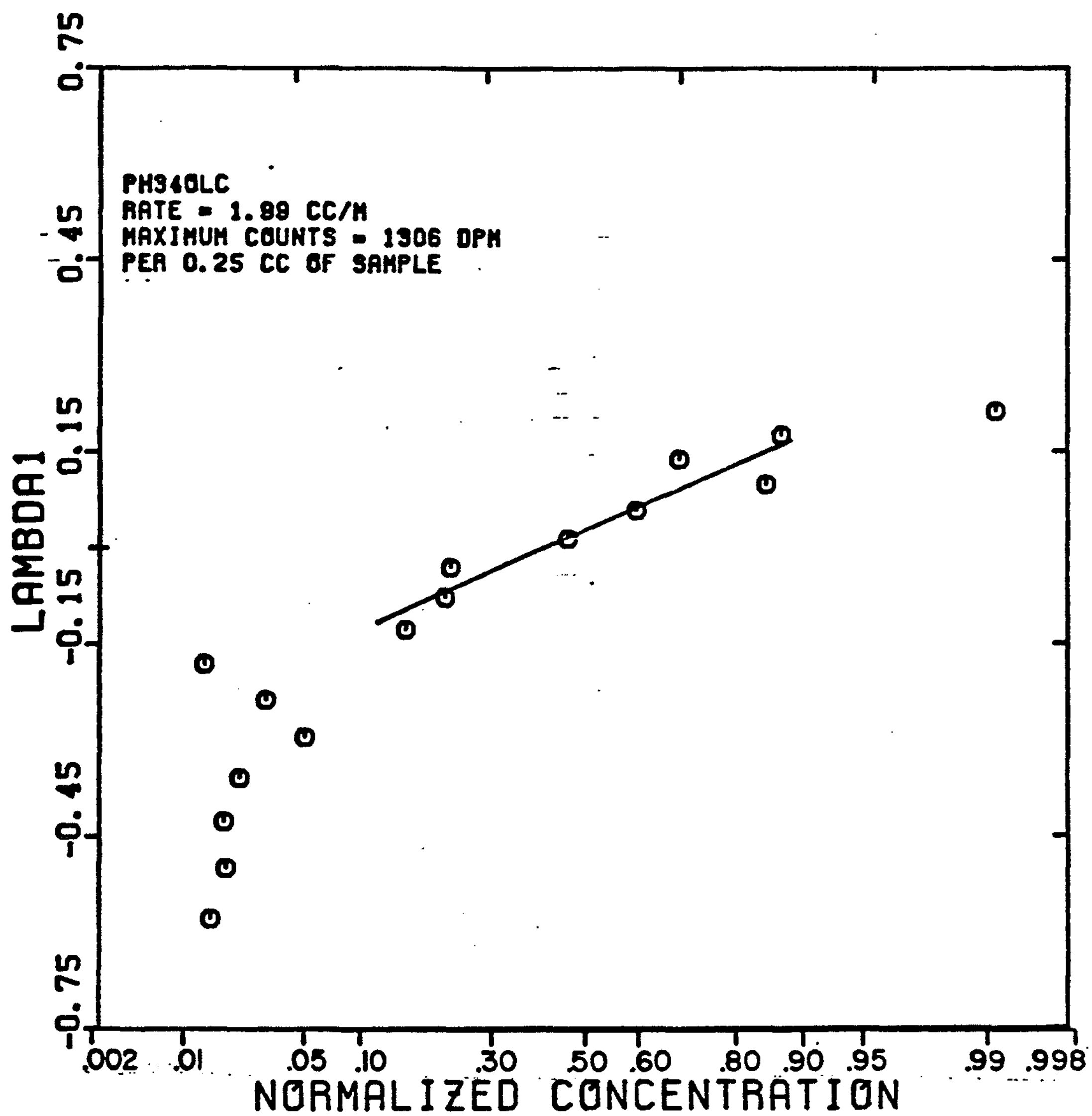

FIGURE 5.168

SANDPACK BREAKTHROUGH CURVE FOR TRITIUM
TRACER IN THE AQUEOUS PHASE
(EXPERIMENT PH35AQ)

$S_w = 0.324 \quad f_w = 0.587$

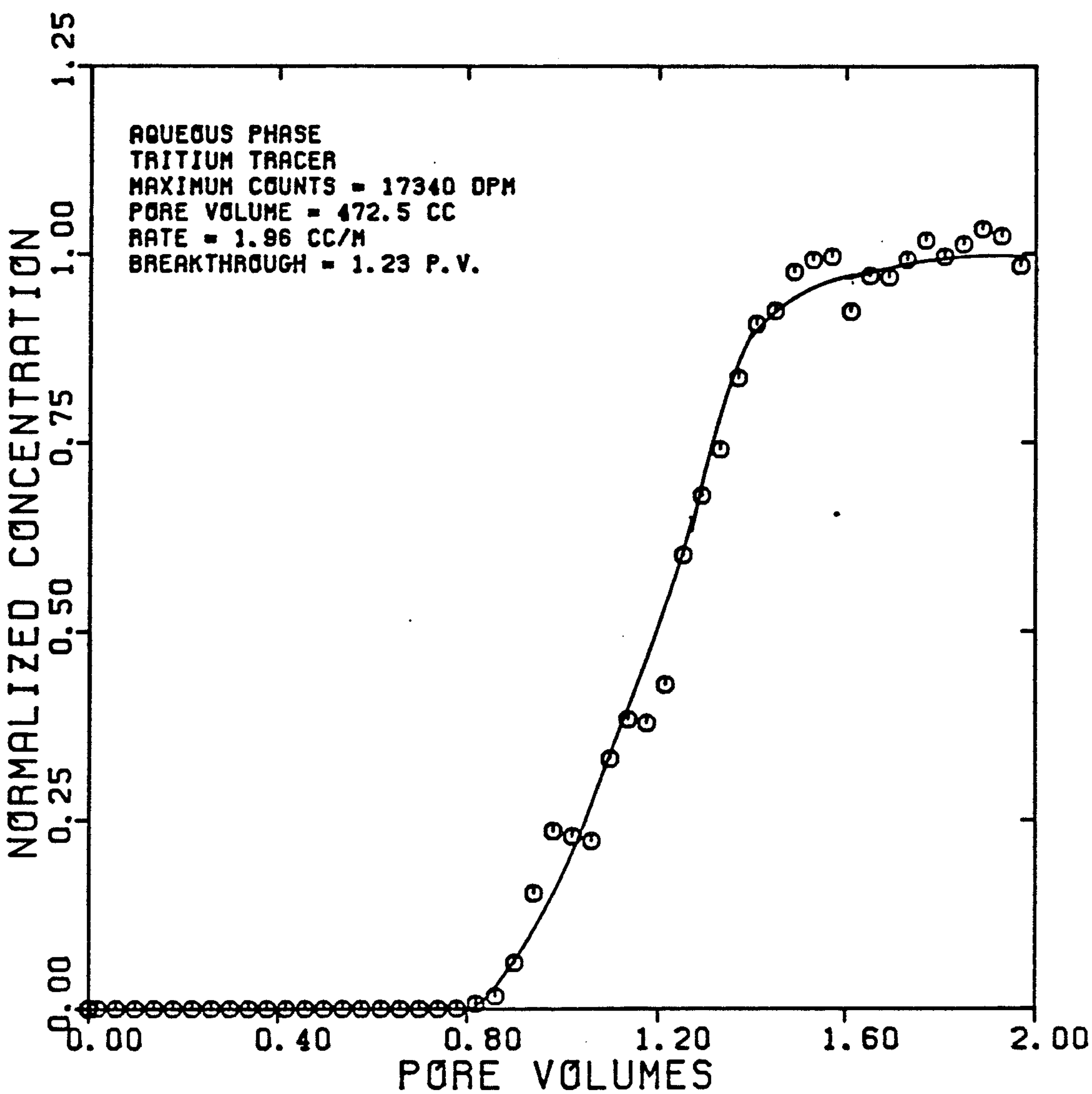

FIGURE 5.169

DISPERSIVITY OF TRITIUM TRACER IN THE AQUEOUS PHASE (EXPERIMENT PH35AQ)

$S_w = 0.324 \quad f_w = 0.587$

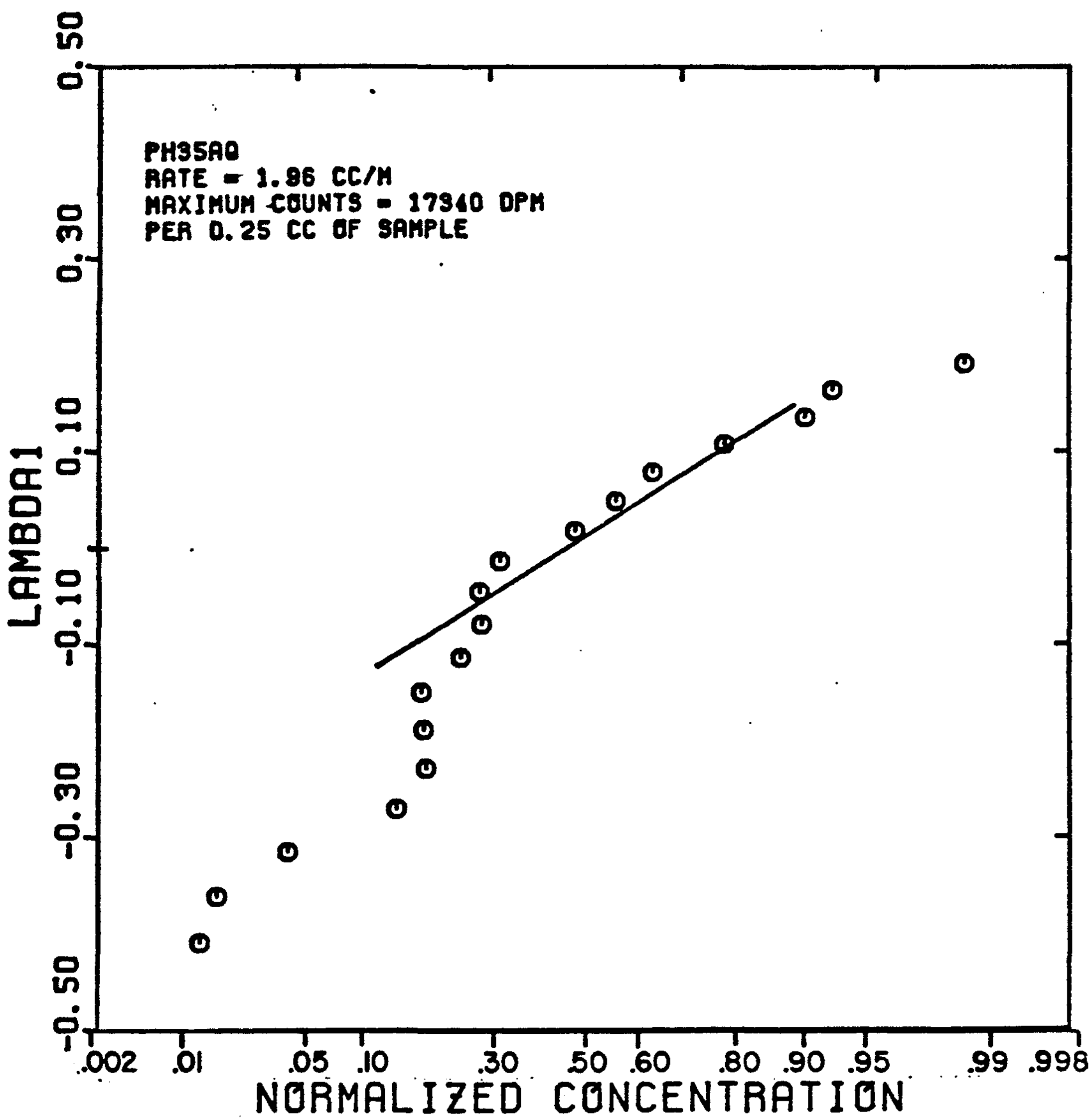

FIGURE 5.170

SANDPACK BREAKTHROUGH CURVE FOR TRITIUM TRACER IN THE MICROEMULSION PHASE (EXPERIMENT PH35MET)

$S_{me} = 0.515 \quad f_{me} = 0.233$

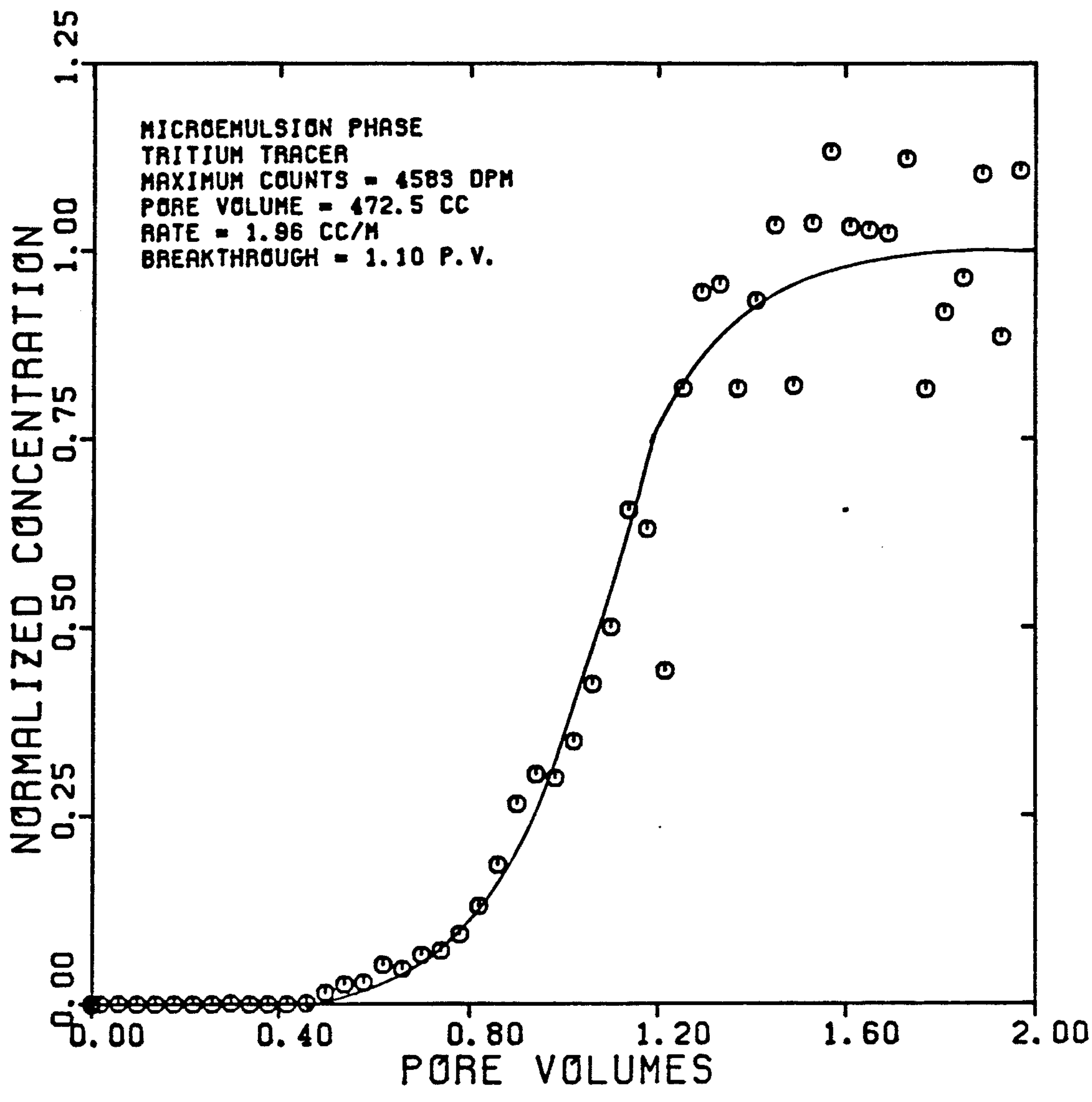

FIGURE 5.171

DISPERSIVITY OF TRITIUM
TRACER IN THE MICROEMULSION PHASE
(EXPERIMENT PH35MET)

$S_{me} = 0.515 \quad f_{me} = 0.233$

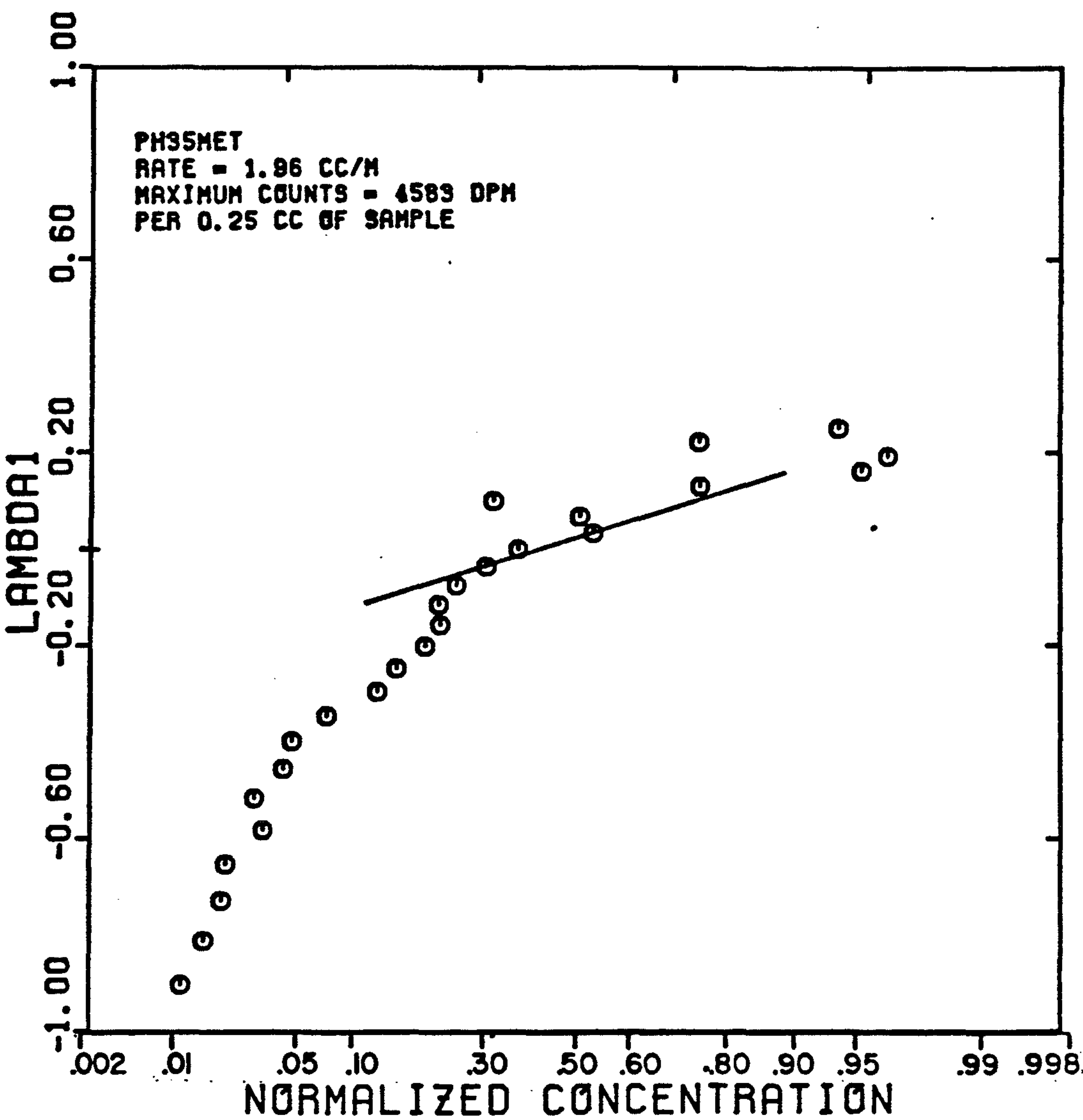

FIGURE 5.172

SANDPACK BREAKTHROUGH CURVE FOR CARBON 14
TRACER IN THE MICROEMULSION PHASE
(EXPERIMENT PH35MEC)

$S_{me} = 0.515 \quad f_{me} = 0.233$

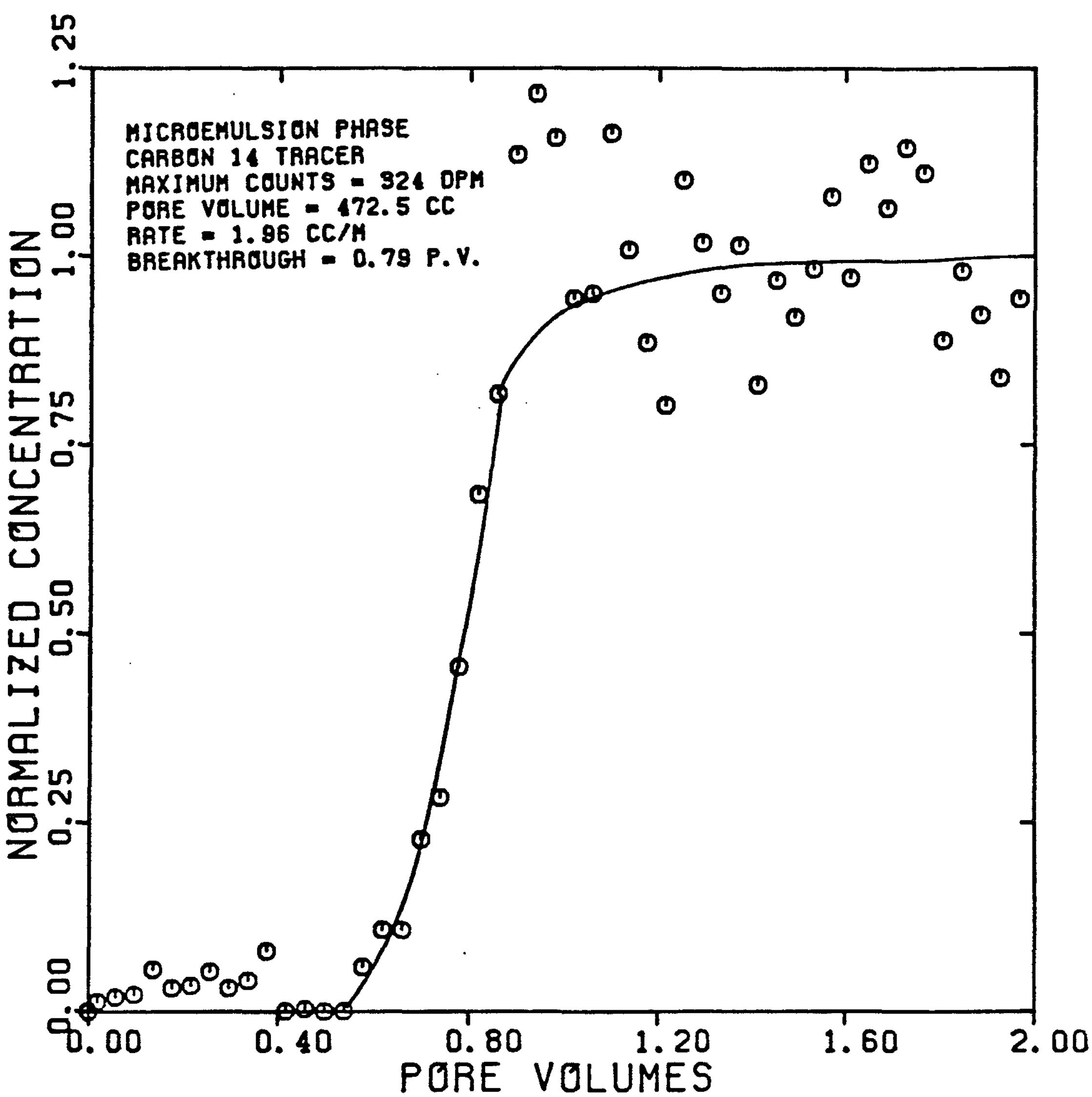

FIGURE 5.173

DISPERSIVITY OF CARBON 14
TRACER IN THE MICROEMULSION PHASE
(EXPERIMENT PH35MEC)

$S_{me} = 0.515 \quad f_{me} = 0.233$

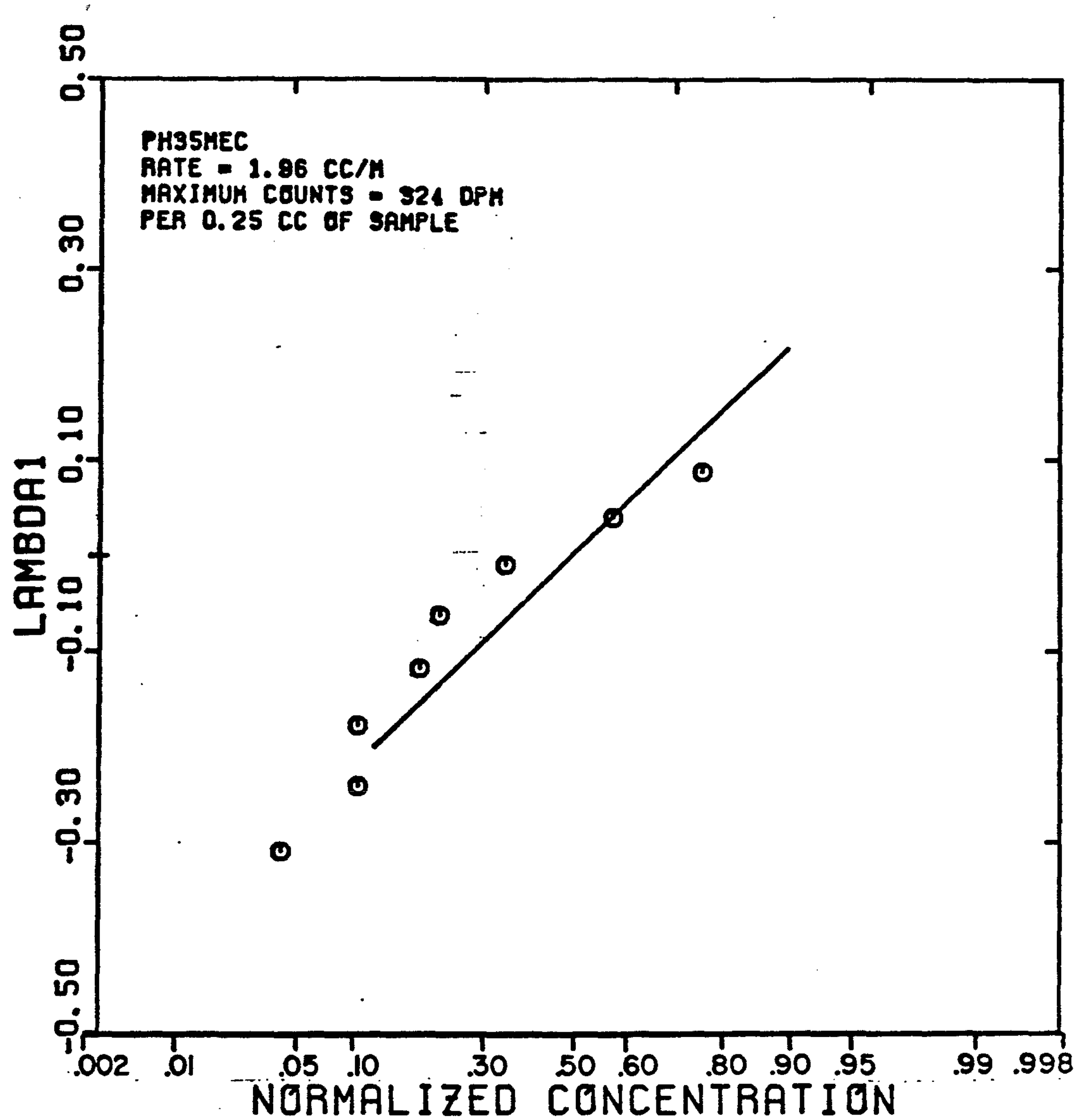

FIGURE 5.174

SANDPACK BREAKTHROUGH CURVE FOR N-NONANE
TRACER IN THE OLEIC PHASE
(EXPERIMENT PH350L)

$S_o = 0.161 \quad f_o = 0.180$

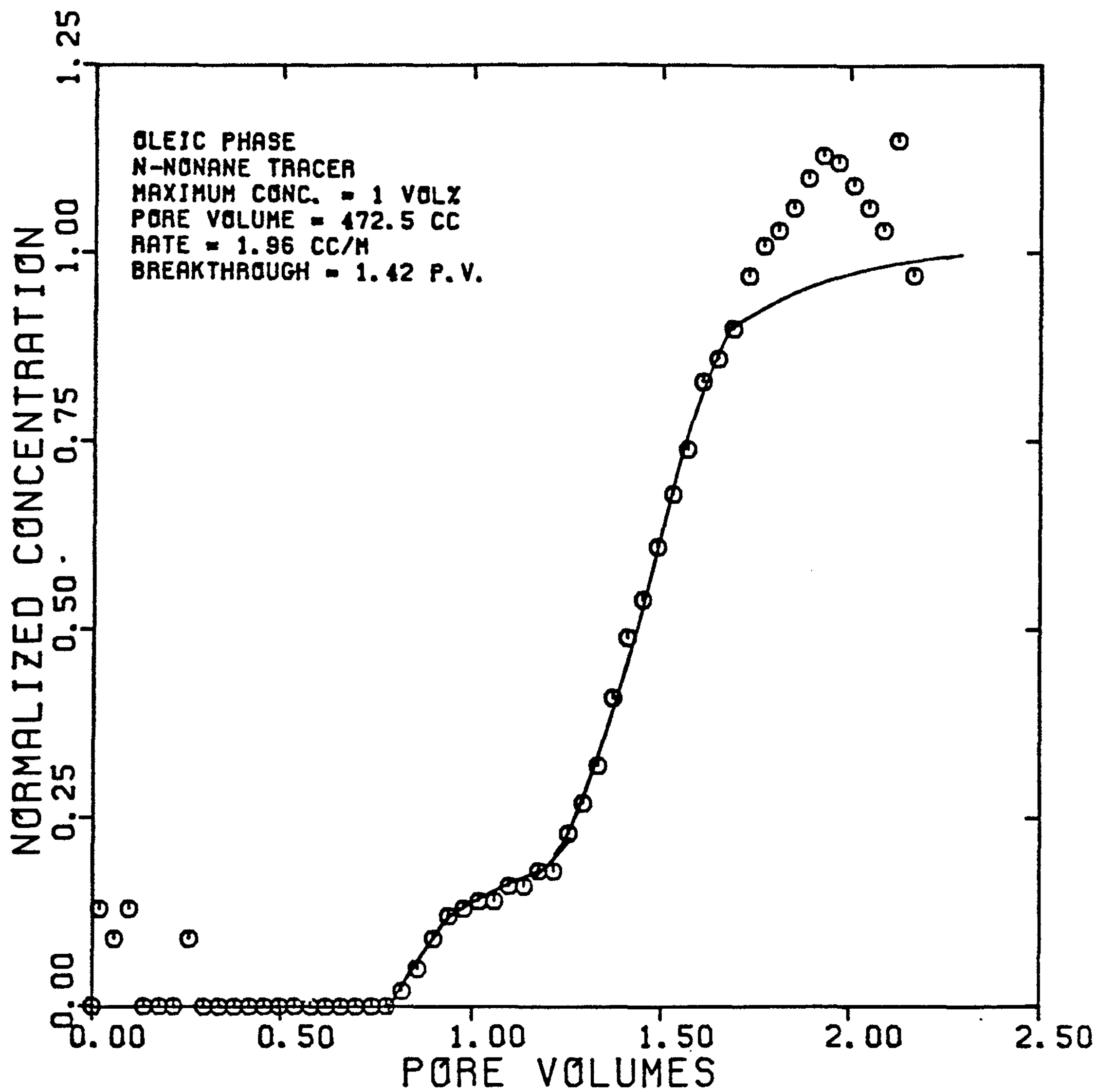

FIGURE 5.175

DISPERSIVITY OF N-NONANE
TRACER IN THE OLEIC PHASE
(EXPERIMENT PH350L)

S_o = 0.161 f_o = 0.180

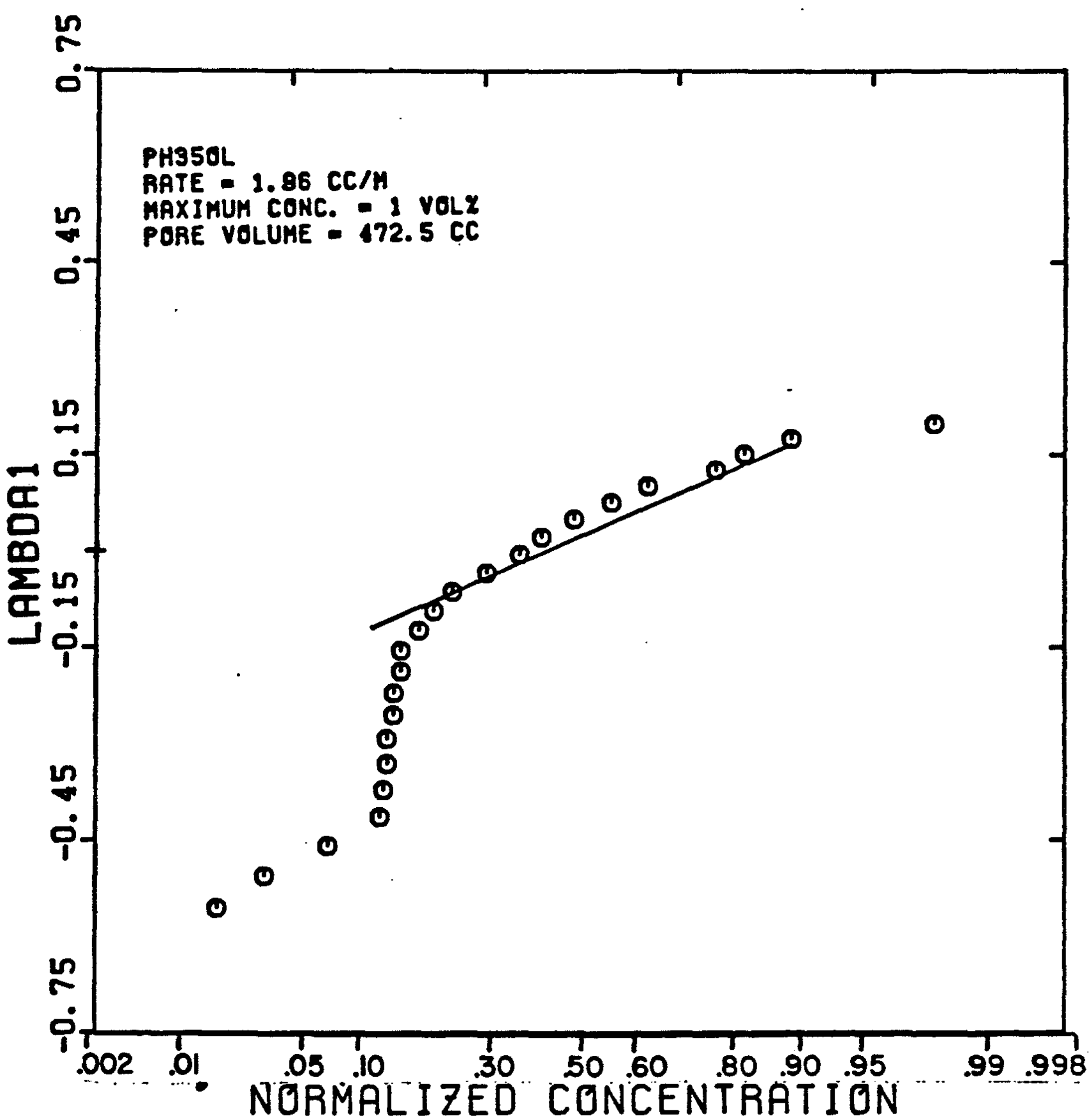

FIGURE 5.176

SANDPACK BREAKTHROUGH CURVE FOR TRITIUM
TRACER IN THE AQUEOUS PHASE
(EXPERIMENT PH36)

$S_w = 0.786 \quad f_w = 1.0$

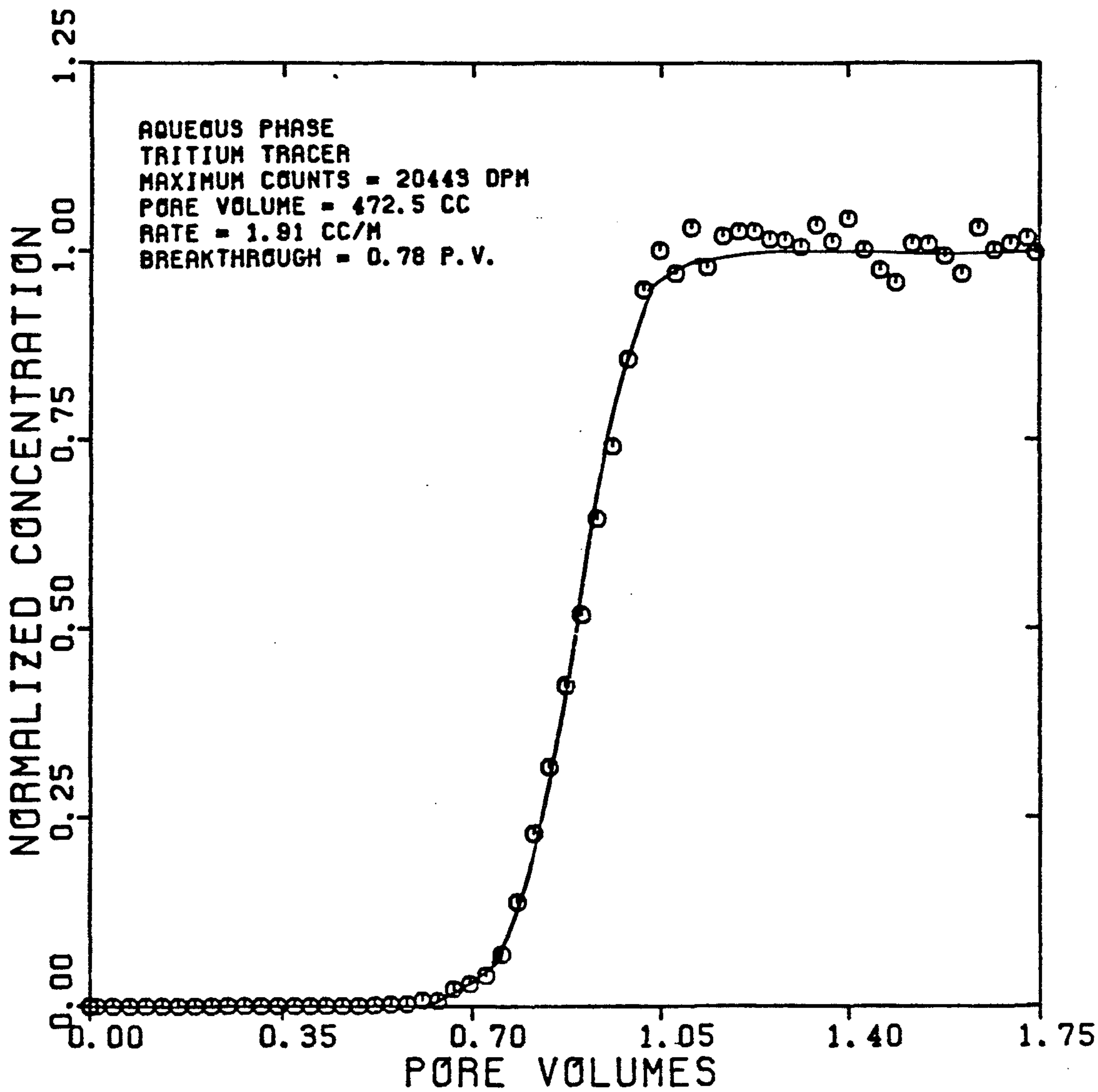

FIGURE 5.177

DISPERSIVITY OF TRITIUM
TRACER IN THE AQUEOUS PHASE
(EXPERIMENT PH36)

$S_w = 0.786 \quad f_w = 1.0$

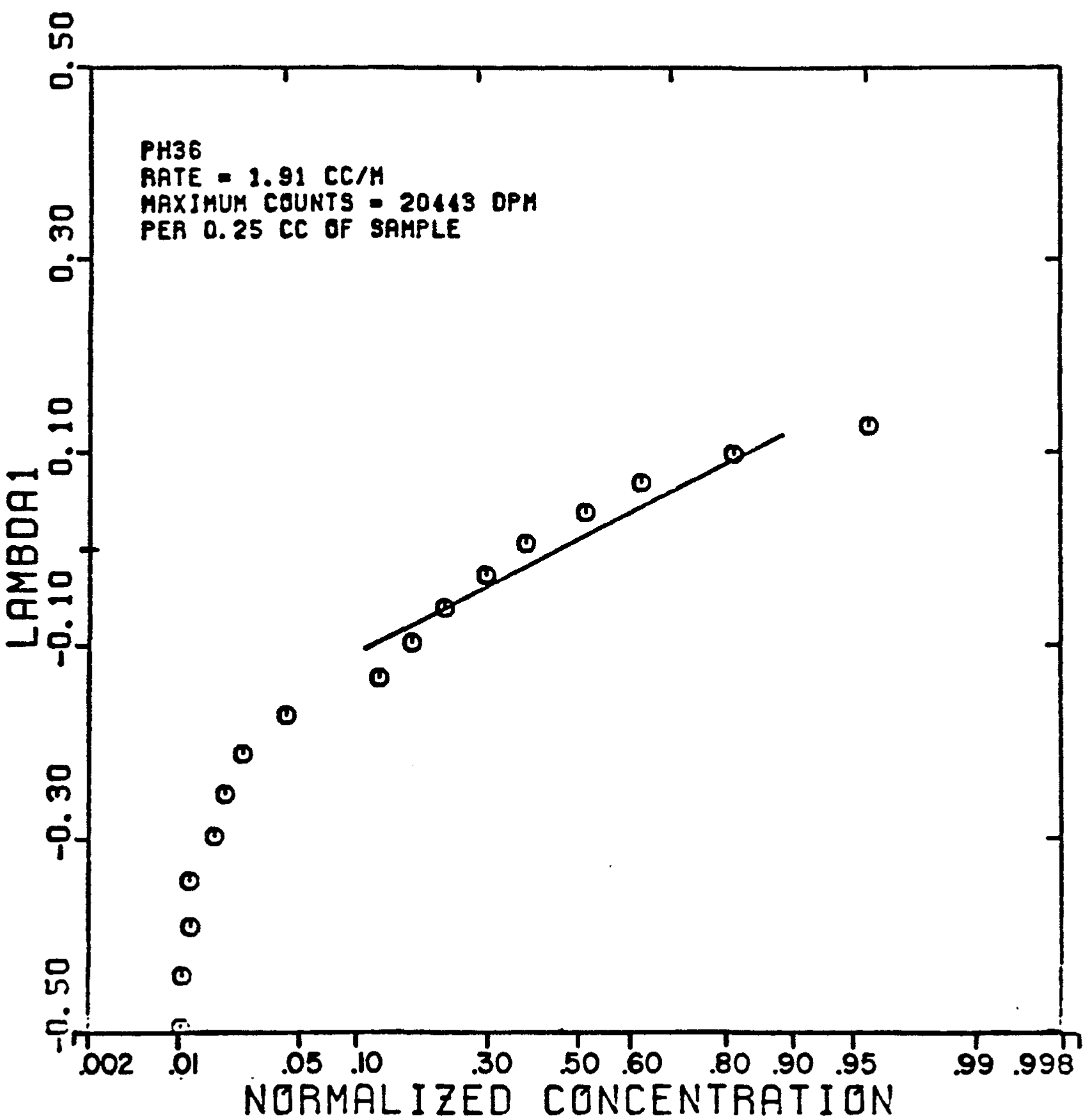

FIGURE 5.178

DISPERSIVITY OF AQUEOUS PHASES IN UNCONSOLIDATED SAND (EXPERIMENT PH3)

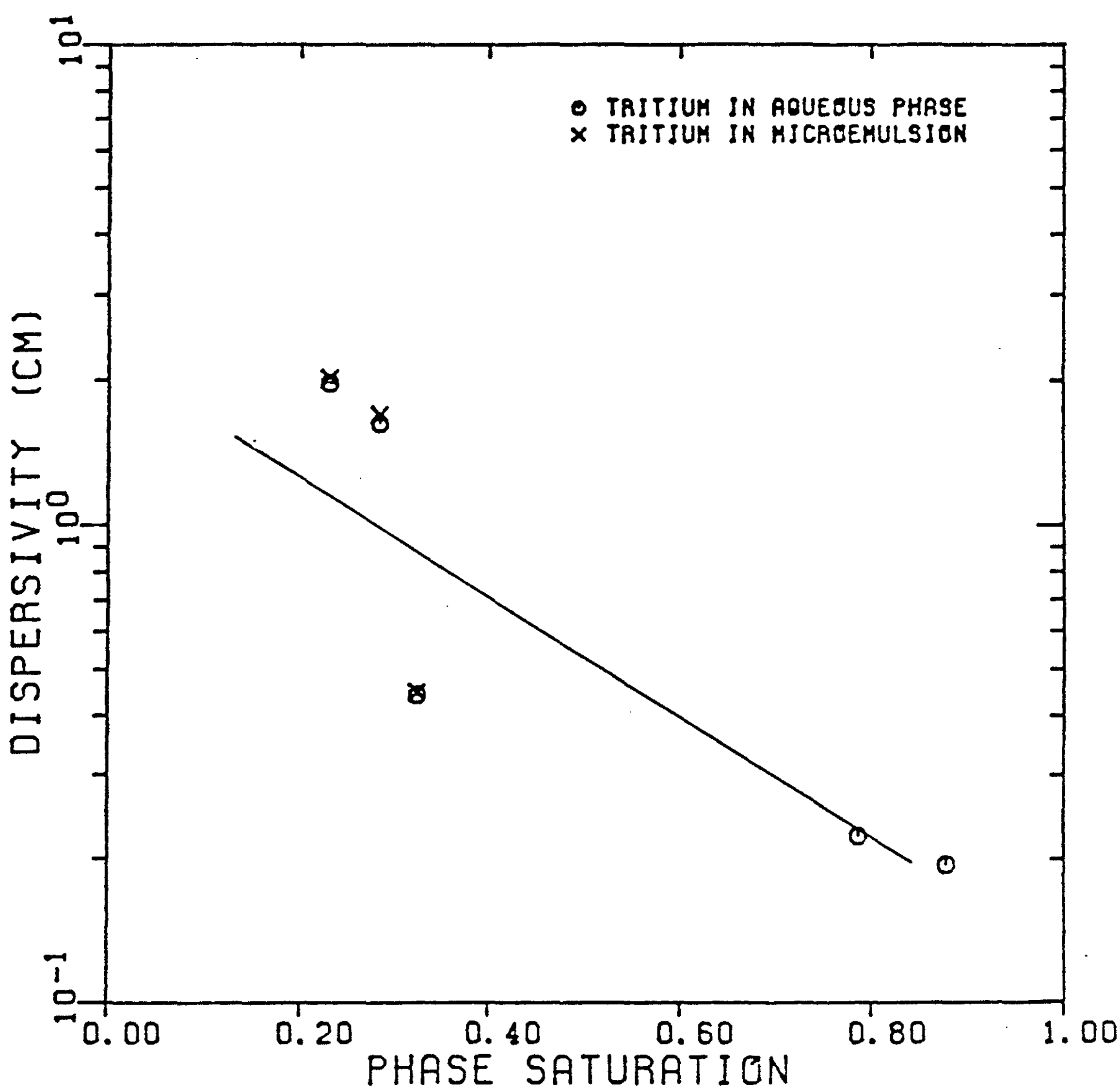

FIGURE 5.179

DISPERSIVITY OF OLEIC
PHASES IN UNCONSOLIDATED SAND
(EXPERIMENT PH3)

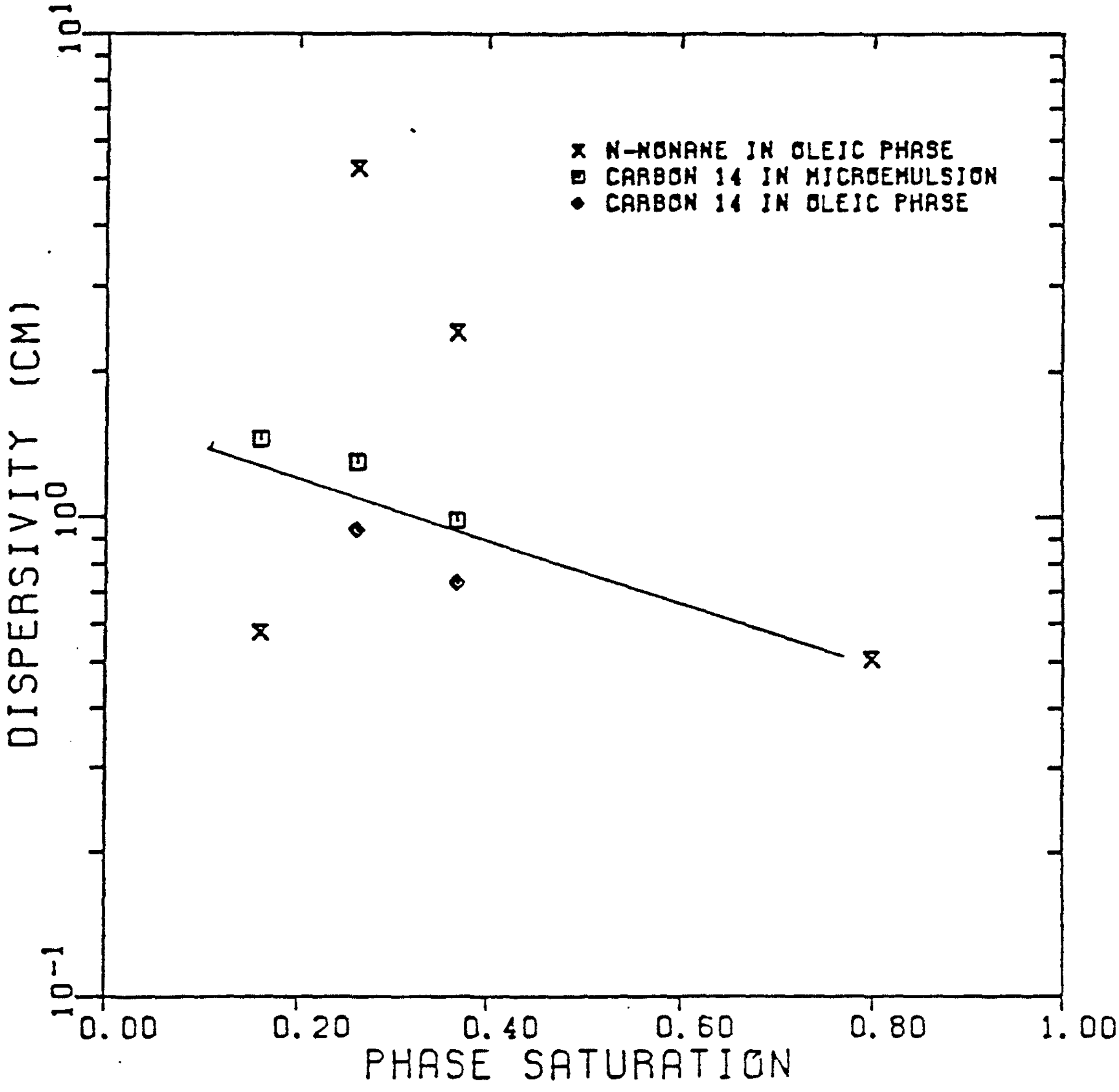

FIGURE 5.180

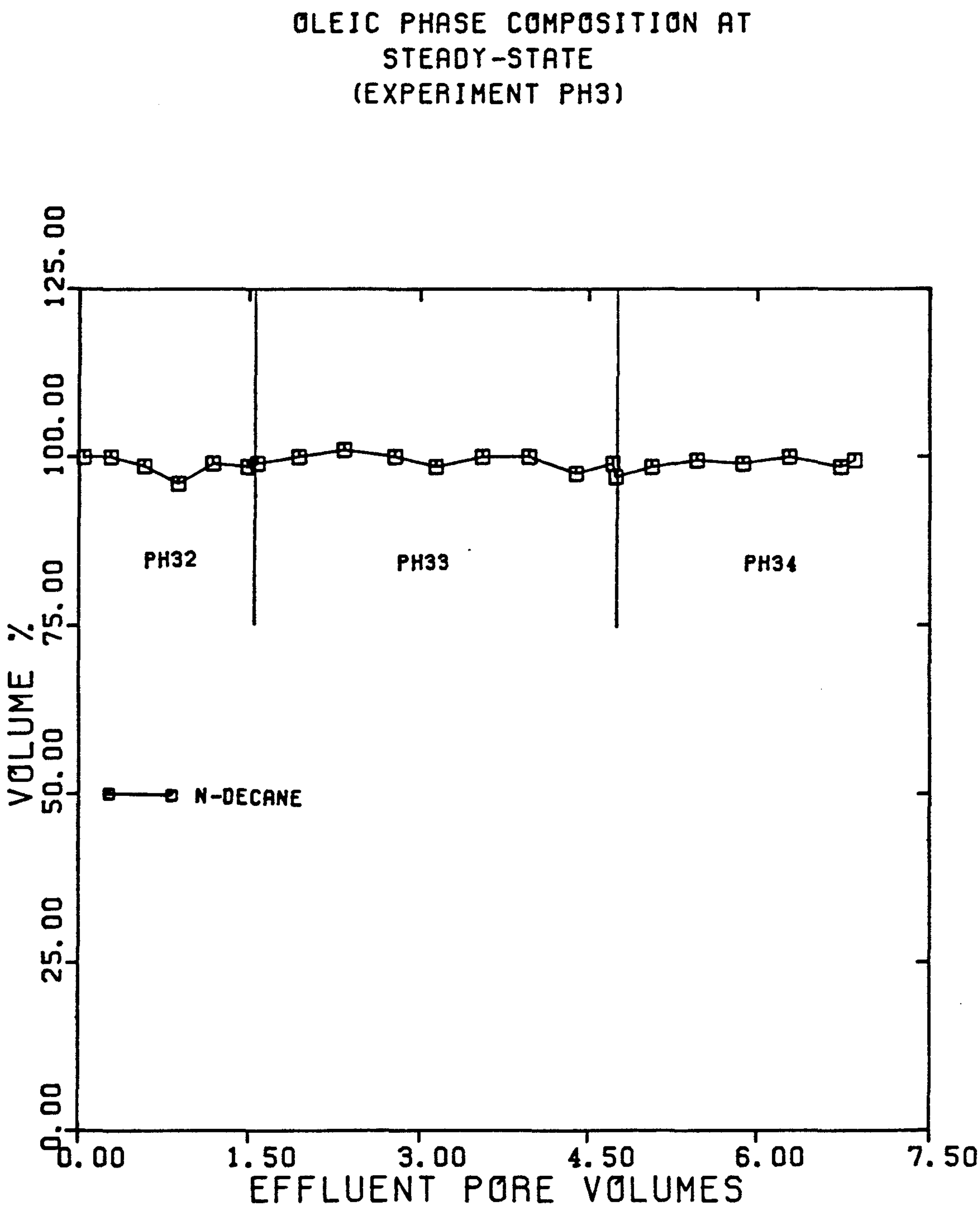
OLEIC PHASE COMPOSITION AT
STEADY-STATE
(EXPERIMENT PH3)
VOLUME %
0.00
25.00
50.00
75.00
100.00
125.00
EFFLUENT PORE VOLUMES
0.00
1.50
3.00
4.50
6.00
7.50
PH32
PH33
PH34
N-DECANE

FIGURE 5.181

MICROEMULSION COMPOSITION AT
STEADY-STATE
(EXPERIMENT PH3)

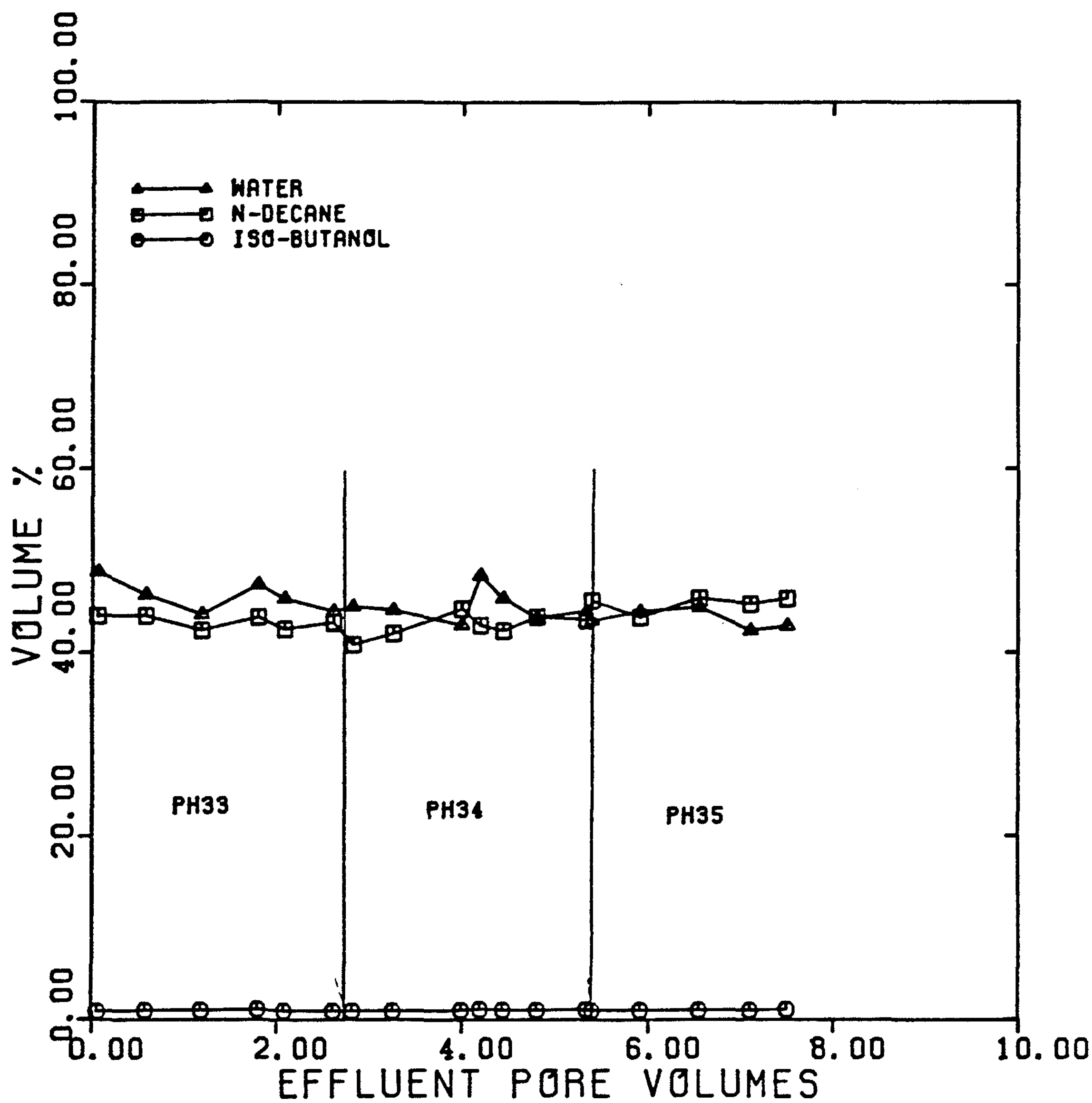

FIGURE 5.182

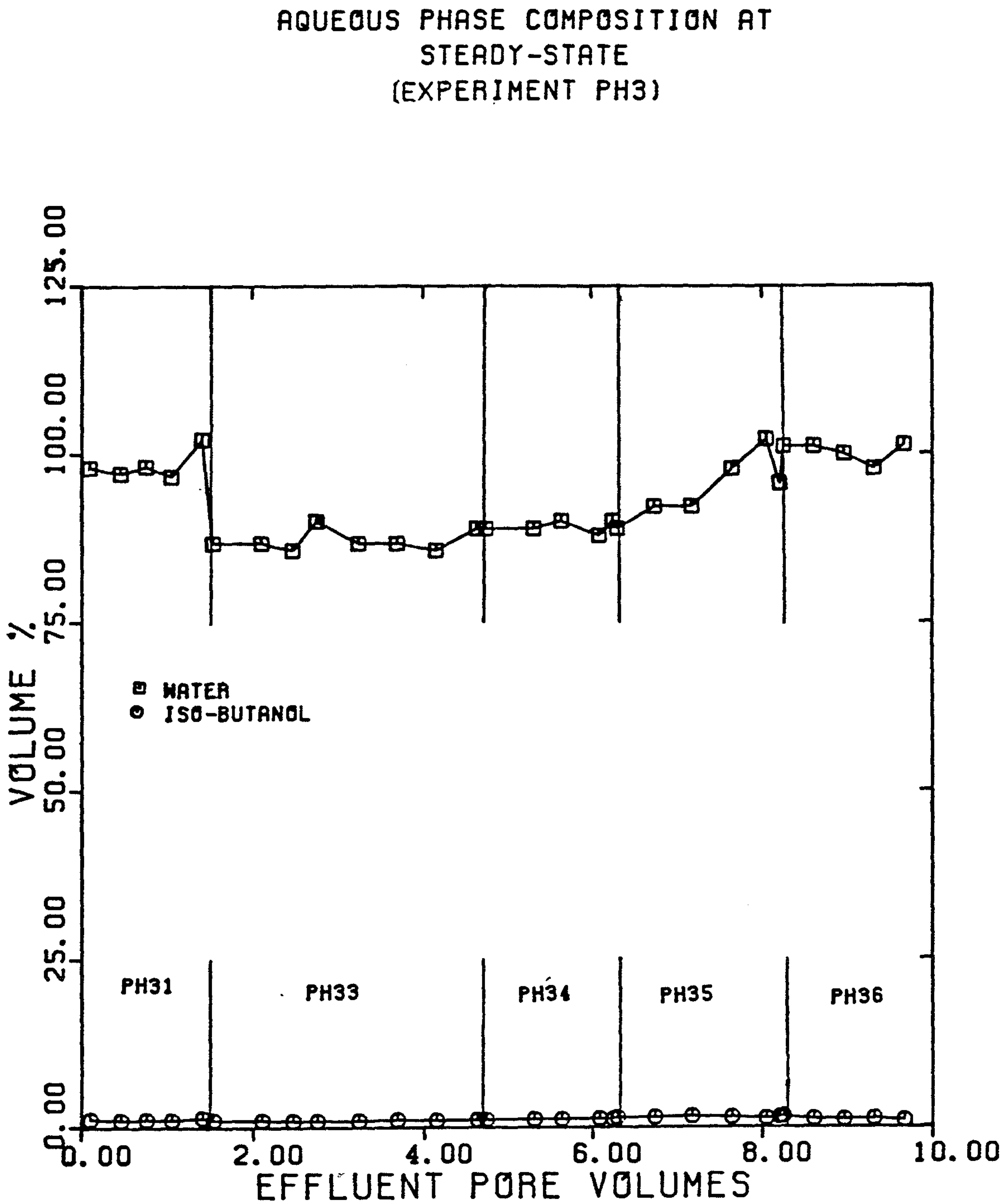
AQUEOUS PHASE COMPOSITION AT
STEADY-STATE
(EXPERIMENT PH3)
VOLUME %
0.00
25.00
50.00
75.00
100.00
125.00
WATER
ISO-BUTANOL
PH31
PH33
PH34
PH35
PH36
0.00
2.00
4.00
6.00
8.00
10.00
EFFLUENT PORE VOLUMES

FIGURE 5.183

INTERFACIAL TENSION BETWEEN PRODUCED MICROEMULSION AND OIL AT STEADY-STATE (EXPERIMENT PH3)

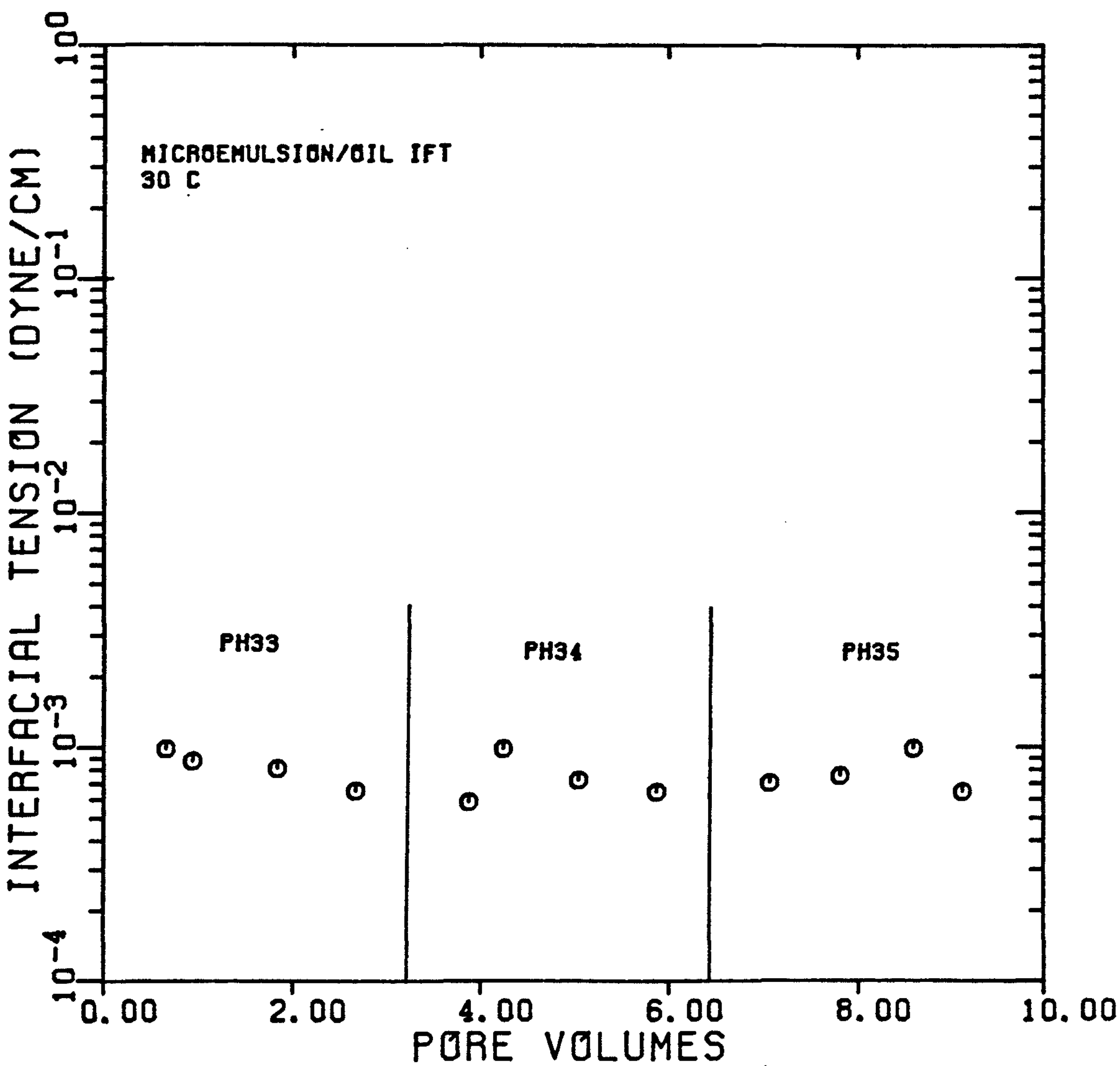

FIGURE 5.184

INTERFACIAL TENSION BETWEEN PRODUCED MICROEMULSION AND BRINE AT STEADY-STATE (EXPERIMENT PH3)

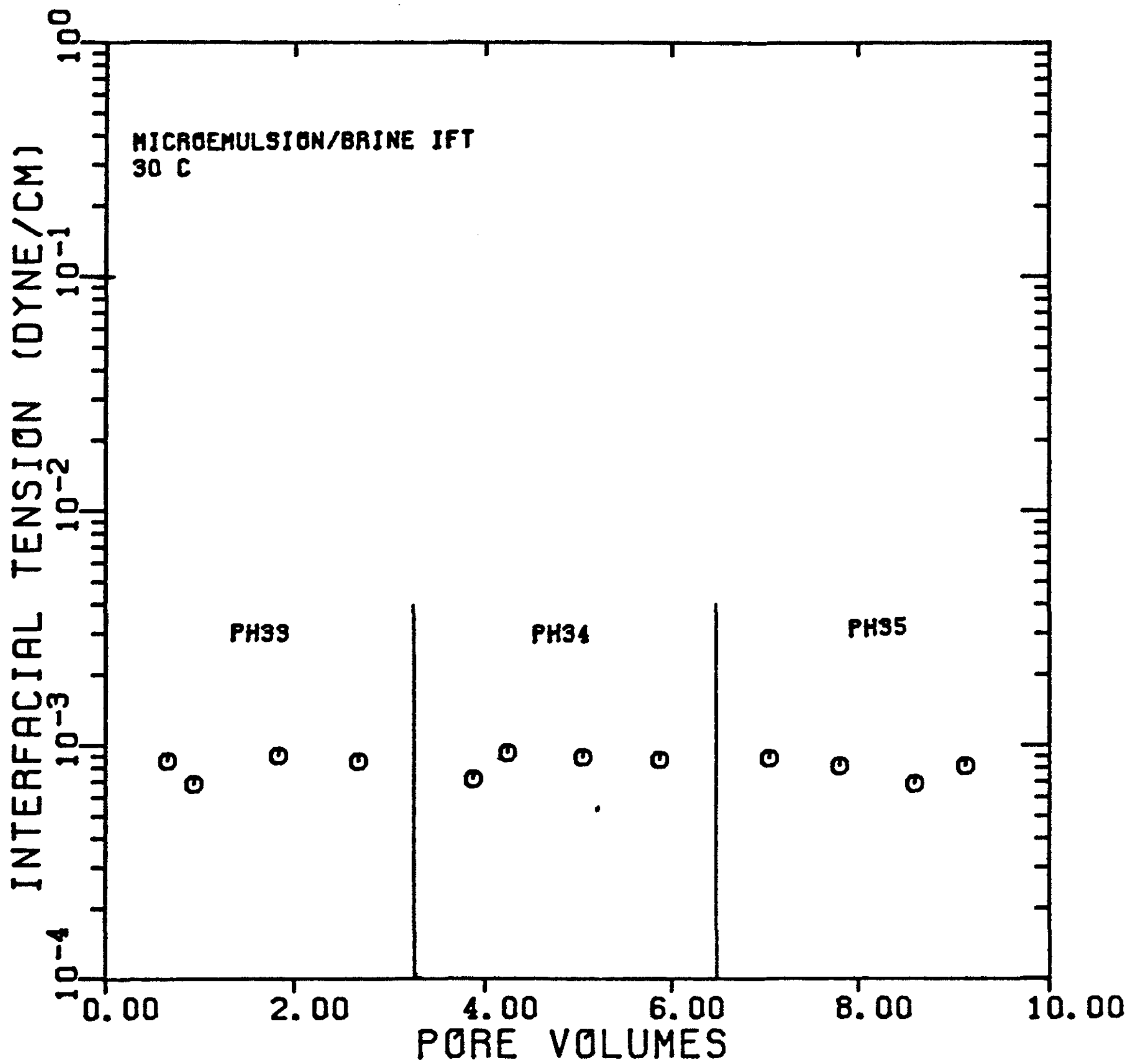

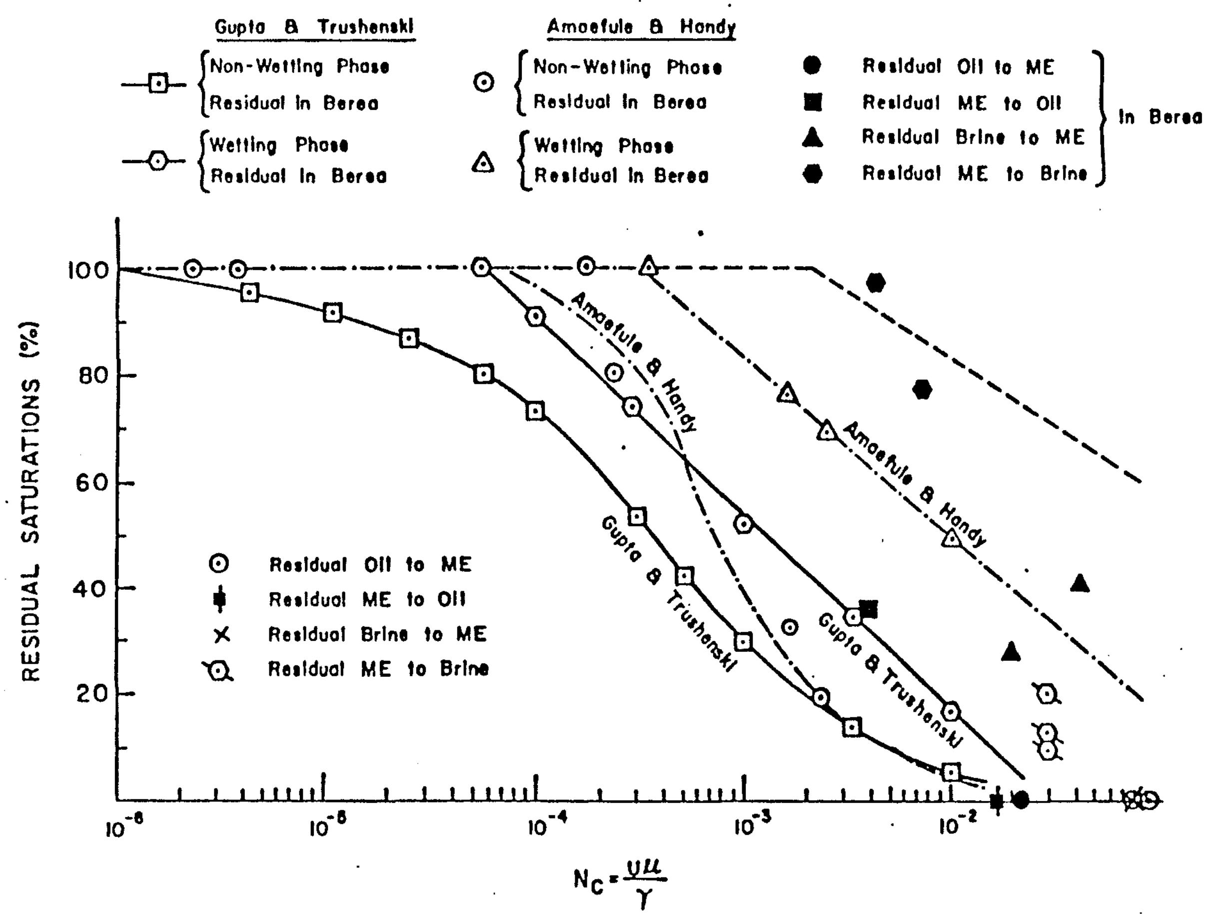

FIGURE 5.185 -- Residual Phase Saturations as a Function of Capillary Number

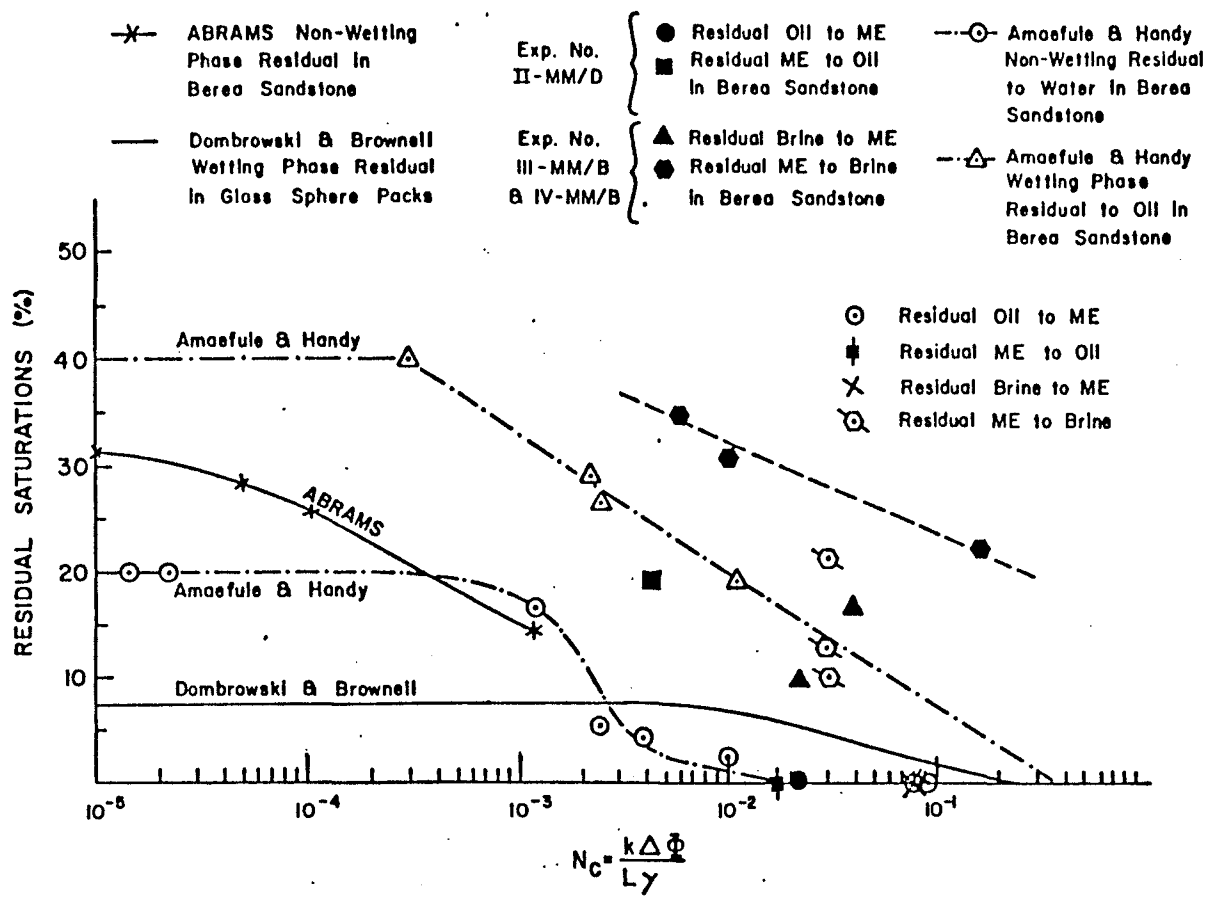

FIGURE 5.186 -- Residual Phase Saturations as a Function of Capillary Number

SUMMARY AND CONCLUSIONS

A brief review of high and low IFT relative permeability and dispersion is presented. Existing dispersion theory is generalized to include the effects of two- and three-phase flow and partitioning tracers. One-, two-, and/or three-phase flow experiments were carried out in sandpacks and Berea sandstone to measure relative premeability and phase dispersivity for both high and low IFT formulations. Relative permeability is measured at steady-state phase fractions followed by injection of a tracer in each flowing phase while at steady-state. Phase saturation and dispersivity are calculated from tracer effluent data. Saturations are also calculated by material balance.

Phase behavior, IFT, and viscosity behavior of Siponate DS-10 and TRS 10-410 formulations were investigated with several alcohol co-surfactants and at several salinities. Siponate DS-10 was determined to be unsuitable for our studies at the compositions investigated, but TRS 10-410 formulations are acceptable. The micellar formulation used in the low IFT flow experiments consists of TRS 10-410 sulfonate, isobutanol, n-decane, and 1.1 wt % NaCl brine. Interfacial tensions between microemulsion and excess brine and microemulsion and excess oil are on the order of 10^{-3} dyne/cm.

The following conclusions can be stated concerning dispersion for the high IFT systems studied:

1. Dispersivity of tritium in the brine phase increases with decreasing brine phase saturation in Berea and the sandpack used in Experiment OW, but no relationship was demonstrated in the sandpack used in Experiment OWZ.
2. Dispersivity of carbon-14 in the oil phase increases with decreasing oil phase saturation in Berea but shows no relationship in the sandpack used in Experiment OWZ.
3. Oil phase dipsersivity is two orders of magnitude greater than brine phase dispersivity in the sandpack used in Experiment OWZ.
4. Brine phase tracer breakthrough curves were smooth and S-shaped and gave saturations in good agreement with material balance.
5. Oil phase tracer breakthrough curves have more of a capacitance-type shape (Chapter 2) and demonstrate early breakthrough resulting in poor agreement with saturations calculated by material balance. (Note that capacitance may account in part for Result 3.)
6. Plateau tracer concentration is very close to injected concentration in the brine phase, but is lower in the oil phase. This result, along with the early breakthrough of oil phase, could indicate the existence of a non-contacted oil volume that

gains tracer by a relatively slow diffusion process compared to the convective process.

The following conclusions can be drawn from the relative permeability studies in the low IFT experiments:

7. Relative permeability increased, but there was significant curvature in both two- and three-phase relative permeability curves.
8. Residual phases in the sand pack at low tension were zero except for residual microemulsion to aqueous phase.
9. Result 8 along with changes in fractional flow diagrams and the essentially identical relative permeability of oleic and aqueous phases in three-phase flow indicate a change in wettability from the initial water-wet state.
10. In three-phase flow, aqueous and oleic phase relative permeabilities appear to be a function of their own saturation. Insufficient data exists for the microemulsion phase.
11. Dispersivity of oleic and aqueous phases increases with decreasing phase saturation.
12. Microemulsion phase dispersivity is essentially unchanged with decreasing microemulsion saturation.

13. Dispersivities measured by partitioning tracers were consistent between the tritiated water and carbon-14 labelled n-decane, but not with n-nonane in n-decane.

The following general conclusions can be drawn:

14. Calcium ion concentration was not significant in the treated sandpack.
15. The composition and IFT analyses of effluent samples (pressure drop and phase volume fractions were constant in all cases) confirm that steady state was achieved with the micellar phases.

More data is needed to confirm and expand the tentative conclusions drawn.

NOMENCLATURE

A = Cross sectional area (cm^2)

$C_{o_{ij}}$ = Injected concentration of component i in phase j

$C_{T_{ij}}$ = Concentration of component i in phase j

$C_{D_{ij}}$ = Normalized concentration of component i in phase j

D_o = Molecular diffusion coefficient (cm^2/sec)

F = Formation electrical resistivity factor

f_j = Fractional flow of phase j

K_l = Longitudinal dispersion coefficient (cm^2/sec)

K_{ij} = Longitudinal dispersion coefficient of tracer i in phase j (cm^2/sec)

K_t = Transverse dispersion coefficient (cm^2/sec)

$\bar{K}_i$ = Average dispersion coefficient of component i (cm^2/sec)

K_{T_i} = Partition coefficient of component i

k = Absolute permeability (D)

k_{ej} = Effective permeability of phase j (D)

k_{rj} = Relative permeability of phase j

L = Total length of porous medium (cm)

M = Mobility (cp^{-1})

M_{rT} = Total relative mobility

N_c = Capillary number

q = Flow rate (cm^3/sec)

S_j = Saturation of phase j

S_{rj} = Residual saturation of phase j

t_D = Time (pore volumes)

t_D^{Bt} = Time where $C_i/C_{oi} = 0.5$ (pore volume)

t_{Dt} = Time normalized for phase fractional flow and saturation in multiphase flow (pore volumes)

U_j = Darcy velocity of phase j (cm/sec)

V = Volume of produced effluent (cm^3)

V_P = Pore volume of porous medium (cm^3)

v_{Tj} = Average interstitial velocity of phase j (cm/sec)

α_l = Longitudinal dispersivity (cm)

α_{ij} = Longitudinal dispersivity of tracer i in phase j (cm)

$\overline{\alpha}_i$ = Average dispersivity of component i (cm)

β = Velocity exponent

ϕ = Porosity (cm^3/cm^3)

λ = Dimensionless function $\frac{t_D - 1}{\sqrt{t_D}}$

λ_1 = Dimensionless function $\frac{t_{Dt} - 1}{\sqrt{t_{Dt}}}$

μ_j = Viscosity of phase j (cp)

σ = Interfacial tension (dyne/cm)

$\Delta\Phi_j$ = Potential difference of phase j (psi)

Subscripts

i = component

i = 1, tritium tracer

i = 2, carbon-14 tracer

i = 2', n-nonane tracer

j = phase

j = 1 or W, aqueous phase

j = 2 or O, oleic phase

j = 3 or ME, microemulsion phase

APPENDIX 1

Construction of Volume Fraction Diagrams

Sample tubes are made up as outlined in Chapter 4 and allowed to reach equilibrium. The volume of each phase is divided by the total phase volume. The resulting phase volumes total 1.0. These points are plotted as in Figure 3.2 with lines connecting the points corresponding to aqueous microemulsion and microemulsion-oleic phase boundaries.

APPENDIX 2

Construction of Pseudo-Ternary Diagrams Using Tie-lines

Figure A2.1[37] illustrates the relationship between distance on the pseudo-ternary diagram and phase volumes of sample tubes. The solid point represents the overall composition. Type II phase compositions correspond to where the tie-lines meet the two-phase envelope. In the ideal Type III phase region, the phases are invarient at constant temperature and pressure and consist of almost pure oil, almost pure brine, and a microemulsion phase of a composition indicated where the one-, two-, and three-phase regions meet (invarient point).

FIGURE A2.1

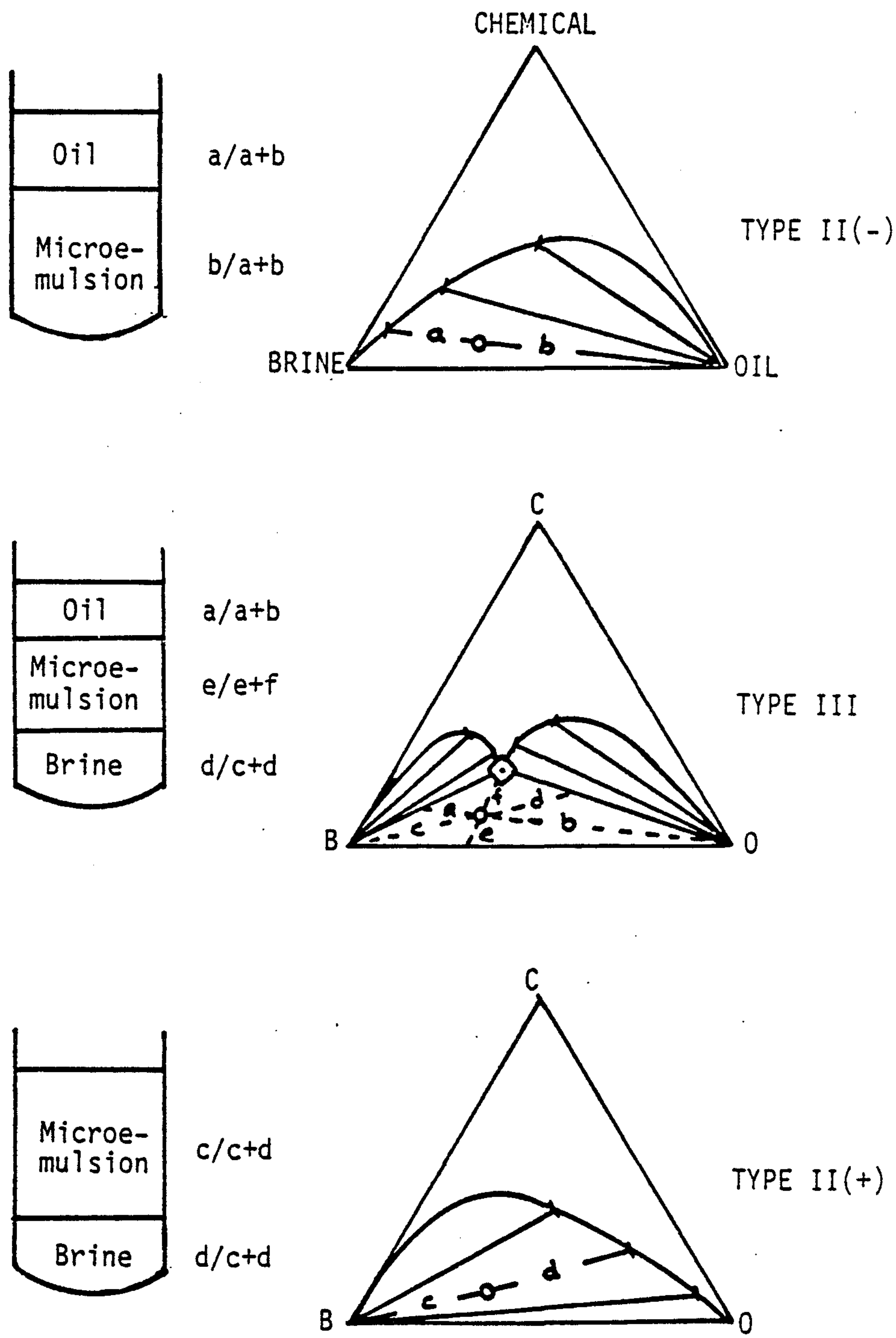

TERNARY REPRESENTATION OF PHASE RELATIONSHIPS

APPENDIX 3

Epoxy Mixing Procedure

Resin (R-829) and hardener (Versamid 125) are available from the Ring Chemical Company. The following procedure is repeated three times:

1. Weigh 70 wt % resin and 30 wt % hardener into a beaker.
2. Stir for five minutes until homogeneous.
3. Pour into a shallow container (such as aluminum foil tray) and allow to set for two hours to attain the proper consistency and to allow air bubbles to escape.
4. Apply epoxy to core as a thin layer.
5. Allow to harden for 24 hours.

APPENDIX 4

Pore Volume by Grain Density

If the weight of sand that is packed into a column of known bulk volume is known, the pore volume can be calculated from the grain density. First, grain density is measured and then the formula for calculating pore volume is presented.

A known weight of sand is weighed into a previously weighed 100 ml volumetric flask. The flask is then filled up the the mark with distilled water and the temperature recorded. Grain density is:

$$\rho_g = \frac{WT_g}{100 - \dfrac{WT_{H_2O}}{\rho_{H_2O}}} \qquad \text{A4.1}$$

The actual values were:

volumetric weight	= 70.28
volumetric + sand weight	= 126.02 g
weight of sand (WT_g)	= 55.74 g
volumetric + sand + H_2O	= 204.61 g
weight of water (WT_{H_2O})	= 78.59 g
water density at 25°C	= .99705 g/ml

$$\rho_g = \frac{55.74\ g}{100\ ml - \dfrac{78.59\ g}{.99705\ g/ml}} = 2.632\ g/ml$$

Pore volume and porosity can be calculated as follows:

$$V_P = \left(V_B - \frac{WT_{sand}}{\rho g} \right) \qquad A4.2$$

$$\phi = \frac{V_P}{V_B} = 1 - \frac{WT_{sand}}{\rho g \; V_B} \qquad A4.3$$

APPENDIX 5

Special Sand Preparation

Ottawa F140 sand (Table 5.1) was divided into component mesh sizes by mechanical shaking. The following mesh sizes were used along with a 400 mesh silica sand supplied by Fisher Scientific Inc.:

Mesh	Grams	Weight Percent
200	246	11.7
230	260	12.4
270	490	23.3
270+	294	14.0
400	810	38.6

Eash mesh size was washed twice in concentrated hydrochloric acid and washed repeatedly with distilled water to neutral pH. The sands were then subjected to sonication for two hours and dried for 48 hours at 110°C. This procedure effectively removed clays from the sand particles (Table 5.45). The mesh mixture mixed well and no segregation of sand was discernable.

APPENDIX 6

Tabular Data for Dispersion Experiments

Experiment	Tables
OWCL	6A1
OW	6A2-6A4
BAOW	6A5-6A13
OWZ	6A14-6A29
MO	6A30-6A40
MW	6A41-6A51
pH3	6A52-6A68

EXPERIMENT CHLOR

TUBE NUMBER	PORE VOLUMES	TOTAL PHASE VOLUME (CC)	PHASE VOLUME (CC)	FRACTIONAL FLOW	NORMALIZED CONCENTRATION	LAMBDA1
1	.022	2.25	0.00	0.0000	.032	-6.549
2	.111	8.95	0.00	0.0000	.000	-2.669
3	.252	16.50	0.00	0.0000	.016	-1.490
4	.413	25.10	0.00	0.0000	.032	-.916
5	.585	33.85	0.00	0.0000	0.000	-.545
6	.759	42.65	0.00	0.0000	.040	-.270
7	.934	51.05	0.00	0.0000	.262	-.070
8	1.108	60.25	0.00	0.0000	.873	.101
9	1.282	69.00	0.00	0.0000	.960	.240
10	1.456	77.75	0.00	0.0000	1.000	.376
11	1.618	85.35	0.00	0.0000	.992	.484

STEADY-STATE PHASE FRACTIONAL FLOW : .0000
50% BREAKTHROUGH (PORE VOLUME) : 1.0016

EXPERIMENT OW1

TUBE NUMBER	PORE VOLUMES	TOTAL PHASE VOLUME (CC)	PHASE VOLUME (CC)	FRACTIONAL FLOW	NORMALIZED CONCENTRATION	LAMBDA1
1	.016	3.55	3.55	1.0000	0.000	-7.895
2	.055	8.85	8.85	1.0000	0.000	-4.050
3	.101	14.00	14.00	1.0000	0.000	-2.845
4	.146	19.00	19.00	1.0000	0.000	-2.250
5	.190	24.00	24.00	1.0000	0.000	-1.870
6	.235	29.00	29.00	1.0000	0.000	-1.594
7	.279	34.00	34.00	1.0000	0.000	-1.370
8	.323	38.95	38.95	1.0000	0.000	-1.204
9	.367	43.95	43.95	1.0000	0.000	-1.057
10	.411	48.95	48.95	1.0000	0.000	-.930
11	.455	53.90	53.90	1.0000	0.000	-.819
12	.499	58.85	58.85	1.0000	0.000	-.720
13	.543	63.85	63.85	1.0000	0.000	-.631
14	.587	68.85	68.85	1.0000	0.000	-.549
15	.631	73.85	73.85	1.0000	0.000	-.474
16	.675	78.75	78.75	1.0000	.002	-.406
17	.719	83.75	83.75	1.0000	.004	-.342
18	.763	88.70	88.70	1.0000	.008	-.282
19	.807	93.70	93.70	1.0000	.012	-.225
20	.851	98.70	98.70	1.0000	.018	-.171
21	.896	103.70	103.70	1.0000	.043	-.121
22	.943	108.65	108.65	1.0000	.192	-.073
23	.984	113.65	113.65	1.0000	.424	-.027
24	1.028	118.65	118.65	1.0000	.551	.017
25	1.072	123.65	123.65	1.0000	.644	.059
26	1.116	128.65	128.65	1.0000	.708	.100
27	1.161	133.65	133.65	1.0000	.886	.139
28	1.205	138.65	138.65	1.0000	.972	.176
29	1.227	138.65	138.65	1.0000	.923	.195
30	1.231	139.60	139.60	1.0000	.911	.198
31	1.257	144.55	144.55	1.0000	1.000	.219
32	1.302	149.60	149.60	1.0000	1.005	.254
33	1.346	154.60	154.60	1.0000	.992	.288
34	1.390	159.60	159.60	1.0000	1.004	.321

STEADY-STATE PHASE FRACTIONAL FLOW : 1.0000

50% BREAKTHROUGH (PORE VOLUME) : 1.0103

EXPERIMENT 0 2

TUBE NUMBER	PORE VOLUMES	TOTAL PHASE VOLUME (CC)	PHASE VOLUME (CC)	FRACTIONAL FLOW	NORMALIZED CONCENTRATION	LAMBDA1
1	.011	2.55	2.20	.8625	1.187	-7.874
2	.044	7.50	6.70	.8933	.915	-3.781
3	.088	12.45	11.00	.8835	1.090	-2.510
4	.132	17.35	15.10	.8703	.939	-1.913
5	.176	22.35	19.40	.8680	.925	-1.534
6	.219	27.25	23.50	.8624	1.111	-1.262
7	.263	32.15	27.65	.8600	.800	-1.054
8	.306	37.10	31.80	.8571	.927	-.884
9	.350	41.95	35.85	.8546	1.010	-.741
10	.393	46.80	39.95	.8536	1.007	-.618
11	.435	51.45	43.85	.8523	.832	-.513
12	.477	56.25	47.90	.8515	.987	-.418
13	.518	60.90	51.75	.8497	.802	-.333
14	.560	65.60	55.65	.8483	.945	-.255
15	.601	70.30	59.55	.8471	.685	-.183
16	.643	75.00	63.40	.8453	.645	-.116
17	.684	79.65	67.20	.8437	.761	-.054
18	.725	84.25	71.00	.8427	.510	.004
19	.766	88.90	74.80	.8414	.388	.059
20	.807	93.45	78.55	.8405	.304	.111
21	.847	97.90	82.15	.8391	.204	.159
22	.885	102.20	85.80	.8395	.202	.204
23	.924	106.55	89.40	.8390	.080	.247
24	.962	110.85	92.90	.8381	.061	.288
25	1.000	115.08	96.50	.8385	.046	.327
26	1.038	119.43	100.10	.8381	.028	.365
27	1.075	123.63	103.60	.8380	.017	.401
28	1.112	127.78	107.05	.8378	.009	.436
29	1.149	131.93	110.40	.8368	.004	.469
30	1.186	136.18	114.00	.8371	0.000	.502

STEADY-STATE PHASE FRACTIONAL FLOW : .8372
50% BREAKTHROUGH (PORE VOLUME) : .7221

EXPERIMENT 044

TUBE NUMBER	PORE VOLUMES	TOTAL PHASE VOLUME (CC)	PHASE VOLUME (CC)	FRACTIONAL FLOW	NORMALIZED CONCENTRATION	LAMBDA1
1	.021	4.70	1.85	.3936	1.021	-6.973
2	.063	9.50	4.15	.4368	.994	-3.848
3	.106	14.40	6.45	.4479	.953	-2.838
4	.149	19.20	8.80	.4583	1.025	-2.285
5	.192	24.15	11.20	.4638	1.008	-1.915
6	.235	29.00	13.65	.4707	1.008	-1.643
7	.278	33.85	16.15	.4771	1.031	-1.431
8	.321	38.75	18.60	.4800	.990	-1.258
9	.364	43.55	21.00	.4822	.990	-1.112
10	.407	48.40	23.40	.4835	.928	-.987
11	.450	53.25	25.85	.4854	.962	-.876
12	.493	58.10	28.30	.4871	1.039	-.777
13	.536	62.95	30.70	.4877	1.036	-.688
14	.578	67.75	33.10	.4886	1.000	-.608
15	.621	72.55	35.50	.4893	1.028	-.534
16	.663	77.40	37.95	.4903	.949	-.465
17	.706	82.25	40.35	.4906	1.006	-.401
18	.749	87.10	42.90	.4925	.966	-.341
19	.792	91.90	45.30	.4929	.931	-.285
20	.835	96.70	47.75	.4938	.962	-.233
21	.877	101.50	50.10	.4936	.961	-.183
22	.919	106.30	52.50	.4939	.790	-.135
23	.962	111.15	54.90	.4939	.786	-.090
24	1.005	115.95	57.30	.4942	.676	-.046
25	1.048	120.80	59.70	.4942	.751	-.005
26	1.090	125.65	62.10	.4942	.664	.036
27	1.133	130.50	64.55	.4946	.479	.074
28	1.176	135.35	66.95	.4946	.416	.111
29	1.219	140.25	69.35	.4945	.364	.147
30	1.263	145.15	71.80	.4947	.329	.183
31	1.306	150.00	74.25	.4950	.294	.216
32	1.349	154.85	76.65	.4950	.261	.249
33	1.392	159.70	79.05	.4950	.228	.280
34	1.435	164.50	81.45	.4951	.236	.311
35	1.477	169.35	83.85	.4951	.194	.341
36	1.521	174.30	86.35	.4954	.154	.370
37	1.564	179.10	88.75	.4955	.099	.399
38	1.606	183.90	91.15	.4956	.064	.426
39	1.649	188.80	93.65	.4960	.047	.453
40	1.692	193.70	96.10	.4961	.029	.480
41	1.736	198.60	98.55	.4962	.017	.506
42	1.779	203.45	100.95	.4962	.009	.531
43	1.822	208.30	103.35	.4962	.003	.556
44	1.865	213.10	105.80	.4965	.001	.580
45	1.937	217.90	108.30	.4970	0.000	.603

STEADY-STATE PHASE FRACTIONAL FLOW : .4971
50% BREAKTHROUGH (PORE VOLUME) : 1.0525

EXPERIMENT BAOH1

TUBE NUMBER	PORE VOLUMES	TOTAL PHASE VOLUME (CC)	PHASE VOLUME (CC)	FRACTIONAL FLOW	NORMALIZED CONCENTRATION	LAMBDA
1	.013	7.30	7.30	1.0000	0.000	-8.797
2	.052	21.20	21.20	1.0000	0.000	-4.287
3	.098	35.20	35.20	1.0000	0.000	-2.893
4	.146	49.00	49.00	1.0000	0.000	-2.242
5	.194	62.85	62.85	1.0000	0.000	-1.837
6	.242	76.70	76.70	1.0000	0.000	-1.547
7	.291	90.70	90.70	1.0000	0.000	-1.323
8	.339	104.50	104.50	1.0000	0.000	-1.142
9	.387	118.40	118.40	1.0000	0.000	-.992
10	.435	132.20	132.20	1.0000	0.000	-.863
11	.483	146.10	146.10	1.0000	0.000	-.750
12	.532	160.00	160.00	1.0000	0.000	-.649
13	.580	173.90	173.90	1.0000	0.000	-.558
14	.629	187.90	187.90	1.0000	0.000	-.475
15	.677	201.80	201.80	1.0000	0.000	-.399
16	.725	215.60	215.60	1.0000	0.000	-.329
17	.773	229.50	229.50	1.0000	0.000	-.264
18	.821	243.30	243.30	1.0000	.008	-.204
19	.869	257.10	257.10	1.0000	.065	-.147
20	.917	270.90	270.90	1.0000	.190	-.093
21	.965	284.60	284.60	1.0000	.375	-.042
22	1.013	298.50	298.50	1.0000	.520	.006
23	1.061	312.30	312.30	1.0000	.687	.053
24	1.109	326.10	326.10	1.0000	.851	.097
25	1.157	340.30	340.00	1.0000	.979	.140
26	1.205	353.80	353.80	1.0000	1.082	.180
27	1.253	367.70	367.70	1.0000	1.082	.220
28	1.302	381.60	381.60	1.0000	1.042	.258
29	1.350	395.40	395.40	1.0000	1.059	.295
30	1.398	409.30	409.30	1.0000	1.033	.330
31	1.446	423.20	423.00	1.0000	.995	.364
32	1.494	436.90	436.90	1.0000	.941	.397
33	1.542	450.60	450.60	1.0000	.993	.430
34	1.589	464.30	464.30	1.0000	.980	.461
35	1.637	478.10	478.10	1.0000	.966	.491
36	1.665	480.20	480.20	1.0000	.988	.509

STEADY-STATE PHASE FRACTIONAL FLOW : 1.0000
50% BREAKTHROUGH (PORE VOLUME) : 1.0066

EXPERIMENT 840H2

TUBE NUMBER	PORE VOLUMES	TOTAL PHASE VOLUME (CC)	PHASE VOLUME (CC)	FRACTIONAL FLOW	NORMALIZED CONCENTRATION	LAMBDA1
1	.016	10.00	10.00	1.0000	0.000	-5.522
2	.050	20.60	20.60	1.0000	0.000	-2.950
3	.083	30.20	30.20	1.0000	0.000	-2.132
4	.116	40.80	40.80	1.0000	0.000	-1.671
5	.152	51.70	51.70	1.0000	0.000	-1.340
6	.192	65.60	65.60	1.0000	0.000	-1.062
7	.238	79.50	79.50	1.0000	0.000	-.827
8	.284	93.50	93.50	1.0000	0.000	-.640
9	.329	107.10	107.10	1.0000	0.000	-.486
10	.374	120.80	120.80	1.0000	0.000	-.356
11	.419	134.40	134.40	1.0000	0.000	-.241
12	.463	148.10	148.10	1.0000	.146	-.139
13	.509	161.90	161.90	1.0000	.363	-.046
14	.553	175.50	175.50	1.0000	.620	.039
15	.598	189.10	189.10	1.0000	.725	.116
16	.643	202.80	202.80	1.0000	.801	.189
17	.688	216.40	216.40	1.0000	.953	.256
18	.732	229.90	229.90	1.0000	1.000	.320
19	.776	243.45	243.45	1.0000	1.076	.379
20	.821	257.15	257.15	1.0000	1.000	.437
21	.866	270.85	270.85	1.0000	.959	.491
22	.911	284.55	284.55	1.0000	.947	.543
23	.956	298.15	298.15	1.0000	1.018	.593

STEADY-STATE PHASE FRACTIONAL FLOW : 1.0000
50% BREAKTHROUGH (PORE VOLUME) : .5326

EXPERIMENT BAOW3AO

TUBE NUMBER	PORE VOLUMES	TOTAL PHASE VOLUME (CC)	PHASE VOLUME (CC)	FRACTIONAL FLOW	NORMALIZED CONCENTRATION	LAMBDA1
1	.032	19.50	1.70	.0874	0.000	-13.603
2	.101	42.30	3.70	.0876	0.000	-7.575
3	.174	63.85	5.40	.0846	.000	-5.709
4	.245	85.45	7.40	.0866	.001	-4.755
5	.316	106.95	9.20	.0861	.007	-4.138
6	.386	128.35	11.15	.0869	.064	-3.695
7	.456	149.85	13.15	.0878	.005	-3.356
8	.526	171.10	15.00	.0877	.032	-3.085
9	.596	192.35	16.90	.0879	.073	-2.862
10	.666	213.45	18.65	.0874	.046	-2.674
11	.735	234.65	20.55	.0876	.111	-2.512
12	.805	255.90	22.35	.0874	.019	-2.369
13	.874	277.15	24.20	.0873	.037	-2.242
14	.944	298.35	26.00	.0872	.022	-2.129
15	1.014	319.55	28.00	.0876	.026	-2.026
16	1.083	340.80	29.70	.0872	.027	-1.933
17	1.153	362.00	31.50	.0870	.035	-1.847
18	1.223	383.25	33.40	.0872	.023	-1.768
19	1.292	404.50	35.10	.0868	.030	-1.695
20	1.362	425.70	36.90	.0867	.030	-1.626
21	1.431	446.90	38.70	.0866	.027	-1.563
22	1.501	468.20	40.60	.0867	.016	-1.503
23	1.571	489.60	42.40	.0866	.039	-1.446
24	1.641	510.80	44.40	.0869	.025	-1.393
25	1.711	532.00	46.20	.0868	.021	-1.342
26	1.780	553.05	47.90	.0866	.016	-1.295
27	1.849	574.15	49.70	.0866	.014	-1.250
28	1.918	595.35	51.50	.0865	.015	-1.206
29	1.988	616.55	53.30	.0865	.024	-1.165
30	2.058	637.85	55.00	.0862	.010	-1.125
31	2.128	659.25	56.80	.0862	.033	-1.087
32	2.198	680.55	58.55	.0860	.018	-1.050
33	2.268	701.95	60.25	.0858	.015	-1.015
34	2.338	723.25	61.95	.0857	.026	-.981
35	2.408	744.55	63.75	.0856	.028	-.948
36	2.478	765.85	65.65	.0857	.014	-.917
37	2.548	787.15	67.45	.0857	.014	-.886
38	2.618	808.55	69.45	.0859	.031	-.857
39	2.688	829.75	71.25	.0859	.017	-.828
40	2.757	851.15	73.05	.0858	.008	-.800
41	2.828	872.50	74.85	.0858	.025	-.773
42	2.898	893.85	76.65	.0858	.008	-.747
43	2.968	915.20	78.45	.0857	.036	-.722
44	3.038	936.55	80.25	.0857	.005	-.697
45	3.108	957.85	82.05	.0857	.058	-.673
46	3.177	979.15	83.85	.0856	.021	-.650
47	3.247	1000.50	85.65	.0856	.014	-.627
48	3.317	1021.80	87.45	.0856	.022	-.604
49	3.387	1043.15	89.25	.0856	.038	-.583
50	3.457	1064.45	91.05	.0855	.034	-.561
51	3.527	1085.65	92.85	.0855	.035	-.541
52	3.597	1106.85	94.65	.0855	.012	-.520
53	3.666	1128.05	96.45	.0855	.028	-.501
54	3.736	1149.25	98.25	.0855	.033	-.481

55	3.805	1170.45	100.05	.0855	.027	-.462
56	3.875	1191.65	101.85	.0855	.046	-.444
57	3.944	1212.85	103.65	.0855	.016	-.426
58	4.014	1234.05	105.45	.0855	.025	-.408
59	4.083	1255.25	107.25	.0854	.014	-.390
60	4.153	1276.45	109.05	.0854	.021	-.373
61	4.223	1297.65	110.85	.0854	.016	-.356
62	4.292	1318.85	112.65	.0854	.013	-.340
63	4.362	1340.05	114.45	.0854	.015	-.323
64	4.441	1367.05	116.65	.0853	.016	-.305
65	4.529	1394.05	118.85	.0853	.025	-.285
66	4.618	1421.05	121.05	.0852	.035	-.266
67	4.707	1448.05	123.25	.0851	.046	-.246
68	4.795	1475.05	125.45	.0851	.061	-.228
69	4.884	1502.05	127.65	.0850	.072	-.209
70	4.972	1529.05	129.85	.0849	.086	-.191
71	5.047	1547.39	131.41	.0849	.106	-.176
72	5.107	1565.73	132.97	.0849	.120	-.164
73	5.167	1584.07	134.53	.0849	.136	-.153
74	5.227	1602.41	136.09	.0849	.165	-.141
75	5.287	1620.75	137.65	.0849	.190	-.129
76	5.348	1639.09	139.21	.0849	.221	-.118
77	5.408	1657.43	140.77	.0849	.242	-.107
78	5.468	1675.77	142.33	.0849	.270	-.096
79	5.528	1694.11	143.89	.0849	.318	-.085
80	5.588	1712.45	145.45	.0849	.350	-.074
81	5.648	1730.79	147.01	.0849	.369	-.063
82	5.709	1749.13	148.57	.0849	.373	-.053
83	5.769	1767.47	150.13	.0849	.403	-.042
84	5.829	1785.81	151.69	.0849	.435	-.032
85	5.889	1804.15	153.25	.0849	.464	-.022
86	5.949	1822.49	154.81	.0849	.478	-.011
87	6.009	1840.83	156.37	.0849	.492	-.001
88	6.070	1859.17	157.93	.0849	.549	.009
89	6.130	1877.51	159.49	.0849	.543	.018
90	6.190	1895.85	161.05	.0850	.554	.028
91	6.250	1914.19	162.61	.0850	.565	.038
92	6.310	1932.53	164.17	.0850	.577	.047
93	6.370	1950.87	165.73	.0850	.588	.057
94	6.431	1969.21	167.29	.0850	.599	.066
95	6.491	1987.55	168.85	.0850	.611	.076
96	6.551	2005.89	170.41	.0850	.636	.085
97	6.611	2024.23	171.97	.0850	.660	.094
98	6.671	2042.57	173.53	.0850	.672	.103
99	6.731	2060.91	175.09	.0850	.683	.112
100	6.792	2079.25	176.65	.0850	.676	.121
101	6.866	2106.40	178.99	.0850	.694	.132
102	6.955	2133.55	181.33	.0850	.664	.145
103	7.044	2160.70	183.67	.0850	.662	.158
104	7.133	2187.85	186.01	.0850	.727	.170
105	7.223	2215.00	188.35	.0850	.716	.183
106	7.312	2242.15	190.69	.0850	.750	.195
107	7.401	2269.30	193.03	.0851	.767	.207
108	7.490	2296.45	195.37	.0851	.787	.219
109	7.579	2323.60	197.71	.0851	.792	.231
110	7.668	2350.75	200.05	.0851	.817	.243
111	7.757	2377.90	202.39	.0851	.807	.255
112	7.846	2405.05	204.73	.0851	.761	.266
113	7.935	2432.20	207.07	.0851	.798	.277
114	8.024	2459.35	209.41	.0852	.771	.289
115	8.113	2486.50	211.75	.0852	.823	.300
116	8.202	2513.65	214.09	.0852	.867	.311

117	8.291	2540.80	216.43	.0852	.895	.322
118	8.380	2567.95	218.77	.0852	.909	.333
119	8.470	2595.10	221.11	.0852	.895	.343
120	8.559	2622.25	223.45	.0852	.879	.354
121	8.648	2649.40	225.79	.0852	.892	.365
122	8.737	2676.55	228.13	.0852	.882	.375
123	8.826	2703.70	230.47	.0852	.899	.385
124	8.915	2730.85	232.81	.0853	.886	.396
125	9.004	2758.00	235.15	.0853	.951	.406
126	9.093	2785.15	237.49	.0853	.939	.416
127	9.182	2812.30	239.83	.0853	.935	.426
128	9.271	2839.45	242.17	.0853	.921	.436
129	9.360	2866.60	244.51	.0853	.945	.445
130	9.449	2893.75	246.85	.0853	.940	.455
131	9.538	2920.90	249.19	.0853	.951	.465
132	9.628	2948.05	251.53	.0853	.969	.474
133	9.717	2975.20	253.87	.0853	.940	.484
134	9.806	3002.35	256.21	.0853	.971	.493
135	9.895	3029.50	258.55	.0853	.924	.502
136	9.984	3056.65	260.89	.0854	.964	.512
137	10.073	3083.80	263.23	.0854	.861	.521
138	10.162	3110.95	265.57	.0854	.964	.530
139	10.251	3138.10	267.91	.0854	1.005	.539
140	10.340	3165.25	270.25	.0854	.971	.548
141	10.429	3192.40	272.59	.0854	.983	.557
142	10.518	3219.55	274.93	.0854	1.012	.566
143	10.607	3246.70	277.27	.0854	.976	.574
144	10.696	3273.85	279.61	.0854	.992	.583
145	10.786	3301.00	281.95	.0854	.971	.592
146	10.875	3328.15	284.29	.0854	.942	.600
147	10.964	3355.30	286.63	.0854	.975	.609
148	11.053	3382.45	288.97	.0854	.973	.617
149	11.142	3409.60	291.31	.0854	.995	.626
150	11.231	3436.75	293.65	.0854	.985	.634
151	11.320	3463.90	295.99	.0855	1.019	.642
152	11.409	3491.05	298.33	.0855	1.009	.651
153	11.498	3518.20	300.67	.0855	.999	.659
154	11.587	3545.35	303.01	.0855	1.015	.667
155	11.676	3572.50	305.35	.0855	1.004	.675
156	11.765	3599.65	307.69	.0855	1.020	.683
157	11.854	3626.80	310.03	.0855	1.039	.691

STEADY-STATE PHASE FRACTIONAL FLOW : .0855
50% BREAKTHROUGH (PORE VOLUME) : 6.0178

EXPERIMENT BAO*30L

TUBE NUMBER	PORE VOLUMES	TOTAL PHASE VOLUME (CC)	PHASE VOLUME (CC)	FRACTIONAL FLOW	NORMALIZED CONCENTRATION	LAMBDA1
1	.032	19.50	17.80	.9126	0.000	-3.032
2	.101	42.30	38.60	.9124	0.000	-1.337
3	.174	63.85	58.45	.9154	0.000	-.728
4	.245	85.45	78.05	.9134	.035	-.374
5	.316	106.95	97.75	.9139	.348	-.118
6	.386	128.35	117.25	.9135	.619	.083
7	.456	149.85	136.95	.9139	.765	.251
8	.526	171.10	156.35	.9138	.881	.396
9	.596	192.35	175.80	.9139	.918	.524
10	.666	213.45	194.90	.9131	.970	.639
11	.735	234.65	214.40	.9137	.953	.740
12	.805	255.90	233.85	.9138	.998	.841
13	.874	277.15	253.20	.9136	1.077	.932
14	.944	298.35	272.70	.9140	1.024	1.017
15	1.014	319.55	292.10	.9141	1.011	1.097
16	1.083	340.80	311.55	.9142	1.022	1.174
17	1.153	362.00	330.85	.9139	1.009	1.247

STEADY-STATE PHASE FRACTIONAL FLOW : .9140
SP1 BREAKTHROUGH (PORE VOLUME) : .3552

EXPERIMENT BAOW4A0

TUBE NUMBER	PORE VOLUMES	TOTAL PHASE VOLUME (CC)	PHASE VOLUME (CC)	FRACTIONAL FLOW	NORMALIZED CONCENTRATION	LAMBDA1
1	.042	25.40	5.27	.2075	0.000	-8.066
2	.132	55.20	11.17	.2024	0.000	-4.379
3	.229	84.20	16.77	.1992	0.000	-3.200
4	.324	113.10	21.57	.1907	0.000	-2.597
5	.418	141.70	26.77	.1889	.012	-2.198
6	.512	170.70	31.57	.1858	.013	-1.906
7	.607	199.20	37.17	.1846	.068	-1.680
8	.701	228.10	42.07	.1844	.016	-1.495
9	.796	257.00	47.47	.1847	.016	-1.340
10	.891	286.00	52.27	.1828	.014	-1.206
11	.972	306.60	56.27	.1835	.051	-1.105
12	1.040	327.50	60.27	.1840	.016	-1.020
13	1.109	348.30	64.27	.1845	.003	-.957
14	1.177	369.00	68.17	.1847	.050	-.892
15	1.244	389.40	71.97	.1848	.030	-.831
16	1.311	409.60	75.67	.1847	.006	-.775
17	1.376	429.50	79.57	.1853	.034	-.723
18	1.442	449.30	83.27	.1853	0.000	-.674
19	1.507	469.10	86.77	.1850	0.000	-.627
20	1.572	489.10	90.47	.1850	.007	-.583
21	1.637	509.00	94.37	.1854	.010	-.541
22	1.702	528.80	98.17	.1856	.016	-.500
23	1.767	548.60	101.77	.1855	.001	-.462
24	1.833	568.50	105.47	.1855	.017	-.425
25	1.898	588.50	109.17	.1855	.013	-.389
26	1.963	608.40	112.87	.1855	.002	-.354
27	2.028	628.10	116.77	.1859	.011	-.321
28	2.094	648.10	120.57	.1860	.015	-.289
29	2.159	667.90	124.57	.1865	.007	-.258
30	2.223	687.50	128.27	.1866	.013	-.229
31	2.288	707.30	131.97	.1866	.013	-.200
32	2.353	726.90	135.77	.1868	.035	-.172
33	2.417	746.70	139.67	.1871	.058	-.145
34	2.482	766.60	143.87	.1877	.115	-.118
35	2.548	786.50	147.67	.1878	.149	-.092
36	2.613	806.30	151.47	.1879	.233	-.067
37	2.678	826.10	155.37	.1881	.352	-.042
38	2.743	845.90	159.37	.1884	.445	-.018
39	2.808	865.60	163.07	.1884	.515	.005
40	2.872	885.40	166.67	.1882	.566	.028
41	2.937	905.00	170.37	.1883	.623	.050
42	3.002	924.90	174.07	.1882	.676	.072
43	3.067	944.70	177.87	.1883	.723	.093
44	3.132	964.60	181.57	.1882	.759	.114
45	3.197	984.50	185.47	.1884	.777	.135
46	3.263	1004.50	189.37	.1885	.785	.155
47	3.328	1024.10	193.17	.1886	.888	.175
48	3.393	1044.10	196.97	.1887	.888	.195
49	3.458	1063.80	200.67	.1886	.810	.214
50	3.522	1083.50	204.37	.1886	.935	.232
51	3.588	1103.50	208.17	.1886	.870	.251
52	3.653	1123.30	211.97	.1887	.988	.269
53	3.718	1143.10	215.87	.1888	.947	.287
54	3.783	1162.90	219.67	.1889	.924	.304

55	3.848	1182.80	223.57	.1890	.968	.322
56	3.913	1202.60	227.47	.1891	.971	.339
57	3.978	1222.40	231.47	.1894	.927	.355
58	4.043	1242.30	235.27	.1894	1.006	.372
59	4.108	1262.20	239.07	.1894	.927	.388
60	4.174	1282.10	242.77	.1894	.957	.404
61	4.239	1302.00	246.67	.1895	.997	.420
62	4.304	1321.80	250.37	.1894	1.021	.436
63	4.369	1341.50	254.17	.1895	.981	.451
64	4.434	1361.40	257.97	.1895	1.034	.466
65	4.499	1381.20	261.67	.1895	1.007	.481
66	4.564	1401.10	265.47	.1895	1.004	.496
67	4.629	1420.80	269.17	.1895	1.037	.510
68	4.694	1440.70	272.97	.1895	1.034	.525

STEADY-STATE PHASE FRACTIONAL FLOW : .1895
50% BREAKTHROUGH (PORE VOLUME) : 2.7935

EXPERIMENT BAOWAOL

TUBE NUMBER	PORE VOLUMES	TOTAL PHASE VOLUME (CC)	PHASE VOLUME (CC)	FRACTIONAL FLOW	NORMALIZED CONCENTRATION	LAMBDA1
1	.042	25.40	20.13	.7925	.004	-2.142
2	.132	55.20	44.03	.7976	.003	-.721
3	.229	84.20	67.43	.8008	.342	-.159
4	.324	113.10	91.53	.8093	.724	.189
5	.418	141.70	114.93	.8111	.884	.440
6	.512	170.70	139.13	.8150	.930	.660
7	.607	199.20	162.03	.8134	1.027	.840
8	.701	228.10	186.03	.8156	.982	.999
9	.796	257.00	209.53	.8153	.938	1.143
10	.891	286.00	233.73	.8172	1.096	1.275
11	.972	306.80	250.53	.8166	.998	1.380

STEADY-STATE PHASE FRACTIONAL FLOW : .8166
50% BREAKTHROUGH (PORE VOLUME) : .2680

EXPERIMENT 8AD-7AQ

TUBE NUMBER	PORE VOLUMES	TOTAL PHASE VOLUME (CC)	PHASE VOLUME (CC)	FRACTIONAL FLOW	NORMALIZED CONCENTRATION	LAMBDA
1	.021	12.50	5.74	.4596	0.000	-7.493
2	.071	30.90	14.64	.4739	0.000	-3.847
3	.132	49.30	24.04	.4877	0.000	-2.678
4	.192	67.70	32.44	.4792	0.000	-2.091
5	.252	86.10	41.24	.4790	0.000	-1.713
6	.313	104.60	50.24	.4803	0.000	-1.440
7	.374	123.20	58.64	.4760	0.000	-1.226
8	.435	142.00	67.84	.4778	0.000	-1.051
9	.497	160.80	77.24	.4804	0.000	-.903
10	.558	179.60	86.44	.4813	0.000	-.776
11	.620	198.30	95.64	.4823	0.000	-.665
12	.681	216.90	104.84	.4834	0.000	-.567
13	.742	235.70	113.84	.4830	0.000	-.478
14	.804	254.50	122.64	.4819	0.000	-.396
15	.865	273.10	131.64	.4820	.013	-.321
16	.927	291.90	140.84	.4825	.071	-.252
17	.988	310.50	150.04	.4832	.171	-.188
18	1.049	329.10	159.14	.4836	.272	-.128
19	1.111	348.10	168.24	.4833	.340	-.070
20	1.173	367.00	177.44	.4835	.463	-.016
21	1.235	385.90	186.14	.4824	.586	.036
22	1.297	404.80	195.44	.4828	.704	.085
23	1.359	423.80	204.54	.4826	.802	.132
24	1.421	442.60	213.54	.4825	.842	.176
25	1.483	461.50	222.84	.4829	.892	.219
26	1.545	480.40	231.84	.4826	.914	.260
27	1.607	499.20	241.24	.4833	.918	.300
28	1.669	518.10	250.44	.4834	.927	.338
29	1.731	536.90	259.44	.4832	.972	.375
30	1.792	555.80	268.44	.4830	.980	.411
31	1.854	574.50	277.54	.4831	.993	.446
32	1.916	593.30	286.94	.4836	.997	.479
33	1.978	612.40	296.24	.4837	1.017	.512
34	2.040	631.10	305.24	.4837	.981	.544
35	2.102	650.10	314.44	.4837	.985	.575
36	2.164	668.90	323.54	.4837	1.009	.605
37	2.226	688.00	332.74	.4836	1.005	.635
38	2.288	707.00	341.94	.4837	1.004	.664
39	2.351	725.90	351.14	.4837	.986	.692
40	2.413	744.90	360.44	.4839	1.014	.720
41	2.475	763.90	369.84	.4842	1.001	.747

STEADY-STATE PHASE FRACTIONAL FLOW : .4842
50% BREAKTHROUGH (PORE VOLUME) : 1.1919

EXPERIMENT BAOW70L

TUBE NUMBER	PORE VOLUMES	TOTAL PHASE VOLUME (CC)	PHASE VOLUME (CC)	FRACTIONAL FLOW	NORMALIZED CONCENTRATION	LAMBDA
1	.021	12.50	6.76	.5404	0.000	-2.871
2	.071	30.90	16.26	.5261	.003	-1.124
3	.132	49.30	25.26	.5123	.076	-.462
4	.192	67.70	35.26	.5208	.439	-.081
5	.252	86.10	44.86	.5210	.667	.193
6	.313	104.60	54.36	.5197	.830	.411
7	.374	123.20	64.56	.5240	.888	.594
8	.435	142.00	74.16	.5222	.948	.755
9	.497	160.80	83.56	.5196	1.004	.898
10	.558	179.60	93.16	.5187	.993	1.028
11	.620	198.30	102.66	.5177	1.015	1.147
12	.681	216.90	112.06	.5166	.971	1.257
13	.742	235.70	121.86	.5170	1.011	1.360
14	.804	254.50	131.86	.5181	1.019	1.457
15	.865	273.10	141.46	.5180	.998	1.549
16	.927	291.90	151.06	.5175	1.067	1.637
17	.988	310.50	160.46	.5168	1.014	1.721
18	1.049	329.10	169.96	.5164	.997	1.800
19	1.111	348.10	179.86	.5167	.913	1.878

STEADY-STATE PHASE FRACTIONAL FLOW : .5167
50% BREAKTHROUGH (PORE VOLUME) : .2081

EXPERIMENT RADW8

TUBE NUMBER	PORE VOLUMES	TOTAL PHASE VOLUME (CC)	PHASE VOLUME (CC)	FRACTIONAL FLOW	NORMALIZED CONCENTRATION	LAMBDA
1	.019	11.50	11.50	1.0000	.033	-5.546
2	.058	24.10	24.10	1.0000	.004	-2.944
3	.100	36.70	36.70	1.0000	0.000	-2.086
4	.141	49.30	49.30	1.0000	.006	-1.614
5	.182	61.90	61.90	1.0000	.006	-1.296
6	.224	74.50	74.50	1.0000	.007	-1.059
7	.265	87.10	87.10	1.0000	.007	-.871
8	.306	99.70	99.70	1.0000	0.000	-.715
9	.348	112.30	112.30	1.0000	.009	-.582
10	.389	124.90	124.90	1.0000	.018	-.466
11	.430	137.45	137.45	1.0000	.019	-.363
12	.471	149.95	149.95	1.0000	.030	-.271
13	.513	162.55	162.55	1.0000	.043	-.186
14	.554	175.20	175.20	1.0000	.130	-.100
15	.595	187.75	187.75	1.0000	.367	-.036
16	.637	200.40	200.40	1.0000	.617	.031
17	.678	213.05	213.05	1.0000	.729	.094
18	.719	225.50	225.50	1.0000	.879	.153
19	.760	238.05	238.05	1.0000	.980	.209
20	.802	250.65	250.65	1.0000	1.000	.262
21	.843	263.30	263.30	1.0000	.939	.313
22	.885	275.95	275.95	1.0000	.980	.362
23	.926	288.40	288.40	1.0000	1.011	.408
24	.967	300.95	300.95	1.0000	1.003	.452
25	1.008	313.55	313.55	1.0000	.997	.495
26	1.049	326.20	326.20	1.0000	.950	.537
27	1.091	338.85	338.85	1.0000	1.012	.577
28	1.132	351.30	351.30	1.0000	.992	.616
29	1.173	363.85	363.85	1.0000	1.004	.653
30	1.214	376.45	376.45	1.0000	1.016	.689

STEADY-STATE PHASE FRACTIONAL FLOW : 1.0000
50% BREAKTHROUGH (PORE VOLUME) : .6175

EXPERIMENT OW1ZA

TUBE NUMBER	PORE VOLUMES	TOTAL PHASE VOLUME (CC)	PHASE VOLUME (CC)	FRACTIONAL FLOW	NORMALIZED CONCENTRATION	LAMBDA1
1	.029	27.25	0.00	0.0000	.001	-5.798
2	.089	55.95	0.00	0.0000	.001	-3.121
3	.150	84.50	0.00	0.0000	.001	-2.247
4	.210	112.15	0.00	0.0000	0.000	-1.770
5	.271	142.95	0.00	0.0000	0.000	-1.447
6	.332	169.50	0.00	0.0000	.000	-1.202
7	.393	198.00	0.00	0.0000	.001	-1.009
8	.454	226.65	0.00	0.0000	.001	-.849
9	.515	255.25	0.00	0.0000	0.000	-.714
10	.576	283.90	0.00	0.0000	0.000	-.595
11	.635	310.35	0.00	0.0000	0.000	-.495
12	.694	338.90	0.00	0.0000	.000	-.404
13	.755	367.55	0.00	0.0000	.000	-.318
14	.816	396.30	0.00	0.0000	.008	-.239
15	.878	425.05	0.00	0.0000	.084	-.166
16	.939	453.85	0.00	0.0000	.283	-.098
17	1.001	482.65	0.00	0.0000	.366	-.035
18	1.062	511.40	0.00	0.0000	.598	.025
19	1.124	540.20	0.00	0.0000	.770	.081
20	1.185	568.75	0.00	0.0000	.895	.134
21	1.244	594.95	0.00	0.0000	.973	.183
22	1.302	623.65	0.00	0.0000	1.000	.229
23	1.364	652.40	0.00	0.0000	1.011	.275
24	1.424	679.85	0.00	0.0000	.993	.319
25	1.484	708.40	0.00	0.0000	1.002	.361
26	1.545	737.05	0.00	0.0000	.983	.402
27	1.606	765.85	0.00	0.0000	.973	.442
28	1.668	794.70	0.00	0.0000	1.008	.480
29	1.730	823.50	0.00	0.0000	.991	.518
30	1.791	852.30	0.00	0.0000	.973	.554
31	1.853	881.10	0.00	0.0000	.992	.589
32	1.904	908.65	0.00	0.0000	.967	.618

STEADY-STATE PHASE FRACTIONAL FLOW : .0000
50% BREAKTHROUGH (PORE VOLUME) : 1.0365

EXPERIMENT OWBZA

TUBE NUMBER	PORE VOLUMES	TOTAL PHASE VOLUME (CC)	PHASE VOLUME (CC)	FRACTIONAL FLOW	NORMALIZED CONCENTRATION	LAMBDA1
1	.025	23.70	0.00	0.0000	0.000	-5.722
2	.079	51.15	0.00	0.0000	0.000	-3.014
3	.137	78.70	0.00	0.0000	.003	-2.120
4	.196	106.20	0.00	0.0000	0.000	-1.635
5	.254	133.75	0.00	0.0000	0.000	-1.312
6	.312	161.20	0.00	0.0000	0.000	-1.071
7	.370	188.50	0.00	0.0000	0.000	-.882
8	.428	215.75	0.00	0.0000	0.000	-.726
9	.485	242.75	0.00	0.0000	0.000	-.593
10	.543	270.00	0.00	0.0000	0.000	-.477
11	.600	297.15	0.00	0.0000	0.000	-.374
12	.658	324.35	0.00	0.0000	.009	-.281
13	.715	351.45	0.00	0.0000	.032	-.197
14	.773	378.60	0.00	0.0000	.147	-.120
15	.830	405.65	0.00	0.0000	.334	-.048
16	.888	433.05	0.00	0.0000	.569	.019
17	.945	460.20	0.00	0.0000	.816	.082
18	1.003	487.25	0.00	0.0000	.894	.141
19	1.060	514.50	0.00	0.0000	1.029	.197
20	1.118	541.70	0.00	0.0000	1.018	.250
21	1.175	568.90	0.00	0.0000	1.027	.301
22	1.233	596.20	0.00	0.0000	1.025	.350
23	1.291	623.55	0.00	0.0000	1.032	.396
24	1.349	650.85	0.00	0.0000	1.033	.441
25	1.406	678.05	0.00	0.0000	.988	.484
26	1.464	705.20	0.00	0.0000	1.009	.525
27	1.521	732.30	0.00	0.0000	.962	.565
28	1.579	759.60	0.00	0.0000	.977	.604
29	1.636	786.70	0.00	0.0000	.989	.642
30	1.694	813.80	0.00	0.0000	.976	.678
31	1.751	840.95	0.00	0.0000	.954	.713
32	1.790	850.55	0.00	0.0000	.998	.736

STEADY-STATE PHASE FRACTIONAL FLOW : .0000
50% BREAKTHROUGH (PORE VOLUME) : .8707

EXPERIMENT OW1Z

TUBE NUMBER	PORE VOLUMES	TOTAL PHASE VOLUME (CC)	PHASE VOLUME (CC)	FRACTIONAL FLOW	NORMALIZED CONCENTRATION	LAMBDA1
1	.012	11.40	11.40	1.0000	0.000	-8.979
2	.039	25.60	25.60	1.0000	0.000	-4.847
3	.069	39.50	39.50	1.0000	.001	-3.540
4	.098	53.40	53.40	1.0000	.000	-2.870
5	.127	67.00	67.00	1.0000	.000	-2.439
6	.156	80.50	80.50	1.0000	.001	-2.131
7	.185	93.90	93.90	1.0000	.001	-1.893
8	.213	107.20	107.20	1.0000	.001	-1.702
9	.241	120.50	120.50	1.0000	0.000	-1.542
10	.269	133.80	133.80	1.0000	.001	-1.405
11	.297	147.10	147.10	1.0000	.000	-1.285
12	.326	160.50	160.50	1.0000	.001	-1.178
13	.354	173.90	173.90	1.0000	.000	-1.082
14	.382	187.30	187.30	1.0000	.000	-.995
15	.411	200.80	200.80	1.0000	0.000	-.916
16	.439	214.20	214.20	1.0000	.000	-.843
17	.467	227.50	227.50	1.0000	0.000	-.775
18	.495	240.70	240.70	1.0000	0.000	-.713
19	.524	254.10	254.10	1.0000	.001	-.655
20	.552	267.60	267.60	1.0000	.001	-.599
21	.581	281.10	281.10	1.0000	0.000	-.547
22	.609	294.60	294.60	1.0000	.001	-.497
23	.637	307.80	307.80	1.0000	.000	-.451
24	.665	321.00	321.00	1.0000	.000	-.407
25	.694	334.50	334.50	1.0000	.000	-.364
26	.722	348.20	348.20	1.0000	.000	-.323
27	.751	361.40	361.40	1.0000	.000	-.284
28	.779	374.80	374.80	1.0000	.001	-.247
29	.808	388.30	388.30	1.0000	.000	-.211
30	.836	401.70	401.70	1.0000	.000	-.176
31	.864	415.20	415.20	1.0000	.013	-.142
32	.893	428.60	428.60	1.0000	.049	-.110
33	.921	441.80	441.80	1.0000	.125	-.079
34	.949	455.20	455.20	1.0000	.222	-.049
35	.978	468.60	468.60	1.0000	.387	-.019
36	1.006	482.10	482.10	1.0000	.557	.009
37	1.034	495.50	495.50	1.0000	.741	.037
38	1.063	508.70	508.70	1.0000	.902	.064
39	1.091	522.10	522.10	1.0000	.956	.090
40	1.119	535.50	535.50	1.0000	1.017	.116
41	1.148	548.90	548.90	1.0000	.995	.141
42	1.176	562.20	562.20	1.0000	1.000	.166
43	1.204	575.70	575.70	1.0000	1.005	.190
44	1.233	589.20	589.20	1.0000	.998	.213
45	1.247	589.50	589.50	1.0000	1.000	.225

STEADY-STATE PHASE FRACTIONAL FLOW : 1.0000
50% BREAKTHROUGH (PORE VOLUME) : .9966

EXPERIMENT OW22

TUBE NUMBER	PORE VOLUMES	TOTAL PHASE VOLUME (CC)	PHASE VOLUME (CC)	FRACTIONAL FLOW	NORMALIZED CONCENTRATION	LAMBDA1
1	.011	10.20	10.20	1.0000	0.000	-6.573
2	.036	24.10	24.10	1.0000	.010	-3.393
3	.066	38.20	38.20	1.0000	.026	-2.352
4	.096	52.20	52.20	1.0000	.054	-1.815
5	.125	66.30	66.30	1.0000	.078	-1.465
6	.155	80.00	80.00	1.0000	.081	-1.211
7	.184	93.70	93.70	1.0000	.112	-1.015
8	.213	107.40	107.40	1.0000	.134	-.853
9	.242	120.90	120.90	1.0000	.198	-.717
10	.270	134.40	134.40	1.0000	.254	-.599
11	.299	147.90	147.90	1.0000	.264	-.495
12	.327	161.40	161.40	1.0000	.308	-.401
13	.356	174.80	174.80	1.0000	.341	-.317
14	.384	188.30	188.30	1.0000	.339	-.239
15	.413	201.80	201.80	1.0000	.397	-.167
16	.441	215.30	215.30	1.0000	.409	-.100
17	.470	228.80	228.80	1.0000	.442	-.037
18	.498	242.10	242.10	1.0000	.535	.022
19	.527	255.50	255.50	1.0000	.508	.077
20	.555	268.80	268.80	1.0000	.574	.129
21	.583	282.20	282.20	1.0000	.567	.179
22	.612	295.70	295.70	1.0000	.617	.227
23	.640	309.10	309.10	1.0000	.640	.273
24	.668	322.50	322.50	1.0000	.692	.316
25	.697	335.90	335.90	1.0000	.645	.359
26	.725	349.25	349.25	1.0000	.692	.399
27	.753	362.55	362.55	1.0000	.745	.438
28	.781	375.85	375.85	1.0000	.763	.476
29	.810	389.25	389.25	1.0000	.761	.512
30	.838	402.55	402.55	1.0000	.776	.548
31	.866	416.05	416.05	1.0000	.786	.582
32	.895	429.45	429.45	1.0000	.766	.616
33	.923	442.95	442.95	1.0000	.870	.649
34	.952	456.55	456.55	1.0000	.835	.681
35	.980	469.95	469.95	1.0000	.828	.713
36	1.009	483.35	483.35	1.0000	.865	.743
37	1.037	496.85	496.85	1.0000	.894	.773
38	1.066	510.25	510.25	1.0000	.852	.802
39	1.094	523.85	523.85	1.0000	.896	.830
40	1.123	537.35	537.35	1.0000	.877	.858
41	1.151	550.75	550.75	1.0000	.930	.886
42	1.180	564.25	564.25	1.0000	.898	.913
43	1.208	577.75	577.75	1.0000	.989	.939
44	1.237	591.15	591.15	1.0000	.945	.965
45	1.266	604.75	604.75	1.0000	1.076	.990
46	1.294	618.05	618.05	1.0000	1.030	1.015
47	1.322	631.45	631.45	1.0000	.966	1.039
48	1.351	645.15	645.15	1.0000	1.031	1.064
49	1.379	658.45	658.45	1.0000	.962	1.087

STEADY-STATE PHASE FRACTIONAL FLOW : 1.0000

50% BREAKTHROUGH (PORE VOLUME) : .4877

EXPERIMENT OH3ZA0

TUBE NUMBER[R]	PORE VOLUMES	TOTAL PHASE VOLUME (CC)	PHASE VOLUME (CC)	FRACTIONAL FLOW	NORMALIZED CONCENTRATION	LAMBDA1
1	.014	13.25	1.61	.1215	.001	-19.626
2	.059	42.75	4.51	.1055	.001	-9.467
3	.121	71.75	7.26	.1012	.002	-6.544
4	.183	101.45	10.21	.1006	.002	-5.259
5	.245	130.35	12.81	.0983	.001	-4.492
6	.306	159.10	15.41	.0969	.002	-3.972
7	.368	188.55	18.51	.0982	.003	-3.581
8	.431	218.35	21.71	.0994	0.000	-3.269
9	.493	247.30	24.46	.0989	.002	-3.018
10	.554	275.90	27.36	.0992	.001	-2.812
11	.614	304.70	30.06	.0987	.001	-2.636
12	.676	333.75	32.96	.0988	.002	-2.482
13	.737	362.60	35.66	.0983	.002	-2.346
14	.798	391.50	38.56	.0985	.002	-2.225
15	.859	420.60	41.56	.0988	.004	-2.115
16	.921	449.60	44.46	.0989	.001	-2.016
17	.982	478.45	47.26	.0988	.001	-1.926
18	1.043	507.30	50.06	.0987	.002	-1.843
19	1.104	536.15	52.86	.0986	.000	-1.766
20	1.165	565.15	55.76	.0987	.003	-1.695
21	1.227	593.95	58.56	.0986	.001	-1.628
22	1.288	622.85	61.51	.0988	.002	-1.566
23	1.349	651.75	64.36	.0987	.001	-1.508
24	1.410	680.65	67.21	.0987	.002	-1.453
25	1.472	710.10	70.56	.0994	.000	-1.400
26	1.534	739.20	73.81	.0999	0.000	-1.350
27	1.596	768.75	77.16	.1004	.001	-1.302
28	1.658	798.45	80.56	.1009	0.000	-1.257
29	1.721	827.90	83.76	.1012	0.000	-1.213
30	1.783	856.90	86.66	.1011	.002	-1.172
31	1.844	886.10	89.86	.1014	0.000	-1.133
32	1.906	915.40	92.86	.1014	.002	-1.095
33	1.968	944.50	95.86	.1015	.001	-1.059
34	2.030	973.70	98.86	.1015	0.000	-1.024
35	2.092	1003.00	101.76	.1015	.000	-.990
36	2.154	1032.20	104.66	.1014	.001	-.958
37	2.216	1061.60	107.86	.1016	0.000	-.926
38	2.278	1090.70	110.86	.1016	.001	-.896
39	2.340	1120.30	113.86	.1016	.000	-.867
40	2.402	1149.70	116.96	.1017	.001	-.838
41	2.464	1178.80	119.96	.1018	.002	-.811
42	2.526	1208.00	122.96	.1018	.001	-.784
43	2.587	1237.00	125.86	.1017	.001	-.758
44	2.649	1266.30	128.86	.1018	0.000	-.733
45	2.711	1295.40	131.76	.1017	.000	-.708
46	2.773	1324.70	134.76	.1017	.001	-.685
47	2.835	1354.00	137.86	.1018	.000	-.661
48	2.897	1383.20	140.76	.1018	.001	-.639
49	2.958	1412.40	143.81	.1018	.001	-.616
50	3.020	1441.70	146.71	.1018	.002	-.595
51	3.082	1471.10	149.61	.1017	.001	-.574
52	3.144	1500.40	152.51	.1016	.001	-.553
53	3.206	1529.60	155.61	.1017	.001	-.533
54	3.268	1559.00	158.81	.1019	.001	-.513

55	3.330	1588.10	161.81	.1019	.001	-.493
56	3.392	1617.70	164.81	.1019	.001	-.474
57	3.455	1646.90	167.81	.1019	.000	-.456
58	3.516	1676.00	170.91	.1020	.000	-.438
59	3.578	1705.20	174.31	.1022	.000	-.420
60	3.640	1734.50	177.11	.1021	.001	-.402
61	3.702	1763.70	180.01	.1021	.001	-.385
62	3.763	1792.75	182.91	.1020	.001	-.368
63	3.825	1821.95	185.91	.1020	.001	-.352
64	3.887	1851.06	188.86	.1020	.000	-.336
65	3.948	1880.16	191.76	.1020	.000	-.320
66	4.010	1909.16	194.61	.1019	.001	-.304
67	4.071	1938.26	197.46	.1019	.001	-.289
68	4.133	1967.56	200.46	.1019	.000	-.273
69	4.195	1996.56	203.31	.1018	.001	-.259
70	4.256	2025.56	206.36	.1019	.001	-.244
71	4.318	2054.66	209.26	.1018	.001	-.229
72	4.379	2083.76	212.31	.1019	.001	-.215
73	4.441	2112.66	215.31	.1019	.000	-.201
74	4.502	2141.26	218.21	.1019	.001	-.188
75	4.562	2170.11	221.26	.1020	.001	-.174
76	4.624	2199.31	224.26	.1020	.002	-.161
77	4.685	2228.41	227.16	.1019	.003	-.147
78	4.747	2257.46	230.16	.1020	.005	-.134
79	4.808	2286.56	232.96	.1019	.007	-.121
80	4.870	2315.56	235.76	.1018	.010	-.109
81	4.931	2344.66	238.76	.1018	.016	-.096
82	4.993	2373.66	241.86	.1019	.020	-.084
83	5.055	2402.86	244.76	.1019	.025	-.071
84	5.116	2431.86	247.71	.1019	.037	-.059
85	5.177	2460.86	250.66	.1019	.079	-.047
86	5.232	2483.71	252.43	.1016	.098	-.037
87	5.274	2500.01	252.43	.1010	.148	-.029
88	5.308	2516.36	252.44	.1003	.195	-.022
89	5.343	2532.86	252.89	.0998	.207	-.016
90	5.378	2549.16	253.64	.0995	.395	-.009
91	5.410	2563.16	254.26	.0992	.433	-.003
92	5.428	2566.26	254.80	.0993	.487	-.000
93	5.432	2566.51	255.34	.0995	.573	.001
94	5.446	2580.11	257.94	.1000	.591	.003
95	5.492	2609.76	262.44	.1006	.597	.012
96	5.553	2638.26	266.24	.1009	.648	.023
97	5.615	2668.26	270.54	.1014	.680	.034
98	5.678	2697.26	274.24	.1017	.760	.045
99	5.738	2725.06	278.34	.1021	.786	.055
100	5.795	2751.36	281.10	.1022	.854	.065
101	5.853	2779.86	284.94	.1025	.893	.075
102	5.915	2809.86	289.24	.1029	.834	.086
103	5.977	2838.86	292.94	.1032	.787	.096
104	6.038	2866.66	297.04	.1036	.930	.106
105	6.095	2892.96	299.84	.1036	.954	.116
106	6.153	2921.46	303.64	.1039	.984	.125
107	6.215	2951.46	307.94	.1043	1.010	.135
108	6.277	2980.46	311.64	.1046	1.042	.145
109	6.337	3008.26	315.74	.1050	.998	.155
110	6.395	3034.56	318.54	.1050	1.025	.164
111	6.453	3063.06	322.34	.1052	.984	.173
112	6.514	3093.06	326.64	.1056	1.010	.183
113	6.577	3122.06	330.34	.1058	1.042	.192
114	6.637	3149.86	334.44	.1062	.998	.201
115	6.694	3176.16	337.24	.1062	1.025	.210
116	6.752	3204.66	341.04	.1064	.984	.219

117	6.814	3234.66	345.34	.1068	1.010	.228
118	6.877	3263.66	349.04	.1069	1.042	.237
119	6.937	3291.46	353.14	.1073	.990	.246
120	6.994	3317.76	355.94	.1073	1.025	.254
121	7.052	3346.26	359.74	.1075	1.001	.262
122	7.114	3376.26	364.04	.1078	.980	.271

STEADY-STATE PHASE FRACTIONAL FLOW : .1079
53% BREAKTHROUGH (PORE VOLUME) : 5.4285

EXPERIMENT OW3ZOL

TUBE NUMBER	PORE VOLUMES	TOTAL PHASE VOLUME (CC)	PHASE VOLUME (CC)	FRACTIONAL FLOW	NORMALIZED CONCENTRATION	LAMBDA
1	.013	9.20	8.94	.9722	0.000	-4.910
2	.034	23.25	21.59	.9288	.085	-2.351
3	.065	37.75	34.69	.9190	.189	-1.479
4	.096	52.75	48.19	.9136	.270	-1.014
5	.127	67.25	61.34	.9122	.304	-.707
6	.158	81.75	74.44	.9106	.331	-.481
7	.189	96.75	87.89	.9085	.407	-.297
8	.220	111.45	101.19	.9080	.430	-.142
9	.251	125.90	114.34	.9082	.496	-.011
10	.282	140.35	127.49	.9084	.538	.104
11	.312	154.65	140.49	.9085	.545	.207
12	.343	169.10	153.64	.9086	.618	.301
13	.373	183.65	166.69	.9077	.554	.388
14	.404	198.55	179.99	.9065	.636	.470
15	.436	213.55	193.39	.9056	.722	.548
16	.468	228.35	206.59	.9047	.708	.621
17	.499	242.75	219.64	.9048	.743	.688
18	.529	257.30	232.79	.9048	.735	.751
19	.560	271.80	245.89	.9047	.859	.812
20	.591	286.35	258.94	.9043	.768	.870
21	.621	300.75	272.04	.9046	.813	.925
22	.652	315.15	285.04	.9045	.862	.978
23	.682	329.60	298.09	.9044	.858	1.030
24	.713	344.20	311.19	.9041	.908	1.079
25	.744	358.60	324.24	.9042	.883	1.128
26	.774	373.05	337.34	.9043	.827	1.174
27	.805	387.55	350.34	.9040	.830	1.219
28	.835	401.95	363.34	.9040	.842	1.263
29	.866	416.35	376.24	.9037	.893	1.306
30	.897	431.05	389.44	.9035	.860	1.348
31	.928	445.55	402.44	.9033	.944	1.389
32	.958	460.05	415.54	.9033	.933	1.428
33	.989	474.45	428.54	.9032	.974	1.467
34	1.019	488.90	441.59	.9032	.912	1.505
35	1.050	503.35	454.59	.9031	.958	1.542
36	1.081	517.75	467.64	.9032	1.022	1.579
37	1.111	532.20	480.69	.9032	.932	1.614
38	1.142	546.60	493.69	.9032	1.008	1.649
39	1.172	561.00	506.69	.9032	.984	1.684
40	1.203	575.60	519.79	.9030	.936	1.717
41	1.233	590.00	532.79	.9030	1.011	1.751
42	1.264	604.40	545.79	.9030	.986	1.783
43	1.294	618.80	558.69	.9029	.975	1.815
44	1.325	633.30	571.74	.9028	.991	1.847
45	1.356	647.70	584.74	.9028	1.040	1.878
46	1.386	662.20	597.79	.9027	1.000	1.909
47	1.417	676.70	610.84	.9027	1.000	1.939
48	1.447	691.10	623.84	.9027	1.025	1.969
49	1.478	705.55	636.79	.9025	1.008	1.999
50	1.509	720.55	649.94	.9020	1.001	2.028
51	1.540	735.05	662.79	.9017	1.065	2.057
52	1.571	749.65	675.79	.9015	.899	2.086

STEADY-STATE PHASE FRACTIONAL FLOW : .9015
50% BREAKTHROUGH (PORE VOLUME) : .2539

EXPERIMENT OW4ZAO

TUBE NUMBER	PORE VOLUMES	TOTAL PHASE VOLUME (CC)	PHASE VOLUME (CC)	FRACTIONAL FLOW	NORMALIZED CONCENTRATION	LAMBDA1
1	.013	12.65	2.02	.1597	.001	-13.865
2	.044	29.15	3.52	.1208	.000	-7.536
3	.073	40.10	5.82	.1451	.001	-5.788
4	.118	71.10	13.72	.1930	.001	-4.488
5	.181	100.10	19.67	.1965	.002	-3.524
6	.240	126.70	25.22	.1991	.002	-2.987
7	.299	155.40	31.02	.1996	.001	-2.612
8	.357	182.00	36.22	.1990	.001	-2.328
9	.416	210.75	41.97	.1991	.003	-2.101
10	.476	239.40	47.52	.1985	.001	-1.908
11	.537	267.85	53.17	.1985	.002	-1.746
12	.598	297.60	59.12	.1987	0.000	-1.605
13	.660	326.45	65.07	.1993	.001	-1.480
14	.721	355.10	71.02	.2000	.002	-1.372
15	.782	383.65	76.82	.2002	.001	-1.275
16	.843	413.20	82.57	.1998	.002	-1.186
17	.905	441.75	88.27	.1998	.002	-1.105
18	.965	470.30	94.02	.1999	.001	-1.032
19	1.026	498.80	99.67	.1998	.002	-.964
20	1.086	527.75	105.72	.2003	.002	-.901
21	1.147	556.35	111.22	.1999	.001	-.841
22	1.208	585.10	117.02	.2000	.001	-.786
23	1.268	612.80	122.52	.1999	.002	-.734
24	1.326	640.60	127.82	.1995	.001	-.686
25	1.386	669.00	133.72	.1999	.001	-.640
26	1.446	697.25	139.62	.2002	.000	-.595
27	1.506	725.85	145.07	.2004	.001	-.553
28	1.566	754.45	151.37	.2006	.001	-.512
29	1.627	782.85	157.17	.2008	.002	-.473
30	1.687	811.25	163.02	.2009	.001	-.436
31	1.747	839.85	168.52	.2007	.000	-.400
32	1.808	868.55	174.32	.2007	.001	-.365
33	1.869	897.25	179.72	.2003	.001	-.332
34	1.930	926.95	185.72	.2004	.000	-.299
35	1.992	955.75	191.57	.2004	.001	-.267
36	2.053	984.45	197.27	.2004	.002	-.237
37	2.114	1013.64	203.42	.2007	.001	-.207
38	2.176	1042.34	209.22	.2007	.001	-.178
39	2.236	1071.14	214.87	.2006	.007	-.151
40	2.298	1100.34	220.67	.2005	.027	-.124
41	2.360	1129.44	226.47	.2005	.076	-.097
42	2.421	1158.14	231.92	.2003	.154	-.071
43	2.482	1187.09	237.62	.2002	.255	-.047
44	2.543	1216.29	243.22	.2000	.377	-.022
45	2.605	1245.19	248.82	.1998	.511	.002
46	2.666	1273.89	254.37	.1997	.609	.025
47	2.727	1302.89	259.87	.1995	.707	.048
48	2.788	1331.74	265.47	.1993	.803	.070
49	2.849	1360.79	271.27	.1993	.897	.092
50	2.911	1389.89	276.97	.1993	.963	.113
51	2.972	1419.04	282.62	.1992	.925	.134
52	3.034	1448.14	288.32	.1991	.956	.155
53	3.096	1477.24	293.87	.1989	.998	.175
54	3.157	1506.49	299.52	.1988	1.014	.195

55	3.219	1535.69	305.32	.1988	.980	.214
56	3.281	1564.59	310.72	.1986	.981	.233
57	3.342	1593.69	316.27	.1985	.990	.252
58	3.404	1623.14	322.07	.1984	1.030	.270
59	3.466	1652.04	327.72	.1984	1.026	.288
60	3.527	1681.04	333.27	.1983	1.034	.306
61	3.589	1710.54	339.27	.1983	.936	.324
62	3.651	1739.94	344.97	.1983	1.043	.341
63	3.713	1769.19	350.47	.1981	1.039	.358
64	3.775	1798.54	356.02	.1979	1.053	.375
65	3.838	1828.04	361.92	.1980	1.022	.392
66	3.900	1857.54	367.77	.1980	1.026	.408
67	3.962	1886.54	373.42	.1979	1.039	.424
68	4.023	1915.54	379.02	.1979	.998	.440
69	4.085	1945.04	384.82	.1978	1.009	.456
70	4.147	1974.24	390.37	.1977	1.033	.471
71	4.209	2003.64	396.47	.1979	1.007	.487
72	4.271	2032.24	401.87	.1977	1.046	.501
73	4.331	2060.89	407.27	.1976	1.032	.516
74	4.392	2089.54	412.92	.1976	.991	.530
75	4.453	2118.19	418.62	.1976	1.013	.545
76	4.514	2147.19	424.37	.1976	1.004	.559
77	4.575	2176.09	430.17	.1977	1.041	.573
78	4.636	2204.89	435.57	.1975	1.021	.586
79	4.697	2233.99	441.42	.1976	1.030	.600
80	4.759	2263.34	447.42	.1977	1.020	.614
81	4.821	2292.24	453.02	.1976	.966	.627
82	4.883	2322.19	459.07	.1977	.977	.641
83	4.945	2351.19	464.67	.1976	1.014	.654
84	5.006	2379.94	470.27	.1976	1.008	.667
85	5.067	2408.54	475.97	.1976	.993	.680
86	5.127	2436.79	481.37	.1975	.992	.692
87	5.187	2465.19	486.82	.1975	1.015	.705
88	5.248	2493.89	492.37	.1974	.994	.717
89	5.308	2522.49	497.92	.1974	1.004	.729
90	5.369	2551.34	503.52	.1974	1.001	.741
91	5.430	2579.94	509.42	.1975	1.001	.753
92	5.491	2609.34	515.72	.1976	1.007	.765
93	5.553	2638.24	521.52	.1977	1.002	.777

STEADY-STATE PHASE FRACTIONAL FLOW : .1977
50% BREAKTHROUGH (PORE VOLUME) : 2.5999

EXPERIMENT OMAZOL

TUBE NUMBER	PORE VOLUMES	TOTAL PHASE VOLUME (CC)	PHASE VOLUME (CC)	FRACTIONAL FLOW	NORMALIZED CONCENTRATION	LAMBDA1
1	.006	5.65	5.24	.9268	0.000	-3.649
2	.019	12.65	10.59	.8369	.079	-1.709
3	.037	22.35	18.89	.8450	.223	-.931
4	.054	29.15	25.59	.8778	.325	-.520
5	.066	32.80	28.94	.8822	.415	-.331
6	.077	40.10	34.24	.8538	.465	-.167
7	.102	56.20	45.54	.8103	.527	.111
8	.135	71.10	57.34	.8064	.567	.393
9	.166	85.40	68.84	.8060	.659	.606
10	.196	100.10	80.39	.8031	.688	.786
11	.225	112.30	89.89	.8004	.666	.933
12	.253	126.70	101.44	.8006	.688	1.065
13	.283	141.10	112.94	.8004	.745	1.196
14	.314	155.40	124.34	.8001	.756	1.316
15	.342	167.70	134.24	.8005	.784	1.420
16	.370	182.00	145.74	.8008	.812	1.518
17	.400	196.35	157.24	.8008	.893	1.618
18	.431	210.75	168.74	.8006	.861	1.714
19	.461	225.05	180.34	.8013	.922	1.805
20	.491	239.40	191.84	.8013	.916	1.891
21	.522	253.65	203.34	.8016	.976	1.974
22	.552	267.85	214.64	.8013	.930	2.054
23	.582	282.25	226.04	.8008	.930	2.131
24	.613	296.60	237.44	.8005	.970	2.206
25	.643	311.10	248.94	.8002	.930	2.279
26	.674	325.45	260.34	.7999	.903	2.350
27	.704	339.90	271.84	.7998	.918	2.419
28	.734	354.10	283.04	.7993	.962	2.486
29	.764	368.35	294.29	.7989	.967	2.551
30	.795	382.65	305.79	.7991	.955	2.614
31	.825	396.95	317.19	.7991	.951	2.676
32	.855	411.20	328.59	.7991	.982	2.736
33	.885	425.40	339.94	.7991	.940	2.795
34	.916	439.75	351.44	.7992	.948	2.853
35	.946	454.05	362.89	.7992	.999	2.911
36	.976	468.30	374.24	.7991	.973	2.966
37	1.006	482.40	385.64	.7994	.978	3.021
38	1.036	496.80	397.09	.7993	.991	3.075
39	1.067	511.40	408.59	.7990	.978	3.129
40	1.098	525.75	419.99	.7988	1.055	3.182
41	1.128	540.05	431.39	.7988	1.044	3.233
42	1.158	554.05	442.79	.7992	1.005	3.283
43	1.188	568.55	454.49	.7994	.956	3.333
44	1.218	582.80	465.74	.7991	1.020	3.382

STEADY-STATE PHASE FRACTIONAL FLOW : .7992
50% BREAKTHROUGH (PORE VOLUME) : .8912

EXPERIMENT OW5ZAQ

TUBE NUMBER	PORE VOLUMES	TOTAL PHASE VOLUME (CC)	PHASE VOLUME (CC)	FRACTIONAL FLOW	NORMALIZED CONCENTRATION	LAMBDA1
1	.020	18.50	6.13	.3316	.001	-11.340
2	.061	37.60	11.73	.3121	0.000	-6.410
3	.102	56.50	17.23	.3050	0.000	-4.869
4	.143	75.60	22.83	.3020	0.000	-4.042
5	.185	94.80	28.43	.2999	0.000	-3.500
6	.226	114.10	34.13	.2992	0.000	-3.107
7	.268	133.40	39.73	.2979	0.000	-2.804
8	.310	152.80	45.43	.2973	0.000	-2.561
9	.352	172.20	51.13	.2969	0.000	-2.360
10	.395	191.80	56.83	.2963	0.000	-2.180
11	.447	220.80	65.53	.2968	0.000	-2.006
12	.510	249.80	74.33	.2976	0.000	-1.824
13	.574	279.20	83.43	.2988	0.000	-1.669
14	.637	308.00	91.93	.2985	0.000	-1.535
15	.699	337.00	100.63	.2986	0.000	-1.419
16	.762	365.60	109.23	.2988	0.000	-1.315
17	.824	394.40	118.03	.2993	0.000	-1.222
18	.885	421.60	125.93	.2987	0.000	-1.139
19	.946	450.70	134.93	.2994	0.000	-1.063
20	1.009	480.30	144.43	.3007	0.000	-.990
21	1.073	509.60	153.33	.3009	0.000	-.922
22	1.137	538.90	162.23	.3010	0.000	-.859
23	1.200	568.00	171.03	.3011	0.000	-.800
24	1.263	597.10	179.63	.3008	0.000	-.745
25	1.326	626.10	188.33	.3008	0.000	-.694
26	1.388	654.30	196.73	.3007	0.000	-.646
27	1.450	683.50	201.83	.2953	0.000	-.600
28	1.514	713.20	210.83	.2956	0.000	-.555
29	1.578	742.10	219.63	.2960	0.000	-.512
30	1.641	771.50	228.73	.2965	0.000	-.472
31	1.704	800.50	237.43	.2966	0.000	-.433
32	1.767	829.40	246.23	.2969	0.000	-.396
33	1.830	858.50	254.93	.2970	0.000	-.360
34	1.893	887.60	263.63	.2970	0.000	-.326
35	1.956	916.70	272.63	.2974	0.000	-.293
36	2.020	946.10	281.83	.2979	0.000	-.261
37	2.083	975.00	290.63	.2981	0.000	-.230
38	2.146	1004.50	299.73	.2984	0.000	-.199
39	2.210	1033.90	308.73	.2986	.005	-.170
40	2.273	1063.00	317.73	.2989	.023	-.142
41	2.336	1091.80	326.23	.2988	.068	-.114
42	2.399	1121.20	335.33	.2991	.134	-.088
43	2.462	1150.00	344.13	.2992	.222	-.062
44	2.525	1178.70	352.83	.2993	.325	-.037
45	2.587	1207.90	361.83	.2996	.447	-.012
46	2.651	1237.30	371.13	.3000	.554	.012
47	2.715	1266.70	380.13	.3001	.650	.036
48	2.778	1295.70	389.13	.3003	.706	.059
49	2.841	1324.80	397.93	.3004	.779	.081
50	2.934	1354.10	406.83	.3004	.740	.103
51	2.968	1383.40	415.83	.3006	.830	.125
52	3.031	1412.30	424.53	.3006	.888	.146
53	3.094	1441.80	433.53	.3007	.904	.167
54	3.158	1471.00	442.23	.3006	.954	.187

55	3.221	1500.00	451.03	.3007	.948	.207
56	3.283	1528.70	459.53	.3006	.967	.227
57	3.346	1558.00	468.33	.3006	.988	.246
58	3.410	1587.00	477.13	.3007	.973	.265
59	3.473	1616.40	486.13	.3008	.968	.283
60	3.537	1645.70	495.13	.3009	.957	.302
61	3.600	1674.70	503.83	.3009	.994	.319
62	3.663	1703.80	512.73	.3009	.989	.337
63	3.726	1733.00	521.83	.3011	.996	.354
64	3.789	1762.30	530.83	.3012	1.003	.372
65	3.852	1791.10	539.23	.3011	.998	.388
66	3.915	1820.10	547.83	.3010	.974	.405
67	3.978	1849.30	556.63	.3010	1.002	.421
68	4.042	1878.70	565.73	.3011	.996	.437
69	4.105	1907.90	574.63	.3012	.978	.453
70	4.169	1937.20	583.43	.3012	.988	.469
71	4.231	1965.90	592.03	.3012	1.017	.484
72	4.294	1995.10	600.63	.3011	.979	.500
73	4.357	2024.10	609.23	.3010	1.017	.515
74	4.420	2053.10	617.93	.3010	1.016	.529
75	4.483	2082.20	626.63	.3009	.993	.544
76	4.544	2109.60	634.73	.3009	.974	.558
77	4.605	2138.50	643.33	.3008	.979	.572
78	4.668	2167.40	651.93	.3008	.987	.586
79	4.731	2196.40	660.43	.3007	1.019	.600
80	4.794	2225.30	669.03	.3006	.976	.614
81	4.856	2254.20	677.63	.3006	1.002	.627
82	4.919	2282.90	686.13	.3006	1.007	.641
83	4.981	2312.00	694.73	.3005	1.006	.654
84	5.044	2340.90	703.33	.3005	1.014	.667
85	5.107	2370.10	712.03	.3004	.992	.680
86	5.171	2399.20	720.73	.3004	.996	.693
87	5.234	2428.20	729.33	.3004	1.005	.706
88	5.296	2457.00	737.83	.3003	.962	.719
89	5.359	2486.00	746.43	.3003	1.006	.731
90	5.422	2514.80	754.93	.3002	1.010	.744

STEADY-STATE PHASE FRACTIONAL FLOW : .3002
50% BREAKTHROUGH (PORE VOLUME) : 2.6190

EXPERIMENT 045ZOL

TUBE NUMBER	PORE VOLUMES	TOTAL PHASE VOLUME (CC)	PHASE VOLUME (CC)	FRACTIONAL FLOW	NORMALIZED CONCENTRATION	LAMBDA
1	.012	11.30	8.33	.7373	0.000	-2.817
2	.336	23.10	16.93	.7330	.119	-1.241
3	.059	32.80	23.73	.7235	.246	-.701
4	.079	42.20	30.43	.7211	.351	-.396
5	.099	51.70	37.23	.7201	.430	-.169
6	.119	61.10	43.83	.7174	.507	.015
7	.139	70.60	50.53	.7157	.537	.170
8	.160	80.20	57.33	.7149	.628	.306
9	.180	89.80	64.13	.7142	.664	.428
10	.200	99.40	70.93	.7136	.704	.538
11	.221	109.00	77.73	.7131	.688	.639
12	.241	118.70	84.53	.7121	.743	.733
13	.261	128.30	91.33	.7119	.810	.820
14	.282	138.00	98.23	.7118	.777	.902
15	.302	147.70	105.13	.7118	.805	.980
16	.323	157.40	111.93	.7111	.864	1.053
17	.343	167.10	118.83	.7111	.828	1.124
18	.364	176.80	125.63	.7106	.856	1.191
19	.385	186.60	132.53	.7102	.870	1.255
20	.405	196.40	139.53	.7104	.865	1.318
21	.431	211.00	149.73	.7096	.878	1.392
22	.462	225.40	159.83	.7091	.881	1.477
23	.492	239.90	169.93	.7083	.925	1.557
24	.523	254.40	180.03	.7077	.967	1.635
25	.554	269.00	190.13	.7068	.943	1.709
26	.585	283.80	200.33	.7059	.984	1.782
27	.616	298.30	210.53	.7058	.993	1.852
28	.646	312.60	220.63	.7058	1.013	1.918
29	.677	327.10	230.73	.7054	.969	1.982
30	.708	341.60	240.93	.7053	1.007	2.045
31	.738	356.00	251.03	.7051	1.001	2.106
32	.768	370.20	260.93	.7048	1.046	2.165
33	.799	384.70	270.93	.7043	.981	2.223
34	.829	399.00	280.93	.7041	1.007	2.279
35	.860	413.40	290.93	.7038	.999	2.334

STEADY-STATE PHASE FRACTIONAL FLOW : .7038
50% BREAKTHROUGH (PORE VOLUME) : .1177

EXPERIMENT OW6ZAQ

TUBE NUMBER[R]	PORE VOLUMES	TOTAL PHASE VOLUME (CC)	PHASE VOLUME (CC)	FRACTIONAL FLOW	NORMALIZED CONCENTRATION	LAMBDA1
1	.015	13.90	7.24	.5208	0.000	-10.285
2	.350	32.90	17.44	.5301	0.000	-5.481
3	.090	52.30	27.44	.5247	0.000	-3.955
4	.131	71.80	37.44	.5214	0.000	-3.186
5	.173	91.50	47.64	.5207	0.000	-2.699
6	.215	111.40	57.74	.5183	0.000	-2.349
7	.257	131.40	67.74	.5155	0.000	-2.081
8	.299	151.30	77.74	.5138	0.000	-1.868
9	.341	171.20	87.54	.5113	0.000	-1.691
10	.384	191.30	97.64	.5104	0.000	-1.541
11	.426	211.40	107.39	.5080	0.000	-1.410
12	.469	231.50	117.19	.5062	0.000	-1.295
13	.511	251.55	126.89	.5044	0.000	-1.193
14	.554	271.55	136.74	.5036	0.000	-1.101
15	.596	291.55	146.49	.5025	0.000	-1.018
16	.638	311.45	156.19	.5015	0.000	-.942
17	.680	331.45	165.74	.5000	0.000	-.871
18	.723	351.35	175.24	.4988	0.000	-.806
19	.765	371.35	185.04	.4983	0.000	-.745
20	.807	391.25	194.54	.4972	0.000	-.688
21	.858	419.25	221.74	.5289	0.000	-.624
22	.917	447.25	249.74	.5584	0.000	-.554
23	.976	475.20	263.84	.5552	0.000	-.490
24	1.036	504.10	277.74	.5510	0.000	-.428
25	1.096	531.55	291.64	.5487	0.000	-.371
26	1.154	559.05	305.64	.5467	0.000	-.319
27	1.213	586.90	319.74	.5448	.001	-.269
28	1.271	614.60	333.84	.5432	.015	-.221
29	1.329	641.70	347.69	.5418	.072	-.176
30	1.387	669.30	361.89	.5407	.150	-.133
31	1.445	696.60	375.79	.5395	.236	-.092
32	1.503	723.90	389.69	.5383	.327	-.053
33	1.561	751.35	403.59	.5372	.444	-.015
34	1.619	778.50	417.29	.5360	.579	.021
35	1.677	805.90	431.29	.5352	.746	.056
36	1.735	833.60	445.39	.5343	.884	.090
37	1.793	860.80	459.19	.5334	.936	.123
38	1.851	888.10	473.09	.5327	.966	.155
39	1.909	915.95	487.09	.5318	1.009	.186
40	1.969	944.40	501.59	.5311	.990	.217
41	2.029	972.90	515.84	.5302	.999	.247
42	2.089	1000.90	529.84	.5294	.995	.277
43	2.148	1029.20	543.94	.5285	1.008	.305
44	2.208	1057.40	557.84	.5276	.993	.333
45	2.268	1085.50	571.74	.5267	1.004	.360
46	2.327	1113.60	585.74	.5260	.993	.386

STEADY-STATE PHASE FRACTIONAL FLOW : .5260

50% BREAKTHROUGH (PORE VOLUME) : 1.5852

EXPERIMENT 046Z0L

TUBE NUMBER	PORE VOLUMES	TOTAL PHASE VOLUME (CC)	PHASE VOLUME (CC)	FRACTIONAL FLOW	NORMALIZED CONCENTRATION	LAMBDA1
1	.005	4.50	2.52	.5600	0.000	-3.110
2	.019	13.90	6.62	.4763	.014	-1.089
3	.039	23.30	10.92	.4687	.289	-.339
4	.059	32.90	15.42	.4687	.557	.075
5	.080	42.50	20.02	.4711	.623	.371
6	.100	52.30	24.82	.4746	.798	.687
7	.121	62.00	29.52	.4761	.807	.805
8	.142	71.80	33.52	.4669	.913	.978
9	.162	81.70	38.32	.4690	.941	1.133
10	.183	91.50	43.02	.4702	.943	1.274
11	.204	101.30	47.82	.4721	.940	1.403
12	.225	111.40	52.82	.4741	.969	1.525
13	.246	121.50	57.92	.4767	.960	1.640
14	.268	131.40	62.82	.4781	.960	1.748
15	.289	141.30	67.72	.4793	.947	1.850
16	.310	151.30	72.72	.4806	.973	1.947
17	.331	161.20	77.72	.4821	.966	2.040
18	.352	171.20	82.82	.4838	.973	2.129
19	.373	181.20	87.82	.4847	1.011	2.215
20	.394	191.30	92.82	.4852	.984	2.299
21	.416	201.40	98.02	.4867	1.013	2.380
22	.437	211.40	103.17	.4880	1.022	2.458
23	.458	221.40	108.32	.4893	.995	2.534
24	.479	231.50	113.47	.4902	.960	2.608
25	.501	241.60	118.67	.4912	1.003	2.680
26	.522	251.55	123.82	.4922	1.012	2.750
27	.543	261.55	128.92	.4929	.971	2.818
28	.564	271.55	133.97	.4934	1.017	2.885
29	.585	281.55	139.12	.4941	1.023	2.950

STEADY-STATE PHASE FRACTIONAL FLOW : .4942
50% BREAKTHROUGH (PORE VOLUME) : .0552

EXPERIMENT DW7ZA0

TUBE NUMBER	PORE VOLUMES	TOTAL PHASE VOLUME (CC)	PHASE VOLUME (CC)	FRACTIONAL FLOW	NORMALIZED CONCENTRATION	LAMBDA1
1	.009	8.50	6.23	.7333	0.000	-11.427
2	.032	22.10	16.13	.7300	.000	-5.904
3	.061	35.60	26.33	.7397	0.000	-4.193
4	.090	49.10	36.73	.7481	0.000	-3.373
5	.118	62.70	47.23	.7533	.000	-2.860
6	.147	76.30	57.63	.7554	0.000	-2.496
7	.176	89.90	67.83	.7545	0.000	-2.220
8	.205	103.50	78.13	.7549	0.000	-2.000
9	.233	117.10	88.43	.7552	0.000	-1.818
10	.262	130.70	98.73	.7554	0.000	-1.664
11	.297	150.30	113.53	.7554	.000	-1.503
12	.339	169.70	128.33	.7562	.000	-1.344
13	.379	188.80	142.63	.7555	0.000	-1.209
14	.420	208.00	157.23	.7559	.000	-1.092
15	.461	227.20	171.93	.7567	0.000	-.988
16	.501	246.50	187.03	.7588	0.000	-.894
17	.542	266.10	201.83	.7585	0.000	-.808
18	.592	293.80	222.63	.7578	0.000	-.714
19	.651	321.70	243.73	.7576	0.000	-.614
20	.710	349.50	264.73	.7575	.000	-.524
21	.770	377.90	286.23	.7574	0.000	-.441
22	.830	406.00	307.53	.7575	0.000	-.365
23	.889	434.00	328.93	.7579	0.000	-.295
24	.948	461.80	349.93	.7578	.000	-.230
25	1.007	490.20	371.43	.7577	.041	-.169
26	1.067	518.50	393.03	.7580	.156	-.111
27	1.127	546.20	413.93	.7578	.303	-.057
28	1.185	573.60	434.83	.7581	.473	-.006
29	1.243	601.20	456.83	.7599	.681	.042
30	1.302	628.90	478.43	.7607	.885	.088
31	1.361	656.90	499.93	.7610	.977	.132
32	1.420	684.60	521.13	.7612	1.006	.175
33	1.479	713.10	543.13	.7617	1.002	.216
34	1.539	741.20	564.63	.7618	1.017	.256
35	1.598	769.00	585.83	.7618	1.001	.294
36	1.657	796.90	607.13	.7619	1.000	.330
37	1.716	824.90	628.63	.7621	.984	.366
38	1.776	853.00	649.43	.7614	1.006	.401
39	1.835	880.90	670.43	.7611	1.024	.434
40	1.894	908.90	691.63	.7610	1.007	.467
41	1.953	936.80	716.13	.7644	1.019	.498
42	2.012	964.80	737.13	.7640	.994	.529
43	2.071	992.70	758.23	.7638	1.053	.559
44	2.130	1020.60	779.43	.7637	1.012	.588
45	2.190	1048.60	800.53	.7634	1.023	.617
46	2.249	1076.70	821.83	.7633	.993	.645
47	2.308	1104.80	843.03	.7631	1.001	.673
48	2.368	1132.90	864.23	.7629	1.043	.700
49	2.428	1161.10	885.83	.7629	1.007	.726
50	2.487	1189.50	907.63	.7630	1.000	.752
51	2.547	1217.50	928.93	.7630	.980	.777
52	2.606	1245.60	950.33	.7630	1.003	.802
53	2.666	1273.70	971.43	.7627	.995	.826
54	2.726	1302.20	992.43	.7621	.962	.850

55	2.786	1330.40	1014.03	.7622	.999	.874
56	2.845	1358.40	1035.23	.7621	1.027	.897
57	2.905	1386.50	1056.43	.7619	.996	.920
58	2.964	1414.30	1077.43	.7618	1.007	.942
59	3.023	1442.40	1098.73	.7617	.966	.964
60	3.082	1470.20	1119.93	.7618	1.000	.986
61	3.141	1498.00	1140.93	.7616	.983	1.007
62	3.200	1526.20	1162.33	.7616	.980	1.028
63	3.260	1554.40	1183.53	.7614	1.021	1.049
64	3.319	1582.20	1204.63	.7614	.989	1.069
65	3.378	1610.10	1225.73	.7613	1.011	1.089
66	3.437	1638.10	1246.73	.7611	.999	1.109

STEADY-STATE PHASE FRACTIONAL FLOW : .7611
50% BREAKTHROUGH (PORE VOLUME) : 1.1925

EXPERIMENT OW7ZOL

TUBE NUMBER	PORE VOLUMES	TOTAL PHASE VOLUME (CC)	PHASE VOLUME (CC)	FRACTIONAL FLOW	NORMALIZED CONCENTRATION	LAMBDA
1	.002	1.80	.55	.3043	.000	-6.059
2	.011	8.50	2.25	.2645	.000	-2.215
3	.025	15.30	4.15	.2711	0.000	-1.126
4	.040	22.10	5.95	.2691	.072	-.632
5	.054	28.90	7.85	.2716	.288	-.313
6	.068	35.60	9.25	.2598	.450	-.077
7	.083	42.40	10.75	.2535	.581	.114
8	.097	49.10	12.35	.2515	.680	.274
9	.111	55.90	13.95	.2495	.742	.414
10	.126	62.70	15.45	.2464	.771	.539
11	.140	69.50	17.05	.2453	.867	.652
12	.154	76.30	18.65	.2444	.839	.756
13	.169	83.10	20.35	.2449	.901	.852
14	.183	89.90	22.05	.2452	.921	.942
15	.197	96.70	23.75	.2456	.904	1.026
16	.212	103.50	25.35	.2449	.943	1.106
17	.226	110.30	26.95	.2443	.957	1.182
18	.241	117.10	28.65	.2446	.913	1.254
19	.255	123.90	30.35	.2449	.931	1.323
20	.269	130.70	31.95	.2444	.922	1.389
21	.287	140.50	34.35	.2445	.940	1.467
22	.308	150.30	36.75	.2445	.957	1.550
23	.328	159.90	38.95	.2436	.976	1.637
24	.349	169.70	41.35	.2437	.969	1.716
25	.369	179.30	43.75	.2440	.988	1.792
26	.390	188.80	46.15	.2444	.973	1.864
27	.410	198.30	48.45	.2443	.996	1.934
28	.430	208.00	50.75	.2440	.981	2.002
29	.450	217.50	52.95	.2434	.993	2.067
30	.471	227.20	55.25	.2432	.984	2.131
31	.491	236.80	57.45	.2426	.992	2.194
32	.511	246.50	59.45	.2412	1.027	2.255
33	.532	256.30	61.85	.2413	1.008	2.315
34	.553	266.10	64.25	.2414	1.031	2.374
35	.573	275.80	66.55	.2413	1.013	2.431

STEADY-STATE PHASE FRACTIONAL FLOW : .2413
50% BREAKTHROUGH (PORE VOLUME) : .0737

EXPERIMENT OW7ZOL

TUBE NUMBER	PORE VOLUMES	TOTAL PHASE VOLUME (CC)	PHASE VOLUME (CC)	FRACTIONAL FLOW	NORMALIZED CONCENTRATION	LAMBDA1
1	.002	1.80	.55	.3043	.000	-6.059
2	.011	8.50	2.25	.2645	.000	-2.215
3	.025	15.30	4.15	.2711	0.000	-1.126
4	.040	22.10	5.95	.2691	.072	-.632
5	.054	28.90	7.85	.2716	.288	-.313
6	.068	35.60	9.25	.2598	.450	-.077
7	.083	42.40	10.75	.2535	.581	.114
8	.097	49.10	12.35	.2515	.680	.274
9	.111	55.90	13.95	.2495	.742	.414
10	.126	62.70	15.45	.2464	.771	.539
11	.140	69.50	17.05	.2453	.867	.652
12	.154	76.30	18.65	.2444	.839	.756
13	.169	83.10	20.35	.2449	.901	.852
14	.183	89.90	22.05	.2452	.921	.942
15	.197	96.70	23.75	.2456	.904	1.026
16	.212	103.50	25.35	.2449	.943	1.106
17	.226	110.30	26.95	.2443	.957	1.182
18	.241	117.10	28.65	.2446	.913	1.254
19	.255	123.90	30.35	.2449	.931	1.323
20	.269	130.70	31.95	.2444	.922	1.389
21	.287	140.50	34.35	.2445	.940	1.467
22	.308	150.30	36.75	.2445	.957	1.550
23	.328	159.90	38.95	.2436	.976	1.637
24	.349	169.70	41.35	.2437	.969	1.716
25	.369	179.30	43.75	.2440	.988	1.792
26	.390	188.80	46.15	.2444	.973	1.864
27	.410	198.30	48.45	.2443	.996	1.934
28	.430	208.00	50.75	.2440	.981	2.002
29	.450	217.50	52.95	.2434	.993	2.067
30	.471	227.20	55.25	.2432	.984	2.131
31	.491	236.80	57.45	.2426	.992	2.194
32	.511	246.50	59.45	.2412	1.027	2.255
33	.532	256.30	61.85	.2413	1.008	2.315
34	.553	266.10	64.25	.2414	1.031	2.374
35	.573	275.80	66.55	.2413	1.013	2.431

STEADY-STATE PHASE FRACTIONAL FLOW : .2413
50% BREAKTHROUGH (PORE VOLUME) : .0737

EXPERIMENT OW8Z

TUBE NUMBER	PORE VOLUMES	TOTAL PHASE VOLUME (CC)	PHASE VOLUME (CC)	FRACTIONAL FLOW	NORMALIZED CONCENTRATION	LAMBDA1
1	.010	9.50	9.50	1.0000	.001	-9.297
2	.035	23.30	23.30	1.0000	0.000	-4.863
3	.064	37.00	37.00	1.0000	0.000	-3.464
4	.093	50.80	50.80	1.0000	0.000	-2.770
5	.122	64.90	64.90	1.0000	0.000	-2.323
6	.152	78.60	78.60	1.0000	0.000	-2.006
7	.181	92.50	92.50	1.0000	0.000	-1.764
8	.213	106.40	106.40	1.0000	0.000	-1.560
9	.240	120.10	120.10	1.0000	0.000	-1.406
10	.269	133.80	133.80	1.0000	0.000	-1.269
11	.298	147.50	147.50	1.0000	0.000	-1.149
12	.327	161.40	161.40	1.0000	0.000	-1.043
13	.356	175.00	175.00	1.0000	0.000	-.947
14	.385	188.80	188.80	1.0000	0.000	-.861
15	.414	202.70	202.70	1.0000	0.000	-.782
16	.444	216.60	216.60	1.0000	0.000	-.709
17	.473	230.50	230.50	1.0000	0.000	-.641
18	.502	244.10	244.10	1.0000	0.000	-.579
19	.531	257.90	257.90	1.0000	.000	-.520
20	.561	271.80	271.80	1.0000	.004	-.465
21	.590	285.70	285.70	1.0000	.005	-.413
22	.619	299.50	299.50	1.0000	.012	-.363
23	.648	313.30	313.30	1.0000	.021	-.317
24	.678	327.20	327.20	1.0000	.031	-.272
25	.707	341.00	341.00	1.0000	.051	-.229
26	.736	354.80	354.80	1.0000	.092	-.189
27	.766	368.60	368.60	1.0000	.149	-.150
28	.795	382.40	382.40	1.0000	.244	-.112
29	.824	396.20	396.20	1.0000	.329	-.076
30	.853	410.00	410.00	1.0000	.447	-.041
31	.882	423.80	423.80	1.0000	.429	-.007
32	.912	437.70	437.70	1.0000	.747	.025
33	.941	451.60	451.60	1.0000	.801	.057
34	.971	465.60	465.60	1.0000	.909	.088
35	1.000	479.30	479.30	1.0000	.896	.118
36	1.029	493.00	493.00	1.0000	.875	.146
37	1.058	506.80	506.80	1.0000	.962	.174
38	1.087	520.70	520.70	1.0000	.864	.202
39	1.117	534.60	534.60	1.0000	.960	.229
40	1.146	548.40	548.40	1.0000	.867	.255
41	1.176	562.50	562.50	1.0000	.921	.280
42	1.205	576.50	576.50	1.0000	.900	.306
43	1.235	590.30	590.30	1.0000	.902	.330
44	1.264	604.10	604.10	1.0000	.904	.354
45	1.293	617.80	617.80	1.0000	1.010	.377
46	1.322	631.90	631.90	1.0000	1.011	.400
47	1.352	646.10	646.10	1.0000	.994	.423
48	1.382	659.80	659.80	1.0000	.948	.445
49	1.411	673.50	673.50	1.0000	1.038	.466

STEADY-STATE PHASE FRACTIONAL FLOW : 1.0000

50% BREAKTHROUGH (PORE VOLUME) : .8889

EXPERIMENT MD1

TUBE NUMBER	PORE VOLUMES	TOTAL PHASE VOLUME (CC)	PHASE VOLUME (CC)	FRACTIONAL FLOW	NORMALIZED CONCENTRATION	LAMBDA1
1	.016	14.70	14.70	1.0000	0.000	-7.987
2	.048	30.60	30.60	1.0000	0.000	-4.404
3	.083	47.40	47.40	1.0000	0.000	-3.237
4	.119	64.80	64.80	1.0000	0.000	-2.595
5	.155	82.10	82.10	1.0000	0.000	-2.176
6	.192	99.20	99.20	1.0000	0.000	-1.876
7	.228	116.70	116.70	1.0000	0.000	-1.644
8	.264	133.10	133.10	1.0000	0.000	-1.459
9	.297	147.10	147.10	1.0000	0.000	-1.319
10	.327	162.30	162.30	1.0000	0.000	-1.202
11	.362	180.10	180.10	1.0000	0.000	-1.085
12	.401	198.60	198.60	1.0000	0.000	-.972
13	.440	217.60	217.60	1.0000	0.000	-.868
14	.481	236.60	236.60	1.0000	0.000	-.774
15	.521	255.60	255.60	1.0000	0.000	-.688
16	.561	274.60	274.60	1.0000	0.000	-.610
17	.601	293.60	293.60	1.0000	.000	-.538
18	.642	312.70	312.70	1.0000	0.000	-.471
19	.682	331.80	331.80	1.0000	.002	-.408
20	.723	351.00	351.00	1.0000	.004	-.350
21	.763	370.20	370.20	1.0000	.009	-.294
22	.804	389.60	389.60	1.0000	.019	-.242
23	.845	408.80	408.80	1.0000	.047	-.192
24	.886	428.20	428.20	1.0000	.110	-.144
25	.927	447.70	447.70	1.0000	.158	-.099
26	.968	467.20	467.20	1.0000	.250	-.055
27	1.009	486.40	486.40	1.0000	.442	-.014
28	1.050	505.60	505.60	1.0000	.610	.026
29	1.091	525.10	525.10	1.0000	.743	.064
30	1.132	544.50	540.50	1.0000	.843	.101
31	1.173	563.90	563.90	1.0000	.811	.137
32	1.214	583.40	583.40	1.0000	.922	.171
33	1.255	602.80	602.80	1.0000	.978	.205
34	1.296	622.30	622.30	1.0000	.989	.237
35	1.338	641.80	641.80	1.0000	1.015	.269
36	1.379	661.40	661.40	1.0000	.981	.300
37	1.421	681.10	681.10	1.0000	.994	.330
38	1.462	700.60	700.60	1.0000	1.028	.359
39	1.503	720.20	720.20	1.0000	.989	.387
40	1.545	739.80	739.80	1.0000	1.002	.415

STEADY-STATE PHASE FRACTIONAL FLOW : 1.0000
50% BREAKTHROUGH (PORE VOLUME) : 1.0232

EXPERIMENT M02LO

TUBE NUMBER	PORE VOLUMES	TOTAL PHASE VOLUME (CC)	PHASE VOLUME (CC)	FRACTIONAL FLOW	NORMALIZED CONCENTRATION	LAMBDA1
1	.018	16.80	12.62	.7514	.028	-8.058
2	.055	35.20	26.42	.7507	.008	-4.435
3	.095	54.50	41.72	.7656	.003	-3.258
4	.136	73.80	56.12	.7605	.001	-2.622
5	.177	93.00	70.82	.7616	.000	-2.211
6	.217	112.30	85.52	.7616	.001	-1.913
7	.258	131.50	100.22	.7622	.001	-1.682
8	.299	150.60	114.82	.7624	.000	-1.495
9	.339	170.00	129.92	.7643	0.000	-1.339
10	.380	189.30	144.82	.7651	.001	-1.204
11	.421	208.50	160.02	.7675	0.000	-1.086
12	.462	227.70	175.72	.7717	0.000	-.983
13	.502	246.90	191.42	.7753	.001	-.889
14	.543	266.30	206.02	.7737	0.000	-.805
15	.584	285.50	221.42	.7756	.001	-.727
16	.625	304.80	236.12	.7747	0.000	-.656
17	.666	324.10	250.72	.7736	.000	-.589
18	.706	343.40	265.32	.7726	0.000	-.527
19	.747	362.80	280.42	.7729	.000	-.469
20	.788	382.10	295.12	.7724	.004	-.415
21	.829	401.50	310.12	.7724	.004	-.363
22	.870	421.00	324.62	.7711	.006	-.314
23	.912	440.40	339.52	.7709	.013	-.267
24	.952	459.60	353.82	.7699	.017	-.223
25	.993	478.90	368.22	.7689	.026	-.181
26	1.034	498.30	383.22	.7691	.056	-.140
27	1.075	517.70	398.32	.7694	.138	-.101
28	1.116	537.10	413.72	.7703	.215	-.064
29	1.157	556.50	428.22	.7695	.427	-.028
30	1.198	575.80	443.22	.7698	.519	.007
31	1.239	594.80	457.82	.7697	.620	.040
32	1.279	614.00	472.02	.7688	.621	.072
33	1.320	633.10	486.82	.7690	.827	.104
34	1.360	652.30	501.52	.7689	.918	.134
35	1.401	671.40	516.22	.7689	.978	.163
36	1.441	690.50	531.42	.7696	.969	.192
37	1.481	709.10	545.72	.7696	.991	.219
38	1.522	727.70	560.42	.7701	1.010	.246
39	1.563	746.80	575.32	.7704	1.010	.272
40	1.601	765.80	590.12	.7706	1.003	.298
41	1.641	785.10	605.32	.7710	1.008	.323
42	1.682	804.10	619.82	.7708	1.000	.348
43	1.721	822.60	634.42	.7712	.970	.371
44	1.761	841.60	649.32	.7715	1.004	.395
45	1.801	860.60	664.22	.7718	1.028	.418

STEADY-STATE PHASE FRACTIONAL FLOW : .7719
50% BREAKTHROUGH (PORE VOLUME) : 1.1898

EXPERIMENT MO2PART

TUBE NUMBER	PORE VOLUMES	TOTAL PHASE VOLUME (CC)	PHASE VOLUME (CC)	FRACTIONAL FLOW	NORMALIZED CONCENTRATION	LAMBDA1
1	.018	16.80	12.62	.7514	0.000	-6.145
2	.055	35.20	26.42	.7507	0.000	-3.304
3	.095	54.50	41.72	.7656	0.000	-2.361
4	.136	73.80	56.12	.7605	0.000	-1.843
5	.177	93.00	70.82	.7616	.005	-1.501
6	.217	112.30	85.52	.7616	0.000	-1.249
7	.258	131.50	100.22	.7622	.005	-1.050
8	.299	150.60	114.82	.7624	0.000	-.888
9	.339	170.00	129.92	.7643	.036	-.750
10	.380	189.30	144.82	.7651	.045	-.629
11	.421	208.50	160.02	.7675	.079	-.523
12	.462	227.70	175.72	.7717	.117	-.429
13	.502	246.90	191.42	.7753	.124	-.343
14	.543	266.30	206.02	.7737	.231	-.264
15	.584	285.50	221.42	.7756	.255	-.191
16	.625	304.80	236.12	.7747	.338	-.123
17	.666	324.10	250.72	.7736	.469	-.060
18	.706	343.40	265.32	.7726	.500	0.000
19	.747	362.80	280.42	.7729	.538	.056
20	.788	382.10	295.12	.7724	.712	.110
21	.829	401.50	310.12	.7724	.729	.161
22	.870	421.00	324.62	.7711	.748	.209
23	.912	440.40	339.52	.7709	.695	.256
24	.952	459.60	353.82	.7699	.769	.300
25	.993	478.90	368.22	.7689	.781	.342
26	1.034	498.30	383.22	.7691	.748	.383
27	1.075	517.70	398.32	.7694	.840	.423
28	1.116	537.10	413.72	.7703	.871	.462
29	1.157	556.50	428.22	.7695	.924	.499
30	1.198	575.80	443.22	.7698	.876	.535
31	1.239	594.80	457.82	.7697	.902	.569
32	1.279	614.00	472.02	.7688	.707	.603
33	1.320	633.10	486.82	.7690	.936	.635
34	1.360	652.30	501.52	.7689	.981	.667
35	1.401	671.40	516.22	.7689	.948	.698
36	1.441	690.50	531.42	.7696	1.012	.728
37	1.481	709.10	545.72	.7696	1.060	.757
38	1.520	727.70	560.42	.7701	.921	.786
39	1.560	746.80	575.32	.7704	.986	.813
40	1.601	765.80	590.12	.7706	.979	.841
41	1.641	785.10	605.32	.7710	1.005	.868
42	1.682	804.10	619.82	.7708	1.014	.895
43	1.721	822.60	634.42	.7712	.960	.921
44	1.761	841.60	649.32	.7715	1.043	.946
45	1.801	860.60	664.22	.7718	1.031	.971

STEADY-STATE PHASE FRACTIONAL FLOW : .7719
50% BREAKTHROUGH (PORE VOLUME) : .7064

EXPERIMENT MO2UP

TUBE NUMBER	PORE VOLUMES	TOTAL PHASE VOLUME (CC)	PHASE VOLUME (CC)	FRACTIONAL FLOW	NORMALIZED CONCENTRATION	LAMBDA1
1	.018	16.80	4.18	.2486	0.000	-6.097
2	.055	35.20	8.78	.2493	0.000	-3.275
3	.095	54.50	12.78	.2344	0.000	-2.330
4	.136	73.80	17.68	.2395	.006	-1.822
5	.177	93.00	22.18	.2384	.008	-1.482
6	.217	112.30	26.78	.2384	0.000	-1.231
7	.258	131.50	31.28	.2378	0.000	-1.034
8	.299	150.60	35.78	.2376	0.000	-.872
9	.339	170.00	40.08	.2357	.019	-.734
10	.380	189.30	44.48	.2349	.058	-.614
11	.421	208.50	48.48	.2325	.085	-.508
12	.462	227.70	51.98	.2283	.114	-.414
13	.502	246.90	55.48	.2247	.145	-.328
14	.543	266.30	60.28	.2263	.229	-.249
15	.584	285.50	64.08	.2244	.242	-.176
16	.625	304.80	68.68	.2253	.355	-.108
17	.666	324.10	73.38	.2264	.386	-.045
18	.706	343.40	78.08	.2274	.539	.015
19	.747	362.60	82.38	.2271	.652	.071
20	.788	382.10	86.98	.2276	.718	.125
21	.829	401.50	91.38	.2276	.709	.175
22	.870	421.00	96.38	.2289	.751	.224
23	.912	440.40	100.88	.2291	.764	.271
24	.952	459.60	105.78	.2301	.820	.315
25	.993	478.90	110.68	.2311	.825	.357
26	1.034	498.30	115.08	.2309	.811	.399
27	1.075	517.70	119.38	.2306	.890	.438
28	1.116	537.10	123.38	.2297	.909	.477
29	1.157	556.50	128.28	.2305	.935	.514
30	1.198	575.80	132.58	.2302	.931	.550
31	1.239	594.80	136.98	.2303	1.016	.585
32	1.279	614.00	141.98	.2312	.992	.618
33	1.320	633.10	146.28	.2310	.992	.651
34	1.360	652.30	150.78	.2311	1.000	.683
35	1.401	671.40	155.18	.2311	.946	.714
36	1.441	690.50	159.08	.2304	1.015	.744
37	1.481	709.10	163.38	.2304	1.015	.773
38	1.522	727.70	167.28	.2299	.925	.801
39	1.563	746.80	171.48	.2296	1.019	.829
40	1.601	765.80	175.68	.2294	1.026	.857
41	1.641	785.10	179.78	.2290	1.013	.884
42	1.682	804.10	184.28	.2292	1.031	.911
43	1.721	822.60	188.18	.2288	1.003	.937
44	1.761	841.60	192.28	.2285	.949	.962
45	1.801	860.60	196.38	.2282	1.005	.987

STEADY-STATE PHASE FRACTIONAL FLOW : .2282

50% BREAKTHROUGH (PORE VOLUME) : .6960

EXPERIMENT MO3LO

TUBE NUMBER	PORE VOLUMES	TOTAL PHASE VOLUME (CC)	PHASE VOLUME (CC)	FRACTIONAL FLOW	NORMALIZED CONCENTRATION	LAMBDA1
1	.010	9.10	4.46	.4896	0.000	-12.387
2	.340	28.50	15.16	.5318	0.000	-5.970
3	.381	47.90	24.46	.5105	0.000	-4.070
4	.122	67.40	33.76	.5008	.000	-3.217
5	.163	86.80	44.36	.5110	0.000	-2.698
6	.204	106.10	53.86	.5076	0.000	-2.339
7	.245	125.50	63.36	.5048	0.000	-2.067
8	.286	145.00	75.46	.5204	0.000	-1.849
9	.327	164.40	85.86	.5222	.000	-1.670
10	.369	183.90	94.56	.5142	0.000	-1.519
11	.410	203.50	103.46	.5084	.002	-1.387
12	.451	223.10	114.76	.5144	.000	-1.272
13	.493	242.70	125.26	.5161	.002	-1.169
14	.534	261.90	136.56	.5214	0.000	-1.077
15	.575	281.20	147.76	.5254	0.000	-.994
16	.615	300.20	158.06	.5265	.000	-.919
17	.656	319.40	167.76	.5252	.000	-.849
18	.696	338.50	176.86	.5225	.001	-.784
19	.736	357.40	186.66	.5223	.000	-.724
20	.777	376.40	197.66	.5251	.003	-.668
21	.817	395.40	207.56	.5249	.001	-.615
22	.857	414.50	216.56	.5224	.001	-.565
23	.887	424.00	220.56	.5202	0.000	-.529
24	.917	442.70	229.96	.5194	.002	-.495
25	.957	461.30	239.06	.5182	.001	-.451
26	.996	480.10	240.56	.5177	0.000	-.410
27	1.036	499.00	259.26	.5195	0.000	-.370
28	1.076	518.00	268.86	.5190	0.000	-.331
29	1.116	537.00	277.86	.5174	.000	-.294
30	1.157	556.20	286.76	.5156	0.000	-.258
31	1.198	575.80	295.86	.5138	.006	-.223
32	1.239	595.40	304.66	.5117	.024	-.189
33	1.281	614.90	313.46	.5098	.052	-.156
34	1.322	634.50	323.06	.5091	.074	-.124
35	1.363	653.80	333.16	.5096	.143	-.093
36	1.404	673.40	343.06	.5106	.256	-.064
37	1.446	693.50	354.66	.5114	.374	-.034
38	1.489	713.30	365.86	.5129	.477	-.005
39	1.531	733.30	377.56	.5149	.595	.022
40	1.573	753.30	388.46	.5157	.709	.050
41	1.615	773.30	398.26	.5150	.821	.076
42	1.658	793.50	407.36	.5134	.862	.102
43	1.701	813.60	415.36	.5105	.930	.128
44	1.743	833.60	425.36	.5103	.963	.152
45	1.786	853.90	436.56	.5112	.988	.177
46	1.829	874.10	447.86	.5124	.966	.201
47	1.871	894.30	460.26	.5147	1.055	.224
48	1.914	914.50	471.76	.5159	1.011	.247
49	1.957	935.00	482.06	.5156	1.017	.269

STEADY-STATE PHASE FRACTIONAL FLOW : .5156

50% BREAKTHROUGH (PORE VOLUME) : 1.4968

EXPERIMENT MO3PART

TUBE NUMBER	PORE VOLUMES	TOTAL PHASE VOLUME (CC)	PHASE VOLUME (CC)	FRACTIONAL FLOW	NORMALIZED CONCENTRATION	LAMBDA1
1	.010	9.10	4.46	.4896	.003	-8.129
2	.040	28.50	15.16	.5318	0.000	-3.812
3	.081	47.90	24.46	.5105	.001	-2.496
4	.122	67.40	33.76	.5008	0.000	-1.886
5	.163	86.80	44.36	.5110	.004	-1.505
6	.204	106.10	53.86	.5076	0.000	-1.234
7	.245	125.50	63.36	.5048	0.000	-1.024
8	.286	145.00	75.46	.5204	0.000	-.852
9	.327	164.40	85.86	.5222	.006	-.708
10	.369	183.90	94.56	.5142	.016	-.580
11	.410	203.50	103.46	.5084	.071	-.474
12	.451	223.10	114.76	.5144	.103	-.375
13	.493	242.70	125.26	.5161	.118	-.286
14	.534	261.90	136.56	.5214	.196	-.205
15	.575	281.20	147.76	.5254	.197	-.132
16	.615	300.20	158.06	.5265	.340	-.063
17	.656	319.40	167.76	.5252	.501	.000
18	.696	338.50	176.86	.5225	.525	.060
19	.736	357.40	186.66	.5223	.451	.116
20	.777	376.40	197.66	.5251	.602	.170
21	.817	395.40	207.56	.5249	.585	.220
22	.857	414.50	216.56	.5224	.691	.269
23	.887	424.00	220.56	.5202	.733	.304
24	.917	442.70	229.96	.5194	.812	.337
25	.957	461.30	239.06	.5182	.779	.380
26	.996	480.10	248.56	.5177	.908	.422
27	1.036	499.00	259.26	.5195	.640	.462
28	1.076	518.00	268.86	.5190	.845	.501
29	1.116	537.00	277.86	.5174	.921	.539
30	1.157	556.20	286.76	.5156	.918	.576
31	1.198	575.80	295.86	.5138	1.193	.612
32	1.239	595.40	304.66	.5117	1.083	.648
33	1.281	614.90	313.46	.5098	.935	.682
34	1.322	634.50	323.06	.5091	.927	.716
35	1.363	653.80	333.16	.5096	.952	.749
36	1.404	673.40	343.86	.5106	.945	.781
37	1.446	693.50	354.66	.5114	.860	.812
38	1.489	713.30	365.86	.5129	.814	.843
39	1.531	733.30	377.56	.5149	.860	.874
40	1.573	753.30	388.46	.5157	.972	.900
41	1.615	773.30	398.26	.5150	.987	.933
42	1.658	793.50	407.36	.5134	1.039	.962
43	1.701	813.60	415.36	.5105	1.083	.990
44	1.743	833.60	425.36	.5103	1.056	1.017
45	1.786	853.90	436.56	.5112	1.001	1.045
46	1.829	874.10	447.86	.5124	1.062	1.072
47	1.871	894.30	460.26	.5147	.956	1.098
48	1.914	914.50	471.76	.5159	.949	1.124
49	1.957	935.00	482.06	.5156	.896	1.149

STEADY-STATE PHASE FRACTIONAL FLOW : .5156

50% BREAKTHROUGH (PORE VOLUME) : .6555

EXPERIMENT MO3UF

TUBE NUMBER	PORE VOLUMES	TOTAL PHASE VOLUME (CC)	PHASE VOLUME (CC)	FRACTIONAL FLOW	NORMALIZED CONCENTRATION	LAMBDA1
1	.010	9.10	4.64	.5104	.005	-8.503
2	.040	28.50	13.34	.4682	0.000	-4.004
3	.081	47.90	23.44	.4895	0.000	-2.638
4	.122	67.40	33.64	.4992	0.000	-2.008
5	.163	86.80	42.44	.4890	0.000	-1.616
6	.204	106.10	52.24	.4924	0.000	-1.338
7	.245	125.50	62.14	.4952	0.000	-1.123
8	.286	145.00	69.54	.4796	.010	-.948
9	.327	164.40	78.54	.4778	.015	-.882
10	.369	183.90	89.34	.4858	.030	-.675
11	.410	203.50	100.04	.4916	.080	-.564
12	.451	223.10	108.34	.4856	.089	-.464
13	.493	242.70	117.44	.4839	.146	-.375
14	.534	261.90	125.34	.4786	.161	-.293
15	.575	281.20	133.44	.4746	.205	-.219
16	.615	300.20	142.14	.4735	.320	-.151
17	.656	319.40	151.64	.4748	.400	-.087
18	.696	338.50	161.64	.4775	.469	-.027
19	.736	357.40	170.74	.4777	.534	.029
20	.777	376.40	178.74	.4749	.600	.082
21	.817	395.40	187.84	.4751	.665	.133
22	.857	414.50	197.94	.4776	.754	.181
23	.887	424.02	203.44	.4798	.834	.216
24	.917	442.70	212.74	.4806	.914	.249
25	.957	461.30	222.24	.4818	.970	.292
26	.996	480.10	231.54	.4823	.941	.333
27	1.036	499.00	239.74	.4805	.743	.373
28	1.076	518.00	249.14	.4810	.841	.411
29	1.116	537.00	259.14	.4826	.939	.449
30	1.157	556.20	269.44	.4844	.956	.485
31	1.198	575.80	279.94	.4862	1.051	.521
32	1.239	595.40	290.74	.4883	1.021	.557
33	1.281	614.90	301.44	.4902	1.011	.591
34	1.322	634.50	311.44	.4909	.985	.624
35	1.363	653.80	320.64	.4904	.966	.656
36	1.404	673.40	329.54	.4894	.995	.688
37	1.446	693.50	338.84	.4886	.935	.719
38	1.489	713.30	347.44	.4871	.986	.749
39	1.531	733.30	355.74	.4851	.988	.779
40	1.573	753.30	364.84	.4843	.956	.809
41	1.615	773.30	375.04	.4850	.935	.837
42	1.658	793.50	386.14	.4866	1.003	.866
43	1.701	813.60	398.24	.4895	1.062	.893
44	1.743	833.60	408.24	.4897	1.068	.920
45	1.786	853.90	417.34	.4888	.990	.947
46	1.829	874.10	426.24	.4876	1.051	.973
47	1.871	894.30	434.24	.4853	.945	.999
48	1.914	914.50	442.74	.4841	.970	1.024
49	1.957	935.00	452.94	.4844	.943	1.050

STEADY-STATE PHASE FRACTIONAL FLOW : .4845

50% BREAKTHROUGH (PORE VOLUME) : .7154

EXPERIMENT MO4LO

TUBE NUMBER	PORE VOLUMES	TOTAL PHASE VOLUME (CC)	PHASE VOLUME (CC)	FRACTIONAL FLOW	NORMALIZED CONCENTRATION	LAMBDA
1	.020	19.00	3.61	.1897	0.000	-10.360
2	.061	38.80	8.01	.2063	0.000	-5.828
3	.103	58.70	12.31	.2096	0.000	-4.399
4	.146	78.90	16.61	.2105	0.000	-3.628
5	.188	99.10	20.61	.2079	0.000	-3.123
6	.231	119.45	24.61	.2060	0.000	-2.758
7	.274	139.65	28.91	.2070	0.000	-2.478
8	.317	159.95	34.01	.2126	0.000	-2.253
9	.360	179.95	39.51	.2195	0.000	-2.067
10	.402	200.15	45.51	.2274	0.000	-1.910
11	.445	220.35	50.61	.2297	0.000	-1.773
12	.488	240.55	56.01	.2328	0.000	-1.652
13	.530	260.45	61.31	.2354	0.000	-1.545
14	.572	280.45	66.51	.2371	0.000	-1.449
15	.615	300.75	72.01	.2394	0.000	-1.361
16	.658	320.95	77.61	.2418	0.000	-1.281
17	.701	341.15	83.01	.2433	0.000	-1.207
18	.744	361.55	88.01	.2430	0.000	-1.138
19	.787	381.95	93.41	.2445	0.000	-1.073
20	.830	402.15	101.81	.2532	0.000	-1.013
21	.873	422.45	109.51	.2592	0.000	-.957
22	.916	442.75	116.61	.2634	0.000	-.904
23	.959	463.15	122.81	.2652	0.000	-.854
24	1.002	483.65	128.81	.2663	0.000	-.806
25	1.045	504.05	134.21	.2663	0.000	-.761
26	1.388	524.25	138.91	.2650	0.000	-.718
27	1.131	544.55	143.91	.2643	0.000	-.677
28	1.175	565.45	149.51	.2644	0.000	-.637
29	1.218	585.70	154.71	.2641	0.000	-.599
30	1.261	606.10	159.71	.2635	0.000	-.563
31	1.304	626.60	164.41	.2624	0.000	-.528
32	1.348	647.00	169.21	.2615	0.000	-.494
33	1.391	667.10	174.21	.2611	0.000	-.462
34	1.433	687.20	179.61	.2614	0.000	-.431
35	1.476	707.40	184.71	.2611	0.000	-.401
36	1.519	727.80	189.71	.2607	0.000	-.372
37	1.561	747.60	194.81	.2606	0.000	-.344
38	1.603	767.60	199.81	.2603	0.000	-.317
39	1.646	787.90	205.01	.2602	0.000	-.290
40	1.689	808.30	209.71	.2594	.000	-.264
41	1.732	828.80	214.31	.2586	.007	-.239
42	1.776	849.30	219.21	.2581	.004	-.214
43	1.819	869.50	224.21	.2579	.029	-.190
44	1.862	890.40	229.81	.2581	.056	-.166
45	1.906	910.80	235.31	.2583	.087	-.143
46	1.949	931.40	241.21	.2590	.106	-.120
47	1.993	951.70	246.51	.2590	.180	-.098
48	2.035	971.60	251.21	.2585	.229	-.077
49	2.077	991.60	255.51	.2577	.281	-.056
50	2.119	1011.30	260.51	.2576	.344	-.036
51	2.161	1031.20	265.81	.2578	.428	-.017
52	2.204	1051.20	271.16	.2579	.511	.003
53	2.246	1071.05	275.81	.2575	.572	.022
54	2.288	1090.85	280.86	.2575	.618	.040

55	2.330	1110.55	286.66	.2581	.716	.058
56	2.372	1130.55	293.76	.2598	.799	.076
57	2.414	1150.40	299.36	.2602	.883	.094
58	2.456	1170.30	304.46	.2602	.889	.111
59	2.498	1190.25	309.11	.2597	.904	.128
60	2.543	1210.20	313.36	.2589	.958	.145
61	2.582	1230.15	317.61	.2582	.965	.161
62	2.628	1253.15	324.41	.2589	.970	.179
63	2.674	1273.35	329.41	.2587	1.001	.196
64	2.716	1293.45	334.61	.2587	1.018	.212
65	2.759	1313.75	339.71	.2586	.996	.228
66	2.802	1333.75	345.11	.2587	.994	.243
67	2.844	1353.60	350.71	.2591	.998	.258
68	2.886	1373.50	355.81	.2590	1.019	.273
69	2.928	1393.45	360.46	.2587	1.023	.288
70	2.970	1413.40	364.71	.2580	1.015	.302

STEADY-STATE PHASE FRACTIONAL FLOW : .2581
50% BREAKTHROUGH (PORE VOLUME) : 2.1979

EXPERIMENT MO4PART

TUBE NUMBER	PORE VOLUMES	TOTAL PHASE VOLUME (CC)	PHASE VOLUME (CC)	FRACTIONAL FLOW	NORMALIZED CONCENTRATION	LAMBDA1
1	.020	19.00	3.61	.1897	.012	-5.753
2	.061	38.80	8.01	.2063	.016	-3.101
3	.103	58.70	12.31	.2096	.003	-2.232
4	.146	78.90	16.61	.2105	0.000	-1.746
5	.188	99.10	20.61	.2079	0.000	-1.418
6	.231	119.45	24.61	.2060	.012	-1.173
7	.274	139.65	28.91	.2070	0.000	-.980
8	.317	159.95	34.01	.2126	0.000	-.821
9	.360	179.95	39.51	.2195	.007	-.686
10	.402	200.15	45.51	.2274	.002	-.569
11	.445	220.35	50.61	.2297	.016	-.464
12	.488	240.55	56.01	.2328	.053	-.371
13	.530	260.45	61.31	.2354	.136	-.286
14	.572	280.45	66.51	.2371	.268	-.209
15	.615	300.75	72.01	.2394	.377	-.137
16	.658	320.95	77.61	.2418	.382	-.069
17	.701	341.15	83.01	.2433	.477	-.006
18	.744	361.55	88.01	.2434	.702	.053
19	.787	381.95	93.41	.2445	.638	.110
20	.830	402.15	101.81	.2532	.437	.163
21	.873	422.45	109.51	.2592	.430	.214
22	.916	442.75	116.61	.2634	.542	.262
23	.959	463.15	122.81	.2652	.632	.308
24	1.002	483.65	128.81	.2663	.752	.353
25	1.045	504.05	134.21	.2663	.895	.396
26	1.088	524.25	138.91	.2650	1.057	.437
27	1.131	544.55	143.91	.2643	.980	.477
28	1.175	565.45	149.51	.2644	.979	.516
29	1.218	585.70	154.71	.2641	.977	.554
30	1.261	606.10	159.71	.2635	.968	.590
31	1.304	626.60	164.41	.2624	.925	.625
32	1.348	647.00	169.21	.2615	.974	.659
33	1.391	667.10	174.21	.2611	.935	.692
34	1.433	687.20	179.61	.2614	.884	.724
35	1.476	707.40	184.71	.2611	.979	.756
36	1.519	727.80	189.71	.2607	1.007	.786
37	1.561	747.60	194.81	.2606	.684	.816
38	1.603	767.60	199.81	.2603	1.048	.845
39	1.646	787.90	205.01	.2602	.997	.874
40	1.689	808.30	209.71	.2594	.751	.902
41	1.732	828.80	214.31	.2586	.972	.930
42	1.776	849.30	219.21	.2581	1.027	.957
43	1.819	869.50	224.21	.2579	1.009	.984
44	1.862	890.40	229.81	.2581	.961	1.010
45	1.906	910.80	235.31	.2583	1.007	1.036
46	1.949	931.40	241.21	.2590	1.001	1.061
47	1.993	951.70	246.51	.2590	1.030	1.086
48	2.035	971.60	251.21	.2585	1.013	1.110
49	2.077	991.60	255.51	.2577	.951	1.134
50	2.119	1011.30	260.51	.2576	1.025	1.157

STEADY-STATE PHASE FRACTIONAL FLOW : .2576
50% BREAKTHROUGH (PORE VOLUME) : .7051

EXPERIMENT MO4UP

TUBE NUMBER	PORE VOLUMES	TOTAL PHASE VOLUME (CC)	PHASE VOLUME (CC)	FRACTIONAL FLOW	NORMALIZED CONCENTRATION	LAMBDA1
1	.020	19.40	15.39	.8103	0.000	-5.724
2	.061	38.80	30.79	.7937	0.000	-3.083
3	.103	58.70	46.39	.7904	0.000	-2.217
4	.146	78.90	62.29	.7895	0.000	-1.733
5	.188	99.10	78.49	.7921	0.000	-1.406
6	.231	119.45	94.84	.7940	.002	-1.162
7	.274	139.65	110.74	.7930	.002	-.969
8	.317	159.95	125.94	.7874	0.000	-.810
9	.360	179.95	140.44	.7805	.002	-.676
10	.402	200.15	154.64	.7726	.009	-.559
11	.445	220.35	169.74	.7703	.028	-.455
12	.488	240.55	184.54	.7672	.057	-.361
13	.530	260.45	199.14	.7646	.129	-.276
14	.572	280.45	213.94	.7629	.277	-.199
15	.615	300.75	228.74	.7606	.391	-.127
16	.658	320.95	243.34	.7582	.460	-.060
17	.701	341.15	258.14	.7567	.502	.003
18	.744	361.55	273.54	.7566	.586	.063
19	.787	381.95	288.54	.7555	.696	.119
20	.830	402.15	300.34	.7468	.737	.173
21	.873	422.45	312.94	.7408	.812	.223
22	.916	442.75	326.14	.7366	.933	.272
23	.959	463.15	340.34	.7348	.977	.318
24	1.002	483.65	354.84	.7337	.996	.363
25	1.045	504.05	369.84	.7337	1.009	.406
26	1.088	524.25	385.34	.7350	.996	.447
27	1.131	544.55	400.64	.7357	.972	.487
28	1.175	565.45	415.94	.7356	.963	.526
29	1.218	585.70	430.99	.7359	.992	.564
30	1.261	606.10	446.39	.7365	1.004	.600
31	1.304	626.60	462.19	.7376	.940	.635
32	1.348	647.00	477.79	.7385	.984	.669
33	1.391	667.10	492.89	.7389	.962	.702
34	1.433	687.20	507.59	.7386	.945	.734
35	1.476	707.40	522.69	.7389	1.000	.766
36	1.519	727.80	538.49	.7399	1.050	.797
37	1.561	747.60	553.39	.7402	1.004	.826
38	1.603	767.60	568.39	.7405	1.042	.855
39	1.646	787.90	583.09	.7401	1.056	.884
40	1.689	808.30	597.99	.7398	1.030	.912
41	1.732	828.80	612.59	.7391	1.046	.940
42	1.776	849.30	627.79	.7392	.968	.968
43	1.819	869.50	643.29	.7398	.971	.994
44	1.862	890.40	659.89	.7411	.996	1.021
45	1.906	910.80	675.29	.7414	1.033	1.047
46	1.949	931.40	690.59	.7415	1.019	1.072
47	1.993	951.70	705.54	.7414	.998	1.097
48	2.035	971.60	720.79	.7419	1.004	1.121
49	2.077	991.60	735.74	.7420	1.038	1.145
50	2.119	1011.30	749.64	.7413	.999	1.168
51	2.161	1031.20	762.44	.7394	.953	1.191
52	2.204	1051.20	776.84	.7390	.998	1.213
53	2.246	1071.05	791.59	.7391	.989	1.236
54	2.288	1090.85	806.74	.7396	.969	1.257

55	2.330	1110.55	822.19	.7403	.980	1.279
56	2.372	1130.55	836.89	.7403	.964	1.300
57	2.414	1150.40	851.39	.7401	1.015	1.321
58	2.456	1170.30	866.64	.7405	.965	1.342
59	2.498	1190.25	881.54	.7406	.992	1.363
60	2.540	1210.20	895.69	.7401	1.035	1.383
61	2.582	1230.15	911.39	.7409	1.008	1.403
62	2.626	1253.15	927.59	.7402	1.013	1.424

STEADY-STATE PHASE FRACTIONAL FLOW : .7403
50% BREAKTHROUGH (PORE VOLUME) : .6984

EXPERIMENT MOS

TUBE NUMBER	PORE VOLUMES	TOTAL PHASE VOLUME (CC)	PHASE VOLUME (CC)	FRACTIONAL FLOW	NORMALIZED CONCENTRATION	LAMBDA1
1	.012	9.00	9.00	1.0000	0.000	-10.165
2	.039	27.90	27.90	1.0000	0.000	-4.871
3	.079	46.80	46.80	1.0000	0.000	-3.281
4	.119	65.50	65.50	1.0000	0.000	-2.561
5	.158	83.60	83.60	1.0000	0.000	-2.125
6	.196	102.00	102.00	1.0000	0.000	-1.817
7	.235	120.00	120.00	1.0000	0.000	-1.582
8	.274	138.60	138.60	1.0000	0.000	-1.392
9	.313	157.20	157.20	1.0000	0.000	-1.231
10	.352	175.20	175.20	1.0000	0.000	-1.097
11	.390	193.30	193.30	1.0000	0.000	-.980
12	.428	211.40	211.40	1.0000	0.000	-.877
13	.467	230.10	230.10	1.0000	0.000	-.783
14	.506	248.20	248.20	1.0000	0.000	-.697
15	.544	266.20	266.20	1.0000	.001	-.621
16	.583	285.00	285.00	1.0000	0.000	-.549
17	.623	303.70	303.70	1.0000	0.000	-.481
18	.663	322.50	322.50	1.0000	.005	-.418
19	.702	341.10	341.10	1.0000	0.000	-.358
20	.741	359.60	359.60	1.0000	.004	-.303
21	.781	378.10	378.10	1.0000	.002	-.251
22	.820	396.40	396.40	1.0000	.015	-.202
23	.859	415.10	415.10	1.0000	.046	-.156
24	.898	433.70	433.70	1.0000	.115	-.110
25	.938	452.30	452.30	1.0000	.221	-.068
26	.977	470.90	470.90	1.0000	.356	-.026
27	1.016	489.40	489.40	1.0000	.573	.013
28	1.055	508.00	508.00	1.0000	.747	.051
29	1.395	527.00	527.00	1.0000	.844	.088
30	1.136	546.10	546.10	1.0000	.918	.124
31	1.176	565.10	565.10	1.0000	.966	.159
32	1.216	584.00	584.00	1.0000	1.000	.193
33	1.256	602.90	602.90	1.0000	.957	.225
34	1.296	621.90	621.90	1.0000	.963	.257
35	1.336	640.70	640.70	1.0000	.973	.288
36	1.376	659.40	659.40	1.0000	.986	.317
37	1.415	678.00	678.00	1.0000	.995	.346
38	1.454	696.40	696.40	1.0000	.973	.374
39	1.494	715.00	715.00	1.0000	1.004	.401
40	1.533	733.50	733.50	1.0000	.995	.427
41	1.572	751.70	751.70	1.0000	1.009	.453
42	1.610	770.10	770.10	1.0000	.991	.478
43	1.649	788.40	788.40	1.0000	.988	.502

STEADY-STATE PHASE FRACTIONAL FLOW : 1.0000
50% BREAKTHROUGH (PORE VOLUME) : 1.0031

EXPERIMENT MW1

TUBE NUMBER	PORE VOLUMES	TOTAL PHASE VOLUME (CC)	PHASE VOLUME (CC)	FRACTIONAL FLOW	NORMALIZED CONCENTRATION	LAMBDA1
1	.018	16.70	16.70	1.0000	0.000	-7.465
2	.054	34.60	34.60	1.0000	0.000	-4.100
3	.092	52.60	52.60	1.0000	.001	-3.020
4	.130	70.70	70.70	1.0000	.001	-2.438
5	.169	88.80	88.80	1.0000	.000	-2.051
6	.208	107.30	107.30	1.0000	0.000	-1.766
7	.247	125.90	125.90	1.0000	.000	-1.541
8	.286	144.50	144.50	1.0000	0.000	-1.358
9	.326	163.10	163.10	1.0000	.001	-1.205
10	.365	181.60	181.60	1.0000	0.000	-1.074
11	.404	200.30	200.30	1.0000	0.000	-.959
12	.444	219.00	219.00	1.0000	.001	-.856
13	.483	237.70	237.70	1.0000	.001	-.764
14	.523	256.40	256.40	1.0000	0.000	-.681
15	.562	275.10	275.10	1.0000	.001	-.604
16	.602	293.90	293.90	1.0000	0.000	-.533
17	.642	312.60	312.60	1.0000	0.000	-.467
18	.682	331.60	331.60	1.0000	0.000	-.406
19	.721	350.20	350.20	1.0000	.005	-.348
20	.761	368.90	368.90	1.0000	.005	-.294
21	.800	387.50	387.50	1.0000	.011	-.243
22	.840	406.10	406.10	1.0000	.026	-.195
23	.879	424.80	424.80	1.0000	.093	-.148
24	.919	443.40	443.40	1.0000	.155	-.104
25	.958	462.10	462.10	1.0000	.258	-.062
26	.998	480.90	480.90	1.0000	.397	-.022
27	1.038	499.60	499.60	1.0000	.583	.017
28	1.077	518.30	518.30	1.0000	.759	.055
29	1.117	537.20	537.20	1.0000	.908	.091
30	1.157	556.00	556.00	1.0000	.931	.126
31	1.197	574.80	574.80	1.0000	.955	.160
32	1.236	593.60	593.60	1.0000	.993	.193
33	1.276	612.40	612.40	1.0000	1.000	.225
34	1.316	631.20	631.20	1.0000	1.008	.256
35	1.356	650.00	650.00	1.0000	1.053	.286
36	1.395	668.70	668.70	1.0000	.998	.315
37	1.435	687.40	687.40	1.0000	.986	.343
38	1.474	706.00	706.00	1.0000	.985	.371
39	1.514	724.50	724.50	1.0000	.979	.398
40	1.554	743.90	743.90	1.0000	1.001	.424

STEADY-STATE PHASE FRACTIONAL FLOW : 1.0000
50% BREAKTHROUGH (PORE VOLUME) : 1.0199

EXPERIMENT MW2LO

TUBE NUMBER	PORE VOLUMES	TOTAL PHASE VOLUME (CC)	PHASE VOLUME (CC)	FRACTIONAL FLOW	NORMALIZED CONCENTRATION	LAMBDA1
1	.018	17.30	2.53	.1461	.002	-6.632
2	.056	35.70	6.33	.1772	0.000	-3.615
3	.095	54.10	10.43	.1927	0.000	-2.640
4	.134	72.60	14.53	.2001	0.000	-2.106
5	.173	91.10	19.03	.2089	0.000	-1.750
6	.212	109.60	23.53	.2147	0.000	-1.488
7	.252	128.30	28.13	.2192	0.000	-1.281
8	.291	146.90	32.43	.2207	0.000	-1.111
9	.330	165.40	35.93	.2172	0.000	-.969
10	.370	184.20	38.13	.2072	0.000	-.846
11	.409	202.60	40.33	.1990	0.000	-.737
12	.449	221.30	43.63	.1971	.001	-.639
13	.488	240.20	47.93	.1995	.006	-.551
14	.528	259.00	52.03	.2009	.166	-.470
15	.568	277.80	56.23	.2024	.201	-.395
16	.608	296.60	60.23	.2031	.223	-.327
17	.648	315.40	64.53	.2046	.298	-.263
18	.688	334.30	69.13	.2068	.340	-.202
19	.728	353.40	73.73	.2086	.344	-.145
20	.768	372.40	78.53	.2109	.380	-.091
21	.808	391.30	83.23	.2127	.443	-.040
22	.848	410.20	87.93	.2144	.512	.008
23	.888	429.30	92.33	.2151	.498	.054
24	.929	448.30	97.53	.2175	.546	.099
25	.969	467.20	102.23	.2188	.605	.141
26	1.009	486.20	107.03	.2201	.609	.182
27	1.049	505.30	111.83	.2213	.719	.221
28	1.089	524.20	116.83	.2229	.710	.259
29	1.129	543.10	121.13	.2230	.736	.295
30	1.169	562.00	126.03	.2242	.783	.331
31	1.210	581.00	130.93	.2253	.935	.365
32	1.250	600.10	136.13	.2268	.977	.398
33	1.290	619.30	140.93	.2276	1.003	.431
34	1.331	638.40	144.93	.2270	1.018	.463
35	1.371	657.20	149.73	.2278	.921	.493
36	1.411	676.10	154.83	.2290	.924	.523
37	1.451	694.90	159.53	.2296	1.012	.552
38	1.491	713.80	164.03	.2298	.932	.580
39	1.531	732.80	168.43	.2298	.953	.607
40	1.571	751.70	172.93	.2300	.980	.635
41	1.611	770.50	177.33	.2301	.944	.661
42	1.651	789.30	181.33	.2297	.932	.687
43	1.690	808.20	185.43	.2294	.970	.712
44	1.730	827.10	189.83	.2295	.916	.737
45	1.763	839.40	192.83	.2297	.969	.757

STEADY-STATE PHASE FRACTIONAL FLOW : .2298
50% BREAKTHROUGH (PORE VOLUME) : .8414

EXPERIMENT MW2PART

TUBE NUMBER	PORE VOLUMES	TOTAL PHASE VOLUME (CC)	PHASE VOLUME (CC)	FRACTIONAL FLOW	NORMALIZED CONCENTRATION	LAMBDA
1	.018	17.30	14.77	.8539	.003	-6.508
2	.056	35.70	29.37	.8228	0.000	-3.541
3	.095	54.10	43.67	.8073	0.000	-2.580
4	.134	72.60	58.07	.7999	0.000	-2.054
5	.173	91.10	72.07	.7911	0.000	-1.703
6	.212	109.60	86.07	.7853	0.000	-1.443
7	.252	128.30	100.17	.7808	0.000	-1.239
8	.291	146.90	114.47	.7793	0.000	-1.070
9	.330	165.40	129.47	.7828	0.000	-.929
10	.370	184.00	145.87	.7928	0.000	-.807
11	.409	202.60	162.27	.8010	0.000	-.699
12	.449	221.30	177.67	.8029	.001	-.602
13	.488	240.20	192.27	.8005	.007	-.513
14	.528	259.00	206.97	.7991	.184	-.433
15	.568	277.80	221.57	.7976	.248	-.359
16	.608	296.60	236.37	.7969	.224	-.290
17	.648	315.40	250.87	.7954	.331	-.226
18	.688	334.30	265.17	.7932	.383	-.166
19	.728	353.40	279.67	.7914	.379	-.109
20	.768	372.40	293.87	.7891	.423	-.055
21	.808	391.30	308.07	.7873	.493	-.004
22	.848	410.20	322.27	.7856	.569	.044
23	.888	429.30	336.97	.7849	.555	.090
24	.929	448.30	350.77	.7825	.608	.135
25	.969	467.20	364.97	.7812	.674	.177
26	1.009	486.20	379.17	.7799	.678	.218
27	1.049	505.30	393.47	.7787	.801	.257
28	1.089	524.20	407.37	.7771	.790	.295
29	1.129	543.10	421.97	.7770	.718	.332
30	1.169	562.00	435.97	.7758	.872	.367
31	1.210	581.00	450.07	.7747	1.041	.402
32	1.250	600.10	463.97	.7732	1.117	.435
33	1.290	619.30	478.37	.7724	1.088	.468
34	1.331	638.40	493.47	.7730	1.133	.500
35	1.371	657.20	507.47	.7722	.924	.530
36	1.411	676.10	521.27	.7710	1.029	.560
37	1.451	694.90	535.37	.7704	1.126	.589
38	1.491	713.80	549.77	.7702	1.004	.617
39	1.531	732.80	564.37	.7702	.986	.645
40	1.571	751.70	578.77	.7700	.876	.672
41	1.611	770.50	593.17	.7699	.983	.699
42	1.651	789.30	607.97	.7703	1.036	.725
43	1.690	808.20	622.77	.7706	1.181	.750
44	1.730	827.10	637.27	.7705	.925	.775
45	1.763	839.40	646.57	.7703	.850	.796

STEADY-STATE PHASE FRACTIONAL FLOW : .7703
50% BREAKTHROUGH (PORE VOLUME) : .8117

EXPERIMENT MW2UP

TUBE NUMBER	PORE VOLUMES	TOTAL PHASE VOLUME (CC)	PHASE VOLUME (CC)	FRACTIONAL FLOW	NORMALIZED CONCENTRATION	LAMBDA1
1	.018	17.30	14.77	.8539	.002	-8.057
2	.056	35.70	29.37	.8228	0.000	-4.459
3	.095	54.10	43.67	.8073	0.000	-3.311
4	.134	72.60	58.07	.7999	0.000	-2.691
5	.173	91.10	72.07	.7911	0.000	-2.283
6	.212	109.60	86.07	.7853	.002	-1.985
7	.252	128.30	100.17	.7898	0.000	-1.752
8	.291	146.90	114.47	.7793	0.000	-1.563
9	.330	165.40	129.47	.7828	0.000	-1.406
10	.370	184.00	145.87	.7928	0.000	-1.270
11	.409	202.60	162.27	.8010	0.000	-1.152
12	.449	221.30	177.67	.8029	.005	-1.047
13	.488	240.20	192.27	.8005	0.000	-.952
14	.528	259.00	206.97	.7991	.001	-.866
15	.568	277.80	221.57	.7976	0.000	-.787
16	.608	296.60	236.37	.7969	0.000	-.715
17	.648	315.40	250.87	.7954	.002	-.648
18	.688	334.30	265.17	.7932	0.000	-.585
19	.728	353.40	279.67	.7914	0.000	-.526
20	.768	372.40	293.87	.7891	0.000	-.471
21	.808	391.30	308.07	.7873	0.000	-.419
22	.848	410.20	322.27	.7856	0.000	-.369
23	.888	429.30	336.97	.7849	0.000	-.322
24	.929	448.30	350.77	.7825	.002	-.277
25	.969	467.20	364.97	.7812	.012	-.235
26	1.009	486.20	379.17	.7799	.033	-.194
27	1.049	505.30	393.47	.7787	.069	-.155
28	1.089	524.20	407.37	.7771	.135	-.117
29	1.129	543.10	421.97	.7770	.226	-.081
30	1.169	562.00	435.97	.7758	.281	-.046
31	1.210	581.00	450.07	.7747	.430	-.012
32	1.250	600.10	463.97	.7732	.617	.020
33	1.293	619.30	478.37	.7724	.755	.052
34	1.331	638.40	493.47	.7730	.954	.083
35	1.371	657.20	507.47	.7722	.980	.113
36	1.411	676.10	521.27	.7710	.988	.142
37	1.451	694.90	535.37	.7704	.973	.170
38	1.491	713.80	549.77	.7702	.963	.197
39	1.531	732.80	564.37	.7702	1.053	.224
40	1.571	751.70	578.77	.7700	.921	.250
41	1.611	770.50	593.17	.7699	1.052	.275
42	1.651	789.30	607.97	.7703	.987	.300
43	1.690	808.20	622.77	.7706	1.091	.324
44	1.730	827.10	637.27	.7705	1.030	.347
45	1.763	839.40	646.57	.7703	.941	.367

STEADY-STATE PHASE FRACTIONAL FLOW : .7703

50% BREAKTHROUGH (PORE VOLUME) : 1.2247

EXPERIMENT M43LO

TUBE NUMBER	PORE VOLUMES	TOTAL PHASE VOLUME (CC)	PHASE VOLUME (CC)	FRACTIONAL FLOW	NORMALIZED CONCENTRATION	LAMBDA1
1	.020	18.80	8.67	.4611	0.000	-5.874
2	.060	38.10	18.07	.4743	0.000	-3.183
3	.101	57.30	27.57	.4811	0.000	-2.308
4	.142	76.50	36.57	.4780	.003	-1.822
5	.182	95.70	45.77	.4783	0.000	-1.494
6	.223	114.70	55.27	.4819	0.000	-1.251
7	.263	133.70	64.77	.4844	.001	-1.060
8	.303	152.70	73.87	.4838	.002	-.901
9	.343	171.70	83.17	.4844	0.000	-.766
10	.383	190.70	92.47	.4849	0.000	-.649
11	.424	210.00	102.57	.4884	.002	-.544
12	.465	229.40	112.07	.4885	.008	-.449
13	.506	248.70	121.47	.4884	.016	-.363
14	.547	268.10	130.67	.4874	.030	-.284
15	.588	287.50	139.97	.4869	.126	-.211
16	.629	306.80	149.27	.4865	.282	-.143
17	.670	326.20	158.57	.4861	.371	-.080
18	.711	345.70	168.17	.4865	.442	-.020
19	.752	364.90	177.17	.4855	.604	.036
20	.793	384.30	185.97	.4839	.629	.089
21	.834	403.70	195.67	.4847	.640	.139
22	.875	423.30	205.47	.4857	.679	.187
23	.916	442.30	215.07	.4863	.732	.233
24	.957	461.80	224.77	.4867	.791	.277
25	.998	481.20	234.77	.4879	.848	.320
26	1.039	500.70	243.87	.4871	.936	.361
27	1.080	520.10	253.67	.4877	.979	.400
28	1.121	539.70	263.67	.4885	1.013	.439
29	1.163	559.30	273.57	.4891	1.059	.476
30	1.204	578.80	283.27	.4894	.936	.512
31	1.246	598.30	292.77	.4893	.997	.547
32	1.287	617.90	302.47	.4895	1.013	.581
33	1.328	637.50	311.87	.4892	1.002	.614
34	1.370	657.10	321.77	.4897	.979	.646
35	1.412	676.80	331.07	.4892	1.000	.678

STEADY-STATE PHASE FRACTIONAL FLOW : .4892
50% BREAKTHROUGH (PORE VOLUME) : .7257

EXPERIMENT MW3PART

TUBE NUMBER	PORE VOLUMES	TOTAL PHASE VOLUME (CC)	PHASE VOLUME (CC)	FRACTIONAL FLOW	NORMALIZED CONCENTRATION	LAMBDA
1	.020	18.80	8.67	.4611	0.000	-5.925
2	.060	38.10	18.07	.4743	0.000	-3.214
3	.101	57.30	27.57	.4811	0.000	-2.333
4	.142	76.50	36.57	.4780	0.000	-1.844
5	.182	95.70	45.77	.4783	0.000	-1.515
6	.223	114.70	55.27	.4819	0.000	-1.271
7	.263	133.70	64.77	.4844	0.000	-1.078
8	.303	152.70	73.87	.4838	0.000	-.919
9	.343	171.70	83.17	.4844	0.000	-.784
10	.383	190.70	92.47	.4849	0.000	-.666
11	.424	210.00	102.57	.4884	0.000	-.561
12	.465	229.40	112.07	.4885	0.000	-.466
13	.506	248.70	121.47	.4884	0.000	-.379
14	.547	268.10	130.67	.4874	.027	-.300
15	.588	287.50	139.97	.4869	.166	-.227
16	.629	306.80	149.27	.4865	.241	-.160
17	.670	326.20	158.57	.4861	.382	-.096
18	.711	345.70	168.17	.4865	.415	-.037
19	.752	364.90	177.17	.4855	.546	.019
20	.793	384.30	185.97	.4839	.733	.072
21	.834	403.70	195.67	.4847	.650	.123
22	.875	423.00	205.47	.4857	.758	.171
23	.916	442.30	215.07	.4863	.604	.217
24	.957	461.80	224.77	.4867	.873	.261
25	.998	481.20	234.77	.4879	.853	.303
26	1.039	500.70	243.87	.4871	.821	.344
27	1.080	520.10	253.67	.4877	.906	.384
28	1.121	539.70	263.67	.4885	.941	.422
29	1.163	559.30	273.57	.4891	.784	.459
30	1.204	578.80	283.27	.4894	1.040	.495
31	1.246	598.30	292.77	.4893	1.035	.530
32	1.287	617.90	302.47	.4895	1.131	.564
33	1.328	637.50	311.87	.4892	1.043	.597
34	1.370	657.10	321.77	.4897	1.228	.629
35	1.412	676.80	331.07	.4892	1.241	.660
36	1.453	696.30	340.57	.4891	.993	.691
37	1.494	715.80	349.87	.4888	.902	.721
38	1.535	735.20	359.47	.4889	.905	.750
39	1.576	754.50	369.37	.4896	.938	.778
40	1.617	773.90	378.77	.4894	1.066	.805
41	1.659	793.60	388.17	.4891	1.171	.833
42	1.700	813.20	397.47	.4888	.971	.860
43	1.742	832.70	407.07	.4889	.911	.886
44	1.783	852.30	416.97	.4892	1.050	.912
45	1.824	871.70	426.47	.4892	1.000	.937
46	1.866	891.30	436.27	.4895	.904	.962
47	1.907	910.90	446.17	.4898	1.118	.986
48	1.949	930.50	455.57	.4896	.802	1.010
49	1.990	950.10	464.77	.4892	.858	1.034
50	2.032	969.70	474.07	.4897	1.146	1.057

STEADY-STATE PHASE FRACTIONAL FLOW : .4898
50% BREAKTHROUGH (PORE VOLUME) : .7377

EXPERIMENT MW3UP

TUBE NUMBER	PORE VOLUMES	TOTAL PHASE VOLUME (CC)	PHASE VOLUME (CC)	FRACTIONAL FLOW	NORMALIZED CONCENTRATION	LAMBDA1
1	.020	18.80	8.67	.4611	.011	-8.710
2	.060	38.10	18.07	.4743	.008	-4.875
3	.101	57.30	27.57	.4811	0.000	-3.662
4	.142	76.50	36.57	.4780	0.000	-3.005
5	.182	95.70	45.77	.4783	0.000	-2.572
6	.223	114.70	55.27	.4819	.011	-2.250
7	.263	133.70	64.77	.4844	.008	-2.015
8	.303	152.70	73.87	.4838	0.000	-1.818
9	.343	171.70	83.17	.4844	0.000	-1.653
10	.383	190.70	92.47	.4849	0.000	-1.512
11	.424	210.00	102.57	.4884	0.000	-1.388
12	.465	229.40	112.07	.4885	0.000	-1.277
13	.506	248.70	121.47	.4884	0.000	-1.178
14	.547	268.10	130.67	.4874	0.000	-1.089
15	.588	287.50	139.97	.4869	0.000	-1.007
16	.629	306.80	149.27	.4865	.011	-.932
17	.670	326.20	158.57	.4861	.008	-.863
18	.711	345.70	168.17	.4865	0.000	-.798
19	.752	364.90	177.17	.4855	0.000	-.738
20	.793	384.30	185.97	.4839	0.000	-.682
21	.834	403.70	195.67	.4847	0.000	-.629
22	.875	423.00	205.47	.4857	0.000	-.579
23	.916	442.30	215.07	.4863	0.000	-.532
24	.957	461.80	224.77	.4867	.006	-.486
25	.998	481.20	234.77	.4879	.006	-.443
26	1.039	500.70	243.87	.4871	0.000	-.402
27	1.080	520.10	253.67	.4877	.003	-.362
28	1.121	539.70	263.67	.4885	0.000	-.324
29	1.163	559.30	273.57	.4891	.003	-.287
30	1.204	578.80	283.27	.4894	.007	-.252
31	1.246	598.30	292.77	.4893	.012	-.218
32	1.287	617.90	302.47	.4895	.036	-.185
33	1.328	637.50	311.87	.4892	.063	-.154
34	1.370	657.10	321.77	.4897	.117	-.123
35	1.412	676.80	331.07	.4892	.146	-.093
36	1.453	696.30	340.57	.4891	.266	-.064
37	1.494	715.80	349.87	.4888	.343	-.036
38	1.535	735.20	359.47	.4889	.468	-.009
39	1.576	754.50	369.37	.4896	.566	.018
40	1.617	773.90	378.77	.4894	.644	.043
41	1.659	793.60	388.17	.4891	.866	.069
42	1.700	813.20	397.47	.4888	.926	.093
43	1.742	832.70	407.07	.4889	1.005	.117
44	1.783	852.30	416.97	.4892	.968	.141
45	1.824	871.70	426.47	.4892	1.066	.164
46	1.866	891.30	436.27	.4895	.947	.186
47	1.907	910.90	446.17	.4898	1.047	.208
48	1.949	930.50	455.57	.4896	1.094	.230
49	1.990	950.10	464.77	.4892	.955	.251
50	2.032	969.70	474.87	.4897	1.133	.272

STEADY-STATE PHASE FRACTIONAL FLOW : .4898
50% BREAKTHROUGH (PORE VOLUME) : 1.5488

EXPERIMENT MW4LO

TUBE NUMBER	PORE VOLUMES	TOTAL PHASE VOLUME (CC)	PHASE VOLUME (CC)	FRACTIONAL FLOW	NORMALIZED CONCENTRATION	LAMBDA1
1	.019	18.25	14.26	.7813	0.000	-6.071
2	.059	37.35	28.96	.7754	0.000	-3.290
3	.099	56.25	43.61	.7753	0.000	-2.388
4	.139	75.25	58.31	.7749	0.000	-1.890
5	.179	94.10	72.86	.7743	0.000	-1.557
6	.219	113.05	87.26	.7719	0.000	-1.309
7	.259	132.05	101.56	.7691	0.000	-1.112
8	.300	151.00	115.86	.7673	0.000	-.950
9	.340	170.05	130.26	.7660	0.000	-.812
10	.380	188.90	144.56	.7653	0.000	-.693
11	.430	217.30	166.01	.7640	0.000	-.564
12	.490	246.05	188.26	.7651	.003	-.428
13	.550	274.15	209.71	.7649	.025	-.310
14	.610	302.20	230.66	.7633	.066	-.207
15	.654	316.15	241.01	.7623	.215	-.136
16	.699	344.20	261.61	.7601	.362	-.070
17	.758	372.45	282.81	.7593	.523	.011
18	.818	400.65	304.06	.7589	.762	.087
19	.868	419.45	318.51	.7593	.882	.146
20	.908	438.15	332.81	.7596	.930	.191
21	.947	457.20	347.26	.7595	.962	.235
22	.988	476.15	361.46	.7591	.962	.276
23	1.028	495.15	375.96	.7593	.949	.317
24	1.068	514.25	390.56	.7595	1.020	.356
25	1.109	533.45	405.26	.7597	.937	.394
26	1.149	552.75	420.06	.7599	.921	.430
27	1.190	571.85	434.66	.7601	1.007	.466
28	1.231	591.05	448.81	.7593	.991	.501
29	1.271	610.25	463.31	.7592	.930	.534
30	1.312	629.65	478.16	.7594	.992	.567
31	1.353	648.95	492.81	.7594	.959	.599
32	1.394	668.15	507.41	.7594	.968	.630
33	1.435	687.60	522.11	.7593	.964	.660
34	1.476	706.85	536.76	.7594	1.008	.690
35	1.517	726.25	551.61	.7595	.954	.719
36	1.558	745.65	566.51	.7598	1.016	.747
37	1.599	765.25	581.46	.7598	.990	.775

STEADY-STATE PHASE FRACTIONAL FLOW : .7599
50% BREAKTHROUGH (PORE VOLUME) : .7498

EXPERIMENT MW4PART

TUBE NUMBER	PORE VOLUMES	TOTAL PHASE VOLUME (CC)	PHASE VOLUME (CC)	FRACTIONAL FLOW	NORMALIZED CONCENTRATION	LAMBDA1
1	.019	18.25	3.99	.2187	0.000	-6.190
2	.059	37.35	8.39	.2246	0.000	-3.362
3	.099	56.25	12.64	.2247	.001	-2.446
4	.139	75.25	16.94	.2251	0.000	-1.942
5	.179	94.10	21.24	.2257	0.000	-1.604
6	.219	113.05	25.79	.2281	0.000	-1.353
7	.259	132.05	30.49	.2309	0.000	-1.155
8	.300	151.00	35.14	.2327	0.000	-.991
9	.340	170.05	39.79	.2340	0.000	-.853
10	.380	188.90	44.34	.2347	0.000	-.733
11	.430	217.30	51.29	.2360	0.000	-.602
12	.490	246.05	57.79	.2349	.010	-.466
13	.550	274.15	64.44	.2351	.021	-.340
14	.610	302.20	71.54	.2367	.139	-.244
15	.654	316.15	75.14	.2377	.246	-.174
16	.699	344.20	82.59	.2399	.425	-.100
17	.758	372.45	89.64	.2407	.356	-.026
18	.818	400.65	96.59	.2411	.792	.050
19	.868	419.45	100.94	.2407	.845	.109
20	.908	438.15	105.34	.2404	.905	.154
21	.947	457.20	109.94	.2405	.925	.197
22	.988	476.15	114.69	.2409	.948	.239
23	1.028	495.15	119.19	.2407	.879	.279
24	1.068	514.25	123.69	.2405	.924	.318
25	1.109	533.45	128.19	.2403	.847	.356
26	1.149	552.75	132.69	.2401	.956	.393
27	1.190	571.85	137.19	.2399	.983	.428
28	1.231	591.05	142.24	.2407	.973	.462
29	1.271	610.25	146.94	.2408	.995	.496
30	1.312	629.65	151.49	.2406	.996	.528
31	1.353	648.95	156.14	.2406	1.048	.560
32	1.394	668.15	160.74	.2406	.988	.591
33	1.435	687.60	165.49	.2407	1.025	.621
34	1.476	706.85	170.09	.2406	.987	.651
35	1.517	726.25	174.64	.2405	1.002	.680
36	1.558	745.65	179.14	.2402	1.001	.708
37	1.599	765.25	183.79	.2402	.951	.736

STEADY-STATE PHASE FRACTIONAL FLOW : .2402

50% BREAKTHROUGH (PORE VOLUME) : .7782

EXPERIMENT MW4UP

TUBE NUMBER	PORE VOLUMES	TOTAL PHASE VOLUME (CC)	PHASE VOLUME (CC)	FRACTIONAL FLOW	NORMALIZED CONCENTRATION	LAMBDA1
1	.019	18.25	3.99	.2187	0.000	-11.037
2	.059	37.35	8.39	.2246	0.000	-6.218
3	.099	56.25	12.64	.2247	0.000	-4.710
4	.139	75.25	16.94	.2251	0.000	-3.904
5	.179	94.10	21.24	.2257	.001	-3.379
6	.219	113.05	25.79	.2281	0.000	-3.000
7	.259	132.05	30.49	.2309	0.000	-2.707
8	.300	151.00	35.14	.2327	0.000	-2.471
9	.340	170.05	39.79	.2340	0.000	-2.276
10	.380	188.90	44.34	.2347	0.000	-2.110
11	.430	217.30	51.29	.2360	.003	-1.934
12	.490	246.05	57.79	.2349	0.000	-1.755
13	.550	274.15	64.44	.2351	0.000	-1.604
14	.610	302.20	71.54	.2367	0.000	-1.475
15	.654	316.15	75.14	.2377	0.000	-1.388
16	.699	344.20	82.59	.2399	.003	-1.309
17	.758	372.45	89.64	.2407	0.000	-1.212
18	.818	400.65	96.59	.2411	0.000	-1.125
19	.868	419.45	100.94	.2407	.001	-1.057
20	.908	438.15	105.34	.2404	0.000	-1.007
21	.947	457.20	109.94	.2405	0.000	-.959
22	.988	476.15	114.69	.2409	0.000	-.913
23	1.028	495.15	119.19	.2407	0.000	-.869
24	1.068	514.25	123.69	.2405	.002	-.828
25	1.109	533.45	128.19	.2403	0.000	-.788
26	1.149	552.75	132.69	.2401	0.000	-.749
27	1.190	571.85	137.19	.2399	.001	-.712
28	1.231	591.05	142.24	.2407	0.000	-.676
29	1.271	610.25	146.94	.2408	.003	-.642
30	1.312	629.65	151.49	.2406	.002	-.609
31	1.353	648.95	156.14	.2406	.007	-.577
32	1.394	668.15	160.74	.2406	.002	-.546
33	1.435	687.60	165.49	.2407	0.000	-.516
34	1.476	706.85	170.09	.2406	.003	-.487
35	1.517	726.25	174.64	.2405	0.000	-.459
36	1.558	745.65	179.14	.2402	.001	-.432
37	1.599	765.25	183.79	.2402	.003	-.405
38	1.640	784.65	188.44	.2402	0.000	-.379
39	1.681	804.20	193.04	.2400	.005	-.354
40	1.723	823.75	197.54	.2398	.008	-.329
41	1.764	842.90	201.84	.2395	.002	-.305
42	1.804	862.05	205.99	.2390	.006	-.282
43	1.845	881.50	210.19	.2384	.005	-.260
44	1.886	900.60	214.44	.2381	.012	-.238
45	1.926	919.70	218.79	.2379	.019	-.216
46	1.967	938.80	223.34	.2379	.031	-.196
47	2.007	957.80	227.64	.2377	.046	-.175
48	2.047	976.60	232.04	.2376	.067	-.155
49	2.087	995.70	236.29	.2373	.091	-.136
50	2.128	1014.80	240.64	.2371	.131	-.117
51	2.168	1033.95	244.99	.2369	.182	-.098
52	2.209	1053.25	249.39	.2368	.239	-.079
53	2.250	1072.65	253.69	.2365	.302	-.061
54	2.291	1092.05	258.24	.2365	.329	-.043

55	2.332	1111.35	262.89	.2366	.398	-.025
56	2.373	1130.85	267.49	.2365	.451	-.008
57	2.414	1150.15	271.89	.2364	.562	.010
58	2.454	1169.25	276.39	.2364	.618	.026
59	2.495	1188.55	280.94	.2364	.675	.043
60	2.536	1207.75	285.24	.2362	.738	.059
61	2.577	1227.10	289.59	.2360	.816	.075
62	2.618	1246.55	293.49	.2354	.839	.091
63	2.659	1266.00	298.24	.2356	.905	.106
64	2.700	1285.40	303.19	.2359	.898	.122
65	2.741	1304.75	308.14	.2362	.954	.137
66	2.782	1324.20	312.99	.2364	.982	.152
67	2.823	1343.70	317.64	.2364	.990	.166
68	2.864	1363.20	322.04	.2362	1.021	.181
69	2.905	1382.45	326.19	.2360	.993	.195
70	2.946	1401.75	330.64	.2359	.996	.209
71	2.973	1408.10	331.89	.2357	1.014	.218

STEADY-STATE PHASE FRACTIONAL FLOW : .2358
50% BREAKTHROUGH (PORE VOLUME) : 2.3909

EXPERIMENT MW5

TUBE NUMBER	PORE VOLUMES	TOTAL PHASE VOLUME (CC)	PHASE VOLUME (CC)	FRACTIONAL FLOW	NORMALIZED CONCENTRATION	LAMBDA1
1	.024	22.95	0.00	0.0000	.003	-5.860
2	.069	42.60	0.00	0.0000	.003	-3.290
3	.111	62.30	0.00	0.0000	.009	-2.468
4	.153	82.15	0.00	0.0000	0.000	-1.989
5	.195	102.00	0.00	0.0000	.002	-1.661
6	.237	121.70	0.00	0.0000	.000	-1.415
7	.278	141.35	0.00	0.0000	.002	-1.221
8	.320	161.00	0.00	0.0000	.001	-1.061
9	.362	180.70	0.00	0.0000	.001	-.924
10	.403	200.40	0.00	0.0000	.001	-.805
11	.445	220.20	0.00	0.0000	.000	-.700
12	.487	239.85	0.00	0.0000	.006	-.606
13	.528	259.45	0.00	0.0000	.013	-.521
14	.570	279.15	0.00	0.0000	.005	-.443
15	.612	298.75	0.00	0.0000	.007	-.371
16	.653	318.50	0.00	0.0000	0.000	-.304
17	.695	338.15	0.00	0.0000	.007	-.241
18	.737	358.00	0.00	0.0000	.050	-.183
19	.778	377.65	0.00	0.0000	.096	-.127
20	.820	397.35	0.00	0.0000	.262	-.075
21	.862	417.55	0.00	0.0000	.394	-.025
22	.904	437.05	0.00	0.0000	.598	.023
23	.946	456.85	0.00	0.0000	.799	.068
24	.988	476.65	0.00	0.0000	.901	.111
25	1.028	494.75	0.00	0.0000	.936	.151
26	1.066	513.00	0.00	0.0000	.941	.180
27	1.106	532.25	0.00	0.0000	.958	.224
28	1.147	551.95	0.00	0.0000	1.007	.261
29	1.189	571.70	0.00	0.0000	.992	.297
30	1.231	591.55	0.00	0.0000	1.003	.332
31	1.273	611.20	0.00	0.0000	.958	.366
32	1.314	630.70	0.00	0.0000	1.009	.399
33	1.355	650.10	0.00	0.0000	1.035	.430
34	1.396	669.45	0.00	0.0000	1.002	.461
35	1.437	688.90	0.00	0.0000	.938	.491
36	1.478	708.20	0.00	0.0000	.969	.520
37	1.519	727.65	0.00	0.0000	.998	.548
38	1.560	746.90	0.00	0.0000	.961	.576
39	1.601	766.20	0.00	0.0000	.977	.603
40	1.641	784.65	0.00	0.0000	1.019	.628

STEADY-STATE PHASE FRACTIONAL FLOW : .0000
50% BREAKTHROUGH (PORE VOLUME) : .8842

EXPERIMENT PH31

TUBE NUMBER	PORE VOLUMES	TOTAL PHASE VOLUME (CC)	PHASE VOLUME (CC)	FRACTIONAL FLOW	NORMALIZED CONCENTRATION	LAMBDA1
1	.014	13.00	13.00	1.0000	.001	-7.743
2	.042	27.10	27.10	1.0000	.001	-4.258
3	.072	41.25	41.25	1.0000	.001	-3.141
4	.102	55.30	55.30	1.0000	.001	-2.542
5	.132	69.25	69.25	1.0000	.001	-2.149
6	.161	83.15	83.15	1.0000	.001	-1.860
7	.191	97.25	97.25	1.0000	.001	-1.639
8	.223	111.00	111.00	1.0000	.001	-1.458
9	.250	125.15	125.15	1.0000	.002	-1.305
10	.279	138.95	138.95	1.0000	.001	-1.173
11	.309	152.80	152.80	1.0000	.001	-1.059
12	.338	166.95	166.95	1.0000	0.000	-.957
13	.368	180.75	180.75	1.0000	0.000	-.865
14	.397	194.60	194.60	1.0000	.000	-.782
15	.426	208.35	208.35	1.0000	0.000	-.706
16	.456	222.15	222.15	1.0000	.001	-.636
17	.485	235.90	235.90	1.0000	0.000	-.572
18	.514	249.75	249.75	1.0000	0.000	-.511
19	.543	263.60	263.60	1.0000	.001	-.454
20	.573	277.65	277.65	1.0000	.001	-.400
21	.602	291.45	291.45	1.0000	.000	-.349
22	.632	305.40	305.40	1.0000	.003	-.301
23	.661	319.25	319.25	1.0000	.003	-.255
24	.690	333.25	333.25	1.0000	.021	-.211
25	.720	346.95	346.95	1.0000	.027	-.169
26	.749	360.85	360.85	1.0000	.049	-.129
27	.779	375.00	375.00	1.0000	.096	-.090
28	.809	389.15	389.15	1.0000	.322	-.052
29	.838	403.10	403.10	1.0000	.452	-.016
30	.868	417.20	417.20	1.0000	.556	.019
31	.898	431.35	431.35	1.0000	.669	.052
32	.928	445.35	445.35	1.0000	.824	.085
33	.958	459.50	459.50	1.0000	.897	.117
34	.987	473.55	473.55	1.0000	.988	.147
35	1.017	487.60	487.60	1.0000	.997	.177
36	1.047	501.70	501.70	1.0000	1.032	.206
37	1.077	515.75	515.75	1.0000	1.041	.234
38	1.106	529.85	529.85	1.0000	1.040	.262
39	1.137	544.30	544.30	1.0000	.983	.289
40	1.167	558.25	558.25	1.0000	1.028	.316
41	1.196	572.35	572.35	1.0000	.974	.341
42	1.226	586.50	586.50	1.0000	1.002	.366
43	1.256	600.65	600.65	1.0000	.995	.391
44	1.286	614.65	614.65	1.0000	1.007	.415
45	1.316	628.70	628.70	1.0000	1.042	.438
46	1.345	642.65	642.65	1.0000	.968	.461
47	1.375	656.70	656.70	1.0000	.987	.483
48	1.405	670.60	670.60	1.0000	.999	.505
49	1.434	684.65	684.65	1.0000	.999	.527

STEADY-STATE PHASE FRACTIONAL FLOW : 1.0000
50% BREAKTHROUGH (PORE VOLUME) : .8521

EXPERIMENT PH32

TUBE NUMBER	PORE VOLUMES	TOTAL PHASE VOLUME (CC)	PHASE VOLUME (CC)	FRACTIONAL FLOW	NORMALIZED CONCENTRATION	LAMBDA
1	.014	13.10	13.10	1.0000	0.000	-7.510
2	.043	27.15	27.15	1.0000	0.000	-4.130
3	.072	41.30	41.30	1.0000	0.000	-3.044
4	.102	55.25	55.25	1.0000	0.000	-2.459
5	.131	68.55	68.55	1.0000	0.000	-2.083
6	.160	82.40	82.40	1.0000	0.000	-1.807
7	.189	96.65	96.65	1.0000	0.000	-1.583
8	.219	110.70	110.70	1.0000	0.000	-1.400
9	.250	125.15	125.15	1.0000	0.000	-1.246
10	.280	139.35	139.35	1.0000	0.000	-1.113
11	.310	153.50	153.50	1.0000	0.000	-.997
12	.340	167.45	167.45	1.0000	0.000	-.896
13	.370	181.75	181.75	1.0000	0.000	-.804
14	.400	195.90	195.90	1.0000	0.000	-.721
15	.433	210.20	210.20	1.0000	0.000	-.640
16	.463	224.80	224.80	1.0000	0.000	-.572
17	.491	238.95	238.95	1.0000	0.000	-.506
18	.521	253.15	253.15	1.0000	0.000	-.445
19	.551	267.60	267.60	1.0000	0.000	-.387
20	.581	281.80	281.80	1.0000	0.000	-.332
21	.611	296.05	296.05	1.0000	.012	-.281
22	.642	310.20	310.20	1.0000	.024	-.233
23	.672	324.40	324.40	1.0000	.060	-.187
24	.702	338.65	338.65	1.0000	.108	-.143
25	.732	352.80	352.80	1.0000	.169	-.101
26	.762	367.05	367.05	1.0000	.157	-.061
27	.792	381.45	381.45	1.0000	.398	-.022
28	.823	396.00	396.00	1.0000	.578	.016
29	.853	410.25	410.25	1.0000	.699	.053
30	.883	424.40	424.40	1.0000	.723	.087
31	.913	438.60	438.60	1.0000	.807	.121
32	.943	452.70	452.70	1.0000	.843	.153
33	.973	467.05	467.05	1.0000	.916	.185
34	1.004	481.40	481.40	1.0000	.916	.215
35	1.034	495.75	495.75	1.0000	.964	.246
36	1.064	509.80	509.80	1.0000	.964	.274
37	1.094	523.85	523.85	1.0000	1.012	.302
38	1.124	538.05	538.05	1.0000	.988	.330
39	1.154	552.20	552.20	1.0000	1.012	.356
40	1.184	566.55	566.55	1.0000	.988	.383
41	1.214	580.80	580.80	1.0000	.976	.408
42	1.245	595.45	595.45	1.0000	1.024	.434
43	1.275	609.75	609.75	1.0000	1.012	.459
44	1.306	623.95	623.95	1.0000	.988	.483
45	1.336	638.30	638.30	1.0000	.988	.506
46	1.366	652.50	652.50	1.0000	.952	.529
47	1.396	666.85	666.85	1.0000	1.012	.552
48	1.426	681.15	681.15	1.0000	.988	.574
49	1.457	695.35	695.35	1.0000	1.012	.596
50	1.487	709.80	709.80	1.0000	1.000	.618
51	1.513	719.85	719.85	1.0000	1.012	.636

STEADY-STATE PHASE FRACTIONAL FLOW : 1.0000
50% BREAKTHROUGH (PORE VOLUME) : .8395

EXPERIMENT PH33A0

TUBE NUMBER	PORE VOLUMES	TOTAL PHASE VOLUME (CC)	PHASE VOLUME (CC)	FRACTIONAL FLOW	NORMALIZED CONCENTRATION	LAMBDA1
1	.019	17.75	3.02	.1699	.001	-7.734
2	.057	36.40	7.32	.2010	.001	-4.278
3	.097	55.55	11.82	.2127	0.000	-3.160
4	.138	75.25	16.52	.2195	0.000	-2.550
5	.179	94.30	20.47	.2170	.000	-2.150
6	.220	113.35	24.42	.2154	0.000	-1.863
7	.260	132.40	28.37	.2142	0.000	-1.639
8	.300	151.55	32.42	.2139	.000	-1.457
9	.341	170.45	36.37	.2133	0.000	-1.304
10	.381	189.40	40.37	.2131	0.000	-1.173
11	.421	208.25	44.17	.2121	0.000	-1.059
12	.461	227.00	47.47	.2091	0.000	-.958
13	.501	246.00	50.87	.2068	.004	-.866
14	.541	264.95	54.27	.2048	.015	-.783
15	.581	283.75	57.87	.2039	.025	-.707
16	.621	302.65	61.62	.2036	.033	-.636
17	.660	321.45	65.07	.2024	.045	-.571
18	.700	340.45	68.22	.2004	.046	-.510
19	.741	359.35	72.37	.2014	.058	-.453
20	.781	378.30	76.27	.2016	.058	-.399
21	.821	397.35	79.97	.2012	.083	-.348
22	.861	416.25	83.82	.2014	.108	-.300
23	.901	435.20	87.87	.2019	.156	-.254
24	.941	454.30	91.97	.2024	.213	-.210
25	.982	473.40	96.12	.2030	.244	-.168
26	1.022	492.40	100.02	.2031	.283	-.127
27	1.062	511.45	103.97	.2033	.306	-.089
28	1.103	530.50	108.07	.2037	.388	-.051
29	1.143	549.55	112.27	.2043	.443	-.015
30	1.183	568.70	116.52	.2049	.573	.019
31	1.224	587.60	120.67	.2054	.616	.053
32	1.264	606.75	124.87	.2058	.747	.085
33	1.305	626.20	129.52	.2068	.694	.117
34	1.345	645.25	133.62	.2071	.727	.148
35	1.386	664.60	137.82	.2074	.817	.178
36	1.427	683.85	141.72	.2072	.889	.207
37	1.467	702.60	145.52	.2071	.907	.235
38	1.508	722.10	149.27	.2067	.874	.262
39	1.549	741.50	153.02	.2064	.872	.289
40	1.590	760.90	156.97	.2063	.951	.316
41	1.631	780.30	160.82	.2061	1.009	.342
42	1.672	799.65	164.77	.2060	.954	.367
43	1.712	818.25	168.57	.2060	1.005	.391
44	1.752	837.70	172.52	.2059	1.003	.415
45	1.793	857.15	176.42	.2058	1.043	.439
46	1.835	876.70	180.42	.2050	1.006	.462
47	1.876	896.20	184.22	.2056	1.043	.485
48	1.917	915.70	188.02	.2053	1.046	.507
49	1.959	935.10	191.82	.2051	.970	.529
50	2.000	954.65	195.52	.2048	1.078	.551
51	2.041	974.25	199.27	.2045	1.005	.572
52	2.083	993.75	203.22	.2045	1.048	.593
53	2.124	1013.25	207.32	.2046	.987	.613
54	2.165	1032.90	211.52	.2048	.991	.634

55	2.207	1052.40	215.52	.2048	1.001	.654
56	2.246	1071.95	219.47	.2047	1.041	.673
57	2.289	1091.50	223.17	.2045	1.009	.692
58	2.331	1111.05	226.87	.2042	1.071	.711
59	2.372	1130.65	230.57	.2039	1.023	.730
60	2.414	1150.25	234.57	.2039	1.019	.749
61	2.455	1169.85	238.47	.2038	1.028	.767
62	2.497	1189.55	242.32	.2037	1.001	.785
63	2.538	1209.15	245.97	.2034	1.030	.803
64	2.580	1228.90	249.77	.2032	1.049	.820
65	2.622	1248.45	253.47	.2030	1.013	.837
66	2.663	1268.15	257.07	.2027	.996	.855
67	2.705	1287.75	260.82	.2025	1.019	.871
68	2.746	1307.30	264.42	.2023	.999	.888
69	2.788	1326.90	268.17	.2021	.889	.904
70	2.829	1346.50	271.97	.2020	1.012	.921
71	2.870	1366.00	275.57	.2017	.980	.937
72	2.912	1385.50	279.27	.2016	.983	.952
73	2.953	1405.10	282.97	.2014	1.036	.968
74	2.994	1424.60	286.57	.2012	.983	.984
75	3.036	1444.15	290.17	.2009	1.013	.999
76	3.077	1463.85	293.77	.2007	.979	1.014
77	3.119	1483.45	297.37	.2005	.994	1.029
78	3.163	1503.00	301.02	.2003	.982	1.044
79	3.202	1522.60	304.62	.2001	1.022	1.059

STEADY-STATE PHASE FRACTIONAL FLOW : .2001
50% BREAKTHROUGH (PORE VOLUME) : 1.1607

EXPERIMENT PH33MEC

TUBE NUMBER	PORE VOLUMES	TOTAL PHASE VOLUME (CC)	PHASE VOLUME (CC)	FRACTIONAL FLOW	NORMALIZED CONCENTRATION	LAMBDA1
1	.019	17.75	4.67	.2630	.028	-8.878
2	.057	36.40	9.12	.2505	.007	-4.952
3	.097	55.55	13.62	.2452	.004	-3.696
4	.138	75.25	18.17	.2414	.024	-3.009
5	.179	94.30	23.27	.2467	.023	-2.565
6	.220	113.35	28.72	.2534	0.000	-2.248
7	.260	132.40	34.27	.2588	.036	-2.002
8	.300	151.55	39.62	.2614	.014	-1.803
9	.341	170.45	44.82	.2629	.001	-1.637
10	.381	189.40	50.02	.2641	.014	-1.496
11	.421	208.25	54.97	.2640	.053	-1.373
12	.461	227.00	59.67	.2629	0.000	-1.264
13	.501	246.00	64.32	.2615	0.000	-1.167
14	.541	264.95	69.02	.2605	.007	-1.079
15	.581	283.75	73.27	.2582	.025	-.998
16	.621	302.65	77.47	.2560	.039	-.925
17	.660	321.45	81.62	.2539	.035	-.856
18	.700	340.45	86.02	.2527	.002	-.793
19	.741	359.35	90.52	.2519	.014	-.733
20	.781	378.30	94.97	.2510	.018	-.677
21	.821	397.35	99.52	.2505	.027	-.624
22	.861	416.25	103.92	.2497	.008	-.575
23	.901	435.20	108.17	.2485	.014	-.527
24	.941	454.30	112.37	.2473	.042	-.482
25	.982	473.40	116.22	.2455	.046	-.439
26	1.022	492.40	119.92	.2435	.043	-.398
27	1.062	511.45	123.57	.2416	.053	-.359
28	1.103	530.50	126.97	.2393	.068	-.321
29	1.143	549.55	130.27	.2370	.075	-.285
30	1.183	568.70	133.32	.2344	.075	-.250
31	1.224	587.60	136.22	.2318	.098	-.216
32	1.264	606.75	139.07	.2292	.095	-.183
33	1.305	626.20	141.62	.2262	.139	-.151
34	1.345	645.25	144.62	.2241	.251	-.121
35	1.386	664.60	147.77	.2223	.314	-.091
36	1.427	683.85	151.52	.2216	.341	-.062
37	1.467	702.60	155.72	.2216	.414	-.034
38	1.508	722.10	160.07	.2217	.463	-.007
39	1.549	741.50	164.52	.2219	.615	.020
40	1.590	760.90	168.92	.2220	.645	.046
41	1.631	780.30	173.27	.2221	.665	.072
42	1.672	799.65	177.47	.2219	.768	.097
43	1.712	818.25	181.42	.2217	.752	.121
44	1.752	837.70	185.57	.2215	.876	.144
45	1.793	857.15	189.72	.2213	.946	.167
46	1.835	876.70	193.77	.2210	.947	.190
47	1.876	896.20	197.87	.2208	.893	.212
48	1.917	915.70	202.07	.2207	.987	.234
49	1.959	935.10	206.27	.2206	1.011	.256
50	2.000	954.65	210.57	.2206	1.046	.277
51	2.041	974.25	214.67	.2203	.993	.297
52	2.083	993.75	218.72	.2201	1.008	.318
53	2.124	1013.25	222.72	.2198	.964	.338
54	2.165	1032.90	226.72	.2195	.835	.357

55	2.207	1052.40	230.82	.2193	.990	.376
56	2.248	1071.95	235.02	.2192	.865	.395
57	2.289	1091.50	239.27	.2192	1.048	.414
58	2.331	1111.05	243.57	.2192	1.064	.432
59	2.372	1130.65	248.02	.2194	1.025	.450
60	2.414	1150.25	252.37	.2194	1.051	.468
61	2.455	1169.85	256.67	.2194	1.016	.486
62	2.497	1189.55	261.17	.2196	.948	.503
63	2.538	1209.15	265.77	.2198	1.050	.520
64	2.580	1228.90	270.27	.2199	1.007	.537
65	2.622	1248.45	274.57	.2199	.969	.553
66	2.663	1268.15	279.07	.2201	.986	.570
67	2.705	1287.75	283.37	.2200	.941	.586
68	2.746	1307.30	287.62	.2200	.982	.602
69	2.788	1326.90	291.87	.2200	.912	.617
70	2.829	1346.50	296.07	.2199	.885	.633
71	2.870	1366.00	300.27	.2198	.959	.648
72	2.912	1385.50	304.52	.2198	.989	.663
73	2.953	1405.10	308.92	.2199	1.008	.678
74	2.994	1424.60	313.32	.2199	.983	.693
75	3.036	1444.15	317.72	.2200	1.040	.707
76	3.077	1463.85	322.17	.2201	1.045	.722
77	3.119	1483.45	326.62	.2202	.976	.736
78	3.160	1503.00	331.02	.2202	.935	.750
79	3.202	1522.60	335.37	.2203	1.047	.764
80	3.228	1527.50	336.47	.2203	1.019	.773

STEADY-STATE PHASE FRACTIONAL FLOW : .2203
50% BREAKTHROUGH (PORE VOLUME) : 1.5178

EXPERIMENT PH33MET

TUBE NUMBER	PORE VOLUMES	TOTAL PHASE VOLUME (CC)	PHASE VOLUME (CC)	FRACTIONAL FLOW	NORMALIZED CONCENTRATION	LAMBDA1
1	.019	17.75	4.67	.2630	.001	-6.584
2	.057	36.40	9.12	.2505	0.000	-3.595
3	.097	55.55	13.62	.2452	0.000	-2.620
4	.138	75.25	18.17	.2414	0.000	-2.077
5	.179	94.30	23.27	.2467	.001	-1.719
6	.220	113.35	28.72	.2534	.000	-1.460
7	.260	132.40	34.27	.2588	0.000	-1.257
8	.300	151.55	39.62	.2614	.001	-1.089
9	.341	170.45	44.82	.2629	.000	-.948
10	.381	189.40	50.02	.2641	.002	-.827
11	.421	208.25	54.97	.2640	.004	-.719
12	.461	227.00	59.67	.2629	.019	-.624
13	.501	246.00	64.32	.2615	.064	-.538
14	.541	264.95	69.02	.2605	.163	-.458
15	.581	283.75	73.27	.2582	.248	-.385
16	.621	302.65	77.47	.2560	.233	-.318
17	.663	321.45	81.62	.2539	.240	-.255
18	.700	340.45	86.02	.2527	.335	-.196
19	.741	359.35	90.52	.2519	.415	-.140
20	.781	378.30	94.97	.2510	.450	-.087
21	.821	397.35	99.52	.2505	.427	-.037
22	.861	416.25	103.92	.2497	.523	.011
23	.901	435.20	108.17	.2485	.600	.057
24	.941	454.30	112.37	.2473	.783	.100
25	.982	473.40	116.22	.2455	.904	.142
26	1.022	492.40	119.92	.2435	.936	.183
27	1.062	511.45	123.57	.2416	.981	.222
28	1.103	530.50	126.97	.2393	.905	.259
29	1.143	549.55	130.27	.2370	.915	.295
30	1.183	568.70	133.32	.2344	1.030	.331
31	1.224	587.60	136.22	.2318	.963	.365
32	1.264	606.75	139.07	.2292	1.024	.398
33	1.305	626.20	141.62	.2262	1.022	.430
34	1.345	645.25	144.62	.2241	1.015	.462
35	1.386	664.60	147.77	.2223	1.099	.492
36	1.427	683.85	151.52	.2216	.977	.522
37	1.467	702.60	155.72	.2216	1.096	.551
38	1.508	722.10	160.07	.2217	1.186	.579
39	1.549	741.50	164.52	.2219	.921	.607
40	1.590	760.90	168.92	.2220	1.020	.635

STEADY-STATE PHASE FRACTIONAL FLOW : .2220
50% BREAKTHROUGH (PORE VOLUME) : .8515

EXPERIMENT PH330L

TUBE NUMBER	PORE VOLUMES	TOTAL PHASE VOLUME (CC)	PHASE VOLUME (CC)	FRACTIONAL FLOW	NORMALIZED CONCENTRATION	LAMBDA1
1	.019	17.75	10.07	.5671	0.000	-6.100
2	.057	36.40	19.97	.5485	0.000	-3.307
3	.097	55.55	30.12	.5422	0.000	-2.389
4	.138	75.25	40.57	.5391	0.000	-1.874
5	.179	94.30	50.57	.5362	0.000	-1.533
6	.220	113.35	60.22	.5312	0.000	-1.285
7	.260	132.40	69.77	.5269	0.000	-1.089
8	.300	151.55	79.52	.5247	0.000	-.927
9	.341	170.45	89.27	.5237	0.000	-.791
10	.381	189.40	99.02	.5228	0.000	-.672
11	.421	208.25	109.12	.5240	.010	-.568
12	.461	227.00	119.87	.5280	.030	-.474
13	.501	246.00	130.82	.5318	.040	-.389
14	.541	264.95	141.67	.5347	.060	-.311
15	.581	283.75	152.62	.5379	.100	-.239
16	.621	302.65	163.57	.5404	.170	-.172
17	.660	321.45	174.77	.5437	.240	-.110
18	.700	340.45	186.22	.5470	.400	-.051
19	.741	359.35	196.47	.5467	.510	.005
20	.781	378.30	207.07	.5474	.570	.058
21	.821	397.35	217.87	.5483	.660	.108
22	.861	416.25	228.52	.5490	.690	.156
23	.901	435.20	239.17	.5496	.770	.201
24	.941	454.30	249.97	.5502	.770	.245
25	.982	473.40	261.07	.5515	.830	.288
26	1.022	492.40	272.47	.5533	.840	.329
27	1.062	511.45	283.92	.5551	.870	.368
28	1.103	530.50	295.47	.5570	.900	.406
29	1.143	549.55	307.02	.5587	.900	.442
30	1.183	568.70	318.87	.5607	.940	.478
31	1.224	587.60	330.72	.5628	.970	.513
32	1.264	606.75	342.02	.5650	1.010	.546
33	1.305	626.20	355.07	.5670	1.010	.579
34	1.345	645.25	367.02	.5688	1.030	.611
35	1.386	664.60	379.02	.5703	.960	.642
36	1.427	683.85	390.62	.5712	1.010	.673
37	1.467	702.60	401.37	.5713	1.010	.702
38	1.508	722.10	412.77	.5716	.970	.731
39	1.549	741.50	423.97	.5718	1.000	.760
40	1.590	760.90	435.02	.5717	1.010	.788

STEADY-STATE PHASE FRACTIONAL FLOW : .5718
50% BREAKTHROUGH (PORE VOLUME) : .7369

EXPERIMENT PH330LC

TUBE NUMBER	PORE VOLUMES	TOTAL PHASE VOLUME (CC)	PHASE VOLUME (CC)	FRACTIONAL FLOW	NORMALIZED CONCENTRATION	LAMBDA1
1	.019	17.75	10.07	.5671	.006	-5.881
2	.057	36.40	19.97	.5485	0.000	-3.173
3	.097	55.55	30.12	.5422	.009	-2.280
4	.138	75.25	40.57	.5391	0.000	-1.778
5	.179	94.30	50.57	.5362	0.000	-1.445
6	.220	113.35	60.22	.5312	.014	-1.202
7	.260	132.40	69.77	.5269	0.000	-1.010
8	.300	151.55	79.52	.5247	.009	-.850
9	.341	170.45	89.27	.5237	0.000	-.715
10	.381	189.40	99.02	.5228	0.000	-.598
11	.421	208.25	109.12	.5240	.013	-.495
12	.461	227.00	119.87	.5280	.018	-.402
13	.501	246.00	130.82	.5318	.029	-.318
14	.541	264.95	141.67	.5347	.044	-.240
15	.581	283.75	152.62	.5379	.090	-.168
16	.621	302.65	163.57	.5404	.169	-.101
17	.660	321.45	174.77	.5437	.312	-.039
18	.700	340.45	186.22	.5470	.599	.020
19	.741	359.35	196.47	.5467	.746	.076
20	.781	378.30	207.07	.5474	1.023	.128
21	.821	397.35	217.87	.5483	.897	.179
22	.861	416.25	228.52	.5490	1.028	.227
23	.901	435.20	239.17	.5496	1.103	.272
24	.941	454.30	249.97	.5502	1.086	.317
25	.982	473.40	261.07	.5515	1.086	.359
26	1.022	492.40	272.47	.5533	.980	.400
27	1.062	511.45	283.92	.5551	1.038	.440
28	1.103	530.50	295.47	.5570	.990	.478
29	1.143	549.55	307.02	.5587	.922	.515
30	1.183	568.70	318.87	.5607	.970	.551
31	1.224	587.60	330.72	.5628	1.023	.586
32	1.264	606.75	342.82	.5650	.952	.620
33	1.305	626.20	355.07	.5670	1.012	.653
34	1.345	645.25	367.02	.5688	.943	.685
35	1.386	664.60	379.02	.5703	.997	.717
36	1.427	683.85	390.62	.5712	1.039	.748
37	1.467	702.60	401.37	.5713	.972	.778
38	1.508	722.10	412.77	.5716	.949	.807
39	1.549	741.50	423.97	.5718	.952	.836
40	1.590	760.90	435.02	.5717	.984	.864

STEADY-STATE PHASE FRACTIONAL FLOW : .5718
50% BREAKTHROUGH (PORE VOLUME) : .6867

EXPERIMENT PH34AQ

TUBE NUMBER	PORE VOLUMES	TOTAL PHASE VOLUME (CC)	PHASE VOLUME (CC)	FRACTIONAL FLOW	NORMALIZED CONCENTRATION	LAMBDA
1	.024	22.50	7.48	.3326	0.000	-5.903
2	.068	41.35	15.08	.3648	0.000	-3.324
3	.108	60.30	22.73	.3770	0.000	-2.505
4	.148	79.30	30.43	.3838	0.000	-2.026
5	.188	98.55	38.10	.3875	0.000	-1.695
6	.229	117.65	45.98	.3909	0.000	-1.447
7	.269	136.70	53.78	.3934	0.000	-1.251
8	.309	155.70	61.63	.3958	0.000	-1.089
9	.350	174.75	69.43	.3973	0.000	-.952
10	.390	193.90	77.13	.3978	0.000	-.832
11	.431	213.30	85.03	.3987	0.000	-.725
12	.472	232.65	92.98	.3997	.001	-.629
13	.513	251.85	101.23	.4020	.006	-.543
14	.553	270.95	109.73	.4050	.019	-.464
15	.594	290.25	118.38	.4079	.027	-.392
16	.635	309.50	126.73	.4095	.063	-.324
17	.675	328.70	134.88	.4104	.099	-.262
18	.716	347.95	142.93	.4108	.164	-.203
19	.757	367.30	150.68	.4102	.273	-.147
20	.798	386.55	157.08	.4064	.271	-.094
21	.838	405.80	163.33	.4025	.338	-.045
22	.879	424.85	170.08	.4003	.510	.003
23	.919	443.90	177.03	.3988	.687	.048
24	.960	463.05	184.08	.3975	.725	.091
25	1.000	482.20	191.23	.3966	.786	.132
26	1.041	501.30	198.58	.3961	.835	.172
27	1.081	520.55	205.98	.3957	.865	.210
28	1.122	539.65	213.53	.3957	.819	.247
29	1.162	558.65	221.23	.3959	.933	.283
30	1.203	578.05	229.23	.3966	.951	.318
31	1.244	597.35	237.38	.3974	.983	.352
32	1.285	616.70	245.53	.3981	.944	.385
33	1.326	635.95	253.78	.3991	.949	.416
34	1.366	655.20	262.03	.3999	.977	.447
35	1.407	674.25	269.98	.4004	.989	.477
36	1.447	693.20	277.18	.3999	.983	.506
37	1.487	712.05	283.73	.3985	1.011	.535
38	1.527	730.95	290.38	.3973	1.033	.562
39	1.567	749.90	296.78	.3958	1.070	.589
40	1.607	769.00	303.28	.3944	1.050	.616

STEADY-STATE PHASE FRACTIONAL FLOW : .3944
50% BREAKTHROUGH (PORE VOLUME) : .8767

EXPERIMENT PH34MEC

TUBE NUMBER	PORE VOLUMES	TOTAL PHASE VOLUME (CC)	PHASE VOLUME (CC)	FRACTIONAL FLOW	NORMALIZED CONCENTRATION	LAMBDA1
1	.324	22.50	4.79	.2130	.012	-6.057
2	.068	41.35	7.99	.1933	.008	-3.420
3	.108	60.30	11.14	.1848	.028	-2.583
4	.148	79.30	14.29	.1802	0.000	-2.095
5	.188	98.55	17.44	.1770	.010	-1.759
6	.229	117.65	20.49	.1742	.012	-1.507
7	.269	136.70	23.59	.1726	.056	-1.308
8	.309	155.70	26.69	.1714	0.000	-1.145
9	.350	174.75	29.94	.1714	.002	-1.006
10	.390	193.90	33.49	.1727	0.000	-.885
11	.431	213.30	37.39	.1753	.012	-.777
12	.472	232.65	41.44	.1781	0.000	-.681
13	.513	251.85	45.64	.1812	.020	-.593
14	.553	270.95	49.94	.1843	0.000	-.515
15	.594	290.25	54.34	.1872	.018	-.442
16	.635	309.50	58.69	.1896	.040	-.374
17	.675	328.70	62.99	.1916	.096	-.311
18	.716	347.95	67.19	.1931	.101	-.252
19	.757	367.30	71.39	.1944	.206	-.196
20	.798	386.55	75.39	.1950	.265	-.143
21	.838	405.80	79.49	.1959	.212	-.093
22	.879	424.85	83.59	.1968	.400	-.046
23	.919	443.90	87.54	.1972	.496	-.001
24	.960	463.05	91.44	.1975	.652	.042
25	1.000	482.20	95.19	.1974	.803	.083
26	1.041	501.30	98.74	.1970	.879	.123
27	1.081	520.55	102.19	.1963	.856	.161
28	1.122	539.65	105.34	.1952	.978	.198
29	1.162	558.85	108.39	.1940	1.028	.234
30	1.203	578.05	111.34	.1926	1.068	.269
31	1.244	597.35	114.09	.1910	1.045	.302
32	1.285	616.70	116.74	.1893	1.025	.335
33	1.326	635.95	119.39	.1877	1.032	.367
34	1.366	655.20	121.89	.1860	.998	.398
35	1.407	674.25	124.54	.1847	1.000	.427
36	1.447	693.20	127.44	.1838	.983	.456
37	1.487	712.05	132.19	.1857	.993	.484
38	1.527	730.95	137.14	.1876	.955	.512
39	1.567	749.90	142.09	.1895	.992	.538
40	1.607	769.00	146.94	.1911	.990	.565

STEADY-STATE PHASE FRACTIONAL FLOW : .1911
50% BREAKTHROUGH (PORE VOLUME) : .9204

EXPERIMENT PH30MET

TUBE NUMBER	PORE VOLUMES	TOTAL PHASE VOLUME (CC)	PHASE VOLUME (CC)	FRACTIONAL FLOW	NORMALIZED CONCENTRATION	LAMBDA1
1	.024	22.50	4.79	.2130	0.000	-5.911
2	.068	41.35	7.99	.1933	.001	-3.329
3	.108	60.30	11.14	.1848	0.000	-2.509
4	.148	79.30	14.29	.1802	0.000	-2.029
5	.188	98.55	17.44	.1770	.000	-1.698
6	.229	117.65	20.49	.1742	0.000	-1.450
7	.269	136.70	23.59	.1726	0.000	-1.254
8	.309	155.70	26.69	.1714	.001	-1.092
9	.350	174.75	29.94	.1714	.001	-.955
10	.390	193.90	33.49	.1727	0.000	-.835
11	.431	213.30	37.39	.1753	0.000	-.728
12	.472	232.65	41.44	.1781	.001	-.632
13	.513	251.85	45.64	.1812	.004	-.546
14	.553	270.95	49.94	.1843	.020	-.467
15	.594	290.25	54.34	.1872	.044	-.395
16	.635	309.50	58.69	.1896	.061	-.327
17	.675	328.70	62.99	.1916	.096	-.264
18	.716	347.95	67.19	.1931	.149	-.205
19	.757	367.30	71.39	.1944	.233	-.150
20	.798	386.55	75.39	.1950	.270	-.097
21	.838	405.80	79.49	.1959	.332	-.047
22	.879	424.85	83.59	.1968	.500	.000
23	.919	443.90	87.54	.1972	.640	.045
24	.960	463.05	91.44	.1975	.765	.088
25	1.002	482.20	95.19	.1974	.813	.129
26	1.041	501.30	98.74	.1970	.857	.169
27	1.081	520.55	102.19	.1963	.880	.208
28	1.122	539.65	105.34	.1952	.894	.245
29	1.162	558.85	108.39	.1940	.906	.280
30	1.203	578.05	111.34	.1926	.954	.315
31	1.244	597.35	114.09	.1910	.989	.349
32	1.285	616.70	116.74	.1893	.999	.382
33	1.326	635.95	119.39	.1877	.996	.414
34	1.366	655.20	121.89	.1860	.998	.445
35	1.407	674.25	124.54	.1847	1.025	.475
36	1.447	693.20	127.44	.1838	1.037	.504
37	1.487	712.05	132.19	.1857	1.002	.532
38	1.527	730.95	137.14	.1876	1.039	.559
39	1.567	749.90	142.09	.1895	1.006	.586
40	1.607	769.00	146.94	.1911	1.108	.613

STEADY-STATE PHASE FRACTIONAL FLOW : .1911
50% BREAKTHROUGH (PORE VOLUME) : .8790

EXPERIMENT PH340L

TUBE NUMBER	PORE VOLUMES	TOTAL PHASE VOLUME (CC)	PHASE VOLUME (CC)	FRACTIONAL FLOW	NORMALIZED CONCENTRATION	LAMBDA1
1	.024	22.50	7.48	.3326	0.000	-6.170
2	.068	41.35	15.08	.3648	0.000	-3.495
3	.108	60.30	22.73	.3770	0.000	-2.645
4	.148	79.30	30.43	.3838	0.000	-2.150
5	.188	98.55	38.18	.3875	0.000	-1.810
6	.229	117.65	45.98	.3909	0.000	-1.555
7	.269	136.70	53.78	.3934	0.000	-1.354
8	.309	155.70	61.63	.3958	0.000	-1.188
9	.350	174.75	69.43	.3973	0.000	-1.048
10	.390	193.90	77.13	.3978	0.000	-.926
11	.431	213.30	85.03	.3987	0.000	-.818
12	.472	232.65	92.98	.3997	0.000	-.720
13	.513	251.85	101.23	.4020	0.000	-.633
14	.553	270.95	109.73	.4050	.010	-.554
15	.594	290.25	118.38	.4079	.030	-.480
16	.635	309.50	126.73	.4095	.040	-.412
17	.675	328.70	134.88	.4104	.070	-.349
18	.716	347.95	142.93	.4108	.120	-.290
19	.757	367.30	150.68	.4102	.170	-.234
20	.798	386.55	157.08	.4064	.190	-.181
21	.838	405.80	163.33	.4025	.250	-.131
22	.879	424.85	170.08	.4003	.330	-.084
23	.919	443.90	177.03	.3988	.410	-.039
24	.960	463.05	184.08	.3975	.510	.004
25	1.000	482.20	191.23	.3966	.570	.046
26	1.041	501.30	198.58	.3961	.610	.085
27	1.081	520.55	205.98	.3957	.650	.124
28	1.122	539.65	213.53	.3957	.660	.161
29	1.162	558.85	221.23	.3959	.690	.196
30	1.203	578.05	229.23	.3966	.730	.231
31	1.244	597.35	237.38	.3974	.770	.264
32	1.285	616.70	245.53	.3981	.790	.297
33	1.326	635.95	253.78	.3991	.810	.329
34	1.366	655.20	262.03	.3999	.830	.359
35	1.407	674.25	269.98	.4004	.840	.389
36	1.447	693.20	277.18	.3999	.880	.418
37	1.487	712.05	283.73	.3985	.900	.446
38	1.527	730.95	290.38	.3973	.910	.473
39	1.567	749.90	296.78	.3958	.970	.500
40	1.607	769.00	303.28	.3944	.990	.526
41	1.648	788.15	309.83	.3931	.990	.552
42	1.688	807.10	316.63	.3923	.990	.577
43	1.726	825.90	323.13	.3913	.990	.601
44	1.768	844.95	329.73	.3902	.990	.625
45	1.809	864.10	336.38	.3893	1.010	.649
46	1.849	883.20	343.18	.3886	1.010	.672
47	1.889	902.25	350.08	.3880	1.020	.695
48	1.930	921.55	357.08	.3875	.990	.717
49	1.971	940.60	363.58	.3865	1.020	.740
50	2.011	959.85	370.53	.3860	.990	.761
51	2.052	979.00	377.53	.3856	1.010	.783
52	2.092	998.10	384.48	.3852	.970	.804
53	2.133	1017.40	391.43	.3847	.990	.824

STEADY-STATE PHASE FRACTIONAL FLOW : .3848

50% BREAKTHROUGH (PORE VOLUME) : .9557

EXPERIMENT PH340LC

TUBE NUMBER	PORE VOLUMES	TOTAL PHASE VOLUME (CC)	PHASE VOLUME (CC)	FRACTIONAL FLOW	NORMALIZED CONCENTRATION	LAMBDA1
1	.024	22.50	7.40	.3326	.009	-6.007
2	.068	41.35	15.08	.3648	.011	-3.309
3	.108	60.30	22.73	.3770	0.000	-2.550
4	.148	79.30	30.43	.3838	.005	-2.073
5	.188	98.55	38.18	.3875	.005	-1.739
6	.229	117.65	45.90	.3909	.005	-1.488
7	.269	136.70	53.70	.3934	.002	-1.290
8	.309	155.70	61.63	.3958	0.000	-1.127
9	.350	174.75	69.43	.3973	.005	-.989
10	.390	193.90	77.13	.3978	.004	-.868
11	.431	213.30	85.03	.3987	.001	-.761
12	.472	232.65	92.98	.3997	.002	-.664
13	.513	251.85	101.23	.4020	.014	-.577
14	.553	270.95	109.73	.4050	.024	-.498
15	.594	290.25	118.38	.4079	.022	-.426
16	.635	309.50	126.73	.4095	.032	-.358
17	.675	328.70	134.88	.4104	.073	-.295
18	.716	347.95	142.93	.4108	.048	-.236
19	.757	367.30	150.68	.4102	.010	-.180
20	.798	386.55	157.08	.4064	.182	-.120
21	.838	405.80	163.33	.4025	.293	-.078
22	.879	424.85	170.08	.4003	.309	-.030
23	.919	443.90	177.03	.3988	.593	.014
24	.960	463.05	184.08	.3975	.718	.057
25	1.004	482.20	191.23	.3966	.879	.099
26	1.041	501.30	198.58	.3961	.783	.139
27	1.081	520.55	205.90	.3957	.892	.177
28	1.122	539.65	213.53	.3957	.983	.214
29	1.162	558.85	221.23	.3959	1.003	.250
30	1.203	578.05	229.23	.3966	1.056	.284
31	1.244	597.35	237.30	.3974	1.039	.310
32	1.285	616.70	245.53	.3981	1.032	.351
33	1.326	635.95	253.78	.3991	1.027	.383
34	1.366	655.20	262.03	.3999	1.003	.414
35	1.407	674.25	269.98	.4004	.957	.443
36	1.447	693.20	277.10	.3999	.960	.472
37	1.487	712.05	283.73	.3985	.952	.500
38	1.527	730.95	290.30	.3973	.985	.528
39	1.567	749.90	296.70	.3958	1.003	.555
40	1.607	769.00	303.28	.3944	1.031	.581

STEADY-STATE PHASE FRACTIONAL FLOW : .3944

50% BREAKTHROUGH (PORE VOLUME) : .9862

EXPERIMENT PH35A0

TUBE NUMBER[R]	PORE VOLUMES	TOTAL PHASE VOLUME (CC)	PHASE VOLUME (CC)	FRACTIONAL FLOW	NORMALIZED CONCENTRATION	LAMBDA1
1	.019	18.10	10.36	.5726	0.000	-7.887
2	.058	36.70	21.41	.5835	.000	-4.387
3	.098	55.60	32.26	.5803	0.000	-3.266
4	.138	74.65	43.11	.5775	0.000	-2.652
5	.178	93.75	54.01	.5761	0.000	-2.246
6	.218	112.35	64.56	.5747	0.000	-1.953
7	.258	131.40	75.31	.5732	0.000	-1.725
8	.298	150.15	85.96	.5725	.000	-1.539
9	.338	168.95	97.01	.5742	0.000	-1.384
10	.377	187.75	108.06	.5756	0.000	-1.251
11	.417	206.65	119.21	.5769	0.000	-1.134
12	.458	225.70	130.46	.5780	0.000	-1.029
13	.498	244.70	141.86	.5797	0.000	-.935
14	.538	263.70	153.01	.5803	0.000	-.850
15	.578	282.75	164.41	.5815	0.000	-.772
16	.619	301.85	174.71	.5788	0.000	-.700
17	.659	320.95	185.01	.5765	0.000	-.634
18	.699	339.95	195.61	.5754	0.000	-.572
19	.739	358.80	206.36	.5751	0.000	-.514
20	.779	377.55	216.91	.5745	.001	-.460
21	.819	396.25	227.61	.5744	.007	-.409
22	.859	415.20	238.86	.5753	.017	-.361
23	.899	434.30	250.16	.5760	.061	-.314
24	.939	453.25	261.46	.5769	.154	-.270
25	.979	472.00	272.86	.5781	.236	-.228
26	1.019	490.95	284.41	.5793	.229	-.188
27	1.059	509.90	296.01	.5805	.223	-.149
28	1.098	527.65	307.06	.5819	.332	-.113
29	1.136	546.15	318.41	.5830	.384	-.079
30	1.175	564.30	329.61	.5841	.379	-.045
31	1.214	582.55	340.81	.5850	.430	-.013
32	1.252	600.95	352.11	.5859	.602	.019
33	1.292	619.55	363.51	.5867	.680	.049
34	1.331	638.10	374.91	.5875	.742	.079
35	1.373	656.60	386.26	.5883	.836	.108
36	1.409	675.15	397.36	.5886	.908	.137
37	1.449	694.05	408.56	.5887	.925	.160
38	1.489	713.00	420.01	.5891	.977	.192
39	1.529	732.00	431.56	.5896	.992	.219
40	1.569	750.75	442.96	.5900	.997	.245
41	1.609	769.60	454.26	.5903	.924	.270
42	1.649	788.40	465.46	.5904	.971	.295
43	1.689	807.25	476.66	.5905	.969	.319
44	1.728	826.10	488.01	.5907	.993	.342
45	1.768	845.00	499.41	.5910	1.018	.366
46	1.808	863.65	510.71	.5913	.997	.388
47	1.848	882.65	522.06	.5915	1.013	.410
48	1.888	901.60	533.46	.5917	1.033	.432
49	1.928	920.45	544.61	.5917	1.024	.454
50	1.968	939.20	555.91	.5919	.984	.475

STEADY-STATE PHASE FRACTIONAL FLOW : .5920

50% BREAKTHROUGH (PORE VOLUME) : 1.2290

EXPERIMENT PH35MEC

TUBE NUMBER	PORE VOLUMES	TOTAL PHASE VOLUME (CC)	PHASE VOLUME (CC)	FRACTIONAL FLOW	NORMALIZED CONCENTRATION	LAMBDA1
1	.019	18.10	4.48	.2473	.012	-6.253
2	.058	36.70	8.88	.2419	.019	-3.412
3	.098	55.60	13.48	.2424	.022	-2.486
4	.138	74.65	18.08	.2421	.056	-1.971
5	.178	93.75	22.73	.2424	.031	-1.625
6	.218	112.35	27.18	.2419	.034	-1.373
7	.258	131.40	31.68	.2411	.052	-1.174
8	.298	150.15	36.03	.2399	.031	-1.010
9	.338	168.95	40.28	.2384	.040	-.871
10	.377	187.75	44.48	.2369	.080	-.751
11	.417	206.65	49.73	.2406	0.000	-.645
12	.458	225.70	54.13	.2398	.003	-.549
13	.498	244.70	58.60	.2398	0.000	-.462
14	.538	263.70	63.43	.2405	0.000	-.382
15	.578	282.75	68.00	.2400	.059	-.309
16	.619	301.85	74.03	.2452	.108	-.241
17	.659	320.95	80.23	.2500	.108	-.177
18	.699	339.95	86.18	.2535	.228	-.110
19	.739	358.80	91.88	.2561	.284	-.062
20	.779	377.55	97.40	.2582	.457	-.010
21	.819	396.25	102.98	.2599	.685	.040
22	.859	415.20	108.18	.2605	.810	.088
23	.899	434.30	113.28	.2608	1.136	.133
24	.939	453.25	118.08	.2605	1.216	.177
25	.979	472.00	122.53	.2596	1.157	.219
26	1.219	490.95	127.18	.2590	.944	.259
27	1.059	509.90	131.88	.2586	.951	.298
28	1.098	527.65	136.03	.2578	1.164	.335
29	1.136	546.15	140.30	.2570	1.009	.370
30	1.175	564.30	144.53	.2561	.886	.404
31	1.214	582.55	148.63	.2551	.802	.437
32	1.252	600.95	152.88	.2544	1.102	.469
33	1.292	619.55	157.13	.2536	1.019	.501
34	1.331	638.10	161.43	.2530	.951	.532
35	1.370	656.60	165.78	.2525	1.015	.562
36	1.409	675.15	170.33	.2523	.830	.591
37	1.449	694.05	175.13	.2523	.969	.620
38	1.489	713.00	179.63	.2519	.920	.649
39	1.529	732.00	184.13	.2515	.985	.677
40	1.569	750.75	188.43	.2510	1.080	.704
41	1.609	769.60	193.08	.2509	.972	.731
42	1.649	788.40	197.68	.2507	1.123	.757
43	1.689	807.25	202.48	.2508	1.065	.782
44	1.728	826.10	207.18	.2508	1.145	.808
45	1.768	845.00	211.83	.2507	1.111	.832
46	1.808	863.65	216.38	.2505	.889	.856
47	1.848	882.65	221.13	.2505	.981	.880
48	1.888	901.60	225.83	.2505	.923	.904
49	1.928	920.45	230.58	.2505	.840	.927
50	1.968	939.20	235.03	.2502	.944	.949

STEADY-STATE PHASE FRACTIONAL FLOW : .2503
50% BREAKTHROUGH (PORE VOLUME) : .7868

EXPERIMENT PH35MET

TUBE NUMBER	PORE VOLUMES	TOTAL PHASE VOLUME (CC)	PHASE VOLUME (CC)	FRACTIONAL FLOW	NORMALIZED CONCENTRATION	LAMBDA1
1	.019	18.10	4.48	.2473	0.000	-7.437
2	.058	36.70	8.88	.2419	.001	-4.120
3	.098	55.60	13.48	.2424	0.000	-3.053
4	.138	74.65	18.08	.2421	0.000	-2.467
5	.178	93.75	22.73	.2424	0.000	-2.078
6	.218	112.35	27.18	.2419	0.000	-1.797
7	.258	131.40	31.68	.2411	0.000	-1.578
8	.298	150.15	36.03	.2399	.001	-1.398
9	.338	168.95	40.28	.2384	0.000	-1.248
10	.377	187.75	44.48	.2369	0.000	-1.118
11	.417	206.65	49.73	.2406	0.000	-1.005
12	.458	225.70	54.13	.2398	.001	-.903
13	.498	244.70	58.68	.2398	.015	-.811
14	.538	263.70	63.43	.2405	.026	-.728
15	.578	282.75	68.08	.2408	.029	-.652
16	.619	301.85	74.03	.2452	.053	-.581
17	.659	320.95	80.23	.2500	.047	-.515
18	.699	339.95	86.18	.2535	.066	-.454
19	.739	358.80	91.88	.2561	.071	-.397
20	.779	377.55	97.48	.2582	.093	-.344
21	.819	396.25	102.98	.2599	.131	-.294
22	.859	415.20	108.18	.2605	.185	-.246
23	.899	434.30	113.28	.2608	.266	-.200
24	.939	453.25	118.08	.2605	.305	-.156
25	.979	472.00	122.53	.2596	.301	-.114
26	1.019	490.95	127.18	.2590	.350	-.074
27	1.059	509.90	131.88	.2586	.425	-.035
28	1.098	527.65	136.03	.2578	.501	.001
29	1.136	546.15	140.38	.2570	.656	.035
30	1.175	564.30	144.53	.2561	.631	.069
31	1.214	582.55	148.63	.2551	.443	.101
32	1.252	600.95	152.88	.2544	.818	.132
33	1.292	619.55	157.13	.2536	.945	.163
34	1.331	638.10	161.43	.2530	.956	.193
35	1.370	656.60	165.78	.2525	.817	.223
36	1.409	675.15	170.33	.2523	.934	.251
37	1.449	694.05	175.13	.2523	1.034	.279
38	1.489	713.00	179.63	.2519	.822	.306
39	1.529	732.00	184.13	.2515	1.037	.333
40	1.569	750.75	188.43	.2510	1.132	.360
41	1.609	769.60	193.08	.2509	1.032	.385
42	1.649	788.40	197.68	.2507	1.028	.410
43	1.689	807.25	202.48	.2508	1.023	.434
44	1.728	826.10	207.18	.2508	1.123	.458
45	1.768	845.00	211.83	.2507	.816	.482
46	1.808	863.65	216.38	.2505	.919	.505
47	1.848	882.65	221.13	.2505	.964	.527
48	1.888	901.60	225.83	.2505	1.102	.549
49	1.928	920.45	230.58	.2505	.885	.571
50	1.968	939.20	235.03	.2502	1.107	.593

STEADY-STATE PHASE FRACTIONAL FLOW : .2503
50% BREAKTHROUGH (PORE VOLUME) : .0973

EXPERIMENT PH350L

TUBE NUMBER	PORE VOLUMES	TOTAL PHASE VOLUME (CC)	PHASE VOLUME (CC)	FRACTIONAL FLOW	NORMALIZED CONCENTRATION	LAMBDA1
1	.019	18.10	3.26	.1801	.130	-8.486
2	.058	36.70	6.41	.1747	.090	-4.741
3	.098	55.60	9.86	.1773	.130	-3.547
4	.138	74.65	13.46	.1803	0.000	-2.895
5	.178	93.75	17.01	.1814	0.000	-2.465
6	.218	112.35	20.61	.1834	0.000	-2.157
7	.258	131.40	24.41	.1858	.090	-1.917
8	.298	150.15	28.16	.1875	0.000	-1.722
9	.338	168.95	31.66	.1874	0.000	-1.561
10	.377	187.75	35.21	.1875	0.000	-1.422
11	.417	206.65	37.71	.1825	0.000	-1.300
12	.458	225.70	41.11	.1821	0.000	-1.192
13	.498	244.70	44.16	.1805	0.000	-1.095
14	.538	263.70	47.26	.1792	0.000	-1.007
15	.578	282.75	50.26	.1778	0.000	-.927
16	.619	301.85	53.11	.1759	0.000	-.853
17	.659	320.95	55.71	.1736	0.000	-.784
18	.699	339.95	58.16	.1711	0.000	-.721
19	.739	358.80	60.56	.1688	0.000	-.662
20	.779	377.55	63.16	.1673	0.000	-.607
21	.819	396.25	65.66	.1657	.020	-.555
22	.859	415.20	68.16	.1642	.050	-.506
23	.899	434.30	70.86	.1632	.090	-.459
24	.939	453.25	73.71	.1626	.120	-.414
25	.979	472.00	76.61	.1623	.130	-.372
26	1.019	490.95	79.36	.1616	.140	-.331
27	1.059	509.90	82.01	.1608	.140	-.292
28	1.098	527.65	84.56	.1603	.160	-.256
29	1.136	546.15	87.36	.1600	.160	-.221
30	1.175	564.30	90.16	.1598	.180	-.188
31	1.214	582.55	93.11	.1598	.180	-.155
32	1.252	600.95	95.96	.1597	.230	-.124
33	1.292	619.55	98.91	.1596	.270	-.093
34	1.331	638.10	101.76	.1595	.320	-.063
35	1.370	656.60	104.56	.1592	.410	-.034
36	1.409	675.15	107.46	.1592	.490	-.006
37	1.449	694.05	110.36	.1590	.540	.022
38	1.489	713.00	113.36	.1590	.610	.049
39	1.529	732.00	116.31	.1589	.680	.076
40	1.569	750.75	119.36	.1590	.740	.102
41	1.609	769.60	122.26	.1589	.830	.127
42	1.649	788.40	125.26	.1589	.860	.151
43	1.689	807.25	128.11	.1587	.900	.175
44	1.728	826.10	130.91	.1585	.970	.199
45	1.768	845.00	133.76	.1583	1.010	.222
46	1.808	863.65	136.56	.1581	1.030	.244
47	1.848	882.65	139.46	.1580	1.060	.266
48	1.888	901.60	142.31	.1578	1.100	.288
49	1.928	920.45	145.26	.1578	1.130	.309
50	1.968	939.20	148.26	.1579	1.120	.330
51	2.008	958.00	151.36	.1580	1.090	.350
52	2.047	976.75	155.31	.1590	1.060	.370
53	2.087	995.45	158.61	.1593	1.030	.389
54	2.127	1014.20	161.91	.1596	1.150	.409
55	2.167	1033.15	165.26	.1600	.970	.428

STEADY-STATE PHASE FRACTIONAL FLOW : .1600
50% BREAKTHROUGH (PORE VOLUME) : 1.4172

EXPERIMENT PH36

TUBE NUMBER	PORE VOLUMES	TOTAL PHASE VOLUME (CC)	PHASE VOLUME (CC)	FRACTIONAL FLOW	NORMALIZED CONCENTRATION	LAMBDA1
1	.014	13.40	13.40	1.0000	0.000	-7.821
2	.044	27.75	27.75	1.0000	0.000	-4.314
3	.074	42.15	42.15	1.0000	0.000	-3.192
4	.104	56.30	56.30	1.0000	0.000	-2.591
5	.134	70.20	70.20	1.0000	0.000	-2.200
6	.163	84.15	84.15	1.0000	0.000	-1.914
7	.193	98.35	98.35	1.0000	0.000	-1.689
8	.223	112.25	112.25	1.0000	0.000	-1.506
9	.252	126.30	126.30	1.0000	0.000	-1.352
10	.282	140.60	140.60	1.0000	0.000	-1.219
11	.313	154.75	154.75	1.0000	0.000	-1.102
12	.342	168.65	168.65	1.0000	0.000	-.999
13	.372	182.60	182.60	1.0000	0.000	-.908
14	.401	196.40	196.40	1.0000	0.000	-.825
15	.431	210.65	210.65	1.0000	0.000	-.748
16	.461	224.55	224.55	1.0000	0.000	-.677
17	.490	238.40	238.40	1.0000	0.000	-.612
18	.519	252.35	252.35	1.0000	.000	-.552
19	.549	266.25	266.25	1.0000	.001	-.494
20	.578	280.15	280.15	1.0000	.002	-.441
21	.608	294.00	294.00	1.0000	.007	-.390
22	.637	307.85	307.85	1.0000	.006	-.342
23	.666	321.75	321.75	1.0000	.022	-.297
24	.696	335.65	335.65	1.0000	.029	-.253
25	.725	349.50	349.50	1.0000	.040	-.211
26	.754	363.45	363.45	1.0000	.068	-.171
27	.784	377.35	377.35	1.0000	.138	-.133
28	.813	391.25	391.25	1.0000	.229	-.096
29	.843	405.20	405.20	1.0000	.317	-.061
30	.872	419.00	419.00	1.0000	.425	-.026
31	.901	432.70	432.70	1.0000	.519	.007
32	.930	446.55	446.55	1.0000	.645	.038
33	.960	460.40	460.40	1.0000	.742	.069
34	.989	474.05	474.05	1.0000	.858	.099
35	1.018	488.00	488.00	1.0000	.949	.128
36	1.048	501.90	501.90	1.0000	1.001	.157
37	1.077	515.80	515.80	1.0000	.970	.185
38	1.106	529.70	529.70	1.0000	1.032	.212
39	1.136	543.45	543.45	1.0000	.979	.238
40	1.165	557.30	557.30	1.0000	1.020	.264
41	1.194	571.20	571.20	1.0000	1.026	.289
42	1.224	585.05	585.05	1.0000	1.026	.314
43	1.253	598.95	598.95	1.0000	1.016	.338
44	1.282	612.80	612.80	1.0000	1.014	.361
45	1.312	626.65	626.65	1.0000	1.005	.384
46	1.341	640.50	640.50	1.0000	1.035	.407
47	1.370	654.40	654.40	1.0000	1.012	.429
48	1.400	668.40	668.40	1.0000	1.043	.451
49	1.430	682.55	682.55	1.0000	1.002	.472
50	1.459	696.50	696.50	1.0000	.975	.493
51	1.489	710.30	710.30	1.0000	.958	.514
52	1.518	724.45	724.45	1.0000	1.010	.534
53	1.548	738.50	738.50	1.0000	1.010	.554
54	1.578	752.65	752.65	1.0000	.994	.574

55	1.606	766.80	766.80	1.0000	.970	.594
56	1.638	780.70	780.70	1.0000	1.031	.613
57	1.667	794.55	794.55	1.0000	1.021	.632
58	1.697	808.70	808.70	1.0000	1.010	.650
59	1.727	823.15	823.15	1.0000	1.017	.669
60	1.743	823.70	823.70	1.0000	.990	.670

STEADY-STATE PHASE FRACTIONAL FLOW : 1.0000
50% BREAKTHROUGH (PORE VOLUME) : .8954

REFERENCES

1. Pope, G. A. : "The Application of Fractional Flow Theory to Enhanced Oil Recovery," Soc. Pet. Eng. J. (June 1980) 20, 191-205.

2. Gupta, S. P. and Trushenski, S. P.: "Micellar Flooding--Compositional Effects on Oil Displacement," Soc. Pet. Eng. J. (April 1979) 116-128.

3. Thomas, C. P., Flemings, III, P. D., and Winter, W. K.: "Application of a General Multiphase, Multicomponent Chemical Flood Model to Ternary, Two-Phase Surfactant Systems," Soc. Pet. Eng. J. (February 1981) 21, 63-76.

4. Bear, J.: Dynamics of Fluids in Porous Media, Elsevier, New York, Chapters 9-10, 1972.

5. Scheidegger, A. E.: The Physics of Flow Through Porous Media, MacMillan, New York, Chapter 8, 1957.

6. Bardon, C. and Longeron, D. G.: "Influence of Very Low Interfacial Tensions on Relative Permeability," Soc. Pet. Eng. J. (October 1980) 20, 391-401.

7. Amaefule, Jude O. and Handy, L. L.: "The Effect of Interfacial Tensions on Relative Oil-Water Permeabilities of Consolidated Porous Media," paper SPE 9783 presented at the 2nd Joint Symposium on Enhanced Oil Recovery, Tulsa, OK (April 5-8, 1981).

8. Labastie, A., Guy, M., and Decalud, J. P.: "Effect of Flow Rate and Wettability on Oil-Water Relative Permeabilities and Capillary Pressure," paper SPE 9236 presented at the 2nd Joint Symposium on Enhanced Oil Recovery, Tulsa, OK (April 5-8, 1981).

9. Leverett, M. C.: "Flow of Oil-Water Mixtures Through Unconsolidated Sands," Trans. AIME (1939) 132, 149-171.

10. Klaus, E. E.: "Enhanced Recovery of Pennsylvania Grade Crude Oil with Surfactant," Annual Report for October 1978-September 1979, Contract No. DE-AS19-78BD20009.

11. Mungan, N.: "Interfacial Effects in Immiscible Liquid-Liquid Displacement on Porous Media," Soc. Pet. Eng. J. (September 1966) 6, 247-253.

12. Lefebvre Du Prey, E. J.: "Factors Affecting Liquid-Liquid Relative Permeabilities of a Consolidated Porous Medium," Soc. Pet. Eng. J. (February 1973) 3, 39-47.

13. Talash, A. W.: "Experimental and Calculated Relative Permeability Data for Systems Containing Tension Additives," paper SPE 5810 presented at Improved Oil Recovery Symposium (March 22-24, 1976) Tulsa, OK.

14. Batycky, J. P. and McCaffery, F. G.: "Low Interfacial Tension Displacement Studies," paper No. 78.29.26 presented at 29th Annual Technical Meeting of the Petroleum Society of CIM, Calgary, Canada (June 13-16, 1978).

15. Geffen, T. M., Owens, W. W., Parrish, D. R., and Morse, R. A.: "Experimental Investigation of Factors Affecting Laboratory Relative Permeability Measurements," Trans., AIME (1951) 192, 99-110.

16. Donaldson, E. C., Lorenz, P. B., and Thomas, R. D.: "The Effects of Viscosity and Wettability on Oil and Water Relative Permeabilities," paper SPE 1562 presented at 41st Annual SPE Fall Meeting, Dallas, TX (Oct. 2-5, 1966).

17. Gogarty, W. B.: "Mobility Control with Polymer Solutions," Soc. Pet. Eng. J. (June, 1967) 7 161-173.

18. Gogarty, W. B., Meabon, H. P., and Milton, Jr., H. W.: "Mobility Control Design for Miscible-Type Waterfloods Using Micellar Solutions," J. Pet. Tech. (Feb. 1970) 22, 141-147.

19. Chang, H. L., Al-Rikabi, H. M., and Pusch, W. H.: "Determination of Oil/Water Bank Mobility in Micellar-Polymer Flooding," J. Pet. Tech. (July, 1978) 30, 1055-1060.

20. Brigham, W. E., Reed, P. W., and Dew, J. N.: "Experiments on Mixing During Miscible Displacement in Porous Media," Soc. Pet. Eng. J. (March 1961) 1 1-8; Trans., AIME, Vo. 222.

21. Perkins, T. K., Jr. and Johnston, O. C.: "A Review of Diffusion and Dispersion in Porous Media," Soc. Pet. Eng. J. (March 1963) 70-84; Trans., AIME, Vol. 228.

22. Lake, L. W. and Hirasaki, G. J.: "Taylor's Dispersion in Stratified Porous Media," Soc. Pet. Eng. J., 21, 731-739.

23. Spence, A. P., Jr., and Watkins, R. W.: "The Effect of Microscopic Core Heterogeneity on Miscible Flood Residual Oil Saturation," paper SPE 9229 presented at the 55th Annual SPE Fall Meeting, Dallas, TX (Sept. 21-24, 1980).

24. Shuler, P. J.: A Study of the Mechanisms Affecting the Enhanced Recovery of Oil by Surfactant Flooding, PhD Thesis, University of Colorado at Boulder (1978).

25. Blackwell, R. J.: "Laboratory Studies of Microscopic Dispersion Phenomena," Soc. Pet. Eng. J. (March, 1962) 2, 1-8.

26. Baker, L. E.: "Effects of Dispersion and Dead-End Pore Volume in Miscible Flooding," Soc. Pet. Eng. J. (June 1977) 17, 219-227.

27. Gupta, S. F.: Dispersion and Adsorption in Porous Media, PhD Thesis, Purdue University (1972).

28. Delshad, M.: "Measurement of Relative Permeability and Dispersion for Micellar Fluids in Berea Rock," MS Thesis, The University of Texas at Austin (1981).

29. Brigham, W. E.: "Mixing Equations in Short Laboratory Cores," Soc. Pet. Eng. J. (Feb. 1974) 14, 91-99; Trans., AIME, Vol. 257.

30. Deans, H. A.: "Using Chemical Tracers to Measure Fractional Flow and Saturations In-Situ," paper SPE 7076 presented at the SPE 5th Symposium on Improved Methods for Oil Recovery, Tulsa, Oklahoma, April 16-19, 1978.

31. Stalkup, F. I.: "Displacement of Oil by Solvent at High Water Saturation," Soc. Pet. Eng. J. (Dec. 1970) 10, 337-348.

32. Coats, K. H. and Smith B. D.: "Dead-End Pore Volume and Dispersion in Porous Media," Soc. Pet. Eng. J. (March 1964) 4, 73-84; Trans., AIME, Vol. 231.

33. Raimondi, P., Torcaso, M. A., and Henderson, J. H.: "The Effect of Interstitial Water on the Mixing of Hydrocarbons During a Miscible Displacement Process," Mineral Industries Experimental Station Circular No. 61, The Pennsylvania State U., University Park, (Oct. 23-25, 1961.

34. Thomas, G. H, Countryman, G. R., and Fatt, Irving: Miscible Displacement in a Multiphase System," Soc. Pet. Eng. J. (Sept. 1963) 3, 189-196.

35. Donaldson, E. C., Kendall, R. F., and Manning F. S.: "Dispersion and Tortuosity in Sandstones," paper SPE 6190 presented at the SPE 51st Annual Fall Meeting, New Orleans, Louisiana, Oct. 3-6, 1976.

36. Nelson, R. C. and Pope, G. A.: "Phase Relationships in Chemical Flooding," SPEJ, 18 325-328 (1978).

37. Tsaur, K.: "A Study of Polymer/Surfactant Interactions for Micellar/Polymer Flooding Applications," MS Thesis, University of Texas at Austin (1978).

38. Healy, R. N. and Reed, R. L.: "Immiscible Microemulsion Flooding," Soc. Pet. Eng. J. (April 1977) 17, 129-139.

39. Glinsmann, G. R.: "Surfactant Flooding with Microemulsions Formed In-Situ--Effect of Oil Characteristics," SPE 8326 presented at the 54th Annual Fall Technical Conference of the SPE, Las Vegas, Nevada, (1979).

40. Darcy, H.: "Les Fountaines Publiques de la Ville de Dijon," Dalmont, Paris, 1856.

41. Hedges, J. H. and Glinsmann, G. R.: "Compositional Effects on Surfactant Flood Optimization," SPE 8324 presented at the 54th Annual Fall Technical Conference of the SPE, Las Vegas, Nevada, (1979).

42. Wade, W. H., Schechter, R. S., Morgan, J. C., and Jacobson, J.: "Low Interfacial Tension Involving Mixtures of Surfactants," SPEJ., 17 122-128 (1977)

43. Wade, W. H., Morgan, J., Jacobson, J., Salager, J. L., and Schechter, R. S.,: "Interfacial Tension and Phase Behavior of Surfactant Systems," SPEJ, 18 242-252 (1978).

44. Morgan, J. C., Schechter, R. S., and Wade, W. H.: "Recent Advances in the Study of Low Interfacial Tensions," Published in "Improved Oil Recovery by Surfactant and Polymer Flooding," D. O. Shah and R. S. Schechter, Editors, Academic Press, 101-118 (1977).

45. Salager, J. L.: "Physico-Chemical Properties of Surfactant-Water-Oil Mixtures: Phase Behavior, Microemulsion Formation, and Interfacial Tension," PhD Dissertation, University of Texas at Austin (1977).

46. Salager, J. L., Morgan, J. C., Schechter, R. S., Wade, W. H., and Vasquez, E.: "Optimum Formulation of Surfactant-Water-Oil Systems for Minimum Interfacial Tension or Phase Behavior," SPEJ, 19 107-115 (1979).

47. Jones, K.: "Rheology of Viscoelastic Fluids for Oil Recovery," MS Thesis, The University of Texas at Austin (1981).

48. "Mobility Control and Scaleup for Chemical Flooding," DOE Report DOE/BC/10095-4, August 1979-July 1980.

49. Cayias, J. L., Schechter, R. S., and Wade, W. H.: "The Measurement of Low Interfacial Tension Via the Spinning Drop Technique," ed. K. L. Mittal, ACS Symposium Series, Adsorption at Interfaces (1975), 8, 234-248.

VITA

Donald James MacAllister was born in Muleshoe, Texas, on January 27, 1953, the son of Neal Daniel MacAllister and Chrys Faye MacAllister. After graduation from Coronado High School, Lubbock, Texas, in 1971, he entered The University of Texas at Austin, Texas. As an undergraduate he co-authored publications for the Society of Petroleum Engineers of AIME and the Journal of Colloid and Interface Science. He received a Bachelor of Science in Chemistry degree in December, 1974, and entered Southwestern Medical School in August, 1975. Feeling that he was more suited to the recovery of oil than the recovery of people, he entered the Graduate School at The University of Texas in September, 1979, after a short stint at Core Laboratories.

Permanent address: 2907 Haymeadow
Carrollton, Texas

This thesis was typed by Lynne K. Smith.